UNIVERSITY OF SOUTHAMPTON

CROSS-AXIS MOVEMEMENTS OF THE SEATED HUMAN BODY IN RESPONSE TO WHOLE-BODY VERTICAL AND FORE-AND-AFT VIBRATION

Naser Nawayseh, B.Sc., M.Sc.

DOCTOR OF PHILOSOPHY

FACULTY OF ENGINEERING, SCIENCE AND MATHEMATICS
INSTITUTE OF SOUND AND VIBRATION RESEARCH

MARCH 2004

UNIVERSITY OF SOUTHAMPTON

ABSTRACT

FACULTY OF ENGINEERING, SCIENCE AND MATHEMATICS

INSTITUTE OF SOUND AND VIBRATION RESEARCH

Doctor of Philosophy

CROSS-AXIS MOVEMENTS OF THE SEATED HUMAN BODY IN RESPONSE TO WHOLE-BODY VERTICAL AND FORE-AND-AFT VIBRATION

By Naser Nawayseh

The dynamic responses of humans to vibration are widely reported in the literature with more focus on vertical excitation than horizontal or rotational excitation. Forces have been measured only on the seat and only in the direction of excitation. The aim of this thesis is to provide insight into the forces in both the direction of excitation and in other directions during whole-body vertical and fore-and-aft excitation. The apparent mass was used to represent the forces in the direction of excitation and cross-axis apparent mass in the other directions.

In all experiments, male subjects were exposed to random vibration at 0.125, 0.25, 0.625 and 1.25 ms^{-2} r.m.s. The frequency range differed between the different studies. However, a frequency range of 0.25 to10 Hz was covered in all the studies. During vertical excitation, the vertical apparent mass, fore-and-aft cross-axis apparent mass and lateral cross-axis apparent mass were measured on the seat and backrest. The vertical apparent mass at the feet was also measured. The vertical apparent mass on the seat showed a resonance in the vicinity of 5 Hz. The fore-and-aft cross-axis apparent masses on the seat and at the backrest were as high as 60% of the static masses of the subjects at some frequencies. The vertical apparent mass at the backrest and the lateral cross-axis apparent masses on both the seat and backrest were small compared to those measured in the vertical and fore-and-aft directions on the seat and in the fore-and-aft direction at the backrest. The apparent mass at the feet showed three vibration modes. In all directions, the responses were non-linear: the resonance frequencies decreased with increasing the vibration magnitude.

During fore-and-aft excitation, the fore-and-aft apparent mass, vertical cross-axis apparent mass and lateral cross-axis apparent mass were measured on the seat and backrest. The fore-and-aft apparent mass and the vertical cross-axis apparent mass at the feet were also measured. When no backrest was used, the fore-and-aft apparent mass on the seat suggested three vibration modes: around 1 Hz, between 1 and 3 Hz, and between 3 Hz and 5 Hz. When a backrest was used, only two modes were evident when the feet were not supported and only one mode when the feet were supported. The fore-and-aft apparent mass at the back suggested a main resonance between 3 and 5 Hz. The vertical cross-axis apparent masses on the seat reached as high as 70% of the static masses of the subjects and showed dependency on the sitting posture. However, the vertical cross-axis apparent mass at the backrest and the lateral cross-axis apparent mass on the seat and backrest were very small compared to the fore-and-aft apparent mass on the seat and backrest and the vertical cross-axis apparent mass on the seat. The fore-and-aft apparent mass and the vertical cross-axis apparent mass at the feet were affected by the use of a backrest. The apparent mass and cross-axis apparent mass on the seat, backrest and footrest were non-linear with vibration magnitude.

The effect of seat surface angle on the 'vertical apparent mass' and 'fore-and-aft cross-axis apparent mass' was studied with vertical excitation. The effect of seat surface angle was more pronounced in the 'fore-and-aft cross-axis apparent mass' than in the 'vertical apparent mass'. Increasing seat surface angle decreased the non-linearity in the 'fore-and-aft' direction, possibly due to an increase in the shear stiffness of the buttocks tissue.

A series of lumped parameter linear models with rotational capabilities were developed for the prediction of the vertical apparent mass and the fore-and-aft cross-axis apparent mass measured on the seat with vertical excitation. The final model suggested that three degrees-of-freedom (rotational, vertical and fore-and-aft) were needed to predict the vertical apparent mass and the fore-and-aft cross-axis apparent mass. The final model also suggested a fore-and-aft sliding motion (or possibly deformation of tissue in contact with the seat) of the human body on the seat when exposed to vertical excitation. A linear lumped parameter model was also developed to predict the fore-and-aft apparent mass and the vertical cross-axis apparent mass measured on the seat with fore-and-aft excitation.

In conclusion, the cross-axis forces during vertical and fore-and-aft excitation indicate that the seated human body moves in two-dimensions when exposed to either vertical excitation or fore-and-aft excitation. The cross-axis forces were found to depend on several factors such as vibration frequency, vibration magnitude, sitting posture and seating condition (e.g. using a backrest or a footrest).

ACKNOWLEDGMENTS

I would like to express my gratitude and thanks to my supervisor Professor Michael Griffin for his invaluable advice and encouragements throughout the period of my research. Words are incapable of describing my appreciation for his help. I would also like to thank my review board members Professor Mike Brennan and Dr Neil Ferguson for their constructive questions and suggestions. I would also like to thank the members of the Human Factors Research Unit for providing a comfortable and friendly research environment. The help provided by Dr Miyuki Morioka, Mr Martin Toward and Mr Barnaby Donohew to get me familiar with the use of the equipment and software when I first started my PhD is very much appreciated. Several discussions with Dr Yi Qui, a former unit member, and Dr Chris Lewis were very helpful. My thanks also go to Mr Gary Parker and Mr Peter Russell for their useful technical advice. I would also like to thank all the subjects who participated in the experimental work. I would like to thank all my friends, especially Sophie, Yioula, Tamer, and Ashraf for the unlimited support offered to me during my study. I would like to thank my parents, brothers and sisters for their constant support, encouragement and prayer for me to achieve my goals.

TABLE OF CONTENTS

LIST OF SYMBOLS x

CHAPTER 1 INTRODUCTION 1

CHAPTER 2 LITERATURE REVIEW 4

2.1 INTRODUCTION 4
2.2 METHODS OF REPRESENTING DYNAMIC RESPONSES 4
2.3 MECHANICAL IMPEDANCE AND APPARENT MASS OF THE HUMAN BODY 5
2.3.1 Vertical excitation 5
2.3.1.1 Effect of posture and seating condition 6
2.3.1.2 Effect of vibration magnitude and vibration waveform 16
2.3.2 Horizontal excitation 23
2.3.3 Rotational excitation 26
2.4 TRANSMISSIBILITY OF THE HUMAN BODY 27
2.4.1 Transmissibility to the pelvis and the spine 28
2.4.1.1 Effect of posture and seating condition on the transmissibility to the pelvis and the spine 31
2.4.2 Transmissibility to the head 35
2.4.2.1 Effect of posture and seating condition on the transmissibility to the head 37
2.4.3 Effect of vibration magnitude on the transmissibility to the human body 41
2.5 POSSIBLE CAUSES OF THE PRINCIPAL RESONANCE OF THE APPARENT MASS (OR MECHANICAL IMPEDANCE) 43
2.6 SUGGESTED MECHANISMS CAUSING THE NON-LINEARITY OF THE HUMAN BODY 45
2.7 CROSS-AXIS FORCES AT THE DRIVING POINT 47
2.8 MODELLING THE DYNAMIC RESPONSES OF THE SEATED HUMAN BODY TO VIBRATION 48
2.8.1 Introduction 48
2.8.2 Lumped parameter modelling of the seated human body 49
2.8.2.1 Apparent mass and mechanical impedance models 49
2.8.2.2 Transmissibility models 57
2.8.3 Modelling of the human body in standing and lying positions 61

2.8.4 Modelling the human body in response to horizontal vibration 64
2.8.5 Other models 65
2.9 SUMMARY OF THE LITERATURE REVIEW AND CONCLUSIONS 68

CHAPTER 3 EXPERIMENTAL APPARATUS AND DATA ACQUISITION AND ANALYSIS 72

3.1 INTRODUCTION 72
3.2 EXPERIMENTAL APPARATUS 72
3.2.1 Vibrators 72
3.2.1.1 One-meter vertical electro-hydraulic vibrator 72
3.2.1.2 One-meter horizontal electro-hydraulic vibrator 73
3.2.2 Transducers 73
3.2.2.1 Force transducers 73
3.2.2.2 Accelerometers 78
3.3 DATA ACQUISITION 79
3.4 DATA ANALYSIS 79
3.4.1 Frequency response functions 79
3.4.1.1 Mass cancellation 81
3.4.2 Statistical analysis 82
3.4.2.1 Friedman two-way analysis of variance 82
3.4.2.2 Wilcoxon matched-pairs signed ranks test 83
3.4.2.3 Spearman rank correlation coefficient, rho 83

CHAPTER 4 FORCES AT THE SEAT AND FOOTREST DURING VERTICAL WHOLE-BODY EXCITATION 84

4.1 INTRODUCTION 84
4.2 APPARATUS, EXPERIMENTAL DESIGN AND ANALYSIS 86
4.2.1 Apparatus 86
4.2.2 Experimental design 87
4.2.3 Analysis 87
4.3 RESULTS 87
4.3.1 Response on the seat in the vertical direction 88

4.3.2 Response in the fore-and-aft direction 92
4.3.3 Response in the lateral direction 94
4.3.4 Response at the feet 96
4.4 DISCUSSION 98
4.4.1 Response in the vertical direction 98
4.4.2 Response in the fore-and-aft direction 100
4.4.3 Response in the lateral direction 102
4.4.4 Response at the feet 102
4.5 CONCLUSION 103

CHAPTER 5 FORCES AT THE SEAT AND BACKREST DURING VERTICAL WHOLE-BODY EXCITATION 104

5.1 INTRODUCTION 104
5.2 APPARATUS, EXPERIMENTAL DESIGN AND ANALYSIS 105
5.2.1 Apparatus 105
5.2.2 Experimental design 106
5.2.3 Analysis 107
5.3 RESULTS 107
5.3.1 Static forces on the backrest 107
5.3.2 Response in the vertical direction 108
5.3.2.1 Apparent mass at the seat 108
5.3.2.2 Apparent mass at the back 110
5.3.3 Response in the fore-and-aft direction 112
5.3.3.1 Response at the seat 112
5.3.3.2 Response at the backrest 114
5.3.4 Response in the lateral direction at the seat and backrest 116
5.3.5 Correlation with body characteristics 118
5.4 DISCUSSION 118
5.4.1 Response in the vertical direction 118
5.4.2 Response in the fore-and-aft direction 121
5.4.3 Response in the lateral direction 123
5.5 CONCLUSIONS 124

CHAPTER 6 FORCES AT THE SEAT AND FOOTREST DURING FORE-AND-AFT WHOLE-BODY EXCITATION 126

6.1 INTRODUCTION 126
6.2 APPARATUS, EXPERIMENTAL DESIGN AND ANALYSIS 127
6.2.1 Apparatus 127
6.2.2 Experimental design 127
6.2.2.1 First experiment 127
6.2.2.2 Second experiment 128
6.2.3 Analysis 128
6.3 RESULTS 129
6.3.1 Responses on the seat 129
6.3.1.1 Response in the fore-and-aft direction 129
6.3.1.2 Responses in the vertical and lateral directions 130
6.3.2 Responses at the feet 137
6.3.2.1 Response in the fore-and-aft direction 137
6.3.2.2 Response in the vertical direction 140
6.4 DISCUSSION 142
6.4.1 Response in the fore-and-aft direction 142
6.4.2 Responses in the vertical and lateral directions 144
6.4.3 Response at the feet 146
6.5 CONCLUSION 147

CHAPTER 7 FORCES AT THE SEAT AND BACKREST DURING FORE-AND-AFT WHOLE-BODY EXCITATION 148

7.1 INTRODUCTION 148
7.2 APPARATUS, EXPERIMENTAL DESIGN AND ANALYSIS 149
7.2.1 Apparatus 149
7.2.2 Experimental design 149
7.2.3 Analysis 150
7.3 RESULTS 151
7.3.1 Responses in the fore-and-aft direction 151
7.3.1.1 Response on the seat 151
7.3.1.2 Response at the backrest 154

7.3.2 Responses in the vertical direction 157
7.3.2.1 Response on the seat 157
7.3.2.2 Response at the backrest 160
7.3.3 Response in the lateral direction (at the seat and the backrest) 161
7.4 DISCUSSION 162
7.4.1 Response in the fore-and-aft direction 162
7.4.2 Response in the vertical and lateral directions 166
7.5 CONCLUSION 168

CHAPTER 8 EFFECT OF SEAT SURFACE ANGLE ON FORCES AT THE SEAT SURFACE DURING WHOLE-BODY VERTICAL EXCITATION 169

8.1 INTRODUCTION 169
8.2 APPARATUS, EXPERIMENTAL DESIGN AND ANALYSIS 171
8.2.1 Apparatus 171
8.2.2 Experimental design 172
8.2.3 Analysis 172
8.3 RESULTS 173
8.3.1 'Vertical apparent mass' 173
8.3.1.1 Effect of vibration magnitude 174
8.3.1.2 Effect of seat angle 176
8.3.1.3 Effect of backrest 177
8.3.2 'Fore-and-aft cross-axis apparent mass' 180
8.3.2.1 Effect of vibration magnitude 181
8.3.2.2 Effect of seat angle 183
8.3.2.3 Effect of backrest 185
8.4 DISCUSSION 187
8.4.1 'Vertical apparent mass' 187
8.4.2 'Fore-and-aft cross-axis apparent mass' 189
8.5 CONCLUSIONS 192

CHAPTER 9 MODELLING THE APPARENT MASS AND THE CROSS-AXIS APPARENT MASS MEASURED ON THE SEAT DURING VERTICAL EXCITATION AND DURING FORE-AND-AFT EXCITATION 193

9.1 INTRODUCTION 193
9.2 MODELLING THE VERTICAL APPARENT MASS AND THE FORE-AND-AFT CROSS AXIS APPARENT MASS DURING VERTICAL EXCITATION 194
9.2.1 Model description 194
9.2.2 Equations describing the model 195
9.2.3 Model parameters 196
9.2.4 Results and discussion 198
9.2.4.1 Modelling median and individual data 198
9.2.4.2 Parameter sensitivity tests 206
9.2.4.3 Non-linearity 208
9.2.4.4 Vertical and fore-and-aft transmissibilities to mass 2 211
9.2.5 Conclusions 213
9.3 ALTERNATIVE MODELS TO IMPROVE THE PREDICTION OF THE VERTICAL APPARENT MASS AND THE FORE-AND-AFT CROSS-AXIS APPARENT MASS DURING VERTICAL EXCITATION 214
9.3.1 Description and parameters of the investigated models 214
9.3.2 Results and discussion 216
9.3.2.1 Modelling of median data 216
9.3.2.2 Modelling of individual data 219
9.3.2.3 Parameter sensitivity tests 224
9.4 MODELLING THE FORE-AND-AFT APPARENT MASS AND THE VERTICAL CROSS AXIS APPARENT MASS DURING FORE-AND-AFT VIBRATION 229
9.5 GENERAL REMARKS AND CONCLUSIONS 235

CHAPTER 10 GENERAL DISCUSSION 239

10.1 INTRODUCTION 239
10.2 SUMMARY OF THE MAIN FINDINGS 239
10.3 USE OF LINEAR TECHNIQUES (CROSS-SPECTRAL DENSITY METHOD) 240
10.4 INVESTIGATING THE NON-LINEARITY OF THE HUMAN BODY USING THE PRINCIPLE OF RECIPROCITY AND THE CROSS-AXIS FORCES 243
10.4.1 Introduction 243
10.4.2 Principle of reciprocity 243
10.4.3 Applying the principle of reciprocity to Model 5 using the cross-axis apparent mass 244

10.4.4 Testing the non-linearity of the human body using the cross-axis apparent mass 245

10.5 EFFECT OF SEATING CONDITION ON THE CORRELATION BETWEEN THE RESONANCE FREQUENCIES OF THE VERTICAL APPARENT MASS AND THE FORE-AND-AFT CROSS-AXIS APPARENT MASS 251

CHAPTER 11 GENERAL CONCLUSIONS AND RECOMMENDATIONS FOR FUTURE WORK 254

11.1 INTRODUCTION 254
11.2 GENERAL CONCLUSIONS 254
11.3 RECOMMENDATIONS FOR FUTURE WORK 255

APPENDICES 258

APPENDIX A INDIVIDUAL DATA: VERTICAL EXCITATION WITHOUT A BACKREST (CHAPTER 4) 259

APPENDIX B INDIVIDUAL DATA: VERTICAL EXCITATION WITH A BACKREST (CHAPTER 5) 272

APPENDIX C INDIVIDUAL DATA: FORE-AND-AFT EXCITATION WITHOUT A BACKREST (CHAPTER 6) 288

APPENDIX D INDIVIDUAL DATA: FORE-AND-AFT EXCITATION WITH A BACKREST (CHAPTER 7) 307

APPENDIX E INDIVIDUAL DATA: VERTICAL EXCITATION WITH DIFFERENT SEAT SURFACE ANGLES (CHAPTER 8) 319

APPENDIX F INDIVIDUAL DATA: MODELLING RESULTS (CHAPTER 9) 330

REFERENCES 342

LIST OF SYMBOLS

a	Acceleration (ms^{-2}).
c	Damping coefficient (Ns/m).
c_t	Rotational damping coefficient (Nms).
CM_m	Experimentally measured fore-and-aft cross-axis apparent mass modulus (kg).
CM_p	Predicted fore-and-aft cross-axis apparent mass modulus from the model (kg).
CPh_m	Experimentally measured fore-and-aft cross-axis apparent mass phase (radian).
CPh_p	Predicted fore-and-aft cross-axis apparent mass phase from the model (radian).
e	The distance between the centre of gravity of the rotating mass and the hinge in the models described in Chapter 9 (m).
F	Arbitrary factor used to improve fitting the models responses to the experimental data (equations 9.3 and 9.6).
f, F	Force (N).
F_f	Force measured parallel to the seat surface in the "fore-and-aft" direction (N).
F_v	Force measured normal to the seat surface in the "vertical" direction (N).
G	Acceleration of gravity (9.81 ms^{-2}).
ImM	Imaginary part of the apparent mass.
J	Moment of inertia (kg m^2)
k	Spring constant (N/m).
k_t	Rotational spring constant (Nm).
m	mass (kg)
M	Apparent mass (kg).
M_m	Experimentally measured apparent mass modulus (kg).
M_{mod}	Modulus of the apparent mass (kg).
M_p	Predicted apparent mass modulus from the model (kg).
M_{ph}	Phase of the apparent mass (radian).
M_{psd}	Apparent mass calculated using the Power Spectral Density (PSD) method.
Ph_m	Experimentally measured apparent mass phase (radian).
Ph_p	Predicted apparent mass phase from the model (radian).
ReM	Real part of the apparent mass.
S_{aa}	Power spectral density of the measured acceleration $(ms^{-2})^2$/Hz.
S_{af}	Cross spectral density between the measured force and acceleration (N ms^{-2})/Hz.
S_{ff}	Power spectral density of the measured force N^2/Hz.
t	Time (second).
v	Velocity (ms^{-1}).
x	Fore-and-aft displacement used in Chapter 9 and Chapter 10 (m).

z Vertical displacements used in Chapter 9 (m).

Z Mechanical impedance (Ns/m).

α The angle that *e* (see above) forms with the horizontal when the models (Chapter 9) are in equilibrium (radian); receptance (Chapter 10).

γ^2 Coherency.

θ Seat angle (Chapter 8); rotational displacement (Chapter 9).

ω Angular frequency (rad/s).

CHAPTER 1 INTRODUCTION

People are exposed to vibration every day either voluntarily (e.g. when they shake hands or a person sits on a swing) or involuntarily by being in an environment containing vibration. For example, vibration is present in all sorts of transportation such as trains, cars and ships. In these environments the source of vibration could be the train track, road roughness and car engine, or water waves hitting a ship. Vibration is transmitted to the person via the points of contact with the seat, bed or floor, depending on whether the person is seated, lying or standing. Vibration can also be felt in our houses (building vibration) due, for example, to the movement of a car on a nearby road. Vibrating power tools, such as grinding tools, are a source of vibration transmitted to the body through the hands and arms.

The transmission of vibration to the human body produces different effects and, in some cases, causes injury. The advance in technology makes people expect great quality of life almost free from disturbances and elements of discomfort and interference with activities during work or travel. Research has started to identify the way the human body responds to vibration and standards have been developed to provide methods for measuring, evaluating and assessing vibration (e.g. BS 6841, 1987; ISO 2631, 1997).

The effects of vibration on humans are judged according to three main criteria: interference with activities, interference with comfort and effects on health (see Griffin, 1990). If the effects of vibration are well defined and understood, vibration limits can be produced and used when designing and controlling environments in which humans are exposed to vibration. However, one should not expect the same limit of vibration exposure in road cars as in military tanks; in road cars vibration limits are based on reduction of discomfort while in military tanks vibration limits are based on prevention of injuries.

There are various factors affecting the degree to which people respond to vibration. Different people have different responses (inter-subject variability). Moreover, the response within the same person might change (intra-subject variability). Age, size, health, gender, fitness and previous exposure to vibration are all factors playing roles in defining the response of people to vibration. The adopted posture can also affect the responses of people to vibration, as will be shown later and, hence, it is of importance to define the posture clearly to people taking part in an experiment involving vibration.

The evaluation of vibration must involve the consideration of its frequency, direction, magnitude and duration. The influence of one frequency in one direction is different from its effect in another direction and the same vibration magnitude, frequency and duration in one direction might have a different effect in another direction.

Human response to vibration can be measured either subjectively or objectively. With subjective responses, human subjects are asked questions about the exposure or are asked to compare between stimuli. The subjects could also be asked about their feeling during the exposure, as happens in motion sickness experiments. With objective responses, measurements of, for example, force and acceleration are taken on different parts of the body (biodynamic responses) to identify how the body moves or behaves when exposed to vibration. Some researchers have investigated the effects of vibration on the physiological system and, hence, they measured heart rate, blood pressure, muscle responses, etc. When sufficient knowledge about the subjective and objective responses is available, models combining both types of response can be built to represent the response of humans to vibration. This thesis is concerned with the biodynamic responses of humans to vibration.

The main objective of this thesis was to improve understanding of how the human body behaves dynamically in response to whole-body vibration. The thesis concentrates on quantifying the characteristics of the responses of humans in both the direction of excitation and in the other directions. Measurements (of force and acceleration) were taken on the seat, backrest and footrest during excitation in both the vertical direction and the fore-and-aft direction. Studying the responses in all directions could help in explaining some of the results that appear in the direction of excitation. Mathematical linear two-dimensional models (lateral forces were small) were developed to predict the responses obtained experimentally in the direction of excitation and in the other directions. These models may be used to predict the performance of seats instead of using human subjects, where lack of repeatability and ethical concerns might cause some difficulties.

This thesis is organised into 11 chapters, including this introductory chapter, and six appendices as follows:

Chapter 2 presents a literature review of the dynamic responses of humans to vertical and horizontal vibration. A review of modelling the dynamic responses of humans to vibration is also presented in this chapter.

Chapter 3 summarises the experimental apparatus and data acquisition and analysis methods used.

Chapter 4 presents measurements of forces on a seat without a backrest in the vertical, fore-and-aft and lateral directions and measurements of forces on a footrest in the vertical direction during vertical excitation.

Chapter 5 shows experimental measures of forces on a seat and a backrest in three directions (vertical, fore-and-aft and lateral) during vertical excitation.

Chapter 6 describes experimental measures of the response of humans to fore-and-aft vibration. Forces in the vertical, fore-and-aft and lateral directions were measured on a seat without a backrest. Forces on a footrest in the vertical and fore-and-aft directions are also shown.

Chapter 7 presents forces measured on a seat and a backrest in three directions (vertical, fore-and-aft, and lateral) during exposure of human subjects to fore-and-aft vibration.

Chapter 8 investigates the effect of seat surface angle on the forces measured on a seat in the 'vertical' direction (i.e. normal to seat surface) and in the 'fore-and-aft' direction (i.e. parallel to seat surface). The effects of vibration magnitude and a backrest are also examined.

Chapter 9 shows the development of mathematical models that take into account forces measured on the seat in the vertical and fore-and-aft directions during vertical excitation and during fore-and-aft excitation.

Chapter 10 presents a general discussion.

Chapter 11 presents general conclusions and recommendations for future work.

In the appendices, the characteristics of the subjects used in the experiments and the instructions given to the subjects before commencing the experiments are documented. The individual data obtained from the experiments and the models are also documented in the appendices.

CHAPTER 2 LITERATURE REVIEW

2.1 INTRODUCTION

Research to identify the biodynamic responses of humans to vibration started more than 40 years ago. The objective of this chapter is to review some of the reported studies of biodynamic response to vibration so as to identify current knowledge of the biodynamic responses and provide guidelines for future research. In this thesis, seated subjects have been studied and, hence, more concentration is placed on reviewing studies of seated subjects than studies of standing or recumbent subjects.

In the first section, methods used to represent the dynamic response of humans to vibration are introduced. Broadband random vibration is used in this thesis and, hence, frequency domain methods (see Section 2.2) will be adopted for analysing the results obtained from the experiments reported in this thesis. The following sections focus on the driving point dynamic responses of the human body to vertical and horizontal excitation, the transmissibility of the human body, the cross-axis forces at the driving point, and mathematical models representing the responses of humans to vibration. The final section presents a summary of the literature review and conclusions.

2.2 METHODS OF REPRESENTING DYNAMIC RESPONSES

The exposure of a rigid body to an alternating force (or vibration) would result in an acceleration of that rigid body. The produced acceleration would be proportional to, and in phase with, the applied force. The constant of proportionality, which is called the 'mass' of the body, is the same (except perhaps at high frequencies) regardless of the exposure frequency. However, when a non-rigid system is exposed to vibration, the 'mass' is expected to be different with different frequency of exposure and, therefore, the phrase 'apparent mass' is used instead of 'mass'.

As a non-rigid system, the human body responds differently at different frequencies. Hence, the dynamic responses of the human body have usually been represented by frequency dependent functions known as frequency response functions. These functions are obtained by exposing subjects to vibration and measuring at least two measurements of motion or force at the same point or at different locations on the body. If the measurements are taken at the same point, force and acceleration (or velocity) are normally measured at the interface between the subject's body and the source of vibration (e.g. seat surface or backrest for seated subjects). The frequency response

function calculated from the measured force and acceleration (or velocity) represents the driving point response (apparent mass or driving point mechanical impedance) as shown in Equations 2.1 and 2.2.

$$M(\omega) = \frac{F(\omega)}{a(\omega)} \tag{2.1}$$

$$Z(\omega) = \frac{F(\omega)}{v(\omega)} \tag{2.2}$$

where,

$M(\omega)$ and $Z(\omega)$ are the apparent mass and the driving point mechanical impedance, respectively, and F, a and v, are the Fourier transforms of the force, the acceleration and the velocity at a particular angular frequency, ω.

The advantage of using the apparent mass over using the mechanical impedance is the presence of a reference value for the apparent mass since at low frequencies the human body behaves like a rigid body and, hence, the apparent mass is equal to the static mass. Moreover, the apparent mass can be obtained directly from measurements of acceleration (using accelerometers) and force.

If the signals are measured at different locations, the same type of measurement (e.g. acceleration) is normally taken at the two points. The transfer function in this case will represent the transmissibility of the body between two locations and can be obtained from the complex ratio of the motion at two different points.

Besides the apparent mass, mechanical impedance, and transmissibility, the power absorbed by the body during vibration, defined as the product of the force and the velocity, has been used by some researchers to represent the dynamic responses of the human body to vibration (e.g. Lundström and Holmlund, 1998; Mansfield and Griffin, 1998; Mansfield *et al.*, 2001). The measured biodynamic responses can be used to develop models that may represent the responses of humans to vibration, as will be shown later. In this thesis the apparent mass concept is used.

2.3 MECHANICAL IMPEDANCE AND APPARENT MASS OF THE HUMAN BODY

2.3.1 Vertical excitation

Measures of mechanical impedance and apparent mass of the human body during vertical excitation are widely available in the literature. Previous studies agree on the

trend in which the mass (or impedance) of the body changes with a change in the frequency of vertical excitation. For example, a principal resonance frequency in the vicinity of 5 Hz is a common finding in previous studies (e.g. Coermann, 1962; Fairley and Griffin, 1989; Mansfield, 1998; Matsumoto, 1999; Matsumoto and Griffin, 2002a). Many studies also report a second resonance between 8 and 13 Hz in the apparent mass of seated subjects (e.g. Fairley and Griffin, 1989; Mansfield and Griffin, 2000; Rakheja *et al.*, 2002). Figure 2.1 shows the apparent masses of 60 seated subjects having different ages, masses and genders as measured by Fairley and Griffin (1989).

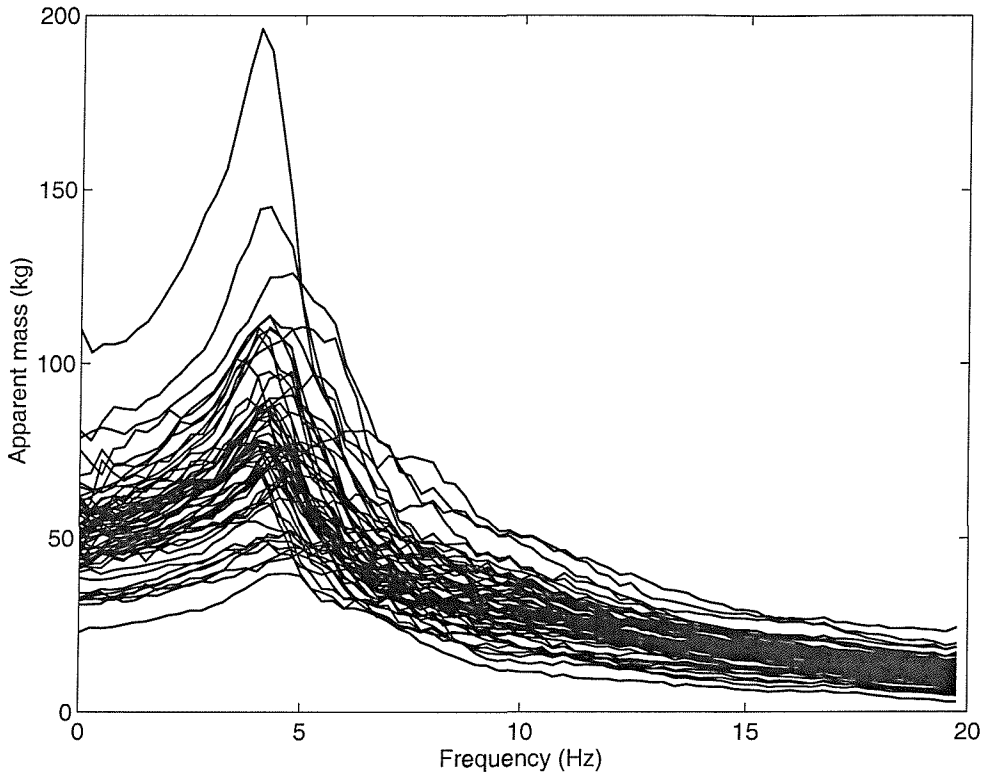

Figure 2.1 Apparent masses of 60 seated subjects having different ages, masses and genders (Fairley and Griffin, 1989).

Different factors have been found to have an effect on the apparent mass. In the next sections, a review of studies that investigated the effects of posture, seating conditions, vibration magnitude and vibration waveform on the apparent mass and mechanical impedance is presented.

2.3.1.1 Effect of posture and seating condition

2.3.1.1.1 Effect of posture

Several researchers have studied the effect of the adopted sitting posture on the apparent mass and mechanical impedance of the human body with vertical excitation.

Fairley (1986) reported a trend for the resonance frequency of the mean apparent mass of eight subjects to increase when the subjects sat with an erect upper body posture (with normal muscle tension) or with tense upper body posture (all muscles in the upper body tensed as much as possible) compared to a normal upper body posture in which the subjects sat in a comfortable upright posture. The effect of upper body posture was further investigated by Fairley and Griffin (1989) using one subject and five sitting postures: slouched, normal, slightly erect, erect and very erect. They reported that 'the change in resonance frequency, over what was an extreme range of postures, was about 1.5 Hz' (see Figure 2.2). Kitazaki (1992) also noticed a slight increase in the apparent mass resonance frequency and magnitude at resonance when a subject changed his posture from normal to erect. Holmlund *et al.* (1995) exposed 30 seated subjects (15 males and 15 females) to sinusoidal vertical whole-body excitation in the frequency range 2-100 Hz and found that an erect sitting posture gave higher impedance magnitude and resonance frequency than a relaxed sitting posture. Since the mass of the upper body did not change with changes to the upper body posture, the change in the resonance frequency mentioned above might be due to a change in the stiffness of the body (probably due to a change in muscle tension) which led to a change in the resonance frequency of the apparent mass: although the subjects in some of the mentioned studies were asked to maintain normal muscle tension when changing upper body posture, change in muscle tension might have been required to support different sitting postures.

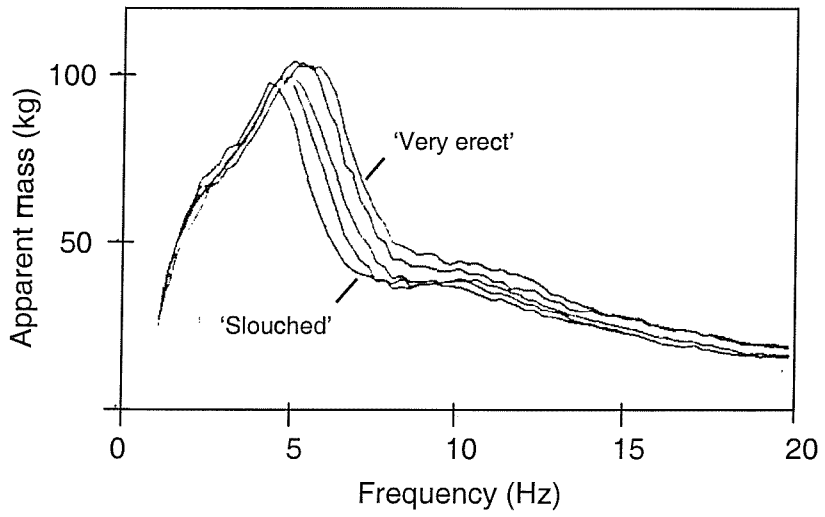

Figure 2.2 Effect of posture on the apparent mass of one subject adopting five sitting postures (Fairley and Griffin, 1989).

Sandover (1978) investigated the effect of constraining the movements of the buttocks tissue and the movement of the viscera on the apparent mass of one subject exposed to random whole-body vertical excitation. He reported an increase in the principal resonance frequency of the apparent mass from 4 Hz to 5.5 Hz when wooden blocks were installed under the ischial tuberosities. Sandover also noticed that constraining the movement of the viscera by wearing many turns of a 4 cm wide webbing belt allowed a 7 to 8 Hz mode to appear in the apparent mass. Kitazaki (1994), using seven subjects, also reported that placing two wooden blocks under the ischial tuberosities and constraining the movement of the viscera, by wearing a wide belt around the abdomen affected the resonance frequency and the magnitude of the apparent mass at resonance: both constraint resulted in an increase in the resonance frequency or a decrease in the apparent mass at resonance, or both. However, using twelve subjects, Mansfield and Griffin (2002) found no significant difference between the apparent mass resonance frequency measured when subjects sat on an inverted SIT-BAR (a rigid indenter that is flat on one side and contoured on the other) and when they sat in an upright posture. They also compared between the responses measured with nine different postures (Figure 2.3 and Figure 2.4). The authors noticed more inter-subject variability for the anterior lean, back-on, and inverted SIT-BAR postures than any of the other postures. However, they reported that 'changes of resonance frequency with posture were generally not significant'.

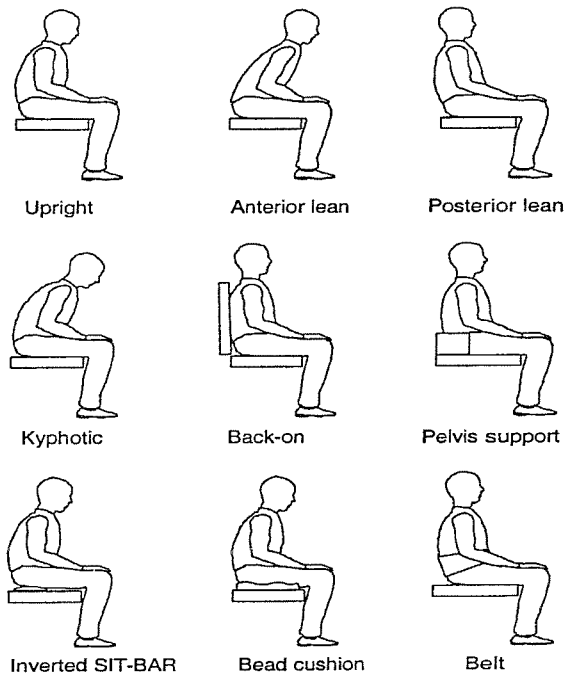

Figure 2.3 The nine postures investigated by Mansfield and Griffin (2002).

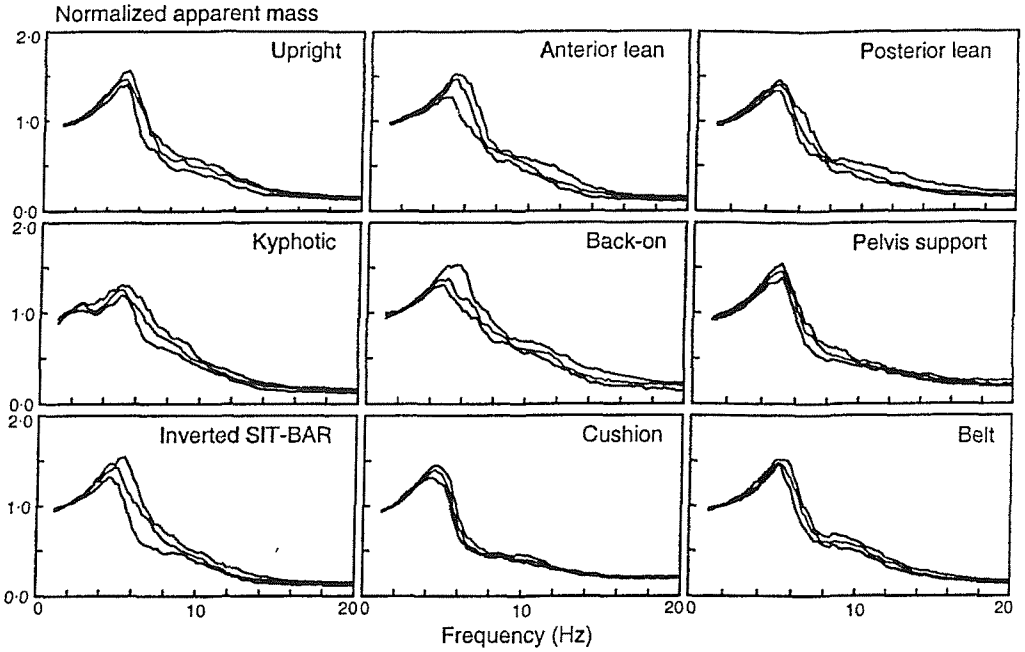

Figure 2.4 Median, first quartile and third quartile of the normalised apparent masses of 12 subjects sitting in the different postures shown in Figure 2.3 (Mansfield and Griffin, 2002).

It can be seen that the effect of increasing the stiffness of the ischial tuberosities by placing rigid objects under the ischial tuberosities is inconsistent between the studies mentioned above, although all studies used similar excitations (random vibration with a magnitude of 1.6 and 2 ms^{-2} r.m.s.). It is possible that the seating conditions caused the inconsistency between the studies: no backrest was used in both Mansfield and Griffin (2002) and Kitazaki (1994) studies but the feet were resting on a footrest moving in phase with the seat in the study of Mansfield and Griffin while the feet were resting on a stationary footrest in Kitazaki's study. Sandover used a backrest and the feet were moving with the seat. These factors (i.e. backrest and footrest) have an effect on the response to vibration as will be shown later in this chapter.

Few studies have measured the apparent mass (or mechanical impedance) of standing subjects. Coermann (1962) measured the mechanical impedance of one subject adopting an erect standing position and an erect sitting position during vertical sinusoidal excitation in the frequency range 1 to 20 Hz. The resonance frequency of the apparent mass in the erect standing position (5.9 Hz) was lower than the resonance frequency of the apparent mass in the sitting position (6.3 Hz). Matsumoto and Griffin (2000) compared the apparent masses of eight subjects in a "normal" standing position with their apparent masses in a "normal" sitting position using random vertical excitation in the frequency range 0.5 to 20 Hz. They reported a resonance frequency in the range 5 to 6 Hz in both

positions, with that of the standing position slightly higher than that of the sitting position, which is opposite to the observation of Coermann (1962). However, the adopted posture was different in the two studies: normal in Matsumoto and Griffin (2000) and erect in Coermann (1962). It is possible that the stiffness of the body can be increased more when using an erect posture in the sitting position than in the standing position. However, the observations of Coermann (1962) are based only on the results of one subject and, hence, need confirmation using more subjects. The magnitude at resonance, as found by Matsumoto and Griffin, was higher in the sitting position than in the standing position (see Figure 2.5).

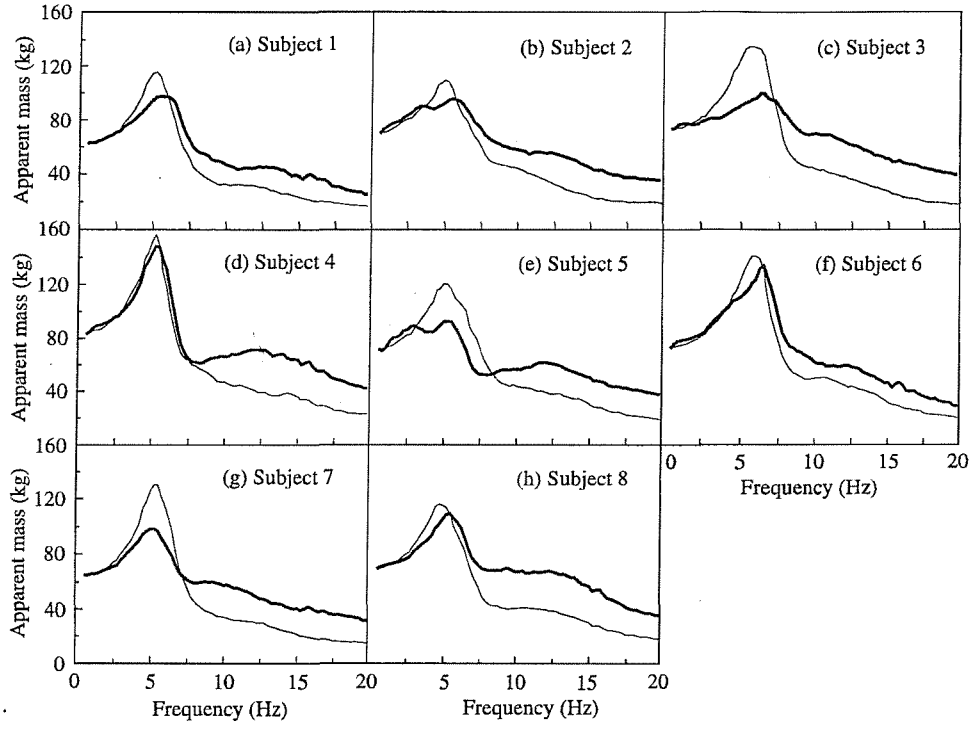

Figure 2.5 Apparent masses in standing and sitting positions: standing ——; sitting ——. Matsumoto and Griffin (2000).

The effects of posture (upper body posture and leg posture) on the mechanical impedance or apparent mass of standing subjects have been reported by a few researchers. Miwa (1975) reported no clear effect of the upper body posture (relaxed or erect) on the mechanical impedance of standing subjects. Matsumoto (1996) studied the effect of posture on the apparent mass of standing subjects. Twelve male subjects were exposed to random vertical excitation in the frequency range 1 to 50 Hz while adopting four standing postures: standing normally, standing with an erect upper body, standing with slouched upper body and standing with legs bent. The resonance frequency

decreased from 5.25 Hz to 4.25 Hz when the posture changed from normal to slouched. The magnitude of the normalised median apparent mass (the apparent mass divided by the static mass of the subjects) at resonance also decreased from 1.41 to 1.26 when the posture changed from normal to slouched. No clear trend for the effect of the erect posture on the apparent mass was found over subjects. The principal resonance was found at 2.75 Hz with the legs bent posture, compared to 5.25 Hz with the normal standing posture. However, the magnitude of the normalised median apparent mass at resonance was higher in the legs bent posture than the normal posture, although the apparent mass at frequencies above resonance decreased dramatically in the legs bent posture.

2.3.1.1.2 Effect of seating conditions

The responses of humans to vibration may also be affected by the seating conditions. For example, the presence of a backrest, the state of the footrest and the inclination of backrest have been found to have an effect on the responses of humans to vibration.

Effect of backrest

Fairley and Griffin (1989) reported a general increase in the apparent mass resonance frequency and the magnitude of apparent mass at frequencies above resonance when subjects leant against the backrest of a seat (inclined 6° from the vertical) compared to not using the backrest of the same seat. Toward (2003) also reported the same finding, although the increase of the resonance frequency when a vertical backrest was used was only 0.2 Hz. Mansfield and Griffin (2002) reported an increase in the apparent mass at frequencies above resonance when a vertical backrest was used compared to no backrest; however, they found no significant difference in the resonance frequency between the two conditions.

Boileau and Rakheja (1998) compared the mechanical impedance of seated subjects adopting an erect sitting posture without backrest with the mechanical impedance of the same subjects while adopting an erect posture with a vertical backrest. No effect of backrest on the mechanical impedance was found at frequencies below 4 Hz. However, the mechanical impedance decreased in the resonance region (between 4 Hz and about 6.5 Hz) and increased above 6.5 Hz when the backrest was employed. No analysis was done to test the effect of using a backrest on the resonance frequency. The authors explained the decrease in the mechanical impedance in the resonance area when a backrest was used as partly due to a decrease in the static weight supported on the seat when a backrest was used: the vertical static load on the seat was 73.6% of total body

weight when no backrest was used and was 68% of total body weight when a vertical backrest was used.

Rakheja *et al.* (2002) found that the principal resonance of the apparent mass with a 'hands on laps' posture occurred at a higher frequency (7-8.1Hz) than those reported in previous studies around 5 Hz. They explained this finding as a result of the inclinations of the seat pan and backrest from the horizontal by 13° and 114°, respectively. The effect of simultaneously changing the backrest angle and the seat surface angle on the dynamic responses of humans to vibration has not been studied. However, the effect of changing the backrest angle while keeping the seat at a fixed angle, or changing the seat surface angle while keeping the backrest angle fixed on the apparent mass have been studied.

Effect of backrest angle

Toward (2003) investigated the apparent mass measured on the seat with backrest angles of 0, 5, 10, 15, 20, 25 and 30°. He found that, below 8 Hz and with a lesser effect between 10 and 15 Hz, the apparent mass decreased with an increase in backrest angle. Above 15 Hz, no effect of backrest inclination was found (see Figure 2.6). The resonance frequency of the apparent mass increased, while the magnitude at resonance decreased, with increasing backrest angle: the resonance frequency and the magnitude at resonance of the median apparent mass were 5.27 Hz and 79.6 kg with 0° backrest angle and were 6.44 Hz and 68.0 kg with a backrest angle of 30°. Wei and Griffin (1999) reported the same effect of backrest angle on the resonance frequency as that reported by Toward (2003), but found no effect on the apparent mass magnitude at resonance with increasing backrest angle. Boileau and Rakheja (1998) compared the mechanical impedance of seated subjects obtained on the seat with backrest angles of 0° and 14° and reported that 'the behaviour of the body leaning against an inclined backrest appears to be more like that of a pure damper at higher frequencies, while being that of a pure mass at low frequencies' (see Figure 2.7).

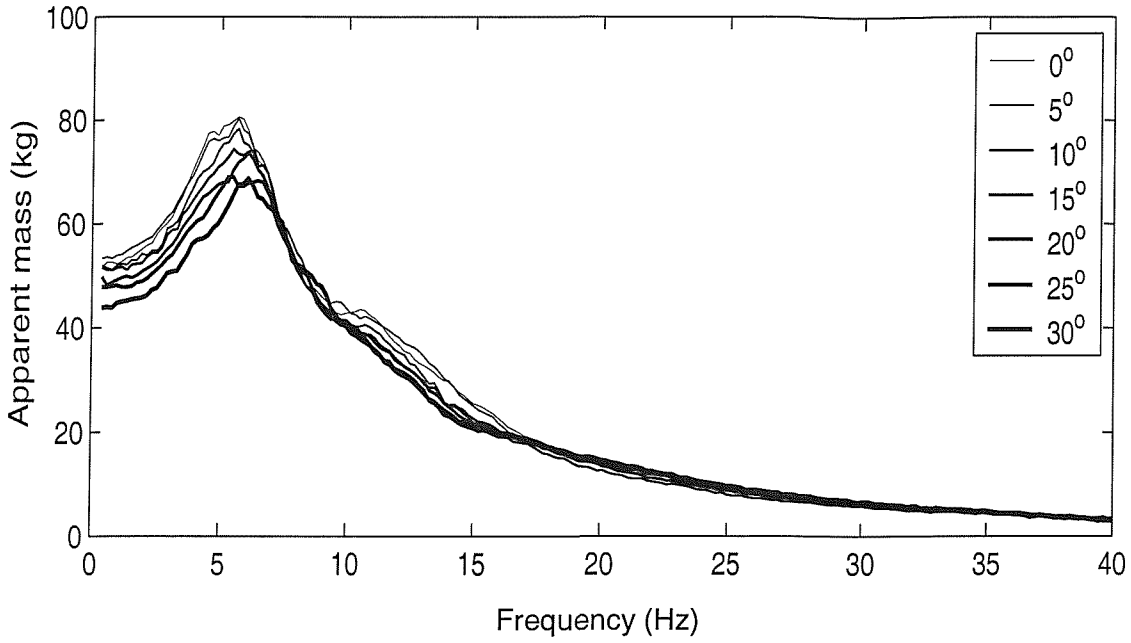

Figure 2.6 Median apparent masses of 12 subjects using a rigid backrest with different angles (Toward, 2003).

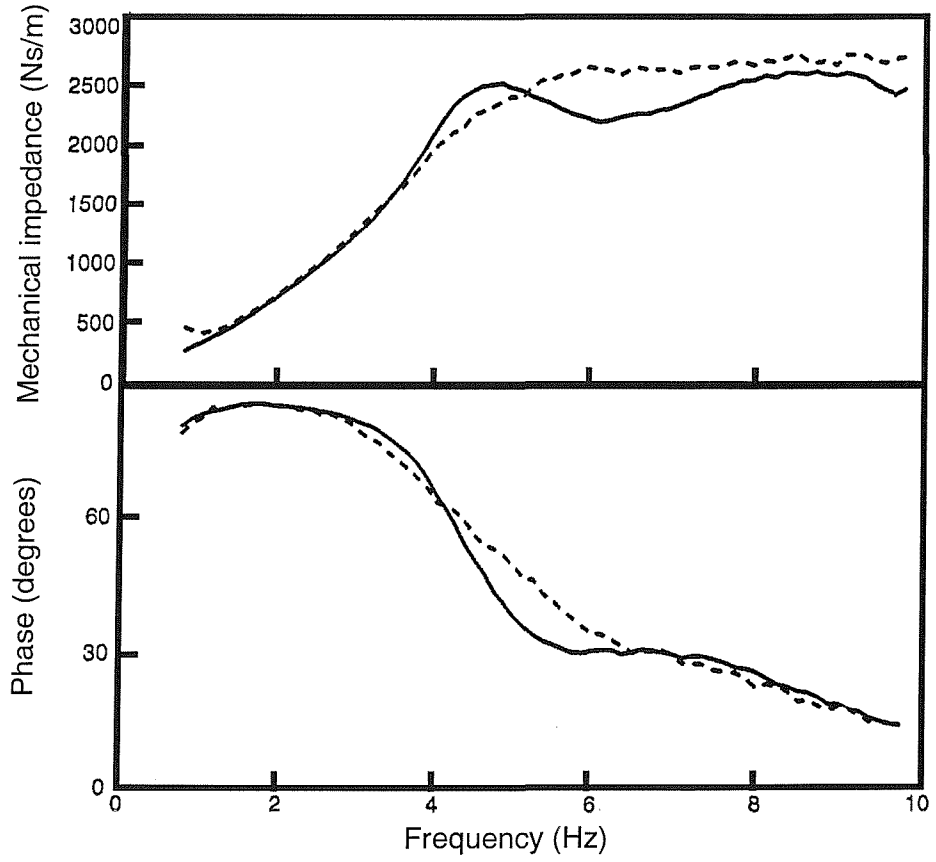

Figure 2.7 Mean driving point mechanical impedance of seated subjects: effect of backrest angle. ———, 0°; – – – –, 14°. (Boileau and Rakheja, 1998).

Effect of seat squab angle

Wei and Griffin (1998a) measured the forces normal to the seat surface with seat cushion inclinations of 0, 5, 10, 15, and 20° and compared the apparent masses obtained from the vertical component of the force and the vertical acceleration. They found that below 5.5 Hz, the apparent mass decreased with increasing seat inclination; however, the decrease was generally small. The mean apparent mass resonance frequencies seem to be not affected by the cushion angle, although this was not mentioned by the authors. The results of Toward (2003) and Wei and Griffin (1998a) may suggest that the high resonance frequency reported by Rakheja *et al.* (2002), mentioned before, was due to backrest inclination and not seat inclination.

Effect of footrest and footrest height

Fairley and Griffin (1989) found that the effect on the apparent mass of using a footrest moving in phase with the seat was different from the effect of using a stationary footrest. With a footrest moving in phase with the seat, the apparent mass tended toward the static mass of the occupant of the seat near zero frequency. This behaviour was expected since the human body was found to behave as a rigid system at very low frequencies. However, when using a stationary footrest, the apparent mass near zero frequency did not tend toward the static mass of the occupant of the seat. Fairley and Griffin further investigated this finding by studying the effect of changing the height of the stationary footrest on the apparent mass. The results showed a slight increase in the apparent mass at frequencies above 10 Hz when lowering the footrest, which is consistent with an increase of the mass on the seat. However, at low frequencies, the apparent mass decreased when lowering the footrest height (see Figure 2.8). This effect was attributed to the relative motion between the platform (the seat) and the footrest: 'the thighs, if they are in contact with the platform, can apply a force in the opposite direction to the force applied by the moving body at some frequencies'.

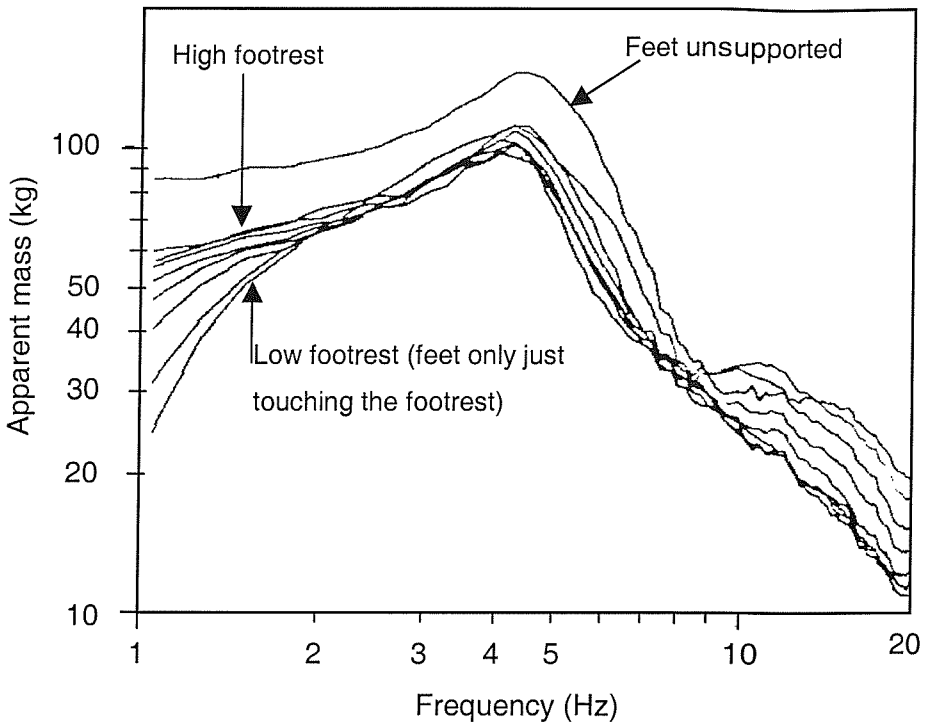

Figure 2.8 Effect of the height of a stationary footrest on apparent mass (one subject, Fairley and Griffin, 1989).

Effect of foot position and hand position

Rakheja *et al.* (2002) investigated the effect of foot position and hand position on the apparent masses of 24 seated subjects (12 males and 12 females) during vertical excitation. The foot positions were a nominal position (feet position selected by the subject, referred to as 'M' position), 7.5 cm ahead of the 'M' position (referred to as 'L' position) and 7.5 cm behind the 'M' position (referred to as 'S' position). The hand positions were described as hands-in-lap (to represent passenger posture) and hands-on-steering wheel (to represent a driver posture). 'The steering column formed an angle of 23° with the horizontal surface of the vibration platform'. A rigid seat with a backrest was used in the study. The seat squab was inclined by 13° with the horizontal while the backrest was inclined by 24° with the vertical. Vertical random vibration in the frequency range 0.5 to 40 Hz was used. The results showed that regardless of the hands posture, the apparent mass was similar in the 'S' and 'M' foot position. With the 'L' foot position, the magnitude of the apparent mass at resonance increased only slightly in the hands-in-lap posture but yielded higher peak magnitude in the hands-on-steering wheel posture (see Figure 2.9). The resonance frequency was not affected by the foot position in any of the hand postures. This might suggest that increasing the stiffness of the thighs (in the 'L' position) or decreasing the stiffness of the thighs (in the 'S' position) has no effect on the principal resonance of the apparent mass. The authors also compared the apparent

masses obtained with the two hand positions. They reported a considerable decrease in the principal resonance frequency and apparent mass at resonance when the hands-on-steering wheel posture was adopted compared to hands-in-laps posture (see Figure 2.9). A second peak at around 11 Hz was clearer in the hands-on-steering wheel posture than in hands-in-lap posture. The authors concluded that 'the biodynamic response of occupants seated with automotive postures and subject to vertical vibration need to be characterized, as a minimum, by two distinct functions for two postures: hands-in-lap and hands-on-steering wheel'.

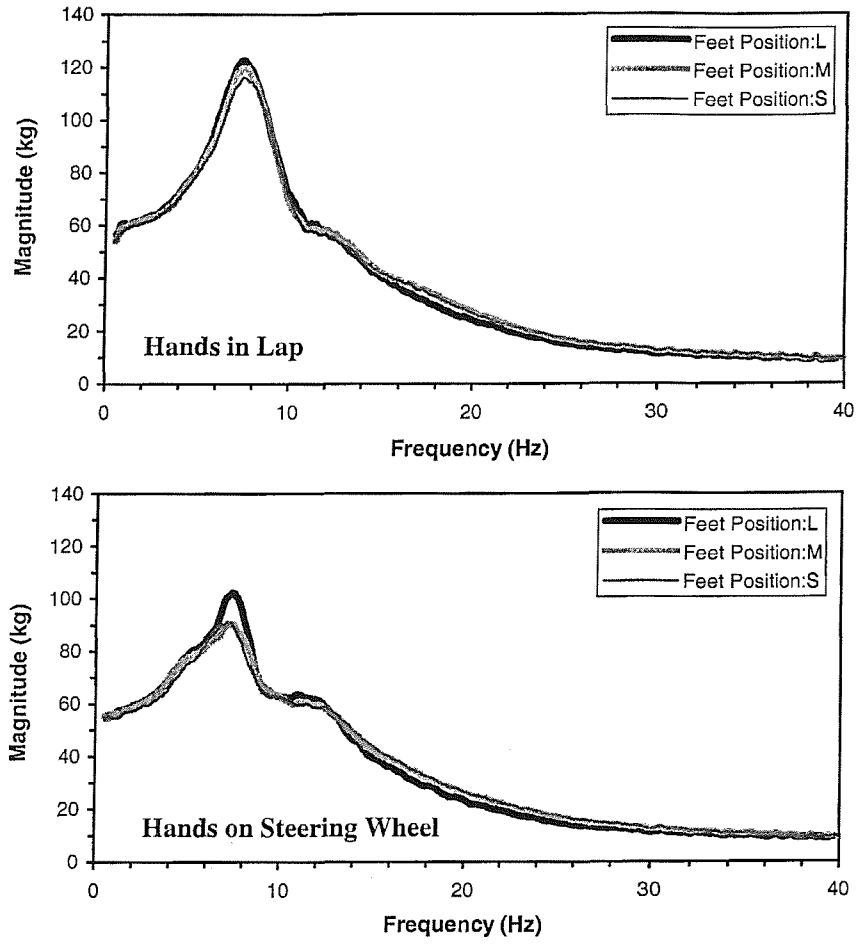

Figure 2.9 Influence of foot position on the magnitude of the apparent mass for two sitting postures (Rakheja *et al.* 2002).

2.3.1.2 Effect of vibration magnitude and vibration waveform

2.3.1.2.1 Effect of vibration magnitude

Many studies have investigated the effect of vibration magnitude on the driving point response (mechanical impedance and apparent mass) to vibration. Almost all studies reported that the human body is a system that responds non-linearly to vibration. Some

studies, however, reported that the human body is a linear system or that the effect of vibration magnitude is small or negligible. Pradko *et al.* (1966) reported that the human body displayed linear characteristics in response to sinusoidal and random vibration. However, no data were shown to support this claim. Coermann (1962) measured the mechanical impedance of one subject exposed to 0.1 g, 0.3 g and 0.5 g vertical sinusoidal vibration. He reported 'in the applicable acceleration range the variation of the impedance was not evident': measurements of impedance magnitude and phase angle at the different vibration magnitudes were within the 10% measurement accuracy. Sandover (1978) measured the apparent mass of one seated subject in the frequency range 1 to 25 Hz using vibration magnitudes of 1 and 2 ms^{-2} r.m.s. and stated that 'any non-linear effects are small'.

Some studies have reported non-linearity in the human body based on observation of distorted output signals (either transmitted force to the body or motion of some parts of the body) obtained as a response to a pure sinusoidal input signals. For example, Wittman and Phillips (1969) found that the amplitude in the transmitted force during 'loading phase' is greater than that obtained during the 'unloading phase'. They also noticed that the time of the 'loading phase' is shorter than that of the 'unloading phase'. For a linear system, the amplitudes and durations in both loading phases are equal and the output signal is sinusoidal as in the input signal. Hinz and Seidel (1987) measured the output force at the seat as well as the acceleration at the head, the shoulder and the fifth thoracic vertebra during sinusoidal whole-body vertical excitation. They reported that the 'accelerations and the force responses exhibited a clear transformation of the sinusoidal input into a non-sinusoidal output' which suggest that the human body acts as a non-linear system when exposed to vibration.

The majority of the studies have reported the non-linearity of the human body as a decrease in the resonance frequencies of the mechanical impedance or the apparent mass of the human body with an increase in the vibration magnitude, suggesting that the human body becomes 'softer' at high vibration magnitudes. Using vertical sinusoidal vibration, Hinz and Seidel (1987) reported a decrease in the average apparent mass resonance frequency of four subjects from 4.5 to 4 Hz with an increase in vibration magnitude from 1.5 to 3.0 ms^{-2} r.m.s. With random vibration, Fairley and Griffin (1989) reported a decrease in the apparent mass resonance frequency from 6 to 4 Hz with an increase in vibration magnitude from 0.25 to 2.0 ms^{-2} r.m.s. The authors hypothesised that at high vibration magnitudes, the stiffness of the body decreases as a result of the greater movement in the musculoskeletal system. Using the same vibration magnitudes,

as those used by Fairley and Griffin, Mansfield and Griffin (2000) found a decrease in the apparent mass resonance frequency from 5.4 to 4.2 Hz with an increase in vibration magnitude from 0.25 to 2.0 ms^{-2} r.m.s. Mansfield *et al.* (2001) reported a similar non-linear phenomenon when using random vibration, repeated shocks, and combinations of random vibration and repeated shocks.

Matsumoto (1999) measured the apparent masses of eight subjects in sitting and standing positions. He used five vibration magnitudes in the range 0.125 to 2.0 ms^{-2} r.m.s. in an attempt to investigate the effect of vibration magnitude on apparent mass in the sitting and standing positions. The vibration frequency range and duration of exposure were 0.5 to 20 Hz and 60 s, respectively. The author noticed that the resonance frequency decreased with increasing vibration magnitude in both positions investigated: increase in the vibration magnitude from 0.125 ms^{-2} r.m.s. to 2.0 ms^{-2} r.m.s. decreased the resonance frequency from 6.75 to 5.25 Hz for the standing position and from 6.4 to 4.75 Hz for the sitting position (see Figure 2.10).

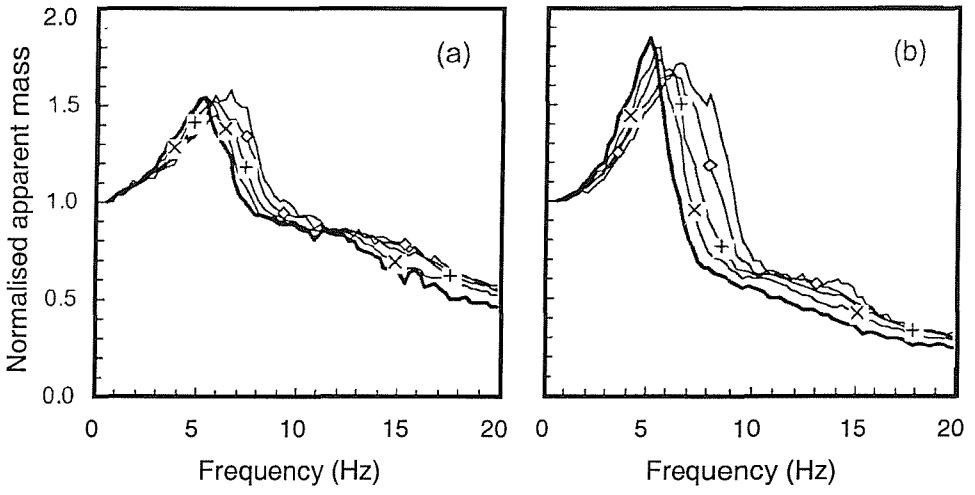

Figure 2.10 Effect of vibration magnitude on the median normalised apparent masses of eight subjects in the standing and sitting positions: (a) standing; (b) sitting. 0.125 ——; 0.25 —◊—; 0.5 —+—; 1.0 —x—; 2.0 ms^{-2} r.m.s. ——. (Matsumoto, 1999).

Smith (1994) studied the effect of vibration magnitude on the mechanical impedance of seated subjects. Four male subjects were exposed to sinusoidal vibration with magnitudes of 0.347, 0.694 and 1.734 ms^{-2} r.m.s. in the frequency range 3 to 20 Hz. Smith identified four regions of resonance in the mechanical impedance: the first region ranged from 5 to 8 Hz, the second region ranged from 7 to 9 Hz, the third region ranged from 12 to 14 Hz and the fourth region ranged from 15 to 18 Hz. The four regions were

more distinct at low vibration magnitudes than at high vibration magnitudes. The first and fourth resonance frequencies showed a significant decrease with an increase in vibration magnitude.

Rakheja *et al.* (2002) studied the effect of vibration magnitude (0.25, 0.5 and 1.0 ms^{-2}) on the apparent masses of seated subjects adopting two different postures, passenger posture and driving posture. They reported a slight decrease in the principal resonance frequency and the magnitude at resonance with increasing vibration magnitude. They noticed that the effect of vibration magnitude was 'slightly more important for the passenger posture (hands-in-lap) than for the driving posture (hands-on-steering wheel)'. However, they concluded that the effect of vibration magnitude on the apparent mass was negligible compared to the effect of hand position. Mansfield and Griffin (2002) studied the effect of nine different sitting postures (see Figure 2.3) and three vibration magnitudes (0.2, 1.0 and 2.0 ms^{-2} r.m.s.) on the resonance frequency of the apparent masses of 12 subjects. They noticed that the effect of vibration magnitude on the apparent mass was greater than the effect of the sitting posture: while the decrease in the resonance frequency with an increase in vibration magnitude was significant with all nine sitting postures, changes in the resonance frequencies with changes in the sitting posture were generally not significant.

Vogt *et al.* (1968) and Mertens (1978) investigated the non-linearity in the mechanical impedance of seated humans with different static accelerations (from 1 G to 3 G in Vogt *et al.*, 1968; from 1 G to 4 G in Mertens, 1978). The different static accelerations were obtained using a centrifuge. The results of both studies showed an increase in the fundamental resonance frequency of the mechanical impedance with increase in static acceleration demonstrating a stiffening effect in contrast to the softening effect of increasing vibration magnitude (see Figure 2.11). For example, Vogt *et al.* showed an increase in the main resonance frequency from 5 Hz with 1 G to 7 Hz with 2 G and to 8 Hz with 3 G. Mertens explained the increase in the resonance frequency as due to an increase in body stiffness resulting from subjects being unable to maintain the upper body posture and, therefore, changed their posture to a curved spine posture. This explanation, however, contradicts the results of some studies which found that changing to a curved spine posture decreased the resonance frequency due to a possible decrease in stiffness. The increase in the resonance frequency with an increase in static acceleration could be the result of the subjects using their muscles in trying to support themselves, or to keep the body posture they were instructed to adopt, at the high acceleration levels.

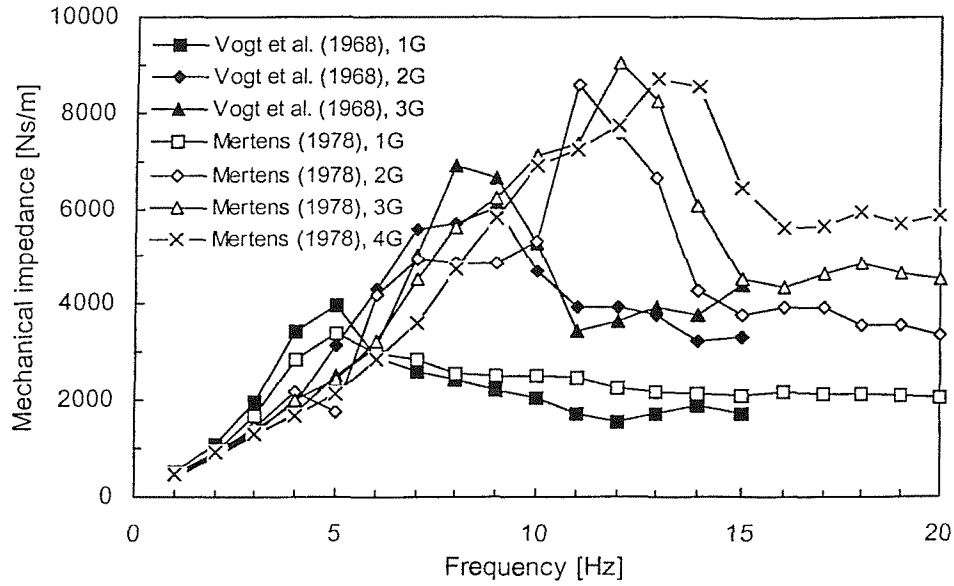

Figure 2.11 Mechanical impedance measured with different static accelerations. Data from Vogt *et al.* (1968) and Mertens (1978). (Data redrawn together by Matsumoto, 1999).

2.3.1.2.2 Effect of vibration waveform

The responses of humans to vibration have been investigated using different types of excitation: sinusoidal, random, transient and motions recorded in real vehicles were used. Two methods have been employed when using a sinusoidal excitation: discrete frequency excitation and frequency sweeps. In the discrete frequency method, the human body is exposed to a single frequency motion and the mechanical impedance (or the apparent mass) is calculated from the ratio of the r.m.s. (or peak value) of the output force to the r.m.s. (or peak value) of the velocity (or acceleration). In the frequency sweep method, the excitation starts at a certain frequency and increases or decreases in frequency at a certain rate until the last frequency is achieved. The driving point response can be obtained from the ratio of the r.m.s. of the output force over a selected period of time to the r.m.s. of the velocity (or acceleration) over the same period of time. When using random, transient or real motions, frequency domain analysis is needed (see Section 3.4.1).

Donati and Bonthoux (1983) compared the mechanical impedance of fifteen seated subjects measured with frequency sweep and random vibration. The same frequency range (1 to 10 Hz) and magnitude of vibration (1.6 ms^{-2} r.m.s.) was used with both waveforms. Figure 2.12 shows the mean mechanical impedance obtained using both waveforms. Although some differences can be seen between the two means, statistical analysis across subjects showed an effect of waveform only at the resonance frequency.

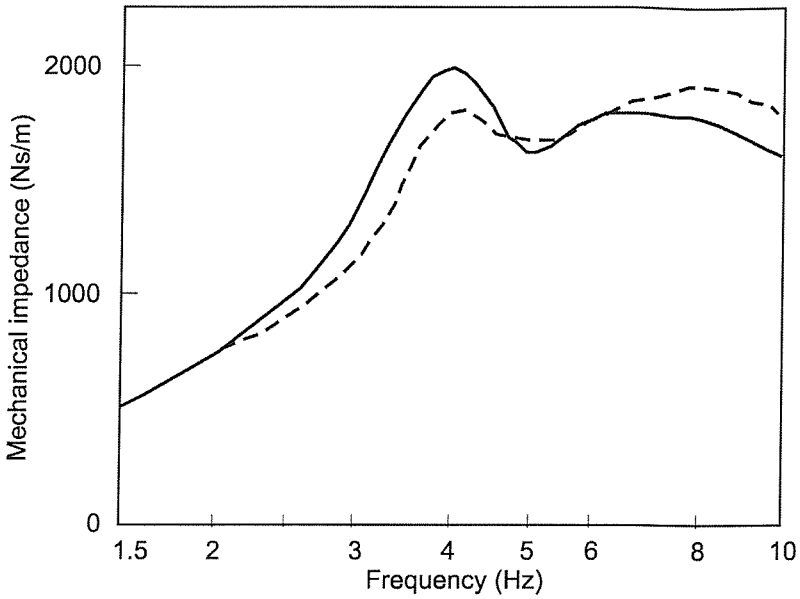

Figure 2.12 Mean mechanical impedance of fifteen subjects measured using different waveforms. ———, swept sinusoidal motion; – – – –, broad band random motion. Donati and Bonthoux (1983).

Wei and Griffin (1999) studied the effect of input spectrum on the apparent masses of seated subjects in six different backrest conditions (no backrest, rigid backrest with angles of 0, 10, 15, and 20°, and soft backrest with 0°). Three different input spectra were used: random vibration with a flat acceleration spectrum over the frequency range 0.5 to 30 Hz, vertical acceleration measured on the floor of a car, and vertical acceleration measured on a seat in the same car. All signals had a magnitude of 0.5 ms^{-2} r.m.s. In all backrest conditions, there were statistically significant differences in the apparent mass between the different spectra at some frequencies; however, the magnitude of the effect of the spectra was small. Rakheja *et al.* (2002) also found negligible differences in the apparent mass obtained using white noise vibration of 1.0 ms^{-2} r.m.s. and track-measured vibration of similar magnitude (1.07 ms^{-2} r.m.s.). Mansfield *et al.* (2001) measured the apparent mass of 24 subjects (11 males and 13 females) using different excitation waveforms with 'nominally identical power spectra' (random vibration, equally spaced shocks, unequally spaced shocks, random combined with equally spaced shocks and random combined with unequally spaced shocks) at each of 0.5, 1.0, and 1.5 ms^{-2} r.m.s. The authors noticed that the resonance frequencies of the apparent masses were slightly higher for exposures to shock; however, they mentioned that the apparent masses were generally similar between the vibration conditions across the frequency range of interest (2-20 Hz).

Toward (2002) investigated the effect of the input spectra on the vertical apparent mass of the human body. Twelve male subjects were exposed to vertical narrowband ½-octave inputs (from 1 to 16 Hz) with magnitudes of 0.25, 0.4, 0.63, 1.0 and 1.6 ms^{-2} r.m.s. The ½-octave narrowband inputs were 'superimposed upon a low-level broadband vibration (at 0.25 ms^{-2} r.m.s.) to obtain good coherency at frequencies below 25 Hz'. The effects of the narrowband input frequency and the vibration magnitude on the resonance frequency of the apparent mass, as reported by Toward (2002) are shown in Figure 2.13. The figure indicates that the non-linearity of the human body depends on both the narrowband input magnitude and frequency. The figure shows greater change in the resonance frequency of the apparent mass with change in input frequency at high input magnitude than at low input magnitudes. The figure also indicates that the non-linearity of the body (change in the resonance frequency of the apparent mass with change in vibration magnitude) is greater with low input frequencies than with high input frequencies.

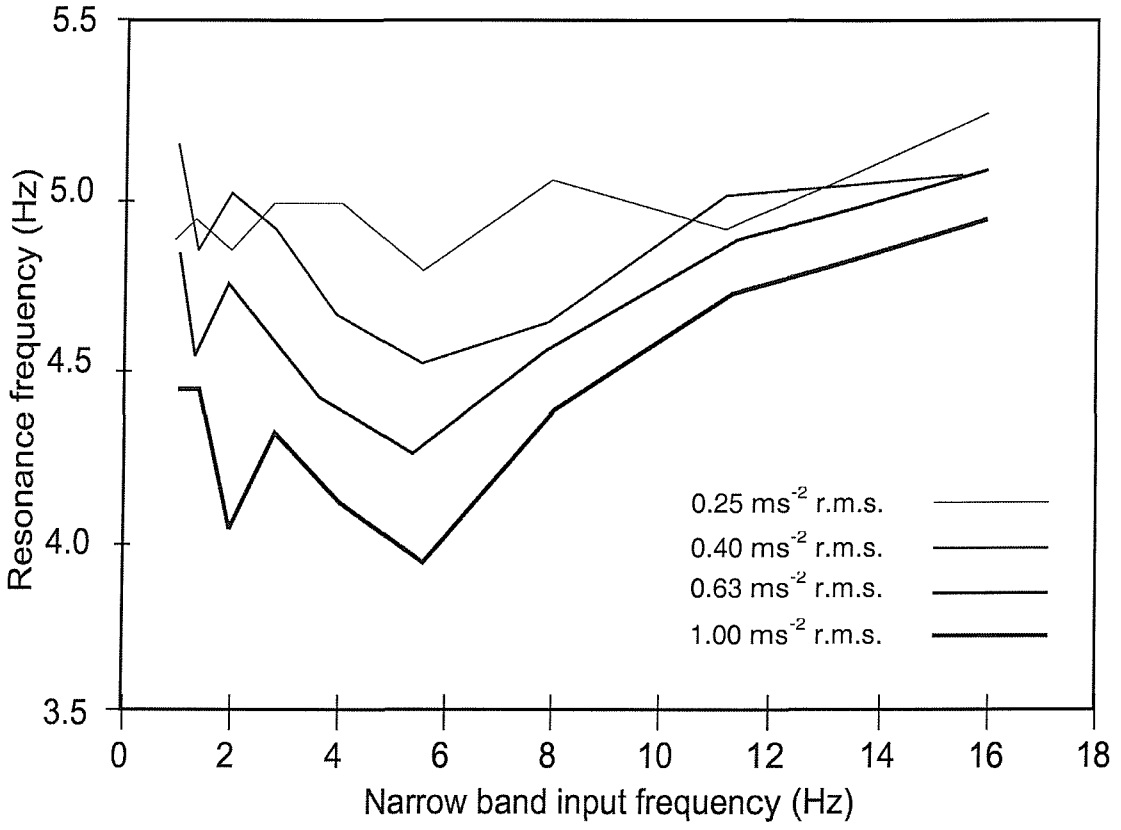

Figure 2.13 Median apparent mass resonance frequencies of 12 subject measured with narrowband inputs at nine ½-octave input frequencies from 1 to 16 Hz and four input magnitudes superimposed on 0.25 ms^{-2} r.m.s. broad band vibration (Toward, 2002).

2.3.2 Horizontal excitation

Studies of human biodynamic responses to horizontal vibration are not common in the literature despite evidences of its importance: Lundström and Lindberg (1983) showed high horizontal vibration component in off-road vehicles. Moreover, subjective studies summarised by Griffin (1990) showed that the perception thresholds during horizontal excitation in the range 1 to 10 Hz are similar to those during vertical excitation. However, only few studies have investigated the responses of humans to horizontal excitation.

Tables of the apparent mass of seated subjects exposed to fore-and-aft random vibration provided by Lee and Pradko (1968) show a peak at 1.3 Hz in the fore-and-aft apparent mass and two peaks at 0.6 Hz and 1.8 Hz in the lateral apparent mass. No detailed description of the exposure or the seating conditions, except that no backrest or armrest was used, was given. Fairley and Griffin (1990) conducted the first fundamental detailed experiments to determine human biodynamic response to horizontal (fore-and-aft and lateral) vibration. Later, a few other studies have been performed in the horizontal direction (Holmlund, 1998; Mansfield and Lundström, 1998; Holmlund and Lundström, 1998; Mansfield and Lundström, 1999a).

Fairley and Griffin (1990) measured the apparent masses of eight seated subjects in the fore-and-aft and lateral directions. The subjects sat on a rigid seat and were exposed to random vibration in the frequency range 0.25 to 20 Hz. The subjects' feet were placed on a footrest moving in phase with the seat. The experiments were conducted once without a backrest and once with a backrest. When no backrest was used, two vibration modes were noticed: around 0.7 Hz and between 1.5 and 3 Hz. However, when a backrest was used, only one vibration mode was evident in the apparent mass with a frequency at about 3.5 Hz for the fore-and-aft direction and at about 1.5 Hz for the lateral direction (see Figure 2.14). Fairley and Griffin (1990) noticed a decrease in the resonance frequency of the second mode, but not the first, with an increase in vibration magnitude in both the fore-and-aft and lateral directions.

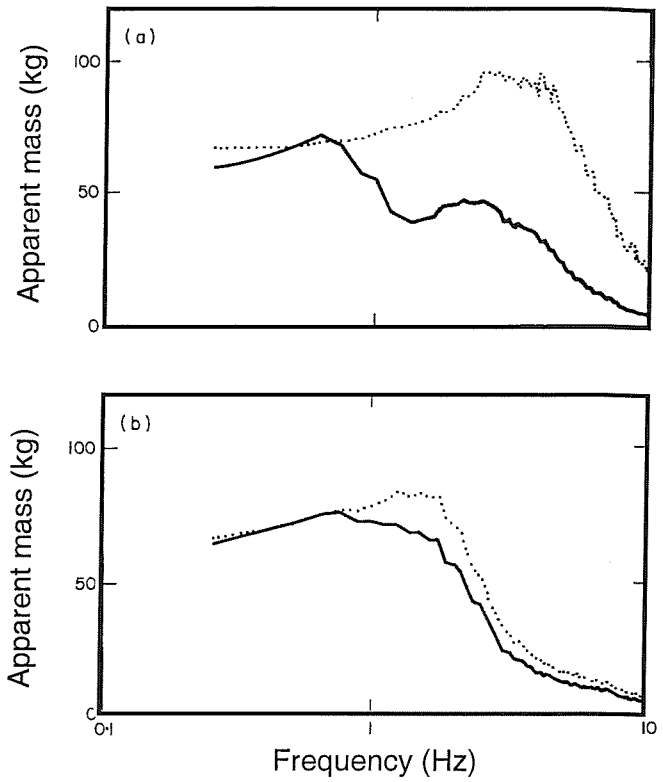

Figure 2.14 Effect of backrest on the mean apparent mass of eight seated subjects during (a) fore-and-aft excitation and (b) lateral excitation. ———, without backrest; ·····, with backrest (Fairley and Griffin, 1990).

Holmlund and Lundström (1998) measured the fore-and-aft and lateral mechanical impedance of 30 subjects (15 males and 15 females) in the frequency range 1.13 to 80 Hz. Sinusoidal vibration with magnitudes between (0.25 and 1.4 ms^{-2} r.m.s.) was used. No backrest was used and the feet were supported on a stationary floor. A vibration mode in the frequency range 2 to 5 Hz, which is consistent with the second mode reported by Fairley and Griffin (1990), was evident in both the fore-and-aft and lateral directions. Obviously, due to the low limit of the frequency range used being above 1 Hz, Holmlund and Lundström were not able to see the first mode reported by Fairley and Griffin (1990). A third mode, in the frequency range 5 to 7 Hz was seen only in the lateral direction (was not found by Fairley and Griffin). An increase in vibration magnitude was found to decrease the resonance frequency in the fore-and-aft mechanical impedance while it had no effect on the resonance frequencies in the lateral direction.

Mansfield and Lundström (1999a) measured the apparent masses of 30 seated subjects (15 males and 15 females) in several directions of horizontal vibration orientated at 0° (fore-and-aft), 22.5°, 45°, 67.5°, and 90° (lateral) with the mid-sagittal plane. The subjects sat on a flat rigid seat with no backrest with their feet stationary on the floor and their arms folded. At each angle, the subjects were exposed to random vibration with

magnitudes of 0.25, 0.5, and 1.0 ms^{-2} r.m.s. in the frequency range 1.5 to 20 Hz. The results showed two peaks in the apparent mass at about 3 Hz and 5 Hz, although the second peak was clearer with greater angles. Both resonance frequencies decreased with an increase in vibration magnitude, which is inconsistent with the effect of vibration magnitude reported by Holmlund and Lundström (1998). The magnitude of the first peak increased while the magnitude of the second peak decreased with an increase in vibration magnitude. The location of only the first resonance depended on the direction of excitation: the first resonance frequency decreased while the second resonance frequency was unaffected by changing the direction of excitation from 0° to 90°.

Mansfield and Lundström (1998) compared the median apparent mass measured using horizontal vibration orientated at 45° to the mid-sagittal plane with the mean of the apparent mass measured using fore-and-aft and lateral excitation. They wanted to test if the response of the human body to horizontal vibration 45° from the mid-sagittal plane could be obtained from the average of the responses in the fore-and-aft and lateral directions. They reported that the peak of the mean apparent mass (i.e. calculated from fore-and-aft and lateral excitation) had greater magnitude than the peak of the apparent mass measured with 45° excitation (Figure 2.15). They also reported significant differences in the apparent mass obtained from the two methods at frequencies below 4 Hz. They suggested that 'it would be beneficial to study the response of the body to other non-orthogonal directions of vibration to identify where the range of angles over which the body can be considered to respond in its fore-and-aft mode or lateral mode'.

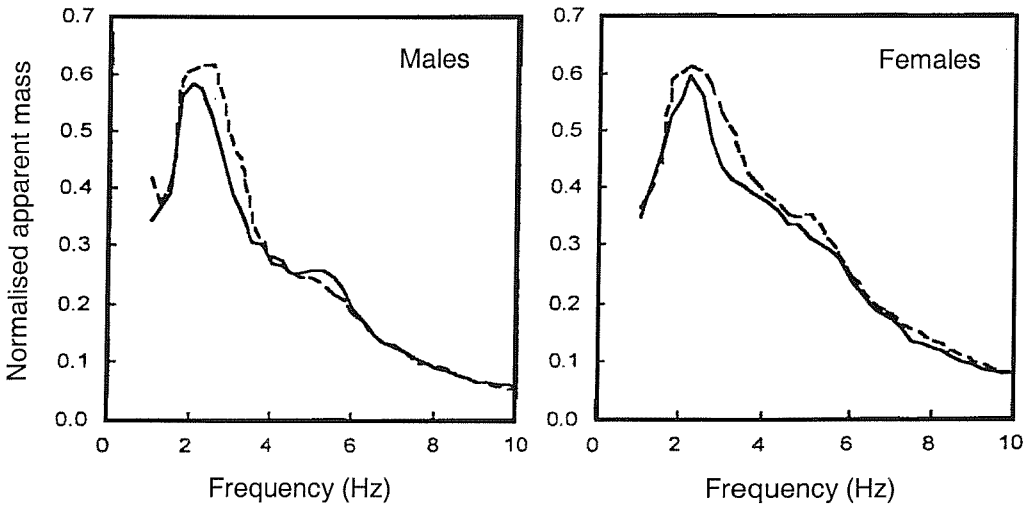

Figure 2.15 Comparison between the median normalised apparent masses measured during horizontal excitation in a direction at 45° from the mid-sagittal plane (——) with the mean of the apparent masses measured during fore-and-aft and lateral excitation (– – –). Data from Mansfield and Lundström (1998).

2.3.3 Rotational excitation

Vibration is not restricted to translational motions (i.e. vertical and horizontal) but may also occur in rotational motions (pitch, yaw and roll). In fact, the acceleration measured in a vehicle in the vertical or the horizontal direction is partly due to rotational motions. For example, vertical motion measured in a car is composed of a component of pure vertical motion, a component due to pitch motion and a component due to roll motion. However, because of the lack of data about the driving point response to rotational motion, it is not known if it was necessary to consider separately the driving response (i.e. apparent mass or mechanical impedance) of the body in translational and rotational directions when evaluating human response to vibration.

Gunston (2003) is the only known study to measure the apparent masses of seated subjects with rotational excitation. He compared the lateral apparent mass in response to lateral excitation with the 'lateral' apparent mass in response to roll excitation (obtained from the force and acceleration measured parallel to the seat surface). Twelve male subjects sat on a rigid seat without backrest and were exposed to random vibration at three different magnitudes (0.05, 0.1, 0.2 ms^{-2} r.m.s.) in the frequency range 0.2 to 2 Hz. With the roll excitation, the centre of rotation was at the surface of the seat. Over the frequency range investigated, the normalised lateral apparent mass (apparent mass divided by the sitting mass of the subjects) was greater in response to roll excitation than in response to lateral excitation (see Figure 2.16). No significant change in the magnitude of the lateral apparent mass was found with change in vibration magnitude at any frequency with either direction of excitation, except at 0.59 Hz and 1.56 Hz with lateral excitation.

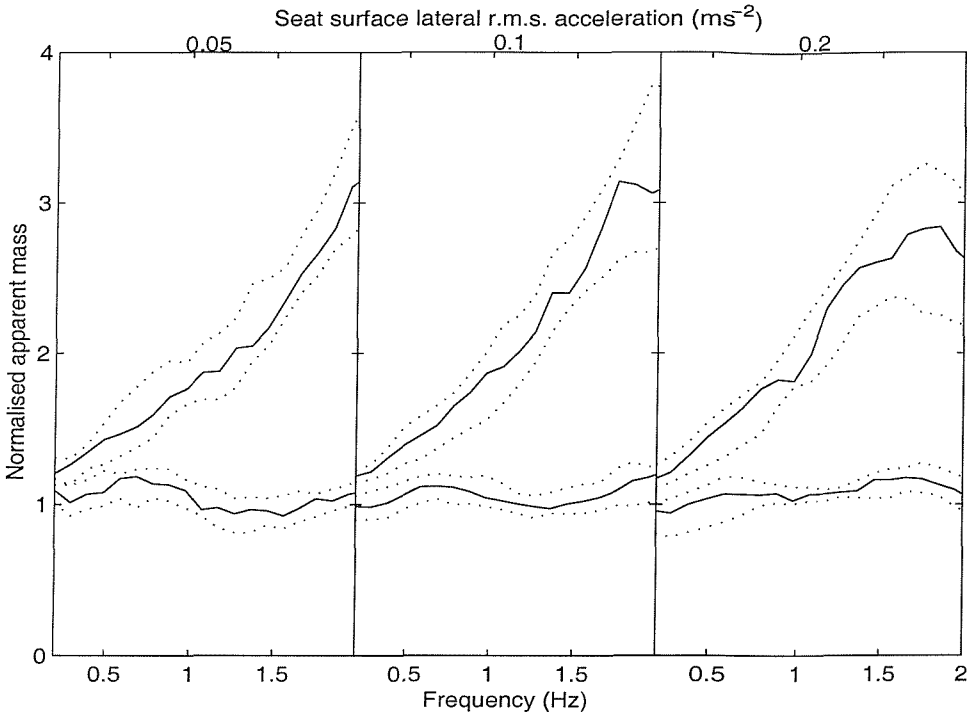

Figure 2.16 Median, first quartile and third quartile of lateral apparent mass measured using lateral excitation (lower lines) and roll excitation (upper lines) at three magnitudes of seat surface lateral acceleration (Gunston, 2003).

2.4 TRANSMISSIBILITY OF THE HUMAN BODY

Measuring the transmissibility of the human body helps in further understanding the movements of the human body when exposed to whole-body vibration. Measuring the dynamic response (transmissibility) of the different parts of the human body can also help in identifying some of the mechanisms that produce certain phenomena in the driving point response such as the resonance and the non-linear phenomena.

Measurements of transmissibility to parts of the body (such as the spine, the pelvis and the viscera) have been reported in the literature. The measurements have been performed using either an invasive method or non-invasive method. In the invasive method, one side of a Kirschner wire (K-wire) is inserted into the spinous processes while the other side of the Kirschner wire (K-wire) is attached to an accelerometer (Panjabi *et al.*, 1986). In the non-invasive method, which is more popular than the invasive method for convenience and ethical reasons, the measurements are taken on the skin and corrected to give the motion of the bone (i.e. the vertebra of interest; e.g. Kitazaki and Griffin, 1998). Transmissibility to the head has been measured by attaching accelerometers on the top of the head or on a helmet, on the forehead or at the mouth using a bite-bar (Paddan and Griffin, 1988a, Figure 2.17).

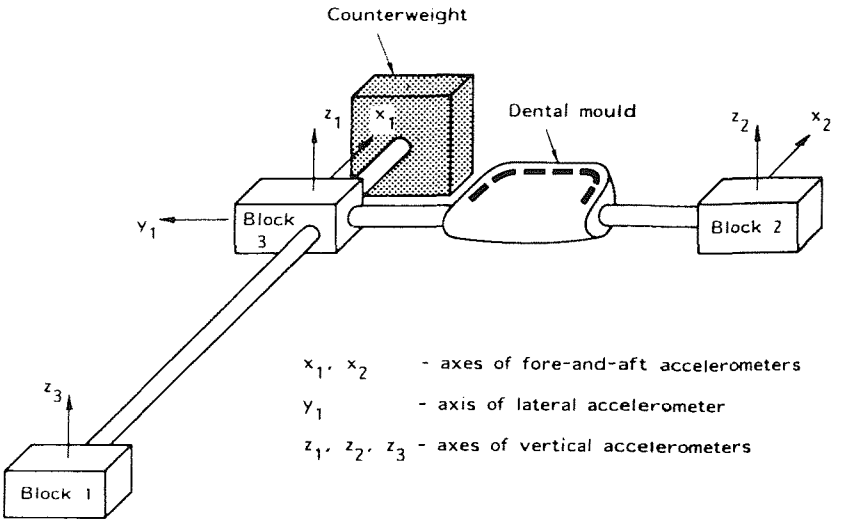

Figure 2.17 Bite-bar used for measuring transmissibility to the head (Paddan and Griffin, 1988a)

Although this thesis is concerned with the driving point response, a review of literature on the transmissibility of the human body is useful and necessary to explain some of the findings of this thesis. A summary of results of studies of the transmissibility of the human body will be given in the following sections.

2.4.1 Transmissibility to the pelvis and the spine

Vertical, fore-and-aft and pitch transmissibilities to the different regions on the spine and the pelvis (see Figure 2.18 and Figure 2.19 for the different components of the pelvis and the spine) have been reported in some studies. Measurements of transmissibility to the pelvis and spine during horizontal excitation or rotational excitation are not known in the literature. This section will review some of the studies of the transmission of vertical seat vibration to the pelvis and spine.

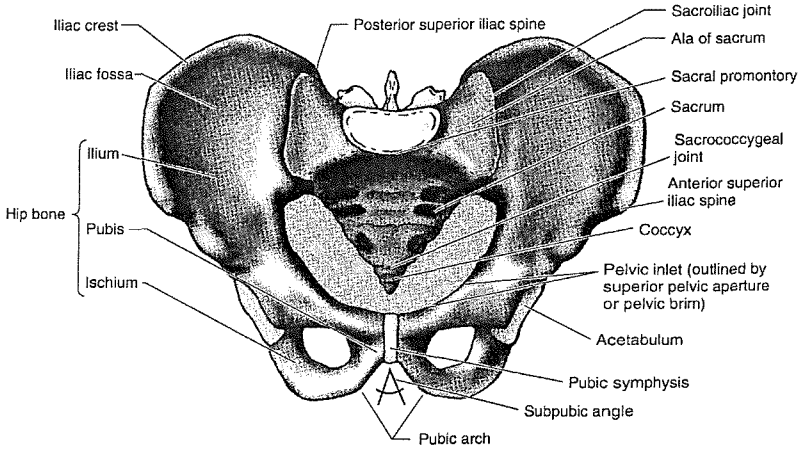

Figure 2.18 Anatomy of the pelvis (Moore and Agur, 2002).

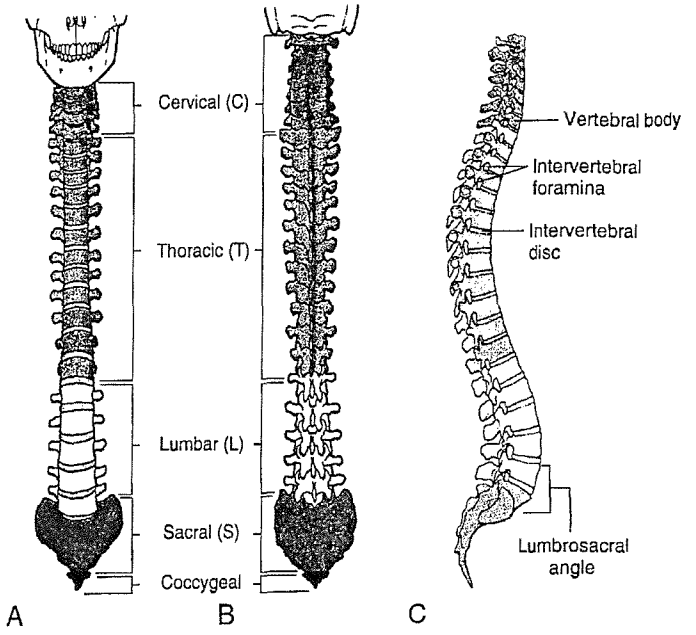

Figure 2.19 Anatomy of the spine. A, anterior view; B, posterior view; C, lateral view (Moore and Agur, 2002).

Using sinusoidal excitation Coermann (1962) and Panjabi *et al.* (1986) reported a resonance in the vicinity of 5 Hz in the vertical transmissibility to the pelvis and the sacrum. A resonance in the vertical motion of the pelvis in the vicinity of 5 Hz was also found using vertical random excitation (Kitazaki and Griffin, 1998; Matsumoto and Griffin, 1998a, Figure 2.20a). A second peak in the range 8 to 10 Hz was also evident in the vertical motion of the pelvis and sacrum (Kitazaki, 1994; Mansfield, 1998; Matsumoto and Griffin, 1998a).

Matsumoto (1999) and Matsumoto and Griffin (1998a) also measured the transmissibility to the fore-and-aft motion of the pelvis and the transmissibility to the pitch motion of the pelvis in the frequency range 0.5 to 10 Hz. They found that the fore-and-aft transmissibility was much less than the vertical transmissibility: the fore-and-aft transmissibilities of eight subjects were less than 0.5 for frequencies below 5 Hz and slightly more than 0.5 at frequencies above 5 Hz (Figure 2.20b). The pelvis pitch motion was very small below 4 Hz but increased above 4 Hz, with some subjects showing peaks in the frequency range 5 to 10 Hz as seen in Figure 2.20c. Mansfield and Griffin (2002) measured the pitch motion of the pelvis in nine postures (see Figure 2.3) during vertical excitation in the frequency range 1 to 20 Hz and reported a peak in the transmissibility at about 12 Hz.

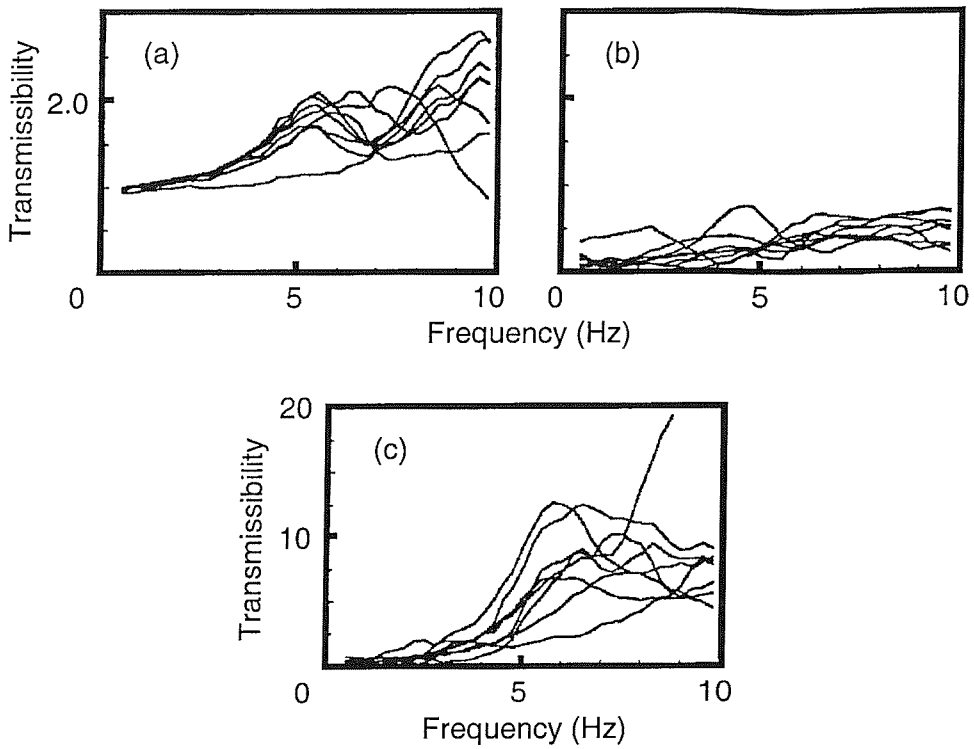

Figure 2.20 Motions of the pelvises of eight subjects with vertical excitation. (a) vertical motion of the pelvis; (b) fore-and-aft motion of the pelvis; (c) pitch motion of the pelvis (Units of pitch transmissibility is $rads^{-2}/ms^{-2}$, Matsumoto and Griffin, 1998a).

Panjabi *et al.* (1986) used the invasive method to measure the vertical, fore-and-aft and pitch motions of the first lumbar vertebra (L1) and the third lumbar vertebra (L3) due to vertical seat excitation. Similar vertical transmissibilities were found at L1 and L3, characterised by a peak with transmissibility around 1.5 at around 4.4 Hz which lead the authors to hypothesise a stiff connection between L1 and L3 in the frequency range of interest (2 to 15 Hz). This peak is in the same region where a peak in the vertical transmissibility to the sacrum (at around 4.7 Hz) was also measured. However, the authors found significant differences between the resonance frequencies measured at L1 and L3 and at the sacrum and concluded that the connection between L3 and the sacrum is flexible that the resonance frequency at L3 was smaller than that at the sacrum. The fore-and-aft transmissibilities to L1 and L3 were less than the vertical transmissibilities and showed no peaks. High inter-subject variabilities were found in the pitch motion of the vertebrae and no trend was clear in the data.

Hinz *et al.* (1988) measured the vertical and fore-and-aft transmissibilities to the third lumbar vertebra (L3) and the fourth lumbar vertebra (L4) during vertical sinusoidal vibration at 4.5 and 8.0 Hz with magnitudes of 1.5 and 3.0 ms^{-2} r.m.s. The measurements were taken on the skin but were corrected to give the motions of the bones. The authors

stated that although the absolute vertical motions at L3 and L4 were greater than the absolute fore-and-aft motions, the relative fore-and-aft motion between L3 and L4 was greater than the relative vertical motion between the two vertebrae. They concluded that 'bidimensional acceleration data confirmed the suggestion that relative motions in the z-direction are combined with angular motions'.

Kitazaki (1994) measured the vertical and fore-and-aft transmissibilities from vertical seat excitation to the first, sixth, and eleventh thoracic vertebrae (T1, T6, T11), the third lumbar vertebra (L3) and the second sacrum (S2). The measurements were taken on the skin but corrected to give the motion of the vertebrae (Kitazaki and Griffin, 1995). Eight subjects adopting a normal sitting posture were exposed to random excitation with magnitude of 1.7 ms^{-2} r.m.s. in the frequency range 0.5 to 35 Hz. Vertical transmissibilities to all locations showed a peak in the vicinity of 5 Hz with greater transmissibility for lower locations on the spine than higher locations. A second peak at around 8 Hz was found in the vertical transmissibilities to the lower locations (i.e. L3 and S2). The fore-and-aft transmissibilities were smaller than the vertical transmissibilities: all fore-and-aft transmissibilities were less than unity except the fore-and-aft transmissibility to T1 at around 5 Hz which was around 1.2. The fore-and-aft transmissibility to the second sacrum, S2 showed two peaks similar, in frequency, to those found in the vertical transmissibility to S2.

2.4.1.1 Effect of posture and seating condition on the transmissibility to the pelvis and the spine

Effect of posture

The effect of the sitting posture and seating conditions on the transmission of vertical seat excitation to the spine has been reported by a few investigators. Kitazaki (1994) compared between the transmissibilities to the spine (T1, T6, T11, L3 and S2) measured with three different sitting postures: normal, erect and slouched. The exposure conditions were described before (see Section 2.4.1). The vertical transmissibilities showed a clear decrease in the 5 Hz resonance frequencies and the magnitude at resonance when subjects changed posture from erect to normal and slouched (Figure 2.21). The decrease in the resonance frequency is consistent with the decrease in the apparent mass resonance frequency when subject changed postures from erect to slouched (Fairley and Griffin, 1989). Above resonance, the vertical transmissibility in the erect posture was higher than in the normal posture and slouched posture especially to T1, T6 and T11. For the fore-and-aft transmissibilities, any change in the resonance frequency with change in posture was small. However, The transmissibility at resonance increased with change in

posture from erect to slouched, especially for the fore-and-aft transmissibility to T1 and T6 (Figure 2.21). In both the vertical transmissibility and fore-and-aft transmissibility the least effect of posture was seen at L3 and S2.

In the same study where Mansfield and Griffin (2002) studied the effect of the sitting posture on the apparent mass, they studied the effect on seat-to-pelvis pitch transmissibility. Twelve male subjects were exposed to vertical random vibration in the frequency range 1.0 to 20 Hz while sitting in nine sitting postures (see Figure 2.3). The authors found only small changes in the apparent mass and pelvis rotation with change in posture.

Effect of seating condition

Magnusson *et al.* (1993) studied the effect of backrest inclination on the transmissibility to the lumbar spine. They reported that the backrest inclination attenuated the vertical vibration at the fourth lumbar vertebra compared to a no backrest condition but the attenuation was small in the resonance region (4 to 6 Hz range). They also reported an increase in fore-and-aft vibration at the fourth lumbar vertebra when a backrest (with angles of 110 and 120°) was used relative to a no backrest condition.

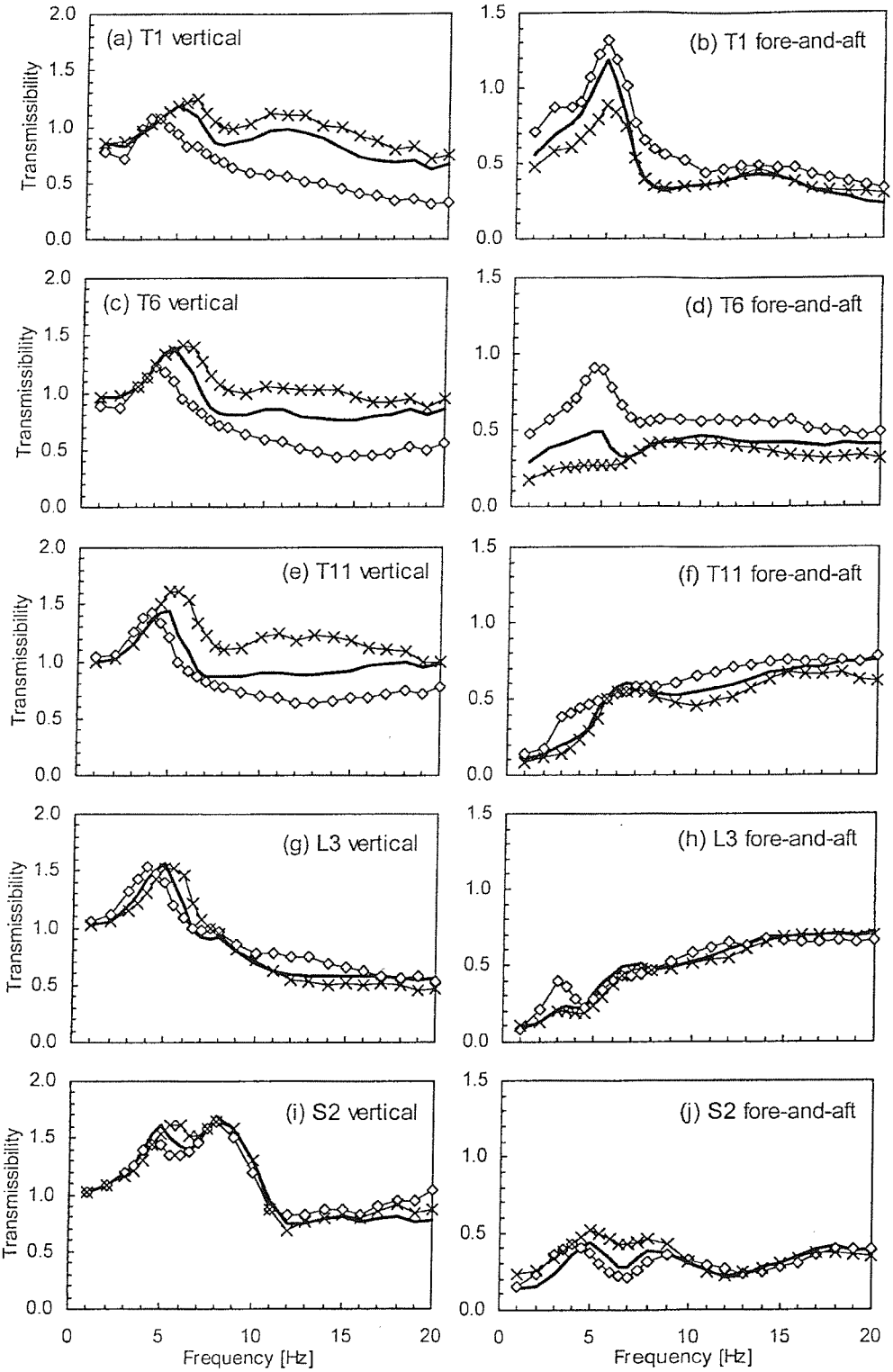

Figure 2.21 Mean vertical transmissibilities and fore-and-aft transmissibilities to the spine: effect of posture ———, normal posture; —x—, erect posture; —◊—, slouched posture (Data from Kitazaki, 1994; redrawn by Matsumoto, 1999).

Lewis and Griffin (1996) studied the effect of using a fixed backrest and a moving backrest on the transmissibility to the seventh thoracic vertebra (T7) and the second sacrum (S2). With the moving backrest, 'the backrest cushion was free to move vertically within guides secured to the seat frame'. The transmissibilities to T7 and S2 in both backrest conditions were compared with the transmissibilities to T7 and S2 measured without a backrest. The vertical transmissibilities to T7 and S2 measured with no backrest conditions were similar to the transmissibilities measured with the moving backrest at frequencies below 6 Hz (see Figure 2.22; the results of two subjects are shown). Above 6 Hz, the transmissibilities measured without backrest were higher than those measured with the moving backrest. The authors also found that the transmissibilities to T7 and S2 were similar to the transmissibilities to the backrest of the seat in both backrest conditions which suggested that the skin of the backs of the subjects was well coupled to the backrest. Hence, in order to find out which backrest reduced the strain in the spine, the authors compared the transmissibility to the seat surface using both backrest conditions and also compared the phase difference between the vibration at the seat surface and the vibration at the backrest in both backrest conditions and found that both (i.e. the seat surface transmissibility at resonance and the phase difference between the seat vibration and the backrest vibration) increased with the fixed backrest. This led the authors to conclude that using a moving backrest might improve comfort and result in less strain in the lumbar region.

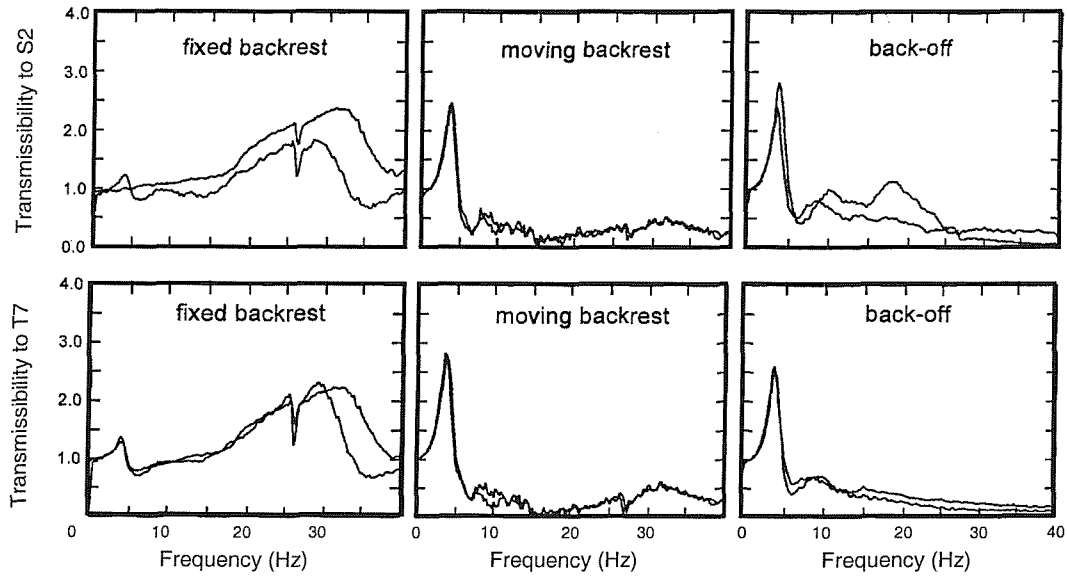

Figure 2.22 Vertical transmissibilities to S2 and T7 with three backrest conditions. Results are shown for two subjects (Lewis and Griffin, 1996).

2.4.2 Transmissibility to the head

Transmissibility to the head during translational (i.e. vertical and fore-and-aft) and rotational excitation has been reported in the literature; however, with more concentration on translational excitation (especially vertical seat excitation) than on rotational excitation. Interests in measuring the transmissibility to the head comes from the link between movements of the head and discomfort and movements of the head and vision. Moreover, measurements of transmissibility to the head, especially with using a bite-bar as explained before, are easier to perform than measurements to other locations such as on the spine. In this section, some results of transmissibility to the heads of seated subjects obtained from previous studies are shown.

Coermann (1962) measured the vertical transmissibility to the head of one subject adopting a relaxed sitting posture. The subject sat on a rigid seat and was exposed to vertical excitation in the frequency range 1 to 20 Hz. The measurements, which were taken on the top of the head, showed a principal peak at around 4.5 Hz and a second peak at around 10.3 Hz.

Paddan and Griffin (1988a) measured the transmission of vertical seat excitation to all six axes of head motion (vertical, fore-and-aft, lateral, pitch, roll and yaw). Twelve male subjects sat in a comfortable upper body posture on a rigid seat without a backrest and rested their feet on a footrest moving in phase with the seat. The subjects were exposed to random vibration of 1.75 ms^{-2} r.m.s. in the frequency range 0.2 to 31.5 Hz. The measurements were obtained using accelerometers mounted on a bite-bar as shown previously in Figure 2.17. The results, shown in Figure 2.23, indicated greatest transmissibility in the mid-sagittal plane (vertical, fore-and-aft and pitch axes). The peaks reported by Coermann (1962) at around 4 and 10 Hz can also bee seen in the data of Paddan and Griffin (1988a).

Paddan and Griffin (1988b) measured the transmissibility to the head in all six axes during horizontal (i.e. fore-and-aft and lateral) excitation. Twelve male subjects sat on a flat rigid seat with no backrest and were exposed to random excitation of 1.75 ms^{-2} r.m.s. in the frequency range 0.2 to 16 Hz, once in the fore-and-aft direction and once in the lateral direction. With fore-and-aft excitation, head motion occurred mainly in the mid-sagittal plane (see Figure 2.24). Lateral seat excitation, however, induces mainly lateral head motion (see Figure 2.25).

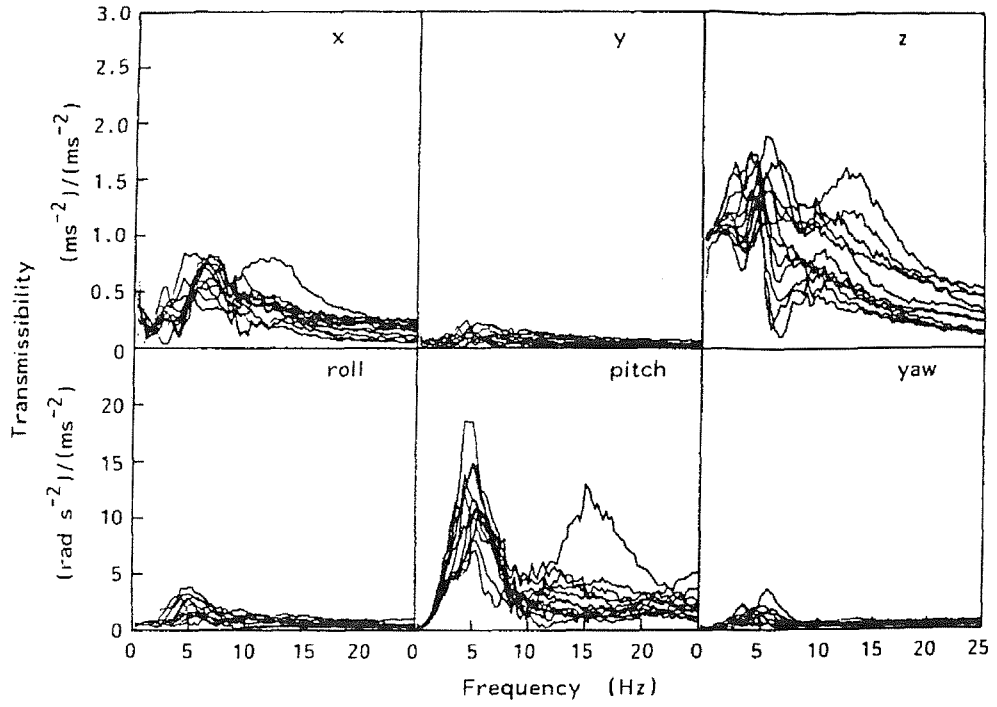

Figure 2.23 Transmissibility of vertical seat excitation to the heads of 12 subjects (Paddan and Griffin, 1988a).

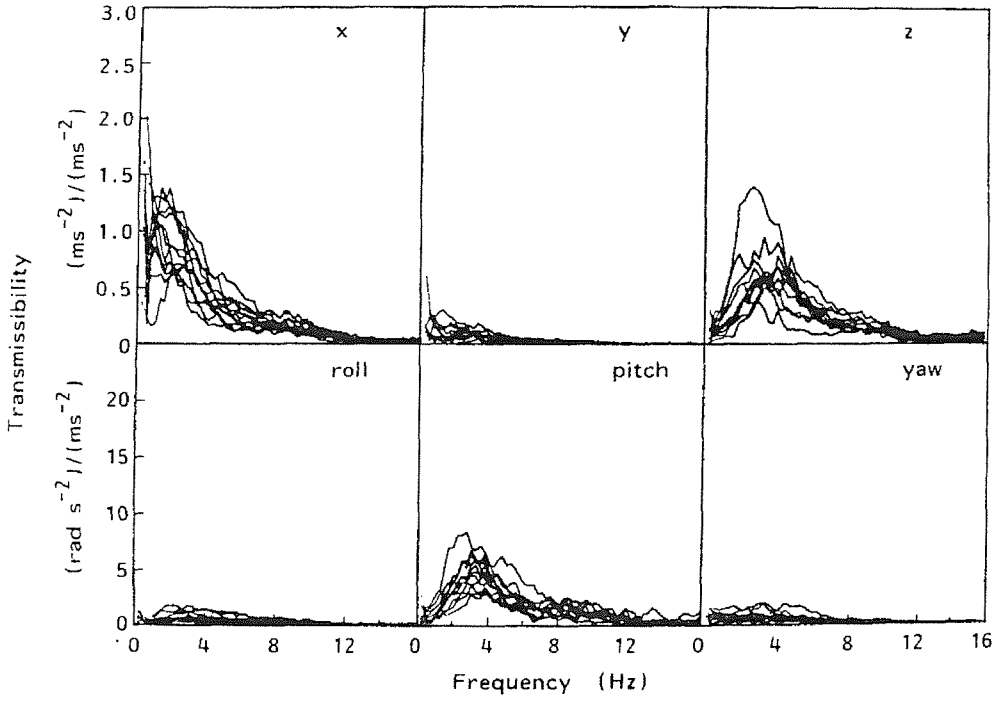

Figure 2.24 Transmissibility of fore-and-aft seat excitation to the heads of 12 subjects (Paddan and Griffin, 1988b).

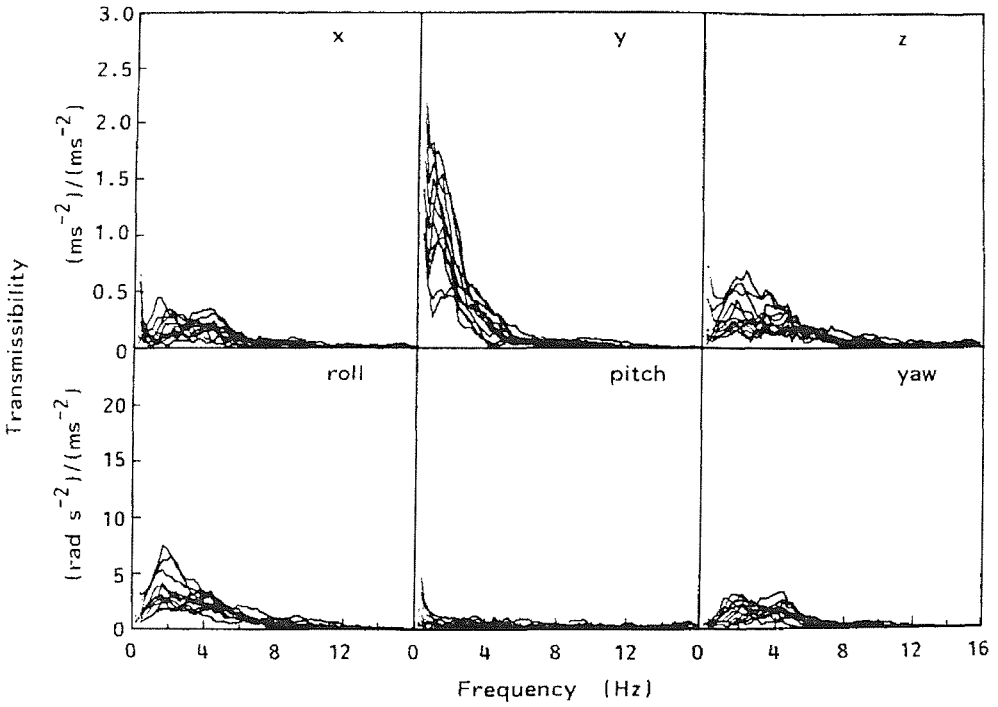

Figure 2.25 Transmissibility of lateral seat excitation to the heads of 12 subjects (Paddan and Griffin, 1988b).

In this thesis only translational excitation will be used while rotational excitation is beyond the interest of this thesis. However, for movements of the head in six axes due to rotational excitation, the reader may refer to Paddan and Griffin (1994) for pitch and roll excitation and to Paddan and Griffin (2000) for yaw excitation.

2.4.2.1 Effect of posture and seating condition on the transmissibility to the head

Effect of posture

Coermann (1962) compared the vertical transmissibility to the head in a relaxed sitting posture with the vertical transmissibility to the head in an erect sitting posture. While there were two peaks in the transmissibility to the head when using a relaxed posture (as was shown before at 4.5 Hz and 10.3 Hz), four peaks were evident when an erect posture was used: a principal peak at around 5 Hz and three other peaks at around 3, 11 and 15 Hz. The transmissibility of the principal peak when the subject adopted an erect posture was lower than when adopting a relaxed posture. However, the transmissibility above resonance was much lower with the relaxed posture than with the erect posture. Griffin *et al.* (1978) also studied the effect of the sitting posture on the transmissibility to the head. Eighteen subjects were exposed to vertical whole-body vibration in the frequency range 1 to 100 Hz while sitting in three different postures: normal upright, relaxed and stiff. The results showed similarity in the transmissibility to the head between the normal upright

posture and the relaxed posture, although the relaxed posture showed slightly lower transmissibility than the normal upright posture at frequencies above about 10 Hz (see Figure 2.26). Compared with the normal and relaxed postures, the stiff posture showed the lowest transmissibility to the head below 6 Hz and the greatest transmissibility to the head above 6 Hz which is consistent with the results of Coermann (1962) mentioned above.

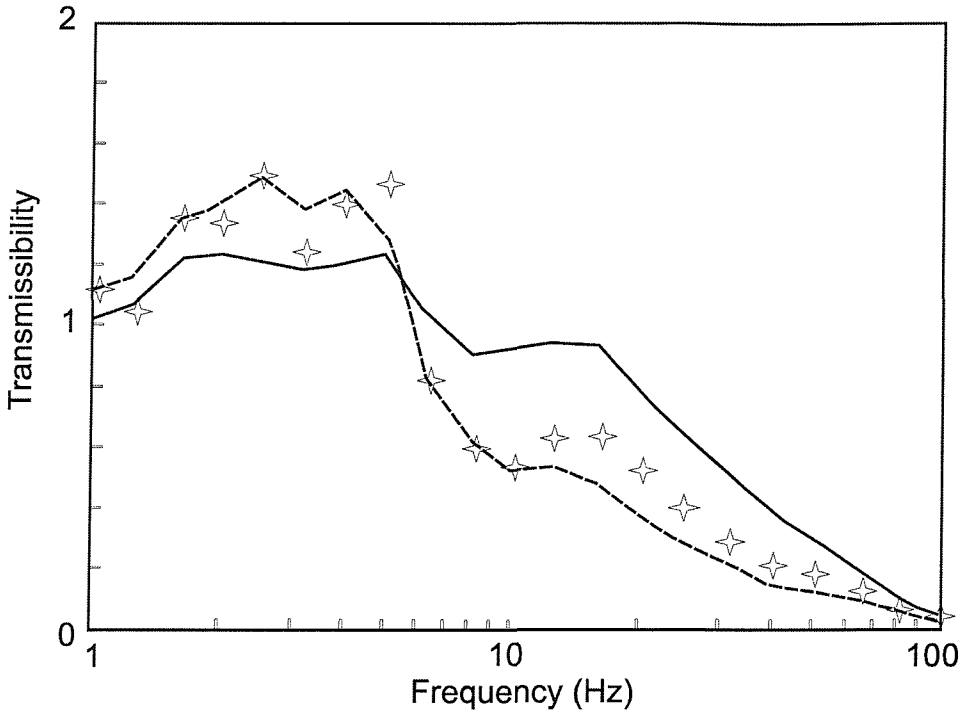

Figure 2.26 Mean seat-to-head-transmissibility of 18 subjects: effect of sitting posture: ☆, "normal upright posture"; ———, "stiff"; – – – –, "relaxed" (Griffin *et al.* 1978).

Effect of seating conditions

The effects of a rigid backrest on the head motion in all six axes have been investigated during vertical and horizontal excitation (Paddan and Griffin,1988a, 1988b). During vertical excitation, Paddan and Griffin (1988a) found an increase in the head motion especially in the range 5 to 10 Hz in the mid-sagittal plane (vertical, fore-and-aft and pitch directions) when a backrest was used compared to no backrest condition (Figure 2.27). Similarly, during fore-and-aft excitation the head motion above 4 Hz increased in the mid-sagittal plane when a backrest was used (Paddan and Griffin, 1988b). Moreover, two peaks were evident in the data (at around 2 Hz and between 6 to 8 Hz) when a backrest was used compared to only one peak at around 2 Hz in the no backrest condition (Figure 2.28). However, little effect of the backrest on the head motion was observed during lateral seat excitation (Figure 2.29; Paddan and Griffin, 1988b).

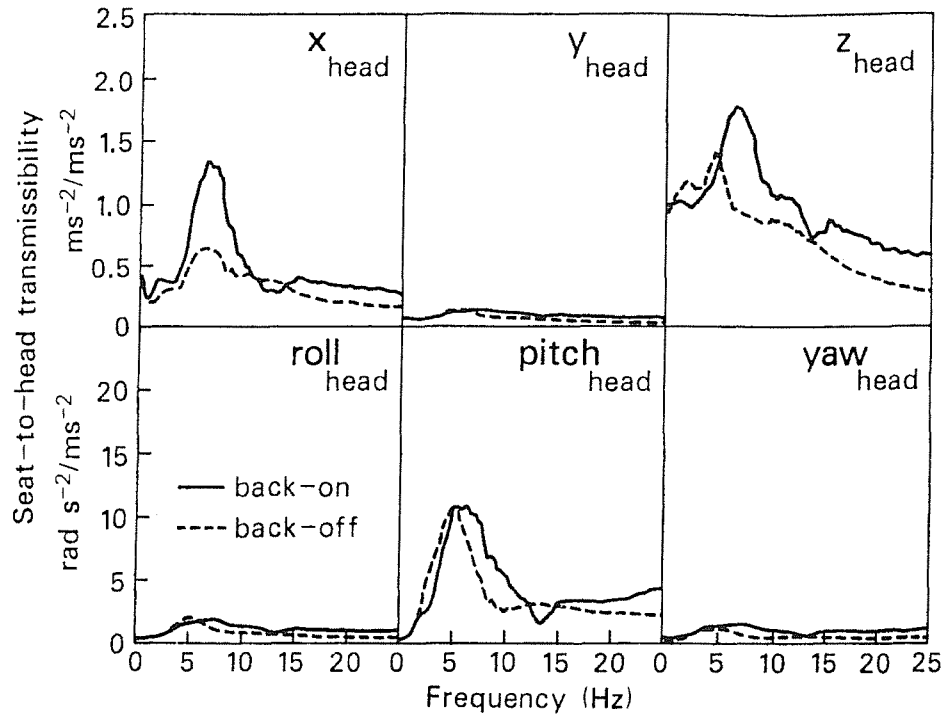

Figure 2.27 Effect of contact with a rigid flat backrest on the mean seat-to-head transmissibility of 12 subjects during vertical seat excitation (Data of Paddan and Griffin, 1988a).

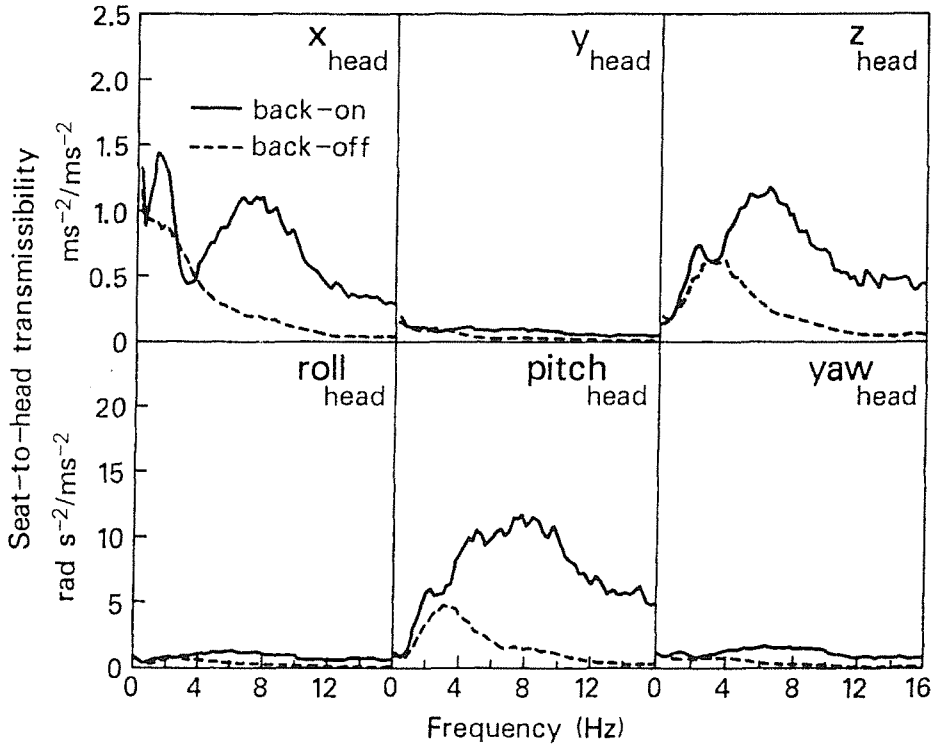

Figure 2.28 Effect of contact with a rigid flat backrest on the mean seat-to-head transmissibility of 12 subjects during fore-and-aft seat excitation (Data of Paddan and Griffin, 1988b).

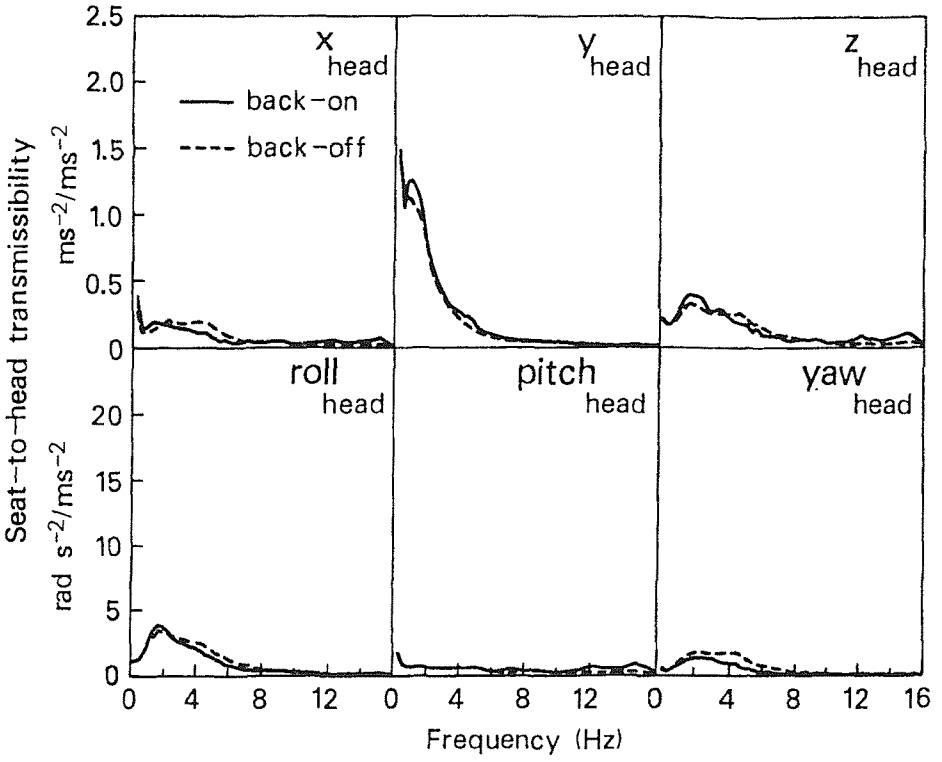

Figure 2.29 Effect of contact with a rigid flat backrest on the mean seat-to-head transmissibility of 12 subjects during lateral seat excitation (Data of Paddan and Griffin, 1988b).

In the same study mentioned in Section 2.4.1.1 where Lewis and Griffin (1996) studied the effect of a moving backrest on the transmissibility to T7 and S2, they also studied the effect on the transmissibility to the head. The principal peak (between 3.5 and 5 Hz) in the transmissibility to the head when a moving backrest was used was of similar frequency to that in the transmissibility to the head when no backrest was used. The frequency of the peak was higher by about 0.5 Hz when a fixed backrest was used. The peak transmissibility was also highest when a fixed backrest was used. The authors suggested that 'moving seat back does not impede movements of the subjects' backs as much as the fixed backrest'.

Howarth (2003) studied the effect of posture and using a headrest on the fore-and-aft and pitch motions of the head during fore-and-aft seat excitation. The subjects sat on a rigid seat inclined at 10° to the horizontal with three different postures. The first posture was 'normal-no-headrest' in which the backs and pelvises of the subjects were in contact with a backrest inclined at 25° to the vertical and no headrest was used. The second posture, 'normal-with-headrest', was the same as the first posture but with the use of a headrest. In the third posture, 'relaxed-no-headrest', the backs of the subjects were in contact with a backrest inclined at 30° from the vertical while their pelvises were moved approximately

5 cm forward from the backrest and no headrest was used. In each posture, twelve male subjects were exposed to fore-and-aft random vibration in the frequency range 0.1 to 5 Hz. The magnitude and duration of the exposure were 0.7 ms^{-2} r.m.s. and 5 minutes. The results showed a peak at around 1 Hz in the pitch motion and between 1 and 1.5 Hz in the fore-and-aft head motion in both the relaxed-no-headrest posture and the normal-no-headrest posture. It was also found that when no headrest was used, similar head motions were found in the relaxed and normal postures (Figure 2.30). When the headrest was used, the fore-and-aft head motion relative to the seat motion was small and the pitch head motion decreased significantly in the region 0.5 to 2 Hz.

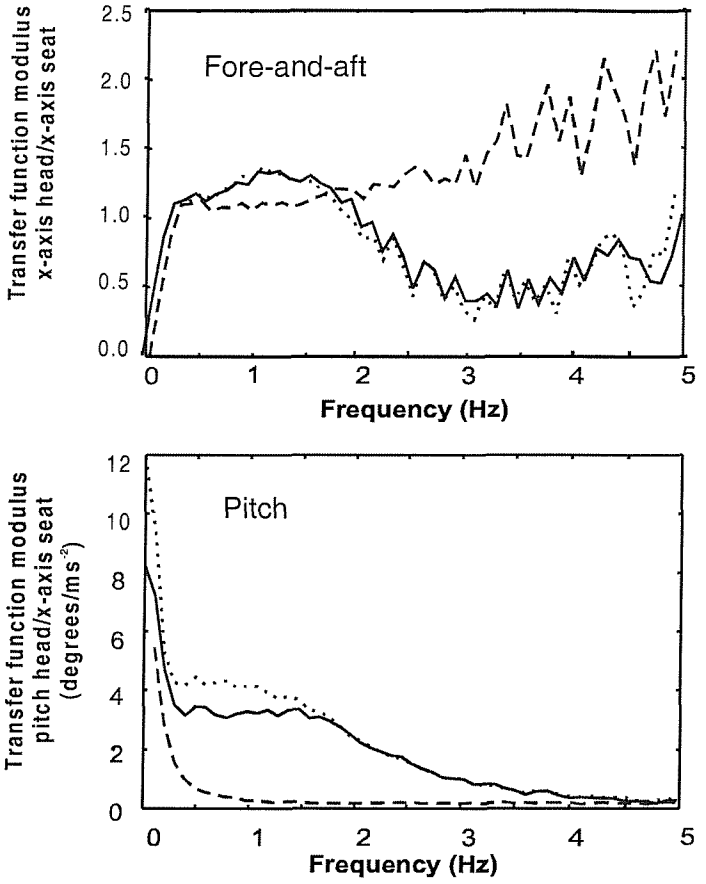

Figure 2.30 Median pitch and fore-and-aft head motion during fore-and-aft seat excitation. ———, normal-no-headrest; – – – –, normal-with-headrest; ·····, relaxed-no-headrest (Howarth, 2003).

2.4.3 Effect of vibration magnitude on the transmissibility to the human body

Reduction in the peak frequencies of the transmissibility to the human body with increase in vibration magnitude has been reported in previous studies. During vertical seat excitation, Mansfield and Griffin (2002) measured the seat-to-pelvis pitch transmissibility

at three vibration magnitudes (0.2, 1, and 2 ms^{-2} r.m.s.) and in nine postures (shown in Figure 2.3). They found that the resonance frequency of the pelvis pitch transmissibility (at around 12 Hz) decreased with increasing the vibration magnitude in all postures.

Matsumoto and Griffin (2002b) measured the transmissibility of the human body to the head, the pelvis and six locations on the spine (T1, T5, T10, L1, L3, L5) in three orthogonal axes in the sagittal plane (i.e. vertical, fore-and-aft and pitch) at five vibration magnitudes (0.125, 0.25, 0.5, 1.0 and 2.0 ms^{-2} r.m.s.). They observed the non-linear phenomenon at most measurement locations and in all axes (Figure 2.31). For example, when the vibration magnitude increased from 0.125 to 2.0 ms^{-2} r.m.s., the resonance frequency in the vertical transmissibility to L3 reduced from 6.25 to 4.75 Hz.

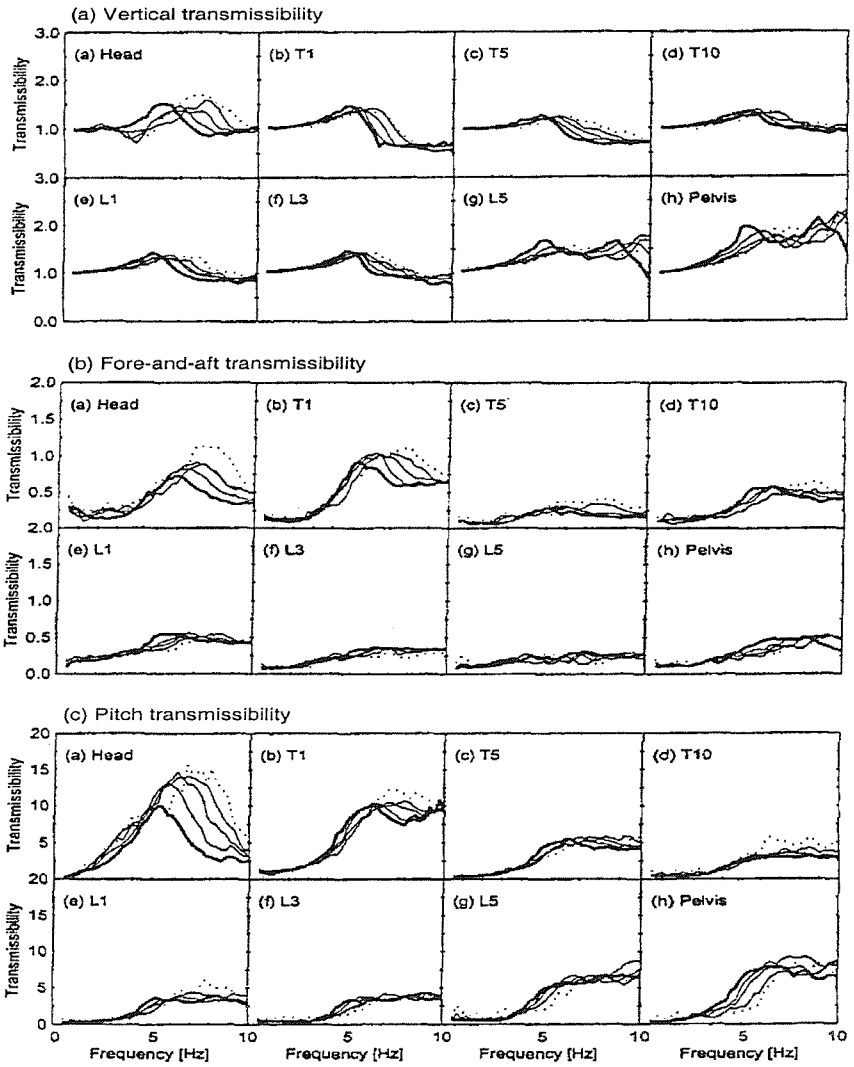

Figure 2.31 Median transmissibilities from vertical seat vibration to vertical, fore-and-aft and pitch vibration at different locations on the body at five vibration magnitudes. ·····, the lowest magnitudes (0.125 ms^{-2} r.m.s.); ———, the greatest magnitude (2.0 ms^{-2} r.m.s). (Units of pitch transmissibility is $rads^{-2}/ms^{-2}$, Matsumoto and Griffin, 2002b).

2.5 POSSIBLE CAUSES OF THE PRINCIPAL RESONANCE OF THE APPARENT MASS (OR MECHANICAL IMPEDANCE)

The precise manner in which the resonance of the body occurs is not yet known. Studies have investigated the parts of the body that cause, or contribute to, the resonance frequency by measuring the transmissibility to specific locations and comparing the results to the resonance frequency of the whole body.

Hagena *et al.* (1985) measured vertical transmissibilities from the platform of a vibrator to vibration at the head, the seventh cervical vertebra, the sixth thoracic vertebra, the first, fourth and fifth lumbar vertebrae and the sacrum with both seated and standing subjects. They found that the transmissibility to each of the measurement locations increased at about 4 Hz, which led them to conclude that the entire body has a resonance at about 4 Hz.

Kitazaki and Griffin (1998) performed an experimental modal analysis to investigate the deformation of the human body at low frequencies and to study the effect of the sitting posture on the deformation at the principal resonance. Measurements of transmissibility in the mid-sagittal plane were taken at the head, the viscera, the right antierior superior iliac spine and the spine (T1, T6, T11, L3, and S2). The apparent mass on the seat was also measured. The authors reported eight vibration modes below 10 Hz (Figure 2.32). The resonance in the apparent mass at about 5 Hz was consistent with the fourth mode which consisted of an entire body mode in which 'the skeleton moved vertically due to axial and shear deformations of the buttocks tissue, in phase with a vertical visceral mode, and a bending mode of the upper thoracic and cervical spine'. The fifth mode was close to the principal mode and involved bending modes in the lumbar and lower thoracic spine together with a pitching mode of the head. The results also indicated that the second resonance in the apparent mass seen at around 8 Hz was caused by pitching of the pelvis and a second visceral mode. The authors also studied the effect of posture on the principal resonance frequency. They noticed a decrease in the resonance frequency from 5.2 Hz to 4.4 Hz when the subjects changed posture from erect to slouch which was consistent with an increase in shear deformation of the buttocks tissue in the entire body mode.

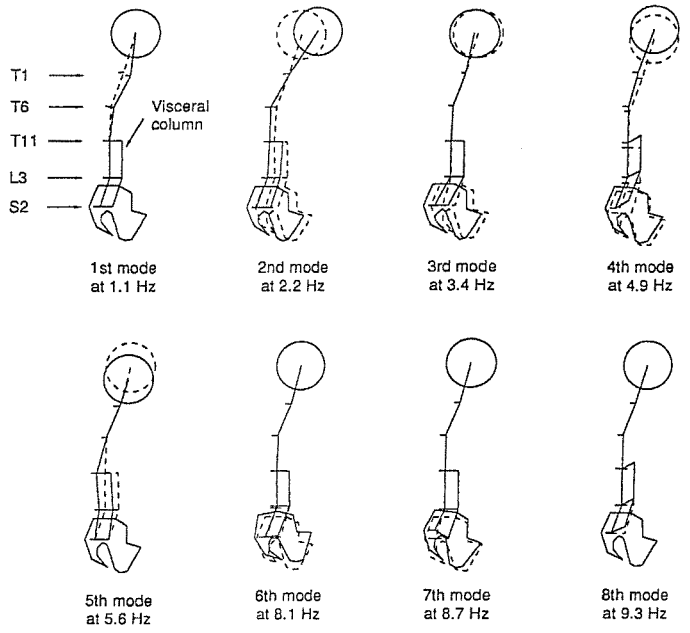

Figure 2.32 Vibration mode shapes extracted from mean transmissibility measurements of eight subjects below 10 Hz (Kitazaki and Griffin, 1998).

Matsumoto and Griffin (1998a) illustrated the movement of the upper bodies of seated subjects at the principal resonance frequency using transmissibilities from vertical seat vibration to vertical, fore-and-aft, and pitch vibration at eight locations on the body (at the first, fifth and tenth thoracic vertebrae, at the first, third and fifth lumbar vertebrae, at the pelvis, and at the head). They concluded that more than one vibration mode may contribute to the principal resonance frequency of the human body but that bending and rocking modes of the spine may contribute to the resonance frequency of the apparent mass. A pitch mode of the pelvis, which might have been accompanied by axial and shear deformation of the pelvis tissue, was noticed close to the resonance frequency. In a later study in which the vertical and the fore-and-aft transmissibilities were modelled (as will be seen in Section 2.7.2.2), Matsumoto and Griffin (2001) suggested that bending or buckling of the vertebral column probably made a minor contribution to the resonance frequency and that the major contribution may come from deformation of the tissue beneath the pelvis and the vertical motion of the viscera. The presence of different modes at and around the resonance frequency may suggest that these modes are closely coupled with each other due to the heavy damping of the body.

The contribution of the tissue of the ischial tuberosities to the principal resonance reported by Kitazaki and Griffin (1998) and Matsumoto and Griffin (1998a, 2001) can be supported by the increase in the resonance frequency of the body when rigid objects

were put under the ischial tuberosities (Sandover, 1978; Kitazaki, 1994) as discussed in Section 2.3.1.1.

Mansfield and Griffin (2000) found that the vertical transmissibility to the spine, posterior superior iliac spine and iliac crest have a resonance frequency similar to that found in the apparent mass and concluded that the peaks in the transmissibilities and apparent mass are influenced by the same mechanisms.

The parts of the body contributing to the principal resonance frequency of the body can also be identified by varying the properties of the parts of the body in a mathematical model and observing the changes to the resonance frequency as will be explained in the modelling section of this Chapter. For example, Kitazaki and Griffin (1997) used a finite element model and found that a shift in the apparent mass resonance frequency associated with altering body posture could be achieved by changing the axial stiffness of the buttocks tissue. This implies that the buttocks tissues might be partly responsible for the resonance frequency.

2.6 SUGGESTED MECHANISMS CAUSING THE NON-LINEARITY OF THE HUMAN BODY

The mechanisms that causes the non-linearity seen in the dynamic responses of the human body are not fully understood. Some suggestions based on experimental observations as well as modelling tests have been reported in the literature. Voluntary change in posture, voluntary and involuntary muscles activity, non-linear properties of the soft tissue of the body, loosening of the skeleton and the geometry of the body were among the suggestions.

Voluntary change in posture as a cause of the non-linearity of the human body was rejected by Mansfield (1998): he compared the non-linearity of the apparent mass of seated subjects in nine different postures (see Figure 2.3) and found no significant differences in the resonance frequencies between the anterior lean posture and the upright posture and between the posterior lean posture and the upright posture. Mansfield also reported that none of the postures, where external control was induced (e.g. SIT-bar posture, belt posture and pelvis support posture), 'eliminated the change in the apparent mass resonance frequency with vibration magnitude'. Mansfield (1998) also concluded that the geometry of the body (e.g. buckling and bending of the spine) is 'most likely' causing the non-linearity of the human body. However, mathematical models (e.g. lumped parameters model by Matsumoto and Griffin, 2001; finite element model by

Kitazaki and Griffin, 1997) suggested that any buckling or bending in the spine was a minor contribution to the principal resonance frequency of the driving point. This suggests that the geometry of the body cannot be the only reason of the non-linearity, as suggested by Mansfield (1998).

Mansfield and Griffin (2000) found that the non-linearity in the seat-to-spine and seat-to-abdomen transmissibilities were greater than the non-linearity in the spine vertical to abdomen vertical transmissibility. They stated that 'the changes observed in the apparent mass of the whole body cannot be accounted for by the change in the response of the viscera alone. They also suggested that the non-linearity in the apparent mass is caused by a 'transmission path common to the spine and the abdomen'.

Matsumoto and Griffin (2002a) investigated the effect of involuntary muscle activities on the non-linearity observed in the apparent mass. The involuntary muscle activity was controlled (minimised) by voluntarily maximising the muscles of the ischial tuberosities in one condition (tensing or stiffening the muscles in that area as much as possible) and the muscles of the abdomen area in another condition (minimising the volume of the abdominal cavity). The apparent masses of eight subjects at five vibration magnitudes: 0.35, 0.5, 0.7, 1.0, and 1.4 ms^{-2} r.m.s. were measured. The non-linearity in both conditions, especially tensing the buttocks muscles condition, was less evident than the non-linearity in a condition where no voluntary muscle control was applied. The authors concluded that 'Involuntary changes in muscle tension during whole-body vibration may be partly responsible for non-linear phenomena in biodynamic responses'.

Fairley and Griffin (1989) reported that the human body became less stiff when exposed to vibration as they noticed a decrease in the mean resonance frequency of eight subjects from 6 to 4 Hz with increase in vibration magnitude from 0.25 to 2 ms^{-2} r.m.s. They hypothesised that 'the effect of vibration magnitude arises from the musculo-skeletal structure of the body: the greater movement that occurs with high magnitudes of vibration reduces the stiffness of the musculo-skeletal structure'. This hypothesis is consistent with the results in some studies which showed softening in the muscles of the finger during and after exposure to vibration (Lakie, 1986): the muscles showed lower viscosity during and after large movements than during and after small movements. If other tissues of the body exhibit the same behaviour, which is called thixotropy, then the effect might appear in the apparent mass and partly explain the non-linearity.

2.7 CROSS-AXIS FORCES AT THE DRIVING POINT

Despite clear rotational modes in the reported transmissibility data (e.g. pitching modes of the pelvis, the spine and the head) and some evidence of shear deformation of the tissue beneath the pelvis as well as fore-and-aft motion of the pelvis during vertical excitation of seated subjects, only one study (Matsumoto and Griffin, 2002a) has measured the fore-and-aft cross-axis forces on the seat. Eight male subjects sat on a force platform that could measure forces in the vertical and fore-and-aft directions simultaneously and were exposed to random vibration in the frequency range 2.0 to 20 Hz. No backrest was used and the feet of the subjects were rested on a stationary footrest. The fore-and-aft forces measured on the seat were related to the vertical acceleration on the seat using a "cross-axis apparent mass function": the cross-axis apparent mass was the complex ratio between the fore-and-aft force and the vertical acceleration. The fore-and-aft cross-axis apparent mass was reported to reach up to 40% of the static mass of some subjects at some frequencies. The median normalised fore-and-aft cross-axis apparent mass is shown in Figure 2.33. This result was consistent with the same authors' previous work (Matsumoto and Griffin, 1998) in which they concluded that the body moves in two dimensions when exposed to vertical vibration. The fore-and-aft cross-axis apparent mass was found to be non-linear: an increase in vibration magnitude produced a decrease in the median fore-and-aft cross-axis apparent mass (see Figure 2.33). It was believed that the cross-axis apparent mass might be a result of some mode of vibration (bending or rocking of the spine) that takes place at frequencies below 2 Hz, as reported previously by Kitazaki and Griffin (1997).

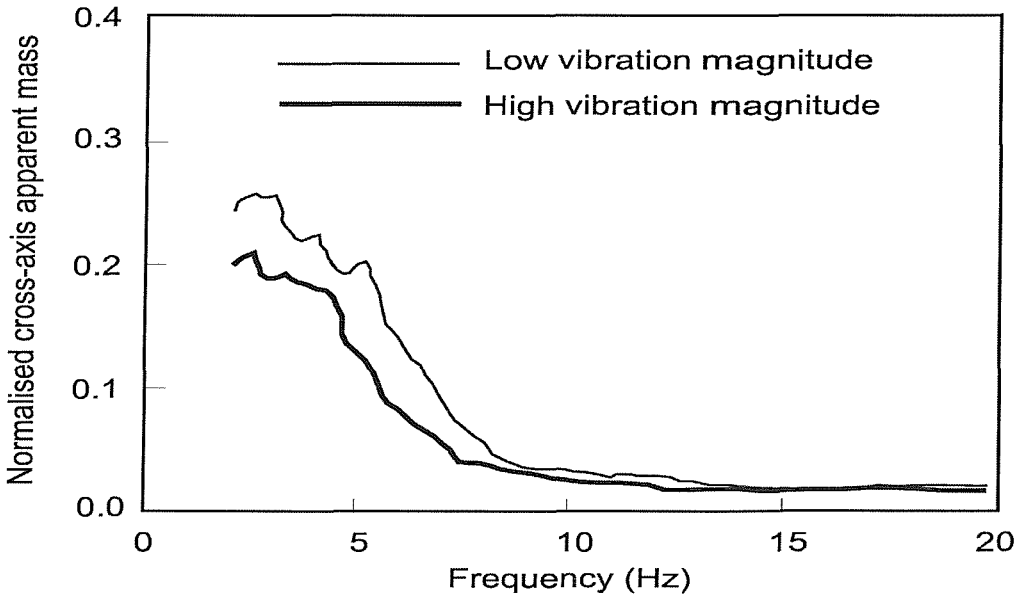

Figure 2.33 Median normalised fore-and-aft cross-axis apparent mass of eight subjects sitting in an upright posture with normal muscle tension. ——, 0.35 ms^{-2} r.m.s.; ——,1.4 ms^{-2} r.m.s. (Matsumoto and Griffin, 2002a).

2.8 MODELLING THE DYNAMIC RESPONSES OF THE SEATED HUMAN BODY TO VIBRATION

2.8.1 Introduction

As was shown in the previous sections, measures of biodynamic responses to vibration, including the mechanical impedance and apparent mass, are widely available in the literature (e.g. Vogt *et al.*, 1968; Fairley and Griffin, 1989; Boileau and Rakheja, 1998; Matsumoto, 1999; Nishiyama *et al.*, 2000). Such measures assist the construction of biodynamic models of the human body that may advance understanding of human responses to vibration. Mechanical dummies may be constructed from such information and used as substitutes for human subjects in seat testing.

Models that describe the responses of humans to vibration can be categorised into three categories: mechanistic models which are representation of how the body moves, quantitative models which summarise biodynamic measurements, and effect models which give indications of the effect of motion on human health, comfort or performance (Griffin, 2001). The complexity of the model would depend on the application for which the model will be used. For example, modelling the apparent mass of the human body in the vertical direction in certain conditions (posture, vibration magnitude, etc.) could be done using a single or two-degree of freedom model (e.g. Wei and Griffin, 1998b). Although this model can be used for seat testing applications (Suggs *et al.*, 1969; Wei, 2000; Lewis, 2001) in the same vibration conditions, it will neither have the capability to explain the characteristics of the response nor have the power to predict the response if the conditions of vibration change.

If the model is to represent the transmissibility to different locations on the body in more than one direction, then the model would act like a mechanistic model if every part of the model represents a particular part of the human body (Kitazaki and Griffin, 1997; Matsumoto and Griffin, 2001). This type of model can further our understanding of the causes of some of the phenomena that characterise the response of humans to vibration such as the resonance and the non-linearity.

Models to predict forces induced in the spine during vibration may need detailed and complex representation of at least the region under study (e.g. lumbar spine). Finite element models have been used for this purpose (e.g. Pankoke *et al.*, 1998; Seidel *et al.*, 2001).

In the following sections some of the literature regarding modelling the human body responses to vibration is presented. Models developed in this thesis (Chapter 9) are lumped parameter models and hence, the literature review focuses on this type of model, with a brief review of other types of model.

2.8.2 Lumped parameter modelling of the seated human body

2.8.2.1 Apparent mass and mechanical impedance models

The simplest form of a lumped parameter model to represent the apparent mass of the human body in the vertical direction is a single degree-of-freedom model (Payne, 1965; Fairley and Griffin, 1989). Payne (1965) used a single degree-of-freedom model (system 2 in Figure 2.34) with a mass representing the upper torso and the head connected to a spring and a viscous damper representing the spine and the tissue associated with it. The model was proposed for the prediction of spinal injury caused by pilot ejection from an aircraft. The damping of the model was obtained by comparing the model response to experimentally measured mechanical impedance. The natural frequency and the damping ratio used in the model were 8.42 Hz and 0.2245.

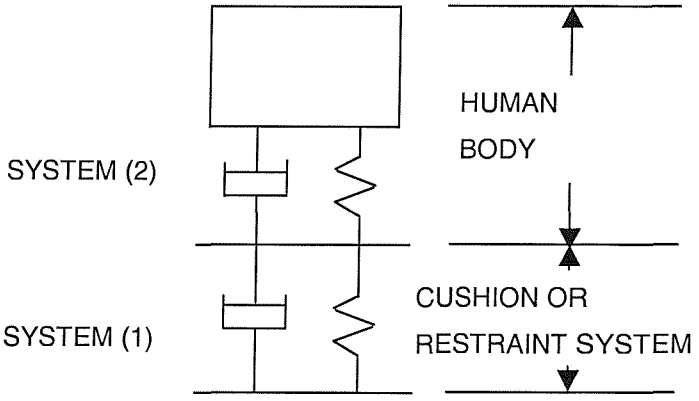

Figure 2.34 Single degree-of-freedom system representing the human body (System 2, Payne, 1965).

Fairley and Griffin (1989) also proposed a single degree-of-freedom model to fit the mean normalised apparent mass of 60 people. The model consisted of two masses with a spring and a damper between the two masses. The upper mass (m_1) represents the mass of the body moving relative to the supporting platform. The lower mass (m_2) represents the mass of the body and legs which does not move relative to the platform (Figure 2.35). The normalised apparent mass magnitude and phase of the model, which had a resonance frequency of 5 Hz and a damping ratio of 0.475, were within one standard deviation of the measured mean normalised apparent mass and phase of the 60 subjects. The second degree-of-freedom (i.e. using m_3, k_t and c_t, where k_t and c_t are the

stiffness and damping of the thighs) was used only when the footrest was stationary and was ignored when the feet were moving with the seat.

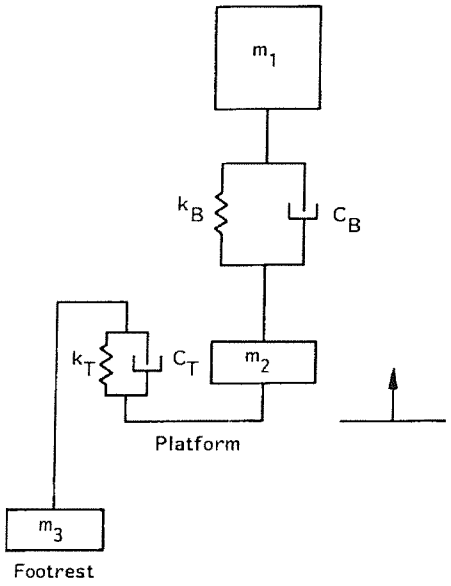

Figure 2.35 Lumped parameter model representing the mechanical impedance of the human body in the vertical direction (Fairley and Griffin, 1989).

Suggs *et al.* (1969) used a two degree-of-freedom model to represent the mechanical impedance of the human body for seat testing applications (Figure 2.36). The parameters of the model were obtained by comparing the response of the model to the measured average mechanical impedance of eleven subjects. The measured mechanical impedance had a first resonance at around 4.5 Hz and a second resonance at around 8 Hz. Suggs *et al.* suggested that the upper mass in the model might be considered to represent the head and chest mass while the lower mass might represent the pelvis and abdomen mass. The frame supporting the two single degree-of-freedom systems was assumed to represent the spinal column. The authors reported that the moduli of the measured and calculated mechanical impedance were similar; however, no phase response data were presented. The mathematical model was transformed to a 'simulator' (testing dummy) for use when measuring seat transmissibility. The authors compared the transmissibility of a tractor seat obtained using the 'simulator' with those obtained with a subject having a sitting mass similar to that of the 'simulator' and with those obtained with a rigid mass similar to that of the 'simulator'. They reported that the seat transmissibility obtained with the subject and the 'simulator' were in agreement up to 6.5 Hz while the seat transmissibility obtained using the rigid mass was 'drastically different' from that obtained using the subject or the 'simulator'.

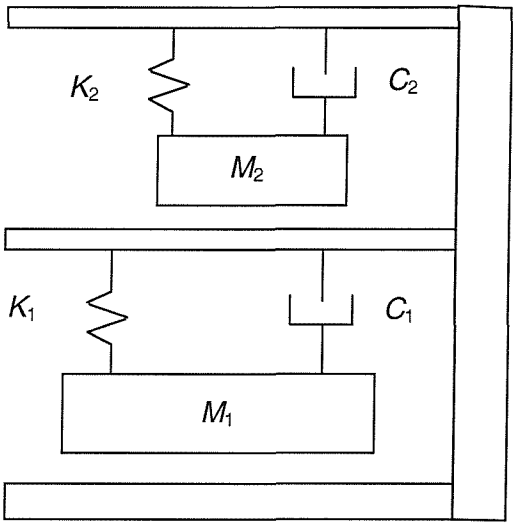

Figure 2.36 Two degree-of-freedom model of the seated human body (Suggs *et al.*, 1969).

Wei and Griffin (1998b) used the same data as Fairley and Griffin (1989) to fit the apparent masses of the 60 subjects to both single-degree-of-freedom and two-degree-of-freedom models (Figure 2.37). Wei and Griffin showed an improvement in the fitting of the experimental data when a two-degree-of-freedom model was used instead of a single-degree-of-freedom model: introducing a second degree of freedom to the model improved the fit to the phase data at frequencies above 8 Hz and improved the fit to the modulus around 5 Hz. Moreover, Wei and Griffin showed an improvement in fitting the data when either the single or the two degree-of-freedom models were supported on a frame (Figure 2.37b, d). However, since these models are just mathematical representation with no parts of the model represent a particular part on the human body, it is difficult to explain why adding the frame improved the agreement between the experimental and theoretical results.

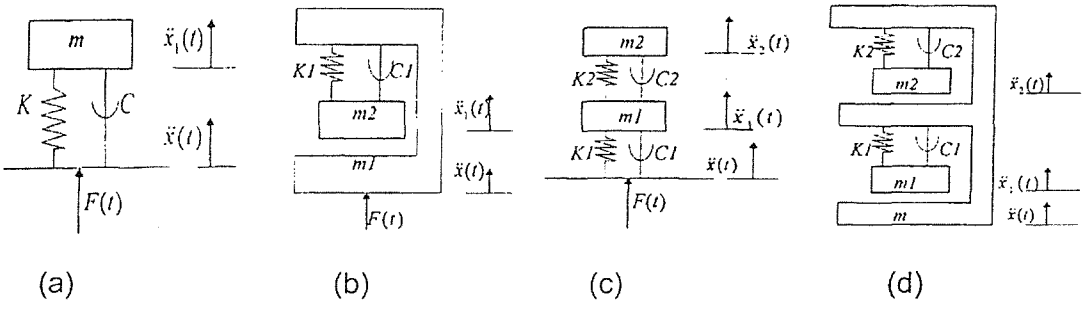

Figure 2.37. Single and two degree-of-freedom models used to represent the apparent mass of 60 subjects (Wei and Griffin, 1998b).

The single and two degree-of-freedom models shown above were usually used to give the response for a specific condition (e.g. specific sitting posture) and, hence, the set of parameters obtained for that particular condition would not necessarily apply to other conditions. For example, an increase in vibration magnitude has been found to change the response (e.g. apparent mass) by shifting the resonance frequency to a lower value (the non-linear response described in previous sections). Hence, different sets of model parameters are expected to be obtained when fitting the model response to experimental results obtained using different vibration magnitudes. Mansfield (1997) used a single degree-of-freedom model (similar in response to that shown in Figure 2.37b) to find out which model parameters needed to be adjusted so as to accommodate the change in the apparent mass with a change in vibration magnitude. A set of model parameters (unsprung mass, sprung mass, stiffness and damping) was obtained for the linear model by fitting the median apparent mass responses measured by Mansfield (1994) at 0.25, 0.5, 1.0, 1.5, 2.0, 2.5 ms^{-2} r.m.s. to the model: the obtained parameters can be used to calculate the apparent mass at all vibration magnitudes, however, with different errors. The optimised parameters were fixed and one parameter at a time was allowed to change to reduce the error between the measured and calculated apparent mass at each vibration magnitude. The author found reduction in the error when varying the stiffness or the mass of the system but not the damping.

International Standard 5982 (1981) proposed a model for the mechanical impedance of seated human subjects exposed to vertical vibration. The model had two degrees of freedom with two masses attached in parallel to a massless frame by springs and dampers (Figure 2.38). The parameters of the model were obtained by comparing the mechanical impedance obtained from the model with a range of mechanical impedance obtained from the literature. Thirty nine subjects with weights from 51 to 93.8 kg were used to obtain the mechanical impedance range. Sinusoidal acceleration amplitudes from 1.0 to 2.0 ms^{-2} were used with subject posture loosely defined, but generally an upright posture. The feet were either supported on a footrest moving in phase with the seat or hanging freely without a support. In the second edition of this standard (final draft International Standard 5982, 2001) the model was replaced by a three degree-of-freedom model that takes into account the transmissibility to the head, as will be explained in Section 2.8.2.2.

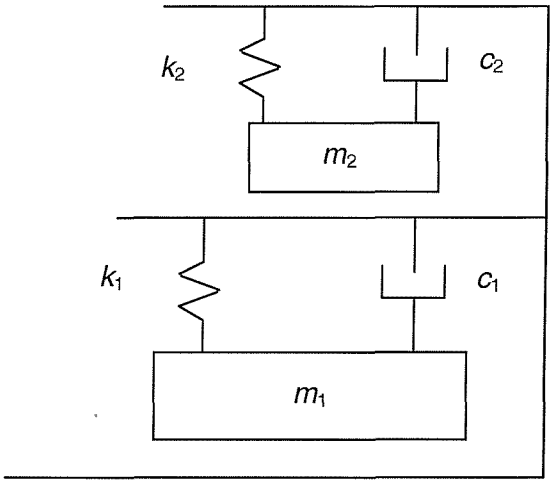

Figure 2.38 Two degree-of-freedom model proposed in International Standard 5982 (1981) to represent the mechanical impedance of the seated human body exposed to vertical vibration.

The human responses to vibration have also been represented by models with more than two degree-of-freedom, with each degree of freedom representing the movement of some part of the human body. For example, a four-degree-of-freedom model was proposed by Payne and Band (1971). The model masses represented the pelvis, viscera, upper thorax, and head and were all to move only in the vertical direction (Figure 2.39). The buttocks, spine, and neck were represented by springs and dampers. The viscera was also connected to the thorax using a spring and damper.

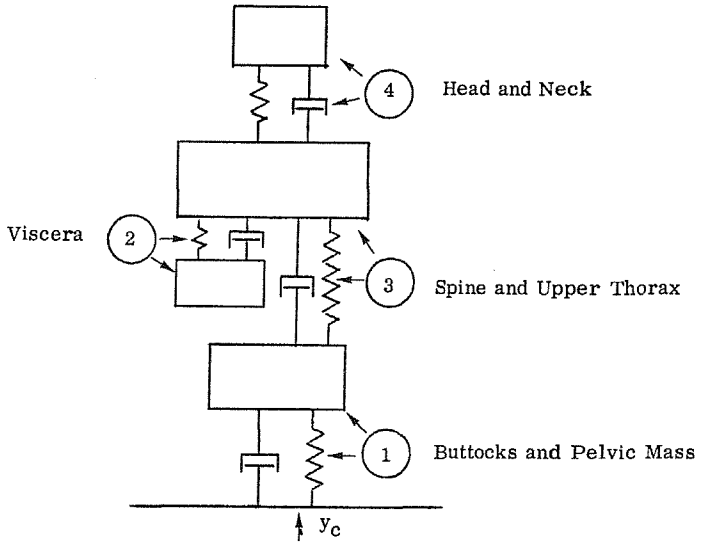

Figure 2.39 Four degree-of-freedom model proposed by Payne and Band (1971).

The masses of the Payne and Band (1971) model were given fixed values obtained from anthropometric data reported in the literature. The stiffness of the viscera and the stiffness and damping of the head were considered 'fairly well established' in the literature and, hence, were also fixed at values obtained from the literature. Other parameters were given initial values found in the literature but were adjusted later so that the model gave better agreement with experimental measurements of driving point impedance. The authors studied the effect of changing the stiffness and damping of the spine and the buttocks and the damping of the viscera on the driving point impedance and concluded that the driving point impedance represented mostly the response of the lower parts of the body such as the pelvis and the buttocks.

Mertens and Vogt (1978) developed a five-degree-of-freedom model to replace the human body in tests where great shocks are the stimulus. The model consisted of parts of the legs, buttocks, viscera, chest and head represented by the masses m_1, m_2, m_4, m_6 and m_7, respectively (Figure 2.40). The masses were fixed to values obtained from anthropometric measurements. The natural frequency of the viscera was also taken from the literature. The remaining parameters (i.e. stiffness and damping parameters) were obtained by comparing the mechanical impedance of the model as well as the transmissibility to the head with those obtained experimentally in previous work (Mertens, 1978). Although the model was supposed to be used for impact conditions, the parameters of the model were obtained under steady state conditions. Different sets of parameters were provided to account for the non-linearity obtained when changing the steady state input acceleration from 1 to 4 G.

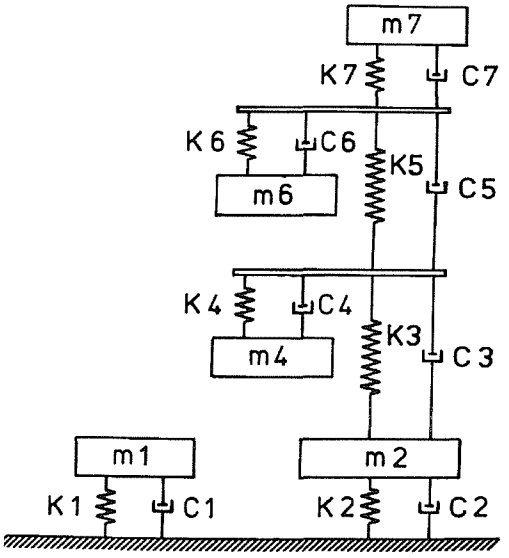

Figure 2.40 Five degree-of-freedom model proposed by Mertens and Vogt (1978) to represent the point mechanical impedance and the transmissibility to the head.

Smith (1994) proposed a base-excited five-degree-of-freedom model (four-degree-of-freedom plus the movement of the base) for quantifying the change in the mass, stiffness and damping of some parts of the body with change in vibration magnitude. The masses of the model (shown in Figure 2.41) were assumed to represent the pelvis, spine, upper torso, lower torso, and the legs. The use of a multi-degree of freedom system was based on observation of four regions of resonance in the mechanical impedance of seated subjects exposed to vertical vibration (Smith, 1993). Good agreement was reported between the modulus obtained experimentally and the modulus obtained theoretically (i.e. from the model). However, a large discrepancy was observed between the experimentally and theoretically obtained phase data, although the phase responses had similar shapes. Three sets of parameters were obtained, each representing the response at each of the three vibration magnitudes used in the study (0.347, 0.694, and 1.734 ms^{-2} r.m.s.).

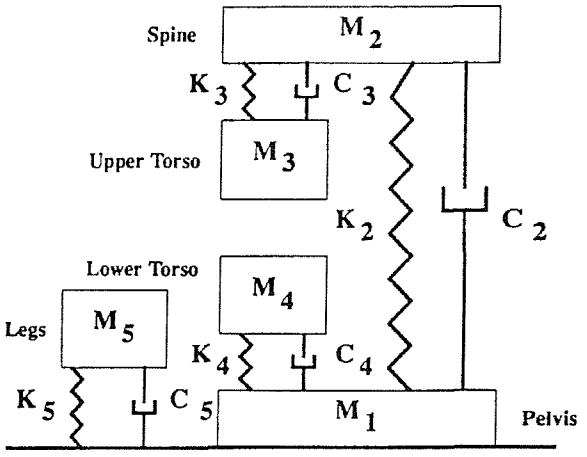

Figure 2.41 Base excited five degree-of-freedom model proposed by Smith (1994).

Boileau and Rakheja (1998) developed a linear four-degree-of-freedom human driver model. The model consisted of four masses connected by linear springs and dampers (Figure 2.42). The masses of the model corresponded to the head and neck (m_1), the chest and upper torso (m_2), the lower torso (m_3), and the thigh and pelvis in contact with the seat (m_4). The springs and dampers in Figure 2.42 represent the stiffness and damping of the buttocks and thighs (K_4 and C_4), the lumbar spine (K_3 and C_3), thoracic spine (K_2 and C_2), and the cervical spine (K_1 and C_1). All parameters of the model were optimised such that the response of the model satisfies both the driving point mechanical impedance and the seat-to-head transmissibility measured experimentally. However, constraints were applied to the optimised parameters such that their values would be in the ranges reported in the literature. The model response showed better agreement,

although agreement only up to 5 Hz, with the mechanical impedance than with the seat-to-head-transmissibility.

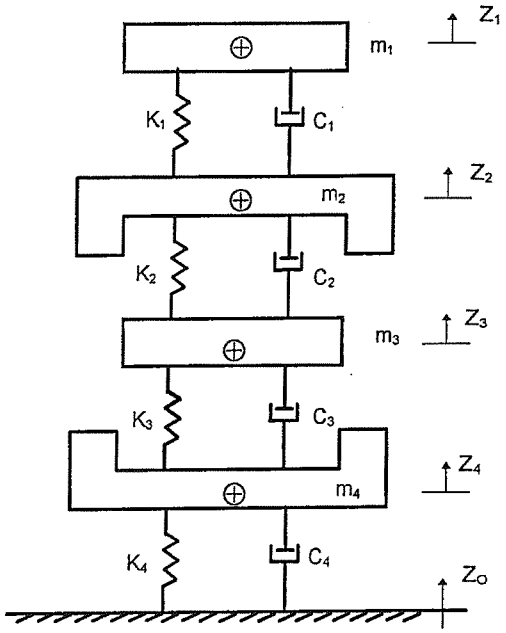

Figure 2.42 Vehicle driver four-degree-of-freedom model (Boileau and Rakheja, 1998).

Boileau *et al.* (2002) developed a three-degree-of-freedom model to predict the apparent mass and the vertical seat-to-head transmissibility of the seated human body. The model consists of two subsystems: a single-degree-of-freedom system and a two-degree-of-freedom system (Figure 2.43). Although none of the masses of the model represent any particular part of the body, m_2 was considered to represent the head when calculating the seat-to-head transmissibility. Three degrees-of-freedom were needed to account for the resonance at around 4 Hz in the mean apparent mass and for the two resonances at 4.5 Hz and 10 Hz in the seat-to-head transmissibility shown in the final draft of the International Standard ISO 5982. Although the responses of the model (i.e. the apparent mass and the seat-to-head-transmissibility) were within the range of the apparent mass and seat-to-head transmissibility defined in ISO 5982 (2001), they were not in good agreement with the mean apparent mass (defined for body mass of 75 kg) or the seat-to-head transmissibility at all frequencies: below 4 Hz and between 10 and 14 Hz, the apparent mass calculated from the model deviated from the mean value given in the standard. For the seat-to-head transmissibility, the model response also deviated from the mean response defined in the standard especially around the resonance area where the model underestimated the peak value.

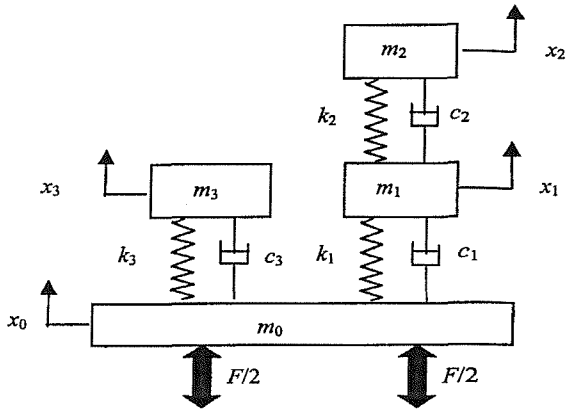

Figure 2.43 Three degree-of-freedom model proposed by Boileau *et al.* (2002)

Boileau *et al.* (2002) found that changes in body mass can be accounted for, in the above model, by changing only m_3: inspection of the model showed that a slight change in m_1 and m_2 'would be likely' to deviate the seat-to-head transmissibility from the idealised range given in ISO 5982. Since there is no clear evidence for the dependency of the seat-to-head transmissibility on the mass of the subjects and also 'there is no basis for deciding how the stiffness and damping characteristics would actually depend on subject mass' the authors decided to vary only the value of m_3 to accommodate change in body mass (to 55 kg and 90 kg) while fixing all the other parameters at the values obtained for a body mass of 75 kg, as was explained in the previous paragraph.

2.8.2.2 Transmissibility models

In this section, a review of some of the models on the transmissibility of the human body will be presented. As was the case for the mechanical impedance models, the transmissibility models depended on experimental measurements to develop the model or tune the model response to match transmissibility experimental measurements.

Latham (1957) proposed the first single degree-of-freedom model representing the transmission of vibration through the human body. The model, which consisted of two masses connected to each other by a spring (see Figure 2.44), was intended to model the seat-man system during pilot ejection situations. The author compared the acceleration response of the mass representing the human body to a step function input with experimental measurements of acceleration at the hip. The calculated and measured acceleration time histories were generally in good agreement. Griffin et al. (1978) also modelled the seat-to-head transmissibility in the frequency range 1 to 100 Hz using a single-degree-of-freedom model. The obtained results were reported to be within the 5th and 95th percentile of the data of all subjects.

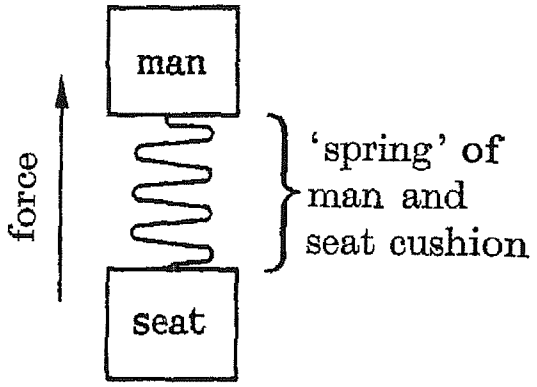

Figure 2.44 Single degree-of-freedom model proposed by Latham (1957) to represent the transmission of vibration through the human body.

Muksian and Nash (1974) used a six-degree of freedom model to predict the response of seated humans to vertical vibration. The model consisted of several masses representing different parts of the human body. The head and the first cervical vertebra (C1) were lumped in one mass called the 'head', m_1. The rest of the vertebrae were assumed to be rigidly connected and were represented by one mass called the 'back', m_2. The thoracic cage was represented by a single body called 'torso', m_3. The viscera of the thorax and the abdomen were represented by three rigid bodies called 'thorax', 'diaphragm', and 'abdomen' shown in Figure 2.45 as m_4, m_5, and m_6. The pelvis and the legs were combined by one mass called 'pelvis', m_7. The masses were fixed to value obtained from the literature. Forces in the gliding joints (between the ribs and vertebrae), the ballistocardiographic force (proportional to heart beat frequency) and the diaphragm muscle forces ('varies linearly with respiration rate') were taken into account. The stiffness and the viscous damping between the head and the back and between the back and the pelvis were assumed linear based on result from other researchers (Pradko *et al.*, 1966). The stiffness and damping in the other parts were assumed non-linear: they were modelled by non-linear cubic springs and non-linear cubic dampers. Springs and damping coefficients were either assumed, or taken from the literature. The results showed that the damping coefficients were frequency dependent: using the estimated damping coefficients, the seat-to-head transmissibility obtained from the model was in good agreement with measured seat-to-head transmissibility only below 8 Hz. The damping coefficients had to be adjusted at frequencies above 8 Hz to improve the prediction of the model.

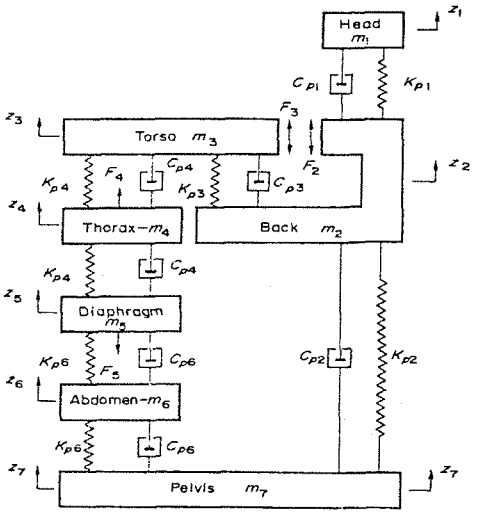

Figure 2.45 Six degree-of-freedom model proposed by Muksian and Nash (1974)

A four degree-of-freedom model was proposed in International Standard 7962 (1987) to represent the mechanical transmissibility to the head in the vertical direction in both sitting and standing positions (see Figure 2.46). The model concerns transmissibility to the head in the frequency range 0.5 to 31.5 Hz. The model was limited to sinusoidal vibration inputs with amplitudes in the range 2 to 4 ms^{-2}. In general, the experimental data used to develop the model were for upright sitting or standing positions, although, the posture in some of the studies was loosely defined. The mean mass of the 50 subjects used in the proposed model was 76 kg. The proposed parameters are also shown in Figure 2.46.

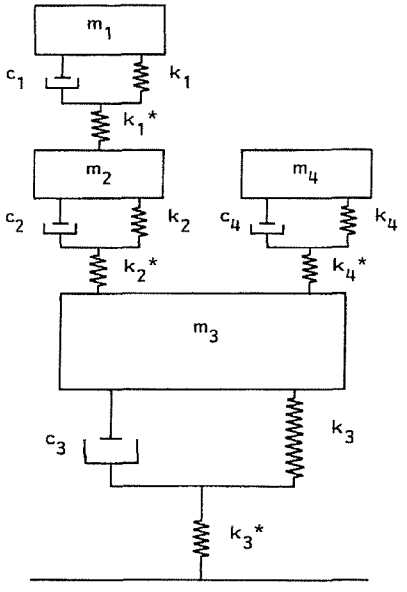

Model parameters	
m_1	8,24 kg
m_2	8,05 kg
m_3	44,85 kg
m_4	13,86 kg
k_1	22 x 10^8 N.m^{-1}
k_2	20,13 x 10^4 N.m^{-1}
k_3	88,56 x 10^3 N.m^{-1}
k_4	36,47 x 10^3 N.m^{-1}
k_1^*	36 x 10^7 N.m^{-1}
k_2^*	65 x 10^9 N.m^{-1}
k_3^*	52,34 x 10^4 N.m^{-1}
k_4^*	69,30 x 10^3 N.m^{-1}
c_1	748,1 N.s.m^{-1}
c_2	578,0 N.s.m^{-1}
c_3	2964,0 N.s.m^{-1}
c_4	901,8 N.s.m^{-1}

Figure 2.46 Four-degree-of-freedom model proposed in International Standard 7962 (1987) to represent the vertical transmissibility to the head of standing and seated people exposed to vertical vibration.

The model described in the International Standard 7962 (1987) was replaced by a three degree-of-freedom model (similar in structure to that shown in Figure 2.43) that accommodate the transmissibility to the head as well as the mechanical impedance/ apparent mass of seated subjects (final draft International Standard 5982, 2001). Although the masses of the model did not represent specific parts of the human body, the transmissibility to mass m_2 (see Figure 2.43) was considered to represent the transmissibility to the head. The model was developed based on data obtained from the literature for seated subjects adopting an erect posture without backrest and with the feet supported on a footrest moving in phase with the seat. Data for seat to head transmissibility (but not the mechanical impedance) where the feet were hanging freely were also considered. The data considered in developing the model were defined for subjects having masses between 49 and 93 kg and exposed to sinusoidal or broad-band random vibration of amplitude less than or equal to 5 ms^{-2} r.m.s. in the frequency range 0.5 to 20 Hz.

Matsumoto (1998) and Matsumoto and Griffin (2001) proposed four and five-degree-of-freedom models to investigate the possible mechanisms associated with the principal resonance at around 5 Hz in the apparent mass of the seated human body. Translational and rotational degrees of freedom were used such that the model would have movements in the mid-sagittal plane (Figure 2.47). Masses 1, 2, and 4 for both models represented the whole legs, the pelvis, and the viscera, respectively. The upper body, excluding the pelvis and the viscera, were represented by mass 3 in model 1 and by masses 3 and 5 in model 2. The linear spring and linear damper beneath mass 1 where assumed to represent the tissue beneath the pelvis and the thighs. The rotational degree-of-freedom of the pelvis was represented by the connection between mass 1 and mass 2. The bending mode of the spine was represented by the connection between masses 2 and 3 in model 1 by the connection between masses 2 and 3 as well as masses 3 and 5 in model 2. The viscera, represented by mass 4, was assumed to move only vertically.

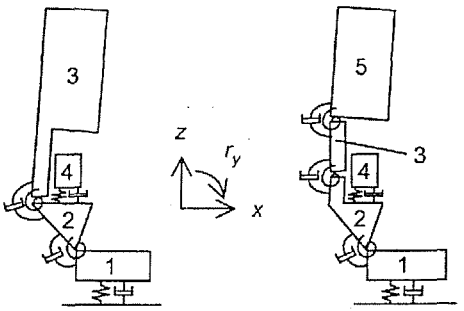

(a) Model 1 (b) Model 2

Figure 2.47 Mechanistic models proposed by Matsumoto and Griffin (2001) to represent the apparent mass as well as vertical and fore-and-aft transmissibilities to several locations on the human body. (a) model 1: four degree-of-freedom; (b) model 2: five degree-of-freedom model.

The masses and geometrical parameters of Matsumoto and Griffin models were taken from Kitazaki and Griffin (1997), while the stiffness and damping coefficients were optimised by comparing the apparent mass and vertical and fore-and-aft transmissibilities to several locations on the upper body calculated from the model with those obtained experimentally by Matsumoto and Griffin (1998a). Using modal analysis and parameter sensitivity tests, the authors concluded that the dominant contributors to the resonance frequency of the human body at about 5 Hz are the vertical motion due to the deformation of the tissue beneath the pelvis and the vertical motion of the viscera. Although a bending mode of the spine was observed experimentally (Matsumoto and Griffin, 1998a), the model showed small contribution of this mode to the apparent mass resonance frequency at 5 Hz. The authors stated that 'the models appear to provide reasonable explanations for the dynamic responses of the seated body exposed to vertical whole-body vibration'.

2.8.3 Modelling of the human body in standing and lying positions

Most available models in the literature deal with the response of seated humans to vertical vibration. Although, the sitting position is the most common position in environments where vibration occurs (such as transportation), there are some cases where people are exposed to vibration while standing or lying. For example, in underground trains people might be exposed to vibration in both standing and sitting positions. Another example is transporting patients in ambulances where the patient has to adopt recumbent position. The following is a review of some of the models that represent the response of standing and lying subjects to vibration.

Matsumoto and Griffin (2003) developed six lumped parameter models (2 single degree-of-freedom and 4 two degree-of-freedom) to represent the apparent mass of the standing human body exposed to vertical vibration (Figure 2.48). The apparent mass of the human body was modelled in three standing postures (standing normally, legs bent posture, and one leg posture) and at four vibration magnitudes (0.25, 0.5, 1.0, 2.0 ms^{-2} r.m.s.). The optimised parameters for the mean and individual response were obtained by comparing the response of the model to the apparent mass measurement reported by Matsumoto and Griffin (1998b).

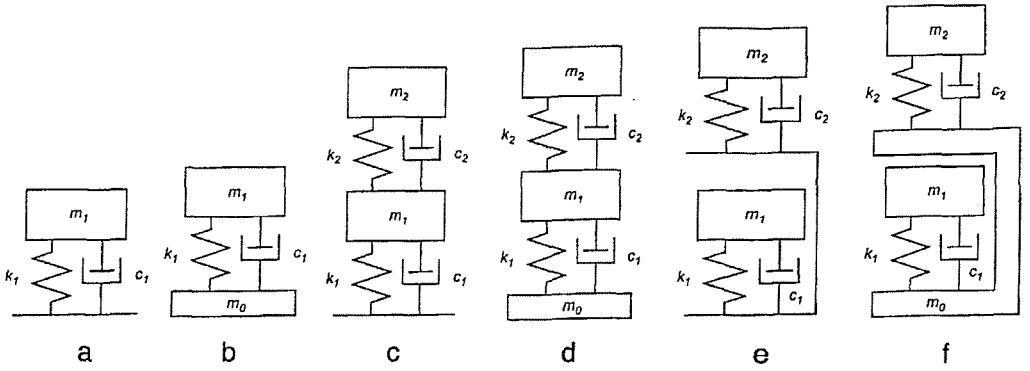

Figure 2.48 Six models proposed by Matsumoto and Griffin (2003) to represent the apparent mass of standing subjects exposed to whole-body vertical vibration: a and b are single degree-of-freedom models; c, d, e and f are two degree-of-freedom models.

Matsumoto and Griffin tabulated the optimised parameters for all models for the mean normalised apparent mass of 12 subjects in the normal standing posture and at 1.0 ms^{-2} r.m.s. They also tabulated the optimised parameters for the two degree-of-freedom models with the massless support at four vibration magnitudes. The two degree-of-freedom models showed better agreement with the measured apparent mass magnitudes and phases than the single degree-of-freedom models, which is the same conclusion of Wei and Griffin (1998b) for similar models representing the apparent mass of seated people. However, the two-degree-of freedom models with massless structure (i.e. model c and model e in Figure 2.48) showed better agreement with the experimental apparent mass than those with a support (i.e. model d and model f in Figure 2.48) which is the opposite of the finding of Wei and Griffin (1998b) for modelling the apparent mass of seated subjects. The authors also found that the effect of vibration magnitude and the effect of posture could be accounted for by changing the stiffness and damping parameters in the two degree-of-freedom models while keeping the masses constant.

International Standard 5982 (1981) proposed models for sitting persons (see Section 2.7.2.1), and also standing and supine persons. The same two degree-of-freedom model structure used to represent the mechanical impedance in the sitting position (see Figure 2.38) was used to represent the mechanical impedance in the standing position but with different model parameters for each position. The parameters of the model in the standing position were obtained by comparing the response of the model with the measured mechanical impedance of five subjects adopting, although it was only loosely defined, 'standing erect' or 'standing relaxed' postures. The weights of the subjects were in the range 78.5 to 100 kg and the data used were for sinusoidal acceleration amplitudes from 1 to 2.5 ms^{-2}.

The model proposed by the International Standard 5982 (1981) for the supine position consisted of three single degree-of-freedom models with parallel arrangement (Figure 2.49). The data used to obtain the parameters of the model were those of 12 subjects exposed to sinusoidal vibration with amplitude in the range 1.0 to 2.5 ms^{-2}.

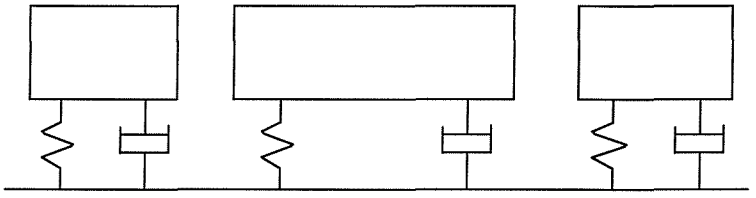

Figure 2.49 Three degree-of-freedom model for the supine position (International Standard 5982, 1981).

Vogt *et al.* (1973) developed a three degree-of-freedom model to represent the mechanical impedance of the human body in the supine position. The model consisted of a single degree-of-freedom and two degree-of-freedom systems supported on a rigid support as shown in Figure 2.50. The parameters of the model were obtained by comparing the mechanical impedance calculated from the model with the mean mechanical impedance of ten subjects measured under vertical sinusoidal excitation with five different sustained accelerations (1 to 5 G). The mechanical impedance in the supine position was found to be dependent on the sustained acceleration and, hence, graphs showing the change in each parameter with change in the sustained acceleration were provided.

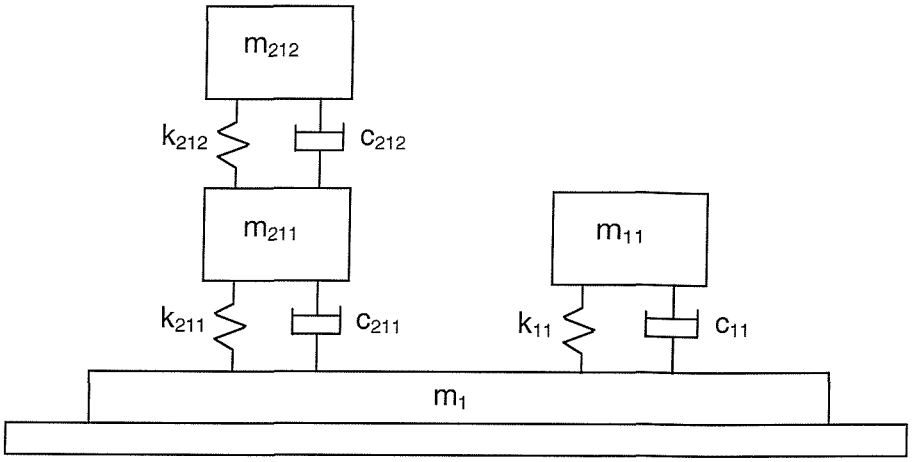

Figure 2.50 Three-degree-of-freedom model for the supine human body (Vogt *et al.*, 1973).

2.8.4 Modelling the human body in response to horizontal vibration

Despite the fact that vibration can occur in the horizontal as well as vertical direction, few studies have measured the response of humans to horizontal (fore-and-aft and lateral) vibration. The work by Mansfield and Lundström (1999b) is the only work to propose models that represent the response of humans to fore-and-aft and lateral excitation. Figure 2.51 shows six lumped parameter models proposed by Mansfield and Lundström to represent the apparent mass of the human body in the lateral and fore-and-aft directions and at 0.5 and 1.0 ms^{-2} r.m.s.

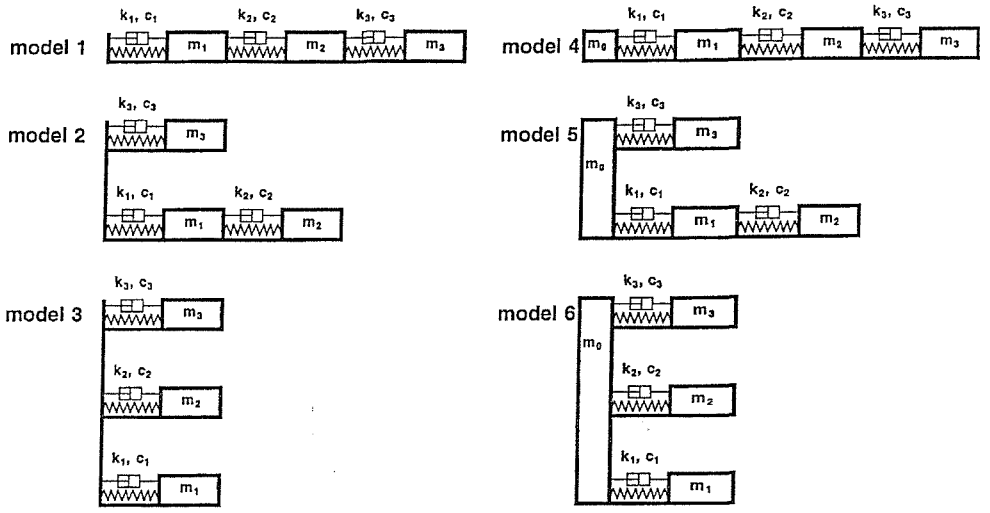

Figure 2.51 Six three degrees of freedom models proposed by Mansfield and Lundström (1999b) to represent the apparent mass of the seated human exposed to fore-and-aft and lateral vibration.

The optimised model parameters were obtained by comparing the response of the models to experimental data reported previously by Fairley and Griffin (1990) and Mansfield and Lundström (1999a). The agreement between the calculated and the measured apparent mass for both directions (i.e. fore-and-aft and lateral) was best (i.e. least error) when the model consisted of three parallel single degree-of-freedom systems attached to a rigid support was used (model 6 in Figure 2.51). However, the calculated and measured phase responses were in good agreement only up to 4 Hz. The stiffness in the model showed a decrease with an increase in vibration magnitude, consistent with the softening effect of vibration magnitude found in the experimental data.

2.8.5 Other models

Some research modelled the human body as a continuous system rather than a lumped parameter system. For example, Liu and Murray (1966) used a continuum model to model the human body in the sitting position while Ji (1995) used a continuum model to represent the response in the standing position. Liu and Murray (1966) represented the human body by a continuum model in which the upper body, from the lumbar region up to the neck, was represented by a uniform homogeneous elastic rod. The head was represented by a mass located at the upper end of the homogeneous rod. The authors studied the longitudinal wave propagation through the body and the stress distribution in response to a step acceleration input. They concluded that stress, and not the acceleration directly, is the cause of injury and, hence, the use of the maximum acceleration as a criterion of tolerance is invalid. Li *et al.* (1971) proposed a simplified continuum dynamic model representation of the curved spine. The torso mass was uniformly distributed along the length of the spine with a mass representing the head on top of the mass of the torso. The spine was chosen to be with constant cross sectional area with sinusoidal curvature. The bending moment contribution of the head-torso eccentricities was not included in the model. The geometrical data as well as the strength properties of the spine were taken from the literature.

The finite element method has also been used to model the response of humans to vibration (e.g. Kitazaki and Griffin, 1997; Pankoke *et al.*, 1998; Seidel *et al.*, 2001, Pankoke *et al.*, 2001). Kitazaki and Griffin (1997) proposed a two-dimensional finite element model to represent the response of humans to whole-body vertical vibration. The spine, viscera, head, pelvis and buttocks tissue were modelled using beam, spring, and mass elements as shown in Figure 2.52.

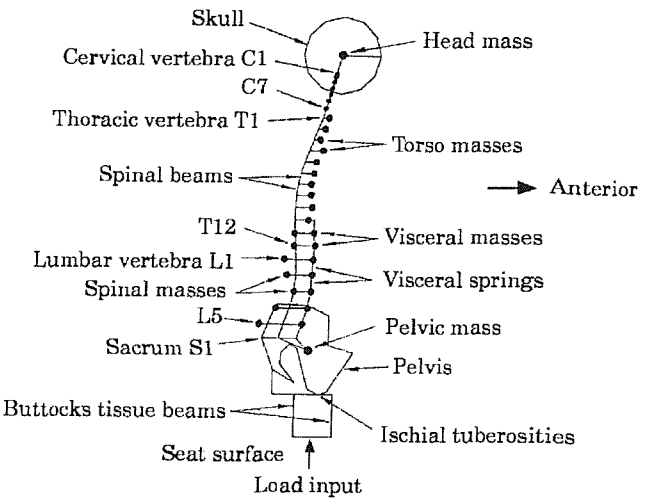

Figure 2.52 Finite element two-dimensional model propose by Kitazaki and Griffin (1997).

The geometrical, inertial and stiffness data were either measured or taken from the literature. The modal damping ratios were obtained by comparing the driving point apparent mass of the model with the measurements obtained in previous work by Kitazaki and Griffin (1998). Seven vibration mode shapes were extracted from the model and were in good agreement with the vibration mode shapes measured experimentally by Kitazaki and Griffin (1998). The results also showed that the principal resonance at about 5 Hz is caused by an entire body mode in which the head, spine and the pelvis move almost rigidly. This mode is accompanied by axial and shear deformation of the tissue beneath the pelvis and vertical visceral mode. The second resonance frequency between 8 and 12 Hz was found to be due to a rotational mode of the pelvis together with a second mode for the viscera. The shift that occurs in the principal resonance frequency of the driving point response when posture changes from erect to slouched was achieved only by changing the axial stiffness of the buttocks tissue in the model. The authors suggested that the increase in contact area between the buttocks and thighs and the seat surface when subject change from erect to slouched posture could have decreased the axial stiffness of the tissue beneath the pelvis resulting in a decrease in the resonance frequency of the body. The conclusions obtained from the model are consistent with the conclusions obtained for the experimental modal analysis (see Kitazaki and Griffin, 1998).

Pankoke *et al.* (1998) developed a finite element model to predict the internal forces in the lumbar spine. The region between the third lumbar vertebra (L3) and the fifth lumbar vertebra (L5) was anatomically represented. It was modelled by rigid bodies connected to each other by linear springs. The regions above L3-L5 (upper torso with the neck, head, and arms) and below L3-L5 (pelvis, thigh, lower leg and foot) were modelled as rigid

masses connected by linear springs but with less detail than between the region between L3 and L5 (Figure 2.53). The viscera was modelled by 'three-mass-chain' with elastic connection with the lumbar spine model. The muscles in the lumbar region were also modelled by linear springs connected to the torso and to the pelvis.

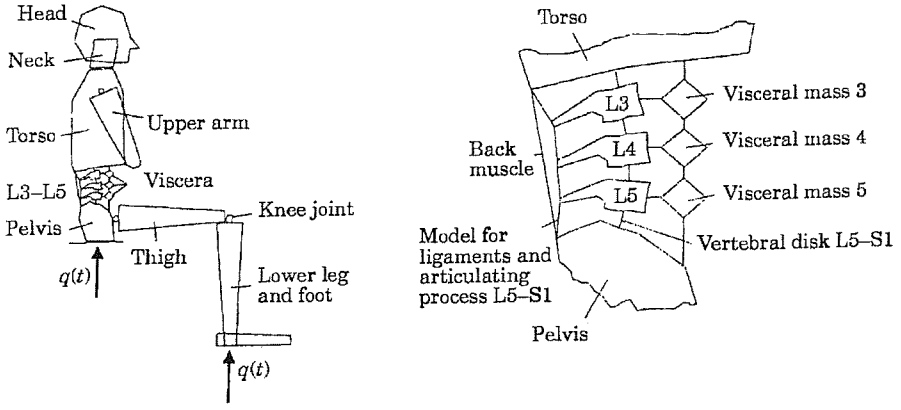

Figure 2.53 Finite element model proposed by Pankoke *et al.* (1998) to predict the internal forces acting on the lumbar spine.

Model parameters such as stiffness, damping and inertia were obtained from the literature. The parameters which were not found in the literature, were obtained by comparing the response of the model to experimental measurements. The effect of subject height and weight as well as posture were included in the model by changing the inertial and geometry properties of the model. However, the stiffness and energy dissipating parameters were fixed. The model was validated using experimental data consisting of vertical and fore-and-aft seat-to-head transmissibilities and mechanical impedance. The experimental data were in agreement with the response of the model only in the frequency range below 5 Hz in both the mechanical impedance and the transmissibility from seat vertical motion to fore-and-aft head motion. No results were shown for the seat vertical motion to the head vertical motion. The authors recommended that the model be used to estimate the forces in the lumbar area when using excitations with spectral density 'biggest in the lower frequency range up to 7 Hz'.

Seidel *et al.* (2001) used the same finite element model developed by Pankoke *et al.* (1998) to predict the static and dynamic forces induced in the spine with different conditions of body mass and height and sitting posture. A multiple regression equation was provided to calculate the compressive static force predicted by the model at the disc L5/S1. The independent variables in the equation were the mass of the body and the angle that the disc makes with the horizontal, which was different with different postures.

The dynamic shear and compression forces were represented by transfer functions calculated using the shear or compression force and the vertical seat acceleration. The transfer function showed dependency of the forces on the body mass and height and sitting posture.

Nicol *et al.* (1995) deployed an artificial neural network (ANN) to predict the non-linear response of the human spine at L4 to shock input at the seat. The acceleration measurement on the spine was taken at the L4 vertebra. The authors used the back propagation algorithm to train the recurrent artificial neural network used to predict the spine response. Three sets of input signals were used, each of which was applied for a duration of 5.5 minutes. All signal sets contained background vibration with an r.m.s value of 0.05 g and periodic shocks that occurred at a rate of 3 shocks per minute. The input shocks, which were single cycle damped sinusoids with frequencies of 2, 4, 6, 8, and 11 Hz, were presented in random order. The shock amplitudes were -1 G, -2 G, and -3 G in the three signal sets. The authors compared the prediction obtained from the non-linear ANN with those obtained by using linear prediction models such as the Dynamic Response Index (DRI, response of a single degree-of-freedom model) and the British Standard 6841 (1987). The comparison was based on calculating the root mean square error between the measured vertical acceleration at L4 and the predicted acceleration at L4 obtained from each of the three methods. The authors reported smaller error when using the ANN than when using DRI or BS 6841. However, caution should be taken when using the model to extrapolate to acceleration time histories far from the training range.

2.9 SUMMARY OF THE LITERATURE REVIEW AND CONCLUSIONS

The literature contains a variety of studies of the biodynamic responses of humans to vibration. Most studies involved the response of the seated human body to vertical excitation; few studies have been concerned with standing or lying bodies and few studies involved horizontal or rotational excitation. In this section of the thesis, the general findings of the previous studies are summarised and conclusions are drawn to provide guidelines and the backbone for this research.

A principal resonance in the vicinity of 5 Hz in the driving point response (apparent mass or mechanical impedance) of seated and standing subjected exposed to vertical excitation, and another resonance in the range 8 to 15 Hz, is a consistent finding in previous work. However, the exact mechanisms responsible for the resonance phenomena are not fully understood. Although some mechanisms are suggested in the literature, based on experimental work or mathematical modelling, the suggested

mechanisms are not consistent. It seems that more than one vibration mode contributes to the principal resonance in the driving point mechanical impedance (or apparent mass) observed at about 5 Hz, although, it is difficult to separate these modes due to the heavy damping of the human body. It is possible that some modes may be major contributors to the resonance behaviour in certain postures or seating conditions while minor in others, which could explain the inconsistency between studies regarding the mechanisms causing the resonance frequency: it is possible that all the suggested mechanism are correct but the extent of their contribution to the resonance frequency depends on factors such as posture and sitting condition.

Non-linearity of the human body is another phenomena reported in the majority of the studies of the effect of vibration magnitude on either the driving point response or the transmissibility to different locations on the body. However, the mechanisms causing the non-linearity are still not understood, especially there is inconsistency in the suggested mechanisms causing the non-linearity of the human body. The complexity of the human body and the difficulty in measuring the properties of the living human tissue are factors restricting the advance in understanding of the non-linearity with the available technology. More data of the response of humans to vibration adopting different postures and different seating conditions is needed to quantify the non-linearity and further understanding of the non-linearity: posture (erect, relaxed, etc.) and seating conditions (using of a backrest, inclination of a backrest, etc.) were found to greatly affect the resonance frequency and magnitude at resonance.

Very few studies have reported the biodynamic response of humans to horizontal (fore-and-aft and lateral) excitation. The driving point response of the human body to horizontal excitation showed a dependency on factors such as sitting posture and vibration magnitude. There are some inconsistencies (e.g. number of vibration modes or effect of vibration magnitude) between the few reported studies, which highlights the need for more data to help explain the inconsistency and to further understanding of the responses of humans to horizontal excitation.

The biodynamic response of humans to rotational excitation is rarely found in the literature. This type of motion could happen in environments such as off-road vehicles. Their effects on the human body could be as serious as the effects induced by translational motion. For example, through a biomechanical model, Deursen *et al.* (2000) stated that a 'small pelvic axial rotation resulted in a significant change of load in the intervertebral discs'.

Various types of mathematical models ranging from simple to complex models have been reported in the literature. The purposes of the models varied from summarising some experimental measurements in a mathematical representation to predicting internal forces acting on the spine due to exposure to vibration. Despite the complexity of the structures of some of the models, they are mainly based on simple assumptions. For example, most models have been assumed to be linear passive models. Due to the lack of information about the properties of the living human tissues, the parameters of the models have usually been obtained using experimental measurements such as the driving point mechanical impedance (or apparent mass) and transmissibility to different locations on the body based on specific excitations levels and specific seating conditions and they are less applicable to other excitation levels and other seating conditions. Models representing the responses of humans to horizontal vibration are hardly available in the literature. Modelling the response in this direction is needed to understand how the human body moves in real life multi-axis vibration environment, such as in transportation.

Footrests and backrests are also interfaces between a seat occupant and the vibration. However, the work reported in the literature have mainly considered forces on the seat. Measurements of forces on the backrest and footrest are relatively easier to perform than measurements of transmissibilities to different locations on the body and could provide information about the movements of the body in response to vibration as well as insight into the dynamic responses of the feet and the back which could help in explaining results obtained in comfort studies.

Vertical and fore-and-aft transmissibilities to different locations on the body during vertical excitation suggest that the human body moves in two directions when exposed to vertical whole-body excitation. Modelling studies have also shown shear deformation of the tissue beneath the pelvis and fore-and-aft motion of the pelvis during vertical excitation. Fritz (2000) concluded, using a biomechanical model, that the 'spinal forces are not only elevated in the direction parallel to the vibration excitation but also in the two other orthogonal vibration directions'. Measurements of forces at the interface between the seat and the seat occupant are easier to obtain than measurements of internal forces and possibly more accurate than predictions obtained from biomechanical models, given the simplification suggested in the models due to the lack of information about the properties of the living tissue and the shortage of understanding of some phenomenon such as the non-linearity. Forces at the interface between a seat and its occupant have only been measured in the direction of excitation, except for one study (Matsumoto and Griffin,

2002a). Knowledge of the nature and the characteristics of these forces (in the direction of excitation and in the other directions) may help identify, through a more representative model, some of the mechanisms causing the resonance and the non-linearity in the human body.

The literature review has identified some areas where research in the field of human response to vibration is needed to further understanding of the responses of humans to vibration. The main objective of this thesis is to provide an insight into the forces in both the direction of excitation and in the other directions at the seat, footrest and backrest during whole-body vertical and fore-and-aft excitation of seated subjects. The characteristics of these forces with different sitting postures, different excitation magnitudes and different seating arrangements will be studied. Linear lumped parameter models will be developed to represent the forces in the direction of excitation and in other directions during both vertical whole-body excitation and fore-and-aft whole-body excitation. The parameters of the models will be optimised by comparing the apparent mass and cross-axis apparent mass (same concept used by Matsumoto and Griffin 2002a, see Section 2.6) obtained experimentally with the apparent mass and cross-axis apparent mass calculated from the models. The models will be used to identify the modes that produce the resonance of both the apparent mass and the cross-axis apparent mass.

CHAPTER 3 EXPERIMENTAL APPARATUS AND DATA ACQUISITION AND ANALYSIS

3.1 INTRODUCTION

This chapter of the thesis describes the apparatus and equipment used in conducting the experimental work. It also shows the data acquisition and analysis techniques used to collect and present the data from the experiments.

3.2 EXPERIMENTAL APPARATUS

3.2.1 Vibrators

Two hydraulic vibrators were used to complete the sets of experiments needed in this work. The description of each vibrator is given in the following sections.

3.2.1.1 One-metre vertical electro-hydraulic vibrator

Experiments carried out during vertical vibration were conducted using a vibrator capable of producing a peak-to-peak displacement of 1 m in the vertical direction and a dynamic load of 10 kN with a preload of 8.8 kN. An aluminium alloy plate with the dimensions 1.5 by 0.89 by 0.015 m was bolted rigidly to the table of the vibrator, which in turn was attached to the servo-hydraulic actuator driving the vibrator. The seat and footrest used in the experiments were mounted on the aluminium alloy plate (Figure 3.1).

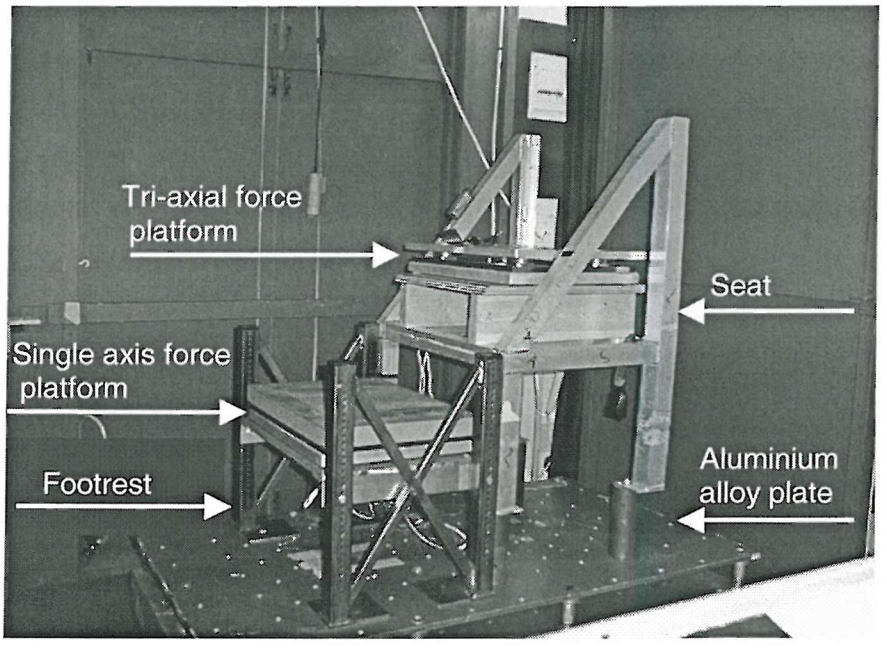

Figure 3.1 Photograph of the seat, footrest, and force platforms mounted on the one-metre vibrator aluminium alloy plate. (Set-up for the first experiment, Chapter 4).

3.2.1.2 One-metre horizontal electro-hydraulic vibrator

This vibrator was used to provide motion for the experiments conducted in the fore-and-aft direction. It is capable of producing 1 m peak-to-peak motion in the horizontal direction. An aluminium alloy plate with the dimensions 1.5 by 1.0 by 0.02 m was mounted rigidly on the table of the horizontal vibrator. The same seat and footrest used in the vertical excitation experiments were used in the fore-and-aft excitation experiments and were mounted on the aluminium alloy plate of the horizontal vibrator.

3.2.2 Transducers

The apparent mass concept was used to present the data in all the experiments conducted in this thesis. Hence, measurements of force and acceleration were required to calculate the apparent mass.

3.2.2.1 Force transducers

Two force platforms type Kistler 9281 B and Kistler Z 13053 were used to measure the forces at the interface between the subject and the seat surface, backrest, and footrest. Both force platforms consisted of four quartz piezo-electric force transducers distributed in a rectangular arrangement. An aluminium alloy plate was bolted on to the force transducers in each of the force platforms. Both plates had the same width and depth of 0.6 by 0.4 m but different thickness (0.02 m for the Kistler 9281 B and 0.047 m for the Kistler Z 13053). The Kistler 9281 B force platform had the capability of measuring the forces in the three directions (*x*, *y*, and *z*) simultaneously. The other force platform could measure the force in the direction perpendicular to its surface. All signals were amplified using Kistler 5001 or Kistler 5007 charge amplifiers before sending them to the computer.

The force platforms were calibrated statically and checked dynamically in all possible directions before the experiment commenced. In the tri-axial force platform, the force measurements in the direction perpendicular to its surface were taken from each cell and summed in the computer, while the forces measured in the other two directions and the force measured using the single axis force platform were summed before sending the signals to the computer. Hence, it was decided to calibrate individually only the cells in the tri-axial force platform in the direction perpendicular to its surface. Figure 3.2 shows the output force from each cell when loaded with 2, 4, and 6 kg masses and unloaded with the same masses. After this static calibration, each cell was loaded by a rigid mass weighing about 4 kg and exposed to vertical random vibration with magnitude of 0.625 ms^{-2} r.m.s. and frequency range 0.25 to 25 Hz. The four cells had a similar sensitivity as

shown in Figure 3.3. Further dynamical calibration was done by bolting the aluminium alloy plate, where the subjects sat, to the cells and vibrate once with no load on the plate and once with a rigid mass of about 22.5 kg placed on the top of the plate. Figure 3.4 shows the result of both of these calibrations indicating that the aluminium alloy plate had a mass of 15 kg. The single-axis force platform was calibrated in a similar procedure to that mentioned above. Figure 3.5 shows the dynamic calibration results when only the aluminium alloy plate (33 kg) was bolted to the cell as well as the result when 10.63 kg mass was placed on the top of the aluminium alloy plate.

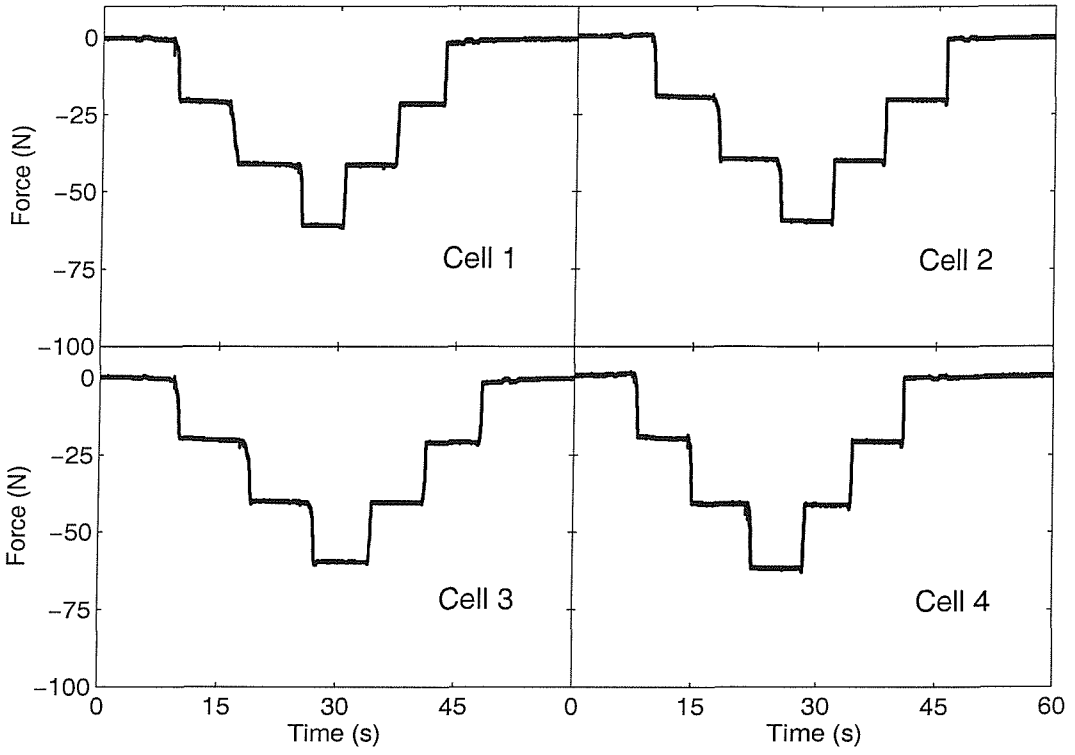

Figure 3.2 Statically calibrated four force transducers using 2, 4, and 6 kg loads.

The force transducers were also calibrated for measurements of forces in the plane of the aluminium plate in two directions parallel to its edges. These forces were the fore-and-aft and lateral forces when the measurements were taken on the seat and the vertical and lateral forces when the measurements were taken on the backrest. The calibration was conducted using a pulley system where several loads were attached to a rope passing through a pulley and connected to the aluminium plate from the other end. The calibration was then checked statically, using a spring balance as shown in Figure 3.6 and dynamically using random vibration in either the fore-and-aft direction or lateral direction.

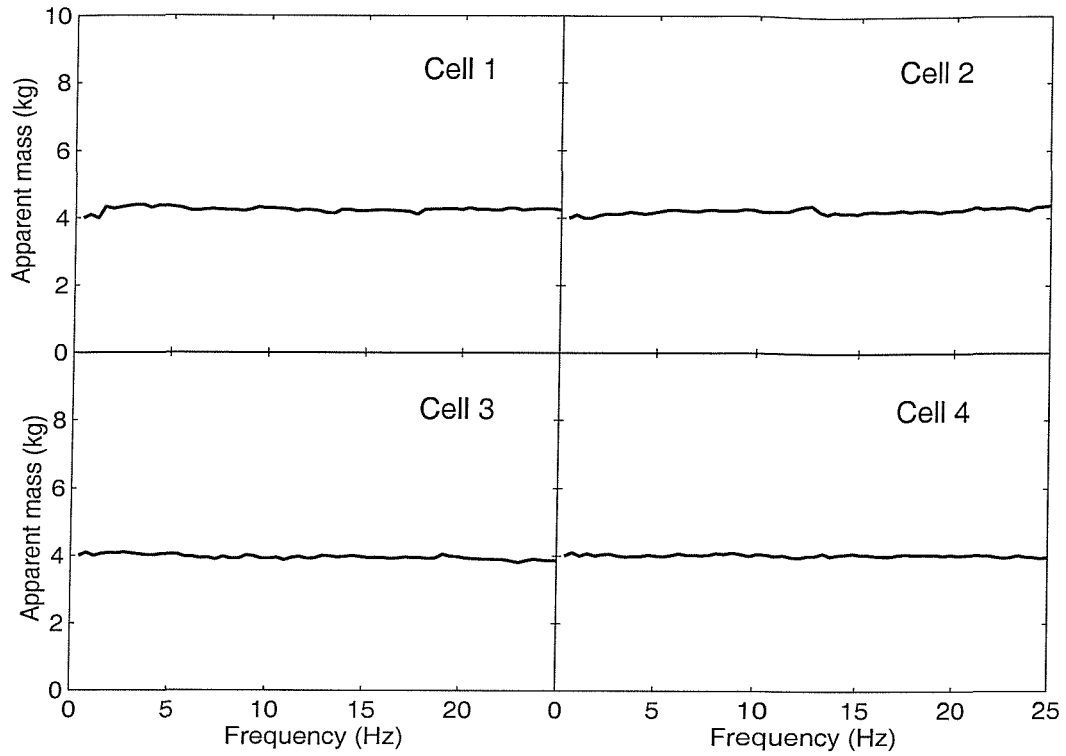

Figure 3.3 Dynamically calibrated four force transducers using a load of about 4 kg mass.

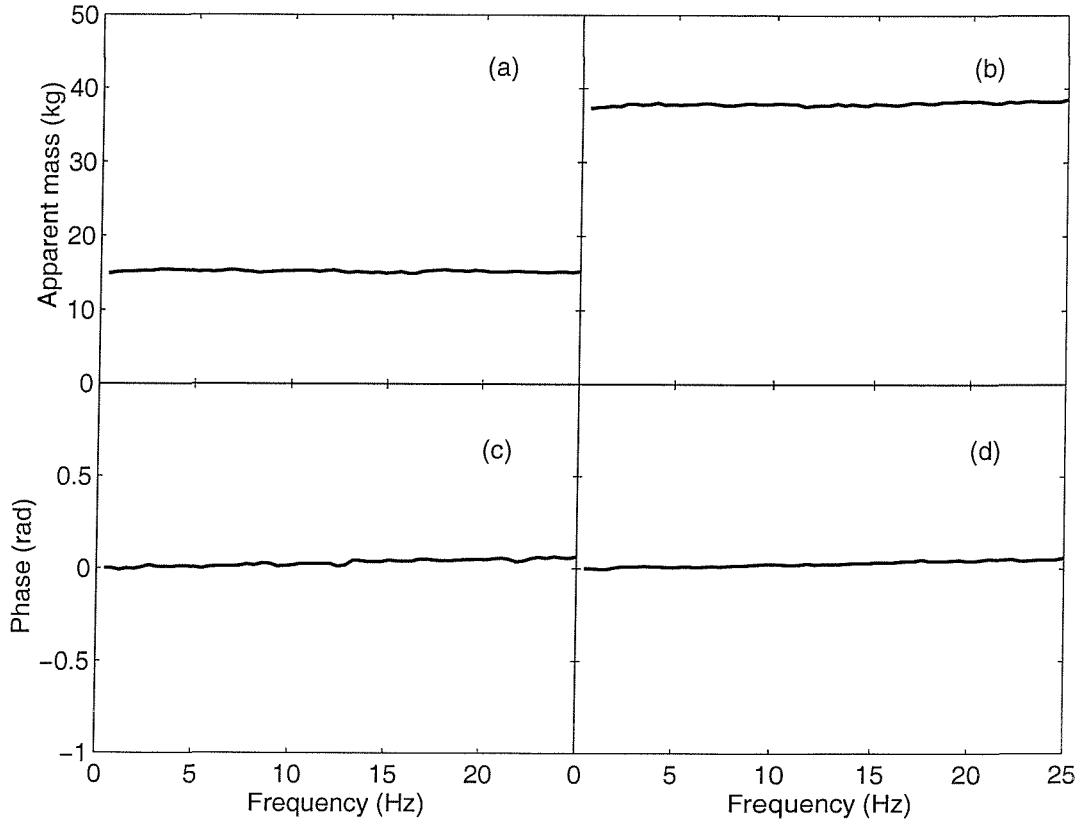

Figure 3.4 Measured apparent mass for the tri-axial force platform: (a) and (c) no load on the aluminium plate; (b) and (d) an addition of 22.5 kg mass.

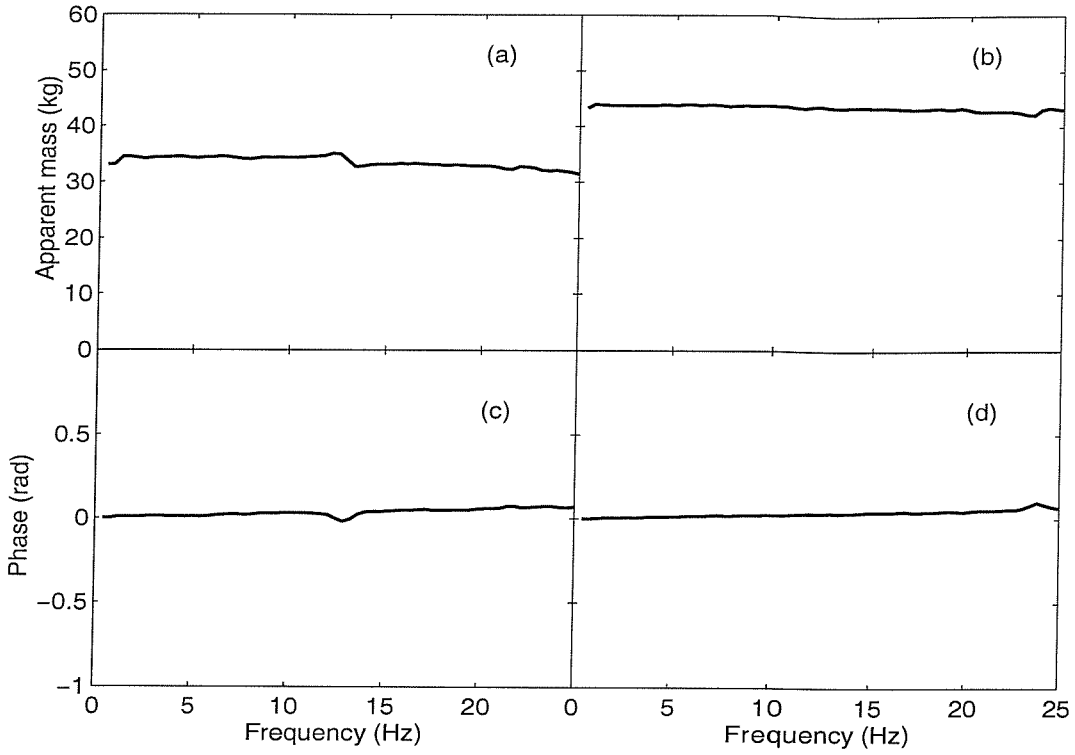

Figure 3.5 Measured apparent mass for the single axial force platform: (a) and (c) no load on the aluminium plate; (b) and (d) an addition of 10.63 kg mass.

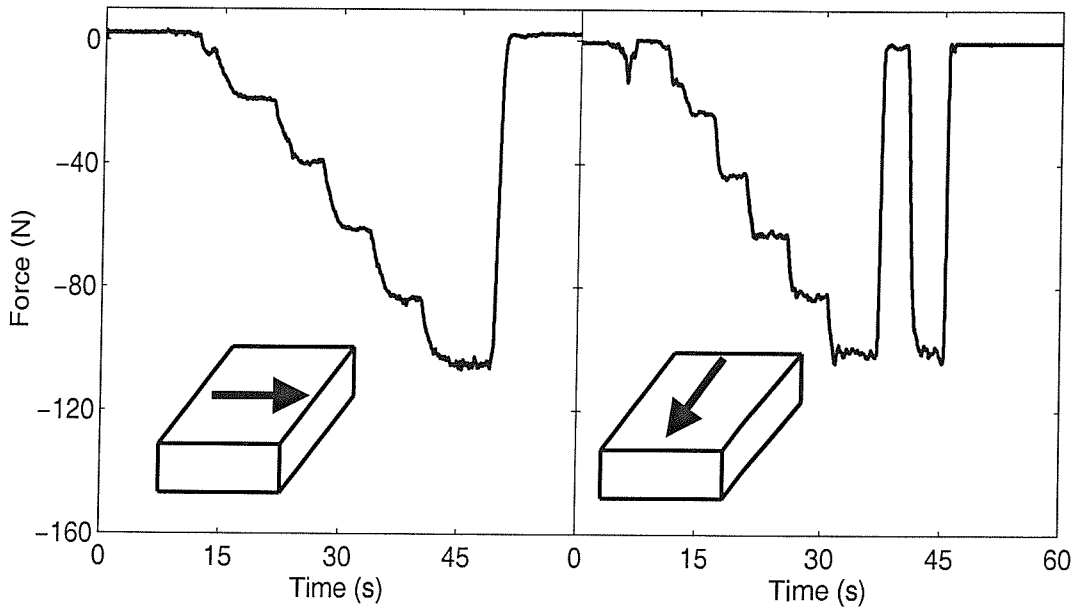

Figure 3.6 Statically calibrated tri-axial force platform in the direction shown in the figure using 20, 40, 60, 80 and 100 N forces.

Figure 3.7 shows the results obtained from the dynamic calibration in the fore-and-aft direction. The figure shows that the upper aluminium plate had a mass of 15 kg, which is consistent with that found from the dynamic calibration in the vertical direction.

In both the tri-axial and the single axis force transducer, the error in the magnitude of the measured apparent mass was less than 3% of the total mass of the rigid loads above the force cells (i.e. the mass of the aluminium plate plus the mass of the load on top of the plate) over the whole frequency range, except for the fore-and-aft apparent mass when the 10 kg load was used (Figure 3.7) where the observed error was around 7% at frequencies greater than 15 Hz. The error in the phase of the apparent masses measured using the tri-axial force platform and the single axis force platform was less than 0.03 radians below 10 Hz and less than 0.05 radians below 25 Hz, except for the phase of the fore-and-aft apparent mass when the 10 kg load was used (Figure 3.7) where the observed error was less than 0.05 radians below 10 Hz and less than 0.1 radians below 25 Hz.

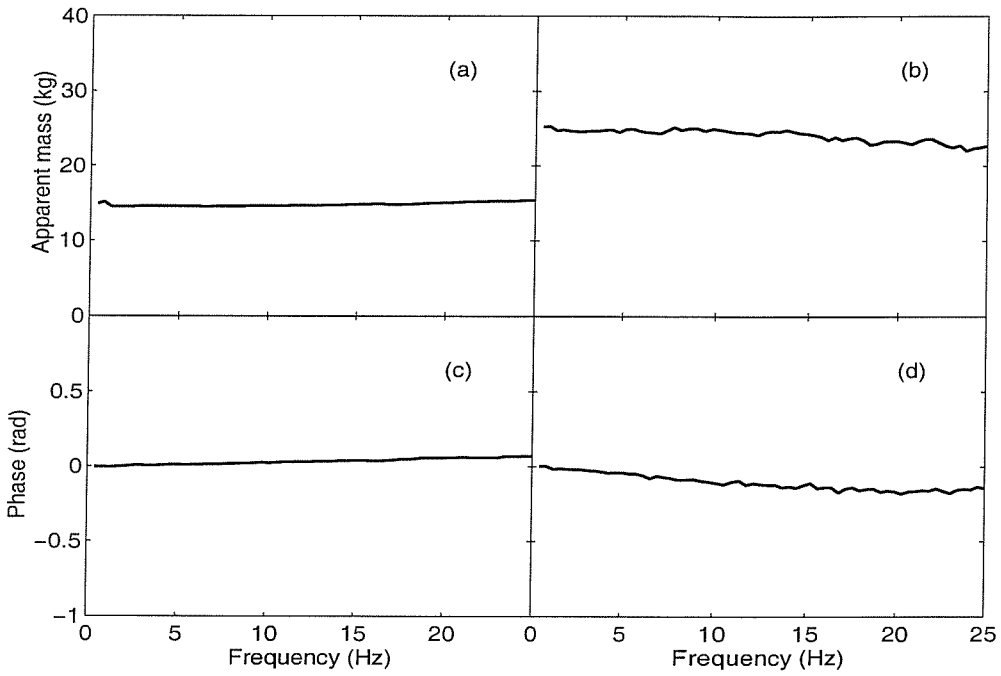

Figure 3.7 Dynamically calibrated tri-axial force platform using vibration in the fore-and-aft direction: (a) and (c) no load on the aluminium plate; (b) and (d) addition of 10 kg mass.

3.2.2.2 Accelerometers

The accelerometers used to measure the motion of the vibrator in the different experiments were piezo-resistive types Entran EGCSY-240D*-10, Entran EGCS-DO-10-/V10/L4M, and Entran EGCSY-240D*-10. The operating range of all the accelerometers used was ±10g while the sensitivity varied between 9.6 to 13.58 mV/g. They were calibrated before the experiments commenced and checked during and after the experiments. In the vertical vibration experiments, the accelerometers were calibrated to give a reading of zero when placed on a horizontal surface and a value of 2 g when turned by 180° on the horizontal surface. In the horizontal vibration experiments, the accelerometers were calibrated to give a reading of zero when attached to a vertical surface and a reading of 1 g when placed on a horizontal surface. Figure 3.8 shows the transfer function between two calibrated accelerometers placed at two different points (on the seat and on a footrest) and vibrated using the one-meter vertical vibrator. The figure reflects a pitching motion at about 13 Hz, which appeared in the data as will be shown later in Chapter 4.

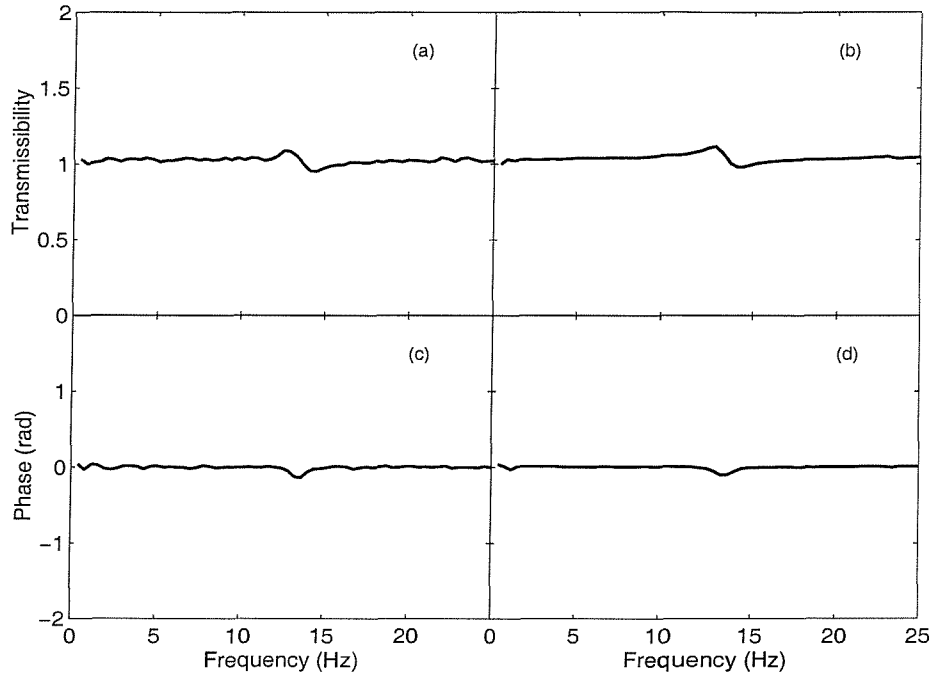

Figure 3.8 Transmissibility and phase angle between two accelerometers mounted on the vertical vibrator (a) and (c) with 0.125 ms^{-2} r.m.s.; (b) and (d) with 1.25 ms^{-2} r.m.s.

3.3 DATA ACQUISITION

Random vibration signals generated using *HVLab* software (version 3.81) were used to drive the vibrators in all the experiments. The generated signals were sent to the controller of the vibrator via a 16-channel *HVLab* data acquisition and analysis system. This system used an Advantech PCL-818 data acquisition card and Techfilter TF-16 anti-aliasing card. Before they were fed to the controller, the input signals were low-pass filtered and displayed on an oscilloscope. The output signals from the accelerometers and the force transducers were acquired using the same *HVLab* system mentioned above. The signals from the force transducers were amplified using charge amplifiers (as mentioned before) before they were acquired. The duration and sampling rate were set in the *HVLab* software. Figure 3.9 illustrates a schematic diagram of the set-up used to drive the vibrators and to acquire the signals.

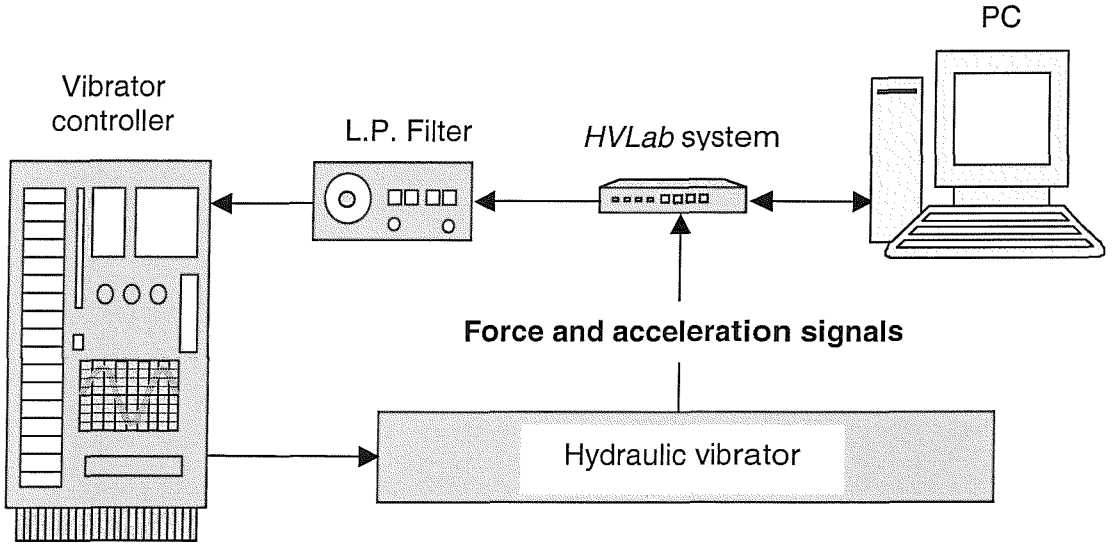

Figure 3.9 Schematic diagram of the set-up used to drive the vibrators and acquire the output signals.

3.4 DATA ANALYSIS

3.4.1 Frequency response functions

The apparent mass concept was used to represent the measured forces and accelerations in the direction of vibration. For the cases where the forces are measured in directions other than the direction of vibration, a cross-axis apparent mass concept was used. In either case, the apparent mass and the cross-axis apparent mass (representing a transfer function between the force and the acceleration, see Figure 3.10) were calculated using the cross-spectral density (CSD) method defined as follows:

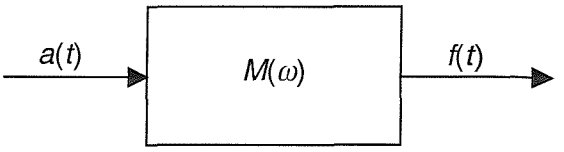

Figure 3.10 Block diagram of a transfer function (the transfer function shown here is the apparent mass or the cross-axis apparent mass).

$$M(\omega) = \frac{S_{af}(\omega)}{S_{aa}(\omega)} \tag{3.1}$$

where $M(\omega)$ is the apparent mass (or the cross-axis apparent mass) in complex numbers, $S_{af}(\omega)$ is the cross spectral density between the force and the acceleration, and $S_{aa}(\omega)$ is the power spectral density of the acceleration measured in the direction of vibration. The frequency response function can also be calculated using the power spectral density (PSD) method defined as:

$$M_{psd}(\omega) = \left[\frac{S_{ff}(\omega)}{S_{aa}(\omega)}\right]^{1/2} \tag{3.2}$$

where $M_{psd}(\omega)$ is the apparent mass in real numbers and $S_{ff}(\omega)$ is the power spectral density of the measured force.

The difference between the CSD and the PSD methods is that the CSD method gives an estimate of the output produced by the input (i.e. the output is linearly dependent on the input) while the PSD method shows how the output is related to the input without assuming any causal relationship between them. Hence, the results obtained using the CSD method are the same as, if the system is linear and there is no noise in the system, or less than those obtained using the PSD method. Comparison between the CSD and the PSD methods is given in Section 10.3.

One advantage of the cross-spectral density method over the power spectral density method is, as a complex function, that it is capable of giving modulus and phase measures, while the power spectral density method gives only the modulus. The modulus $M_{mod}(\omega)$ and phase $M_{ph}(\omega)$ of the apparent mass, or the cross-axis apparent mass, calculated using the CSD method are found using the following relations:

$$M_{mod}(\omega) = \sqrt{(ReM(\omega))^2 + (ImM(\omega))^2} \tag{3.3}$$

$$M_{ph}(\omega) = \tan^{-1} \frac{ImM(\omega)}{ReM(\omega)} \tag{3.4}$$

where $ReM(\omega)$ and $ImM(\omega)$ are the real and imaginary parts of the apparent mass, $M(\omega)$. Another approach to test the linearity of a system is to calculate the coherency (γ^2_{af}) over the frequency range of interest.

$$\gamma^2_{af}(\omega) = \frac{|S_{af}(\omega)|^2}{S_{aa}(\omega)S_{ff}(\omega)} \tag{3.5}$$

where (γ^2_{af}) is the coherency of the system and always lies between 0 and 1. For ideal linear systems with no noise, the coherency would have the maximum value of one at all frequencies. However, for non-linear systems, or with the presence of noise, the coherency is expected to drop. Coherencies obtained from the different experiments in this thesis are shown in Section 10.4.4 and in the Appendices.

3.4.1.1 Mass cancellation

The masses of the aluminium plates bolted to the force transducers would be included in the apparent mass measured during vibration and must be subtracted from the apparent mass to obtain the apparent mass of the subject. This mass cancellation can be conducted in either the frequency domain or in the time domain. In the frequency domain, the mass of the plate (assuming phase of zero for the rigid mass) is subtracted from the real part of the transfer function measured when using a subject. Alternatively, the real and imaginary parts of the transfer function calculated without a subject are subtracted from the real and imaginary parts of the transfer function calculated when using a subject. In the time domain, the force acting on the plate of the force platform is subtracted from the total measured force acting with the subject and the plate. The modulus of the apparent mass was found not to be greatly affected by the method used for mass cancellation (Figure 3.11). However, this is not the case for the coherency. The coherency is more accurate when calculated in the time domain than when calculated in the frequency domain because the effect of the mass plate is removed before calculating the coherency. Mass cancellation in the frequency domain and in the time domain was used to calculate the apparent masses reported in this thesis: time domain method was used when the coherency was shown.

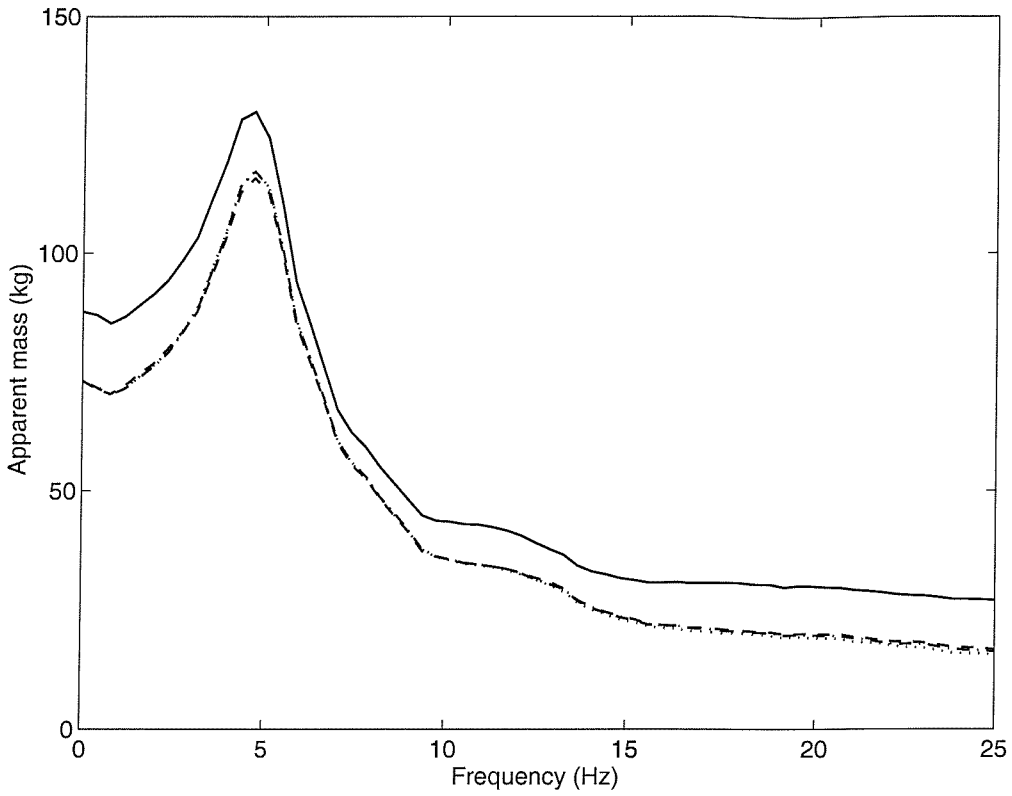

Figure 3.11 Mass cancellation of the 15 kg mass of the plate 'above' the force transducers: ———, apparent mass magnitude before mass cancellation; ·····, apparent mass magnitude after subtracting 15 kg from the real part of the measured transfer function; –·–·–·–, apparent mass magnitude after subtracting transfer functions in the frequency domain; – – – –, apparent mass magnitude after mass cancellation in the time domain.

3.4.2 Statistical analysis

Statistical analysis was used in this thesis to compare results between the different conditions used and to test for correlations between different variables. Due to the unknown distribution of the population from which the samples of subjects were drawn, it was decided to use the non-parametric statistical techniques. SPSS statistical analysis software was used to perform the statistical tests. In the following subsections, a brief description of each statistical test used in this thesis is given together with cases for which it was used. For more detailed examples about these tests and how they work, the reader is recommended to see Clegg (1990) or Siegel and Castellan (1988).

3.4.2.1 Friedman two-way analysis of variance

The Friedman two-way analysis of variance was used to test the null hypothesis that *k* matched samples have been drawn from the same population. In the experiments in this thesis, the samples were matched since the same group of subjects were studied under

each of the *k* different conditions. The Friedman test was applied in this thesis to examine whether a certain variable was dependent on the vibration conditions used. For example, the Friedman test was employed to test if the resonance frequency of the human body measured for 12 subjects differed significantly by using four vibration magnitudes: 0.125, 0.25, 0.625 and 1.25 ms^{-2} r.m.s. In this case, *k* is equal to 4. If no significant difference (0.05 level of significance was mainly used) was found in the resonance frequency between the four vibration magnitudes, then it could be concluded that the resonance frequency was independent of the vibration magnitude and, hence, the null hypothesis is accepted. However, if a significant difference was found in the resonance frequencies then there was difference between at least two of the conditions. To find out the conditions where the differences occurred, another statistical test, which deals with two sets of data, was needed.

3.4.2.2 Wilcoxon matched-pairs signed ranks test

The Wilcoxon matched-pairs signed ranks test was used to examine whether two related samples (conditions) were different from each other. The power in this test comes from the fact that it uses information about the direction and the magnitude of the difference within pairs of the two samples under investigation. For example, if the resonance frequency in the above example was dependent on the vibration magnitude, the Wilcoxon test could be used to find out between which two conditions (i.e. vibration magnitudes) there was a difference in the resonance frequency. This means that the resonance frequencies in each condition must be compared to the resonance frequencies in the other conditions. In the example here, six tests are needed.

3.4.2.3 Spearman rank correlation coefficient, *rho*

The Spearman rank correlation coefficient was used to investigate associations between two variables. For example, this statistics was used to investigate whether there was a correlation between the physical characteristics of the human body (e.g. weight, height, etc.) and the resonance frequency and the magnitude at resonance of the apparent mass. It is also useful to explore if two phenomena are related. For example, significant correlation between two resonance frequencies measured on different parts of the human body may indicate that they are produced by a common mechanism.

CHAPTER 4 FORCES AT THE SEAT AND FOOTREST DURING VERTICAL WHOLE-BODY EXCITATION

4.1 INTRODUCTION

When exposed to vertical vibration the human body exhibits various resonances, especially a resonance at about 5 Hz, seen as increased apparent mass and increased transmission of vibration to the body at this frequency. However, as was shown in the literature review (Chapter 2), the biodynamic responses to whole-body vertical vibration depend on many factors, especially body posture (e.g. Coerman, 1962; Fairley and Griffin, 1989; Kitazaki, 1992; Holmlund *et al.*, 1995; Matsumoto and Griffin, 1998b; Mansfield and Griffin, 2000) and vibration magnitude (e.g. Hinz and Seidel, 1987; Griffin, 1990; Mansfield and Griffin, 2000; Smith, 2000; Matsumoto and Griffin, 2002a,b).

Posture affects the geometry of the body and the muscles that support the body. Fairley and Griffin (1989), Kitazaki (1992), and Holmlund *et al.* (1995) concluded that an erect body posture increased mechanical impedance (or apparent mass) and increased the resonance frequency of the body relative to a relaxed posture. The transmission of vibration to the spine and to the head is also increased in an erect posture (e.g. Griffin, 1975). These findings appear consistent with increased body stiffness in an erect posture.

Muscle tension may also affect the responses of the body to vibration. For example, Fairley and Griffin (1989) noticed an increase in the resonance frequency when subjects were instructed to tense their upper body muscles as much as possible.

Studies investigating the linearity of the apparent mass of the body have concluded that there is a 'softening' with increased vibration magnitude: the resonance frequency reduces at higher magnitudes of vibration (e.g. Mansfield and Griffin, 2000; Matsumoto and Griffin, 2002b). For example, an increase in the vibration magnitude from 0.125 ms^{-2} r.m.s. to 2.0 ms^{-2} r.m.s. decreased the resonance frequency from 6.75 to 5.25 Hz in standing subjects (Matsumoto and Griffin, 1998b) and reduced the resonance frequency from 6.4 to 4.75 Hz in sitting subjects (Matsumoto and Griffin, 2002a).

Several researchers have hypothesised that the tissues beneath the ischial tuberosities might contribute to the non-linearity (e.g. Kitazaki, 1994; Matsumoto and Griffin, 2001). In an investigation of the effect of buttocks tissues on the non-linearity, Matsumoto and

Griffin (2002a) instructed subjects to tense buttocks muscles to increase their stiffness. Using eight subjects at five vibration magnitudes (0.35, 0.5, 0.7, 1.0, and 1.4 ms^{-2} r.m.s.), they found the non-linearity decreased with increased muscle tension, implying that buttocks tissues may be partly responsible for the non-linearity.

Almost all studies of the point response of the body (apparent mass or impedance) have been restricted to responses in the direction of the applied vibration. Measurements of acceleration on the body in the fore-and-aft direction (e.g. on the head, the abdomen, and the spine) caused by vertical vibration show appreciable movements in the fore-and-aft direction (e.g. Panjabi *et al.*, 1986; Kitazaki and Griffin, 1998; Matsumoto and Griffin, 1998a). In one experiment with vertical excitation, forces have been measured in the fore-and-aft direction on a seat excited in the vertical direction (see Matsumoto and Griffin, 2002a). At resonance, it was found that the 'cross-axis apparent mass' (i.e. the ratio of the force in the fore-and-aft direction to the acceleration in the vertical direction), could reach up to 40% of the static masses of the subjects.

Understanding the mechanisms that produce the non-linear behaviour of the human body and the forces in directions other than the direction of excitation is important to improve the biodynamic modelling of humans' response to vibration. Such models are required to test the performance and response of vibration isolation devices (such as vehicle seats) that are influenced by the dynamic responses of the body and therefore vary with vibration magnitude.

This chapter presents an experimental investigation of the forces at the seat and footrest in the directions of excitation (i.e. vertical direction) and at the seat in directions other than the direction of excitation (i.e. fore-and-aft and lateral direction). The effect of vibration magnitude and posture on the forces will be presented. It was hypothesised that the human body would show non-linear response but the non-linearity would decrease by raising the feet so as to increase the mass of the body supported on the ischial tuberosities. The increase of mass on the ischial tuberosities would increase the pressure on the tissue beneath the pelvis and would lead to increase in the stiffness of the tissue. This could help in reducing the involuntary change in muscle tension; Matsumoto and Griffin (2002a) reported that reducing involuntary muscle tension by maximising voluntary muscle tension in the ischial tuberosities area reduced the non-linearity of the body. Kitazaki (1997) reported that the response at a footrest depended on the posture of the legs; hence, it was hypothesised that the response of the feet would differ when changing the footrest height. It was further hypothesised that there would be appreciable forces in

the fore-and-aft direction and that these forces would also show a non-linear response. It was anticipated that forces on the seat in the lateral direction would be relatively small.

4.2 APPARATUS, EXPERIMENTAL DESIGN AND ANALYSIS

4.2.1 Apparatus

Subjects were exposed to vertical whole-body vibration using an electro-hydraulic vibrator (see Chapter 3). A rigid seat and an adjustable footrest (to give different foot heights) were mounted on the platform of the vibrator. A force plate (Kistler 9281 B) capable of measuring forces in three directions simultaneously was secured to the supporting surface of the seat so as to measure forces in the vertical, fore-and-aft, and lateral directions. Another force platform (Kistler Z 13053) was secured to the footrest so as to measure forces at the feet in the vertical direction. Signals from both force platforms were amplified using Kistler 5001 and Kistler 5007 charge amplifiers. Acceleration was measured at the centre of both force platforms using piezo-resistive accelerometers (Entran EGCSY-240D-10 and Entran EGCS-DO-10-/V10/L4M). The signals from the accelerometers and the force transducers were acquired at 200 samples per second via 67 Hz anti-aliasing filters with an attenuation rate of 70 dB in the first octave.

Four different foot heights, and hence four different sitting postures, were achieved using an adjustable footrest (Figure 4.1). The four postures were: (i) 'feet hanging' with no foot support, (ii) feet supported with 'maximum thigh contact' (i.e. heels just in contact with the footrest), (iii) 'average thigh contact' (i.e. upper legs horizontal, lower legs vertical and supported on the footrest), and (iv) 'minimum thigh contact' (i.e. the footrest 160 mm above the position with 'average thigh contact' in position (iii)). The postures were achieved solely by altering the height of the footrest. The footrest was exposed to the same vertical vibration as the seat. No backrest was used in this experiment.

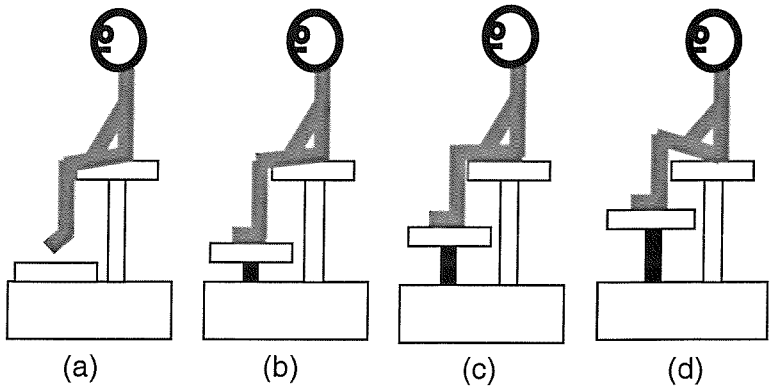

Figure 4.1 Schematic diagrams of the four sitting postures: (a) feet hanging; (b) maximum thigh contact; (c) average thigh contact; (d) minimum thigh contact.

4.2.2 Experimental design

Twelve male subjects with average age 31.4 years (range 20 to 47 years), weight 74.6 kg (range 57 to 106 kg), and stature 1.78 m (range 1.68 to 1.86 m), were exposed to random vertical vibration with an approximately flat constant bandwidth acceleration power spectrum over the frequency range 0.25 to 25 Hz. Subjects' ages, weights and heights are given in Appendix A. The duration of each exposure was 60 seconds.

In each posture, the twelve subjects were exposed to four vibration magnitudes (0.125, 0.25, 0.625, and 1.25 ms^{-2} r.m.s.). The presentation of the four postures and the four vibration magnitudes was balanced across subjects.

4.2.3 Analysis

The measured data are partly presented as apparent masses in the vertical direction, calculated from the vertical force and vertical acceleration at the seat and footrest. The forces in the fore-and-aft and lateral directions were related to the acceleration measured on the seat in the vertical direction using the concept of 'cross-axis apparent mass'. In both cases, the apparent mass and the cross-axis apparent mass, were calculated using the cross spectral density method:

$$M(\omega) = \frac{S_{af}(\omega)}{S_{aa}(\omega)} \qquad (4.1)$$

where, $M(\omega)$ is the apparent mass (or the cross-axis apparent mass), $S_{af}(\omega)$ is the cross spectral density between the force and the acceleration, and $S_{aa}(\omega)$ is the power spectral density of the acceleration. All spectra were calculated by using a resolution of 0.39 Hz. The aluminium plates of the force platforms 'above' the force transducers behaved as rigid bodies (giving constant mass and zero phase over the frequency range of interest) when tested with vertical vibration without a subject. Hence, the static masses of the plates of the force platforms (15 kg for the seat and 33 kg for the footrest) were subtracted from the real parts of the transfer functions measured in the vertical direction.

4.3 RESULTS

The apparent mass data were used to present the results rather than the normalised apparent mass data (the apparent mass divided by the static mass) in order to show the differences between the different postures. It was found that the medians of the normalised apparent masses of the individuals were mostly within 5% (a maximum of 10% at some frequencies) of the normalised median apparent masses. Individual responses are given in Appendix A.

4.3.1 Response on the seat in the vertical direction

The apparent masses of the 12 subjects were calculated for each posture and each vibration magnitude. Individual data were of a form similar to those previously published (e.g. Fairley and Griffin, 1989; Mansfield and Griffin, 2000). A non-linearity was evident for all subjects in all postures. Figure 4.2 shows the median apparent masses of the twelve subjects in the vertical direction at the seat in each posture and at each vibration magnitude. There is a clear decrease in the resonance frequency with an increase in vibration magnitude and a trend towards a reduction in the magnitude of the apparent mass at resonance with an increase in vibration magnitude. Table 4.1 shows the median resonance frequencies and median apparent masses at resonance for the twelve subjects obtained after calculating the median apparent mass at each frequency. Statistical analysis showed significant reductions in the resonance frequencies with increases in vibration magnitudes for all postures ($p < 0.05$; Wilcoxon matched-pairs signed ranks) except between 0.125 and 0.25 ms^{-2} r.m.s. for the maximum thigh contact posture and for the minimum thigh contact posture (Table 4.2).

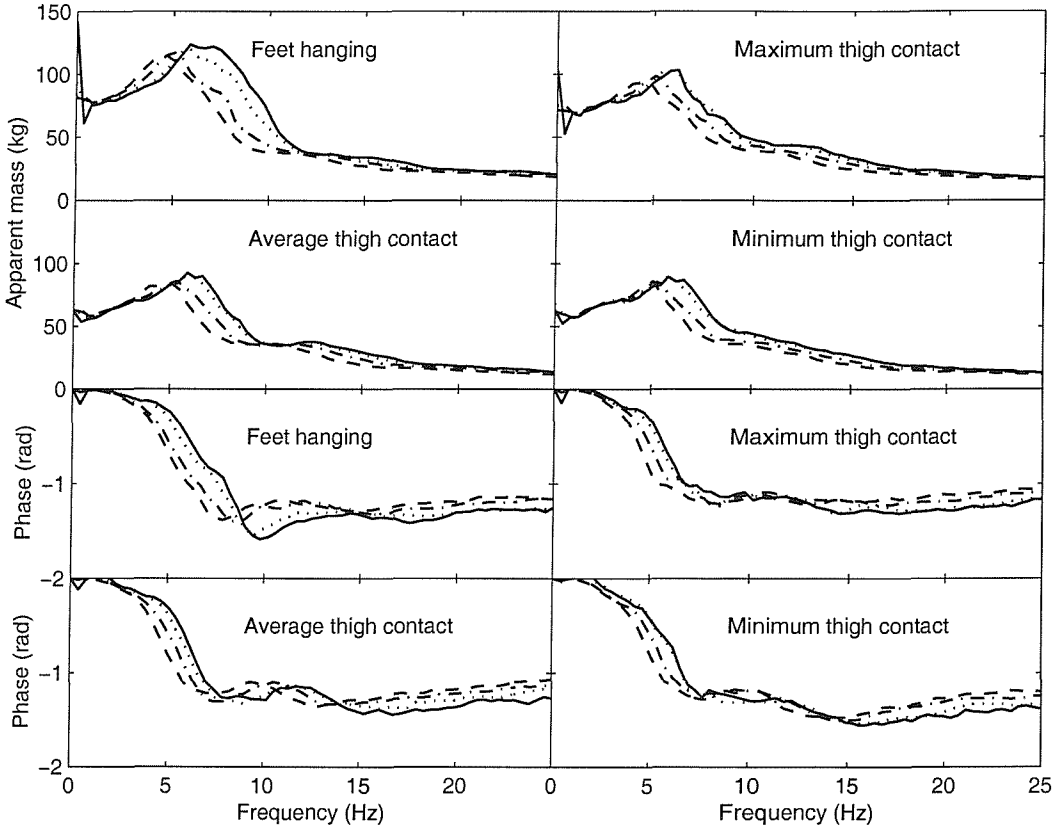

Figure 4.2 Median apparent mass and phase angle of twelve subjects in the vertical direction: effect of vibration magnitude. ———, 0.125 ms^{-2} r.m.s.; ·····, 0.25 ms^{-2} r.m.s.; —·—·—, 0.625 ms^{-2} r.m.s.; – – –, 1.25 ms^{-2} r.m.s.

Table 4.1 Median resonance frequencies and magnitudes of apparent mass at resonance for four postures at four vibration magnitudes.

Vibration magnitude (ms^{-2} r.m.s.)	Resonance frequency (Hz), Resonance Magnitude (kg)			
	Feet hanging	Maximum thigh contact	Average thigh contact	Minimum thigh contact
0.125	5.85, 123.4	6.24, 103.1	5.85, 92.2	5.85, 89.5
0.250	5.85, 119.6	5.85, 102.3	5.85, 89.7	5.85, 89.5
0.625	5.07, 117.0	5.07, 98.4	5.46, 84.5	5.07, 85.3
1.250	4.68, 114.3	4.68, 95.1	4.68, 84.6	5.07, 85.6

Table 4.2 The *p* values for differences in resonance frequencies of apparent mass: effect of vibration magnitude.

Posture	Vibration magnitude (ms^{-2} r.m.s.)	0.125	0.250	0.625	1.250
Feet hanging	0.125	-	0.014	0.014	0.002
	0.250		-	0.005	0.002
	0.625			-	0.002
	1.250				-
Maximum thigh contact	0.125	-	0.055	0.002	0.002
	0.250		-	0.002	0.002
	0.625			-	0.002
	1.250				-
Average thigh contact	0.125	-	0.027	0.002	0.002
	0.250		-	0.002	0.002
	0.625			-	0.004
	1.250				-
Minimum thigh contact	0.125	-	0.389	0.005	0.002
	0.250		-	0.003	0.002
	0.625			-	0.029
	1.250				-

Further statistical analysis was conducted to investigate whether subject posture affected the size of the change in the resonance frequency between the two lower vibration magnitudes (i.e. 0.125 and 0.25 ms^{-2} r.m.s.) and between the two higher vibration magnitudes (i.e. 0.625 and 1.25 ms^{-2} r.m.s.). The results, shown in Table 4.3, indicate that the sizes of differences in the resonance frequencies obtained at the two lower vibration magnitudes did not depend on body posture. However, at the higher vibration magnitudes, there was a significant difference ($p < 0.05$) in the size of the absolute change in the resonance frequencies between the feet hanging posture and the minimum thigh contact posture, and between the maximum thigh contact posture and the minimum

thigh contact posture. The changes in the resonance frequencies between the two higher vibration magnitudes in the minimum thigh contact posture were less than those in the feet hanging posture and the maximum thigh contact posture. The change in the magnitude of the apparent mass with change in vibration magnitude was further explored at three frequencies: (a) at resonance, (b) at a frequency below resonance (i.e. 3.12 Hz), and (c) at a frequency above resonance (i.e. 8.2 Hz). The results indicate that the non-linearity decreased when adopting the minimum thigh contact posture (Table 4.4).

Table 4.3 The *p* values for differences in the absolute change in resonance frequencies. H: feet hanging; Max: maximum thigh contact; Av: average thigh contact; Min: minimum thigh contact; Vibration magnitudes: 1: 0.125; 2: 0.25; 3: 0.625; 4: 1.25 ms^{-2} r.m.s.

(a) Lower vibration magnitudes (0.125 and 0.25 ms^{-2} r.m.s.)

	H1-H2	Max1-Max2	Av1-Av2	Min1-Min2
H1-H2	-	0.083	0.119	0.118
Max1-Max2		-	0.234	0.493
Av1-Av2			-	0.834
Min1-Min2				-

(b) Higher vibration magnitudes (0.625 and 1.25 ms^{-2} r.m.s.)

	H3-H4	Max3-Max4	Av3-Av4	Min3-Min4
H3-H4	-	0.414	0.931	0.014
Max3-Max4		-	0.720	0.021
Av3-Av4			-	0.166
Min3-Min4				-

Table 4.4 Statistically significant differences between apparent mass magnitudes for four postures. Comparisons shown where $p < 0.05$; Wilcoxon matched-pairs signed ranks test. H: feet hanging; Max: maximum thigh contact; Av: average thigh contact; Min: minimum thigh contact; Vibration magnitudes: 1: 0.125; 2: 0.25; 3: 0.625; 4: 1.25 ms^{-2} r.m.s.

	At the resonance frequency	Below resonance (3.12 Hz)	Above resonance (8.2 Hz)	Total out of 18 possible combinations
Feet hanging	H1 / H2 H1 / H3 H1 / H4 H2 / H3	H1 / H2 H1 / H3 H1 / H4 H2 / H3 H2 / H4 H3 / H4	H1 / H3 H1 / H4 H2 / H3 H2 / H4 H3 / H4	15
Maximum thigh contact	Max2 / Max3 Max2 / Max4	Max1 / Max3 Max1 / Max4 Max2 / Max4 Max3 / Max4	Max1 / Max4 Max2 / Max3 Max2 / Max4 Max3 / Max4	10
Average thigh contact	Av1 / Av3 Av2 / Av3 Av2 / Av4	Av1 / Av4 Av2 / Av4 Av3 / Av4	Av1 / Av3 Av1/ Av4 Av2/ Av3 Av2 / Av4 Av3 / Av4	11
Minimum thigh contact	Min1 / Min4	Min2 / Min4	-	2

At each vibration magnitude, the median apparent mass also depended on the posture. Like the median apparent masses shown in Figure 4.3, the individual data showed a decrease over the whole frequency range when the thigh contact reduced. This is consistent with reduced thigh contact increasing the mass supported on the footrest and decreasing the mass supported on the seat. However, the resonance frequency of the apparent mass of the body was little affected by the posture, as shown in the median results and the statistical analysis in Table 4.5. There was no statistical significant difference in the resonance frequencies between the four postures except between the feet hanging posture and both the minimum thigh contact posture and the average thigh contact posture at 0.125 ms^{-2} r.m.s.

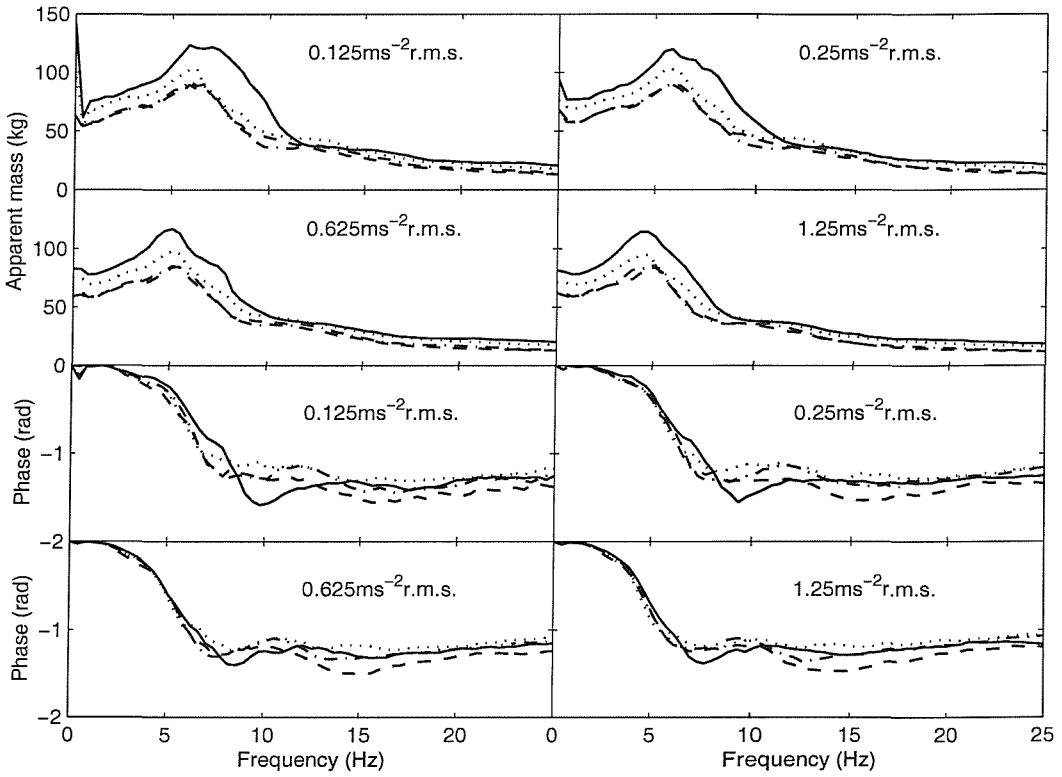

Figure 4.3 Median apparent mass and phase angle of twelve subjects in the vertical direction: effect of posture. ———, feet hanging; ·····, maximum thigh contact; —·—·—, average thigh contact; – – – –, minimum thigh contact.

Table 4.5 The *p* values for differences between resonance frequencies of apparent mass: effect of the sitting posture. H: feet hanging; Max: maximum thigh contact; Av: average thigh contact; Min: minimum thigh contact; vibration magnitudes: 1: 0.125; 2: 0.25; 3: 0.625; 4: 1.25 ms^{-2} r.m.s.

	H1	Max1	Av1	Min1
H1	-	0.057	0.002	0.010
Max1		-	0.831	0.339
Av1			-	0.537
Min1				-

	H2	Max2	Av2	Min2
H2	-	0.068	0.287	0.250
Max2		-	0.518	0.671
Av2			-	1.0
Min2				-

	H3	Max3	Av3	Min3
H3	-	0.146	0.236	0.083
Max3		-	0.931	0.299
Av3			-	0.255
Min3				-

	H4	Max4	Av4	Min4
H4	-	0.068	0.072	0.473
Max4		-	0.943	0.49
Av4			-	0.366
Min4				-

4.3.2 Response in the fore-and-aft direction

The fore-and-aft forces on the seat were related to the acceleration measured in the vertical direction using the 'cross-axis apparent mass' concept. Figure 4.4 shows the variability between subjects (inter-subject variability) in the fore-and-aft response measured at 1.25 ms^{-2} r.m.s. for the four postures. There were considerable forces on the seat in the fore-and-aft direction as a result of vertical seat excitation. In all postures, the resonance frequency is in the vicinity of 5 Hz, similar to that for the vertical apparent mass. There were high correlations between the resonance frequencies in the vertical response and the resonance frequencies of the fore-and-aft response. In all four postures the correlations were significant at the two higher vibration magnitudes ($p < 0.001$; Spearman rank correlation). However the correlations were not statistically significant at the two lower magnitudes with the feet hanging or with the average thigh contact postures ($p > 0.05$).

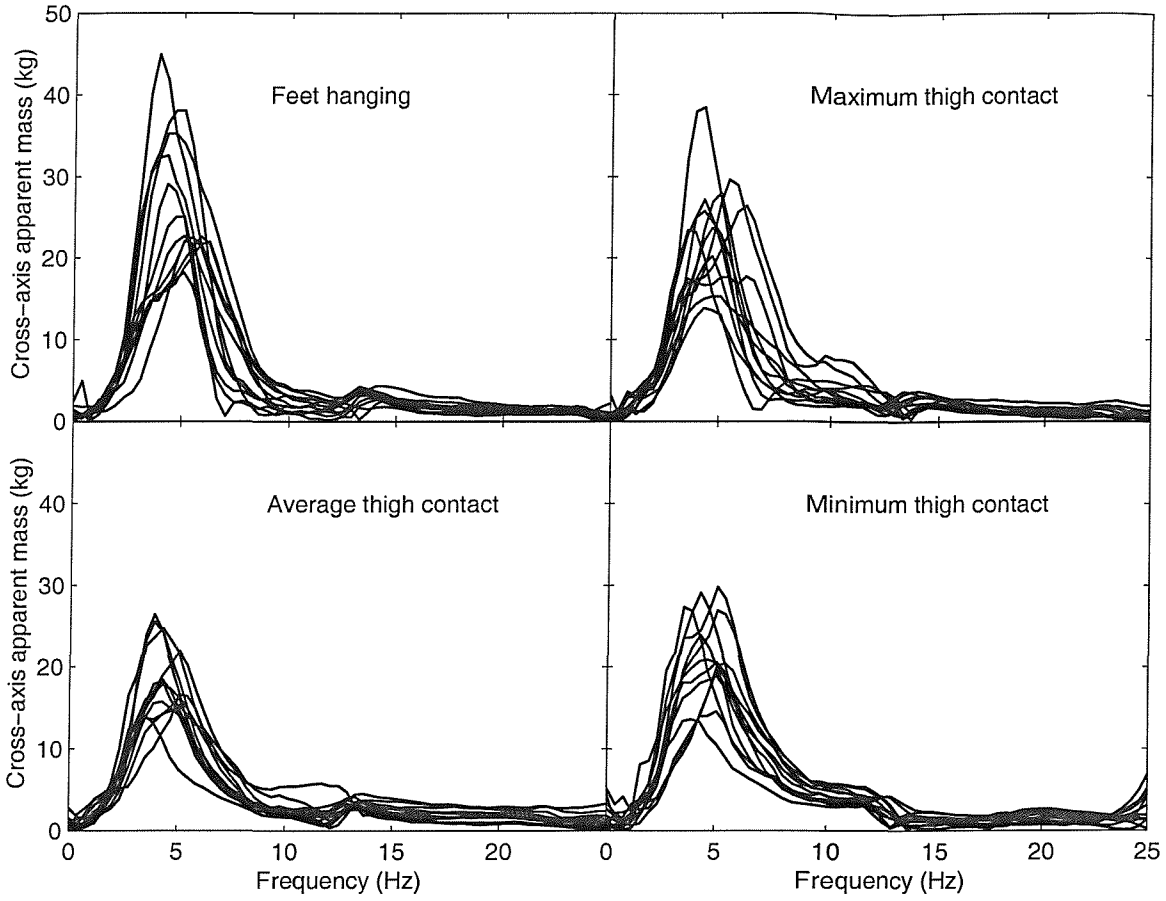

Figure 4.4 Inter-subject variability in the cross-axis apparent mass in the fore-and-aft direction for each posture at 1.25 ms^{-2} r.m.s.

The resonance frequency apparent in the median fore-and-aft cross-axis apparent mass decreased with increasing vibration magnitude, similar to the non-linearity in the vertical apparent mass (Figure 4.5).

The cross-axis apparent mass in the fore-and-aft direction shows changes with posture: it seems that changing from a posture with no foot support to a posture in which the feet were more supported decreased the forces in the fore-and-aft direction. An exception is the minimum thigh contact posture where the forces were more than those with average thigh contact and slightly less, similar, or more than those with the maximum thigh contact posture, depending on the frequency (Figures 4.4 and 4.5). There were no significant differences in the magnitude of the cross-axis apparent mass at resonance between the minimum thigh contact posture and maximum thigh contact posture at any vibration magnitude ($p > 0.1$).

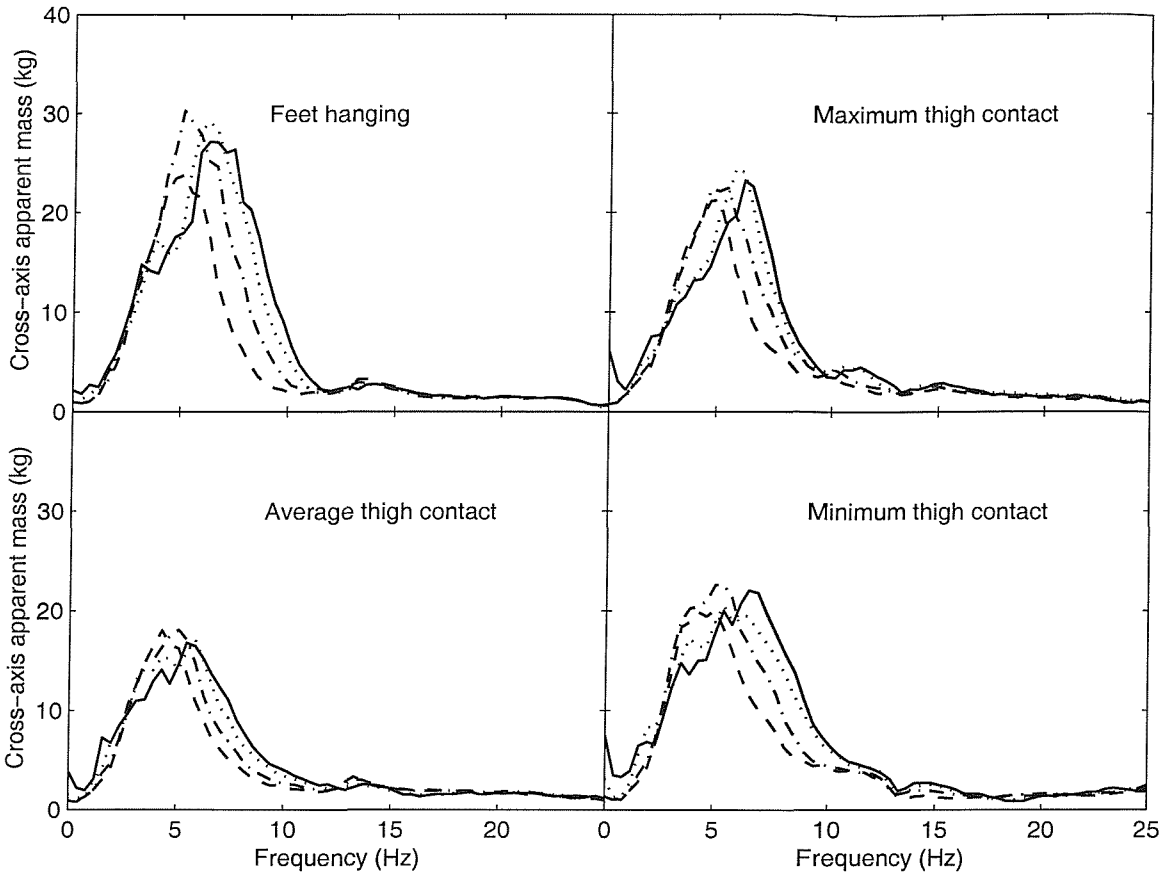

Figure 4.5 Median cross-axis apparent masses of twelve subjects in the fore-and-aft direction: effect of vibration magnitude. ———, 0.125 ms^{-2} r.m.s.; ·····, 0.25 ms^{-2} r.m.s.; —·—·—, 0.625 ms^{-2} r.m.s.; – – – –, 1.25 ms^{-2} r.m.s.

4.3.3 Response in the lateral direction

The lateral forces were calculated using the same cross-axis apparent mass concept: forces in the lateral direction were related to the seat acceleration in the vertical direction. Figure 4.6 shows the inter-subject variability in cross-axis apparent mass when subjects were exposed to 1.25 ms^{-2} r.m.s in the vertical direction. Figure 4.7 shows the median cross-axis apparent masses of the 12 subjects in each posture and at each vibration magnitude. Both figures indicate that, in comparison with the forces in the vertical and fore-and-aft directions, the forces in the lateral direction were low during excitation with vertical vibration. Figure 4.7 shows no clear effect of vibration magnitude on the cross-axis apparent mass in the lateral direction. At some frequencies the cross-axis apparent mass in the lateral direction is low and only slightly in excess of the 'noise' measured with no subject (about 0.2 kg). Measurements are not shown at frequencies in excess of 10 Hz due to a lateral resonance in the system at about 13 Hz.

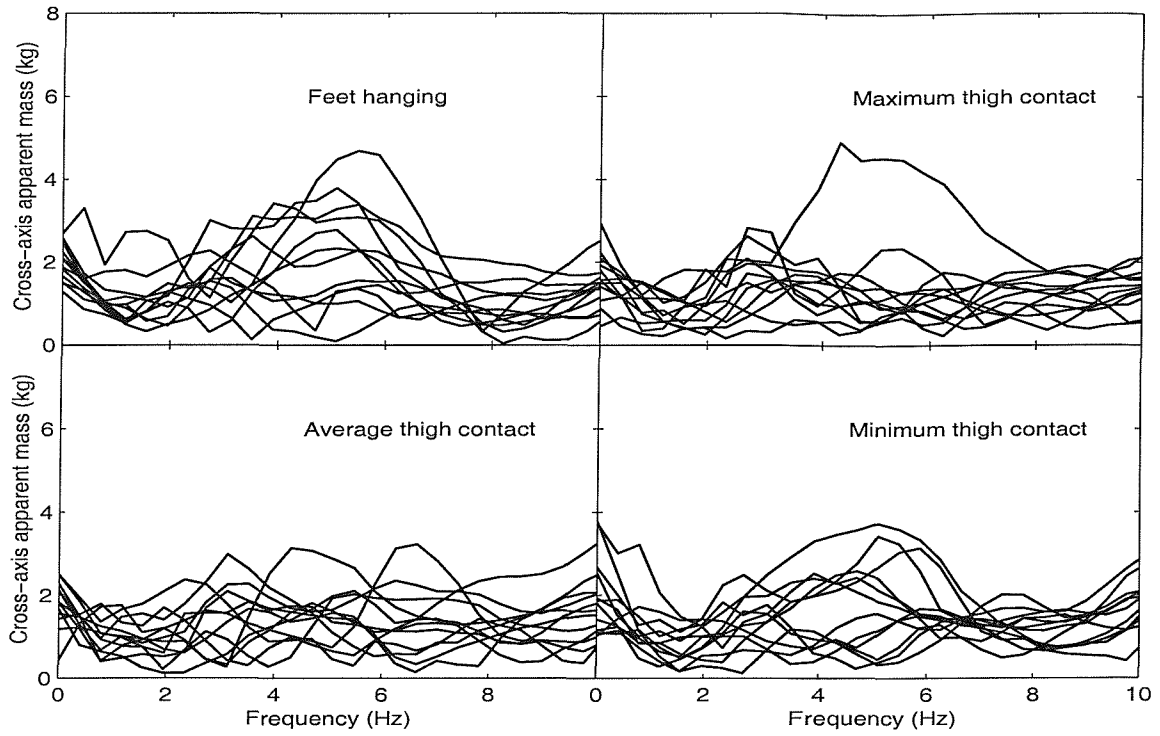

Figure 4.6 Inter-subject variability in the cross-axis apparent mass in the lateral direction for each posture at 1.25 ms^{-2} r.m.s.

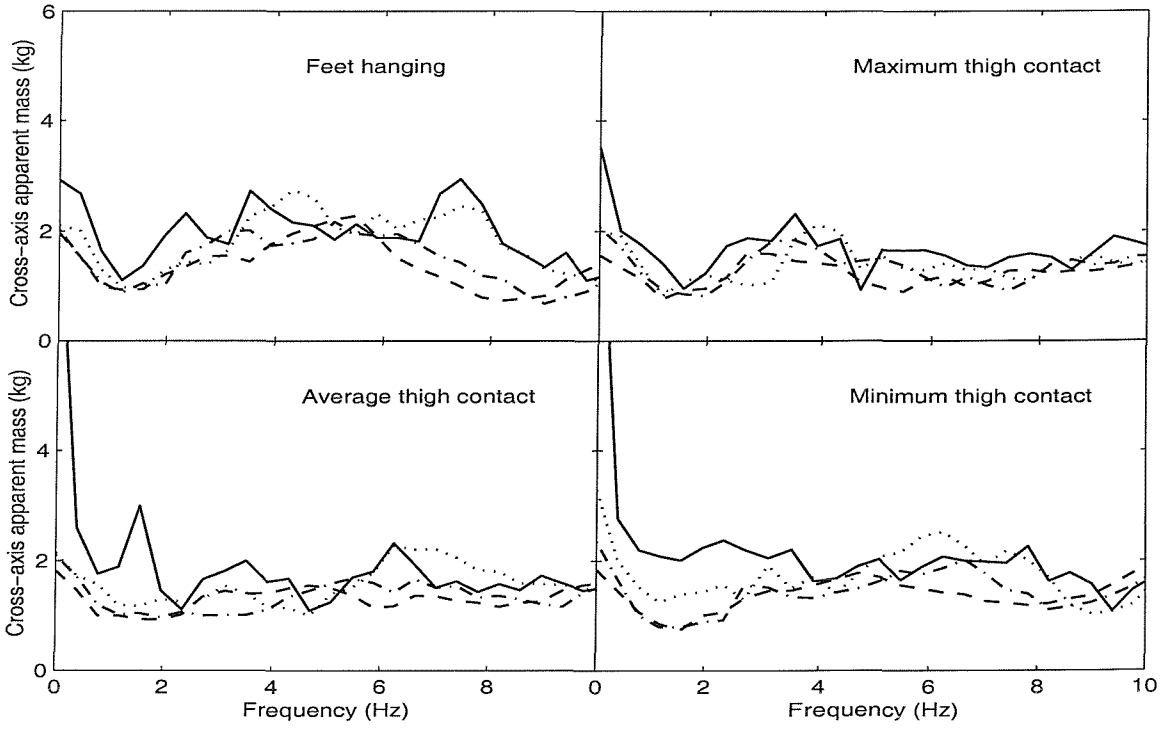

Figure 4.7 Median cross-axis apparent mass of twelve subjects in the lateral direction: effect of vibration magnitude. ———, 0.125 ms^{-2} r.m.s.; ·····, 0.25 ms^{-2} r.m.s.; —·—·—, 0.625 ms^{-2} r.m.s.; – – – –, 1.25 ms^{-2} r.m.s.

4.3.4 Response at the feet

The dynamic response at the feet was measured for the three postures in which the feet were supported on the footrest. In the maximum thigh contact posture, where the mass of the body supported on the footrest was least, one resonance frequency was found between 5 and 10 Hz. With average thigh contact and with minimum thigh contact, the responses were more complex and more than one resonance appeared for all subjects: at 1.25 ms^{-2} r.m.s. the average thigh contact posture showed two resonances (at 5 and 11 Hz), while the minimum thigh contact posture showed three resonances (at 5, 7.5 and 11 Hz). Some subjects also showed a resonance around 14 Hz in both postures (see Appendix A). This behaviour is clear in Figure 4.8, which also shows the inter-subject variability in responses at the feet.

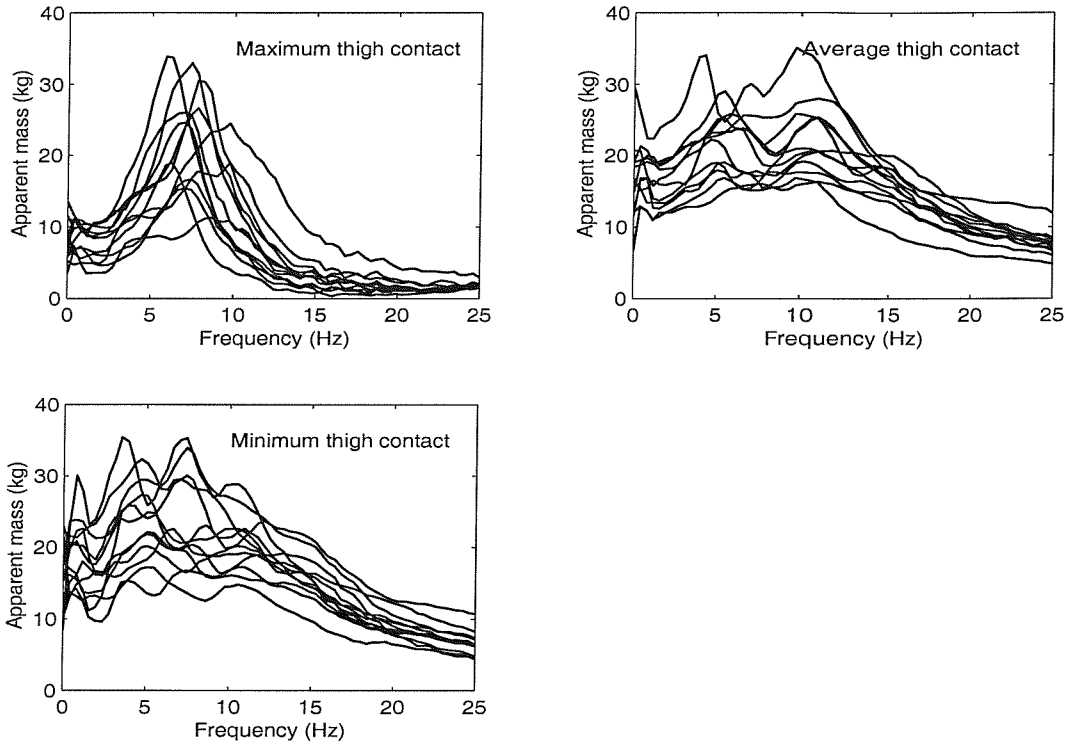

Figure 4.8 Inter-subject variability in the apparent mass at the feet in the vertical direction for each posture at 1.25 ms^{-2} r.m.s.

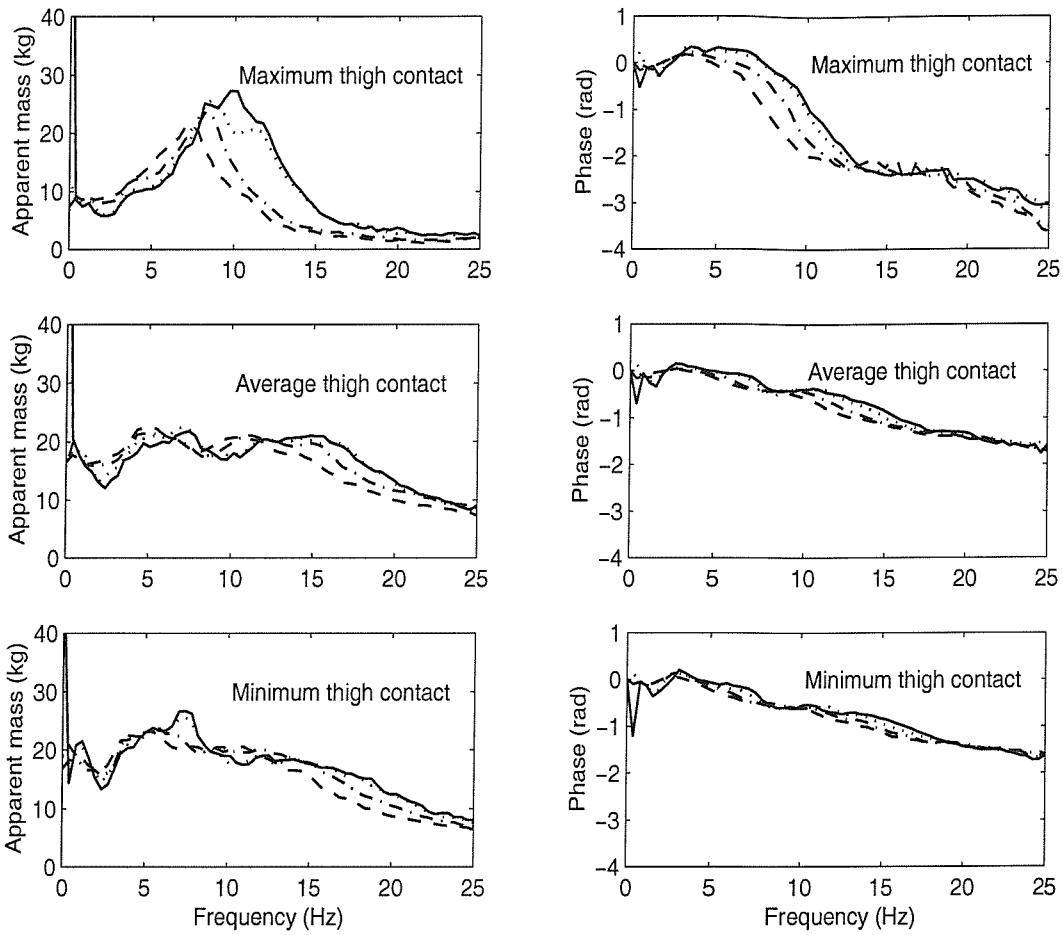

Figure 4.9 Median apparent mass and phase angle at the feet of twelve subjects in the vertical direction: effect of vibration magnitude. ———, 0.125 ms^{-2} r.m.s.; ·····, 0.25 ms^{-2} r.m.s.; —·—·—, 0.625 ms^{-2} r.m.s.; – – – –, 1.25 ms^{-2} r.m.s.

The three postures show some non-linear behaviour in the response at the feet (Figure 4.9). The median resonance frequency in the maximum thigh contact posture reduced from 9.75 Hz to 7.02 Hz when the vibration magnitude increased from 0.125 to 1.25 ms^{-2} r.m.s. However, statistical analysis (Table 4.6) showed that the non-linearity decreased when the feet were more supported. It is also clear that the phase lag between acceleration and force at the feet was greater when the feet were less supported.

Table 4.6 Statistically significant differences between apparent mass magnitudes at the feet for three postures. Comparisons shown where $p < 0.05$; Wilcoxon matched-pairs signed ranks test. Max: maximum thigh contact; Av: average thigh contact; Min: minimum thigh contact; vibration magnitudes: 1: 0.125; 2: 0.25; 3: 0.625; 4: 1.25 ms^{-2} r.m.s.

	At 3.1 Hz	At 5.1 Hz	At 8.2 Hz	At 12.1 Hz	Total out of 24 possible combinations
Maximum thigh contact	Max1 / Max3 Max1 / Max4 Max2 / Max3 Max2 / Max4 Max3 / Max4	Max1 / Max3 Max1 / Max4 Max2 / Max3 Max2 / Max4 Max3 / Max4	Max2 / Max4 Max3 / Max4	Max1 / Max2 Max1 / Max3 Max1 / Max4 Max2 / Max3 Max2 / Max4 Max3 / Max4	18
Average thigh contact	Av1 / Av3 Av1 / Av4 Av2 / Av3 Av2 / Av4 Av3 / Av4	Av1 / Av2 Av1 / Av3 Av1 / Av4 Av2 / Av3 Av2 / Av4	Av1 / Av3	Av1 / Av4 Av2 / Av4 Av3 / Av4	14
Minimum thigh contact	Min1 / Min3 Min1 / Min 4 Min2 / Min4	-	Min2 / Min4	-	4

4.4 DISCUSSION

4.4.1 Response In the vertical direction

In all of the postures investigated, the apparent mass of the human body showed a principal resonance in the vicinity of 5 Hz and a second resonance in the range 7 to 14 Hz. Both resonances decreased with an increase in vibration magnitude, showing a 'non-linearity' as noticed previously (e.g. Hinz and Seidel, 1987; Fairley and Griffin, 1989; Mansfield and Griffin, 2000). Some subjects exhibited a principal resonance frequency as high as 8.6 Hz, which is higher than previously reported. This high value occurred at the lowest vibration magnitude (0.125 ms^{-2} r.m.s.), which is lower than used in previous studies.

The differences in the apparent masses between the four postures (as shown in Figure 4.3) arise because with the feet hanging the whole of the body mass is supported on the seat. Increasing the height of the footrest increased the mass of the body supported on the footrest and decreased the mass supported on the seat. Hence, the minimum thigh contact posture exhibited the lowest apparent mass. However, this change in the distribution of mass between the footrest and the seat had little or no effect on the resonance frequency of the body. The absence of a significant change in the resonance frequency with the changes in posture in this study could suggest that the principal

resonance frequency depends on the motion of the upper body regardless of the changes at the thighs and the legs. This hypothesis might be supported by the similarity of the resonance frequencies between the standing and the sitting positions measured in previous studies (e.g. Miwa, 1975; Matsumoto and Griffin, 2000).

An alternative explanation for the resonance frequency being independent of the postures studied here could be that changing from one posture to another not only changed the distribution of the subject mass on the seat and the footrest but also changed the stiffness of the thighs. This may have maintained the same proportional contribution of the mass and the stiffness to the resonance frequency in the four postures.

A non-linear response of the human body to vibration has been found in transmissibility measurements to various parts of the body (e.g. Mansfield, 1998; Matsumoto and Griffin, 2002b) as well as in mechanical impedance and apparent mass measurements. In the present study, where only apparent mass was measured, the extent of the non-linearity differed between the four postures: a finding that may assist the identification of the mechanisms that cause non-linearity. The position of the feet changed the degree to which the thighs were in contact with the seat and also changed the pressure on tissues beneath the pelvis. For example, changing from the maximum thigh contact posture to the minimum thigh contact posture increased the mass supported on the footrest, reduced the mass supported on the seat and reduced the area of contact at the seat, so increasing the pressure on the pelvis tissue and increasing the stiffness of these tissues. Sandover (1978) noticed an increase in the resonance frequency of the body from 4 to 6 Hz when two 25 mm cubes were placed under the ischial tuberosities, implying an increase in the stiffness of these tissues by increasing the pressure on them. An increase in the stiffness of the tissues of the ischial tuberosities might be the reason for a decrease in the non-linearity in the minimum thigh contact posture: a previous study found decreased non-linearity when the buttocks were tensed and the effect of involuntary muscle tension was reduced (Matsumoto and Griffin, 2002a). This is also consistent with previous suggestions that deformation of tissues beneath the pelvis contribute to the non-linearity of the body in response to vibration (Kitazaki, 1994; Matsumoto and Griffin, 2002a).

It has been suggested that involuntarily muscle activity may contribute to the non-linearity of the human body in response to vibration. Matsumoto and Griffin (2002a) reported less clear non-linear characteristics in the apparent masses of seated subjects when involuntary muscle activity was reduced by controlling muscle tension in the abdomen

and the buttocks. It was reported by some subjects in the present study that maintaining an upright upper body posture with minimum thigh contact was more difficult than with the other three postures. Subjects may have used their muscles to keep the required upright posture and hence reduced the effect of involuntarily changes in muscle tension during vibration. This may be another reason for the reduced non-linearity in the minimum thigh contact posture.

In all postures, the apparent masses at very low frequencies were equal to the static masses of the subjects supported on the seat. At all frequencies, increasing the footrest height decreased the apparent mass of the body measured at the seat due to the increased mass supported at the feet. However, this seems to be only true for a footrest vibrating in phase with the seat. Fairley and Griffin (1989) found a dramatic effect of the height of a stationary footrest on the apparent mass of the body at low frequencies where the apparent mass did not tend toward the static mass on the seat but decreased with a decrease in the height of the footrest. The authors attributed this observation to relative movement between the feet and the seat.

4.4.2 Response in the fore-and-aft direction

The forces measured in the fore-and-aft direction are consistent with the only previous study (Matsumoto and Griffin, 2002a) to have quantified these forces. The individual data in the present study showed that, at resonance, the cross-axis apparent mass in the fore-and-aft direction could reach up to 60% of the static mass of the subject. Matsumoto and Griffin (2002a) did not observe the clear peaks apparent in this study around 5 Hz, possibly due to the different conditions in which the feet of their subjects rested on a stationary footrest. A two dimensional motion is consistent with the fore-and-aft and pitch transmissibilities measured on the body during vertical vibration (Matsumoto and Griffin, 1998a) and the high shear forces at the third lumbar vertebra predicted by Fritz (2000) for a biomechanical model of responses to vertical vibration.

The high forces measured in the fore-and-aft direction might be attributed to some combination of bending or rotational modes of the upper thoracic and cervical spine at the principal resonance frequency or a bending mode of the lumbar and lower thoracic spine, as found by Kitazaki and Griffin (1997) at a mode close to the principal resonance. The fore-and-aft and pitch transmissibilities from vertical seat vibration to six locations on the spine, the head and the pelvis reported by Matsumoto and Griffin (1998a) showed high values around the resonance frequency especially at the head and the first thoracic vertebra. The forces measured in the fore-and-aft direction in this study may be assumed

to be associated with the motions found by Kitazaki and Griffin (1997) and Matsumoto and Griffin 1998a, but their full explanation must await an improved biodynamic model of the linear and non-linear motions of the body.

It was expected that postures with less foot support would produce greater forces in the fore-and-aft direction due to increased free movement of the body. This was true for all postures except with minimum thigh contact, which showed forces more than those found with average thigh contact and similar or more than those found with maximum thigh contact. It seems that with minimum thigh contact it was easy for the body to pivot around the pelvis with a pitching motion that was translated into forces in the fore-and-aft direction.

When a driver is exposed to multi-axis vibration in a vehicle, there will be two fore-and-aft force components contributing to the total force in the fore-and-aft direction on the seat surface. One component of force comes from the reaction of the body to fore-and-aft seat vibration. The other component comes from fore-and-aft forces arising from the responses of the body to vertical vibration, as shown in this study. Since magnitudes of vertical vibration can often be much greater than magnitudes of fore-and-aft vibration, the contribution to the total fore-and-aft force from the component caused by vertical vibration may be significant. In which case, this force may appreciably enhance (or cancel) the fore-and-aft force arising from fore-and-aft vibration. The prediction of the fore-and-aft transmissibilities of seat cushions may need to take this additional force into account.

The well-known non-linearity in the apparent mass of the body in the vertical direction was also evident in the cross-axis apparent mass measured in the fore-and-aft direction. However, in the fore-and-aft cross-axis apparent mass, the non-linearity was less with the average thigh contact posture than with the other three postures. This may imply that the mechanisms that affected the non-linearity in the vertical direction had a different effect on the non-linearity in the fore-and-aft direction: increasing the pressure on the tissue beneath the pelvis in the minimum thigh contact posture reduced the non-linearity in the vertical direction only. This is consistent with the result of Matsumoto and Griffin (2002a) who showed that tensing the muscles of the tissue beneath the pelvis had an effect on the non-linearity in the vertical direction but not the fore-and-aft direction. Since tensing the buttocks muscles in the Matsumoto and Griffin study is assumed to have increased the stiffness of the tissue beneath the pelvis in the vertical and the fore-and-aft direction, it may be hypothesised that neither the axial nor the shear deformation of the buttocks tissue affects the non-linearity found in the fore-and-aft response.

4.4.3 Response in the lateral direction

Forces measured in the lateral direction were small compared to those in the fore-and-aft direction. The lower forces in the lateral direction than in the fore-and-aft direction are presumably the consequences of the symmetry of the human body either side of the mid-sagittal plane. The centre of gravity of the seated human body is in the mid-sagittal plane but forward of the ischial tuberosities where the vibration enters the upper body. This makes it easier for the body to pitch around the lateral axis than to roll around the fore-and-aft axis of the body.

4.4.4 Response at the feet

Only a few studies have investigated the biodynamic response at the feet to vibration. Kitazaki (1997) studied the response of the feet to vertical vibration at 1.0 ms^{-2} r.m.s. With subjects sitting in an inclined rigid seat with an inclined backrest but with knees at angle of 90°, he found resonance frequencies at about 5, 7.5, and 12 Hz, similar to those found in this study at 1.25 ms^{-2} r.m.s. with the minimum thigh contact posture. In the study by Kitazaki, the 12 Hz resonance frequency disappeared when the subjects changed the knee angle from 90° to 110°. In this study, the 7.5 Hz resonance disappeared when the subjects adopted the average thigh contact posture.

The forces measured at the feet in this study were due to the point impedance of the feet but may also have arisen from forces transmitted from the upper body down the legs. Kitazaki (1997) compared the response of the feet with whole-body vibration with their response when only the feet were excited. There were similar response characteristics in both conditions but the apparent mass of the feet during whole-body vibration was higher than when only the feet were excited.

In the present study, the non-linearity in the responses at the seat were also apparent in the apparent mass measured at the feet. A similar finding was reported by Kitazaki (1997): the resonance frequencies of the feet decreased when the vibration magnitude increased. The non-linearity in the response of the feet may be partly due to the deformation of tissues of the feet, similar to the hypothesised deformation of the tissues under the pelvis. This proposition is supported by the decrease in non-linearity of both the upper body and the feet in the minimum thigh contact posture, where the tissues under the pelvis and the feet may have been stiffer due to increased forces at both locations. The non-linearity might alternatively, or additionally, have arisen from rotational motions of the joints or as a reflection of the non-linearity that takes place in the upper body.

The phase lag between the force and the acceleration measured at the feet was less when there was more mass of the body supported on the footrest. One of the possible explanations for this is that the stiffness of the feet tissues might have increased when the feet were more supported.

4.5 CONCLUSION

Varying degrees of non-linearity of the human body have been observed in response to vertical vibration with four postures differing in the degree of thigh contact with the seat, with least non-linearity in a posture having least thigh contact. The results imply little effect of thigh stiffness on the non-linear behaviour but are consistent with the buttocks tissue affecting the non-linearity. Compressing the tissue beneath the ischial tuberosities in the minimum thigh contact posture may have increased the tissue stiffness and reduced the non-linearity.

Forces on the seat in the fore-and-aft direction, produced by vibration of the seat in the vertical direction were high (could reach up to 60% of the static mass of some subjects) and varied with posture. Forces in the lateral direction were relatively small. The study confirms that the human body has appreciable movements in two dimensions when exposed to vertical vibration. The feet showed a complex response with multiple resonances that varied with posture: the position of the feet affected the forces measured at the feet.

CHAPTER 5 FORCES AT THE SEAT AND BACKREST DURING VERTICAL WHOLE-BODY EXCITATION

5.1 INTRODUCTION

Whole-body vibration can cause discomfort and interfere with activities and may cause back problems (Griffin, 1990). During vertical whole-body vibration, the human spine is alternately compressed and extended while bending and rocking. The axial and shear forces in the spine may be expected to influence the various effects of vibration, but are difficult to measure. Forces at the interfaces of the body with the source of vibration (such as the seat and the backrest) reflect how the body moves during vibration and are relatively easy to measure. For example, forces in the vertical and fore-and-aft directions at the seat reflect two-dimensional movement of the body during vertical excitation as was shown in Chapter 4 and by Matsumoto and Griffin (2002a).

Backrests affect the posture of the body by changing the spine curvature, which changes the geometry and stiffness of the body and the body's response to vibration (Griffin, 1990). With horizontal vibration, backrests may restrict body movements (at low frequencies) and may act as an additional source of vibration (at high frequencies), as reported by Fairley and Griffin (1990).

A few studies have investigated the effect of a backrest on the vertical apparent mass of seated subjects. Fairley and Griffin (1989) found that sitting with a backrest increased the resonance frequency of the body and increased the apparent mass at frequencies above resonance. Mansfield (1998) also found an increase in the apparent mass above resonance when using a backrest but found no significant differences between the resonance frequencies with a normal upright posture and a back-on posture (i.e. the back in contact with the backrest).

Studies of the transmission of vertical seat vibration to various locations up the spine have been conducted using seats without a backrest (e.g. Matsumoto and Griffin, 1998a). Because of practical limitations, studies with backrests have mainly measured transmissibility to the head (e.g. Paddan and Griffin, 1988a) with a few studies reporting transmissibility to the pelvis and lower spine (e.g. Magnusson *et al.*, 1993; Mansfield, 1998). Paddan and Griffin (1988a,b, 1994, 2000) studied the effect of a rigid backrest on seat-to-head transmissibility with six directions of excitation (vertical, fore-and-aft, lateral, roll, pitch and yaw) and six directions of head movement. With vertical excitation, they

reported a decrease in inter-subject variability with a backrest but an increase in head vibration, especially in the mid-sagittal plane in the frequency range 5 to 10 Hz. They also reported a small lateral head motion during vertical and fore-aft excitation with back-on and back-off postures. Mansfield (1998) reported an increase in pelvis rotation at resonance when a backrest was used, compared with an upright posture without backrest. He also mentions an increase in inter-subject variability with a backrest, opposite to that for seat-to-head transmissibility reported by Paddan and Griffin (1988a). A minor effect of backrests, attenuating vibration at the third lumbar vertebra, was reported by Magnusson *et al.* (1993).

Although some form of backrest is present on most seats, there appears to have been no study of the apparent mass measured at the back with any axis of vibration: fore-and-aft, lateral or vertical. The experiment described in the present chapter investigated forces at the seat and the backrest in three axes (vertical, fore-and-aft, and lateral) during whole-body vertical excitation. Based on observations from the previous studies, the use of a backrest was expected to increase the resonance frequency of the body and increase the vertical forces on the seat at frequencies greater than resonance compared to those measured without a backrest (Chapter 4). Fore-and-aft forces on the seat were also anticipated to be affected by the use of a backrest: the backrest was expected to restrain the rotational motions of the upper body. It was hypothesised that there would be appreciable forces at the backrest in the fore-and-aft direction but small forces at the backrest in the vertical and lateral directions.

5.2 APPARATUS, EXPERIMENTAL DESIGN AND ANALYSIS

5.2.1 Apparatus

Subjects were exposed to random vertical vibration using an electro-hydraulic vibrator capable of producing a peak-to-peak displacement of 1 metre. A rigid seat with a vertical rigid backrest was mounted on the platform of the vibrator. The backrest was fixed and not adjustable to subject height, and hence different subjects had different contact areas between the back and the backrest. An adjustable footrest (to give different foot heights) moved vertically in phase with the seat. Signals from a tri-axial force plate (Kistler 9281 B) and a single axis force plate (Kistler Z 13053) were amplified by Kistler 5007 charge amplifiers so as to measure the forces at the backrest and the seat. Vertical acceleration was measured at the centre of both force platforms using piezo-resistive accelerometers (Entran EGCSY-240D-10). The signals from the accelerometers and the force transducers were digitised at 200 samples per second via 67 Hz anti-aliasing filters.

5.2.2 Experimental design

Twelve male subjects with average age 29.9 years (range 20 to 46 years), weight 77.2 kg (range 62 to 106 kg), and stature 1.78 m (range 1.68 to 1.86 m), were exposed to random vertical vibration with an approximately flat constant bandwidth acceleration power spectrum over the frequency range 0.25 to 20 Hz. These subjects were the same as those used in the experiment conducted without backrest (Chapter 4) except for subject number 5. In the experiment without a backrest, subject 5 was 47 years old and had a weight and height of 57 kg and 1.7 m while in the experiment conducted with a backrest, subject 5 was 29 years old and had a weight and height of 88 kg and 1.72 m. The duration of each exposure was 60 seconds.

Sixteen different conditions consisted of four vibration magnitudes (0.125, 0.25, 0.625, and 1.25 ms^{-2} r.m.s.) and four sitting postures. The four sitting postures were the same as those used in Chapter 4. However, in the experiment reported here, a backrest was used (see Figure 5.1). In each posture, the twelve subjects were exposed to four vibration magnitudes. The presentation of the four postures and the four vibration magnitudes was balanced across subjects.

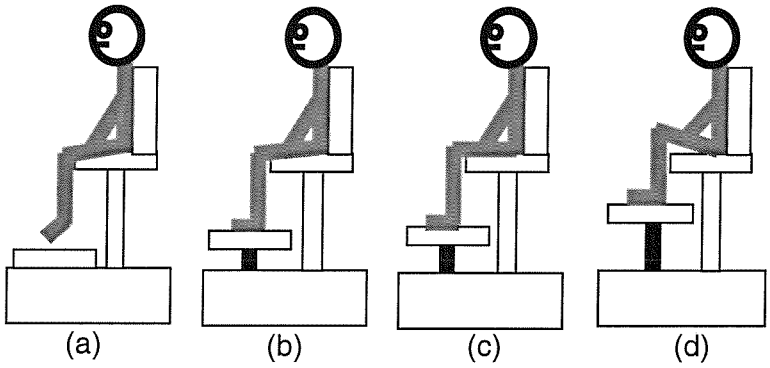

Figure 5.1 Schematic diagrams of the four sitting postures: (a) feet hanging; (b) maximum thigh contact; (c) average thigh contact; (d) minimum thigh contact.

The experiment was carried out in two sessions. In the first session, the tri-axial force platform was secured to the rigid backrest and the single-axis force platform was secured to the seat. In the second session, the force platforms were swapped between the seat and the backrest so that tri-axial forces on both the seat and backrest in the fore-and-aft, lateral and vertical directions could be obtained.

5.2.3 Analysis

The data are partly presented as apparent masses in the vertical direction, calculated from the vertical force and vertical acceleration at the seat and backrest. The forces in the fore-and-aft and lateral directions on the seat and the backrest were related to the acceleration measured on the seat in the vertical direction using the concept of 'cross-axis apparent mass'. In both cases, the apparent mass and the cross-axis apparent mass were calculated using the cross spectral density method:

$$M(\omega) = \frac{S_{af}(\omega)}{S_{aa}(\omega)} \tag{5.1}$$

where, $M(\omega)$ is the apparent mass (or the cross-axis apparent mass), $S_{af}(\omega)$ is the cross spectral density between the force and the acceleration, and $S_{aa}(\omega)$ is the power spectral density of the acceleration. All spectra were calculated by using a resolution of 0.39 Hz. The masses of the aluminium plates of the force platforms 'above' the force transducers (15 kg for the tri-axial force plate and 33 kg for the single axis force plate) were included in the forces measured in the vertical direction and hence mass cancellation was performed in order to remove the effect of these masses. Mass cancellation was performed in the time domain by subtracting the time history of the force on the aluminium plate (the mass of the plate multiplied by the measured acceleration time history) from the time history of the measured force.

5.3 RESULTS

Median responses are mainly shown in the results section. Individual responses are given in Appendix B.

5.3.1 Static forces on the backrest

The static forces that the backs of the subjects exerted on the backrest in the fore-and-aft direction in the four sitting postures were measured without vibration. The static forces were greater in the minimum thigh contact posture than in the feet hanging posture. The medians of the static forces were 42, 44.5, 52.5 and 79.5 N with inter-quartile ranges of 27, 19, 22, and 25.75 N for the feet hanging, maximum thigh contact, average thigh contact and minimum thigh contact postures, respectively. There were statistically significant differences ($p < 0.05$) in the static forces between postures, except between the feet hanging posture and the maximum thigh contact posture ($p = 0.82$). This seems reasonable since the maximum thigh contact posture is similar to the feet hanging

posture except that the feet are just touching the footrest in the maximum thigh contact posture.

5.3.2 Response in the vertical direction

5.3.2.1 Apparent mass at the seat

In both sessions, the vertical apparent mass was measured on the seat. The apparent masses of each of the 12 subjects measured in the first session were within 8% of those measured in the second session in all postures over the whole frequency range of interest (0.25 to 20 Hz). There were no significant differences in the resonance frequencies of the 12 subjects measured in the two sessions for any combination of posture and vibration magnitude.

Figure 5.2 compares the vertical apparent masses of the 12 subjects measured at four vibration magnitudes in the average thigh contact posture in the second session using the tri-axial force platform. There was a decrease in both the first and the second resonance frequencies of the body with an increase in vibration magnitude. A similar non-linearity was also evident in the other three postures (Figure 5.3). Significant differences were found between the resonance frequencies of the apparent mass measured at different vibration magnitudes ($p < 0.05$; except between 0.125 and 0.25 ms^{-2} r.m.s. in both the maximum thigh contact posture and the minimum thigh contact posture, and between 0.625 and 1.25 ms^{-2} r.m.s. in the average thigh contact posture). The effect of changing the height of the footrest on the apparent mass magnitude was the same as that found in Chapter 4; the apparent mass magnitude on the seat decreased with increasing footrest height and decreasing the body mass on the seat.

Further statistical analysis investigated whether subject posture affected the size of the change in the resonance frequency between the two lower vibration magnitudes (i.e. 0.125 and 0.25 ms^{-2} r.m.s.) and between the two higher vibration magnitudes (i.e. 0.625 and 1.25 ms^{-2} r.m.s.). The results indicated no significant difference in the change of the resonance frequency between postures between the two lower vibration magnitudes and the two higher vibration magnitudes.

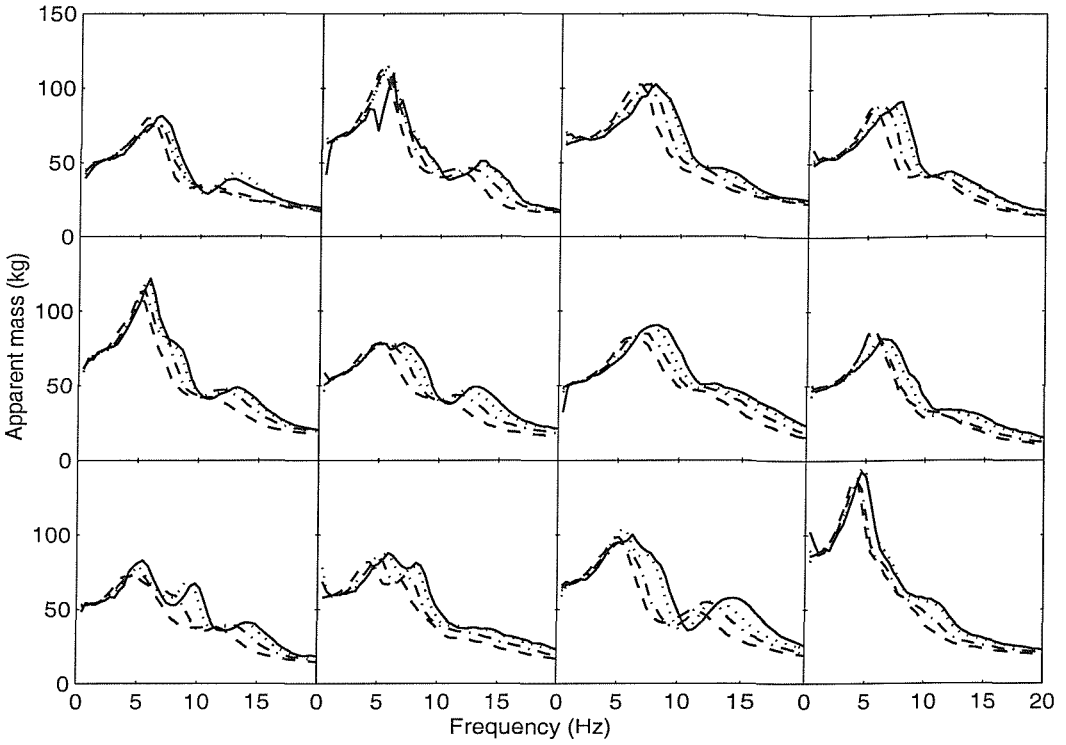

Figure 5.2 Apparent masses of 12 subjects measured in the average thigh contact posture at four vibration magnitudes. ———, 0.125 ms^{-2} r.m.s.; ·····, 0.25 ms^{-2} r.m.s.; –·–·–, 0.625 ms^{-2} r.m.s.; – – – –, 1.25 ms^{-2} r.m.s.

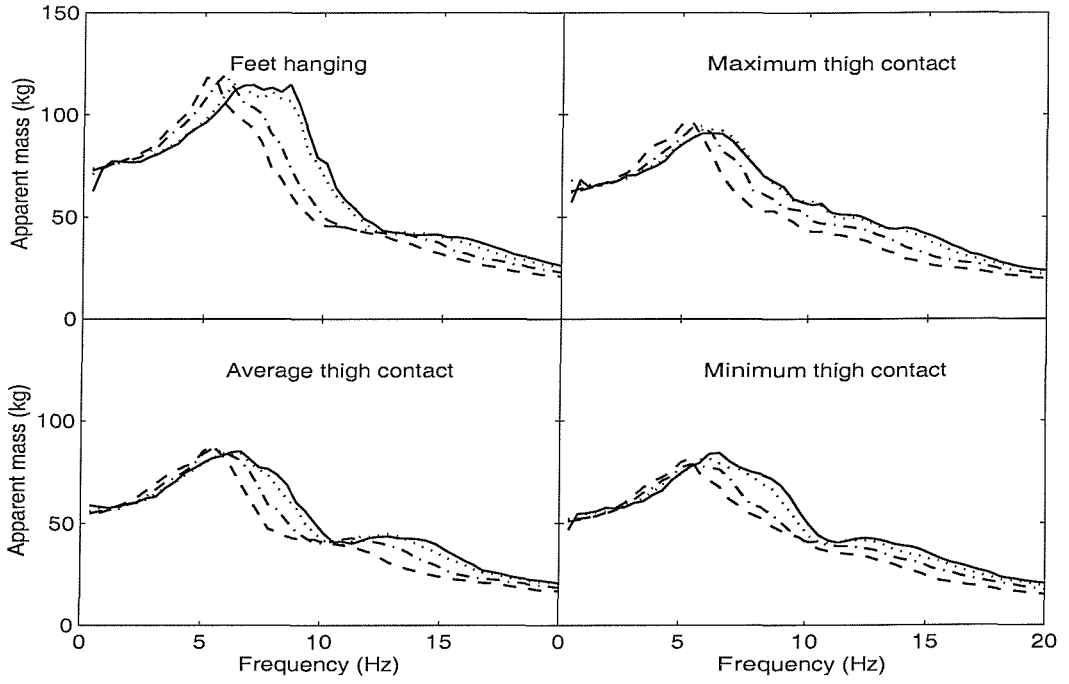

Figure 5.3 Median apparent mass of 12 subjects in the vertical direction: effect of vibration magnitude. ———, 0.125 ms^{-2} r.m.s.; ·····, 0.25 ms^{-2} r.m.s.; –·–·–, 0.625 ms^{-2} r.m.s.; – – – –, 1.25 ms^{-2} r.m.s.

5.3.2.2 Apparent mass at the back

Figure 5.4 shows the inter-subject variability in the vertical apparent mass measured in four sitting postures at the backrest during exposure to 1.25 ms^{-2} r.m.s. There is high subject variability, with a resonance frequency in the vicinity of 5 Hz. The forces produced at the back in the vertical direction were small relative to those at the seat in the vertical direction.

Apparent masses at the backs of 12 subjects adopting the minimum thigh contact posture show resonance frequencies in the range 5 to 7 Hz (depending on the subject and vibration magnitude), with some subjects having two resonances in this range (Figure 5.5). The second resonance appears more pronounced at low vibration magnitudes. There seemed to be a small effect of vibration magnitude on apparent mass at frequencies less than the principal resonance frequency and at high frequencies. At other frequencies, the vertical apparent mass measured at the back decreased with an increase in vibration magnitude. The resonance frequency also decreased with increasing vibration magnitude. The same effect was seen in all four postures (Figure 5.6).

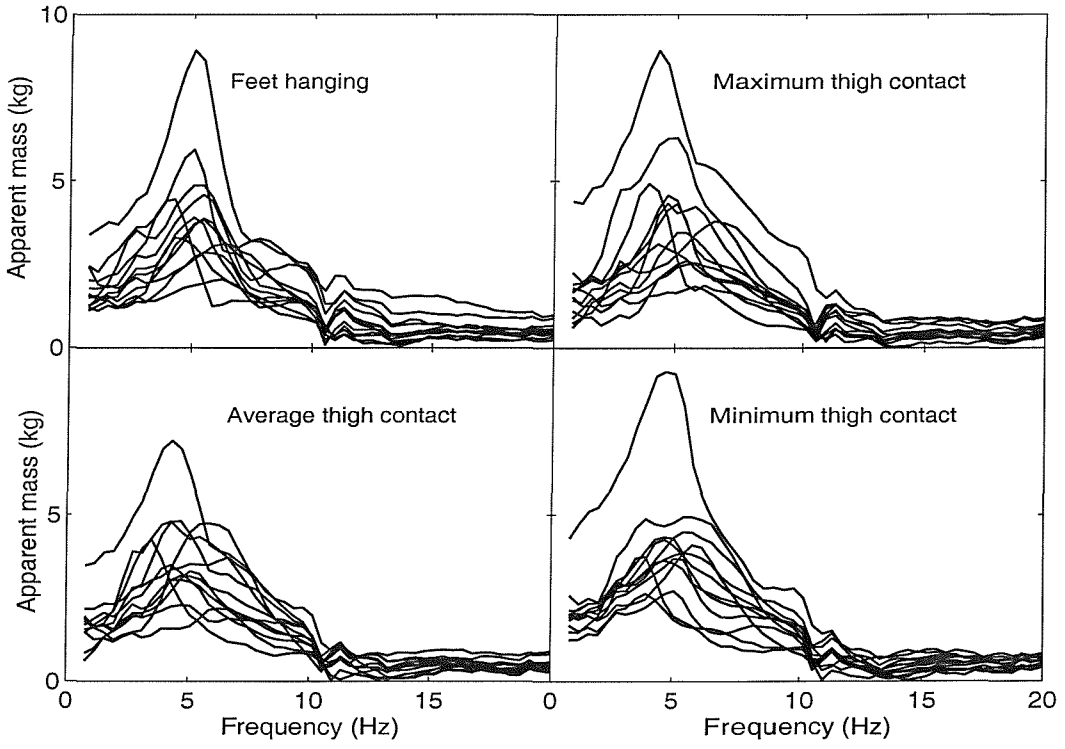

Figure 5.4 Inter-subject variability in the apparent mass measured at the back in the vertical direction for each posture at 1.25 ms^{-2} r.m.s.

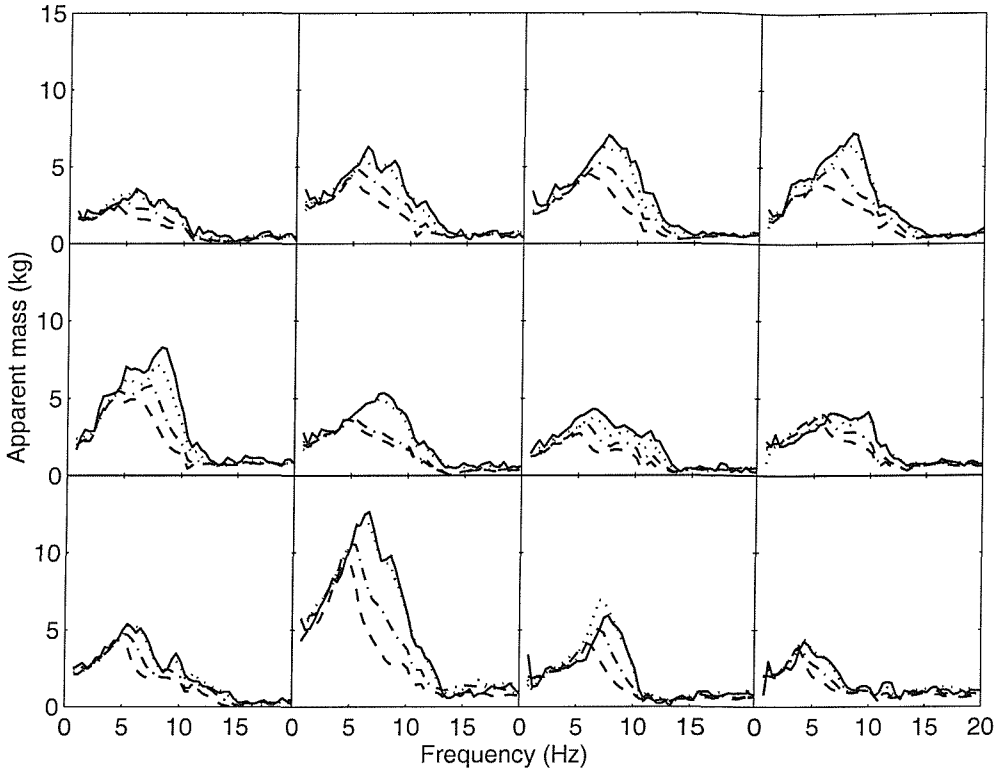

Figure 5.5 Vertical apparent masses of 12 subjects measured at the back in the minimum thigh contact posture at four vibration magnitudes. ———, 0.125 ms^{-2} r.m.s.; ·····, 0.25 ms^{-2} r.m.s.; –·–·–, 0.625 ms^{-2} r.m.s.; – – – –, 1.25 ms^{-2} r.m.s.

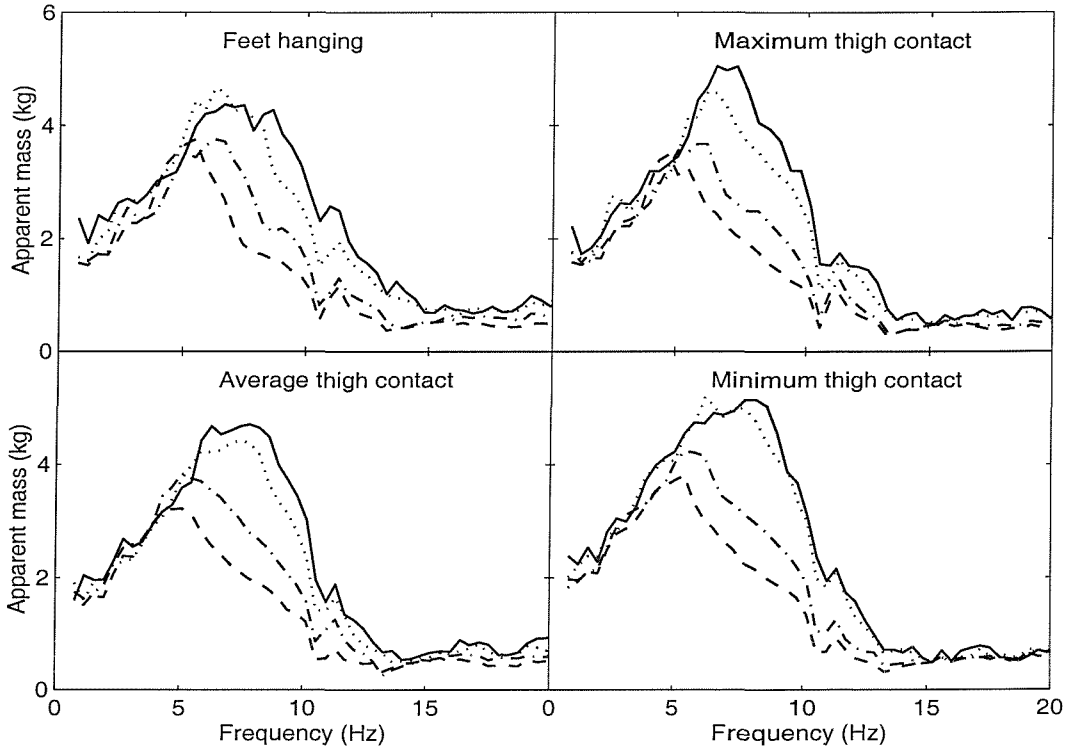

Figure 5.6 Median apparent mass of 12 subjects measured at the back in the vertical direction: effect of vibration magnitude. ———, 0.125 ms^{-2} r.m.s.; ·····, 0.25 ms^{-2} r.m.s.; –·–·–, 0.625 ms^{-2} r.m.s.; – – – –, 1.25 ms^{-2} r.m.s.

Statistical analysis showed significant reductions in the resonance frequencies with increases in vibration magnitudes for all postures ($p < 0.05$; except between 0.125 and 0.25 ms^{-2} r.m.s. in the average thigh contact posture). No significant differences were found between the apparent masses at resonance measured with 0.125 and 0.25 ms^{-2} r.m.s. in any posture. In the feet hanging posture there were no significant differences between the apparent masses at resonance measured with 0.625 and 1.25 ms^{-2} r.m.s.

Statistical analysis showed no significant difference between postures in the resonance frequencies of apparent mass in the vertical direction at the back at any vibration magnitude (except between the feet hanging posture and the maximum thigh contact posture at 0.25 ms^{-2} r.m.s. and between the feet hanging posture and the average thigh contact posture at 1.25 ms^{-2} r.m.s.). The apparent mass at resonance showed a statistically significant difference only between the average thigh contact posture and the minimum thigh contact posture at 0.625 ms^{-2} r.m.s.

5.3.3 Response in the fore-and-aft direction

5.3.3.1 Response at the seat

The cross-axis apparent masses of the 12 subjects measured in the fore-and-aft direction on the seat during vertical excitation show high values (Figures 5.7 and 5.8). The principal resonance frequency, around 5 Hz, decreased with increasing vibration magnitude. A second resonance frequency, between 10 to 15 Hz, is also clear in most of the individual data (in the posture shown in Figure 5.7 and in the other three postures).

There were significant differences between the principal resonance frequencies measured at the four vibration magnitudes in all postures (except between 0.125 and 0.25 ms^{-2} r.m.s. in the feet hanging posture and in the minimum thigh contact posture). Statistical analysis showed no significant differences ($p > 0.05$) between the cross-axis apparent mass at resonance (except between 0.125 and 1.25 ms^{-2} r.m.s. between 0.25 and 1.25 ms^{-2} r.m.s. and between 0.625 and 1.25 ms^{-2} r.m.s. in the feet hanging posture, and between 0.625 and 1.25 ms^{-2} r.m.s. in the maximum thigh contact posture, average thigh contact posture and minimum thigh contact posture).

There were no statistically significant differences in the cross-axis apparent mass at resonance between the feet hanging posture and the minimum thigh contact posture at any vibration magnitude. Similarly, there were no significant differences between the average thigh contact posture and the maximum thigh contact posture.

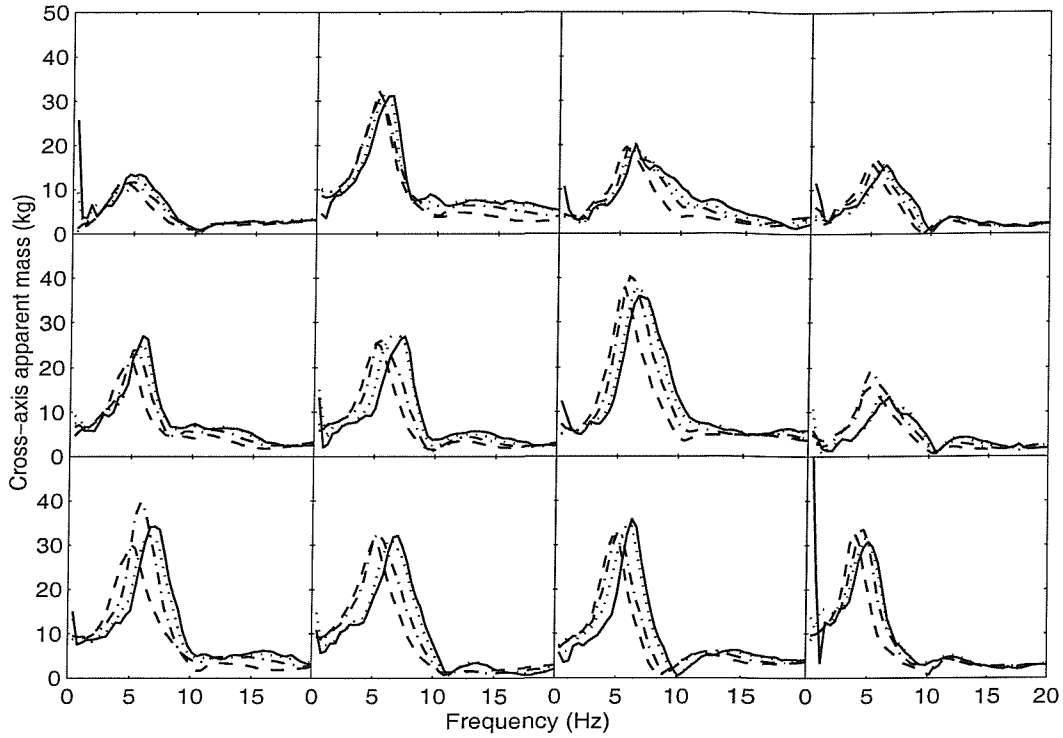

Figure 5.7 Fore-and-aft cross-axis apparent masses of 12 subjects measured on the seat in the minimum thigh contact posture at four vibration magnitudes. ———, 0.125 ms^{-2} r.m.s.; ·····, 0.25 ms^{-2} r.m.s.; –·–·–, 0.625 ms^{-2} r.m.s.; – – – –, 1.25 ms^{-2} r.m.s.

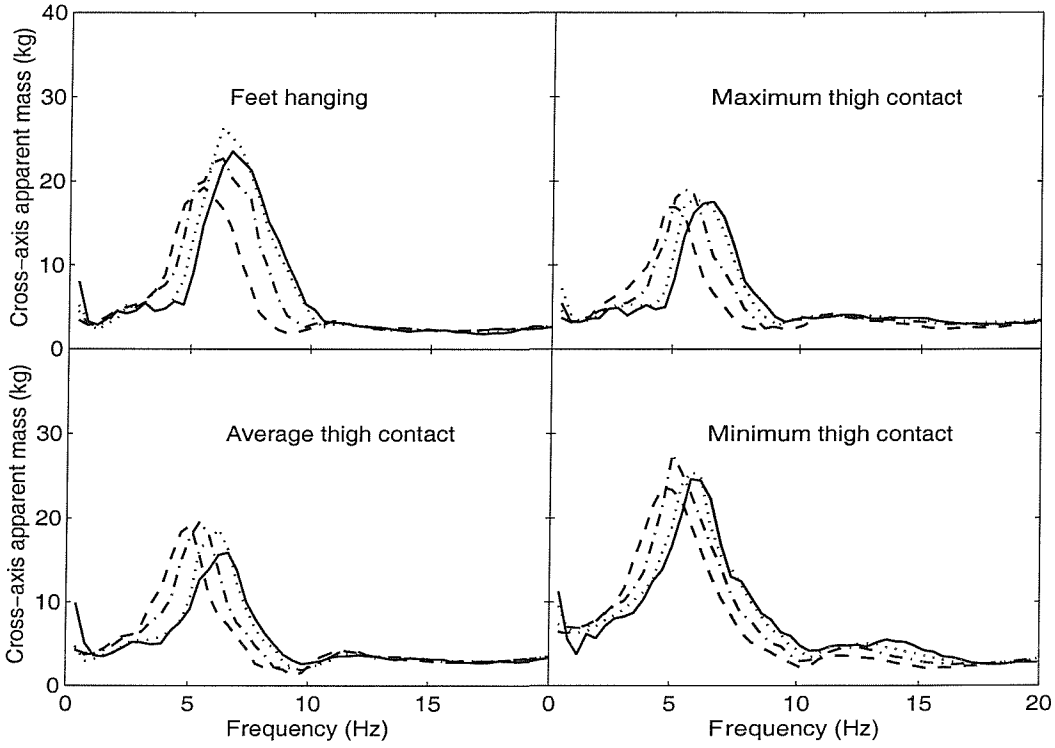

Figure 5.8 Median fore-and-aft cross-axis apparent mass of 12 subjects measured on the seat: effect of vibration magnitude. ———, 0.125 ms^{-2} r.m.s.; ·····, 0.25 ms^{-2} r.m.s.; –·–·–, 0.625 ms^{-2} r.m.s.; – – – –, 1.25 ms^{-2} r.m.s.

5.3.3.2 Response at the backrest

The cross-axis apparent mass in the fore-and-aft direction at the backrest showed high inter-subject variability in all postures, especially at frequencies below 10 Hz (Figure 5.9). Some subjects showed a first resonance frequency in the range 2 to 3 Hz, but all subjects showed a higher resonance frequency, in the range 5 to 10 Hz depending on the subject and vibration magnitude, with a few subjects showing two resonance frequencies in the 5 to 10 Hz range (Figures 5.10 and 5.11).

The fore-and-aft cross-axis apparent mass at the back is non-linear. Statistical analysis showed significant differences between the resonance frequencies (around 5 Hz) measured at four vibration magnitudes (except between 0.125 and 0.25 ms^{-2} r.m.s. in the feet hanging posture). There were significant differences in the fore-and-aft cross-axis apparent mass at resonance between 0.125 and 0.625 ms^{-2} in the maximum thigh contact posture and between 0.125 and 0.25 ms^{-2} and 0.125 and 1.25 ms^{-2} in the minimum thigh contact posture.

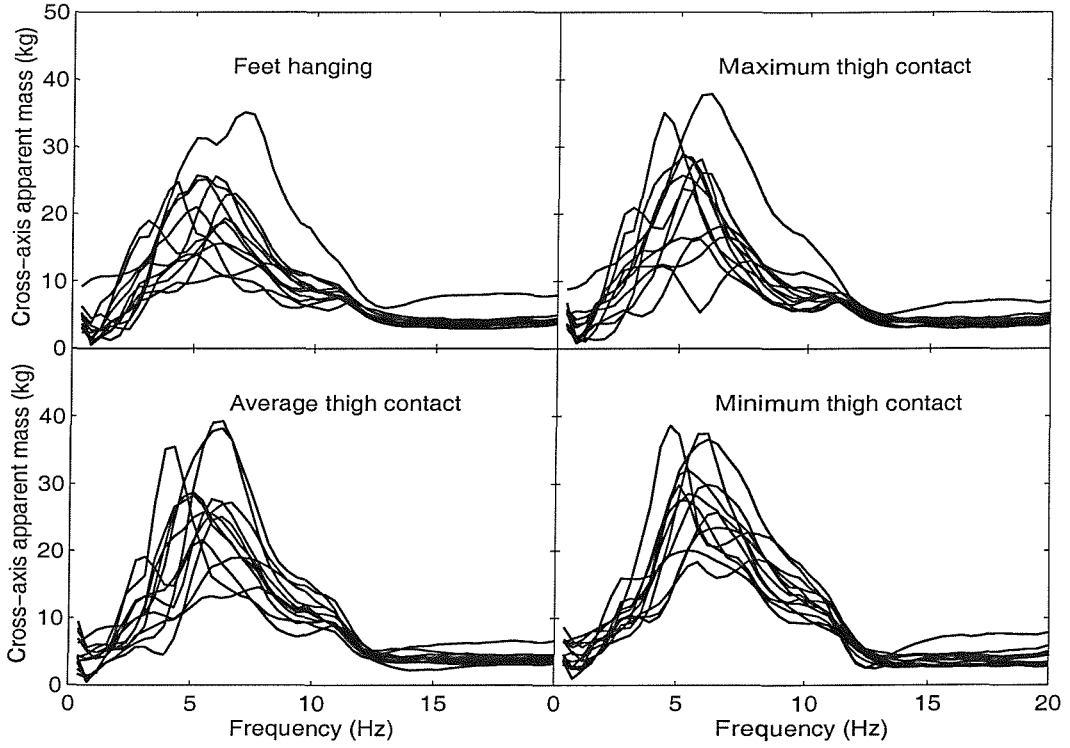

Figure 5.9 Inter-subject variability in the fore-and-aft cross-axis apparent mass measured at the back for each posture at 1.25 ms^{-2} r.m.s.

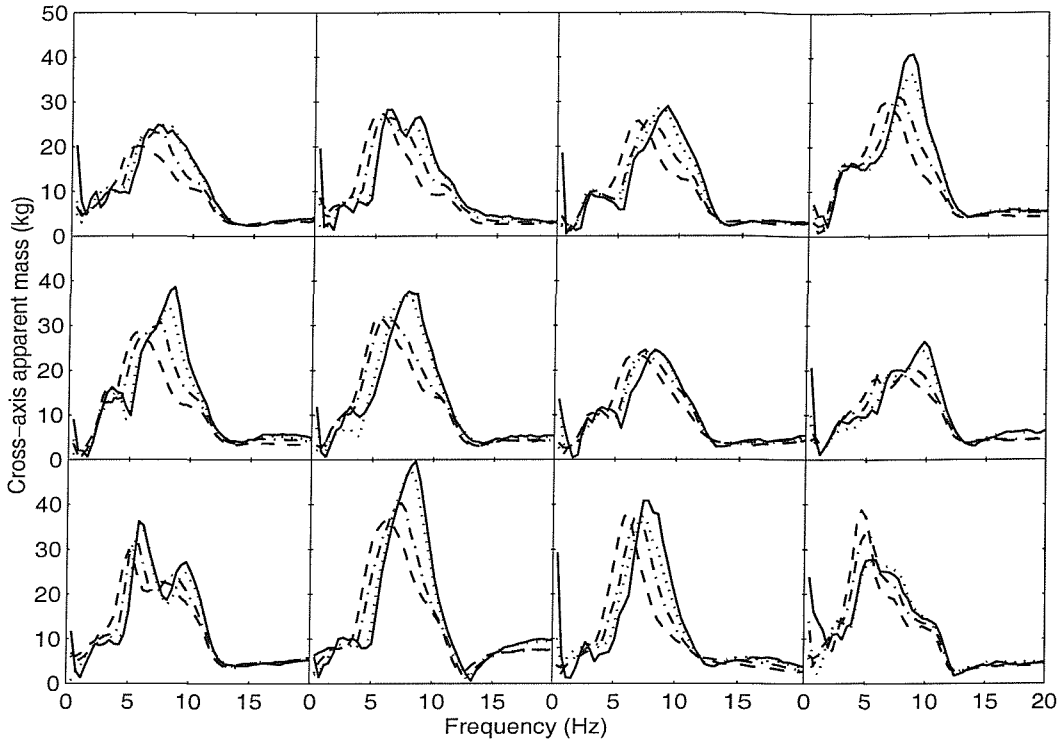

Figure 5.10 Fore-and-aft cross-axis apparent masses of 12 subjects measured at the back in the minimum thigh contact posture at four vibration magnitudes. ———, 0.125 ms^{-2} r.m.s.; ·····, 0.25 ms^{-2} r.m.s.; –·–·–, 0.625 ms^{-2} r.m.s.; – – – –, 1.25 ms^{-2} r.m.s.

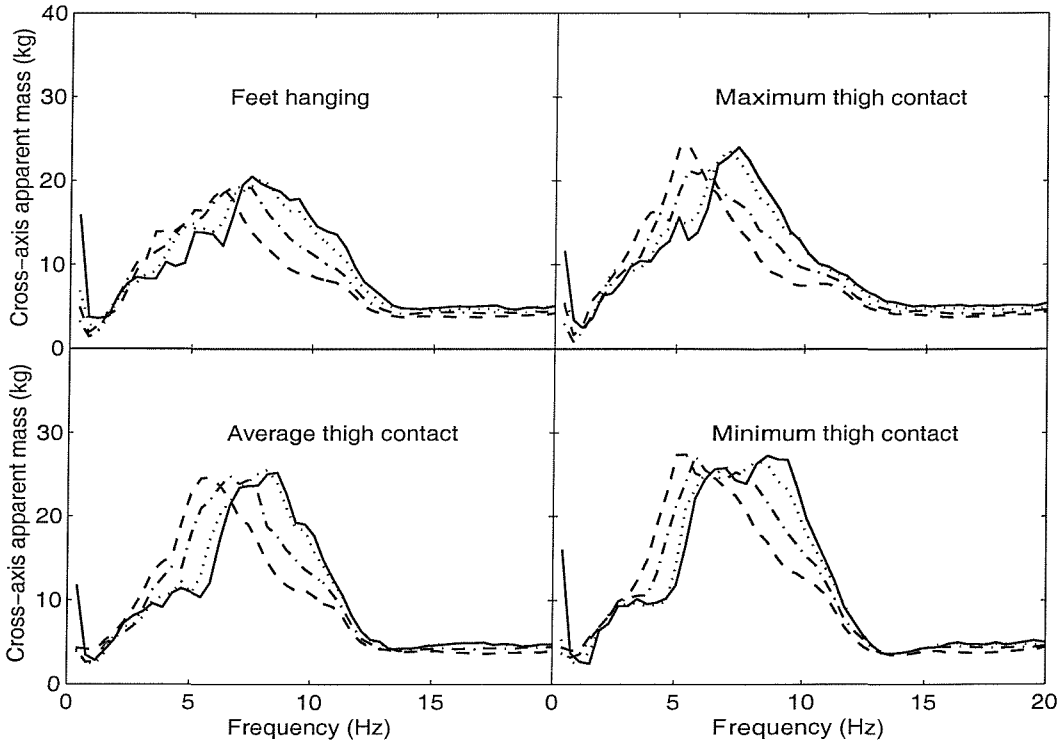

Figure 5.11 Median fore-and-aft cross-axis apparent mass of 12 subjects measured at the back: effect of vibration magnitude. ———, 0.125 ms^{-2} r.m.s.; ·····, 0.25 ms^{-2} r.m.s.; –·–·–, 0.625 ms^{-2} r.m.s.; – – – –, 1.25 ms^{-2} r.m.s.

Figure 5.12 indicates that below 3 Hz and above 10 Hz, there was little effect of posture on fore-and-aft cross-axis apparent mass at the back. However, around the resonance frequency, the fore-and-aft cross-axis apparent mass increased with increasing contact between the back and the backrest (see Section 5.3.1). Statistically significant differences were found in the magnitude of the fore-and-aft cross-axis apparent mass at resonance between the minimum thigh contact posture and both the feet hanging posture and the maximum thigh contact posture at all vibration magnitudes. Significant differences were also found between the average thigh contact posture and the feet hanging posture at all vibration magnitudes.

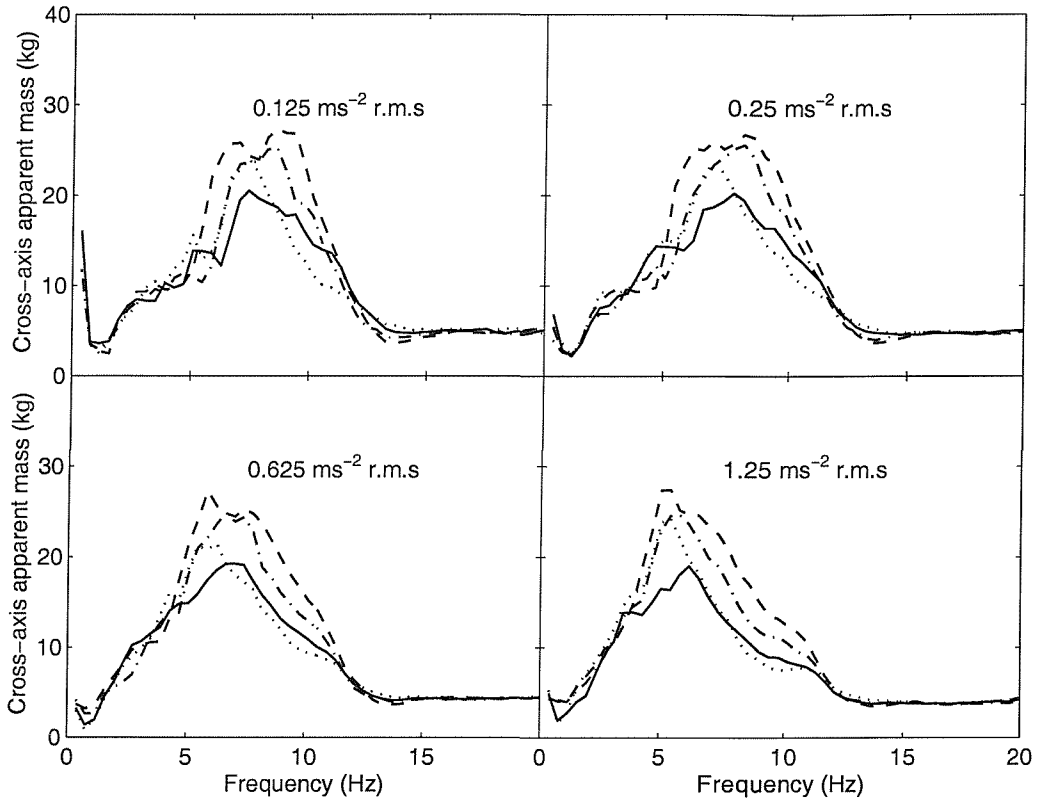

Figure 5.12 Median fore-and-aft cross-axis apparent mass of 12 subjects measured at the back: effect of posture. ———, feet hanging; ·····, maximum thigh contact; –·–·–·–, average thigh contact; – – – –, minimum thigh contact.

5.3.4 Response in the lateral direction at the seat and backrest

The median lateral cross-axis apparent mass at the seat and backrest were small in all postures and at all vibration magnitudes (Figures 5.13 and 5.14) but in excess of the 'noise' measured with no subject (between 0 and 0.3 kg). Although the forces are small, the cross-axis apparent mass tends to decrease with increasing vibration magnitude, showing the same non-linear behaviour apparent in other axes.

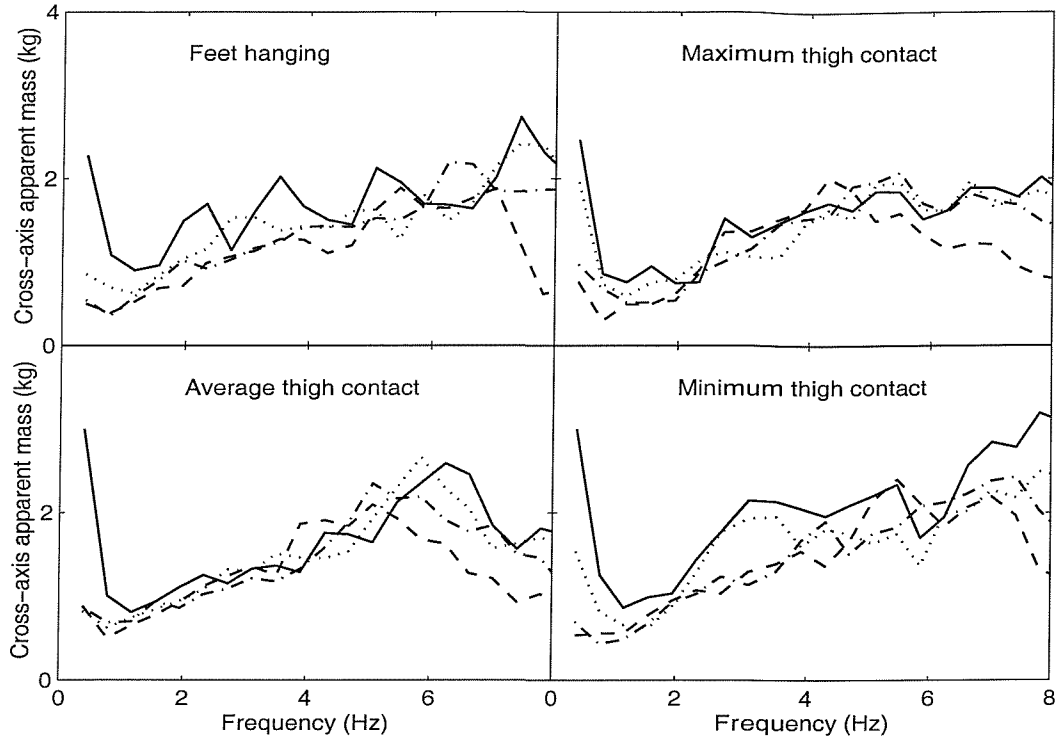

Figure 5.13 Median lateral cross-axis apparent mass of 12 subjects measured on the seat: effect of vibration magnitude. ———, 0.125 ms^{-2} r.m.s.; ·····, 0.25 ms^{-2} r.m.s.; –·–·–, 0.625 ms^{-2} r.m.s.; – – – –, 1.25 ms^{-2} r.m.s.

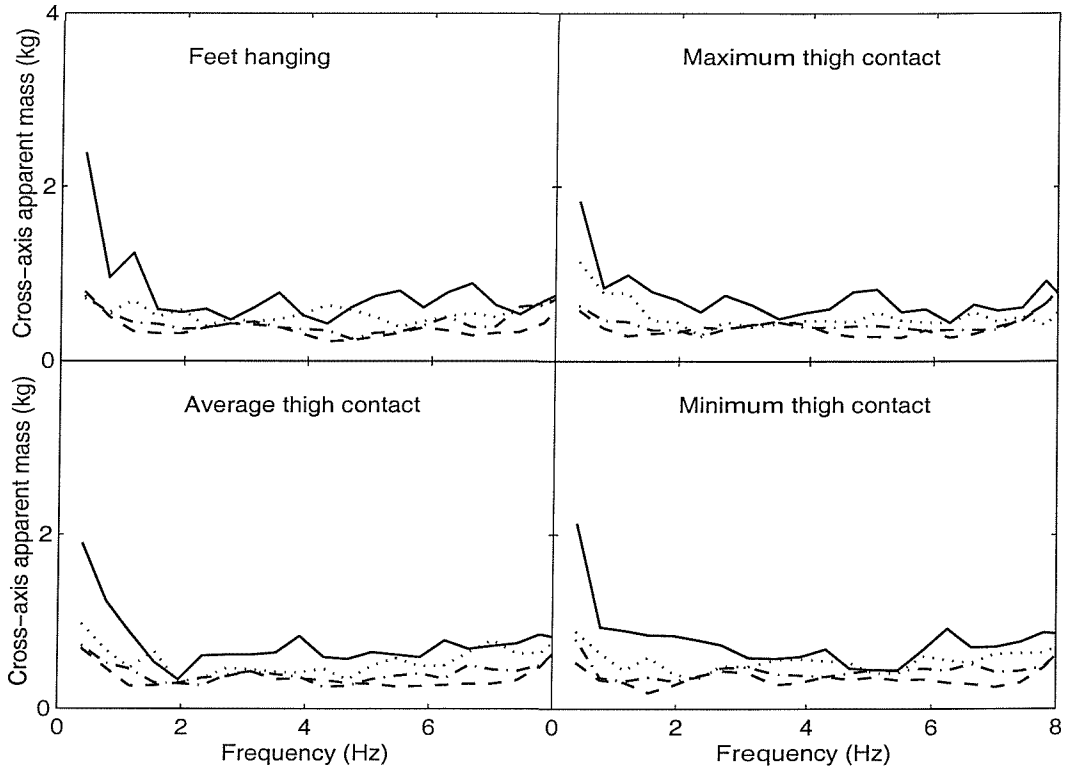

Figure 5.14 Median lateral cross-axis apparent mass of 12 subjects measured at the back: effect of vibration magnitude. ———, 0.125 ms^{-2} r.m.s.; ·····, 0.25 ms^{-2} r.m.s.; –·–·–, 0.625 ms^{-2} r.m.s.; – – – –, 1.25 ms^{-2} r.m.s.

5.3.5 Correlation with body characteristics

The resonance frequency and apparent mass at resonance in the vertical direction at the back, and the resonance frequency and cross-axis apparent mass in the fore-and-aft direction at the back measured at 1.25 ms^{-2} r.m.s. were investigated to determine whether they were correlated with body characteristics (mass, sitting mass, height and ratio of mass to height) or the static force measured at the back. In the vertical direction at the back, positive correlations were found between the body characteristics and the magnitudes at resonance as well as between the static force and the magnitude at resonance, although these were statistically significant only for the body mass ($p = 0.036$) and the sitting mass ($p = 0.007$) in the average thigh contact posture. The increased correlation with the sitting masses, as opposed to the total masses, of the subjects suggests that the upper-body caused the correlation in this posture. There were generally negative correlations, although not statistically significant, between the body characteristics and the resonance frequencies of the vertical apparent mass at the back.

Correlations between the resonance magnitudes of the fore-and-aft cross-axis apparent mass at the back and the body characteristics were, generally, positive although statistically significant only with the heights of the subjects in the average thigh contact posture ($p = 0.011$). There was also a negative correlation, although significant only in the feet hanging posture ($p = 0.002$), between the masses of the subjects and their resonance frequencies for fore-and-aft cross-axis apparent mass at the back.

5.4 DISCUSSION

5.4.1 Response in the vertical direction

The apparent masses measured on the seat in the vertical direction were compared with those obtained without a backrest in Chapter 4. The median apparent masses of 11 of the same subjects used in the two studies with and without a backrest at 1.25 ms^{-2} r.m.s. are shown in Figure 5.15. At low frequencies (less than 4 Hz), statistically significant differences were found between the apparent masses measured with backrest and the apparent masses measured without backrest in all postures (first column, Table 5.1). At frequencies above about 4 Hz, the difference in the apparent mass measured with and without a backrest was significant in some frequency ranges ($p < 0.05$) and insignificant in others (Table 5.1). The effect of the backrest on the apparent mass is more pronounced when the contact between the body and the backrest increased as the feet were raised to the average thigh contact posture and the minimum thigh contact postures (see last two columns in Table 5.1).

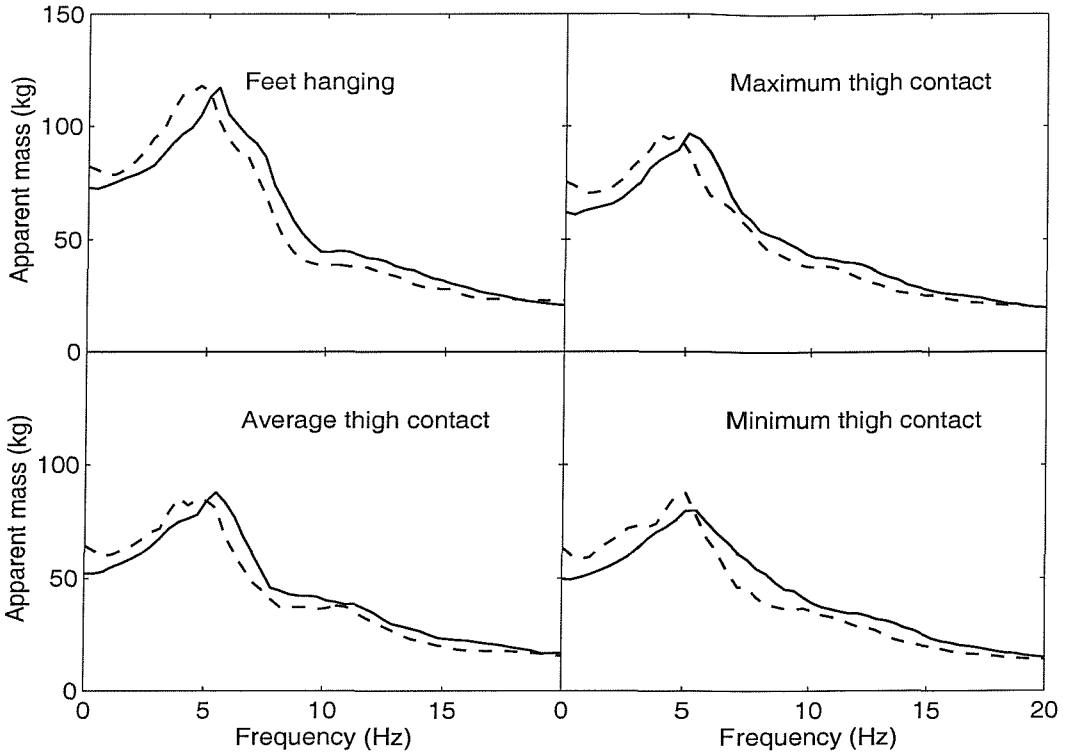

Figure 5.15 Median vertical apparent mass of 11 subjects measured on the seat at 1.25 ms^{-2} r.m.s. in four sitting postures: effect of backrest. ———, with backrest; – – – –, without backrest.

Table 5.1 Ranges of frequencies where there was, or was not, a statistically significant difference between the vertical apparent mass measured on the seat with and without backrest. (Significant differences occur at $p < 0.05$).

Posture	Frequency range (Hz)		Out of 52 frequencies	
	Significant difference	Non-significant difference	Significant difference	Non-significant Difference
Feet hanging	0.39 – 4.29 7.02 – 9.75 12.09 – 14.04	4.68 – 6.63 10.14 – 11.70 14.43 – 20.0	25	27
Maximum thigh contact	0.39 – 4.29 7.02 – 14.04	4.68 – 6.63 14.43 – 20.0	30	22
Average thigh contact	0.39 – 4.68 5.85 – 13.65	5.07 – 5.46 14.04 – 20.0	33	19
Minimum thigh contact	0.39 – 4.68 7.02 – 18.33	5.07 – 6.63 18.72 – 20.0	42	10

Since the human body moves as a rigid body at very low frequencies, the vertical forces measured on the seat without a backrest may be expected to be the same as the vector addition of the vertical forces measured on the seat and the backrest when using the backrest. This hypothesis was tested in all postures at 0.78 Hz and 0.25 ms^{-2} r.m.s. In all postures, there were no significant differences ($p > 0.05$) between the apparent mass measured on the seat without a backrest and the apparent mass obtained from adding the forces on the seat and backrest in the vertical direction at 0.78 Hz at 0.25 ms^{-2} r.m.s.

The median results show a tendency for the resonance frequency to increase with the use of a backrest (Figure 5.15). This increase in the resonance frequency was explained previously (e.g. Fairley and Griffin, 1989) as an increase in body stiffness when in contact with a backrest. Statistical analysis showed significant difference ($p < 0.05$) in the resonance frequency of the apparent mass measured at 1.25 ms^{-2} r.m.s. with and without a backrest in all sitting postures, except in the minimum thigh contact posture. In the minimum thigh contact posture, and when not using a backrest, the subjects needed to tense their muscles to keep the upright posture.

Significant correlations ($p \leq 0.03$) were found between the resonance frequencies measured with a backrest and the resonance frequencies measured without a backrest in all postures and at all vibration magnitudes, except at 0.125 ms^{-2} r.m.s. in the feet hanging posture and at 0.25 and 0.625 ms^{-2} r.m.s. in the minimum thigh contact posture. Significant correlations ($p \leq 0.047$) were also found between the apparent mass at resonance measured with and without a backrest, except at 0.125 and 0.25 ms^{-2} r.m.s. in the feet hanging posture. These correlations may be used to predict the resonance frequency and apparent mass at resonance that would be obtained with a backrest in studies conducted without a backrest.

The vertical apparent masses measured at the back were small and varied across subjects from 5 kg to 10 kg in the frequency range 5 to 7 Hz. This peak is at a frequency similar to the peak in the vertical transmissibility to the spine (to T1, T6, T11, L3, and S2) and the pelvis (Matsumoto and Griffin, 1998a; Kitazaki, 1994). The vertical forces measured at the back arise from the vertical force applied at the backs of the subjects by the vertical movement of the backrest as well as from the pitch movement, expansion and contraction of the upper body produced by the vertical oscillation of the body. If the backrest had been stationary, only a friction force would have been produced to oppose the motion in the vertical direction. If an inclined backrest had been used, vertical force on the backrest would have arisen from the mass of the parts of the upper body supported

on the backrest as well as from the pitching movements of the upper body. In this case, the total vertical force on the backrest would depend on the phase between the forces produced by the mass on the backrest and the forces produced by the upper body pitching modes.

The high variability between subjects in the vertical apparent mass at the back could be attributed to several factors. As was seen in Section 5.3.5, there were positive correlations between the total masses and the sitting masses of the subjects and the magnitude of the vertical apparent mass measured at the back. Although no significant correlations were found between the heights of the subjects and the magnitude at resonance of the apparent mass at the back, the location of the point of contact between the back and the backrest could be a source of variability.

In all four postures there was a decrease in the resonance frequencies of the apparent masses of the body with an increase in vibration magnitude. With a backrest, statistical analysis showed no effect of posture on the non-linearity as opposed to the reduced non-linearity in the minimum thigh contact posture when no backrest was used in Chapter 4. Matsumoto and Griffin (2002a) found that increased muscle tension reduce the non-linearity of the body. Possibly, without a backrest, the subjects tensed their muscles to maintain the upright posture in the minimum thigh contact posture but did not need the same muscle tension when a backrest was used.

No significant difference was found in the absolute change in resonance frequency with and without a backrest in any of the cases mentioned above. This means that, although the backrest seemed to increase the stiffness of the body and shift the resonance frequency to higher values, it did not affect the non-linearity of the body. Comparing this with the results of Matsumoto and Griffin mentioned above, one might conclude that the non-linearity is affected by the stiffness of only particular parts of the body.

5.4.2 Response in the fore-and-aft direction

The high forces in the fore-and-aft direction on the seat are consistent with the results of Matsumoto and Griffin (2002a) and the results obtained without a backrest in Chapter 4. These forces may be attributed to rotational modes of the upper body segments. The first resonance frequency, between 5 and 8 Hz, changed with a change of vibration magnitude. The second resonance (a small peak between 10 and 15 Hz) is consistent with a rotational mode of the pelvis and the lower upper-body (T11-L3) found using a biodynamic model with rotational capabilities (see Matsumoto and Griffin, 2001). The

origin of this peak may be the same as that of the small peak in the vertical apparent mass of seated person in the same frequency range.

As was found without a backrest, the feet hanging posture and the minimum thigh contact posture gave the highest forces in the fore-and-aft direction on the seat, possibly due to greater pitching motions in these two postures.

The forces on the seat in the fore-and-aft direction (cross-axis apparent masses) with a backrest were compared with those obtained in Chapter 4 without a backrest (Figure 5.16). Statistical analysis showed significant differences in the cross-axis apparent masses at resonance measured with and without a backrest at every vibration magnitude only in the feet hanging posture and in the maximum thigh contact posture ($p < 0.05$). The presence of the backrest restrained the upper body and helped in reducing the pitching motion that was difficult to reduce without a backrest, especially when the feet were not supported.

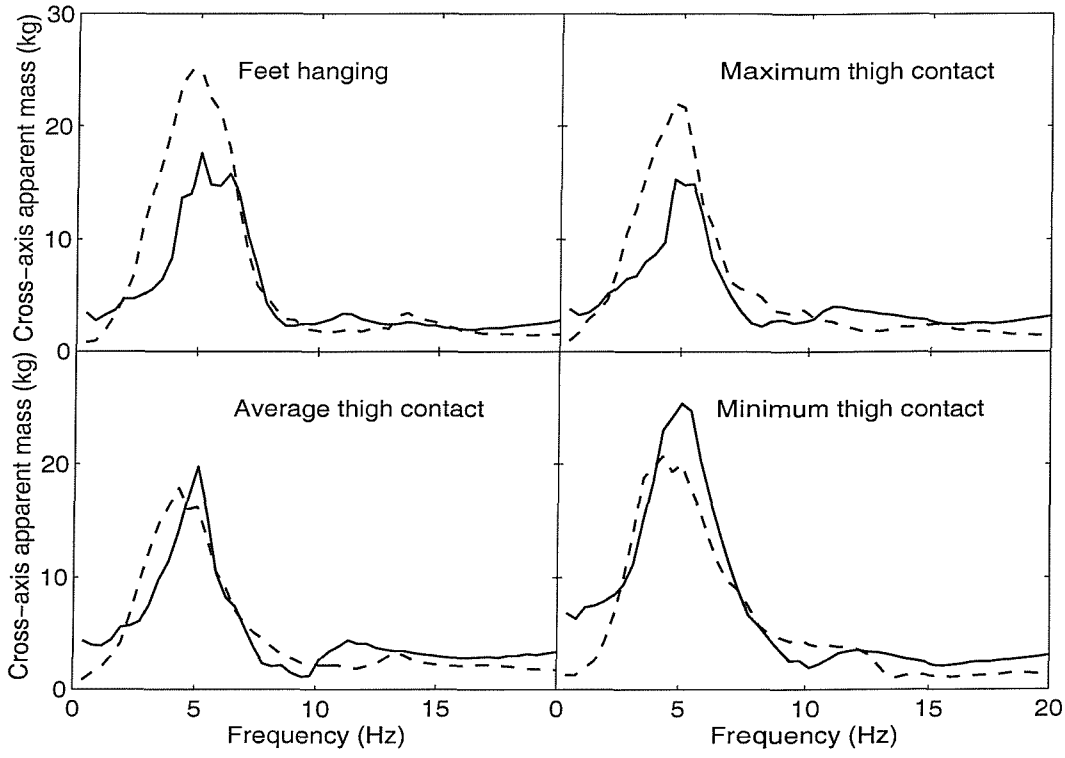

Figure 5.16 Median fore-and-aft cross-axis apparent mass of 11 subjects measured on the seat at 1.25 ms^{-2} r.m.s. in four sitting postures: effect of backrest. ———, with backrest; – – – –, without backrest

There were high forces (i.e. high fore-and-aft cross-axis apparent masses) at the back. Similar to the forces measured in the fore-and-aft direction on the seat, the fore-and-aft forces measured at the back may have arisen from rotational motions of some parts of the body caused by the vertical oscillation of the body (at the seat and at the backrest). The first resonance frequency, which appeared between 2 and 3 Hz, is consistent with a dominant upper-body pitch mode found in this frequency range by Matsumoto and Griffin (2001). It is also consistent with a peak found in the transmission of vertical seat vibration to fore-aft head vibration and in the transmission of vertical seat vibration to horizontal motion of the third lumbar vertebra (Paddan and Griffin, 1988a; Kitazaki and Griffin, 1994; Matsumoto and Griffin, 1998a). A peak in the same frequency range was more pronounced in the fore-and-aft motion of the head during fore-and-aft seat vibration than during vertical seat vibration (Paddan and Griffin, 1988b). In the present study, a vertical force was applied by the backrest on the backs of the subjects; this may have caused the upper body to pitch, producing a fore-and-aft vibration in the head-neck system. Similarly, pitch motion of the body resulting from vertical oscillation will have produced a horizontal force to the head-neck system. The second mode between 5 and 10 Hz is consistent with horizontal motions of the spine at this frequency (e.g. Kitazaki, 1994).

The cross-axis apparent mass at the back in the fore-and-aft direction was greater when there was greater contact force between the backs of the subjects and the backrest (i.e. the minimum thigh contact posture). This trend for increased cross-axis apparent mass with increased static force is similar to the increase in apparent mass on the seat with heavier subjects. In postures where the feet were more supported on the footrest (and there was increased static force on the backrest) there would have been a force from the feet to react to the pitch movement during vibration, and so push the upper body against the backrest, which may have increased the dynamic force on the backrest in the fore-and-aft direction.

The oscillatory fore-and-aft forces at the back (caused by solely vertical vibration) may be a source of discomfort. Studies have shown that fore-and-aft oscillation of a backrest causes discomfort (e.g. Parsons *et al.*, 1982) but oscillatory force without motion has not been investigated.

5.4.3 Response in the lateral direction

Lateral forces measured on the backrest and on the seat were small in comparison to the forces measured in the vertical and fore-and-aft directions. Furthermore, there were no large changes in forces at the seat with and without a backrest (see Figure 5.17). The

high inter-subject variability indicates that, although the human body is roughly symmetrical in the mid-sagittal plane, some roll or yaw oscillation may have occurred and produced a lateral force. This is consistent with measurements of the transmission of vertical seat vibration to lateral, roll, and yaw motion at the head (Paddan and Griffin, 1988a).

The forces measured in this study were obtained with a rigid seat and a rigid backrest. Cushioned seats and backrests may modify the results. For example, whereas a rigid backrest tends to prevent movement at the back, a compliant backrest will allow fore-and-aft movement of the back.

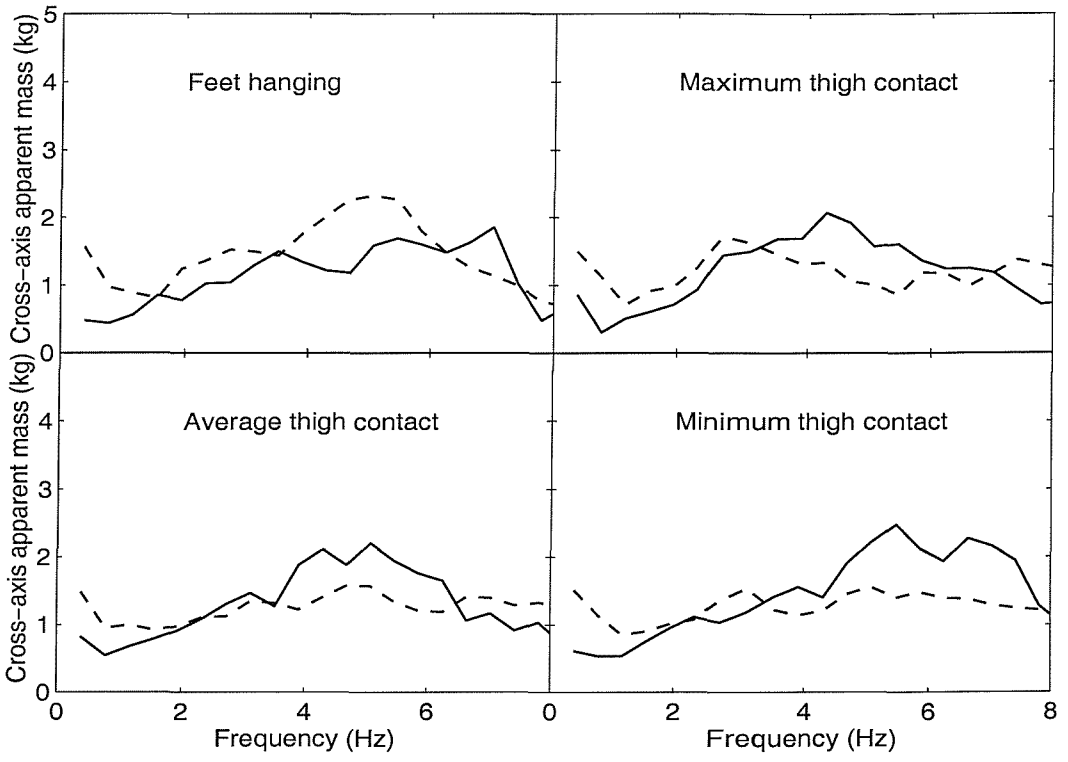

Figure 5.17 Median lateral cross-axis apparent mass of 11 subjects measured on the seat at 1.25 ms^{-2} r.m.s. in four sitting postures: effect of backrest. ———, with backrest; – – – –, without backrest

5.5 CONCLUSIONS

During vertical whole-body vibration, in addition to vertical forces at the seat, there are high forces in the fore-and-aft direction on the seat and backrest (could reach up to 30 to 50% of the static mass of some subjects). Forces in the lateral direction were small, compared to the fore-and-aft forces, as were forces in the vertical direction on the

backrest. Forces in all directions showed a similar non-linear response characterised by decreases in resonance frequencies with increases in vibration magnitude. The presence of the backrest modified the forces in the fore-and-aft and vertical direction on the supporting seat surface. The high forces at the backrest as well as on the seat in directions other than the direction of excitation merit further investigation for their effect on dynamic models of seat-person systems.

CHAPTER 6 FORCES AT THE SEAT AND FOOTREST DURING FORE-AND-AFT WHOLE-BODY EXCITATION

6.1 INTRODUCTION

Horizontal vibration can be dominant in some vehicles such as tractors, earth-moving machines and trains (Griffin, 1990; Lundström and Lindberg, 1983). However, few studies have reported biodynamic responses of the human body to horizontal vibration.

Some measures of the driving point response of the seated body to horizontal vibration have been reported (e.g. Fairley and Griffin, 1990; Holmlund and Lundström, 1998; Mansfield and Lundström, 1998; Mansfield and Lundström, 1999). As was shown in Chapter 2, there is some inconsistency in the modes reported to be associated with horizontal vibration but three vibration modes have been suggested. The first is below 1 Hz, the second is between 1 and 3 Hz, and the third has a resonance around 5 Hz. Only Fairley and Griffin (1990) investigated frequencies below 1 Hz and, hence, only their study reported a mode below 1 Hz.

With an increase in vibration magnitude, in both the fore-and-aft and lateral directions, Fairley and Griffin (1990) noticed a decrease in the resonance frequency of the second mode, but not the first mode. Holmlund and Lundström (1998) noticed the same effect on the frequency of the second mode (they did not measure the first mode), but only in the fore-and-aft direction. Mansfield and Lundström (1999) reported a decrease in the frequency of both the second and the third mode with an increase in vibration magnitude.

This chapter presents two experimental studies of the responses of seated subjects to whole-body fore-and-aft excitation. In the first experiment forces on the seat in the fore-and-aft, vertical and lateral directions were measured. In the second experiment, forces at the feet in the fore-and-aft and vertical directions were measured. It was hypothesised that significant forces would be found in the fore-and-aft and vertical directions on the seat and footrest but with less force in the lateral direction. It was also hypothesised that the response at the feet would depend on the body posture, and that forces at both the seat and the feet would be non-linear.

6.2 APPARATUS, EXPERIMENTAL DESIGN AND ANALYSIS

6.2.1 Apparatus

Two separate experiments were conducted to measure the dynamic responses at the seat and the feet of seated subjects. In both experiments, subjects were exposed to fore-and-aft whole-body vibration using an electro-hydraulic vibrator capable of producing peak-to-peak displacements of 1 metre. A rigid seat and an adjustable footrest (to give different foot heights) were mounted on the platform of the vibrator. A force plate (Kistler 9281 B) capable of measuring forces in three directions simultaneously was secured to the supporting surface of the seat (in the first experiment) and the feet (in the second experiment) in order to measure forces in the vertical, fore-and-aft, and lateral directions. The force plates are described in Chapter 3. Signals from the force platform were amplified using Kistler 5007 and Kistler 5001 charge amplifiers. Acceleration was measured at the centre of the force platform in each experiment using piezo-resistive accelerometers (Entran EGCSY-240D-10). The signs of the fore-and-aft acceleration and fore-and-aft force were positive in the forward direction. In the vertical direction, the force was positive in the upward direction. All signals were acquired at 200 samples per second via 67 Hz anti-aliasing filters with an attenuation rate of 70 dB in the first octave.

6.2.2 Experimental design

6.2.2.1 First experiment

Twelve male subjects with average age 31.1 years (range 24 to 47 years), weight 77.5 kg (range 63 to 106 kg), and stature 1.79 m (range 1.68 to 1.91 m), were exposed to random fore-and-aft vibration with an approximately flat constant bandwidth acceleration power spectrum over the frequency range 0.25 to 20 Hz. The age, weight and height of the subjects participated in the experiment are given in Appendix C. The same four sitting postures as those used during vertical excitation (Chapter 4) were used here. The postures are shown again in Figure 6.1 for convenience. A footrest was supported on the vibrator platform and therefore exposed to the same fore-and-aft vibration as the seat. The subjects placed their hands in their laps. No backrest was used in the first experiment.

In each sitting posture, the twelve subjects were exposed to four vibration magnitudes (0.125, 0.25, 0.625, and 1.25 ms^{-2} r.m.s.). The presentation of the four postures and the four vibration magnitudes was balanced across subjects. Each vibration exposure lasted 60 seconds.

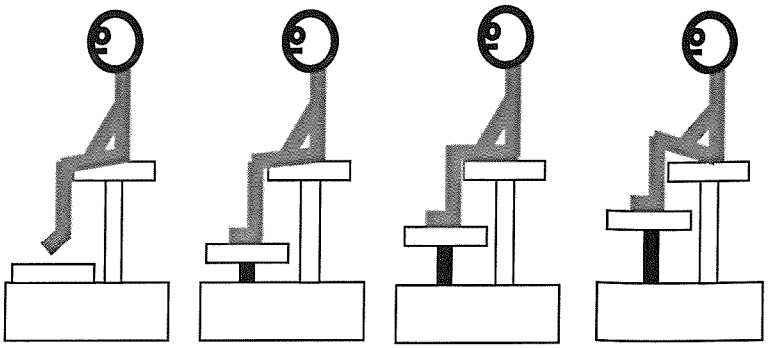

Figure 6.1 Schematic diagrams of the four sitting postures: (a) feet hanging; (b) maximum thigh contact; (c) average thigh contact; (d) minimum thigh contact.

6.2.2.2 Second experiment

Six male subjects with average age 28 years (range 21 to 38 years), weight 71.3 kg (range 56 to 87 kg), and stature 1.72 m (range 1.63 to 1.83 m) participated in the second experiment (see Appendix C for individual data). Three vibration magnitudes were used (0.125, 0.250, and 0.625 ms^{-2} r.m.s.). The same frequency range (0.25 to 20 Hz) and duration (60 seconds) were used as in the first experiment. For each vibration magnitude, the subjects in this experiment adopted the average thigh contact posture (posture C in Figure 6.1) with a backrest and without a backrest.

6.2.3 Analysis

In the first experiment, the forces were measured in the vertical, fore-and-aft and lateral directions on the seat. In the second experiment, the forces were measured in the fore-and-aft and vertical directions on the footrest. For the fore-and-aft direction, the forces are presented as apparent masses calculated from the fore-and-aft acceleration and the fore-and-aft force at either the seat or the footrest. For the vertical and lateral directions, the forces were related to the fore-and-aft acceleration using the concept of 'cross-axis apparent mass'.

The apparent mass and the cross-axis apparent mass were calculated using the cross spectral density method:

$$M(\omega) = \frac{S_{af}(\omega)}{S_{aa}(\omega)} \qquad (6.1)$$

where, $M(\omega)$ is the apparent mass (or the cross-axis apparent mass), $S_{af}(\omega)$ is the cross spectral density between the force and the acceleration, and $S_{aa}(\omega)$ is the power spectral density of the acceleration. All spectra were calculated by using a resolution of 0.195 Hz. In the fore-and-aft direction, mass cancellation was needed to remove the effect of the aluminium plate ('above' the force transducers) where the subjects sat. Mass cancellation was performed in the frequency domain: the transfer function measured without a subject was subtracted from the transfer functions obtained when subjects were used.

6.3 RESULTS

As in the previous chapters, mainly median responses will be shown in the results section. Individual results are given in Appendix C.

6.3.1 Responses on the seat

6.3.1.1 Response in the fore-and-aft direction

There was appreciable inter-subject variability in the magnitude of the fore-and-aft apparent mass in all postures (Figure 6.2). In all postures, the average coefficient of variation (the average of the ratios of the standard deviation to the mean calculated at each frequency) indicated greater variability at 0.125 ms^{-2} r.m.s. than at 1.25 ms^{-2} r.m.s. The average coefficient of variation also showed greater inter-subject variability in the magnitude and the phase of the apparent mass in the minimum thigh contact posture than in the other postures.

In most subjects, three vibration modes are apparent in the frequency range 0 to 10 Hz. The first vibration mode has a frequency around 1 Hz and is evident in all subjects in the feet hanging posture, the maximum thigh contact posture and the average thigh contact posture (although not at all vibration magnitudes), and in only six subjects in the minimum thigh contact posture (see Appendix C). The second mode has a peak in the frequency range 1 to 3 Hz and is apparent in the response of all subjects in all postures and most vibration magnitudes. The third mode occurs at frequencies between 3 Hz and 5 Hz and is evident in all subjects in the feet hanging posture, eleven subjects in the maximum thigh contact posture, eight subjects in the average thigh contact posture, and seven subjects in the minimum thigh contact posture (Appendix C).

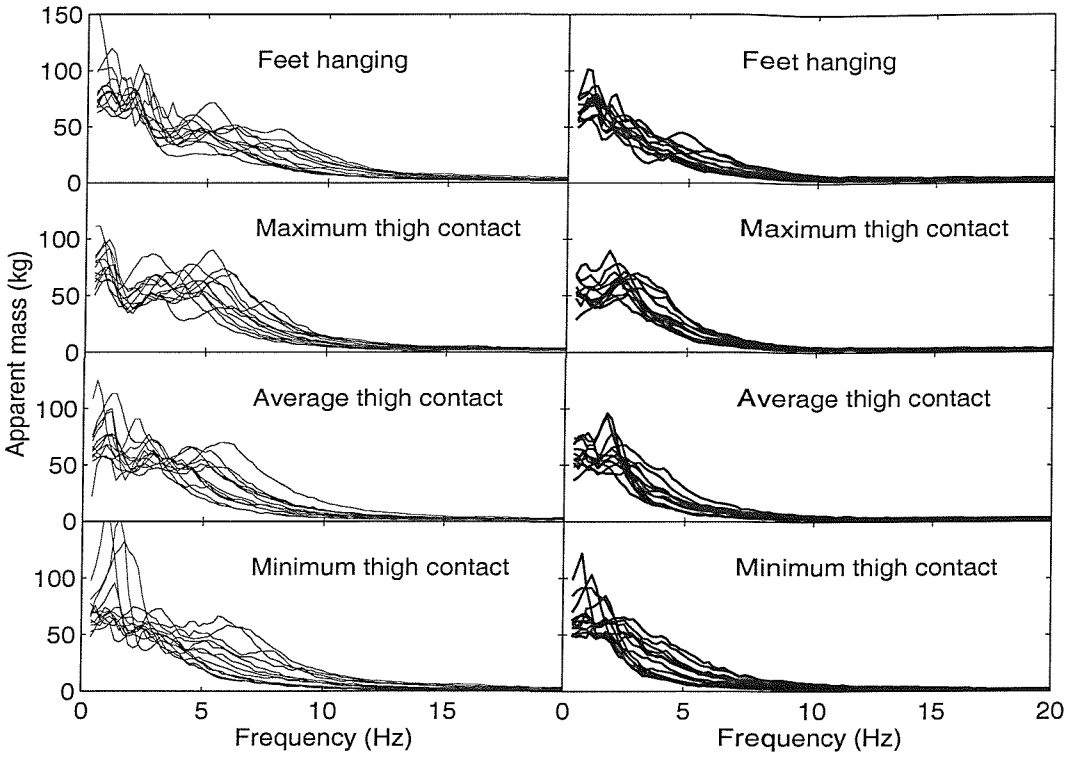

Figure 6.2 Inter-subject variability in the fore-and-aft apparent mass at the seat for each posture at two vibration magnitudes. ———, 0.125 ms^{-2} r.m.s.; ———, 1.25 ms^{-2} r.m.s.

The median magnitude and phase of the apparent mass showed a non-linear response in all postures (Figure 6.3). The apparent mass magnitudes at the frequencies of the three vibration modes and at higher frequencies (0.78, 2.15, 4.1, 6.05, 8.0 and 12.1 Hz) were used to quantify the non-linearity. Above 6 Hz, statistical analysis using Wilcoxon matched-pairs signed ranks tests showed significant differences ($p < 0.05$) in the apparent mass magnitudes measured at the four vibration magnitudes. Below 6 Hz, least non-linearity was found in the average thigh contact posture and the minimum thigh contact posture at 2.15 Hz (Table 6.1).

6.3.1.2 Responses in the vertical and lateral directions

Considerable vertical forces, represented as vertical cross-axis apparent mass, were found on the seat during fore-and-aft excitation (Figure 6.4). The average coefficient of variation over the whole-frequency range indicated greater subject variability at 0.125 ms^{-2} r.m.s. than at 1.25 ms^{-2} r.m.s. in all postures (see Figure 6.4 and Appendix C). In the feet hanging posture, all subjects show a resonance frequency in the range 4 to 8 Hz. Eleven subjects show another resonance (although not at all vibration magnitudes) at a lower frequency (2 to 3 Hz). In the maximum thigh contact posture, vibration modes around 1 Hz, around 3 Hz and around 4 to 7 Hz can be identified (although all three

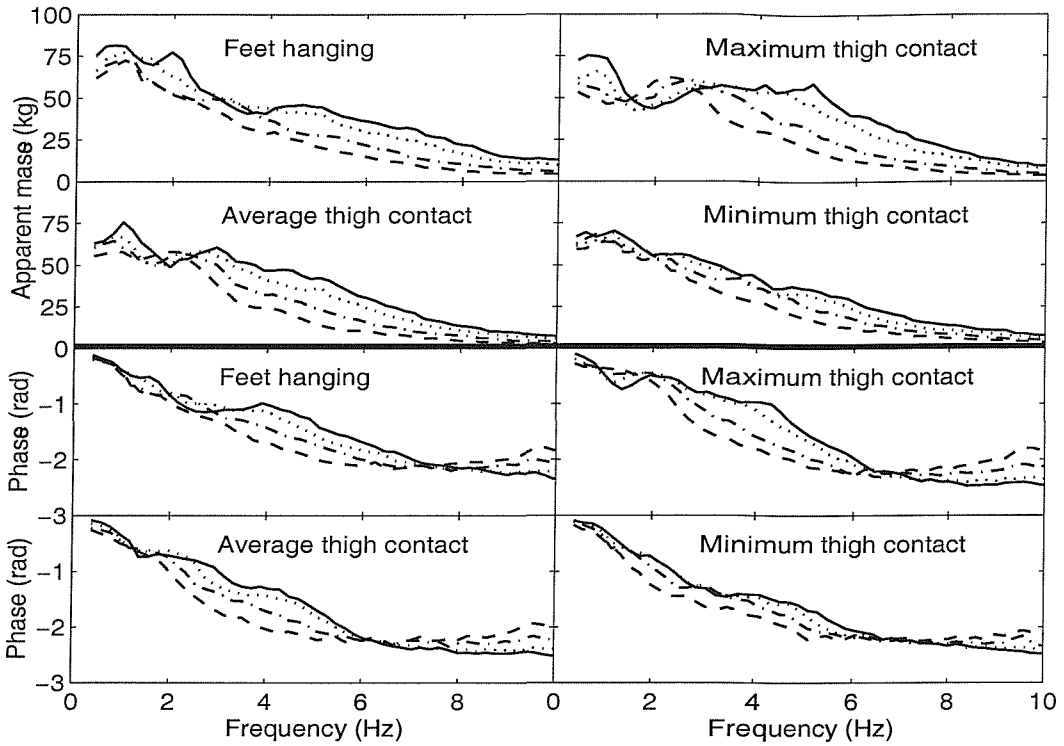

Figure 6.3 Median fore-and-aft apparent mass and phase angle of twelve subjects at the seat: effect of vibration magnitude. ———, 0.125 ms^{-2} r.m.s.; ·····, 0.25 ms^{-2} r.m.s.; —·—·—, 0.625 ms^{-2} r.m.s.; – – – –, 1.25 ms^{-2} r.m.s.

modes are not visible for all subjects). In the average thigh contact posture and in the minimum thigh contact posture, most subjects showed modes with frequencies around 1 Hz and 3 Hz, with a few showing a mode at a higher frequency.

Median data show that the vertical cross-axis apparent mass magnitudes tended to decrease with increasing vibration magnitude (Figure 6.5). Statistical analysis using Wilcoxon matched-pairs signed ranks test showed that the change in the vertical cross-axis apparent mass with vibration magnitude depended on the frequency and the posture. For example, at four vibration magnitudes, there was no significant difference in the cross-axis apparent mass at either 0.78 Hz or 2.15 Hz with the feet hanging posture. However, there was a significant difference in the cross-axis apparent mass obtained with the four vibration magnitudes at higher frequencies (Table 6.2). The phases of the vertical cross-axis apparent masses on the seat are also shown in Figure 6.5. These phases can be understood by reference to the sign convention for the fore-and-aft acceleration and the vertical force mentioned in Section 6.2.1. For example, at 4.4 Hz, the median phase in the feet hanging posture at 0.125 ms^{-2} r.m.s. is -3.14 radians. This means that at this frequency, a forward acceleration produced a downward vertical force.

Table 6.1 Statistically significant differences between fore-and-aft apparent mass magnitudes. Comparisons shown where $p < 0.05$; Wilcoxon matched-pairs signed ranks test: effect of vibration magnitude. H: feet hanging; Max: maximum thigh contact; Av: average thigh contact; Min: minimum thigh contact; Vibration magnitudes: 1: 0.125; 2: 0.25; 3: 0.625; 4: 1.25 ms^{-2} r.m.s.

Posture	0.78 Hz	2.15 Hz	4.1 Hz	6.05 Hz	8.0 Hz	12.1 Hz	Total out of 36 possible combinations
Feet hanging	H1 / H2 H1 / H3 H1 / H4 H2 / H3	H1 / H2 H1 / H3 H1 / H4 H2 / H4	H1 / H3 H1 / H4 H2 / H3 H2 / H4 H3 / H4	All combinations	All combinations	All combinations	31
Maximum thigh contact	Max1 / Max2 Max1 / Max3 Max1 / Max4 Max2 / Max3 Max2 / Max4	Max1 / Max2 Max1 / Max3 Max1 / Max4 Max2 / Max3 Max2 / Max4	Max1 / Max4 Max2 / Max3 Max2 / Max4 Max3 / Max4	All combinations	All combinations	All combinations	32
Average thigh contact	Av1 / Av2 Av1 / Av3 Av1 / Av4 Av2 / Av3 Av2 / Av4	None	All combinations	All combinations	All combinations	All combinations	29
Minimum thigh contact	Min1 / Min 4 Min2 / Min4 Min3 / Min4	Min1 / Min 2	All combinations	All combinations	All combinations	All combinations	28

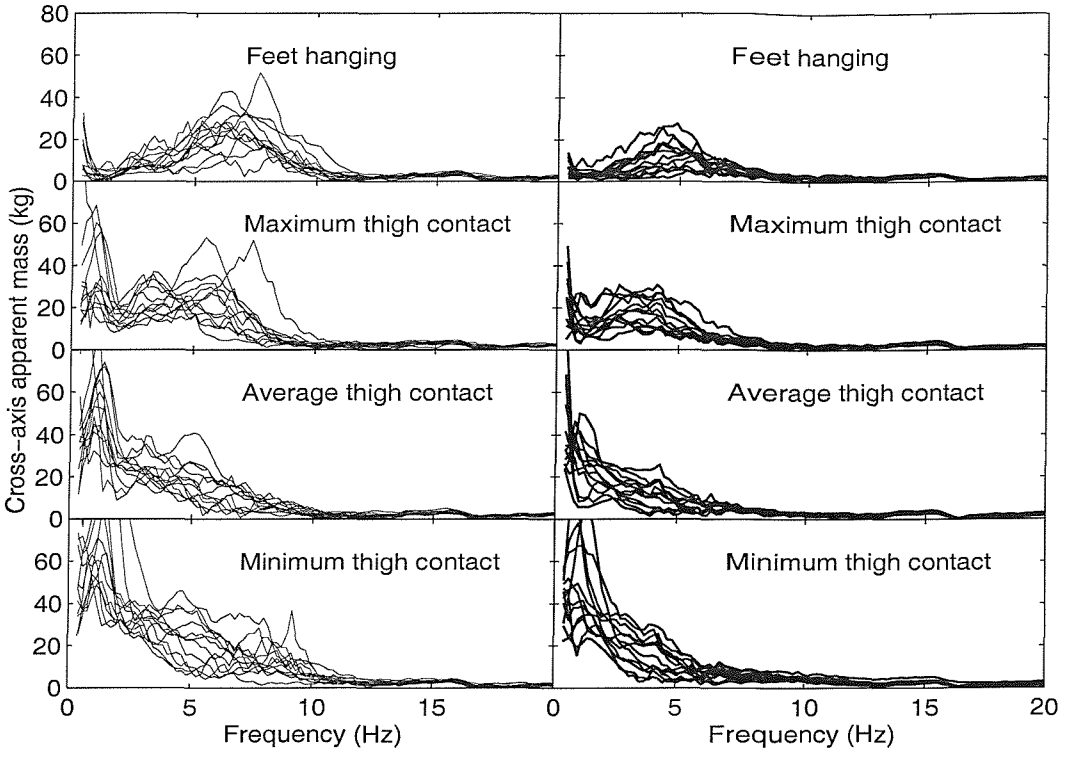

Figure 6.4 Inter-subject variability in the vertical cross-axis apparent mass at the seat for each posture at two vibration magnitudes. ———, 0.125 ms^{-2} r.m.s.; ———, 1.25 ms^{-2} r.m.s.

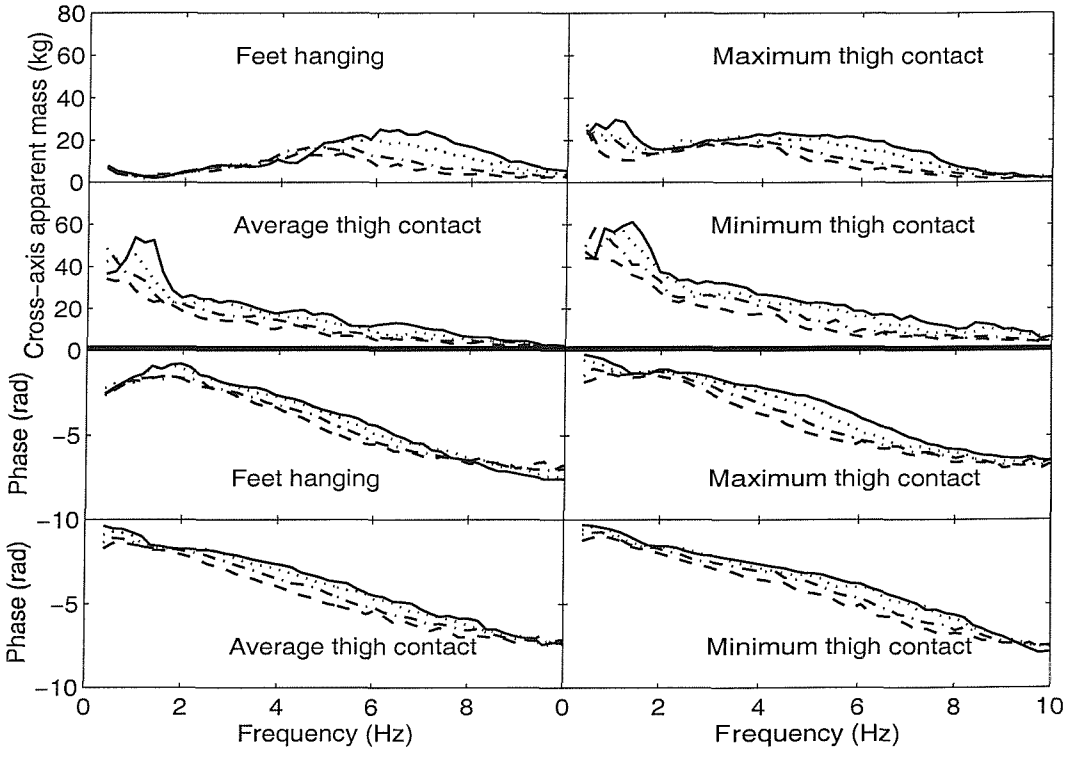

Figure 6.5 Median vertical cross-axis apparent mass and phase angle of twelve subjects at the seat: effect of vibration magnitude. ———, 0.125 ms^{-2} r.m.s.; ·····, 0.25 ms^{-2} r.m.s.; —·—·—, 0.625 ms^{-2} r.m.s.; – – – –, 1.25 ms^{-2} r.m.s.

Table 6.2 Statistically significant differences between the vertical cross-axis apparent mass magnitudes. Comparisons shown where $p < 0.05$; Wilcoxon matched-pairs signed ranks test: effect of vibration magnitude. H: feet hanging; Max: maximum thigh contact; Av: average thigh contact; Min: minimum thigh contact; Vibration magnitudes: 1: 0.125; 2: 0.25; 3: 0.625; 4: 1.25 ms^{-2} r.m.s.

	At 0.78 Hz	At 2.15 Hz	At 4.10 Hz	At 6.05 Hz	At 8.0 Hz	At 12.1 Hz	Total out of 36 possible combinations
Feet hanging	None	None	H1 / H2	All combinations	All combinations	H1 / H4 H2 / H4 H3 / H4	16
Maximum thigh contact	Max1 / Max3 Max1 / Max4 Max2 / Max3 Max2 / Max4 Max3 / Max4	None	Max2 / Max4	All combinations	All combinations	Max1 / Max2 Max1 / Max4 Max3 / Max4	21
Average thigh contact	Av1 / Av3 Av1 / Av4 Av2 / Av3 Av2 / Av4	Av1 / Av2 Av1 / Av3 Av1 / Av4	Av1 / Av3 Av1 / Av4 Av2 / Av3 Av2 / Av4 Av3 / Av4	Av1 / Av3 Av1 / Av4 Av2 / Av3 Av2 / Av4 Av3 / Av4	Av1 / Av3 Av1 / Av4 Av2 / Av3 Av2 / Av4 Av3 / Av4	None	22
Minimum thigh contact	Min3 / Min4	Min1 / Min2 Min1 / Min3 Min1 / Min4 Min2 / Min3 Min2 / Min4	Min1 / Min2 Min1 / Min3 Min1 / Min4 Min2 / Min3 Min2 / Min4	All combinations	All combinations	None	23

At frequencies below about 5 Hz, the median vertical cross-axis apparent mass magnitudes tended to increase with increasing support for the feet (Figure 6.6). However, at frequencies between 4 and 10 Hz, median results show the lowest cross-axis apparent mass in the average thigh contact posture. At higher frequencies, the vertical cross-axis apparent mass is low in all postures.

In all postures, the lateral cross-axis apparent masses were small relative to those in the vertical direction. The high inter-subject variability seen in the lateral direction was less at higher vibration magnitudes (Figure 6.7). The median lateral cross-axis apparent mass was in excess of the 'noise' measured with no subject (between 0 and 0.3 kg) at most frequencies. The median lateral cross-axis apparent mass shows a non-linear characteristic with vibration magnitude (Figure 6.8). The lateral cross-axis apparent masses are shown at frequencies below 10 Hz due to a lateral resonance in the system at about 13 Hz.

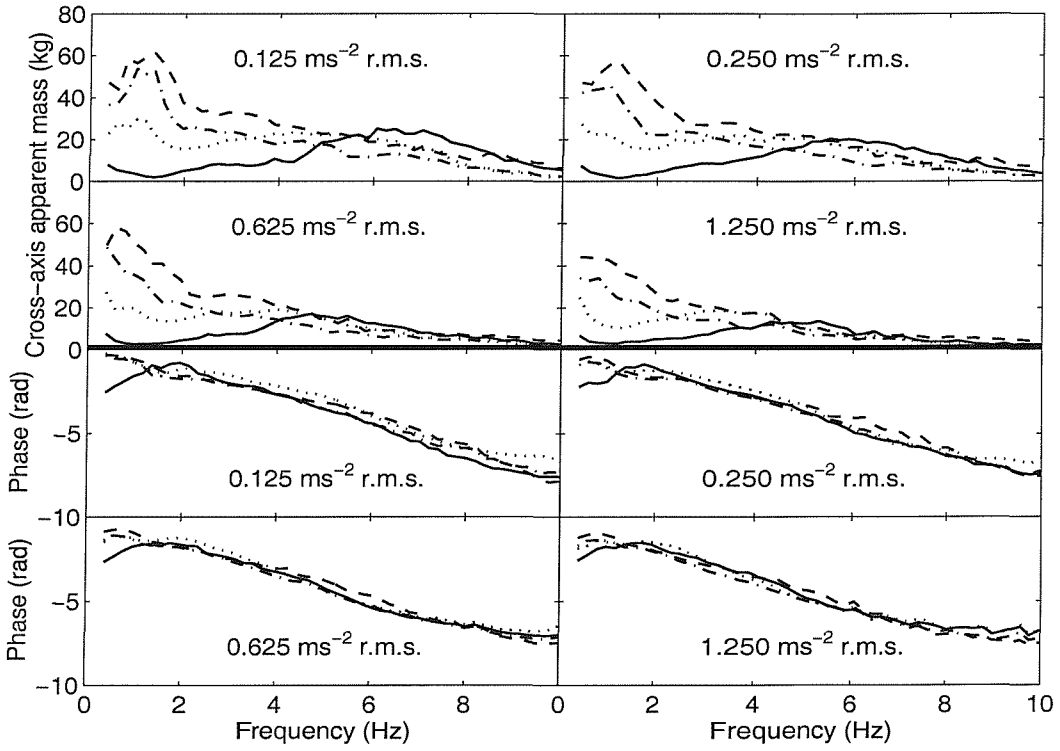

Figure 6.6 Median vertical cross-axis apparent mass and phase angle of twelve subjects at the seat: effect of posture. ———, feet hanging; ·····, maximum thigh contact; —·—·—, average thigh contact; – – – –, minimum thigh contact.

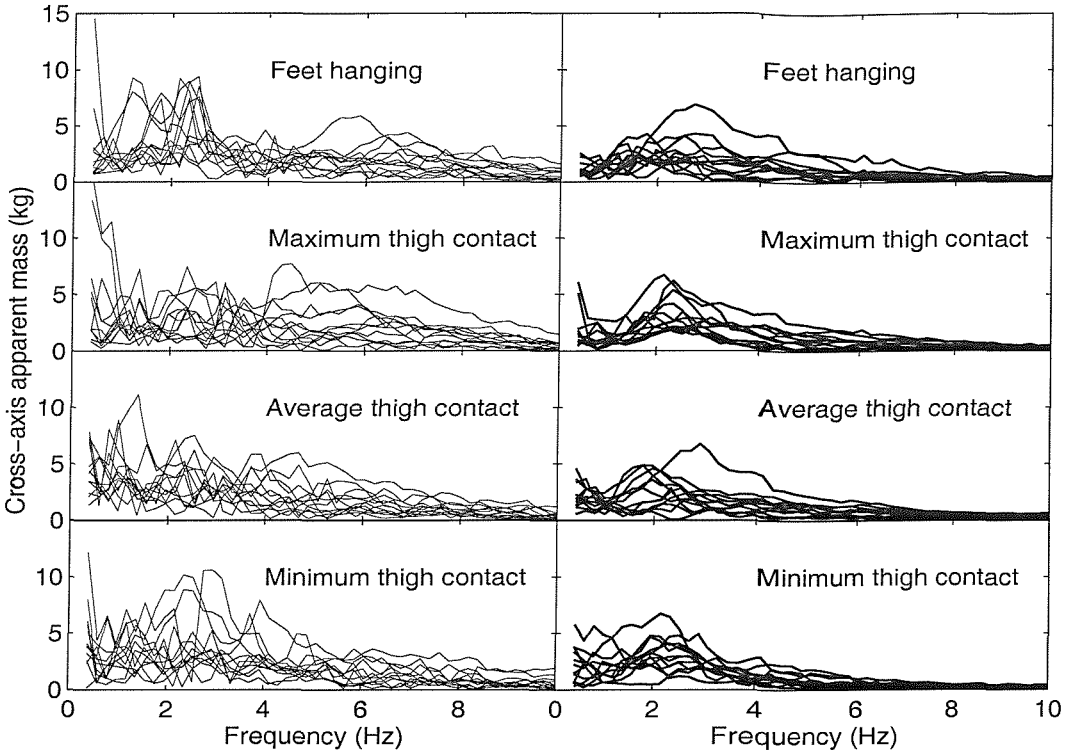

Figure 6.7 Inter-subject variability in the lateral cross-axis apparent mass at the seat for each posture at two vibration magnitudes. ———, 0.125 ms^{-2} r.m.s.; ———, 1.25 ms^{-2} r.m.s.

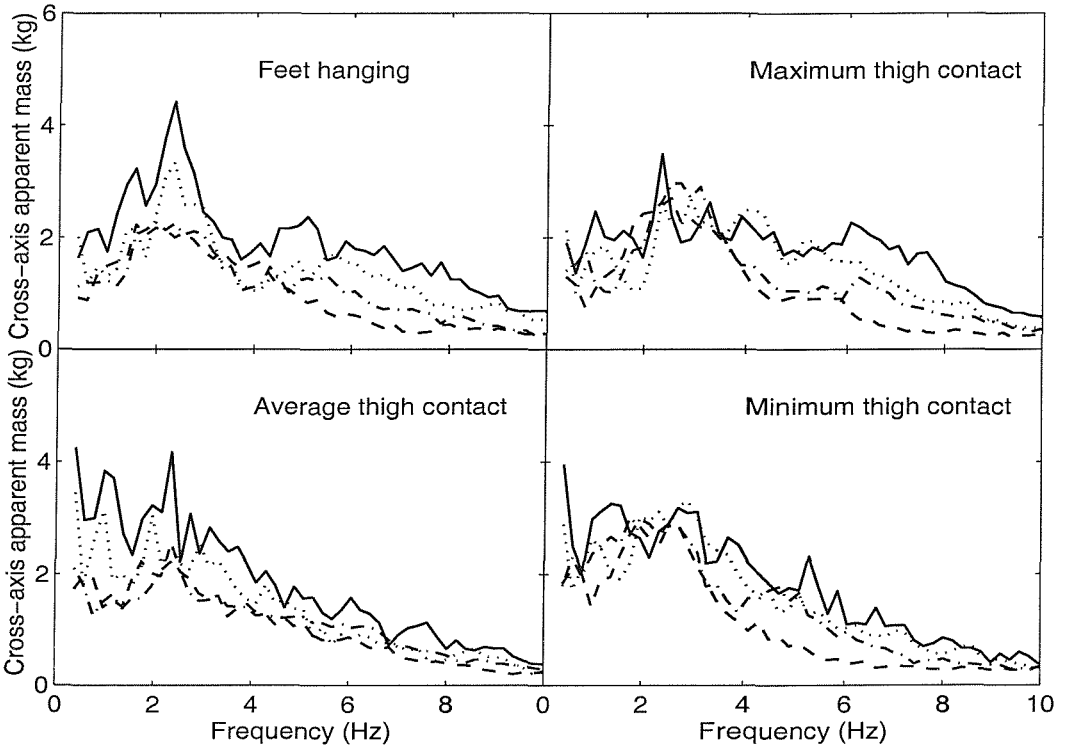

Figure 6.8 Median lateral cross-axis apparent mass of twelve subjects at the seat: effect of vibration magnitude. ———, 0.125 ms^{-2} r.m.s.; ·····, 0.25 ms^{-2} r.m.s.; –·–·–, 0.625 ms^{-2} r.m.s.; – – – –, 1.25 ms^{-2} r.m.s.

6.3.2 Responses at the feet

6.3.2.1 Response in the fore-and-aft direction

With and without a backrest, the inter-subject variability in the fore-and-aft apparent mass at the feet is shown in Figure 6.9. There appears to be a resonance in the apparent mass at the feet in the frequency range 3 to 5 Hz (depending on the subject and vibration magnitude), both with and without the backrest (Figures 6.10 and 6.11). The variation in apparent mass magnitude with change in vibration magnitude was investigated at six frequencies (0.78, 2.15, 4.1, 6.05, 8.0, and 12.1 Hz). Statistical analysis (Wilcoxon matched-pairs signed ranks test) showed that the change in apparent mass magnitude with vibration magnitude was dependent on the frequency: at some frequencies the effect of vibration magnitude on the apparent mass magnitude was clearer than at others (Table 6.3).

The backrest seemed to increase the median resonance frequency and the magnitude of the apparent mass at resonance, while decreasing the median apparent mass at frequencies below resonance (Figure 6.12).

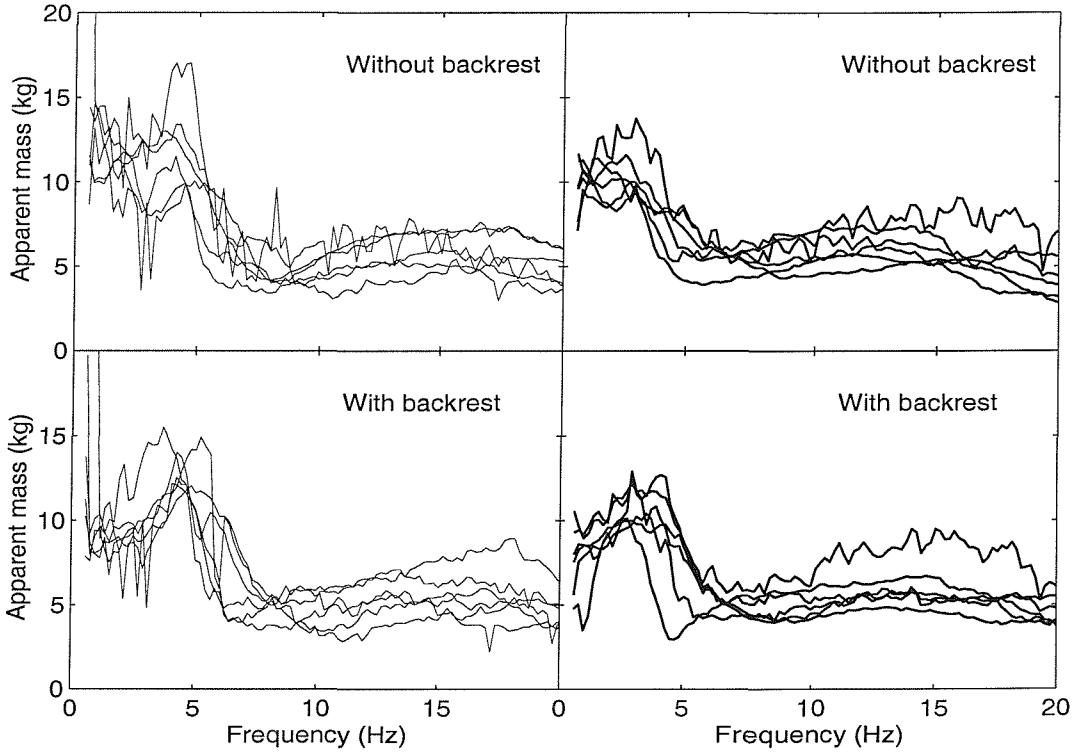

Figure 6.9 Inter-subject variability in the fore-and-aft apparent mass at the feet for two postures at two vibration magnitudes. ———, 0.125 ms^{-2} r.m.s.; ———, 0.625 ms^{-2} r.m.s.

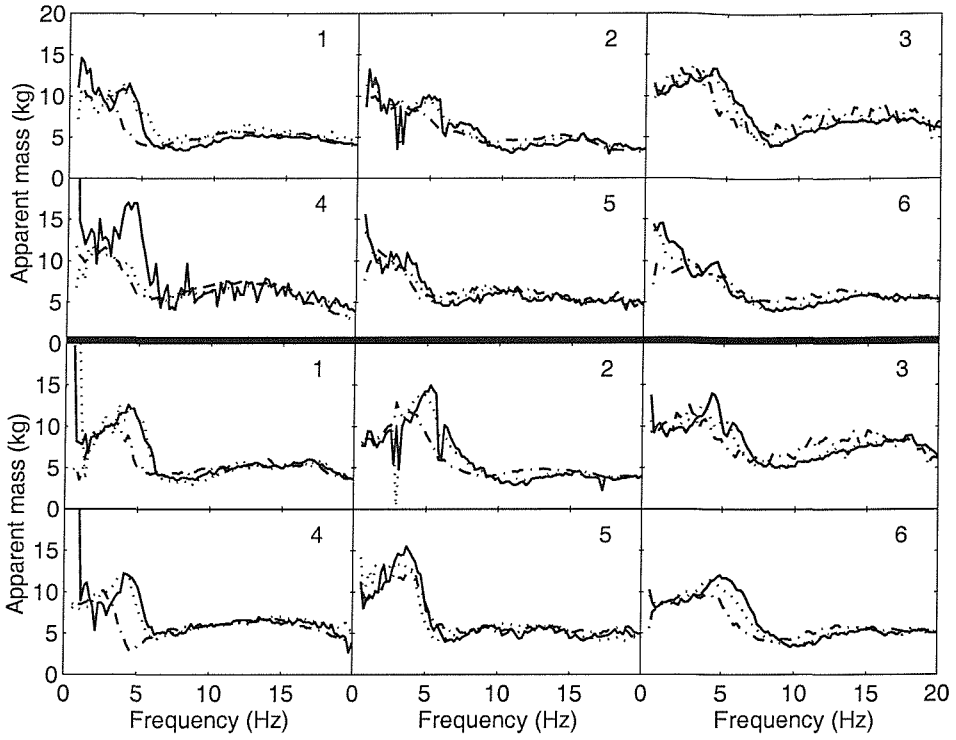

Figure 6.10 Fore-and-aft apparent masses at the feet of six subjects. ———, 0.125 ms^{-2} r.m.s.; ·····, 0.25 ms^{-2} r.m.s.; –·–·–, 0.625 ms^{-2} r.m.s. First two rows of figures without backrest; second two rows with backrest.

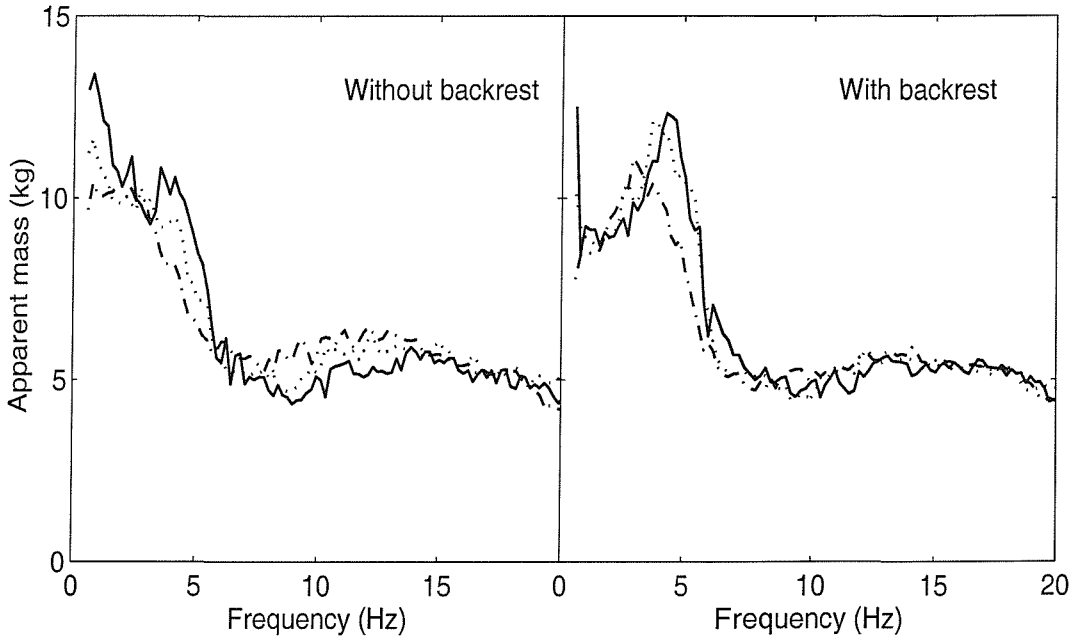

Figure 6.11 Median fore-and-aft apparent masses at the feet of six subjects: effect of vibration magnitude. ———, 0.125 ms^{-2} r.m.s.; ·····, 0.25 ms^{-2} r.m.s.; –·–·–, 0.625 ms^{-2} r.m.s.

Table 6.3 Statistically significant differences between the fore-and-aft apparent mass magnitudes at the feet, and between the vertical cross-axis apparent mass magnitudes at the feet. Comparisons shown where $p < 0.05$; Wilcoxon matched-pairs signed ranks test: effect of vibration magnitude. WO: without backrest; W: with backrest. Vibration magnitudes: 1: 0.125; 2: 0.25; 3: 0.625 ms^{-2} r.m.s.

	Fore-and-aft		Vertical	
	Without backrest	With backrest	Without backrest	With backrest
At 0.78 Hz	WO1 / WO3	-	WO1 / WO3 WO2 / WO3	-
At 2.15 Hz	-	-	WO1 / WO2	-
At 4.10 Hz	WO1 / WO2 WO1 / WO3 WO2 / WO3	W1 / W3 W2 / W3	WO1 / WO3 WO2 / WO3	W1 / W3
At 6.05 Hz	-	-	WO2 / WO3	W1 / W2 W1 / W3
At 8.00 Hz	-	-	WO1 / WO3 WO2 / WO3	W1 / W3 W2 / W3
At 12.1 Hz	WO1 / WO2 WO1 / WO3	W2 / W3	-	W1 / W2

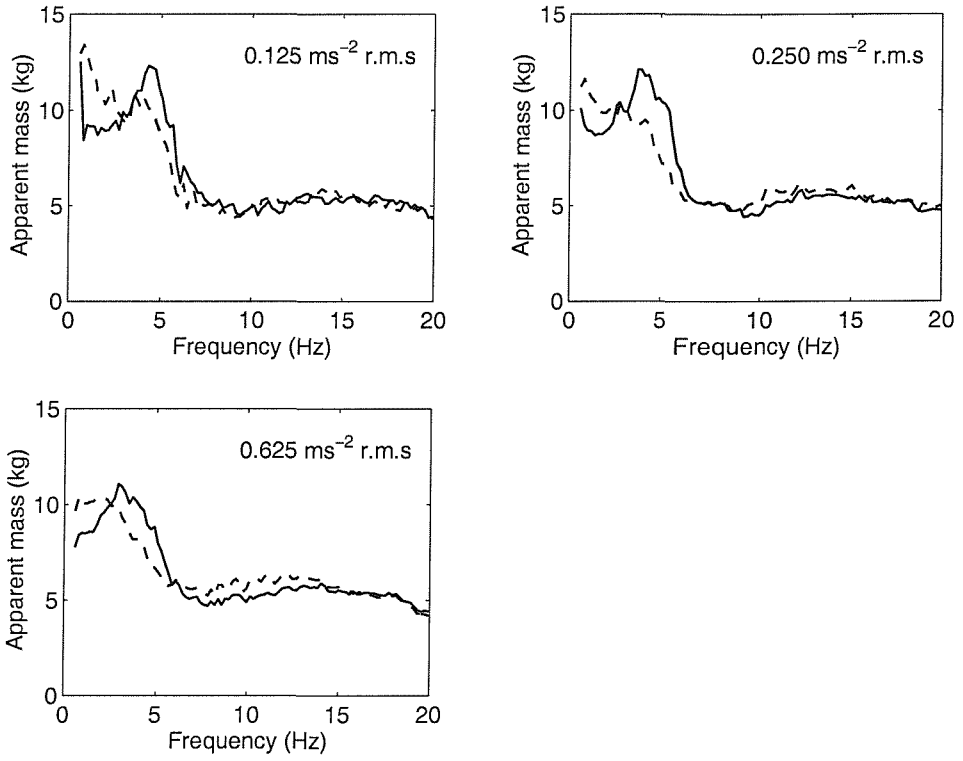

Figure 6.12 Median fore-and-aft apparent masses at the feet of six subjects: effect of backrest. ———, with backrest; – – – –, without backrest.

6.3.2.2 Response in the vertical direction

Variability between subjects in the vertical cross-axis apparent mass is shown in Figure 6.13 for two vibration magnitudes and two sitting conditions. The Figure also shows a resonance around 1 Hz when no backrest was used, but a resonance around 5 Hz when the backrest was used.

The response at the feet in the vertical direction depended on vibration magnitude (Figure 6.14 and Figure 6.15). As noticed in the fore-and-aft apparent mass measured at the feet, the variation in the vertical cross-axis apparent mass at the feet with change in vibration magnitude was dependent on the frequency (Table 6.3).

Below 4 Hz, there was greater median vertical cross-axis apparent mass at the feet when subjects did not use the backrest (see Figure 6.16). At the same vibration magnitude, there were statistically significant differences in the vertical cross-axis apparent masses measured with and without a backrest at 0.78, 2.15, 6.05, 8.0, and 12 Hz ($p < 0.05$). No significant effect of backrest was found at 4.1 Hz.

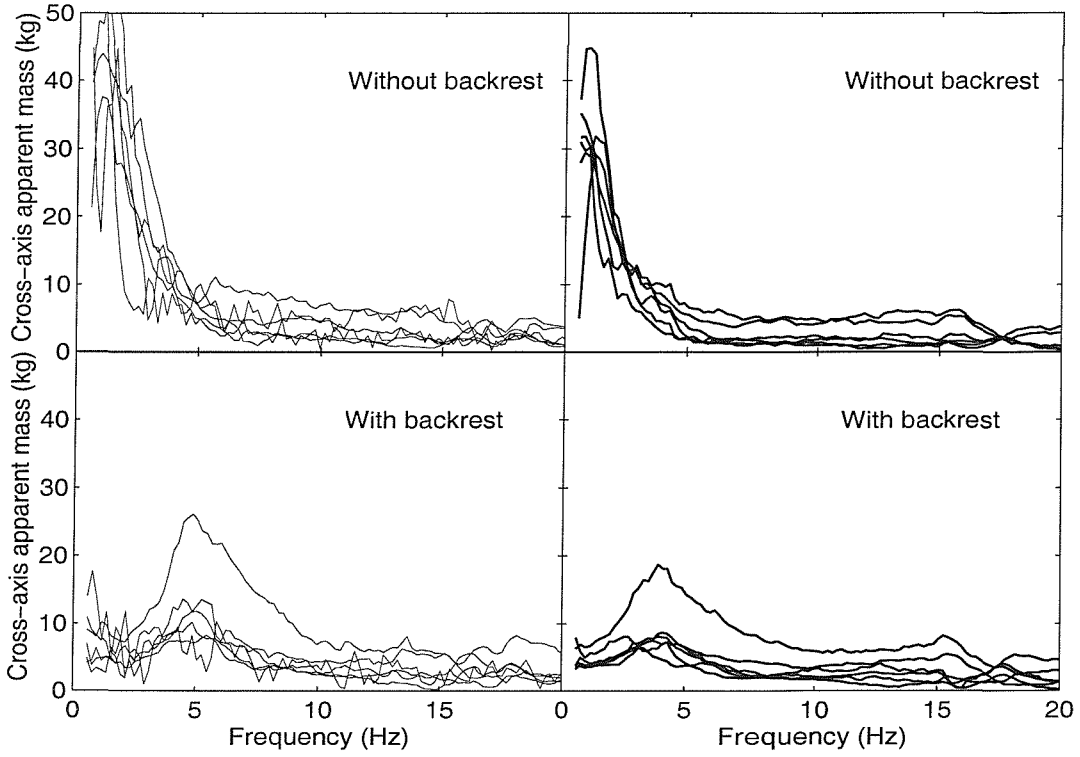

Figure 6.13 Inter-subject variability in the vertical cross-axis apparent mass at the feet for two postures at two vibration magnitudes. ———, 0.125 ms^{-2} r.m.s.; ———, 0.625 ms^{-2} r.m.s.

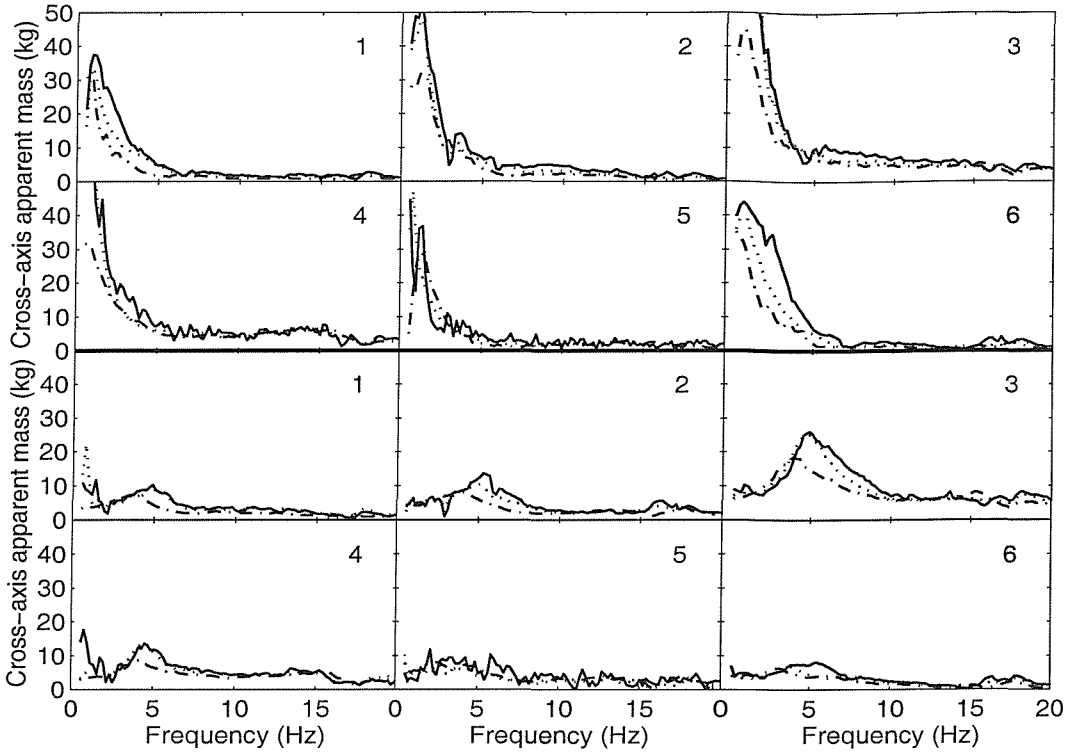

Figure 6.14 Vertical cross-axis apparent masses at the feet of six subjects. ———, 0.125 ms^{-2} r.m.s.; ·····, 0.25 ms^{-2} r.m.s.; –·–·–, 0.625 ms^{-2} r.m.s. First two rows of figures without backrest; second two rows with backrest.

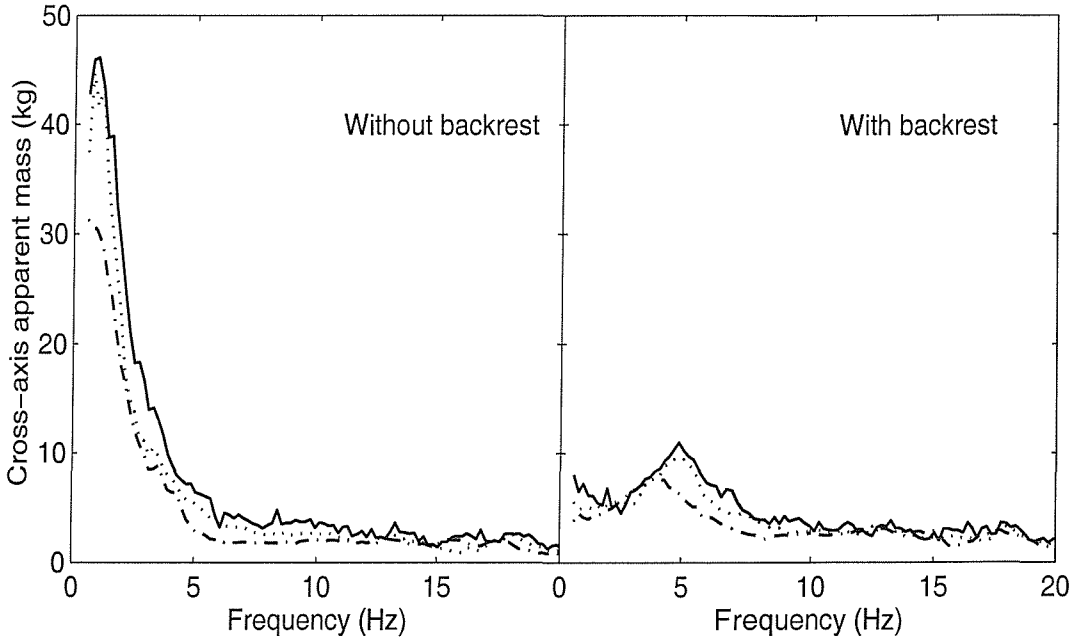

Figure 6.15 Median vertical cross-axis apparent masses at the feet of six subjects: effect of vibration magnitude. ———, 0.125 ms^{-2} r.m.s.; ·····, 0.25 ms^{-2} r.m.s.; –·–·–, 0.625 ms^{-2} r.m.s.

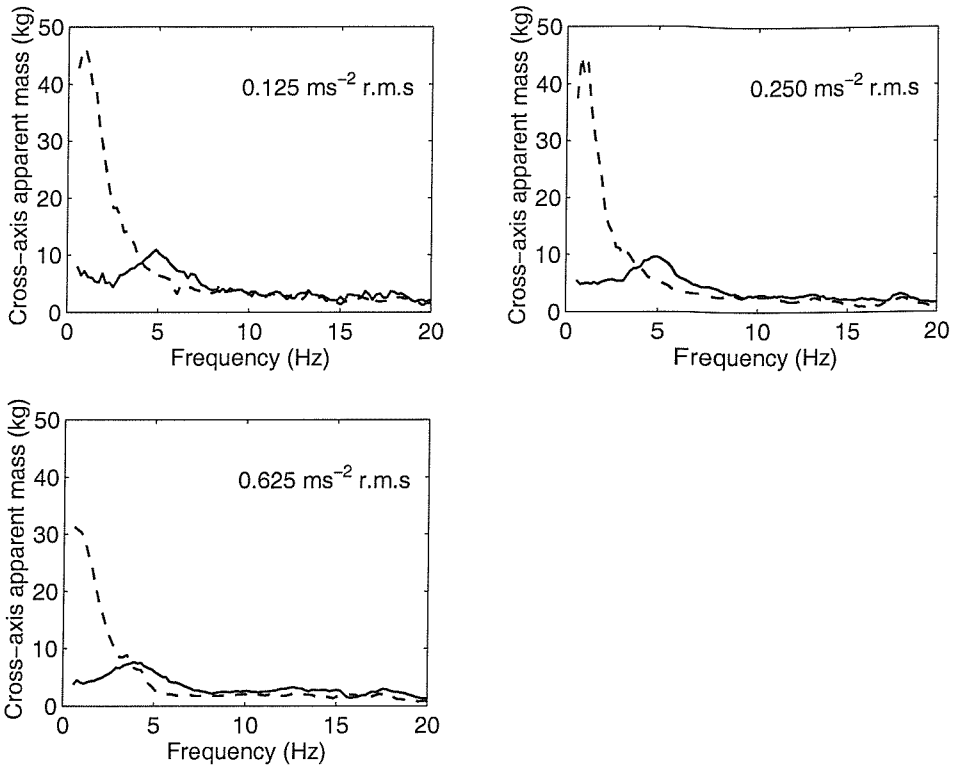

Figure 6.16 Median vertical cross-axis apparent masses at the feet of six subjects: effect of backrest. ———, with backrest; – – – –, without backrest

6.4 DISCUSSION

6.4.1 Response in the fore-and-aft direction

More than one resonance, high subject variability, and a non-linearity in the fore-and-aft apparent mass are consistent findings in previous studies. Three vibration modes were found in the present study (around 1 Hz, between 1 and 3 Hz and between 3 and 5 Hz). Fairley and Griffin (1990) reported modes similar to the first and second mode found here but no third mode. Holmlund and Lundström (1998) and Mansfield and Lundström (1999) only investigated frequencies above 1 Hz; Holmlund and Lundström reported mainly one mode, similar to the second mode in this study, while Mansfield and Lundström reported modes similar to the second and third modes found here.

Some of the differences in apparent mass between studies may be due to the use of different vibration magnitudes and waveforms, different sitting postures, and whether the feet were moving in phase with the seat or supported on a stationary footrest. The angle between the upper leg and lower leg, as well as the height of the footrest with respect to the seat, may also have contributed to differences between the studies.

Vibration magnitude affected the visibility of the third vibration mode above 3 Hz: the third mode was mainly evident at low vibration magnitudes, diminishing with increasing vibration magnitude as the apparent mass decreased in that region. Fairley and Griffin (1990) used a minimum vibration magnitude of 0.5 ms^{-2} r.m.s., compared to 0.125 ms^{-2} r.m.s. in the present study and 0.25 ms^{-2} r.m.s. in the study reported by Mansfield and Lundström (1999). Although, Holmlund and Lundström (1998) used vibration magnitude as low as 0.25 ms^{-2} r.m.s., they employed sinusoidal vibration where the energy at each frequency would have been higher than when using broad-band random vibration at the same overall r.m.s. vibration magnitude. Fairley (1986) compared the vertical apparent mass of the body at 1.0 ms^{-2} r.m.s. using random vibration over the range 1.5 to 20 Hz and a frequency sweep. There was a reduced resonance frequency with the sinusoidal vibration, consistent with the expected non-linearity and offering an explanation of the difference between the results obtained in this study with random vibration at 0.25 ms^{-2} r.m.s. and those obtained by Holmlund and Lundström (1998) with sinusoidal vibration of the same magnitude. Mansfield and Lundström suggested that (1999) placing the hands on the knees, or in the laps, might have damped the third mode, but this may be excluded since subjects in the present study also placed their hands in their laps.

In contrast to the present study, where an adjustable footrest was used, all previous studies have used a fixed distance between the seat surface and the footrest. If the range of subject heights was wide, the previous studies would have been a mixture of results from the four postures used in the present study (perhaps excluding the feet hanging posture). Neither Fairley and Griffin (1990) nor Mansfield and Lundström (1999) reported the heights of their subjects. In the Holmlund and Lundström (1998) study the subject heights were in the range 167 to 188 cm. The mixture of postures resulting from using the same seat with different subject sizes, may have increased inter-subject variability and increased the difficulty of comparing results from the different studies: in the present study there were statistically significant differences in apparent masses obtained with different postures.

Another difference between studies is whether the footrest moved with the seat (as in this study and in Fairley and Griffin, 1990) or was stationary (as in Holmlund and Lundström, 1998 and Mansfield and Lundström, 1999). Different forces on the seat should be expected with a moving footrest and a stationary footrest, due to different phases between the seat and the feet.

With a stationary footrest, forces measured on the seat might be affected by the height of the footrest, as found with vertical vibration by Fairley and Griffin (1989). With a decrease in the height of a stationary footrest, they reported a decrease in the apparent mass on the seat at low frequencies, as opposed to the increase in apparent mass with a decrease in the height of a footrest that moved in phase with the seat. Although the difference has only been reported for vertical vibration, it might be wise to assume that the results obtained with a moving footrest at low frequencies (below 1 Hz) in the present study and in Fairley and Griffin (1990) may not be the same as those with a stationary footrest.

All relevant previous studies reported a decrease in the resonance frequency of the second mode with an increase in vibration magnitude. Mansfield and Lundström (1999) also reported a decrease in the third mode resonance frequency with an increase in vibration magnitude. Fairley and Griffin (1990) (the only previous study to measure the first mode) found no effect of vibration magnitude on the resonance frequency of this mode. With an increase in vibration magnitude, although Mansfield and Lundström reported an increase in the apparent mass magnitude at resonance for the second mode, Holmlund and Lundström (1998) reported a decrease in the magnitude of the mechanical impedance at resonance, and over the whole frequency range. None of the previous studies provided evidence that the apparent changes were statistically significant. In the present study, the change in the magnitude of the fore-and-aft apparent mass with a change in vibration magnitude was used as a measure of the non-linearity, because not all subjects showed clear resonances at all vibration magnitudes (see Table 6.1). The non-linear response in the fore-and-aft direction depended on the height of the footrest and the vibration frequency.

An additional explanation for differences in modes between studies is that because not all modes are at the same frequency in all subjects, they become 'smeared out' by averaging when calculating a mean or median response.

6.4.2 Responses in the vertical and lateral directions

High vertical forces on the seat, but low lateral forces, are consistent with unpublished data mentioned by Holmlund and Lundström (2001). The results are also similar to the high fore-and-aft forces and low lateral forces arising from vertical excitation (see Chapter 4 and Chapter 5).

In the present study, within the range 4 to 7 Hz, individual vertical cross-axis apparent mass was up to 70% of the static subject mass in the feet hanging posture. At frequencies below 5 Hz, the vertical cross-axis apparent mass increased with increasing support for the feet, and reached up to 100% of the static mass of some subjects in the minimum thigh contact posture. The magnitudes of the vertical cross-axis apparent mass were then similar to the fore-and-aft apparent mass. For example, in the minimum thigh contact posture, the median vertical cross-axis apparent mass was 64% of the fore-and-aft apparent mass at 5 Hz and 86% of the fore-and-aft apparent mass around 1.0 Hz. Using a biomechanical model, Fritz (2000) reported a ratio of 1.3 to 1 between shear and compressive forces predicted during fore-and-aft excitation.

Only the vertical forces measured with the feet hanging posture are similar to the fore-and-aft forces measured on the seat during vertical excitation (see Chapter 4): both forces had low values at low frequencies and had a resonance in the vicinity of 5 Hz. When the feet were supported, there were high vertical forces at frequencies lower than 5 Hz, which might have masked the peak in the vertical cross-axis apparent mass at 5 Hz in some subjects. Any swinging of the feet when they are not supported might primarily affect fore-and-aft forces on the seat. When the feet are supported on a footrest, the subjects may stabilise their body by exerting greater force on the footrest when moving forward and greater force on the seat when moving backward. Some subjects reported difficulty in preventing themselves from sliding on the seat when the body was less supported and said they needed to push down on the footrest to prevent sliding.

At 5 Hz, the vertical forces may have been caused by similar modes to the fore-and-aft forces presented in Chapter 4 for vertical excitation. With the feet hanging, the response in the vertical direction resembles transmissibilities from fore-and-aft seat vibration to vertical and pitch vibration at the head, where resonances around 2 Hz and between 6 and 10 Hz have been reported (Paddan and Griffin, 1988b). Using a biodynamic model with rotational capability, Matsumoto and Griffin (2001) obtained three pitch modes: around 2.5 Hz (pitching motion of the pelvis together with a bending mode of the spine), 5.7 Hz (bending of the spine) and 8.6 Hz (bending in the spine). From experimental data with vertical seat vibration, Matsumoto and Griffin (1998a) also determined rotational modes in the range 5 to 7 Hz for pitch motion of the head and motion of first thoracic vertebra. Since the pitch modes occur in the mid-sagittal plane (the *x*-*z*) plane, it is reasonable that the same rotational modes are obtained during vertical and fore-and-aft vibration. However, a full explanation of the forces in the vertical direction must await experimental studies of transmissibility from fore-and-aft seat vibration to parts of the

body and the development of biodynamic models describing the motion of the human body caused by fore-and-aft excitation.

6.4.3 Response at the feet

A previous study (e.g. Kitazaki, 1997) and the results in Chapter 4 showed that during vertical vibration, the response at the feet is complex, with multiple resonances that vary with posture. However, no previous study has reported biodynamic responses at the feet with horizontal vibration.

With and without a backrest, the fore-and-aft apparent mass at the feet showed a peak in the frequency range 3 to 5 Hz. At the same vibration magnitude, the resonance frequency and the apparent mass at resonance increased when using a backrest (Figure 6.12), showing a similar trend to the effect of a backrest on the apparent mass of seated subjects during fore-and-aft vibration (Fairley and Griffin, 1990). At frequencies below resonance, the fore-and-aft apparent mass at the feet is less with a backrest than without a backrest, showing another similar trend to the effect of a backrest on the fore-and-aft apparent mass of seated subjects (Fairley and Griffin, 1990; see also Chapter 7). This shows that the response at the feet is affected by the posture of the upper body: when a subject leans against a backrest, the upper body is restrained from swaying backward and forward, so reducing the force on the legs arising from the motion. Kitazaki (1997) also showed that the response at the feet is affected by the condition of the upper body: he compared the response of the feet with whole-body vertical vibration with the response when only the feet were excited and found similar response characteristics in both conditions but the apparent mass of the feet during whole-body vibration was higher than when only the feet were excited. This indicates that some of the forces measured at the feet came from forces transmitted from the upper body down the legs to the feet.

The vertical cross-axis apparent mass at the feet also depended on the presence of a backrest. The high vertical cross-axis apparent mass at the feet at low frequencies (Figure 6.13) is consistent with the explanation for the high forces in the vertical direction on the seat: the subjects may have applied forces in the vertical direction on the footrest when they pitched forward and applied vertical forces on the seat when they pitched backward. The decrease in the vertical forces at low frequencies at the feet when using a backrest is similar to the decrease in the vertical forces measured at the seat when a backrest was used during fore-and-aft vibration as will be shown in Chapter 7.

6.5 CONCLUSION

The apparent mass responses of seated subjects to fore-and-aft vibration suggest three modes: around 1 Hz, between 1 and 3 Hz, and between 3 Hz and 5 Hz. The three modes varied between subjects, and depended on the vibration magnitude and the sitting posture.

Fore-and-aft vibration caused considerable vertical forces at the seat and at the footrest. The vertical forces are assumed to arise from pitching of all or parts of the upper body. At the seat and at the footrest, the vertical forces were influenced by sitting posture: with increasing height of the footrest, the vertical forces on the seat increased at low frequency; when a backrest was used, the vertical forces on the footrest decreased at low frequencies.

On the seat and the footrest, the dynamic responses in all directions showed a non-linear behaviour. The extent of the non-linearity depended on the posture, the vibration frequency, measurement location and direction.

CHAPTER 7 FORCES AT THE SEAT AND BACKREST DURING FORE-AND-AFT WHOLE-BODY EXCITATION

7.1 INTRODUCTION

Chapter 4 and Chapter 5 showed appreciable cross-axis forces in the fore-and-aft direction on the seat and backrest during exposure of subjects to vertical vibration which is also consistent with the previous finding of Matsumoto and Griffin (2002a). Chapter 6 showed high vertical cross-axis forces on the seat without a backrest during exposure to fore-and-aft vibration. The high cross-axis forces suggest that there is two-dimensional movement of the seated human body when it is exposed to single-axis vibration in either the vertical or fore-and-aft direction.

The use of a backrest has been found to affect the apparent mass of the body during fore-and-aft vibration (e.g. Fairley and Griffin, 1990), and both the apparent mass and fore-and-aft cross-axis apparent mass during exposure to vertical vibration (see Chapter 5). While three vibration modes were found in the fore-and-aft apparent masses of subjects sitting without a backrest, only one vibration mode was evident in the apparent mass calculated from forces measured at the seat and backrest when there was also motion applied to the back (Fairley and Griffin, 1990). In Chapter 5, it was demonstrated that during vertical vibration, the frequency of the principal resonance around 5 Hz increased when using a backrest. Fairley and Griffin (1989) reported the same observation. Also with vertical vibration, there are significant differences in the fore-and-aft cross-axis apparent mass measured on a seat with and without a backrest in a maximum thigh contact posture and in a feet hanging posture as shown in Chapter 5. Transmissibilities to the head during vertical and fore-and-aft vibration are also modified, especially for motions in the mid-sagittal plane, when a backrest is used (Paddan and Griffin, 1988a,b).

Although backrests modify the vibration responses of the seated body, there are no known studies of the forces on backrests during horizontal (i.e. fore-and-aft or lateral) vibration. The study presented in this chapter investigated tri-axial (i.e. fore-aft, lateral and vertical) forces at the seat and the backrest during fore-and-aft whole-body excitation. It was expected that considerable forces would be found in the fore-and-aft direction on the seat and backrest. It was also anticipated that high forces would be found in the vertical direction on the seat, with low vertical forces on the backrest and low lateral forces on both the seat and backrest. It was hypothesised that the addition of a backrest

would modify the fore-and-aft, lateral and vertical forces measured on the same seat but without a backrest (Chapter 6).

7.2 APPARATUS, EXPERIMENTAL DESIGN AND ANALYSIS

7.2.1 Apparatus

Subjects were exposed to fore-and-aft whole-body vibration using an electro-hydraulic vibrator capable of producing peak-to-peak displacements of 1 metre. A rigid seat with a rigid backrest and an adjustable footrest (to give different foot heights) were mounted on the platform of the vibrator. A force plate (Kistler 9281 B) capable of measuring forces in three directions simultaneously was secured to the supporting surface of the seat in order to measure forces in the vertical, fore-and-aft and lateral directions. Another force plate (Kistler Z 13053) was bolted to the backrest so as to measure forces at the back in the fore-and-aft direction. The forces at the back in the vertical and lateral directions were also measured for one subject using the Kistler 9281 force platform. A description of the force plates can be found in Chapter 3. Signals from the force platforms were amplified using Kistler 5007 charge amplifiers. Acceleration in the fore-and-aft direction was measured at the centre of the force platforms using piezo-resistive accelerometers (Entran EGCSY-240D-10). The signs of the fore-and-aft acceleration and fore-and-aft forces on both the seat and backrest were positive in the forward direction. In the vertical direction, the force was positive in the upward direction. The signals from the accelerometers and the force transducers were sampled at 200 samples per second via 67 Hz anti-aliasing filters with an attenuation rate of 70 dB in the first octave.

7.2.2 Experimental design

Twelve male subjects, with average age 30.8 years (range 24 to 47 years), weight 76.1 kg (range 63 to 103 kg), and stature 1.79 m (range 1.68 to 1.91 m), were exposed to random fore-and-aft vibration with an approximately flat constant bandwidth acceleration power spectrum over the frequency range 0.25 to 10 Hz. The upper frequency was limited to 10 Hz because of a fore-and-aft resonance in the backrest at 16 Hz. The subjects were the same as those used in Chapter 6 (fore-and-aft excitation without backrest) except for subject 2. In this experiment subject 2 was 34 years old and had a height and weight of 1.8 m and 83 kg. Four sitting postures were used. The four postures were the same as those used in Chapter 6 but with the use of a vertical backrest (Figure 7.1). In each sitting posture, the twelve subjects were exposed to four vibration magnitudes (0.125, 0.25, 0.625, and 1.25 ms^{-2} r.m.s.). The presentation of the four postures and the four vibration magnitudes was balanced across subjects. The forces in

the vertical and lateral directions at the backrest were measured for only one subject in the four sitting postures and at three vibration magnitudes (0.125, 0.25, and 0.625 ms^{-2} r.m.s.).The duration of each exposure lasted 60 seconds.

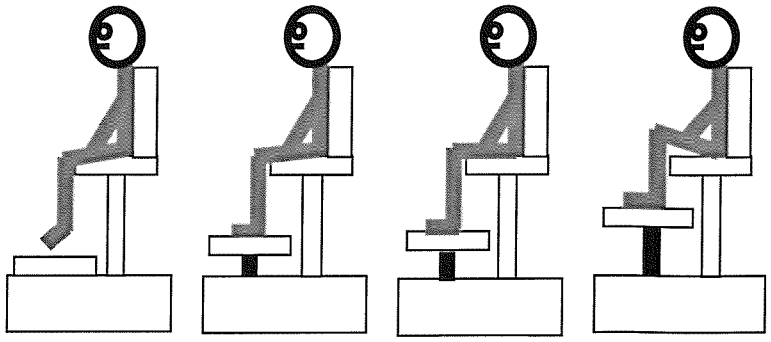

Figure 7.1 Schematic diagrams of the four sitting postures: (a) feet hanging; (b) maximum thigh contact; (c) average thigh contact; (d) minimum thigh contact.

7.2.3 Analysis

The data are partly presented as apparent masses in the fore-and-aft direction, calculated from the fore-and-aft force and fore-and-aft acceleration at the seat and backrest. The forces in the vertical and lateral directions measured on the seat for twelve subjects, and on the back for one subject, were related to the acceleration measured on the seat or backrest in the fore-and-aft direction using the concept of 'cross-axis apparent mass'. The apparent mass and the cross-axis apparent mass were calculated using the cross spectral density method:

$$M(\omega) = \frac{S_{af}(\omega)}{S_{aa}(\omega)} \tag{7.1}$$

where, $M(\omega)$ is the apparent mass (or the cross-axis apparent mass), $S_{af}(\omega)$ is the cross spectral density between the force and the acceleration, and $S_{aa}(\omega)$ is the power spectral density of the acceleration. All spectra were calculated by using a resolution of 0.195 Hz.

To calculate the apparent masses of subjects in the fore-and-aft direction, the forces due to the masses of the aluminium plates of the force platforms 'above' the force transducers were subtracted from the total measured masses (mass of the subject and plate) in the frequency domain: the real and imaginary parts of the transfer function measured without a subject were subtracted from the real and imaginary parts of the transfer functions obtained with subjects.

7.3 RESULTS

In this section, median responses and some individual responses are shown. The rest of the individual responses are shown in Appendix D.

7.3.1 Responses in the fore-and-aft direction

7.3.1.1 Response on the seat

High inter-subject variability was found in the responses of the twelve subjects, with a tendency towards less variability at higher vibration magnitudes (Figure 7.2). In all postures, the average coefficient of variation, defined as the average of the ratios of the standard deviations to the means calculated at each frequency, showed a higher variability at 0.125 ms^{-2} r.m.s. than at 1.25 ms^{-2} r.m.s.

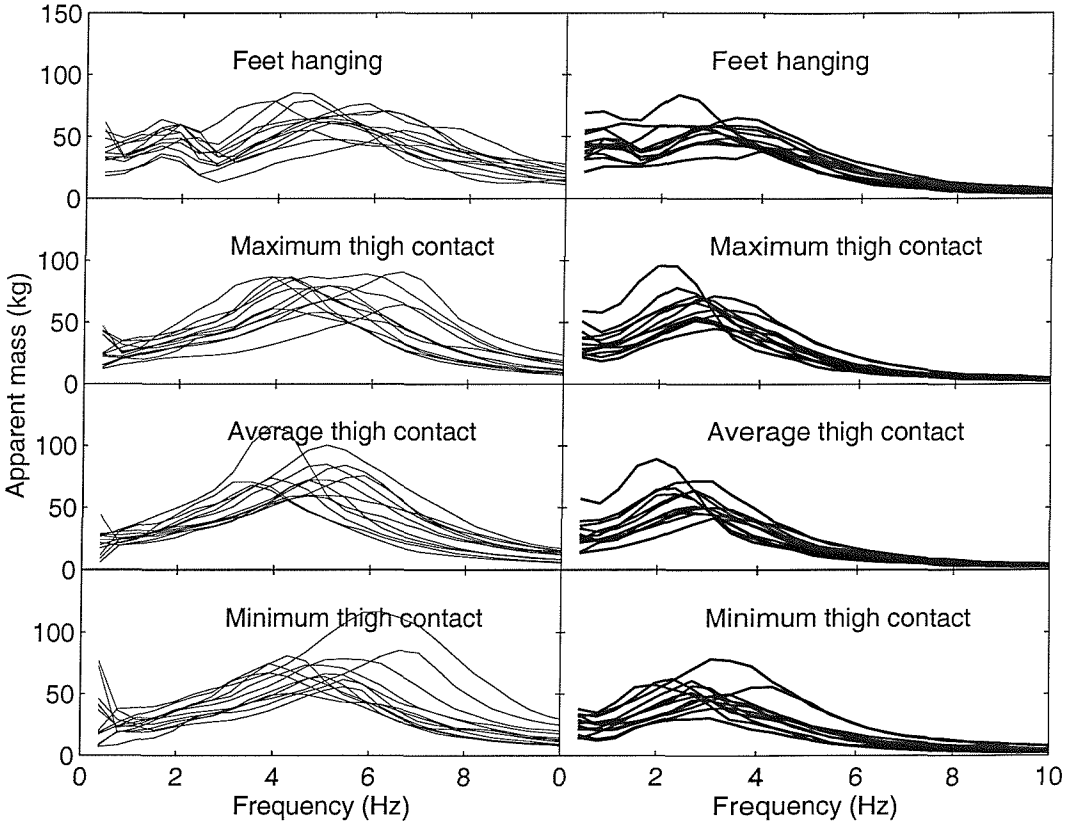

Figure 7.2 Inter-subject variability in the fore-and-aft apparent mass on the seat for each posture at two vibration magnitudes. ———, 0.125 ms^{-2} r.m.s.; ———, 1.25 ms^{-2} r.m.s.

In all postures, there was a peak in the fore-and-aft apparent mass on the seat in the frequency range 2 to 6 Hz (depending on the subject and vibration magnitude). An additional peak in the frequency range 1 to 2 Hz was found only in the feet hanging

posture (Figure 7.2). In all postures, both the median and the individual data showed a decreased resonance frequency and decreased apparent mass magnitude at resonance with increasing vibration magnitude (see Figures 7.3, 7.4) except for subject 12 (Figure 7.3). Statistical analysis showed significant differences ($p < 0.05$) in the resonance frequencies (around 1 to 2 Hz in the feet hanging posture, and in the range 2 to 6 Hz in all postures) measured at the four vibration magnitudes. Subject posture did not affect the size of the change in the resonance frequency: there were no statistically significant differences between postures in the size of the change in the resonance frequency between the two lower vibration magnitudes (i.e. 0.125 and 0.25 ms^{-2} r.m.s.) and the two higher vibration magnitudes (i.e. 0.625 and 1.25 ms^{-2} r.m.s.).

A change of vibration magnitude also caused significant differences ($p < 0.05$) in the magnitudes of the apparent mass at resonance, except between 0.25 and 0.625 ms^{-2} r.m.s., between 0.25 and 1.25 ms^{-2} r.m.s., and between 0.625 and 1.25 ms^{-2} r.m.s. in the feet hanging posture (for both peaks), and between 0.625 and 1.25 ms^{-2} r.m.s. in the maximum thigh contact posture and the average thigh contact posture.

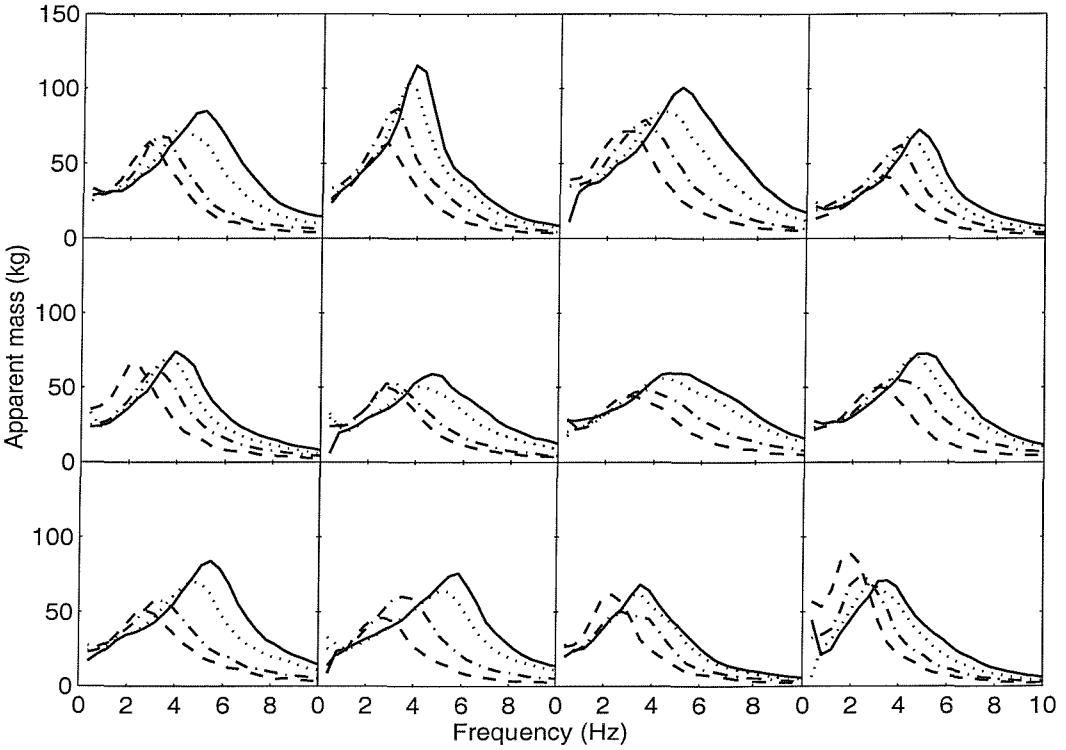

Figure 7.3 Fore-and-aft apparent masses of 12 subjects measured on the seat in the average thigh contact posture at four vibration magnitudes. ———, 0.125 ms^{-2} r.m.s.; ·····, 0.25 ms^{-2} r.m.s.; –·–·–, 0.625 ms^{-2} r.m.s.; – – – –, 1.25 ms^{-2} r.m.s.

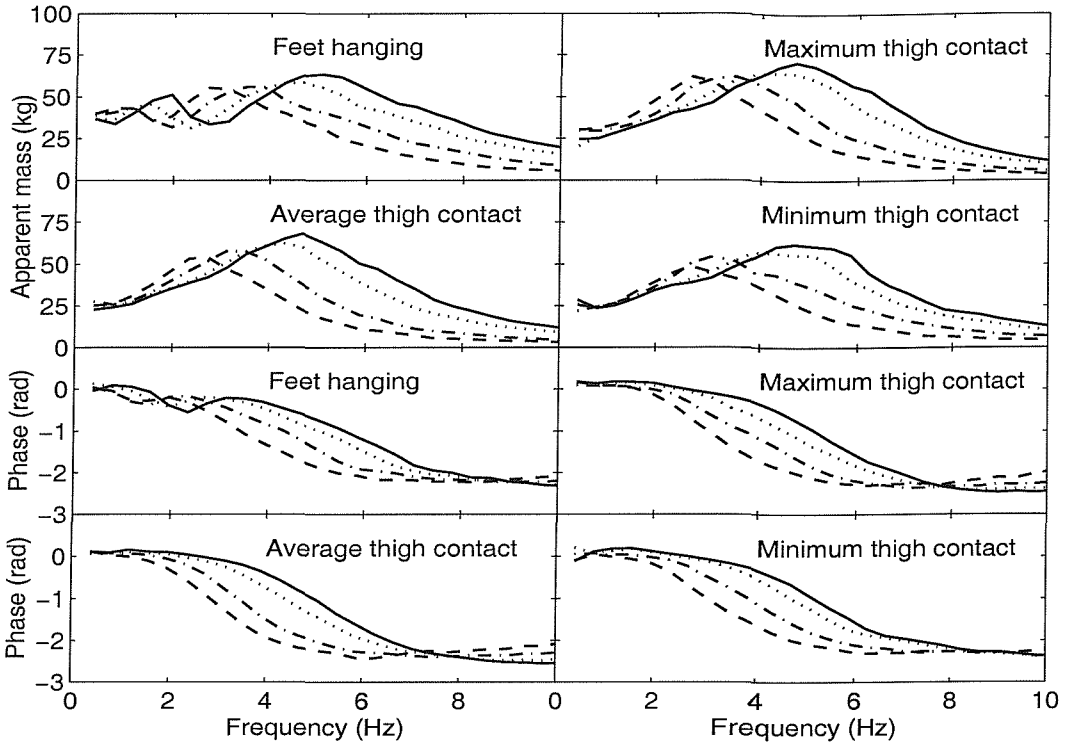

Figure 7.4 Median apparent mass and phase angle of twelve subjects measured on the seat in the fore-and-aft direction: effect of vibration magnitude. ———, 0.125 ms^{-2} r.m.s.; ·····, 0.25 ms^{-2} r.m.s.; –·–·–, 0.625 ms^{-2} r.m.s.; – – – –, 1.25 ms^{-2} r.m.s.

At all vibration magnitudes, there were significant differences in the fore-and-aft apparent masses at resonance between the feet hanging posture and the maximum thigh contact posture ($p < 0.05$), with the apparent mass magnitude at resonance higher in the maximum thigh contact posture than in the feet hanging posture. However, there were no significant differences in the fore-and-aft apparent mass between the maximum thigh contact posture, average thigh contact posture, and minimum thigh contact posture at any vibration magnitude, except between the maximum thigh contact posture and both the average thigh contact posture and the minimum thigh contact posture at 1.25 ms^{-2} r.m.s.

There was a trend for the resonance frequency to decrease with an increase in sitting mass (statistically significant at $p < 0.05$ for more than 50% of the combinations of posture and vibration magnitude). The correlation between the sitting mass (and the total body mass) and the magnitude of the apparent mass at resonance depended on the support of the feet: when there was no support of the feet (i.e. feet hanging posture) or minimal support of the feet (maximum thigh contact posture), the correlation was significant at all vibration magnitudes. However, when the feet were supported (average

thigh contact posture and minimum thigh contact posture), the correlation was not significant at any vibration magnitude.

7.3.1.2 Response at the backrest

The high subject variability in the fore-and-aft response on the seat was also present in the fore-and-aft response at the backrest (Figure 7.5). In all sitting postures, there is a first peak with a frequency less than 2 Hz in most individual data. A second, clearer, peak is present in all individuals between 3 and 5 Hz, except for subject 11 in the feet hanging posture, average thigh contact posture and minimum thigh contact posture and for subject 12 in all postures where the second peak appeared below 3 Hz (Table 7.1). A third broad peak in the frequency range 4 to 7 Hz appeared in the responses of a few subjects. The first and third peaks were clearer at low vibration magnitudes than at high vibration magnitudes.

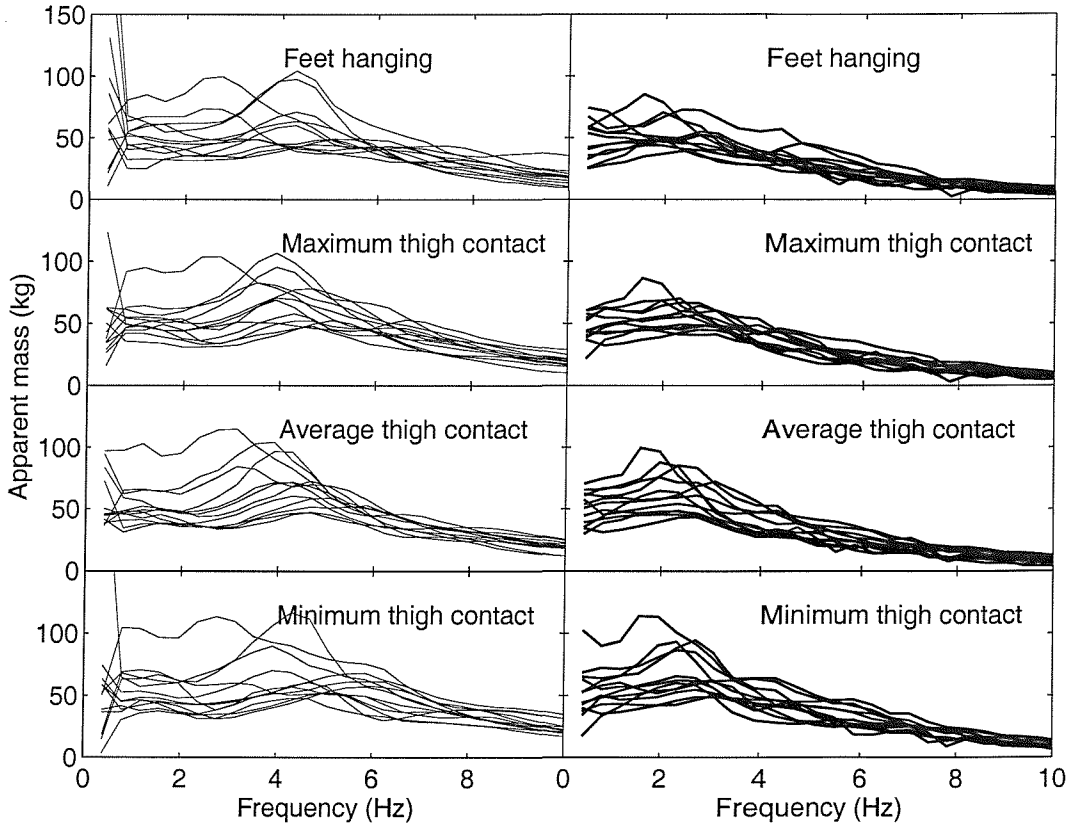

Figure 7.5 Inter-subject variability in the fore-and-aft apparent mass at the back for each posture at two vibration magnitudes. ———, 0.125 ms^{-2} r.m.s.; ———, 1.25 ms^{-2} r.m.s.

Table 7.1 Peak frequencies and corresponding fore-and-aft apparent mass at the back measured at 0.25 ms^{-2} r.m.s. *f*: resonance frequency; *m*: magnitude at resonance; 1: first peak; 2: second peak; - :peak not clear.

Subj. No.	Feet hanging				Maximum thigh contact			
	f_1 (Hz)	m_1(kg)	f_2 (Hz)	m_2 (kg)	f_1 (Hz)	m_1 (kg)	f_2 (Hz)	m_2 (kg)
1	1.95	43.0	4.10	42.4	1.76	44.6	3.71	51.2
2	0.98	69.4	3.71	98.0	0.78	62.7	3.52	95.0
3	1.76	45.6	3.5	42.3	1.56	49.0	3.71	50.4
4	1.76	44.8	3.52	62.0	1.56	51.0	3.52	62.9
5	-	-	3.52	91.3	0.98	62.4	3.52	102
6	1.17	47.4	3.32	32.3	1.17	50.9	3.32	64.7
7	-	-	4.10	67.6	1.37	54.9	4.10	76.0
8	-	-	4.30	43.5	1.37	37.3	4.49	53.3
9	1.17	41.8	3.91	58.5	1.17	48.7	3.52	53.3
10	0.78	49.1	3.32	48.2	1.17	48.4	3.52	56.2
11	0.78	70.3	2.54	81.9	1.56	65.2	3.32	81.1
12	1.17	94.8	1.76	101	1.56	102	2.54	104
Subj. No.	Average thigh contact				Minimum thigh contact			
	f_1 (Hz)	m_1 (kg)	f_2 (Hz)	m_2 (kg)	f_1 (Hz)	m_1 (kg)	f_2 (Hz)	m_2 (kg)
1	1.56	39.8	3.91	47.4	-	-	4.10	52.1
2	-	-	3.71	98.1	0.78	66.5	3.71	104
3	1.56	46.1	3.91	55.4	1.56	45.3	5.08	51.2
4	1.37	49.7	4.29	76.3	1.76	62.4	3.91	59.4
5	0.98	67.9	3.32	114	0.98	62.1	3.13	91.3
6	1.17	56.2	3.32	66.1	1.17	52.9	3.71	69.1
7	0.98	54.9	3.91	71.9	1.37	47.8	5.08	57.6
8	-	-	4.49	49.8	1.56	39.6	4.88	56.0
9	0.78	47.3	3.52	58.1	1.17	48.2	4.30	59.2
10	1.17	42.4	3.72	48.9	1.17	54.8	4.88	68.0
11	0.78	63.9	2.93	86.2	0.78	70.5	2.73	65.2
12	1.17	100	2.54	114	1.37	110	2.54	112

With a change in vibration magnitude, both the individual data and the median data showed changes in the fore-and-aft apparent mass measured at the back (Figures 7.6 and 7.7). There were significant differences in the resonance frequency (between 3 and 5 Hz) at the four vibration magnitudes ($p < 0.05$), except between 0.25 and 0.625 ms^{-2} r.m.s. in all postures and between 0.125 and 0.625 ms^{-2} r.m.s. in the minimum thigh contact posture. The median phases are also shown in Figure 7.7. These phases can be understood by reference to the sign convention for the fore-and-aft acceleration and the fore-and-aft force at the backrest (Section 7.2.1).

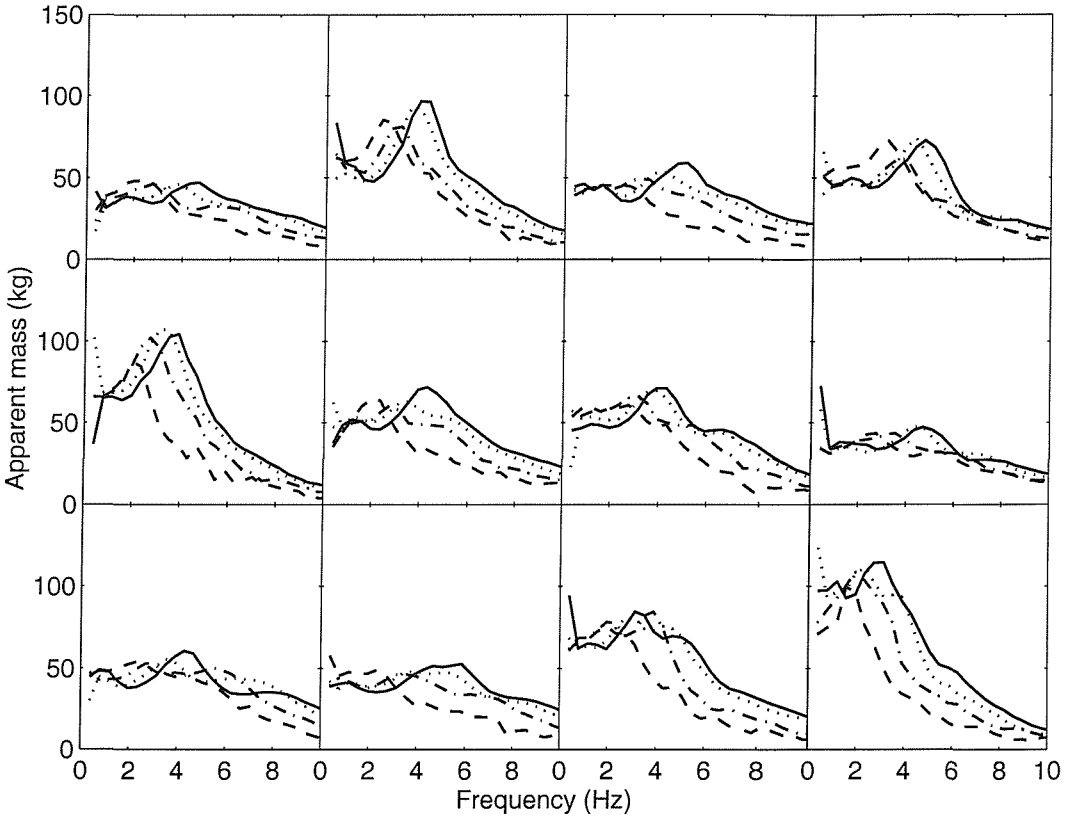

Figure 7.6 Fore-and-aft apparent masses of 12 subjects measured at the back in the average thigh contact posture at four vibration magnitudes. ———, 0.125 ms^{-2} r.m.s.; ·····, 0.25 ms^{-2} r.m.s.; –·–·–, 0.625 ms^{-2} r.m.s.; – – – –, 1.25 ms^{-2} r.m.s.

There were positive correlations between both the sitting mass (weight supported on the seat) and the total body mass and the magnitude of the first peak and the second peak (appearing at about 1 and 4 Hz, respectively, $p < 0.05$) in all 16 conditions (combination of 4 postures and 4 vibration magnitudes). There was no significant correlation between the sitting masses of the subjects and either the first resonance frequency or the second resonance frequency ($p > 0.1$) except marginally between the second resonance

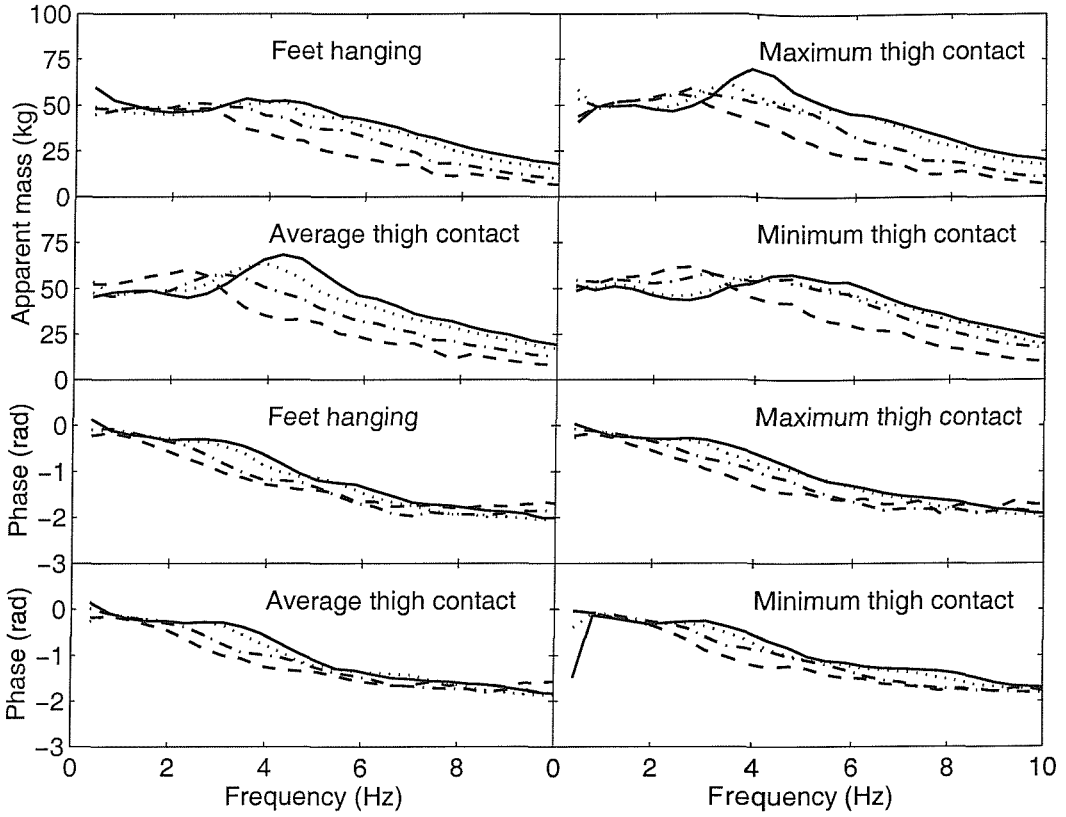

Figure 7.7 Median fore-and-aft apparent mass and phase angle at the back of twelve subjects: Effect of vibration magnitude. ———, 0.125 ms^{-2} r.m.s.; ·····, 0.25 ms^{-2} r.m.s.; —·—·—, 0.625 ms^{-2} r.m.s.; – – – –, 1.25 ms^{-2} r.m.s.

frequency and the sitting masses of the subjects in the minimum thigh contact posture (p = 0.078). The statures (i.e. standing heights) of the subjects were not correlated with either the first or the second resonance frequencies or the apparent masses at resonance in any posture except marginally correlated with the second resonance frequency in the feet hanging posture (p = 0.064).

7.3.2 Responses in the vertical direction

7.3.2.1 Response on the seat

The vertical forces on the seat were related to the acceleration measured in the fore-and-aft direction using the concept of 'cross-axis apparent mass'. For the four sitting postures, Figure 7.8 shows the variability between subjects in the vertical responses measured with fore-and-aft excitation at 0.125 and 1.25 ms^{-2} r.m.s. In all postures, the median resonance frequencies were in the range 6 to 8 Hz, depending on vibration magnitude. A trough can be seen around 5 Hz.

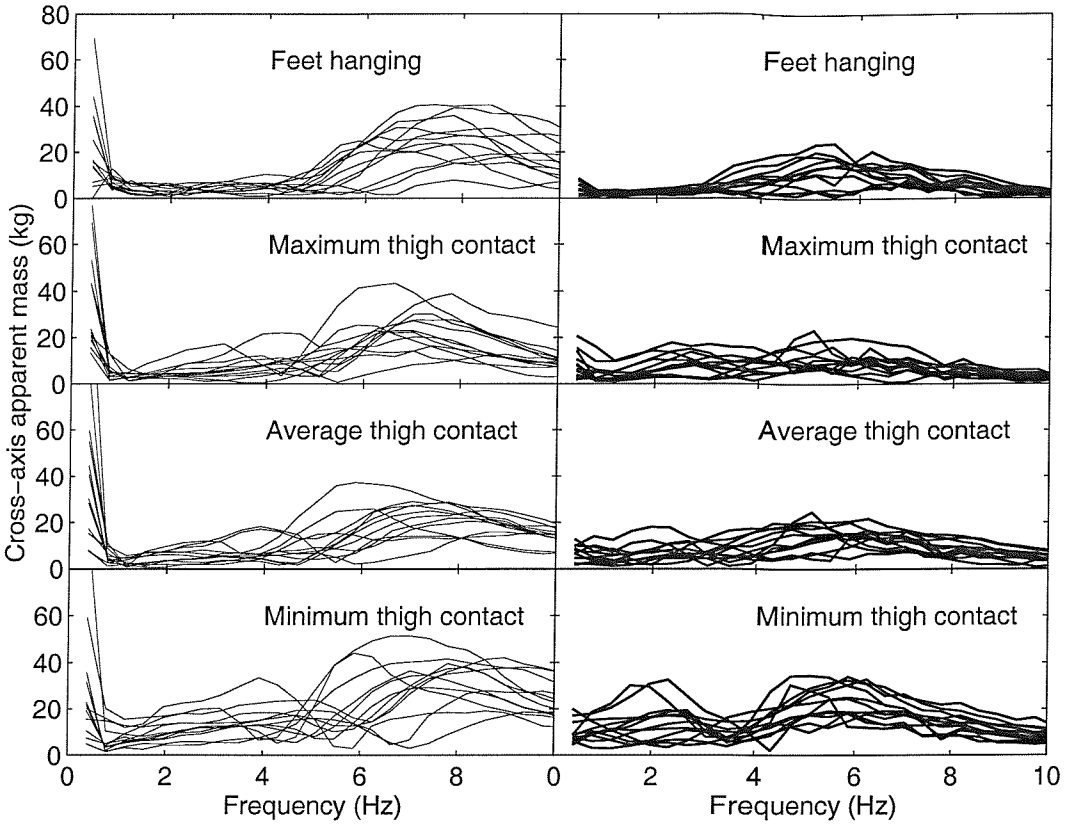

Figure 7.8 Inter-subject variability in the vertical cross-axis apparent mass on the seat for each posture at two vibration magnitudes. ———, 0.125 ms^{-2} r.m.s.; ———, 1.25 ms^{-2} r.m.s.

The resonance frequency and, generally, the cross-axis apparent mass at resonance, decreased with increasing vibration magnitude, following the same non-linear behaviour found in the fore-and-aft response (Figure 7.9 and 7.10). There were significant differences in the resonance frequencies measured with the four vibration magnitudes ($p < 0.05$), except between 0.125 and 0.25 ms^{-2} r.m.s. in the maximum thigh contact posture and between 0.625 and 1.25 ms^{-2} r.m.s. in both the maximum thigh contact posture and the average thigh contact posture. There were also significant differences in the cross-axis apparent mass at resonance measured at the four vibration magnitudes ($p < 0.05$), except between 0.125 and 0.25 ms^{-2} r.m.s. in both the average thigh contact posture and the minimum thigh contact posture, and between 0.625 and 1.25 ms^{-2} r.m.s. in the average thigh contact posture ($p < 0.05$).

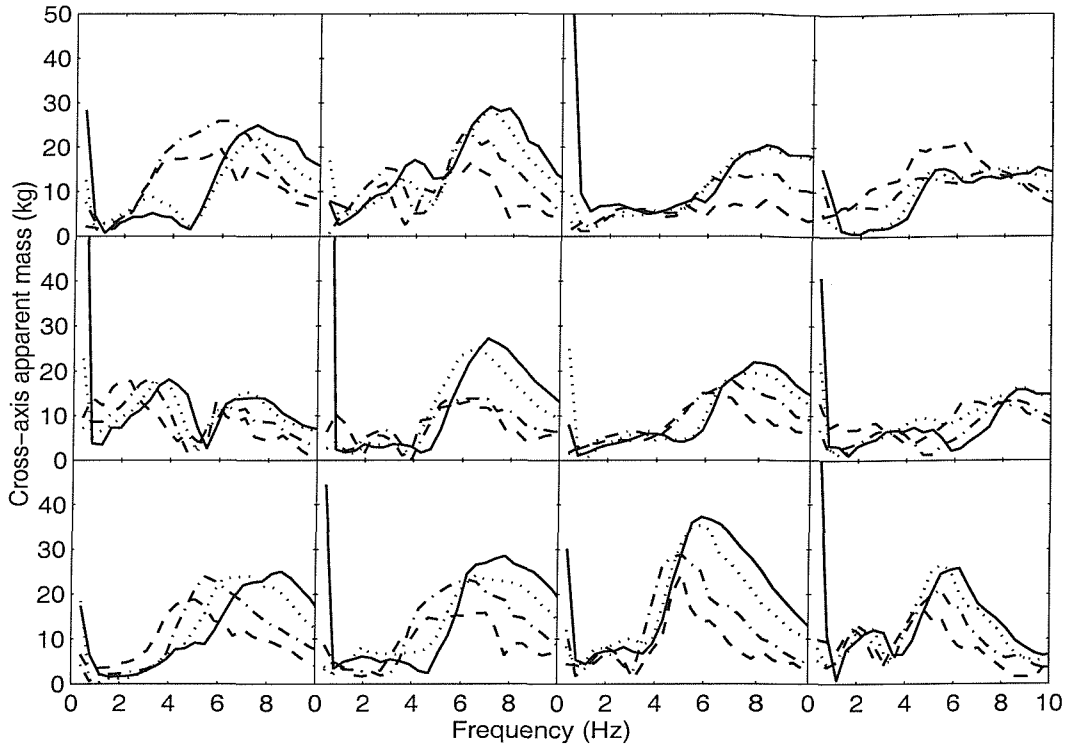

Figure 7.9 Vertical cross-axis apparent masses of 12 subjects measured on the seat in the average thigh contact posture at four vibration magnitudes. ———, 0.125 ms^{-2} r.m.s.; ·····, 0.25 ms^{-2} r.m.s.; –·–·–, 0.625 ms^{-2} r.m.s.; – – – –, 1.25 ms^{-2} r.m.s.

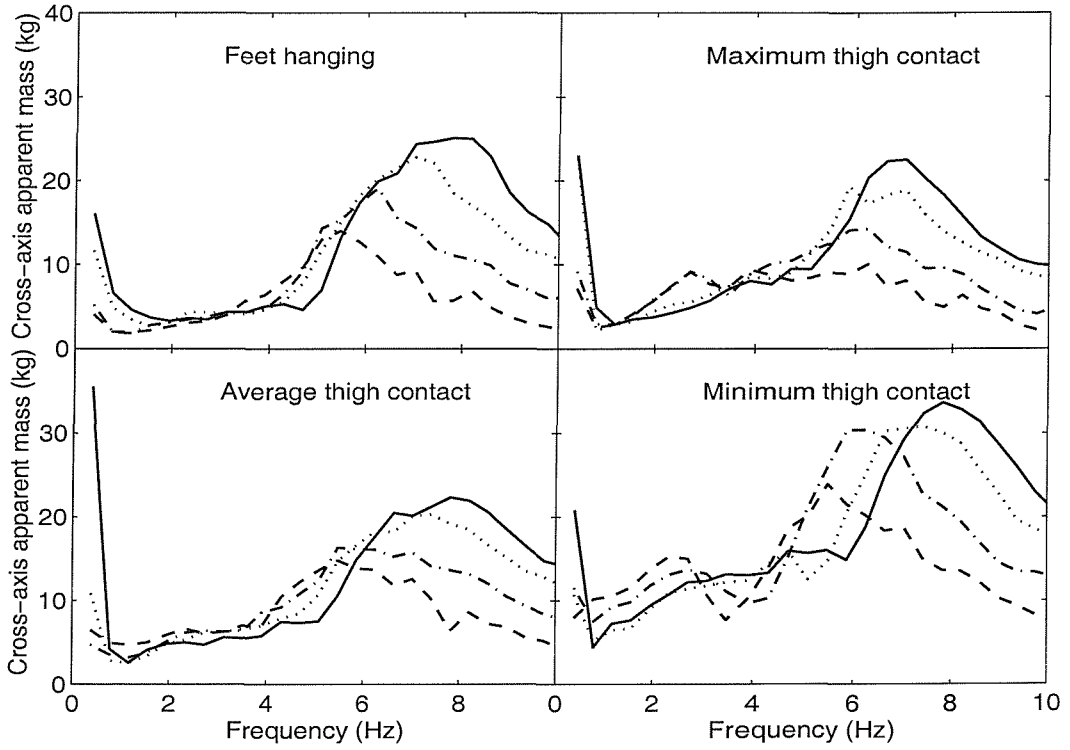

Figure 7.10 Median vertical cross-axis apparent mass of twelve subjects measured on the seat: Effect of vibration magnitude. ———, 0.125 ms^{-2} r.m.s.; ·····, 0.25 ms^{-2} r.m.s.; –·–·–, 0.625 ms^{-2} r.m.s.; – – – –, 1.25 ms^{-2} r.m.s.

At resonance, the minimum thigh contact posture gave a greater vertical cross-axis apparent mass than the other three postures. There was no significant difference in the vertical cross-axis apparent mass at resonance between the feet hanging posture, maximum thigh contact posture, and average thigh contact posture at any vibration magnitude ($p > 0.05$). There were significant differences between these three postures and the minimum thigh contact posture at all four vibration magnitudes. There were no significant differences in resonance frequencies between postures at any vibration magnitude ($p > 0.05$).

7.3.2.2 Response at the backrest

The force in the vertical direction at the back was measured for one subject in the four sitting postures and at three vibration magnitudes (0.125, 0.25, and 0.625 ms^{-2} r.m.s.). The vertical cross-axis apparent mass at the back was low and, mostly, did not exceed 3 kg at a resonance appearing between 5 and 7 Hz, depending on the vibration magnitude (Figure 7.11). In all postures, the resonance frequency decreased with increasing vibration magnitude.

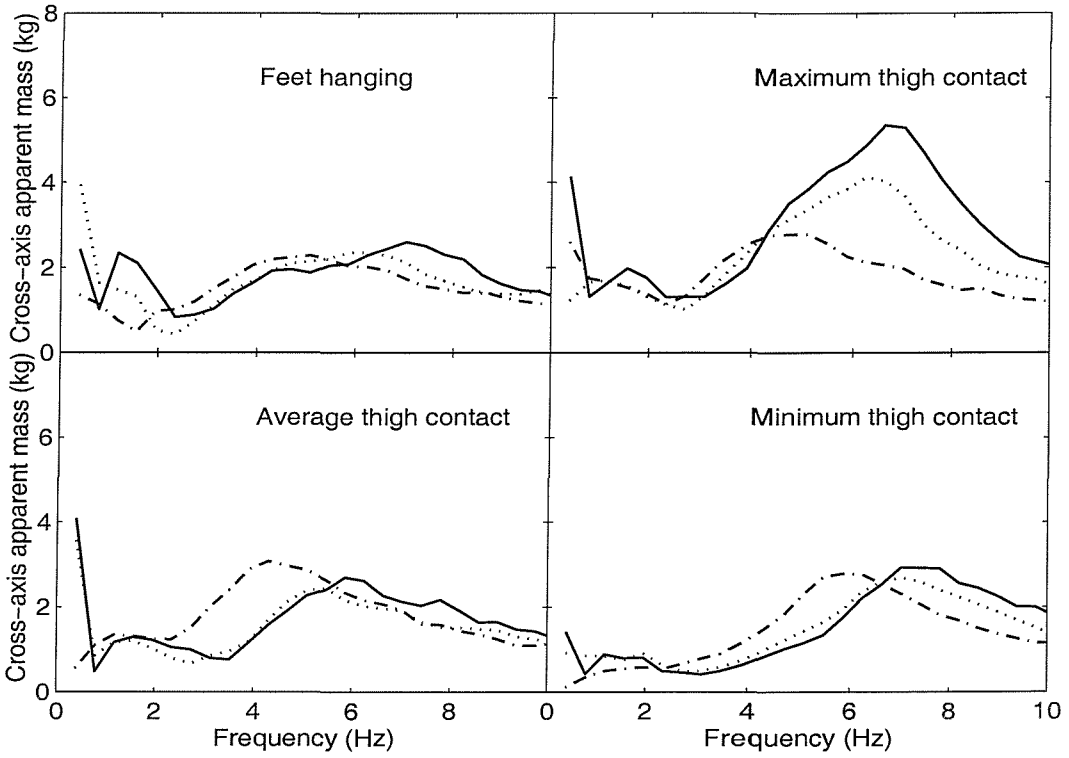

Figure 7.11 Vertical cross-axis apparent mass of one subject measured at the back at three vibration magnitudes. ———, 0.125 ms^{-2} r.m.s.; ·····, 0.25 ms^{-2} r.m.s.; —·—·—, 0.625 ms^{-2} r.m.s.

7.3.3 Response in the lateral direction (at the seat and the backrest)

The lateral cross-axis apparent masses measured on the seat and backrest were low in all postures (Figures 7.12 and 7.13). At the backrest, the lateral cross-axis apparent mass was slightly greater than the 'noise' measured without subjects (0 to 0.3 kg). On the seat, increasing the vibration magnitude decreased the resonance frequency in the lateral cross-axis apparent mass from about 5 Hz to around 2 to 3 Hz.

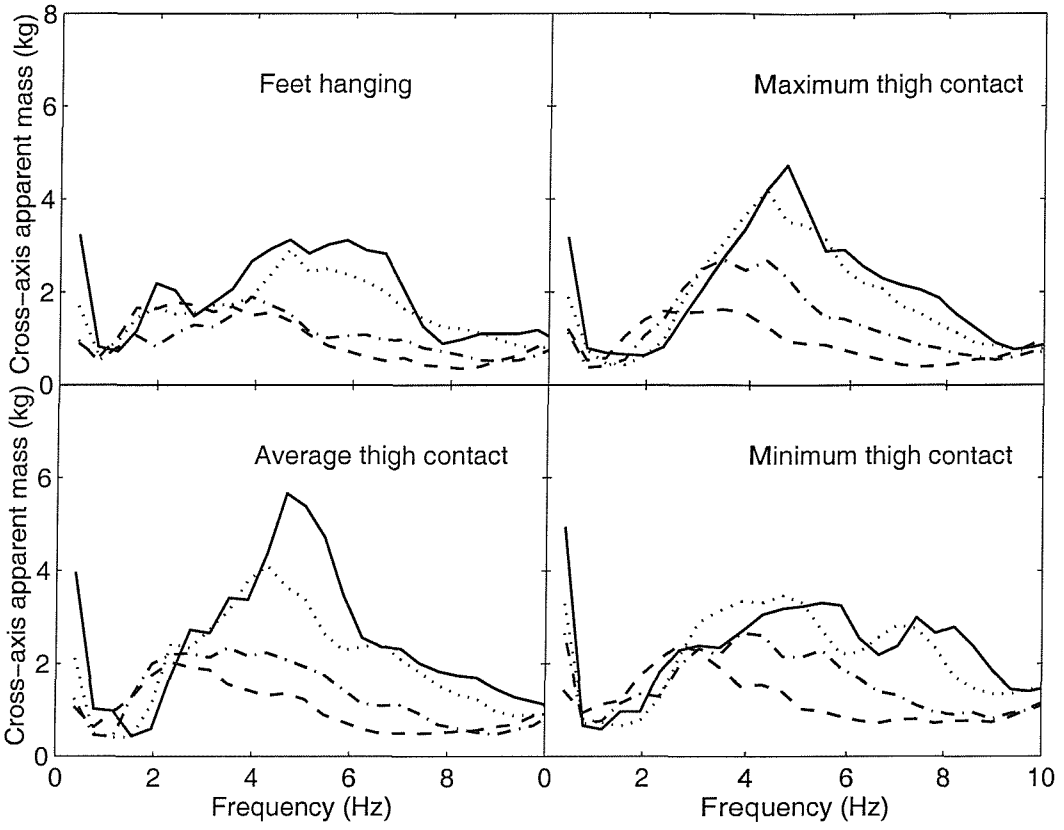

Figure 7.12 Median lateral cross-axis apparent mass of twelve subjects measured on the seat: effect of vibration magnitude. ———, 0.125 ms^{-2} r.m.s.; ·····, 0.25 ms^{-2} r.m.s.; —·—·—, 0.625 ms^{-2} r.m.s.; – – – –, 1.25 ms^{-2} r.m.s.

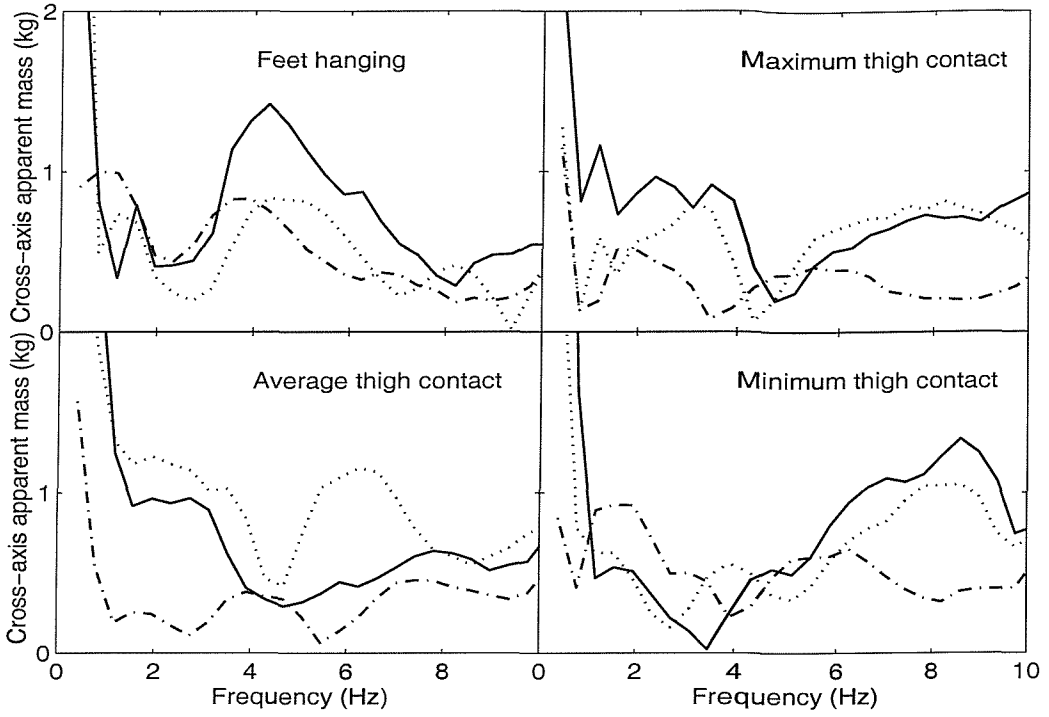

Figure 7.13 Lateral cross-axis apparent mass of one subject measured at the back at three vibration magnitudes. ———, 0.125 ms^{-2} r.m.s.; ·····, 0.25 ms^{-2} r.m.s.; –·–·–, 0.625 ms^{-2} r.m.s.

7.4 DISCUSSION

7.4.1 Response in the fore-and-aft direction

The response on the seat in the fore-and-aft direction showed a dependency on the status of the feet: when the feet were not supported there were two resonance frequencies, compared to one resonance frequency when the feet were supported. In comparison with the result obtained in Chapter 5 using vertical vibration, supporting the feet on a footrest moving in phase with the seat tended to reduce the apparent mass measured on the seat (due to the reduced mass on the seat) without changing the shape of the response.

The responses measured in the four postures in the present study can be compared with the responses measured in the same postures in Chapter 6 without a backrest (Figure 7.14). The comparison is shown for the median of the eleven subjects who participated in both the experiment described in this chapter and the experiment described in Chapter 6. Without a backrest, there was evidence of three modes, irrespective of whether the feet were supported (Figure 7.14). When a backrest was used, there were two modes in the feet unsupported posture (i.e. feet hanging) but only one mode when the feet were supported.

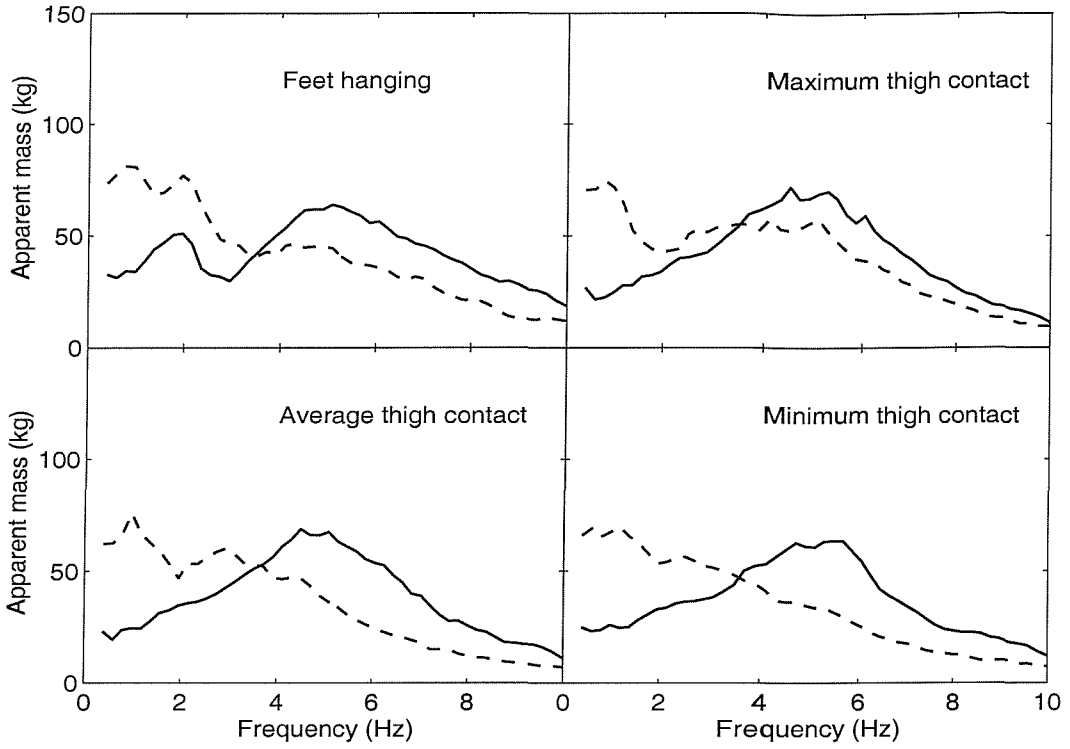

Figure 7.14 Median fore-and-aft apparent masses of eleven subjects measured on the seat at 0.125 ms^{-2} r.m.s. in four sitting postures: effect of backrest. ———, with backrest; – – – –, without backrest.

The one mode in the fore-and-aft apparent mass when the feet were supported is consistent with the single mode found by Fairley and Griffin (1990) with 1.0 ms^{-2} r.m.s. in a feet supported posture. Fairley and Griffin, who reported only two modes (at 0.7 and 1.5 to 3 Hz) without a backrest, suggested that the single mode found when using a backrest might be associated with the second mode measured without backrest. However, a third mode found above 3 Hz without a backrest in Chapter 6 and by Mansfield and Lundström (1999) was more pronounced at low vibration magnitudes (0.125 and 0.25 ms^{-2} r.m.s.) than at high vibration magnitudes. This, together with the results in the feet hanging posture (where two modes were found when using a backrest, see Figure 7.14) suggest that the second mode in the feet hanging posture and the single mode in the other postures when using a backrest may be associated with the third mode found without a backrest.

High forces were found in the fore-and-aft direction at the backrest. With a backrest, the 'total apparent mass' of the body can be calculated from the sum of the forces measured at the seat and the backrest. Although this summation may be applicable where the human body behaves linearly in response to vibration (e.g. at very low frequencies, below

1 Hz), it is not applicable at higher frequencies where the body behaves non-linearly and the superposition principle will not apply. The apparatus used by Fairley and Griffin (1990) was designed to combine the force at the back with that on the seat (a vertical flat backrest was welded to the top plate of the force platform mounted on the seat, so giving measurements of forces transmitted to the body from both the seat and the back). This would explain the higher apparent mass obtained by Fairley and Griffin than measured on the seat in this chapter. Fairley and Griffin found an increase in their measure of apparent mass at frequencies above 0.8 Hz when the body made contact with the backrest.

The increased apparent mass in all postures at high frequencies when using a backrest is similar to the increased head motion (in vertical, fore-and-aft, lateral, pitch, roll, and yaw axes) when subjects use a backrest during exposure to translational or rotational whole-body vibration (Paddan and Griffin, 1988a,b; 1994; 2000). Clearly, the backrest can be a source of vibration transmission to the body and so reduction in the vibration on a backrest may reduce some adverse human responses to vibration. However, with the non-rigid seats used in many vehicles the forces at the seat and backrest will not be in phase (unlike this study) and the vibration at the seat and backrest may be expected to combine in a phase-dependent manner. Furthermore, at low frequencies, a backrest may provide postural stability and reduce some effects of vibration, even though there is an increased apparent mass when using a backrest.

The correlation between the sitting mass (or the total body mass) of the subject and the apparent mass on the seat at resonance was found to depend on the support of the feet: significant correlations were found with feet hanging and maximum thigh contact postures while insignificant correlations were found with average thigh contact and minimum thigh contact postures. It seems that the response on the seat in the fore-and-aft direction depends on the foot posture in a complex manner that not only changes the shape of the response but also affects the correlations.

The significant correlations between the masses of subjects and the apparent masses measured at the back at resonance in all conditions are similar to the high correlation between sitting mass and vertical apparent mass at resonance during vertical vibration (e.g. Fairley and Griffin, 1989; Rakheja *et al.*, 2002). The way that fore-and-aft vibration is applied to the back resembles the way vertical vibration is applied to the seat: both applied forces are normal to the body, in contrast to the shear force applied by the seat during fore-and-aft vibration.

The mode between 1 Hz and 2 Hz seen in the fore-and-aft apparent mass on the seat in the feet hanging posture disappeared when the feet were supported. This mode might be associated with the second mode found in Chapter 6 between 1 and 3 Hz in all sitting postures (i.e. feet hanging, maximum thigh contact, average thigh contact and minimum thigh contact) when no backrest was used (see feet hanging posture in Figure 7.14). At a similar frequency, Matsumoto and Griffin (2001) found a pitching mode in the pelvis and the upper body during vertical vibration. Kitazaki and Griffin (1997) reported an out-of-phase fore-and-aft motion of the head and pelvis at about 1 and 2 Hz caused by bending deformation of the spine during vertical vibration. When using a backrest, a 1 to 2 Hz peak is also pronounced in measures of the transmissibility of fore-and-aft seat vibration to fore-and-aft head vibration (Paddan and Griffin, 1988b). Although the feet were supported, when no backrest was used the rotational modes were clearer, consistent with the upper body being free to pitch. When the subjects leant on a backrest, the presence of a backrest together with the foot support reduced the freedom of the body to pitch forward and backward. However, this was not the case with the feet hanging posture where the body still has some degree of freedom to pitch. This might explain the presence of the 1 to 2 Hz mode in all sitting postures when no backrest was used but only in the feet hanging posture when a backrest was used. A mode in a similar frequency range was also found in the fore-and-aft apparent mass at the back in all postures. The mode measured at the back at 1 to 2 Hz might be associated with a pitching mode also seen at the head in this frequency range, as reported by Paddan and Griffin (1988b).

The body movements responsible for the peaks appearing in the fore-and-aft apparent mass on the seat and backrest, as well as the causes of the non-linearity, are not yet well established. The resonance in the vicinity of 4 Hz in the fore-and-aft apparent mass on the seat could reflect a response of the tissues of the buttocks. Kitazaki and Griffin (1997) noticed shear deformation of buttocks tissue beneath the pelvis and fore-and-aft movement of the pelvis in the range 4 to 6.5 Hz. The peaks in the fore-and-aft apparent mass could also be the result of bending modes in the spine or a pitching mode of the pelvis (the spine and the pelvis appear to have rotational modes at these frequencies, Sandover and Dupuis, 1987; Kitazaki and Griffin, 1998). The mechanisms producing the resonance frequencies and the non-linearity are gradually being uncovered from measures of the transmissibilities to different locations on the body and measures of the apparent mass, both allowing the gradual development of improved biodynamic models (see e.g. Matsumoto and Griffin, 2001; Kitazaki and Griffin, 1997).

7.4.2 Response in the vertical and lateral directions

On the seat and backrest, vertical forces (presented as cross-axis apparent masses) indicated a resonance between 5 and 8 Hz, decreasing in frequency with increasing vibration magnitude. However, the magnitudes of these forces were only considerable on the seat. The considerable forces on the seat in the fore-and-aft direction during vertical excitation, were attributed to rotational modes of different parts of the upper body. If a segment of the upper body has a pitch mode during vertical excitation, the same mode may be expected during fore-and-aft excitation. The rotational modes in the mid-sagittal plane of the pelvis, the spine and the head seen in both transmissibility studies (e.g. Paddan and Griffin, 1988a; Matsumoto and Griffin, 1998a) and biodynamic models (e.g. Kitazaki and Griffin, 1997; Matsumoto and Griffin, 2001) could be responsible for both the vertical forces on the seat during fore-and-aft vibration and the fore-and-aft forces on the seat during vertical vibration. The low vertical forces at the backrest could be the result of some vertical motion of the spine accompanying the pitching mode of the pelvis, spine and upper body.

The vertical cross-axis apparent mass on the seat at resonance was greatest in the minimum thigh contact posture. The fore-and-aft cross-axis apparent mass on the seat during vertical excitation was also greater in the minimum thigh contact posture than in the other postures as was shown in Chapter 5. In this posture (i.e. the minimum thigh contact posture) the body is resting on a small area (around the ischial tuberosities) allowing easier pitching of the upper body in the minimum thigh contact posture than in the other postures as was explained in Chapter 4 and Chapter 5.

The vertical cross-axis apparent masses measured on the seat were compared to those measured on the seat without a backrest as was shown in Chapter 6. The presence of the backrest shifted the resonance frequency to a higher frequency (see the feet hanging posture and the maximum thigh contact posture in Figure 7.15). The high vertical forces on the seat at low frequencies with no backrest were explained in Chapter 6 by the subjects applying forces on the seat in the vertical direction when they sway backward, and applying a vertical force on the footrest when they sway forward (Figure 7.15). The subjects in the present study did not apply a vertical force on the seat at low frequencies since the backrest restrained the body from swaying backward. The increase in the vertical forces at high frequencies (Figure 7.15) is not surprising given that the backrest transmits vibration to the body at high frequencies: the backrest increased the pitching motion of the upper body by applying a fore-and-aft force on the upper body.

There were low forces in the lateral direction on the seat and at the backrest. This is consistent with the body being roughly symmetrical about the mid-sagittal plane. The lateral forces on the seat, are slightly greater than those measured on the seat without a backrest (see Chapter 6 and Figure 7.16). The slight increase in the lateral forces when using the backrest is consistent with a slight increase in the lateral motion of the head when a similar backrest was used (Paddan and Griffin, 1988b).

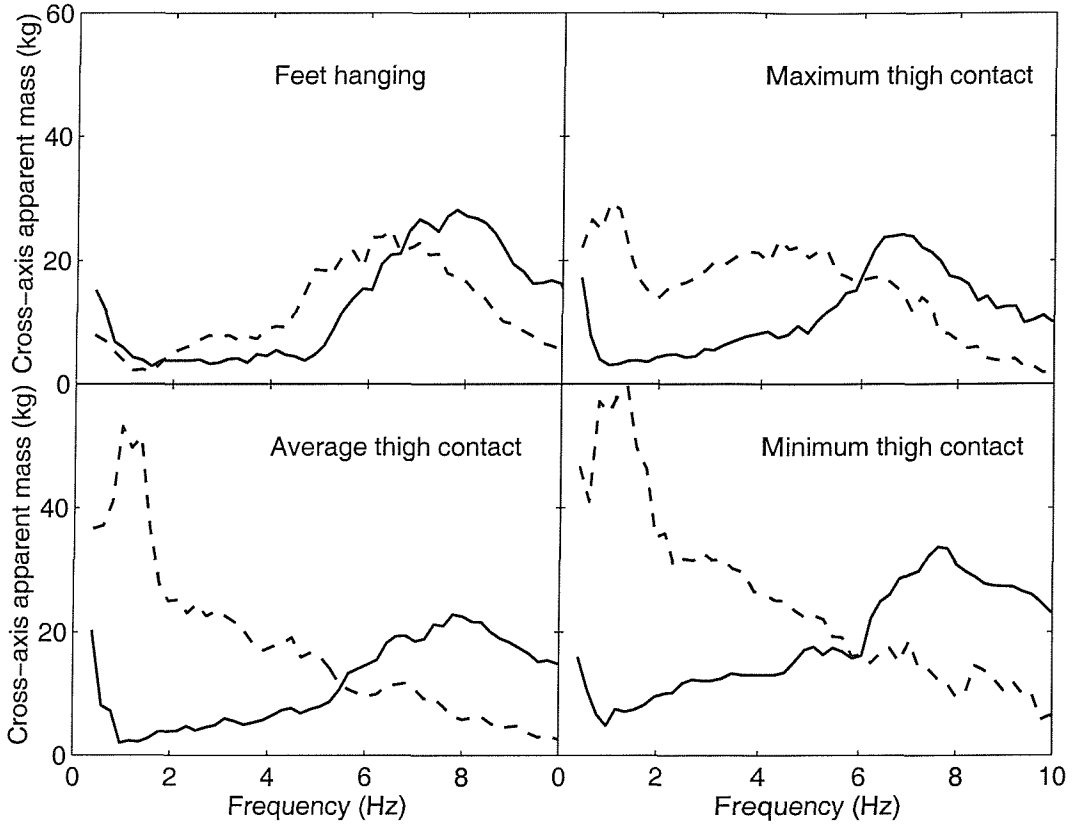

Figure 7.15 Median vertical cross-axis apparent masses of eleven subjects measured on the seat at 0.125 ms^{-2} r.m.s. in four sitting postures: effect of backrest. ———, with backrest; – – – –, without backrest.

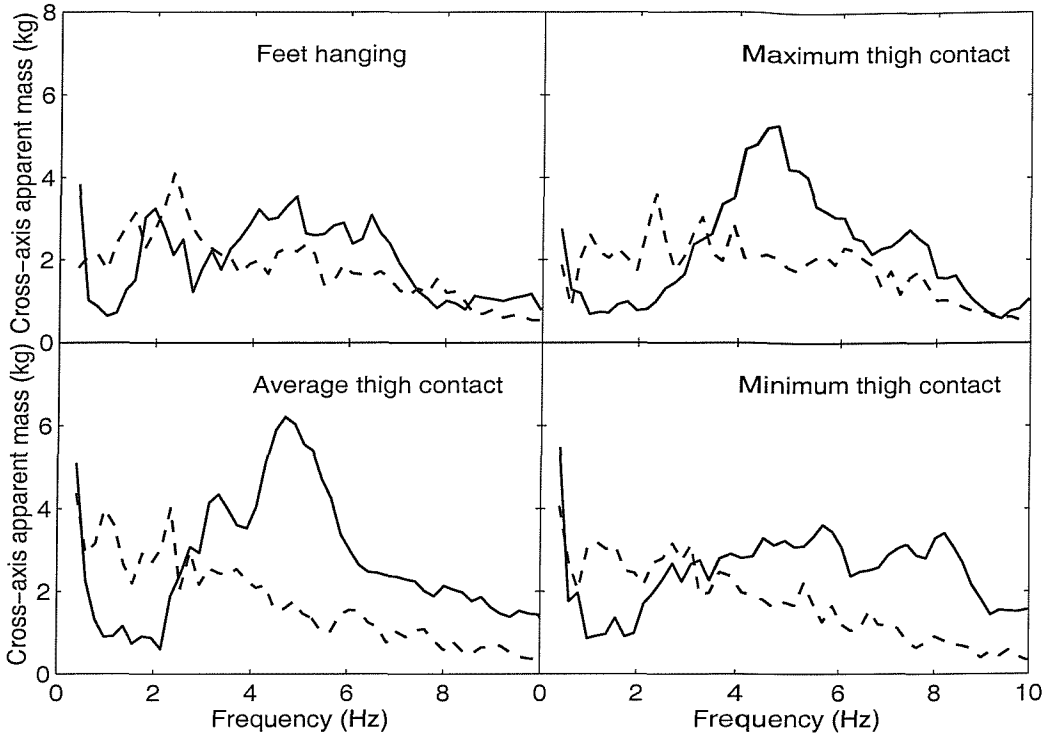

Figure 7.16 Median lateral cross-axis apparent masses of eleven subjects measured on the seat at 0.125 ms^{-2} r.m.s. in four sitting postures: effect of backrest. ———, With backrest; – – – –, Without backrest.

7.5 CONCLUSION

Fore-and-aft vibration of subjects sitting in a rigid seat with a rigid flat vertical backrest resulted in high forces in the fore-and-aft and vertical directions on the seat and high forces in the fore-and-aft direction on the backrest. Lateral forces on the seat and backrest, and vertical forces at the backrest, are relatively small.

The characteristics of the fore-and-aft forces on the seat depended on whether the feet were supported on a footrest: two resonance frequencies were found when the feet were not supported compared to only one resonance frequency when the feet were supported. Forces in all directions on the seat and backrest showed non-linear behaviour.

In comparison with measurements with no back support, the backrest reduced forces in the fore-and-aft and vertical directions on the seat at low frequencies and increased forces at high frequencies.

The high fore-and-aft forces at the backrest confirm the need to consider the contribution of backrests and footrests to vibration of the body.

CHAPTER 8 EFFECT OF SEAT SURFACE ANGLE ON FORCES AT THE SEAT SURFACE DURING WHOLE-BODY VERTICAL EXCITATION

8.1 INTRODUCTION

It has been shown in the previous chapters that the response of humans to vibration depends on several factors. Vibration characteristics (i.e. magnitude, frequency, and direction), the adopted sitting posture and the seating arrangement are among these factors. For example, when exposed to vertical vibration the human body behaves like a pure mass at low frequencies (below 2 Hz) but there is a resonance in the vicinity of 5 Hz. A second resonance appears in the range 8 to 13 Hz while at higher frequencies the response seems to that of a spring-damper combination. The biodynamic responses of the human body also show a dependency on the vibration magnitude: reductions in the principal resonance frequency of the apparent mass of the body with increases in vibration magnitude have been shown.

A seat-person system behaves like a dynamically coupled system when exposed to whole-body vibration. This means that the responses of the occupant of a compliant seat affect the responses of the seat. Changing seat dynamics may also change the responses of the seat occupant to vibration by altering the way the body is coupled to the seat, for example by changing the point of contact of the subject with the seat or changing the sitting posture. Fairley and Griffin (1989) noticed that the vertical apparent mass of the body at low frequencies increased with increasing height of a stationary footrest, in contrast to decreased apparent mass with increasing height of a footrest moving in phase with the seat. It was found in Chapter 4 that the fore-and-aft cross-axis apparent mass (the ratio of the fore-and-aft force on the seat to vertical acceleration) depended on support for the lower legs on a moving footrest. It is therefore of interest to clarify the effect of seat characteristics (e.g. with or without a backrest, backrest inclination, seat surface angle, presence of a footrest, etc.) when studying the responses of humans to vibration.

Although the supporting surfaces of vehicle seats are often inclined, most studies of the dynamic responses of the body have involved horizontal supporting seat surfaces. In a study of the effect of seat inclination on both seat transmissibility and the apparent mass

of the body, Wei and Griffin (1998) found that increasing the seat inclination from 0 to 20° decreased the seat cushion transmissibility at frequencies below 6 Hz and increased seat transmissibility above 6 Hz. Subject vertical apparent mass decreased with increasing seat angle at frequencies below 5.5 Hz, although the change was generally small.

As was seen in the previous chapters, the human body moves in two-dimensions (in the mid sagittal plane) when exposed to vertical or fore-and-aft vibration (see also Matsumoto and Griffin, 2002a). High fore-and-aft forces have been found on the seat during vertical excitation and high vertical forces have been found during fore-and-aft excitation. The high cross-axis forces were attributed to pitching modes in the body. These measurements were obtained on a horizontal seat surface. There are no known measurements of the effects of seat surface angles or seat backrest angles on the vertical and fore-and-aft forces at the seat surface and the backrest.

This study investigated the effect of variations in seat surface angle on the 'vertical apparent mass' (calculated from the force normal to the seat surface and vertical acceleration) and 'fore-and-aft cross-axis apparent mass' (calculated from the force parallel to the seat surface and vertical acceleration) during exposure to whole-body vertical vibration. There is an evidence of a decrease in the non-linearity in the vertical direction when tensing or stiffening the muscles of the ischial tuberosities (Matsumoto and Griffin, 2002a). However, it is not clear whether the stiffening in the axial, shear or both directions reduced the non-linearity. In the present study, It was hypothesised that increasing seat surface angle would result in an increase in shear stiffness of tissue at the ischial tuberosities and that this increase in stiffness might affect the non-linearity in the 'vertical' as well as in the 'fore-and-aft' direction. It was also hypothesised that there would be only small variations in the 'vertical' forces with variation in seat angles between 0 and 15°; assuming little change in body posture with these changes in seat angle, the vertical forces will vary with the cosine of the seat angle, which is close to unity for the angles employed. With a horizontal seat (i.e. at 0°), the fore-and-aft cross-axis apparent mass is mainly produced by the pitching modes of the upper body. However, with inclinations of 5, 10, and 15°, the 'fore-and-aft cross-axis apparent mass' has two main components: one is produced by the pitching movements of the body and the other by the force exerted on the mass of the body in the direction parallel to the seat surface. The latter was expected to increase with increasing seat surface inclination. The addition of a backrest was expected to reduce both the 'vertical apparent mass' and the 'fore-and-aft cross-axis apparent mass' at low frequencies.

8.2 APPARATUS, EXPERIMENTAL DESIGN AND ANALYSIS

8.2.1 Apparatus

Subjects were exposed to whole-body vertical vibration using an electro-hydraulic vibrator capable of peak-to-peak displacements of 1 metre. A rigid seat, with a flat supporting surface that could be adjusted to different angles was mounted on the platform of the vibrator. The seat had a rigid flat vertical backrest, the bottom of which was level with the upper surface of the seat while the top was 52 cm above the seat surface. When subjects were not using the backrest, they sat in an upright posture without their backs touching the backrest by leaving a gap between the back and the backrest. When the backrest was used, the subjects were asked to maintain full contact with the backrest. Subjects supported their feet on a footrest that was inclined by 45° and moved in phase with the seat (Figure 8.1).

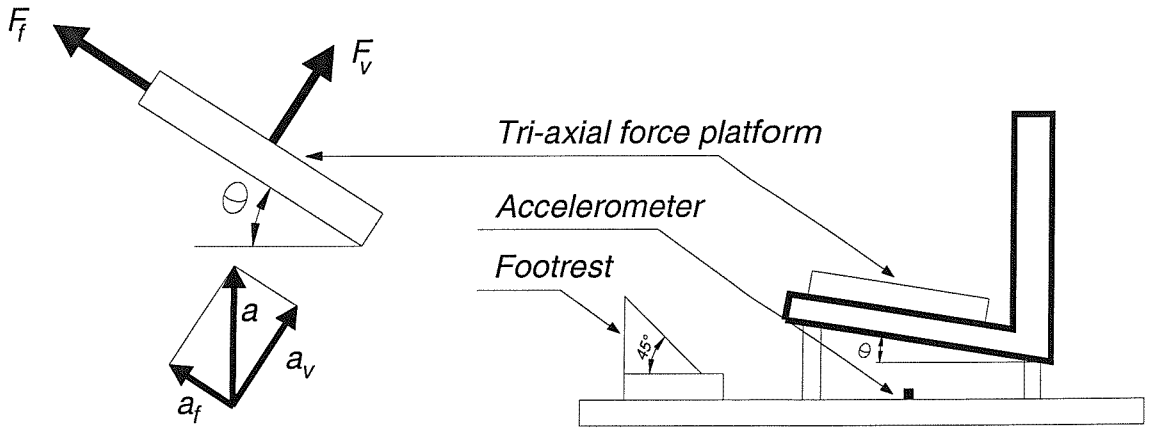

Figure 8.1 Schematic diagram of the seat, force platform and accelerometer arrangements.

A tri-axial force platform (Kistler 9281 B) was used to measure the forces normal and parallel to the supporting seat surface (i.e. 'vertical' and 'fore-and-aft', respectively, Figure 8.1). The force platform has been described in Chapter 3. Signals from the force platform were amplified using charge amplifiers (Kistler 5007). Acceleration was measured in the vertical direction at the centre of the force platform using a piezo-resistive accelerometer (Entran EGCSY-240D-10). The acceleration and force were acquired at 200 samples per second via 67 Hz anti-aliasing filters with an attenuation rate of 70 dB in the first octave. The duration of each vibration exposure was 60 seconds.

8.2.2 Experimental design

Twelve male subjects with an average age 30.9 years (range 24 to 47 years), weight 76.5 kg (range 65 to 103 kg), and stature 1.77 m (range 1.64 to 1.86 m), were exposed to random vertical vibration with an approximately flat constant bandwidth acceleration power spectrum over the frequency range 0.25 to 15 Hz. Characteristics of all subjects are given in Appendix E.

The experiment was conducted using four seat surface angles: 0, 5, 10, and 15°. The subjects held an emergency STOP button with their hands in their laps. The subjects were instructed to stretch their legs forward and rest their feet on the inclined footrest. The footrest was moved toward the seat when the seat angle was increased, so as to maintain similar thigh contact with the seat in all conditions. With each seat angle, the twelve subjects were exposed to four vibration magnitudes (0.125, 0.25, 0.625, and 1.25 ms^{-2} r.m.s.), both with and without the vertical backrest. The presentation of the four seat angles and the four vibration magnitudes was balanced across subjects.

8.2.3 Analysis

The components of acceleration in the directions normal and parallel to the seat surface (a_v and a_f in Figure 8.1) could be used with the forces measured normal and parallel to the seat surface to calculate a 'vertical apparent mass' and a 'fore-and-aft cross-axis apparent mass'. However, with the seat angle changing, the magnitude of acceleration in these directions also changed during the experiment. The 'vertical apparent masses' at different seat angles and the 'fore-and-aft cross-axis apparent masses' measured with different seat angles will therefore have varied due to the combined effects of changing the seat surface angle and the non-linearity of the body. An alternative analysis is for the force measured normal to the seat surface, F_v, to be resolved into vertical and fore-and-aft components, and the force measured parallel to the seat surface, F_f, to be resolved into vertical and fore-and-aft components so as to calculate resultant forces in the vertical and fore-and-aft directions. However, given the non-linearity of the human body, this simple resolving and adding of force components may be suspect. It was therefore decided to directly compare the measured forces (i.e. the forces normal and parallel to the seat surface) with the applied vertical acceleration

The forces measured normal to the seat surface (F_v) and parallel to the seat surface (F_f) were analysed relative to the vertical acceleration (see Figure 8.1), producing two frequency response functions: one normal to the seat surface (i.e. 'vertical apparent mass') and the other parallel to the seat surface ('fore-and-aft cross-axis apparent mass'). The two frequency response functions were calculated using the cross-spectral density method:

$$M(\omega) = \frac{S_{af}(\omega)}{S_{aa}(\omega)} \tag{8.1}$$

where, $M(\omega)$ is the 'vertical apparent mass' (or 'fore-and-aft cross-axis apparent mass'), in kg, $S_{af}(\omega)$ is the cross spectral density between the force measured normal (or parallel) to the seat surface and the applied vertical acceleration, and $S_{aa}(\omega)$ is the power spectral density of the applied vertical acceleration. All spectra were calculated by using a resolution of 0.39 Hz. Before calculating $M(\omega)$, mass cancellation was needed to remove the effect of the mass of the aluminium plate of the force platform (15 kg) mounted 'above' the force cells. The force produced by the aluminium plate of the force platform in the direction normal to the seat surface (15 kg $\cdot$ a $\cdot$ cos θ, Figure 8.1) was subtracted in the time domain from the force measured normal to the seat surface, F_v. The force produced by the aluminium plate in the direction parallel to the seat surface (15 kg $\cdot$ a $\cdot$ sin θ) was subtracted in the time domain from the force measured in the direction parallel to the seat surface, F_f. The coherency between the force and acceleration was calculated after mass cancellation in the time domain and found to be above 0.96 over the whole frequency range for the 'vertical apparent mass' and above about 0.85 over the whole frequency range for the 'fore-and-aft cross-axis apparent mass' except in the region 5 to 7 Hz where a trough was evident in the data (see Section 8.3.2).

8.3 RESULTS

As in the previous chapters, mainly median responses will be shown in the results section while individual responses are given in Appendix E.

8.3.1 'Vertical apparent mass'

The 'vertical apparent masses' of 12 subjects (obtained from the force normal to the seat surface and the vertical applied acceleration) measured at 1.25 ms^{-2} r.m.s. with four seat angles are shown in Figure 8.2. All subjects and all seat angles showed a similar response characteristic: the modulus increased with increasing frequency up to a peak in

the vicinity of 5 Hz, and then decreased with increasing frequency. The phase lag between the vertical acceleration and the 'vertical' force was zero at very low frequencies and increased with frequency up to 1.5 radians, with no big change in the phase angle at high frequencies.

The coefficient of variation (defined as the ratio of the standard deviation to the mean) showed that at all seat angles and with all vibration magnitudes, the inter-subject variability was greatest around the resonance frequency.

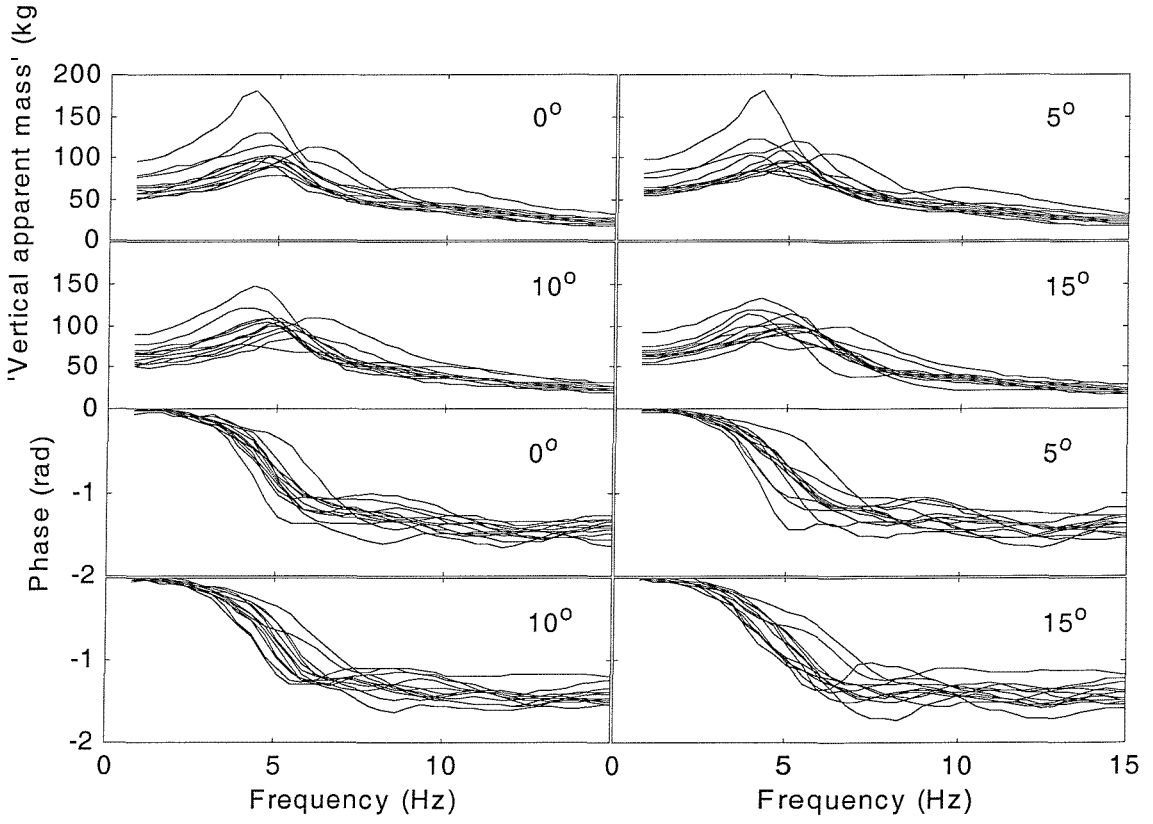

Figure 8.2 Inter-subject variability in the 'vertical apparent masses' measured at 1.25 ms^{-2} r.m.s. with four different seat angles and without a backrest.

8.3.1.1 Effect of vibration magnitude

With all seat angles, the 'vertical apparent mass' showed a non-linear characteristic (Figure 8.3): statistically significant differences were found between the resonance frequencies at the different vibration magnitudes ($p < 0.05$), except between 0.125 and 0.25 ms^{-2} r.m.s. with seat angles of 5 and 15°. Further statistical analysis was conducted to investigate whether the seat angle affected the size of the change in the resonance frequency between the two lower vibration magnitudes (i.e. 0.125 and 0.25 ms^{-2} r.m.s.) and between the two higher vibration magnitudes (i.e. 0.625 and 1.25 ms^{-2} r.m.s.). The

results indicate that the sizes of differences in the resonance frequencies obtained at the two lower vibration magnitudes and the sizes of differences in the resonance frequencies obtained at the two higher vibration magnitude did not depend on the seat angle (Friedman, $p > 0.7$).

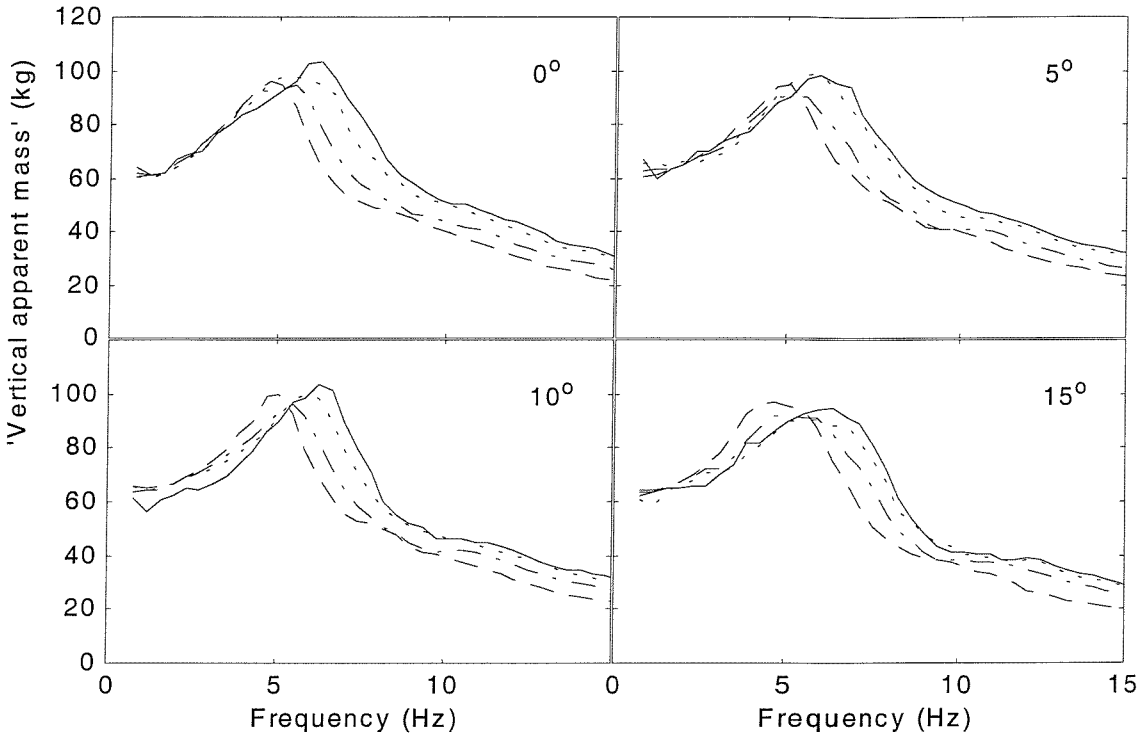

Figure 8.3 Effect of vibration magnitude on median 'vertical apparent masses' of twelve subjects measured without a backrest: ———, 0.125 ms^{-2} r.m.s.; ·····, 0.25 ms^{-2} r.m.s.; –·–·–, 0.625 ms^{-2} r.m.s.; – – – –, 1.25 ms^{-2} r.m.s. with four seat angles of 0, 5, 10 and 15°.

The effect of vibration magnitude on the 'vertical apparent mass' magnitude at resonance was clearer at low seat angles: statistically significant differences were found in the 'vertical apparent mass' at resonance measured at the different vibration magnitudes only when the seat angle was 0° or 5° (Friedman, $p < 0.05$). At 0°, significant differences in the apparent mass magnitude at resonance were found between 0.125 and 0.25, between 0.625 and 1.25 ms^{-2} r.m.s., and between 0.25 and 0.625 ms^{-2} r.m.s. (Wilcoxon, $p < 0.05$). At 5°, significant differences were found between 0.125 and 0.625 ms^{-2} r.m.s. and between 0.25 and 0.625 ms^{-2} r.m.s. (Wilcoxon, $p < 0.05$). Where there were differences, the magnitude at resonance at the lower vibration magnitude was higher than the magnitude at the higher vibration magnitude. The median resonance frequencies and the median 'vertical apparent masses' at resonance obtained with the four vibration magnitudes and the four seat angles are shown in Table 8.1.

Table 8.1 Median resonance frequencies and magnitudes at resonance of the 'vertical apparent mass' for four seat angles at 0.125, 0.250, 0.625 and 1.25 ms^{-2} r.m.s. (Without backrest)

Seat angle (°)	Resonance frequency (Hz)				Magnitude at resonance (kg)			
	0.125	0.250	0.625	1.250	0.125	0.250	0.625	1.250
0	6.25	5.47	5.47	4.69	103.4	97.6	94.3	95.8
5	5.86	5.86	5.47	5.08	97.9	99.1	90.1	94.8
10	6.25	5.86	5.47	5.08	103.4	99.9	96.4	99.5
15	6.25	5.47	4.69	4.69	94.8	90.7	92.0	96.6

8.3.1.2 Effect of seat angle

At all vibration magnitudes, the 'vertical apparent masses' were similar at each of the four seat angles (Figure 8.4 and 8.5). There were no statistically significant differences in the resonance frequencies, or the magnitudes at resonance, with changing seat surface angle at any vibration magnitude (Friedman, $p > 0.1$). There were also no significant differences between the 'vertical apparent masses' measured with 0° and the 'vertical apparent masses' measured with 5, 10, or 15° at any frequency (0.25 to 15 Hz, $p > 0.1$).

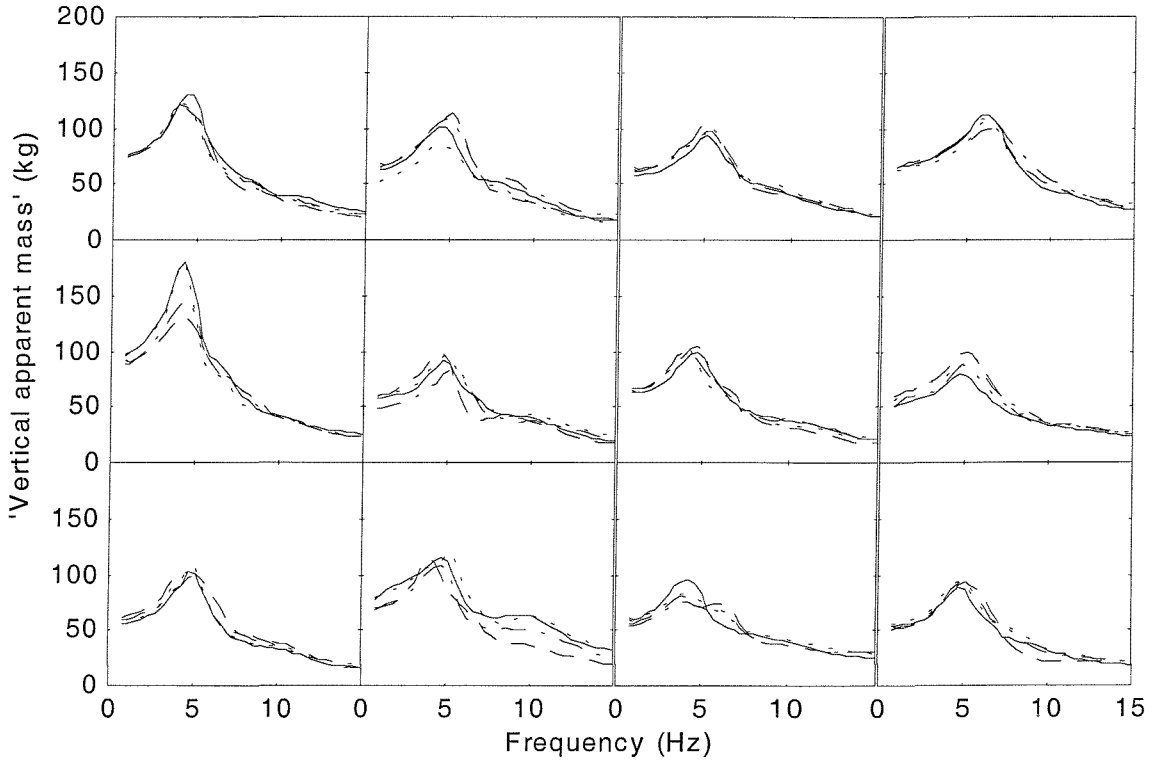

Figure 8.4 'Vertical apparent masses' of 12 subjects measured at 1.25 ms^{-2} r.m.s. without a backrest: ———,0°; ·····, 5°; –·–·–, 10°; – – – –, 15°.

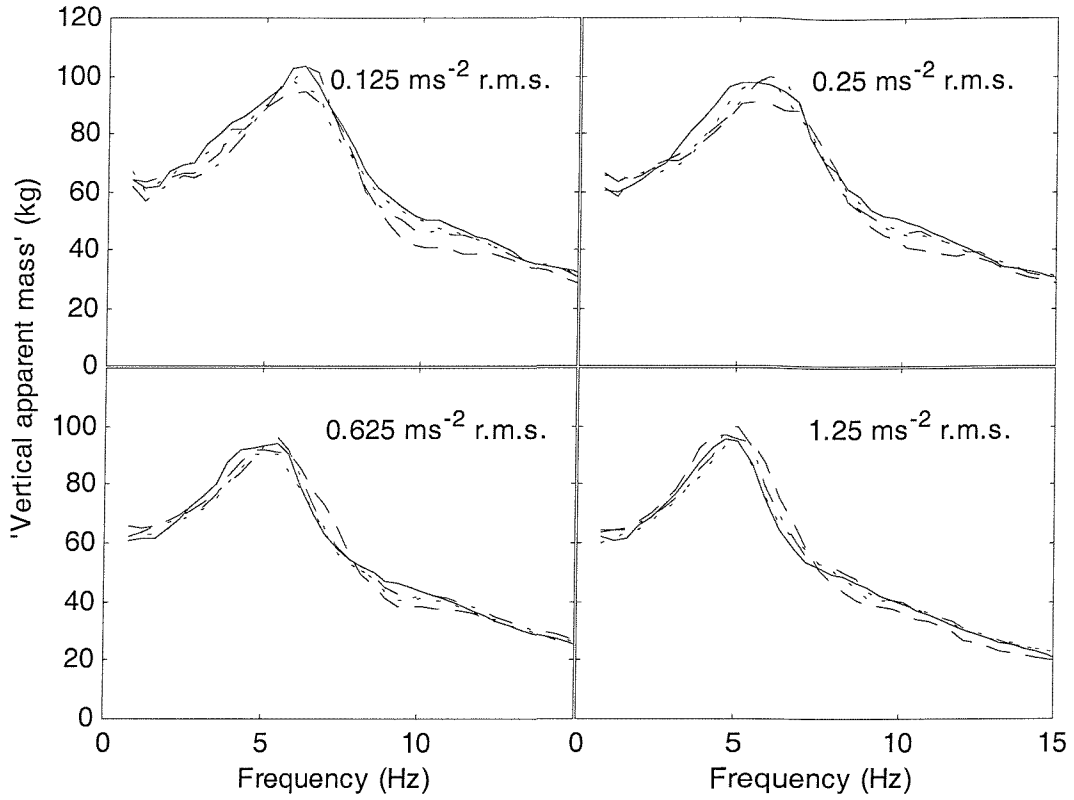

Figure 8.5 Effect of seat angle on median 'vertical apparent masses' of twelve subjects measured without a backrest:. ———,0°; ·····, 5°; –·–·–, 10°; – – – –, 15°.

8.3.1.3 Effect of backrest

At each seat angle and at all vibration magnitudes, the 'vertical apparent masses' measured without a backrest were compared to those measured with a backrest (Figures 8.6 and 8.7). There was no statistically significant difference between the resonance frequencies of the 'vertical apparent mass' measured with a backrest and the resonance frequencies of the 'vertical apparent mass' measured without a backrest when using seat angles of 0, 5 or 10° at any vibration magnitude ($p > 0.05$). However with a seat angle of 15°, there were statistically significant differences between the resonance frequencies of the 'vertical apparent mass' measured with a backrest and the resonance frequencies of the 'vertical apparent mass' measured without a backrest, except with a vibration magnitude of 0.125 ms^{-2} r.m.s. Table 8.2 shows the median resonance frequencies and median 'vertical apparent mass' magnitudes at resonance measured in all conditions with a backrest.

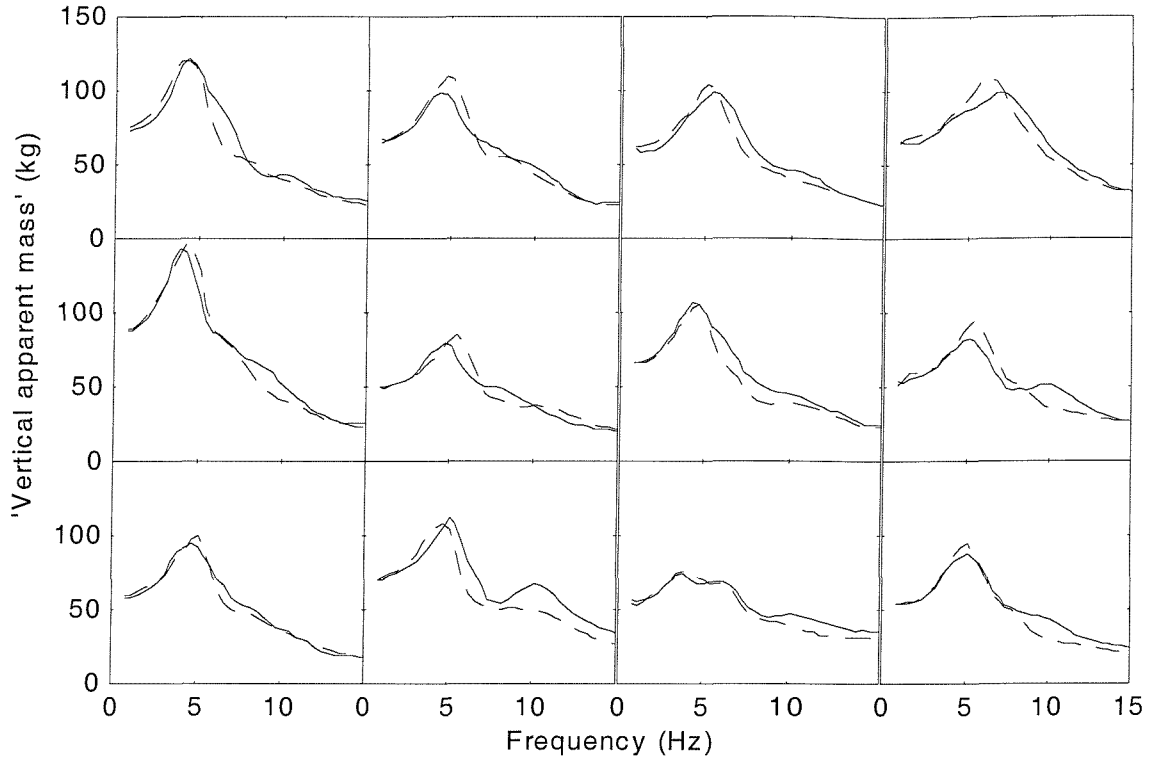

Figure 8.6 Effect of backrest on 'vertical apparent masses' of 12 subjects measured at 1.25 ms^{-2} r.m.s. with seat angle of 10°: ———, with backrest; – – – –, without backrest.

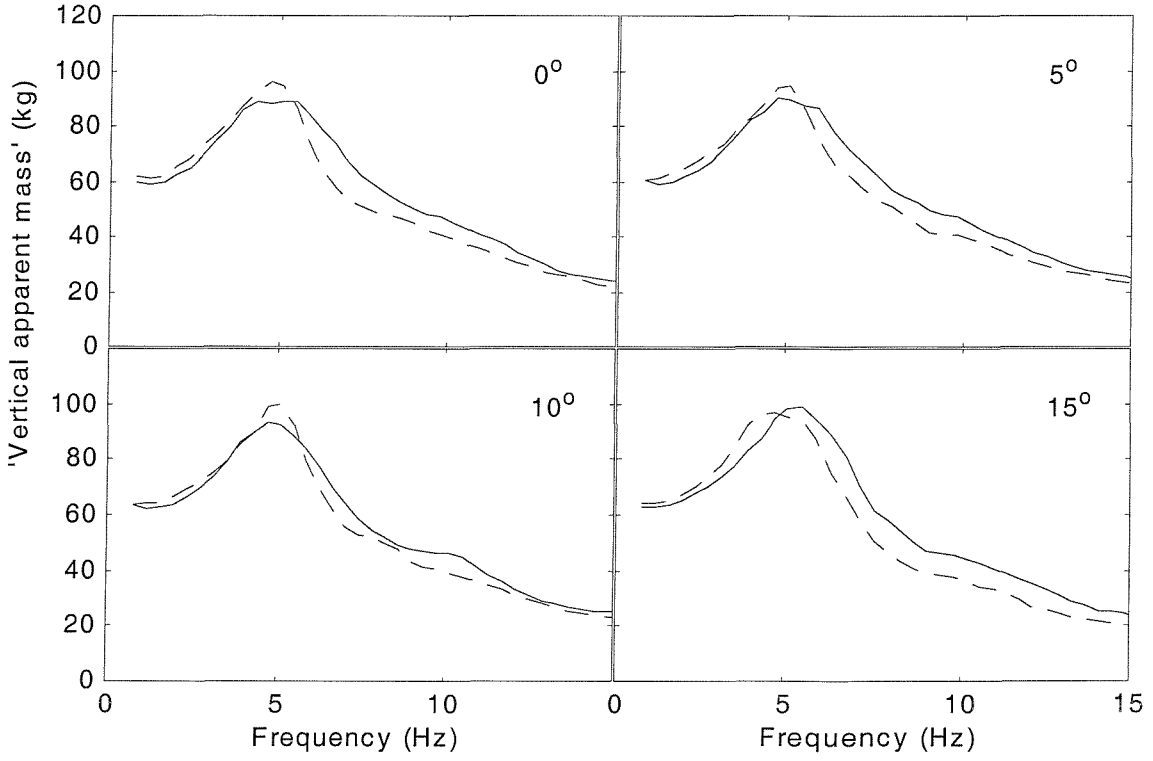

Figure 8.7 Effect of backrest on median 'vertical apparent masses' of twelve subjects measured at 1.25 ms^{-2} r.m.s.: ———, with backrest; – – – –, without backrest.

The backrest tended to reduce the 'vertical apparent mass' at low frequencies and increase the 'vertical apparent mass' at high frequencies (see Figure 8.7). The effect of the backrest on the 'vertical apparent mass' over the whole frequency range (obtained with 1.25 ms^{-2} r.m.s.) is shown in Table 8.3. The table shows a greater effect of the backrest at small seat angles than at large seat angles.

Table 8.2 Median resonance frequencies and magnitudes at resonance of the 'vertical apparent mass' for four seat angles at 0.125, 0.250, 0.625 and 1.25 ms^{-2} r.m.s. (With backrest)

Seat angle (°)	Resonance frequency (Hz)				Magnitude at resonance (kg)			
	0.125	0.250	0.625	1.250	0.125	0.250	0.625	1.250
0	6.25	6.25	5.86	5.08	97.3	94.9	89.0	89.1
5	7.03	6.25	5.08	4.69	97.9	91.2	90.6	89.8
10	5.86	5.86	5.47	4.69	97.3	95.4	95.8	93.4
15	5.86	5.86	5.47	5.47	98.0	93.8	93.2	98.8

Table 8.3 Ranges of frequencies where there was, or was not, a statistically significant difference in the 'vertical apparent mass' measured with and without a backrest at 1.25 ms^{-2} r.m.s.

Seat angle (°)	Frequency range (Hz)		Out of 39 frequencies	
	Significant difference	Non-significant difference	Significant difference	Non-significant difference
0	0.39 – 15.0	-	39	-
5	1.17 – 4.30 6.25 – 15.0	0.39 - 0.78 4.69 – 5.86	33	6
10	1.56 – 2.73 4.69 – 5.08 7.03 – 12.50 14.84 – 15.0	0.39 – 1.17 3.12 – 4.30 5.47 – 6.64 12.89 – 14.45	23	16
15	5.86 – 15.0	0.39 – 5.47	25	14

8.3.2 'Fore-and-aft cross-axis apparent mass'

With all seat angles, the 'fore-and-aft cross-axis apparent masses' (obtained from the force measured parallel to seat surface and the vertical applied acceleration) had magnitudes comparable to the 'vertical apparent mass'. The 'fore-and-aft cross-axis apparent mass' increased with increasing frequency up to a peak in the vicinity of 4 Hz, after which the 'fore-and-aft cross-axis apparent mass' reduced to a trough (Figure 8.8). The coefficient of variation had its greatest value between 5 and 7 Hz, where the trough occurred with all seat angles and all vibration magnitudes. The coefficient of variation in the 5 to 7 Hz region decreased with increasing seat angle. Consequently, the average coefficient of variation over the whole frequency range decreased with increasing seat angle: the average coefficient of variation decreased by about 25% when the seat angle was increased from 0 to 15° at 0.125 ms^{-2} r.m.s. and by about 30% when the seat angle was increased from 0 to 15° at 1.25 ms^{-2} r.m.s.

The resonance frequencies of the 'fore-and-aft cross-axis apparent masses' were tested for correlation with the resonance frequencies of the 'vertical apparent masses'. In none of the 16 conditions (4 seat angles and 4 vibration magnitudes) was there a significant correlation between the resonance frequencies measured in the 'fore-and-aft' and 'vertical' directions (Spearman, $p > 0.1$).

At all angles and at all vibration magnitudes, subject mass and subject stature were correlated with the magnitude of the 'fore-and-aft cross-axis apparent mass' at resonance ($p < 0.01$, Spearman), but they were not correlated with the resonance frequency of the 'fore-and-aft cross-axis apparent mass'.

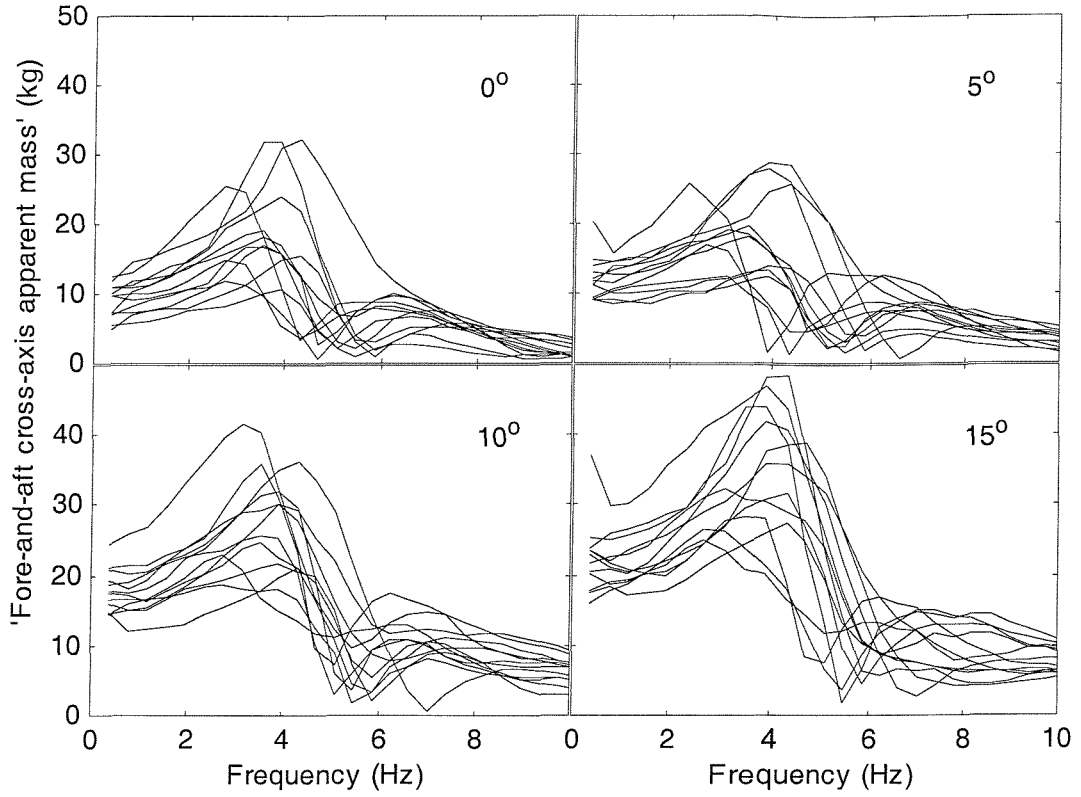

Figure 8.8 Inter-subject variability in the 'fore-and-aft cross-axis apparent mass' measured at 1.25 ms^{-2} r.m.s. with four different seat angles and no backrest.

8.3.2.1 Effect of vibration magnitude

The effect of vibration magnitude on the resonance frequency of the 'fore-and-aft cross-axis apparent mass' decreased with increasing seat angle (Figure 8.9 and Table 8.4): Table 8.4 indicates that the least effect of vibration magnitude on the resonance frequency occurred with the seat inclined at 15°. For the 'fore-and-aft cross-axis apparent mass' at resonance, there were no statistically significant differences between the different vibration magnitudes at any seat angle (Friedman, $p > 0.05$); except between 0.125 and 1.25 ms^{-2} r.m.s. at 15° (Wilcoxon, $p < 0.05$). Table 8.5 shows the changes of the median resonance frequency and median magnitude at resonance with changes in vibration magnitude.

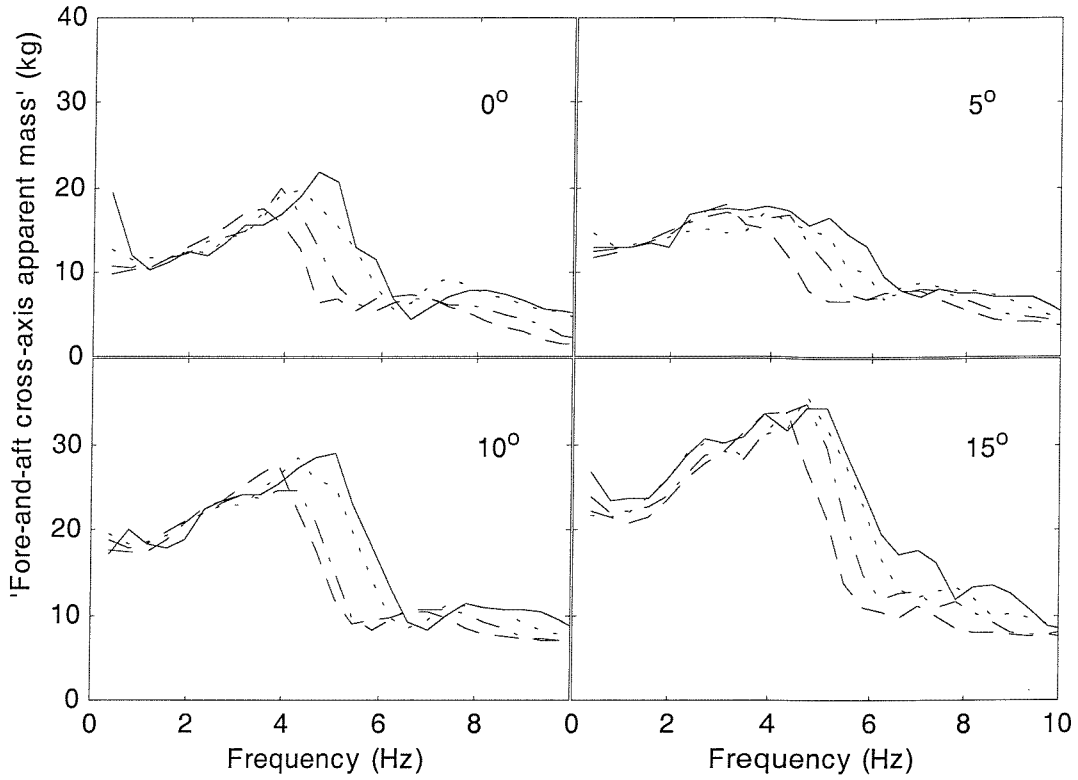

Figure 8.9 Effect of vibration magnitude on median 'fore-and-aft cross-axis apparent mass' of twelve subjects measured without a backrest: ———, 0.125 ms^{-2} r.m.s.; ·····, 0.25 ms^{-2} r.m.s.; –·–·–, 0.625 ms^{-2} r.m.s.; – – – –, 1.25 ms^{-2} r.m.s.

Table 8.4 Wilcoxon matched-pairs signed-ranks test for the resonance frequency of the 'fore-and-aft cross-axis apparent mass': effect of vibration magnitude. *$p < 0.1$, **$p < 0.05$, ***$p < 0.01$, ns: $p > 0.1$

Seat angle (°)	Vibration magnitude (ms^{-2} r.m.s.)	0.125	0.250	0.625	1.250
0	0.125	-	**	***	***
	0.250		-	***	***
	0.625			-	**
	1.250				-
5	0.125	-	ns	***	**
	0.250		-	**	**
	0.625			-	*
	1.250				-
10	0.125	-	ns	**	**
	0.250		-	ns	ns
	0.625			-	ns
	1.250				-
15	0.125	-	ns	ns	ns
	0.250		-	ns	ns
	0.625			-	**
	1.250				-

Table 8.5 Median resonance frequencies and magnitudes at resonance of the 'fore-and-aft cross-axis apparent mass' for four seat angles at 0.125, 0.250, 0.625 and 1.25 ms^{-2} r.m.s. (Without backrest).

Seat angle (°)	Resonance frequency (Hz)				Magnitude at resonance (kg)			
	0.125	0.25	0.625	1.25	0.125	0.25	0.625	1.25
0	4.69	4.30	3.91	3.52	21.8	19.7	20.0	17.6
5	3.91	3.91	3.12	3.12	17.6	17.1	16.9	17.9
10	5.08	4.30	3.91	3.91	28.9	28.3	24.6	27.7
15	5.08	4.69	4.69	4.30	34.2	35.6	34.8	33.8

8.3.2.2 Effect of seat angle

The resonance frequencies and the 'fore-and-aft cross-axis apparent mass' magnitude at resonance with different seat angles were compared at each vibration magnitude. No statistically significant difference in the resonance frequency was found between the different seat angles at any vibration magnitude (Friedman, $p > 0.05$). However, there were significant differences in the apparent mass magnitude at resonance between seat inclinations of 0, 10, and 15° at all vibration magnitudes, but no significant difference in the magnitude at resonance between 0 and 5° at any vibration magnitude. There was also a significant difference between the magnitude of the 'fore-and-aft cross-axis apparent mass' measured with a 0° seat angle and the 'fore-and-aft cross-axis apparent mass' measured with 5, 10 or 15° seat angle at all frequencies in the range 0.25 to 10 Hz (at a magnitude of 1.25 ms^{-2} r.m.s.) ($p < 0.05$), except in the range 2.73 to 7.03 Hz with seat angles of 0 and 5°. Between 5, 10, and 15°, the 'fore-and-aft cross-axis apparent mass' increased with increasing seat angle at frequencies below 5 Hz, although the greatest differences occurred in the resonance area (Figure 8.10). Above 5 Hz, no significant differences were found in the 'fore-and-aft cross-axis apparent mass' between 10 and 15°. A similar trend was found with the other vibration magnitudes (Figure 8.11).

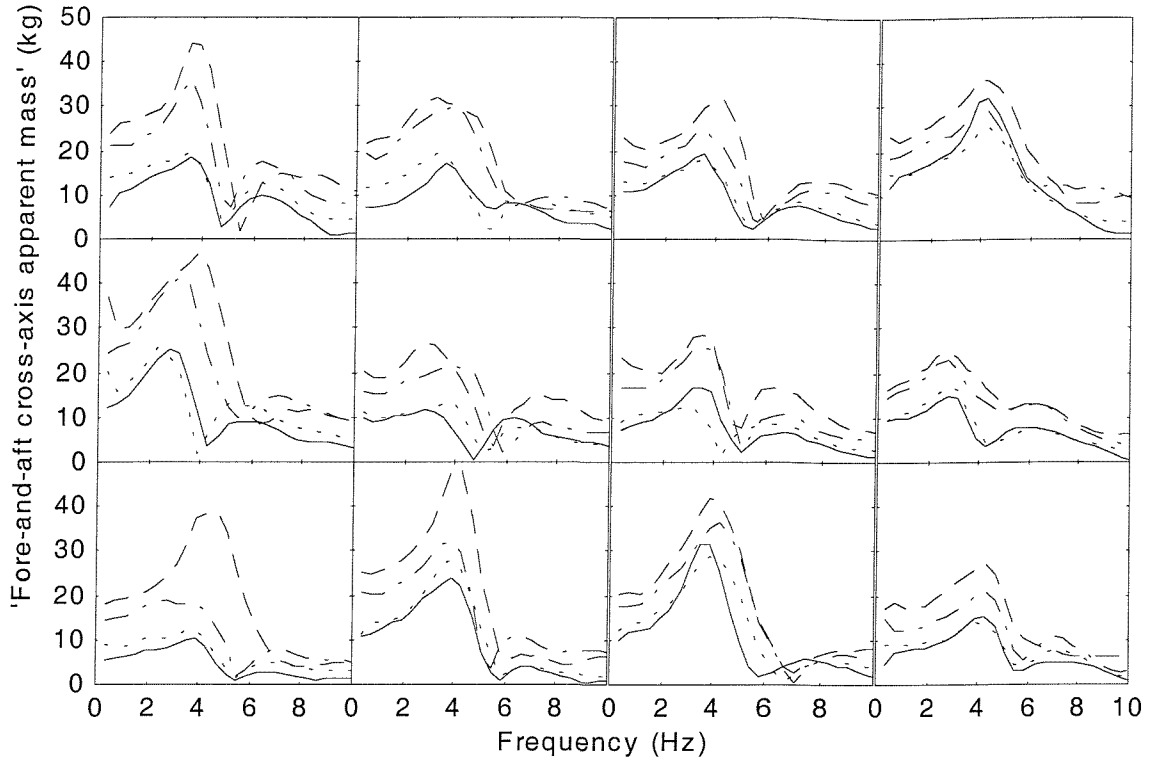

Figure 8.10 'Fore-and-aft cross-axis apparent masses' of 12 subjects measured at 1.25 ms^{-2} r.m.s. without a backrest. ———,0°; ·····, 5°; —·—·—, 10°; – – – –, 15°.

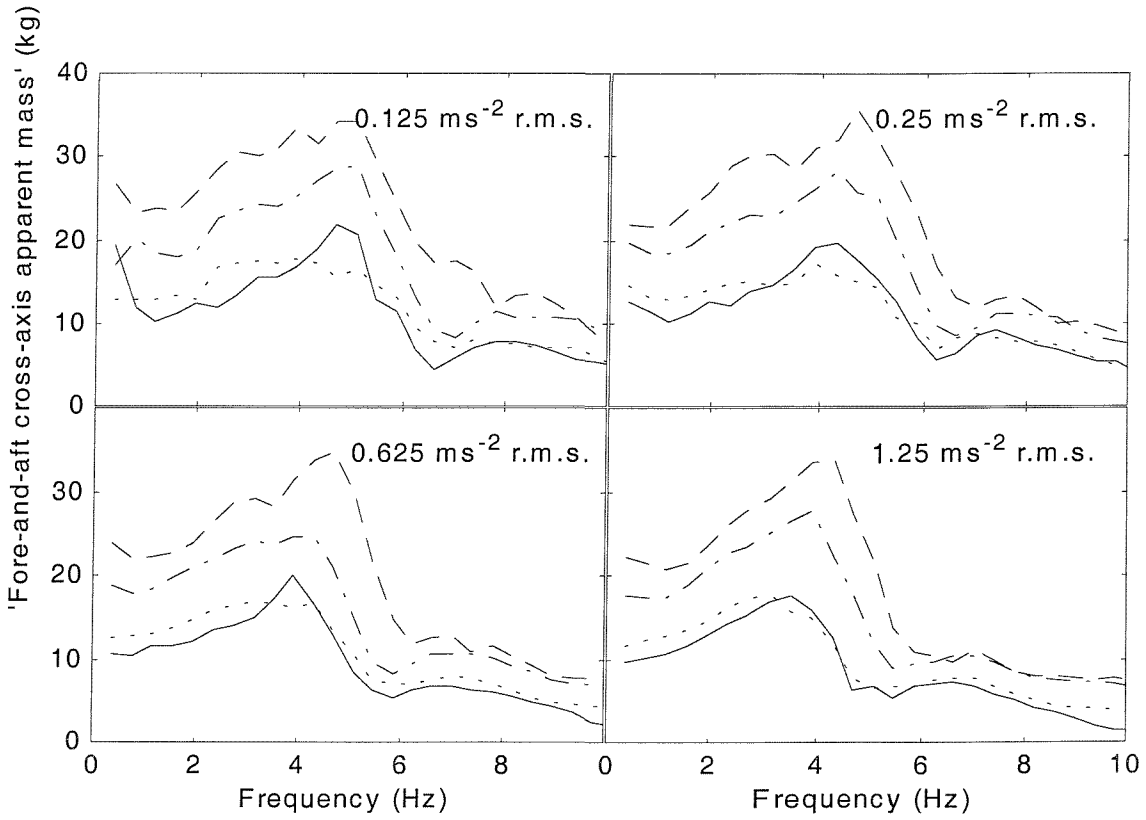

Figure 8.11 Effect of seat angle on median 'fore-and-aft cross-axis apparent masses' of twelve subjects measured without a backrest: ———,0°; ·····, 5°; —·—·—, 10°; – – – –, 15°.

8.3.2.3 Effect of backrest

The median resonance frequencies and magnitudes of the 'fore-and-aft cross-axis apparent mass' at resonance with a backrest are shown in Table 8.6. In comparison with Table 8.5 (where the median 'fore-and-aft cross-axis apparent mass' at resonance without a backrest are shown), there is a trend for the 'fore-and-aft cross-axis apparent mass' magnitude at resonance to decrease when using a backrest. With all seat surface angles, the effect of the backrest was evident at low frequencies: there were statistically significant differences in the magnitude of the 'fore-and-aft cross-axis apparent mass' measured with and without a backrest only below about 6 Hz at 0.125 and at 0.25 ms^{-2} r.m.s. and below about 4 Hz at 0.625 and at 1.25 ms^{-2} r.m.s. (Figures 8.12 and 8.13).

Table 8.6 Median resonance frequencies and magnitudes at resonance of the 'fore-and-aft cross-axis apparent mass' for four seat angles at 0.125, 0.250, 0.625 and 1.25 ms^{-2} r.m.s. (With backrest)

Seat angle (°)	Resonance frequency (Hz)				Magnitude at resonance (kg)			
	0.125	0.25	0.625	1.25	0.125	0.25	0.625	1.25
0	4.69	5.47	4.30	4.30	8.2	9.4	7.3	8.1
5	5.47	4.69	4.30	3.91	9.09	9.09	7.68	7.49
10	5.08	5.08	3.91	3.12	17.94	16.76	12.69	11.6
15	4.69	5.08	3.12	3.52	20.52	19.28	14.10	13.36

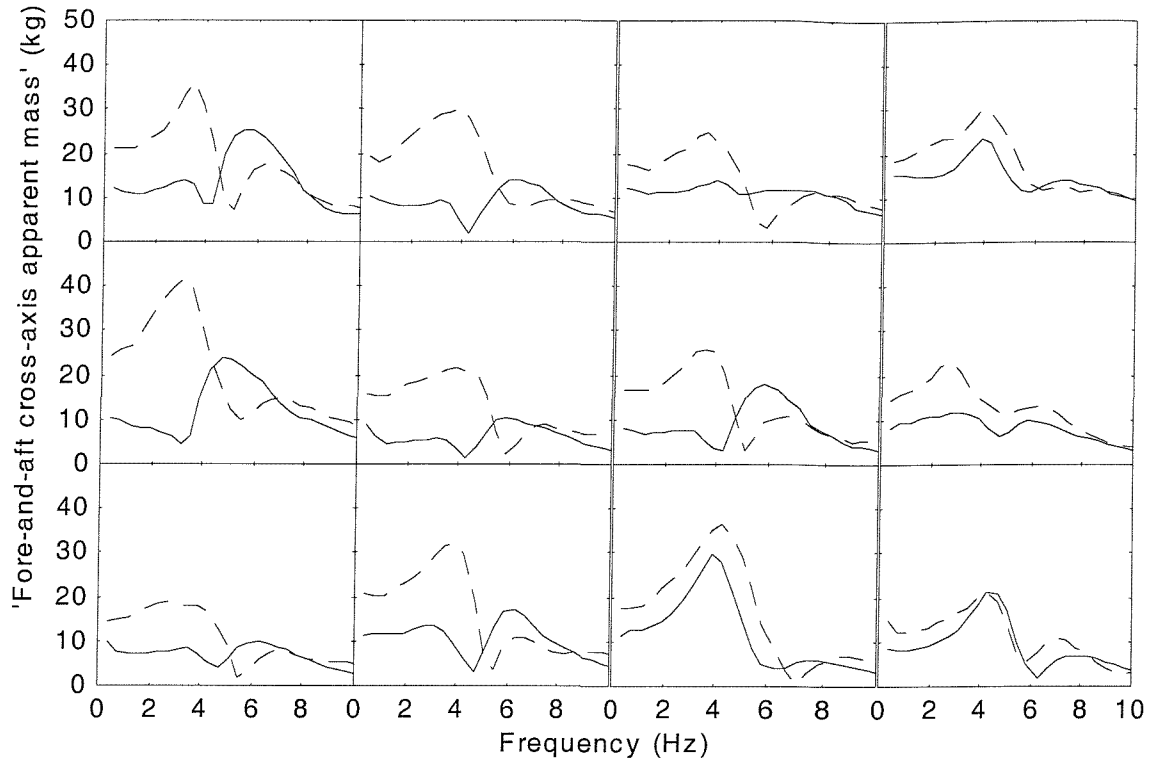

Figure 8.12 Effect of backrest on 'fore-and-aft cross-axis apparent masses' of 12 subjects measured at 1.25 ms^{-2} r.m.s. with seat angle of 10°. ———, with backrest; – – – –, without backrest.

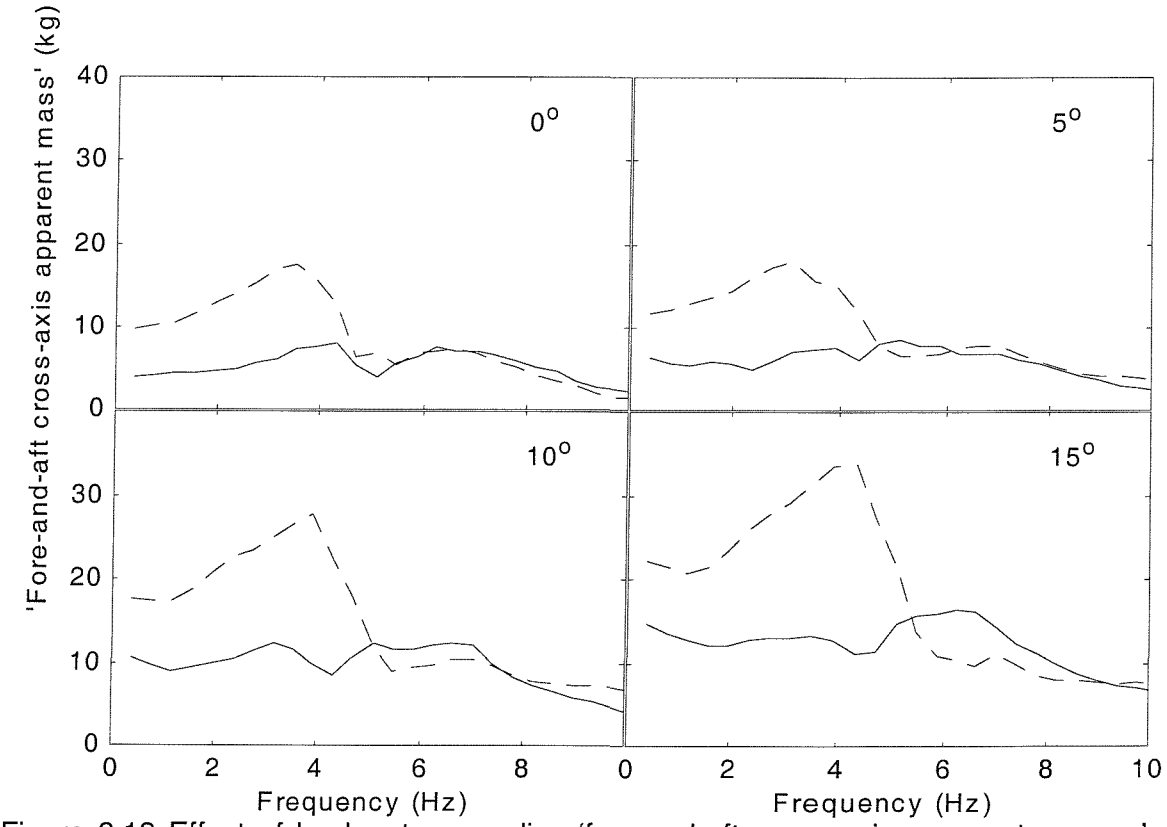

Figure 8.13 Effect of backrest on median 'fore-and-aft cross-axis apparent masses' of twelve subjects measured at 1.25 ms^{-2} r.m.s.: ———, with backrest; – – – –, without backrest.

8.4 DISCUSSION

8.4.1 'Vertical apparent mass'

At all seat angles, the moduli and phases of the 'vertical apparent mass' were similar to the vertical apparent mass moduli and phases reported previously (e.g. Mansfield, 1998; Wei, 2000). The decrease in the inter-subject variability (decrease in the average coefficient of variation) with an increase in vibration magnitude is consistent with that noticed by Mansfield and Griffin (2002) where they found a higher average coefficient of variation over the frequency range 1 to 20 Hz at 0.2 ms^{-2} r.m.s. than at 1.0 or 2.0 ms^{-2} r.m.s. in seven out of nine postures.

The non-linearity observed here in the 'vertical apparent mass' with all seat angles (the softening effect) is consistent with the decrease in the resonance frequency with an increase in vibration magnitude found previously in measures of apparent mass and mechanical impedance (e.g. Hinz and Seidel, 1987; Matsumoto and Griffin, 2002a) and in measures of transmissibility to different parts of the body (e.g. Mansfield and Griffin, 2000; Matsumoto and Griffin, 2002b) when horizontal supporting seat surfaces were used. The mechanisms that cause the decrease in the resonance frequency with an increase in vibration magnitude are not known, but some suggestions have been offered. Matsumoto and Griffin (2002a) noticed a decrease in the non-linearity when subjects sat with tensed buttocks tissue compared to a normal sitting posture, which implies that these tissues are partly responsible for the non-linearity. This is consistent with the conclusion in Chapter 4: a decrease in the non-linearity when the upper body was resting on the tissue of the buttocks in a minimum thigh contact posture was found compared to other postures with greater thigh contact. In the present study, it was expected that increasing the seat surface angle would increase the shear stiffness of the ischial tuberosities and this might affect the non-linearity in the 'vertical' direction. However, the results showed no effect of seat surface angle on the non-linearity, suggesting that shear movement of tissues at the ischial tuberosities was not a principal mechanism causing non-linearity in the 'vertical' direction. This might imply that the decrease in the non-linearity noticed by Matsumoto and Griffin (2002a) when subjects tensed their buttocks tissue was due to an increase in axial stiffness of the buttocks tissue rather than an increase in shear stiffness of the tissue.

Vibration magnitude had a greater effect on the 'vertical apparent mass' at resonance when the seat was at 0° (i.e. horizontal). However, unlike the effect of vibration

magnitude on the resonance frequency, the effect of vibration magnitude on the modulus of the apparent mass at resonance is inconsistent in previous studies. For example, while Matsumoto (1999) found no significant differences in the magnitude of the apparent mass at resonance measured with different vibration magnitudes, Mansfield and Griffin (2000) found a slight, but statistically significant, increase in the normalised apparent mass magnitude at resonance with increasing vibration magnitude, using similar vibration magnitudes to those used by Matsumoto. The results obtained in this study at 0° show a statistically significant decrease in the apparent mass magnitude at resonance with increasing vibration magnitude. For example, the median vertical apparent mass at resonance decrease from about 103 kg to about 95 kg when the vibration magnitude increased from 0.125 ms^{-2} r.m.s. to 1.25 ms^{-2} r.m.s. Understanding the factors that affect the changes in apparent mass at resonance may assist understanding of the non-linearity.

The 'vertical apparent masses' had similar resonance frequencies and similar magnitudes at resonance, irrespective of seat angle. Wei and Griffin (1998) measured the forces normal to the seat surface with cushion inclinations of 0, 5, 10, 15, and 20° and compared the apparent masses obtained from the vertical component of the measured force and the vertical acceleration. They found, generally, only small changes in the apparent mass below 5.5 Hz with the different seat angles. However, they found that with increasing seat inclination the seat transmissibility tended to decrease below 6 Hz and increase above 6 Hz. Wei and Griffin concluded that the small change in the apparent mass with different seat angles could not explain the change in the transmissibility of the seat. In this study, the absence of a considerable change in the 'vertical apparent mass' with a change in seat angle (up to 15°) over the whole frequency range may suggest only a small, if any, postural change accompanied the change in seat angle. Alternatively, a change in posture with change in seat angle might have been offset by changes in the force normal to the seat surface (i.e. change in the cosine of the seat angle) so that the responses at the different seat angles remained similar: a change in the upper body posture might have accompanied the change in the seat angle so that the force measured normal to the seat surface was not greatly affected.

The results showed no significant differences in the resonance frequency measured with and without a backrest at 0, 5, and 10°. It seems that no study has previously compared the resonance frequency of the body with and without a backrest with seat angles other than 0°. At 0°, the insignificant effect of the backrest on the resonance frequency in this

study is consistent with the results of Mansfield and Griffin (2002), but inconsistent with the results in Chapter 5 where significant differences in the resonance frequencies measured with and without a backrest were found. At 0°, one difference between this study and that reported in Chapter 5 is the position of the lower legs: they were vertical in the experiment reported in Chapter 5 but not vertical in the experiment presented in this Chapter. However, this explanation might be excluded because the lower legs were also vertical in the study by Mansfield and Griffin. This is also supported by Rakheja *et al.* (2002) who found no effect on the resonance frequency when moving the feet from far away to close to a seat. The reason for the differences in the effect of the backrest on the resonance frequencies between studies may be the type of backrest employed. In the experiment reported in this Chapter, the full length of the back of each subject (including the lumbar and pelvis areas) was in contact with the backrest, whereas in Chapter 5, the lumbar spine and the pelvis area were not in contact with the backrest.

The backrest was found to generally reduce the 'vertical apparent mass' at frequencies below resonance while increasing the 'vertical apparent mass' at frequencies above resonance. This is consistent with the effect of a backrest in a previous study (Fairley and Griffin, 1989) and the result reported in Chapter 5. The effect of the backrest on the 'vertical apparent mass' magnitude was greater with a decreased seat surface angle (see Table 8.3), although the effect of a backrest on the resonance frequency of the 'vertical apparent mass' was greater with increased seat angle. However, the effect of the backrest on the vertical apparent mass during vertical excitation is small compared to the effect of the backrest on fore-and-aft apparent mass during fore-and-aft excitation. During fore-and-aft excitation, a backrest considerably increases the fore-and-aft apparent mass at frequencies above about 1 Hz (e.g. Fairley and Griffin, 1990).

Among the different factors studied (vibration magnitude, seat angle and backrest), vibration magnitude had the greatest effect on the resonance frequency of the 'vertical apparent mass'.

8.4.2 'Fore-and-aft cross-axis apparent mass'

The 'fore-and-aft cross-axis apparent masses' (calculated from forces measured parallel to the seat surface and vertical applied acceleration) were large, but less than those in the 'vertical' direction at all seat angles and at all vibration magnitudes. The resonance frequencies of the 'fore-and-aft cross-axis apparent masses' were also lower than the 'vertical apparent masses'.

With the seat at 0° (i.e. horizontal), the high 'fore-and-aft cross-axis apparent masses' on the seat surface are likely to have been due to pitching modes of parts of the upper body, as suggested in Chapter 4. However, in Chapter 4, small fore-and-aft forces at low frequencies (below 1 Hz) were found, in contrast to high forces at low frequencies measured in this study. In the four postures used in Chapter 4, the lower legs were vertical and therefore did not contribute to fore-and-aft forces on the seat. In the present study, the lower legs were stretched forward and the feet rested on a footrest inclined at 45° (see Figure 8.1). In this seating arrangement, forces at the feet may have contributed to fore-and-aft forces at the seat and may be responsible for the forces measured at low frequencies. The decrease in the fore-and-aft forces seen between 5 and 7 Hz (i.e. where the troughs occurred) may be due to forces coming from the feet through the legs to the seat, since measures of apparent mass at the feet show resonances at similar frequencies (see Chapter 4, and Kitazaki, 1997).

The increase in the 'fore-and-aft cross-axis apparent mass' at low frequencies as the seat angle increased (to 5, 10 and 15°) seems to be caused mostly, if not totally, by the increase in the component of the mass in the 'fore-and-aft' direction (i.e. parallel to seat surface). When the seat was at 0°, the measured fore-and-aft force was perpendicular to the applied vertical acceleration and, hence, the measured fore-and-aft cross-axis apparent masses at low frequencies (around 1 Hz) may be assumed to come from forces applied at the feet, as explained above. Assuming the human body moves as a rigid body at very low frequencies, an increase in seat angle from θ_1 to θ_2 will increase the 'fore-and-aft cross-axis apparent mass' by the mass of the subject multiplied by (sin θ_2-sin θ_1). For example, subject 1 had a sitting mass of 74.0 kg (see apparent mass around 1 Hz in Figure 8.4). When the seat angle increased between 5 and 15°, an increase of 12.7 kg (74 kg * (sin 15° - sin 5°)) would be expected in the 'fore-and-aft' component of the mass. From Figure 8.10, at 1 Hz the difference between the 'fore-and-aft cross-axis apparent mass' measured at 15° and that measured at 5° is 12.6 kg (26.8 kg at 15° and 14.2 at 5°), consistent with the expected increase. These calculations assume that the forces coming from the feet do not change, or have a small change, with the variation in seat angle. Around the resonance frequency, these simple calculations will not apply because the resonance is associated with pitching modes of the body and there is a large non-linearity.

The resonance frequencies from the two responses (i.e. 'vertical apparent mass' and 'fore-and-aft cross-axis apparent mass') were not correlated in any condition, implying a

different mechanism produced the two resonances. Kitazaki and Griffin (1997, 1998) reported two separate vibration modes at 3.4 and 4.9 Hz produced by two different mechanisms. The mode at 3.4 Hz was a bending mode of the entire spine, which caused fore-and-aft motion of the pelvis in phase with fore-and-aft motion of the head. The 4.9 Hz mode was the principal mode: an 'entire body mode in which the head, spinal column and the pelvis moved vertically due to axial and shear deformations of the buttocks tissue, in phase with a vertical visceral mode, and a bending mode of the upper thoracic and cervical spine'. Matsumoto and Griffin (2001) also reported two vibration modes at 2.53 Hz and 5.66 Hz when modelling the dynamic responses (apparent mass and transmissibility) of the human body to vibration using multi-degree of freedom models with rotational capability. The 2.53 Hz mode was produced by pitching motion of the pelvis in phase with a bending mode of the spine. The mode at 5.66 Hz was thought to be due to deformation of the buttocks tissues together with a vertical mode of the viscera and bending mode of the spine. The mode measured in the 'fore-and-aft' direction in the present study might be the same mode reported at 3.4 Hz (or 2.53 Hz) in the previous studies, while the mode measured in the vertical direction in the present study may be the 4.9 Hz (or the 5.66 Hz) mode measured in the previous studies.

Similar non-linear behaviour to that with the 'vertical apparent mass' was found in the 'fore-and-aft cross-axis apparent mass': a decrease in the resonance frequency with an increase in vibration magnitude. The effect of vibration magnitude on the resonance frequency decreased with increasing seat angle. Since the mass in the 'fore-and-aft' direction increases with an increase in seat surface angle, the insignificant change in the resonance frequency found in the 'fore-and-aft cross-axis apparent mass' with the increase in seat surface angle suggests an increase in stiffness of the ischial tuberosities, where shear stiffness increases with the increase in seat surface angle. The increase in stiffness might have been the factor that reduced the softening effect of the vibration magnitude in the 'fore-and-aft' direction with the increase in seat angle, although this increase in stiffness had no effect on the non-linearity in the 'vertical' direction.

The effect of the backrest on the 'fore-and-aft cross-axis apparent mass' was more pronounced than the effect on the 'vertical apparent mass'. The median fore-and-aft force at resonance decreased by, at least, 38% (at 10° with 0.125 ms^{-2} r.m.s.) and by, at most, 64% (at 0° and 0.625 ms^{-2} r.m.s.) when a backrest was used. At low frequencies, the high forces that were assumed to have transferred from the feet through the legs to the seat when no backrest was used also decreased when a backrest was used. The pitching of

the upper body might have been damped or suppressed when using a backrest: although the great effect of the backrest on the fore-and-aft cross-axis apparent mass was not seen in Chapter 5, the position of the feet in this study might have reduced forward pitching of the body when the backrest reduced backward pitching.

8.5 CONCLUSIONS

With four angles of a supporting seat surface (0, 5, 10, and 15°), the resonance frequencies and the magnitudes at resonance were greater in the 'vertical apparent masses' (calculated from the forces measured normal to the seat surface and the applied vertical acceleration) than in the 'fore-and-aft cross-axis apparent masses' (calculated from forces measured parallel to the seat surface and the applied vertical acceleration). The resonance frequencies in the two directions were not correlated.

At seat angles up to 15°, there were negligible changes in the 'vertical apparent mass' but considerable changes in the 'fore-and-aft cross-axis apparent mass', which increased with increasing seat angle. In both the 'vertical' and 'fore-and-aft' directions, the resonance frequencies decreased with increasing vibration magnitude, with least decrease of resonance frequency in the 'fore-and-aft cross-axis apparent mass' at the maximum inclination of 15°.

The presence of a backrest decreased both the 'vertical apparent mass' and the 'fore-and-aft cross-axis apparent mass' at low frequencies, with the greatest reduction in the 'fore-and-aft cross-axis apparent mass'. The 'fore-and-aft cross-axis apparent mass' at resonance, but not the resonance frequency, was correlated with the masses and statures of the subjects.

CHAPTER 9 MODELLING THE APPARENT MASS AND THE CROSS-AXIS APPARENT MASS MEASURED ON THE SEAT DURING VERTICAL EXCITATION AND DURING FORE-AND-AFT EXCITATION

9.1 INTRODUCTION

The experimental results reported in the previous chapters suggest that the seated human body moves in two dimensions when exposed to whole-body vertical excitation or to whole-body fore-and-aft excitation. The fore-and-aft forces on the seat during vertical vibration and the vertical forces measured on the seat during fore-and-aft vibration were of considerable values and should be taken into account when modelling the responses of humans to vibration.

The two dimensional motion might suggest axial as well as shear forces applied to the spine when the body is exposed to vertical vibration and fore-and-aft vibration, as was reported by Fritz (2000). Attenuating the cross-axis movement as well as attenuating the movement in the direction of vibration should help in reducing the discomfort, interference with activities and the effects on health associated with exposure to vibration.

Previous, single degree-of-freedom and multi degree-of-freedom models have concentrated on modelling the force response in the direction of excitation (e.g. Payne, 1965; Suggs *et al.*, 1969; Fairley and Griffin, 1989; Wei and Griffin, 1998; Boileau and Rakheja, 1998; Matsumoto and Griffin, 2003). A few models have taken into account, using transmissibility measurements, the cross-axis movements of the upper body associated with vertical vibration (e.g. Belytscko and Privitzer, 1978; Kitazaki and Griffin, 1997; Matsumoto and Griffin; 2001). However, no known work has attempted to include in a model the cross-axis forces on the seat induced by vertical or fore-and-aft excitation.

In this chapter, mathematical models taking into account the cross-axis forces measured on the seat are developed. The chapter is divided into three main parts. In the first part an initial two degree-of-freedom model was developed to predict the vertical apparent mass and the fore-and-aft cross-axis apparent mass obtained on the seat during vertical excitation. In the second part, a series of models were investigated to improve the quality of the prediction of the responses measured experimentally during vertical vibration. In the third part, a model to predict the forces obtained during fore-and-aft excitation is proposed.

9.2 MODELLING THE VERTICAL APPARENT MASS AND THE FORE-AND-AFT CROSS AXIS APPARENT MASS DURING VERTICAL EXCITATION

9.2.1 Model description

A lumped parameter model with two degrees-of-freedom (translational in the vertical direction and rotational in the mid-sagittal plane) was used to represent the dynamic responses of seated humans to vertical whole-body excitation. The model is similar to those used by Matsumoto and Griffin (2001, see Figure 2.47) but with reduced degrees-of-freedom. Since only two functions would be predicted in the model described here, it was decided to use only two degree-of-freedom model at this stage of this chapter. The model consisted of two masses, a linear translational spring and damper and a linear rotational spring and damper, as shown in Figure 9.1. Mass 1 is capable of moving only vertically. Mass 2, is attached to mass 1 using a hinge so that mass 2 can move vertically with mass 1 and rotate in the mid-sagittal plane. This rotational motion produces a fore-and-aft motion which will be used to predict the forces in the fore-and-aft direction.

Mass 1 in Figure 9.1 may be assumed to represent the mass of the upper legs carried by the seat, while mass 2, may be assumed to represent the total mass of the upper body parts, including the pelvis. The translational spring and damper represent the stiffness of the thighs and the tissue under the ischial tuberosities. The rotational spring and damper could be thought to represent the resultant rotational stiffness and damping of the different parts of the upper body or the rotational degree-of-freedom of the upper body.

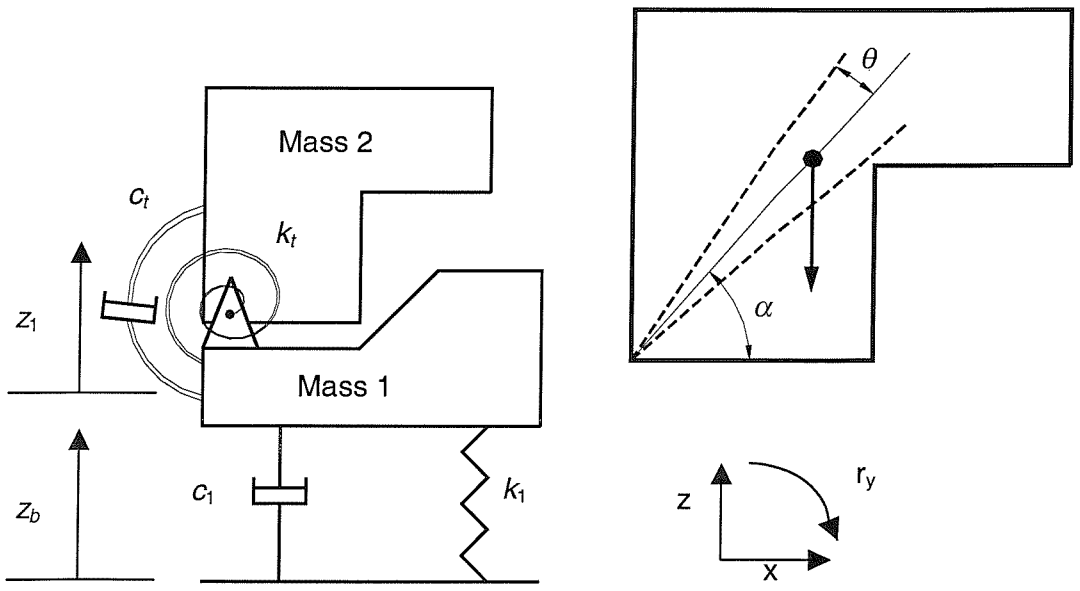

Figure 9.1 Two degree-of-freedom model.

9.2.2 Equations describing the model

As seen in Figure 9.1, mass 1 can move only vertically while mass 2 has vertical and pitching motions. The linearised equations of motion that describe the model are given by equations 9.1 and 9.2. The effect of gravity was not considered when deriving the equations of motion and hence, it is expected that the effect of gravity will be included in the optimised rotational stiffness as will be discussed in Section 9.5.

$$(m_1 + m_2)\frac{d^2 z_1}{dt^2} + m_2 e\cos\alpha\frac{d^2\theta}{dt^2} + k_1(z_1 - z_b) + c_1(\frac{dz_1}{dt} - \frac{dz_b}{dt}) = 0 \qquad (9.1)$$

$$m_2 e\cos\alpha\frac{d^2 z_1}{dt^2} + (m_2 e^2 + J_2)\frac{d^2\theta}{dt^2} + k_t\theta + c_t\frac{d\theta}{dt} = 0 \qquad (9.2)$$

where,

m_1 and m_2 are the masses of mass 1 and mass 2, respectively
J_2 is the moment of inertia of mass 2 about its centre of gravity
k_1 and c_1 are the vertical stiffness and damping beneath mass 1
k_t and c_t are the rotational stiffness and damping of mass 2
e is the distance between the centre of gravity of mass 2 and the hinge
α is the angle that e has with the horizontal when the model is in equilibrium
z_b is the vertical displacement of the base
z_1 is the vertical displacement of mass 1
θ is the pitch displacement of mass 2

The vertical and fore-and-aft forces produced in the model are given by the following equations:

$$f_z(t) = m_1\frac{d^2 z_1}{dt^2} + m_2(\frac{d^2 z_1}{dt^2} + e\cos\alpha\frac{d^2\theta}{dt^2}) \qquad (9.3)$$

$$f_x(t) = m_2 e\sin\alpha\frac{d^2\theta}{dt^2} \qquad (9.4)$$

where,

$f_z(t)$ is the force in the vertical direction
$f_x(t)$ is the force in the fore-and-aft direction

The vertical apparent mass of the model is then calculated from the total force in the vertical direction, f_z, and the acceleration, z_b. The fore-and-aft cross-axis apparent mass is calculated from the force in the fore-and-aft direction, f_x and the acceleration, z_b.

9.2.3 Model parameters

The model was used to compare four postures having the same upper body mass but different masses of the upper legs supported on the seat. Hence, mass 1 (assumed to represent the upper legs carried by the seat when the feet were supported and the lower and upper legs when the feet were not supported) was variable in the model while mass 2 (assumed to represent the upper body) was fixed in the model to a value corresponding to the total mass of the upper body parts calculated from the percentage of each part of the total mass of the body (e.g. National Aeronautics and Space Administration, 1978). The total mass of the body was assigned as 78.0 kg, which corresponds to the median vertical apparent mass at 1 Hz found in the experiment in the feet hanging posture (Chapter 4). The centre of gravity and the moment of inertia of mass 2 were calculated from those of each part of the upper body as given by National Aeronautics and Space Administration (1978). For a seated subject with similar mass to the total median mass used here (78 kg), the ischial tuberosities lie on the seat at a distance of about 10 cm from a vertical plane at the back of the subject (Singley and Haley, 1978). The centre of gravity and the moment of inertia of each body segment were calculated with respect to the origin placed at the ischial tuberosities. Table 9.1 and Figure 9.2 show the different segments of the upper body and their geometric parameters. From Table 9.1, the values of e and α used in the equations above can be shown to be equal to 0.39 m and 84°, respectively.

Table 9.1 Geometric parameters of the different parts of mass 2

Segment	Mass (kg)	Centre of gravity (x,z) [a] (m)	Moment of inertia [b] (kg m^2)
Head	6.40	(0.00, 0.76)	0.903
Torso	39.1	(0.03, 0.34)	1.189
Upper arms	4.4	(0.03, 0.43)	0.035
Fore arms	2.5	(0.15, 0.25)	0.093
Hands	0.95	(0.47, 0.16)	0.226
Mass 2	53.4	(0.04, 0.39)	2.446

[a] With respect to the reference origin at the ischial tuberosities.

[b] About the centre of gravity of mass 2.

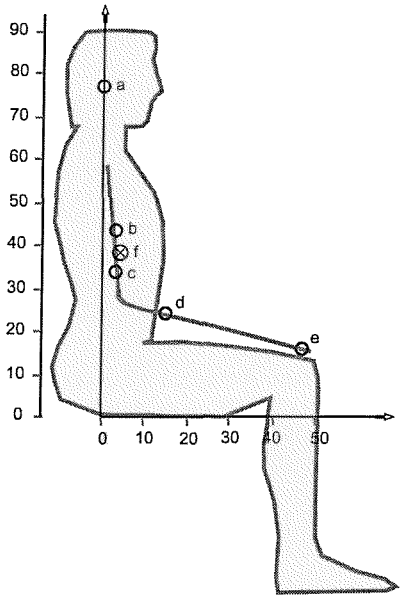

Figure 9.2 Locations of the centre of gravity of different parts of the upper body. a, of the head; b, of the upper arm; c, of the torso; d, of the fore-arm; e, of the hand; f, of mass 2. *x* and *y* scales are in cm.

Stiffness and damping properties of the human body are not available in the literature and, hence, the stiffness and damping of the model were determined by comparing the response of the model with the experimental vertical apparent mass and the fore-and-aft cross-axis apparent mass measured in the first experiment (Chapter 4).

When the response of the model was fitted to individual data, the value of mass 2, the location of the centre of gravity of mass 2 and the moment of inertia of mass 2 were recalculated to correspond to those of the individuals. For simplicity, the density of the human body was assumed to be constant and, therefore, the mass of some parts of the body will be proportional to its volume. The same assumption was used previously by Matsumoto and Griffin (2001). Based on this assumption, the following scaling factors were used: (m_s/m_o) for the mass, $(m_s/m_o)^{1/3}$ for the length (location of the centre of gravity), and $(m_s/m_o)^{5/3}$ for the moment of inertia, where m_s is the mass of the subject and m_o is the initial mass of the model (78.0 kg). Following these criteria, m_2, J_2, and e used for the 12 subjects are shown in Table 9.2.

Table 9.2 Mass, moment of inertia around the centre of gravity of mass 2, and location of centre of gravity of mass 2 (the upper body) used for 12 subjects.

Subject	1	2	3	4	5	6	7	8	9	10	11	12
m_2 (kg)	44	62	58	50	40	50	51	44	55	55	60	78
J_2 (kg m^2)	1.70	3.04	2.71	2.11	1.44	2.12	2.16	1.73	2.47	2.50	2.90	4.44
e (m)	0.38	0.43	0.42	0.40	0.37	0.40	0.40	0.38	0.41	0.41	0.43	0.46

The error function used to optimise the parameters was based on minimising the squared error over the whole frequency range for both the vertical apparent mass magnitude and the fore-and-aft cross-axis apparent mass magnitude. The optimised parameters were obtained using a MATLAB non-linear search method. Initial runs of the model showed better fit for the vertical apparent mass than the fore-and-aft cross-axis apparent mass. So, it was decided to give more weight to the fore-and-aft cross-axis apparent mass function by multiplying its error function by a factor of F, as shown in the following equation:

$$\text{err} = \sum_{i=1}^{N} (M_p - M_m)_i^2 + F * \sum_{i=1}^{N} (CM_p - CM_m)_i^2 \qquad (9.5)$$

where,

M_p and CM_p are the predicted vertical apparent mass magnitude and fore-and-aft cross-axis apparent mass magnitude, respectively.

M_m and CM_m are the measured vertical apparent mass magnitude and fore-and-aft cross-axis apparent mass magnitude, respectively.

F is an arbitrary factor used to improve the fitting of the fore-and-aft cross-axis apparent mass. The value of F varied between subjects.

9.2.4 Results and discussion

9.2.4.1 Modelling median and individual data

Experimental data obtained in the first experiment were used to develop the model and to extract the optimum parameters. The data consisted of vertical apparent mass and fore-and-aft cross-axis apparent mass as measured on the seat during random vertical vibration with magnitudes of 0.125, 0.25, 0.625, 1.25 ms^{-2} r.m.s. in four sitting postures as shown in Figure 9.3. The biodynamic responses obtained at 1.25 ms^{-2} r.m.s. will be modelled in this section. The data obtained at the four vibration magnitudes will be used to investigate the non-linearity of the human body as will be shown in Section 9.2.4.3.

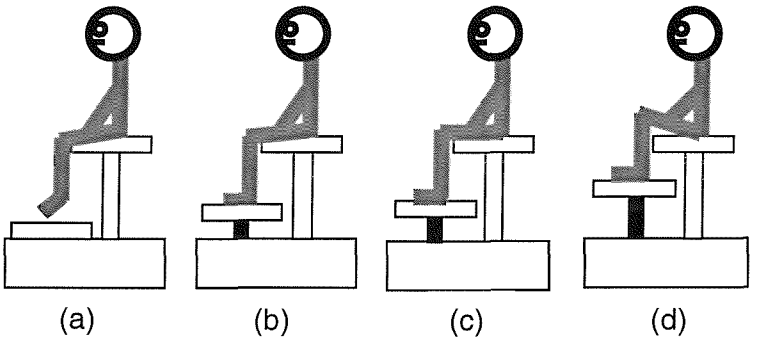

Figure 9.3 Schematic diagrams of the four sitting postures: (a) feet hanging; (b) maximum thigh contact; (c) average thigh contact; (d) minimum thigh contact.

Figure 9.4 to Figure 9.7 show the experimental and predicted median responses at 1.25 ms^{-2} r.m.s. for the four postures. The figures show that the experimental and predicted results are in good agreement only for the magnitude response. The measured and predicted vertical median apparent mass phases were in agreement up to only about 8 Hz. Wei and Griffin (1998) showed that fitting the model response to the experimental results could be improved by increasing the degrees-of-freedom of the model: the agreement between the experimental and predicted results improved when Wei and Griffin used a two degree-of-freedom model rather than a single degree-of-freedom model.

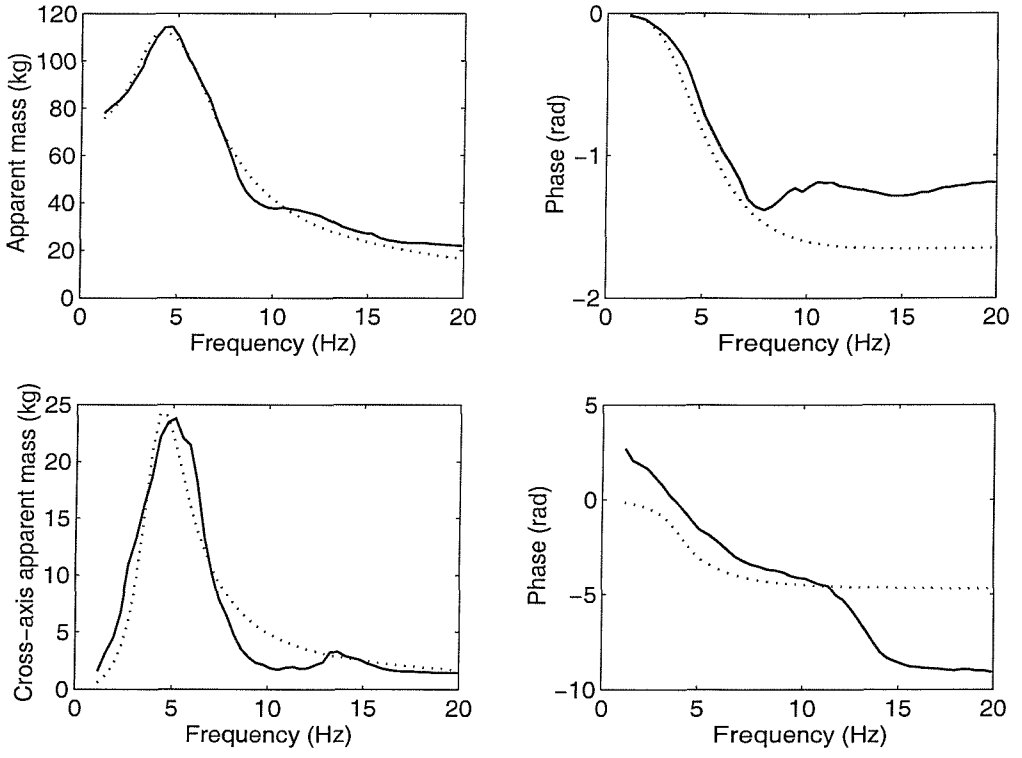

Figure 9.4 Vertical apparent mass and fore-and-aft cross-axis apparent mass magnitudes and phases calculated from the model and median experimental data in the feet hanging posture: ———,experiment; ·····,model.

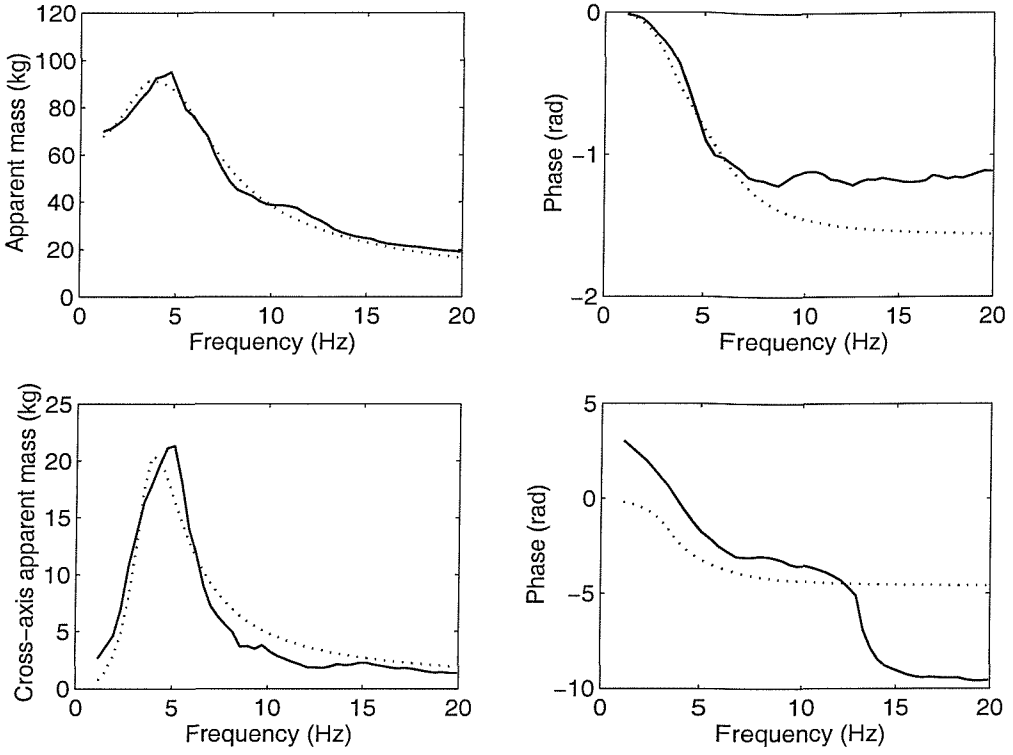

Figure 9.5 Vertical apparent mass and fore-and-aft cross-axis apparent mass magnitudes and phases calculated from the model and median experimental data in the maximum thigh contact posture: ———, experiment; ·····, model.

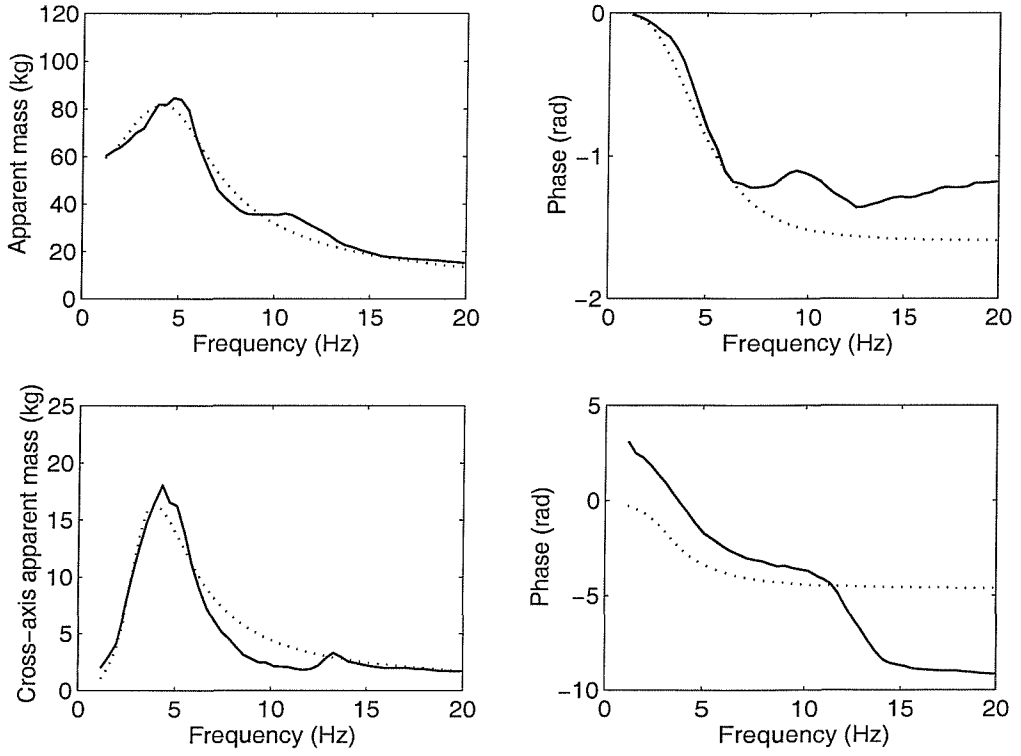

Figure 9.6 Vertical apparent mass and fore-and-aft cross-axis apparent mass magnitudes and phases calculated from the model and median experimental data in the average thigh contact posture: ———, experiment; ·····, model.

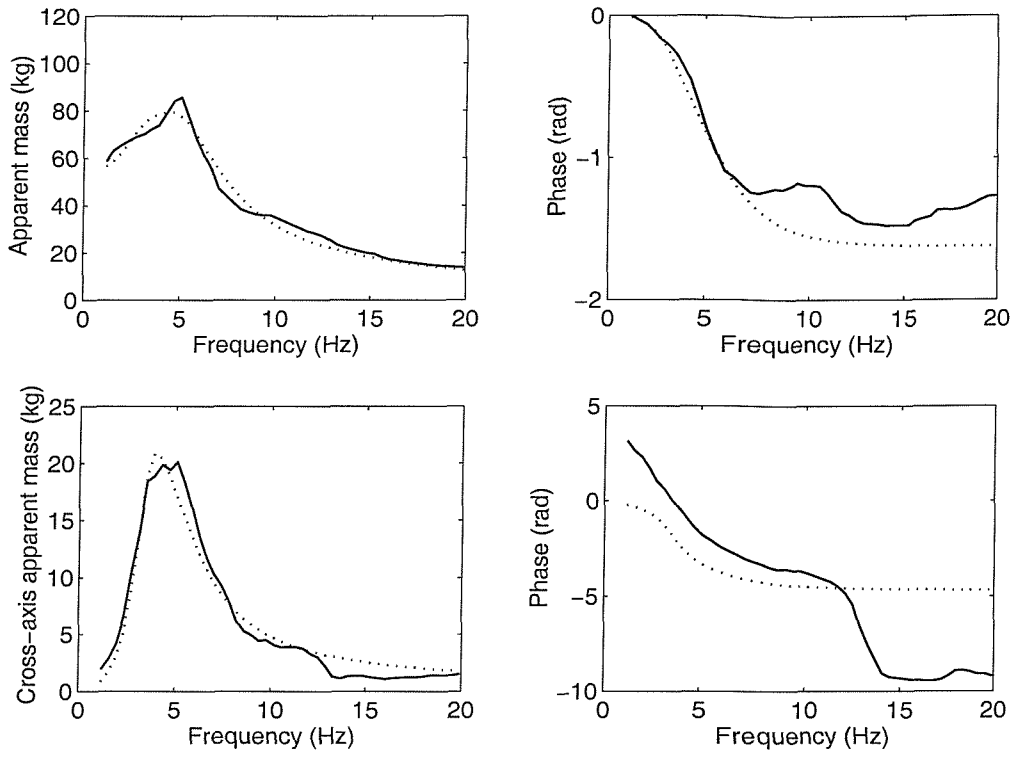

Figure 9.7 Vertical apparent mass and fore-and-aft cross-axis apparent mass magnitudes and phases calculated from the model and median experimental data in the minimum thigh contact posture: ———, experiment; ·····, model.

Despite using a two-degree of freedom model, the model failed to predict the phase response at high frequencies. This could be because although the model accommodates responses in two directions, both degree of freedom have a resonance frequency around 5 Hz. This could have prevented the model from predicting the second resonance frequency appearing between 8 and 13 Hz in the experimental data. It might be possible to improve the response of this model at higher frequencies by adding another degree-of-freedom to the model.

The optimised parameters for the four postures at 1.25 ms^{-2} r.m.s. are shown in Table 9.3. The table shows that the predicted value of mass 1 (m_1) is consistent with the difference between the four postures: changing from the feet hanging posture to the minimum thigh contact posture decreases the mass of the upper legs carried by the seat. As mentioned previously, there are no reliable data in the literature about the measured properties of the living human tissues. Nevertheless, the trend in which the predicted stiffness and damping change between postures seems reasonable. For example, the predicted values of k_1 (shown in Table 9.3) decrease when the thigh contact decreases: changing from the feet hanging posture to the minimum thigh contact posture reduces the stiffness of the thighs. However, the predicted vertical stiffness, k_1 was greater for the minimum thigh contact posture than for the average thigh contact posture. The same

observations were found, for more than 50% of the subjects, when predicting the parameters of the model using the individual data (see Table 9.4). The increase in stiffness in the minimum thigh contact posture could be a reflection of the increased pressure on the tissue under the ischial tuberosities in the minimum thigh contact posture. The rotational damping showed similar values for the feet hanging, maximum thigh contact and minimum thigh contact postures, which were less than that for the average thigh contact posture. This is consistent with lower values of fore-and-aft cross-axis apparent mass found experimentally in the average thigh contact posture than in the other three postures.

Table 9.3 Optimised parameters for four sitting postures.

Posture	m_1 (kg)	k_1 (N/m)	c_1 (Ns/m)	k_t (Nm)	c_t (Nms)
Feet hanging	18	74414	1888	7365	129
Maximum thigh contact	11	61552	1947	5986	127
Average thigh contact	3	52101	1570	4557	147
Minimum thigh contact	0.03	55310	1484	5481	125

Figures 9.8 to 9.11 show the experimental and predicted apparent masses of 12 subjects at 1.25 ms^{-2} for the feet hanging posture. The results of the other postures are shown in Appendix F. As in the median results, good agreement in the magnitude responses were found between the experimental and predicted values (Figures 9.8 and 9.9) while the phase response was in agreement up to only about 8 Hz for the vertical apparent mass phase (Figures 9.10).

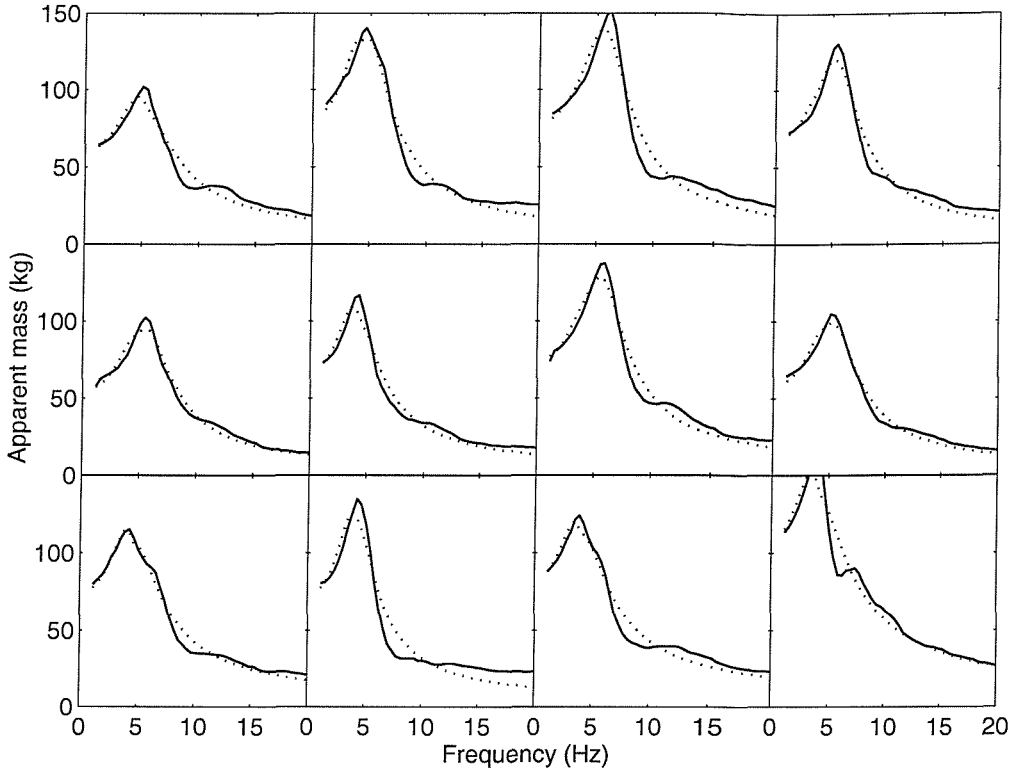

Figure 9.8 Vertical apparent masses of 12 subjects calculated from the model and obtained from the experiment in the feet hanging posture: ———, experiment; ·····, model.

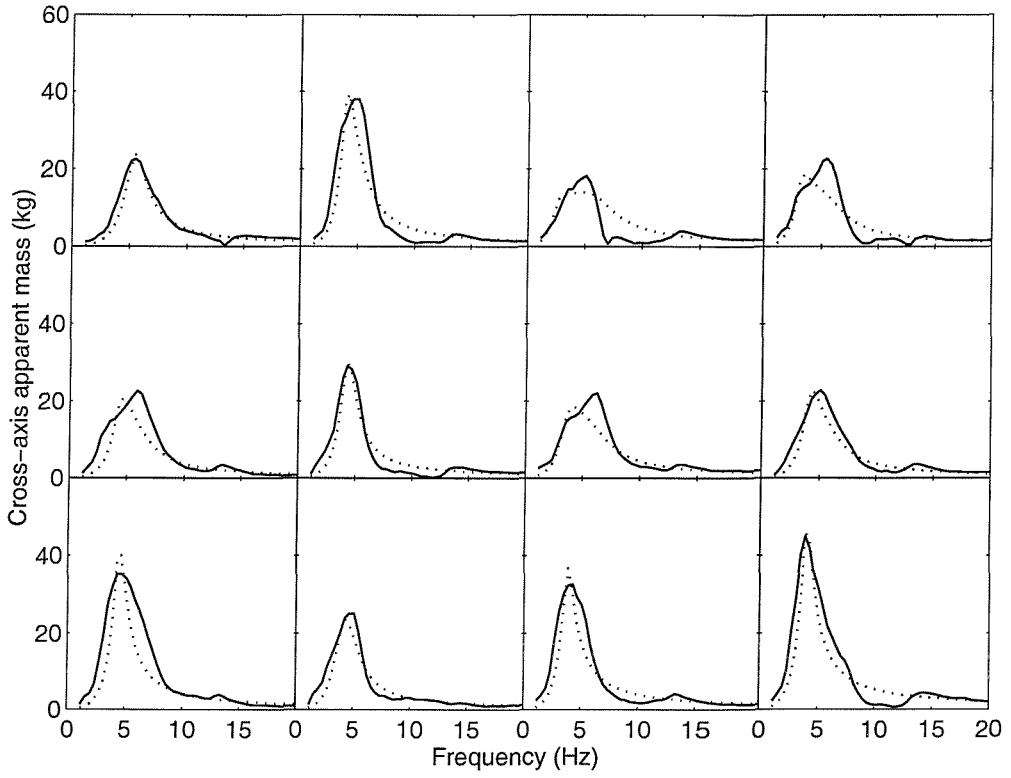

Figure 9.9 Fore-and-aft cross-axis apparent masses of 12 subjects calculated from the model and obtained from the experiment in the feet hanging posture: ———, experiment; ·····, model.

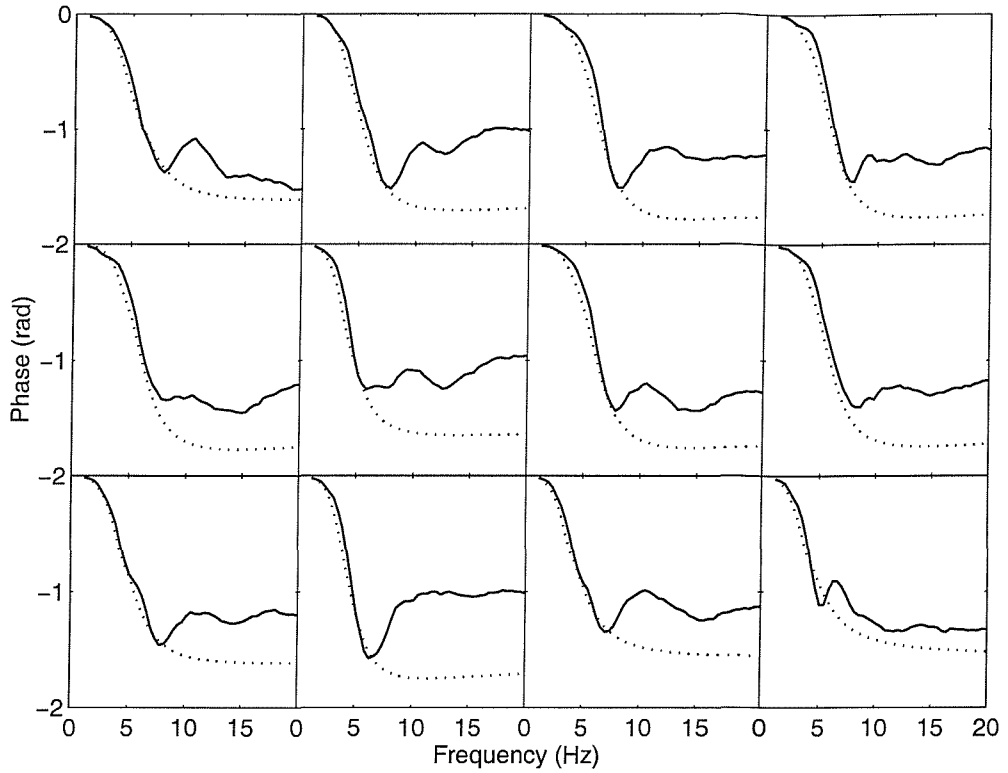

Figure 9.10 Vertical apparent masses phase of 12 subjects calculated from the model and obtained from the experiment in the feet hanging posture: ———, experiment; ·····, model.

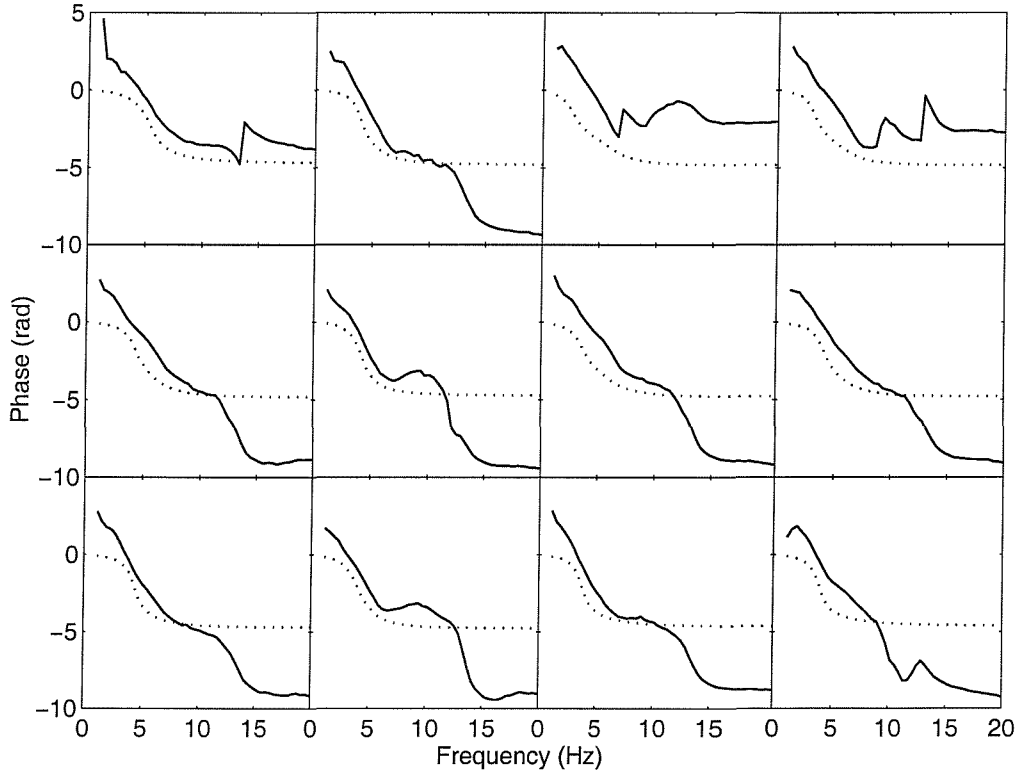

Figure 9.11 Fore-and-aft cross-axis apparent masses phase of 12 subjects calculated from the model and obtained from the experiment in the feet hanging posture: ———, experiment; ·····, model.

Table 9.4 shows the model parameters obtained for 12 subjects. The table also shows that the model parameters fitting the median experimental apparent masses of 12 subjects are similar to the median of the model parameters obtained from the individual prediction, except for the rotational damping.

Table 9.4 Individual model parameters obtained for four sitting postures.

Subject	Feet hanging					Maximum thigh contact				
	m_1 (kg)	k_1 (N/m)	c_1 (Ns/m)	k_t (Nm)	c_t (Nsm)	m_1 (kg)	k_1 (N/m)	c_1 (Ns/m)	k_t (Nm)	c_t (Nsm)
1	17	72326	1843	8913	75	14	53114	1966	4160	88
2	21	84618	1998	8765	90	13	70134	2004	7206	114
3	20	112547	2011	3598	127	10	107611	2237	5318	110
4	19	86234	1690	3816	77	11	80941	1955	10481	77
5	15	75749	1415	4973	60	10	78406	1639	8125	51
6	18	52862	1566	7007	68	11	54483	1595	6541	84
7	24	103169	1947	5339	102	16	89921	2336	5064	108
8	15	73144	1487	5321	69	12	49050	1453	5398	72
9	19	72537	2026	8718	63	12	54502	1800	9670	86
10	17	58462	1466	7979	127	7	40966	1538	5045	82
11	22	64009	2305	7602	77	13	50122	2127	9058	97
12	30	78308	3180	12648	114	20	68014	2484	12495	138
Median of 12 subjects	19	74447	1895	7305	77	12	61258	1961	6874	87
Fit median of 12 subjects	18	74414	1888	7365	129	11	61552	1947	5986	127

Table 9.4 (Continued)

Subject	Average thigh contact					Minimum thigh contact				
	m_1 (kg)	k_1 (N/m)	c_1 (Ns/m)	k_t (Nm)	c_t (Nsm)	m_1 (kg)	k_1 (N/m)	c_1 (Ns/m)	k_t (Nm)	c_t (Nsm)
1	6	55658	2000	7504	87	3	46035	1466	5516	91
2	5	57148	1669	6219	113	2	60248	1701	8700	117
3	4	96558	2239	4357	137	0	84290	1542	8096	114
4	6	56973	1495	4241	93	3	59455	1286	4502	74
5	4	52470	1124	4436	51	2	55598	936	3565	45
6	5	45974	1320	5200	112	1	52708	1411	4682	87
7	5	82687	1755	5143	124	5	75446	1830	9603	120
8	4	48036	1147	3721	82	3	51654	1305	7478	89
9	0	53120	1510	6078	83	0	60849	1486	8239	88
10	3	36286	1359	3310	136	3	41234	1378	4404	154
11	6	49201	1789	6565	159	3	46729	1684	8517	117
12	7	58546	1783	10492	252	3	56263	1769	7833	194
Median of 12 subjects	5	54389	1590	5172	113	3	55931	1476	7656	103
Fit median of 12 subjects	3	52101	1570	4557	147	0.03	55310	1484	5481	125

9.2.4.2 Parameter sensitivity tests

In mechanistic models, which provide understanding of how the human body moves, parameter sensitivity tests are useful to find out which part of the body is responsible of producing the resonance frequency: a parameter whose change shows an appreciable change in the resonance frequency might be the reason for the resonance to happen. As mentioned in Section 9.2.3, mass 1 in the model can be assumed to represent the mass of the upper legs supported on the seat while mass 2 can be assumed to represent the mass of the upper body. The model described here might be assumed to be a very simple mechanistic model for the very complex movements of the human body. Table 9.5 and Table 9.6 show the change in the resonance frequency and the change in the magnitude at resonance of both the vertical apparent mass and the fore-and-aft cross-axis apparent mass in the average thigh contact posture when the model parameters were changed by ±40% of the optimised values. Figures 9.12 and 9.13 show the change in the vertical apparent mass and fore-and-aft cross-axis apparent mass, respectively, over the whole frequency range when the parameters of the model were changed by ±40% of the optimised values.

Table 9.5 Effect of ±40% change in parameters values on the resonance frequency and the magnitude at resonance of the vertical apparent mass in the average thigh contact posture.

	Frequency (Hz)			Magnitude (kg)		
	-40%	Initial	+40%	-40%	Initial	+40%
Vertical stiffness	2.73	4.30	5.08	76.29	82.37	90.41
Rotational stiffness	4.30	4.30	3.91	83.05	82.37	83.54
Vertical damping	4.69	4.30	3.52	111.66	82.37	72.18
Rotational damping	4.30	4.30	4.30	81.00	82.37	83.39

Table 9.6 Effect of ±40% change in parameters values on the resonance frequency and the magnitude at resonance of the fore-and-aft cross-axis apparent mass in the average thigh contact posture.

	Frequency (Hz)			Magnitude (kg)		
	-40%	Initial	+40%	-40%	Initial	+40%
Vertical stiffness	3.52	3.91	4.30	14.31	16.41	16.59
Rotational stiffness	3.91	3.91	4.30	13.02	16.41	19.13
Vertical damping	4.30	3.91	3.91	21.33	16.41	14.31
Rotational damping	3.52	3.91	4.30	25.30	16.41	12.70

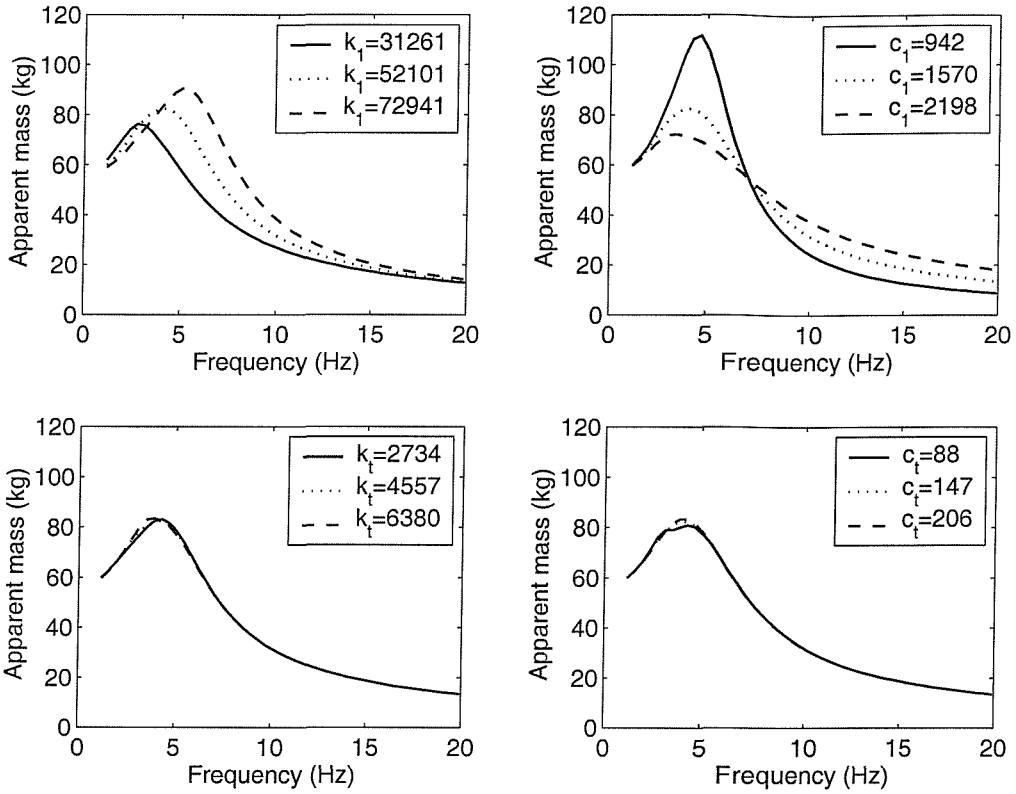

Figure 9.12 Sensitivity of the vertical apparent mass prediction to ±40% changes in the parameters of the model. Results are shown for the average thigh contact posture. Units of k_1, k_t, c_1 and c_t are as in Table 9.4 .

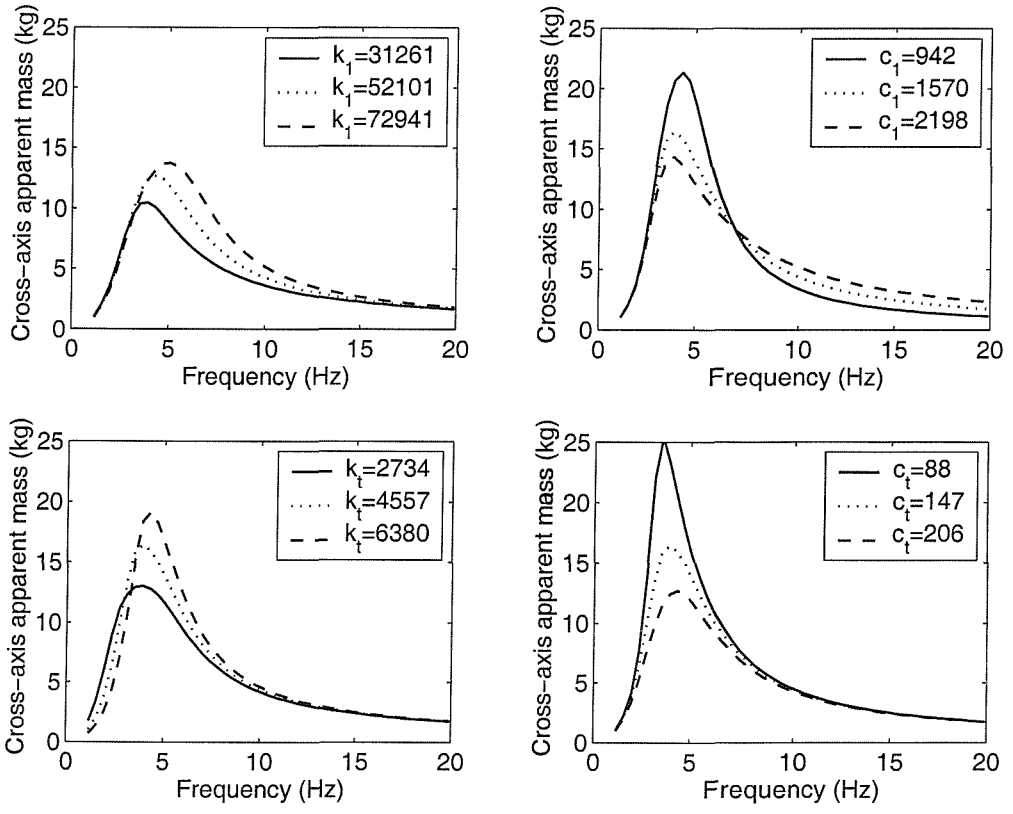

Figure 9.13 Sensitivity of the fore-and-aft cross-axis apparent mass prediction to ±40% changes in the parameters of the model. Results are shown for the average thigh contact posture Units of k_1, k_t, c_1 and c_t are as in Table 9.4.

Table 9.5 and Figure 9.12 show that the resonance frequency and the magnitude at resonance of the vertical apparent mass are affected mainly by changes in the translational stiffness and damping, the same finding as reported before by Matsumoto and Griffin (2001) with a different model. Using a model that predict transmissibilities in the vertical and fore-and-aft directions as well as the apparent mass in the vertical direction, Matsumoto and Griffin found that the major contribution to the resonance behaviour came from the tissue beneath the pelvis and the vertical movement of the viscera, with minor contribution from the bending and rocking modes of the upper body. Table 9.5 also shows that increasing the rotational damping in the model increases the vertical apparent mass at resonance. The reason for this might be that the vertical component of the rotational motion of mass 2 is out of phase with the vertical motion of mass 1, leading to subtraction of the forces in the vertical direction when calculating the vertical apparent mass. When the rotational damping increases, the rotational motion decreases and hence the force that is subtracted to calculate the total force is less.

Table 9.6 and Figure 9.13, show that the resonance frequency and the magnitude at resonance of the fore-and-aft cross-axis apparent mass are affected by both translational and rotational stiffness and damping. If this model represented the exact movement of the human body, it would be concluded that the tissues beneath the ischial tuberosities are contributors to the vertical apparent mass resonance frequency and the bending modes of the upper body make little contribution to the vertical apparent mass resonance frequency. However, this may not be the case if the human body moves in a different way from that described by the model.

9.2.4.3 Non-linearity

Human response to vibration is non-linear: the resonance frequency of the human body decreases with an increase in the vibration magnitude. The cause of the non-linearity, however, is not known. The model developed here was used to investigate which part of the model could contribute to the non-linearity. This was done by fitting the model to the median experimental vertical apparent mass and median fore-and-aft cross-axis apparent mass measured at four vibration magnitudes and quantify the changes in the model parameters due to the change in the vibration magnitude. Figure 9.14 and Figure 9.15 show the experimental and the predicted median responses in the average thigh contact posture at four vibration magnitudes. Similar agreement between the experimental and predicted median responses were found in the other postures at all vibration magnitudes. The model parameters obtained at different vibration magnitudes are shown in Table 9.7.

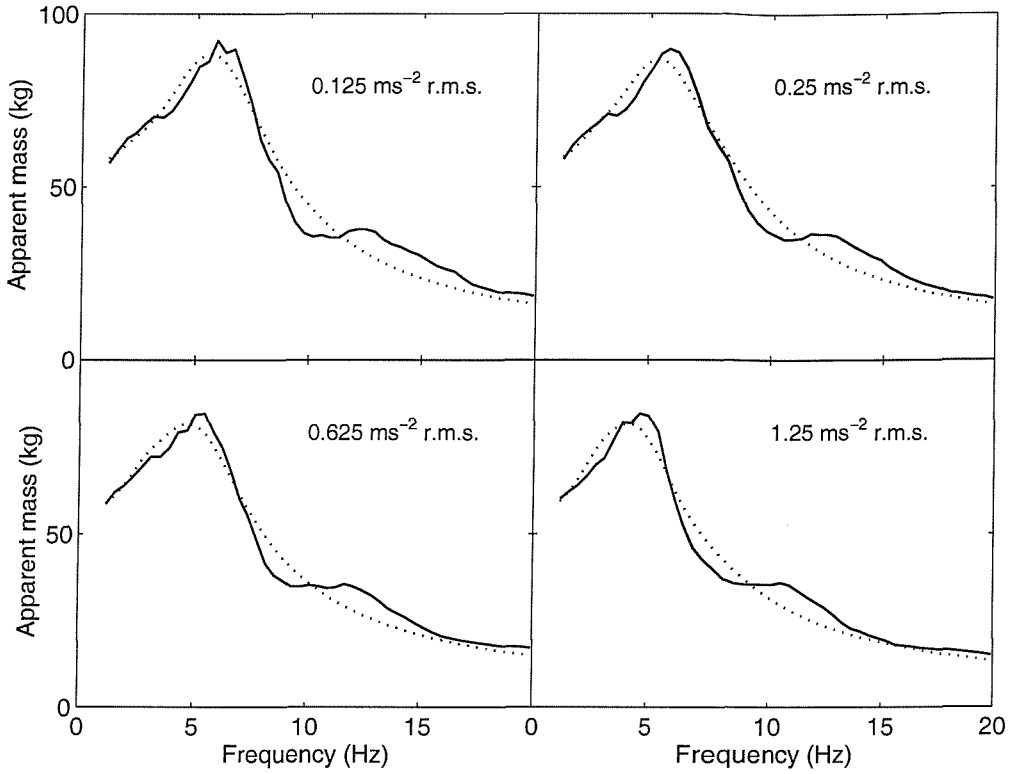

Figure 9.14 Vertical apparent mass calculated from the median experimental data and the fitted model at four vibration magnitudes in the average thigh contact posture: ———, experiment; ·····, model.

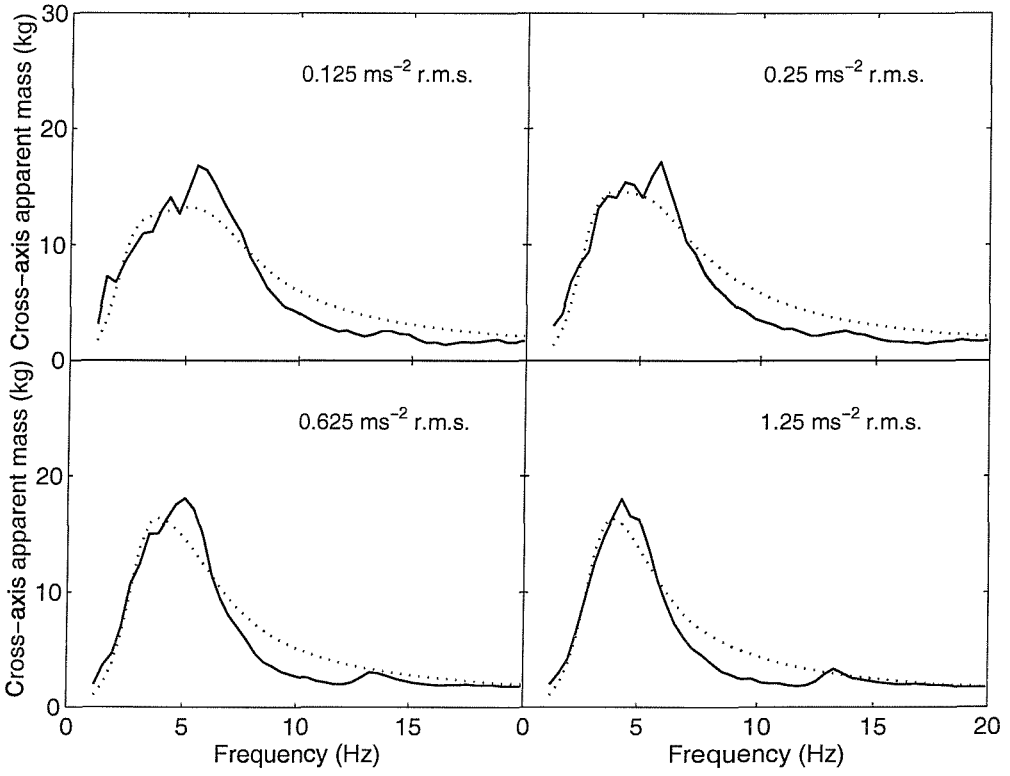

Figure 9.15 Fore-and-aft cross-axis apparent mass calculated from the median experimental data and the fitted model at four vibration magnitudes in the average thigh contact posture: ———, experiment; ·····, model.

Table 9.7 Model parameters obtained for different postures by fitting the model to the median experimental responses at four vibration magnitudes

Posture	Vibration Magnitude (ms^{-2} r.m.s.)	m_1 (kg)	k_1 (N/m)	c_1 (Ns/m)	k_t (Nm)	c_t (Nsm)
Feet hanging	0.125	18	139382	2007	10457	165
	0.25	18	122436	2090	12391	156
	0.625	18	91408	2013	9746	114
	1.250	18	74414	1888	7365	129
Maximum thigh contact	0.125	11	99920	2252	8053	172
	0.25	11	97444	2141	8573	163
	0.625	11	76733	2099	7153	128
	1.250	11	61552	1947	5986	127
Average thigh contact	0.125	3	85418	1764	2770	136
	0.25	3	80249	1777	3573	134
	0.625	3	63916	1720	4436	140
	1.250	3	52101	1570	4557	147
Minimum thigh contact	0.125	0	91224	1649	6861	155
	0.25	0.5	85934	1675	5745	133
	0.625	0	67141	1575	5931	113
	1.250	0.03	55310	1484	5481	125

It seems that the greatest change in parameter with change in vibration magnitude occurs in the vertical stiffness. Statistical analysis using Wilcoxon matched-pairs singed ranks test was used to investigate the difference between the model parameters obtained at 0.125 ms^{-2} r.m.s. and at 1.25 ms^{-2} r.m.s. in the four sitting postures (Table 9.8). No statistically significant difference was found in the value of mass 1 obtained using the two vibration magnitudes in any posture. A significant difference ($p < 0.01$) was found in the vertical stiffness obtained at the two vibration magnitude in all postures, while a significant difference ($p < 0.05$) in the rotational stiffness was found only when the feet were not supported or were just in touch with the footrest. These results suggest that the tissue beneath the ischial tuberosities may contribute to the non-linear behaviour found in the response of humans to vibration, the same conclusion as noticed before by Matsumoto and Griffin (2002a) and in the results of the first experiment of this thesis. The results might also suggest that common non-linear mechanisms, such as deformation in the buttocks tissue acted in all postures, while some other mechanisms, such as bending in the upper body, acts in other postures. This illustrates the importance of precisely define the sitting posture when studying the non-linearity: the different mechanisms reported by different researchers to have caused the non-linearity could be partly due to the different postures used in the different studies.

Table 9.8 Statistical analysis for the difference between the parameters obtained at 0.125 and 1.25 ms^{-2} r.m.s. for four sitting postures (-, no significant difference, $p < 0.05$ *, $p < 0.01$ **)

	Feet hanging	Maximum thigh contact	Average thigh contact	Minimum thigh contact
m_1	-	-	-	-
k_1	**	**	**	**
c_1	-	*	-	*
k_t	*	*	-	-
c_t	-	-	-	-

9.2.4.4 Vertical and fore-and-aft transmissibilities to mass 2

The vertical transmissibility and fore-and-aft transmissibility obtained from the model at the centre of gravity of mass 2 were compared with those measured experimentally in previous studies (Kitazaki, 1994; Matsumoto and Griffin, 2002b). The vertical transmissibility was calculated from the vertical acceleration at the centre of gravity of mass 2 and the vertical acceleration at the base. The fore-and-aft transmissibility was calculated from the fore-and-aft acceleration at the centre of gravity of mass 2 and the vertical acceleration at the base. The following formulae were used:

$$T_v = \frac{Z_1(s)}{Z_b(s)} + e\cos\alpha\frac{\Theta(s)}{Z_b(s)} \tag{9.6}$$

$$T_f = e\sin\alpha\frac{\Theta(s)}{Z_b(s)} \tag{9.7}$$

where,

T_v and T_f are the vertical and fore-and-aft transmissibilities, respectively

$Z_b(s)$, $Z_1(s)$ and $\Theta(s)$ are the Laplace transform of z_b, z_1, and θ, respectively (see Section 9.2.2)

e and α are as described in Section 9.2.2

$s = j \cdot \omega$, where $j = \sqrt{-1}$ and ω is the angular velocity in rad s^{-1}

The vertical and fore-and-aft transmissibilities in the four postures are shown in Figure 9.16.

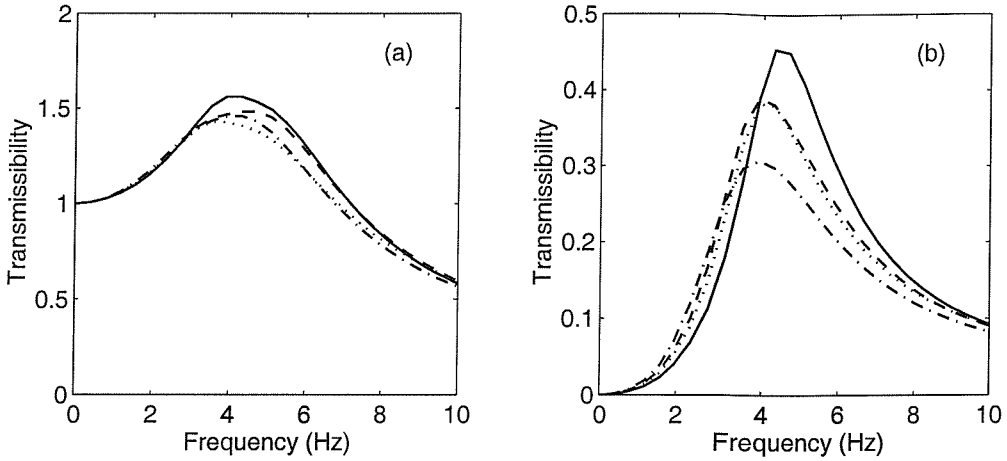

Figure 9.16 Transmissibilities to the centre of gravity of mass 2: (a) vertical transmissibility (b) fore-and-aft transmissibility. ———, feet hanging; ·····, maximum thigh contact; –·–·–·–, average thigh contact; – – – –, minimum thigh contact.

The location of the centre of gravity of mass 2 with respect to the origin located on the seat at the ischial tuberosities is similar to the location of the centre of gravity of the lower thoracic (T10-T12) for a person sitting in an upright posture with a mass similar to that of the model (Singley and Haley, 1978). The vertical transmissibility and fore-and-aft transmissibility are consistent with those to T11 reported by Kitazaki (1994; see Figure 2.21) and to T10 reported by Matsumoto and Griffin (2002b; see Figure 2.31) for frequencies below 6 Hz. However, above 6 Hz, the model seems to under-predict the transmissibility. The measurements reported by Matsumoto and Griffin and by Kitazaki were taken close to the vertebrae, while this model gives a prediction for the transmissibility to the centre of gravity of the T10 to T12 region. Moreover, in the experiments, the transmissibility measured at T10 and T11 might have been affected by the response of the vertebrae below T10 and T11, and by the response of the pelvis, while in this model the whole upper body was assumed to be a rigid body. It is more likely, however, that the incorrect prediction of the transmissibility above 6 Hz is due to the insufficient number of degrees-of-freedom in the model which also caused the incorrect prediction of the phase of the apparent mass above 8 Hz, as was shown in Section 9.2.4.1.

The greatest vertical transmissibility at resonance occurred in the feet hanging posture, while the smallest vertical transmissibility at resonance occurred with the maximum thigh contact posture. The feet hanging posture had the highest stiffness and mass among the four postures (see Table 9.3). Despite the fact that the maximum thigh contact posture had greater stiffness and greater mass than the average thigh contact posture and the minimum thigh contact posture, the vertical transmissibility at resonance in the maximum thigh contact posture was smaller than the vertical transmissibility in both the average

thigh contact posture and the minimum thigh contact posture. This is due to greater vertical damping in the maximum thigh contact posture than in the other two postures, as shown in Table 9.3.

The fore-and-aft transmissibility at resonance is greatest when the feet were less supported (feet hanging and maximum thigh contact postures) or with the minimum thigh contact posture. The fore-and-aft transmissibility in this model is produced by the rotational motion of mass 2, as was shown in the equations above. When the feet were less supported, the upper body could pitch more freely than when the feet were supported. However, in the minimum thigh contact posture the body was supported on a smaller area (mainly the ischial tuberosities) which made it easier for the body to pitch in the mid-sagittal plane (as was explained in Chapter 4). The average thigh contact posture had the smallest rotational displacement, and hence, the least fore-and-aft transmissibility at resonance. This was reflected in the model by a greater rotational damping in the average thigh contact posture than in the other three postures.

9.2.5 Conclusions

A two degree-of-freedom model with rotational capability was developed to represent the dynamic response of the seated human body in the vertical and fore-and-aft directions measured on the seat. The model response showed good agreement with both the experimental median apparent mass and the individual apparent mass at frequencies below 8 Hz. The model implies that the resonance frequency of the human body (around 5 Hz) could be due to the vertical deformation of the tissue beneath the pelvis. The pitching mode of the upper body seemed to make a minor contribution to the 5 Hz resonance frequency of the vertical apparent mass. The greatest change in the model parameters with change in vibration magnitude was found in the stiffness representing the lower legs and the tissues beneath the pelvis, suggesting that this part of the body contributes to the non-linear behaviour observed in the responses of humans to vibration. However, these preliminary conclusions need confirmation in a more representative model of movement of the human body. The model described here, which is simple and based on some crude assumptions, is intended as a step towards models representing the response of the human body in directions of vibration other than the direction of excitation.

9.3 ALTERNATIVE MODELS TO IMPROVE THE PREDICTION OF THE VERTICAL APPARENT MASS AND THE FORE-AND-AFT CROSS-AXIS APPARENT MASS DURING VERTICAL EXCITATION

In this section, five alternative linear lumped parameter models have been investigated in an attempt to obtain better predictions for the magnitudes and phases of the vertical apparent mass and the fore-and-aft cross-axis apparent mass than those obtained by the model used in the previous section. The feet hanging posture and the average thigh contact posture are used in this section.

9.3.1 Description and parameters of the investigated models

The five investigated models are shown in Figure 9.17.

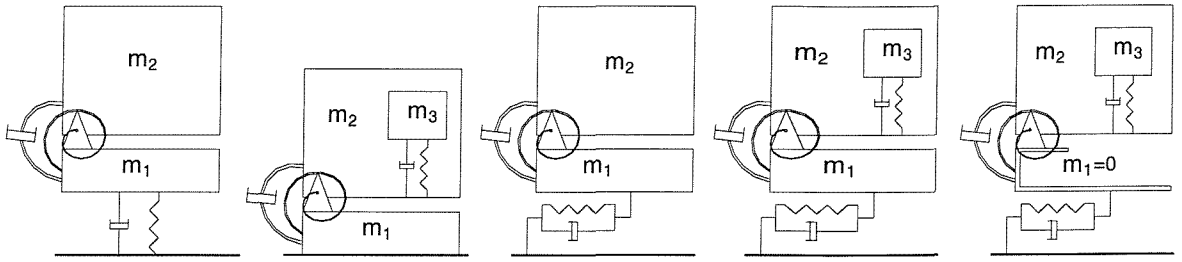

Figure 9.17 Alternative lumped parameter models.

Model 1: Model 1 is the same two degree-of-freedom model used in the previous section. However, in this section all model parameters including the masses, the location of the centre of gravity and the moment of inertia will be optimised.

Model 2: Two degree-of-freedom model. In this model, the input to the vertical degree of freedom is the pitching motion of mass 2 which is opposite to what happens in Model 1 where the vertical motion of mass 1 provides the input to mass 2. The centre of gravity of mass 2 and mass 3 lie on the same vertical line and mass 3 is restricted to vertical motion.

Model 3: Two degree-of-freedom model. The pitching motion of mass 2 is expected to induce fore-and-aft motion in mass 1 and mass 2 and, hence, a horizontal spring and a horizontal damper were installed beneath mass 1 to represent the fore-and-aft motion. The horizontal degree-of-freedom could be considered to represent any shear deformation in the tissue beneath the pelvis.

Model 4: Three degree-of-freedom model. This model is a combination of Model 2 and Model 3.

Model 5: The same as Model 4 but with mass 1 set to zero.

The equations of motion of each model were derived using Lagrange's equations. An example of the equations of motion developed for Model 1 was shown in Section 9.2.2. In this section, the following nomenclatures will be used when referring to the parameters of the models:

m_1, m_2 and m_3 are the masses of mass 1, mass 2 and mass 3, respectively
J_2 is the moment of inertia of mass 2 about the connection point
k_{1z} and c_{1z} are the vertical stiffness and damping beneath mass 1 in Model 1
k_{1x} and c_{1x} are the fore-and-aft stiffness and damping beneath mass 1 in Model 3, Model 4 and Model 5
k_2 and c_2 are the rotational stiffness and damping of mass 2
k_{3z} and c_{3z} are the vertical stiffness and damping beneath mass 3 in Model 2, Model 4 and Model 5
e is the distance between the centre of gravity of mass 2 and the connection point
α is the angle that e has with the horizontal when the model is in equilibrium

All model parameters (inertia properties, stiffness, damping coefficients, and location of the centre of gravity of mass 2) were optimised using the Nelder Meade simplex search method provided in MATLAB by comparing the results obtained experimentally (Chapter 4) with the responses of the models. The moduli and phases of both the vertical apparent mass and the fore-and-aft cross-axis apparent mass were used in the error function used for the optimisation process as follows:

$$\text{err} = \sum_{i=1}^{N}(M_\text{p} - M_\text{m})_i^2 + \text{F}_1 * \sum_{i=1}^{N}(CM_\text{p} - CM_\text{m})_i^2 + \text{F}_2 * \sum_{i=1}^{N}(Ph_\text{p} - Ph_\text{m})_i^2 + \text{F}_3 * \sum_{i=1}^{N}(CPh_\text{p} - CPh_\text{m})_i^2 \quad (9.8)$$

where,

M_p and CM_p are the predicted vertical apparent mass and fore-and-aft cross-axis apparent mass, respectively.
M_m and CM_m are the measured vertical apparent mass and fore-and-aft cross-axis apparent mass, respectively.

Ph_p and CPh_p are the predicted phases of the apparent mass and cross-axis apparent mass, respectively.
Ph_m and CPh_m are the measured phases of the apparent mass and cross-axis apparent mass, respectively.
F_1, F_2 and F_3 are arbitrary factors used to improve the prediction

9.3.2 Results and discussion

9.3.2.1 Modelling of median data

Starting from Model 1, the models were developed in stages until reasonable agreements between the experimental and theoretical results in the magnitudes and phases of the vertical apparent mass and the fore-and-aft cross-axis apparent mass were achieved. The parameters of only the final models were analysed.

In the first stage, Model 1 (which was developed in Section 9.2.2) was used with optimisation of all the model parameters, as opposed to optimising only the stiffness and damping as in Section 9.2.2. This was done to ensure that fixing some of the parameters had no effect on the quality of the curve fitting. However, no improvement in the quality of the curve fitting was obtained when all the parameters were optimised in either the feet hanging posture (Figure 9.18) or the average thigh contact posture (Figure 9.19).

In the second stage, the vertical degree of freedom beneath mass 1 was removed while a vertical degree of freedom and mass 3 were added to be driven initially by mass 2 as shown in Model 2 (Figure 9.17). The vertical degree of freedom beneath mass 1 in Model 1 was removed in Model 2 since a previous study by Wei and Griffin (1998) showed that a model with two degrees of freedom was sufficient to provide reasonable prediction for the vertical apparent mass. The response of Model 2 showed good agreement with the vertical apparent mass magnitude and phase but not with the cross-axis apparent mass, as shown in Figures 9.18 and 9.19. In models with rotational degrees-of-freedom, Matsumoto (1999) found that adding a vertical degree of freedom (representing the viscera in Matsumoto's model) above a pitching mass (representing the pelvis) in an arrangement similar to that of Model 2 was necessary to improve the quality of the model prediction.

In the third stage, the vertical degree of freedom beneath mass 3 was replaced by a fore-and-aft degree of freedom beneath mass 1 in an attempt to improve the prediction in the fore-and-aft direction. The prediction showed good agreement with the vertical apparent mass but not with the fore-and-aft cross-axis apparent mass (Figures 9.18 and 9.19). Although this model is not a mechanistic model, there is evidence in previous mechanistic

models that some mechanisms involving fore-and-aft motion of the pelvis and shear deformation of the buttocks tissue, together with bending modes in the upper body, contribute to the principal mode in the vertical apparent mass (4.9 Hz) and to a mode at a higher frequency (5.6 Hz; Kitazaki and Griffin, 1997). The interactions between these two modes in Model 3 might have helped in improving the prediction in the vertical apparent mass magnitude and phase.

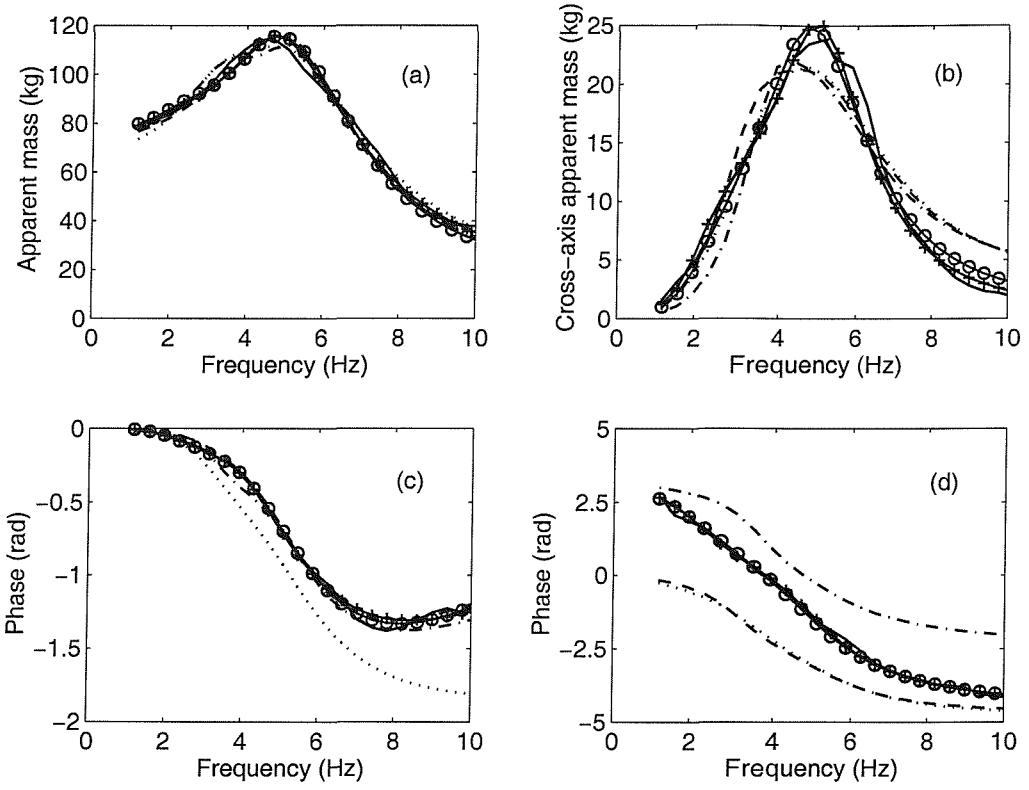

Figure 9.18 Median responses obtained experimentally and calculated using 5 models in the feet hanging posture. (a) and (c), vertical apparent mass; (b) and (d) fore-and-aft cross-axis apparent mass. ———, experimentally; ·····, Model 1; –·–·–, Model 2; – – – –, Model 3; —+—, Model 4; —o—, Model 5.

In the fourth stage, it was clear that a third degree of freedom was necessary to improve the prediction of the fore-and-aft cross-axis apparent mass, as a two degree of freedom model will be sufficient only to give a good prediction for the vertical apparent mass. It was then decided to re-insert the degree of freedom beneath mass 3 (see Model 4, Figure 9.17). At this stage, good agreement between the experimental and theoretical responses was achieved in both the vertical apparent mass and the cross-axis apparent mass. However, the value of m_1 was always zero in Model 4.

In the final stage, m_1 in Model 4 was set to zero producing Model 5. It seems that m_1 had no effect on the response of the final model, as shown in Figures 9.18 and 9.19. The final model (i.e. Model 5) is shown in Figure 9.20 with all the parameters.

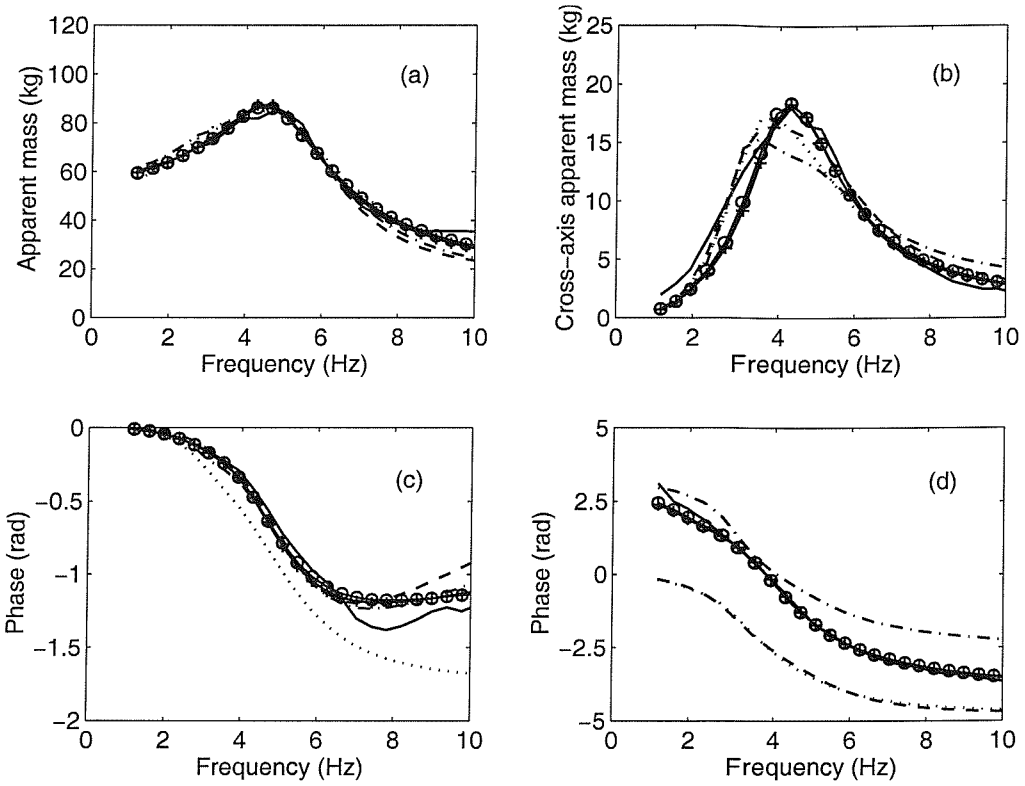

Figure 9.19 Median responses obtained experimentally and calculated using 5 models in the average thigh contact posture. (a) and (c), vertical apparent mass; (b) and (d) fore-and-aft cross-axis apparent mass. ———, experimentally; ·····, Model 1; —·—·—, Model 2; – – – –, Model 3; —+—, Model 4; —o—, Model 5.

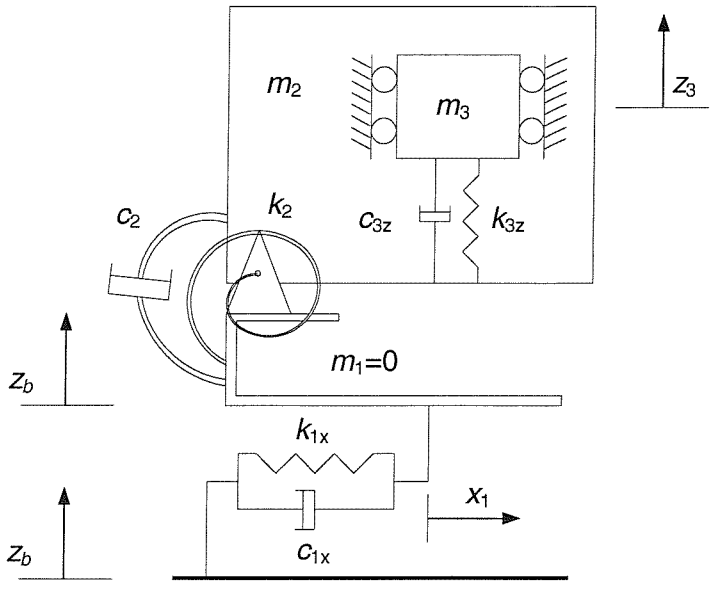

Figure 9.20 Model 5.

9.3.2.2 Modelling of individual data

Model 5 was used to predict the magnitudes and phases of both the vertical apparent masses and fore-and-aft cross-axis apparent masses of 12 subjects sitting in the feet hanging posture and the average thigh contact posture. The calculated and the measured responses were in good agreement as shown in Figure 9.21 to Figure 9.24 in the feet hanging posture and in Figure 9.25 to Figure 9.28 in the average thigh contact posture.

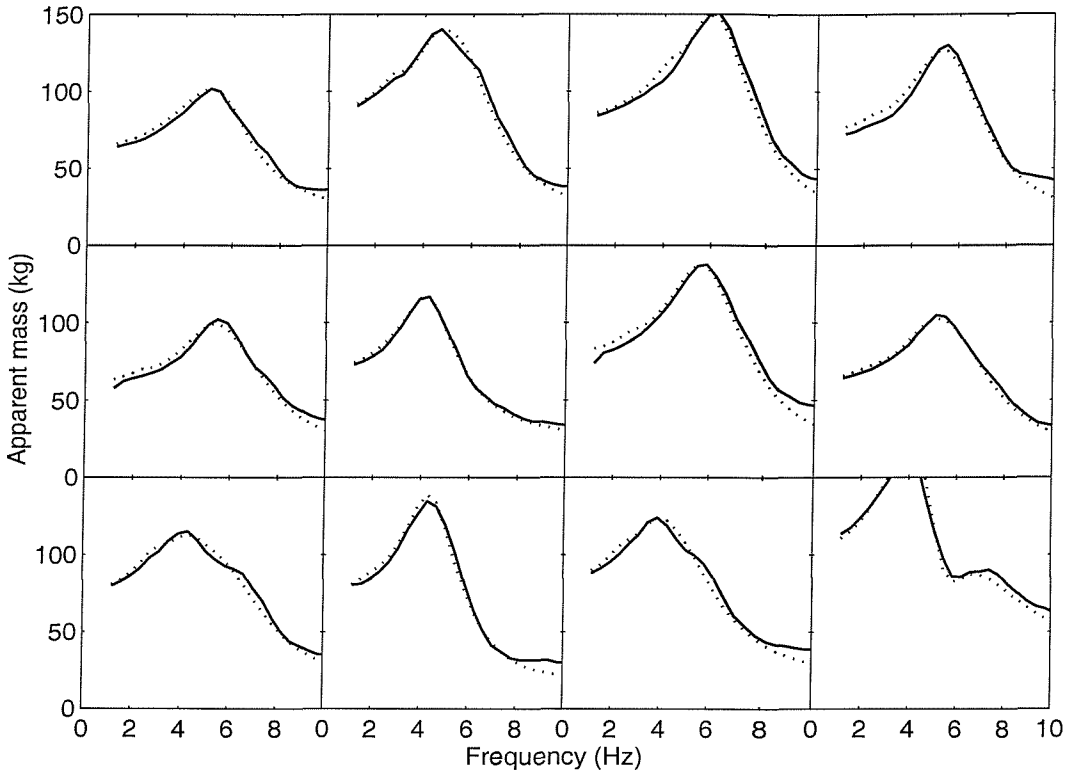

Figure 9.21 Vertical apparent masses of 12 subjects calculated from Model 5 and obtained from the experiment in the feet hanging posture: ———, experiment; ·····, model.

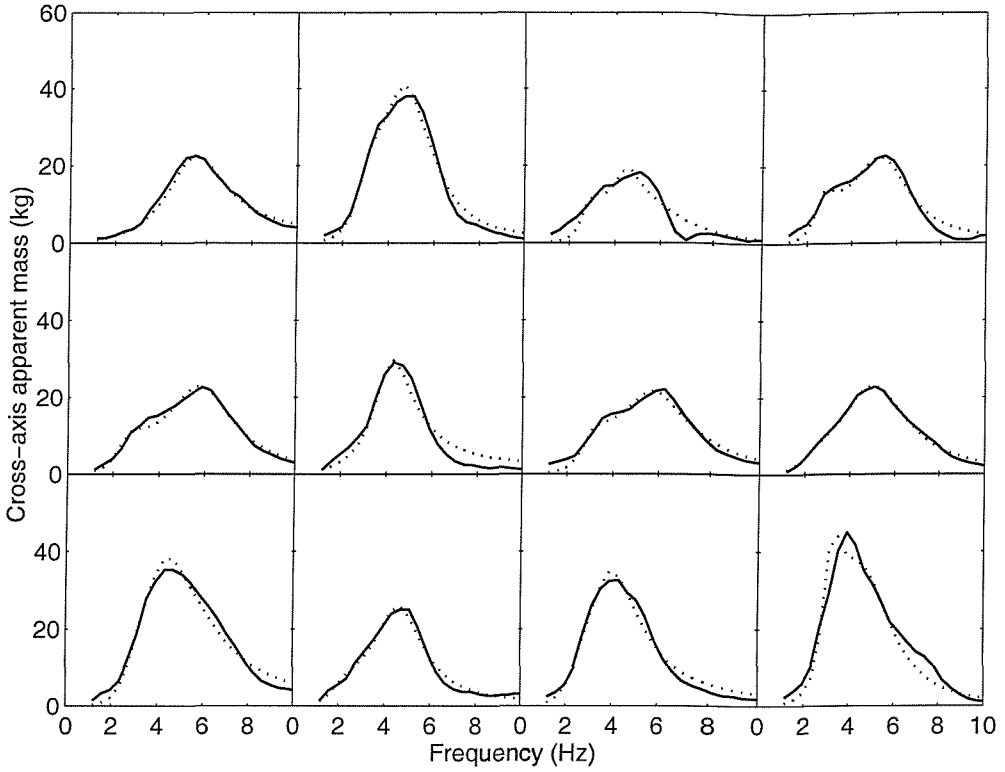

Figure 9.22 Fore-and-aft cross-axis apparent masses of 12 subjects calculated from Model 5 and obtained from the experiment in the feet hanging posture: ———, experiment; ·····, model.

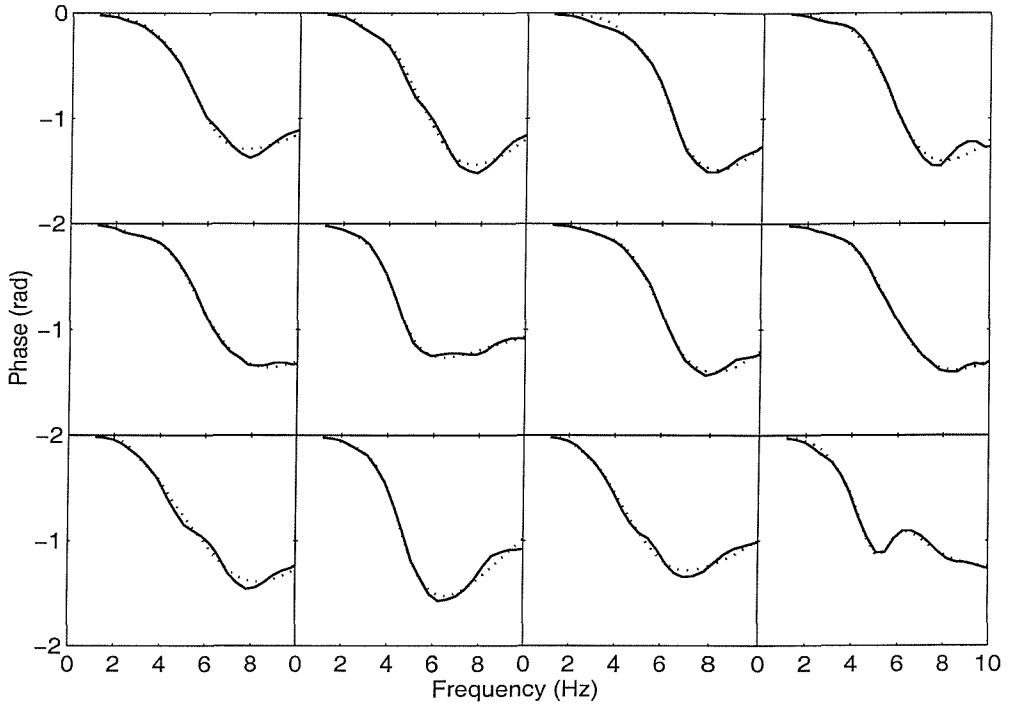

Figure 9.23 Vertical apparent masses phase of 12 subjects calculated from the model and obtained from the experiment in the feet hanging posture: ———, experiment; ·····, model.

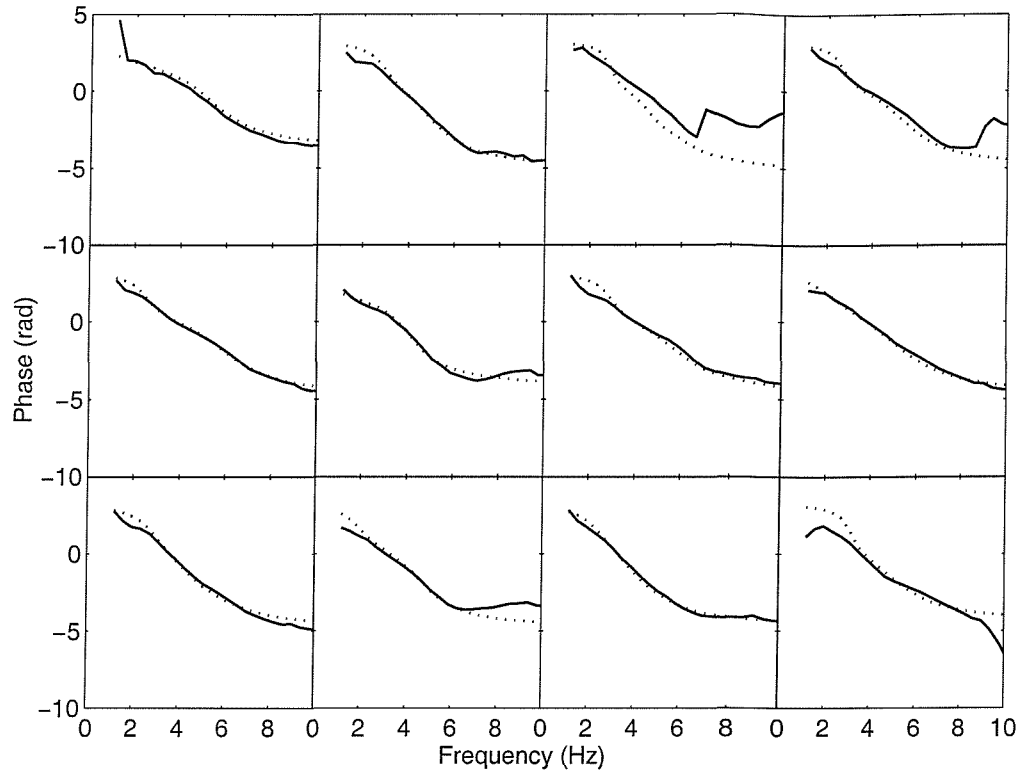

Figure 9.24 Fore-and-aft cross-axis apparent masses phase of 12 subjects calculated from the model and obtained from the experiment in the feet hanging posture: ———, experiment; ·····, model.

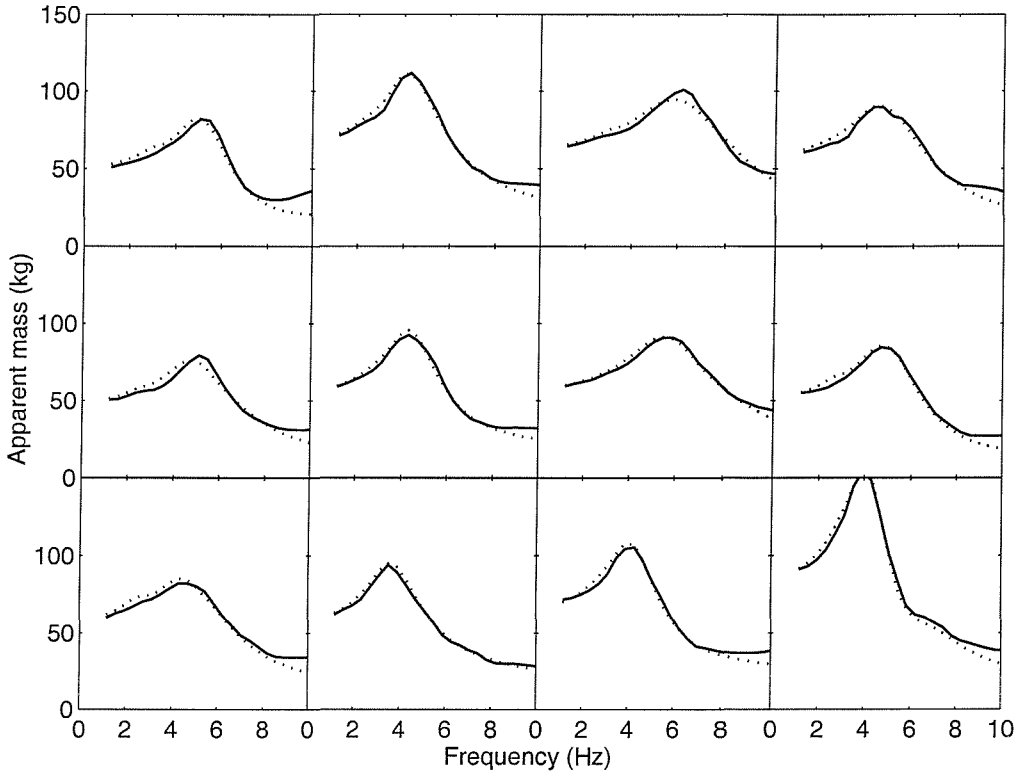

Figure 9.25 Vertical apparent masses of 12 subjects calculated from Model 5 and obtained from the experiment in the average thigh contact posture: ———, experiment; ·····, model.

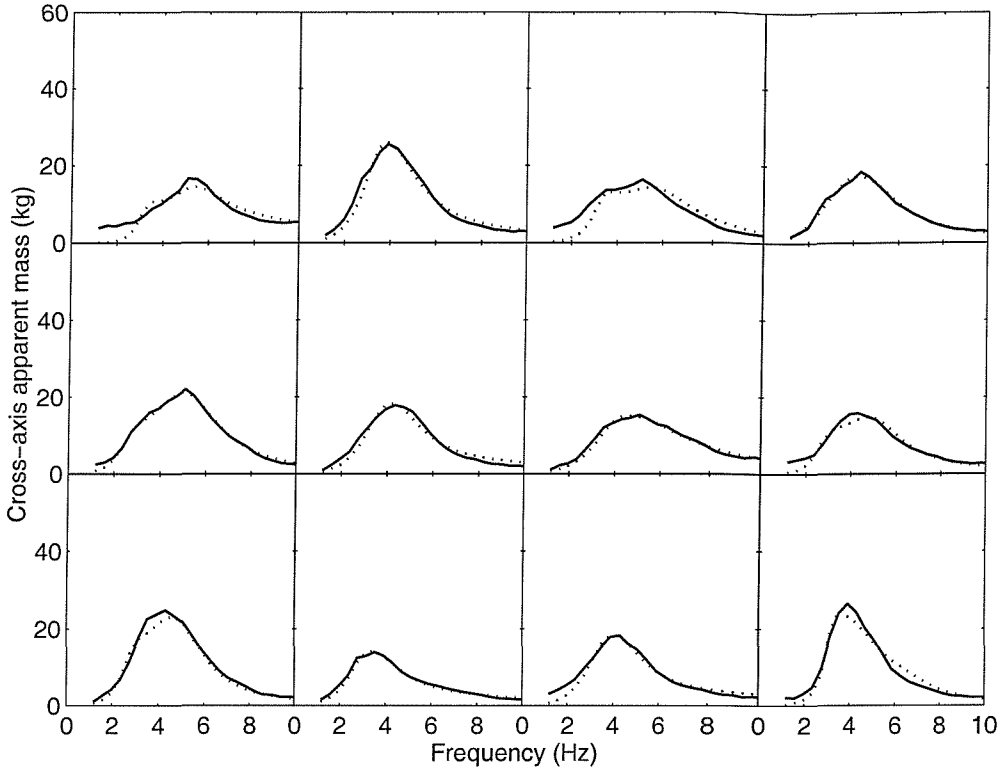

Figure 9.26 Fore-and-aft cross-axis apparent masses of 12 subjects calculated from Model 5 and obtained from the experiment in the average thigh contact posture: ———, experiment; ·····, model.

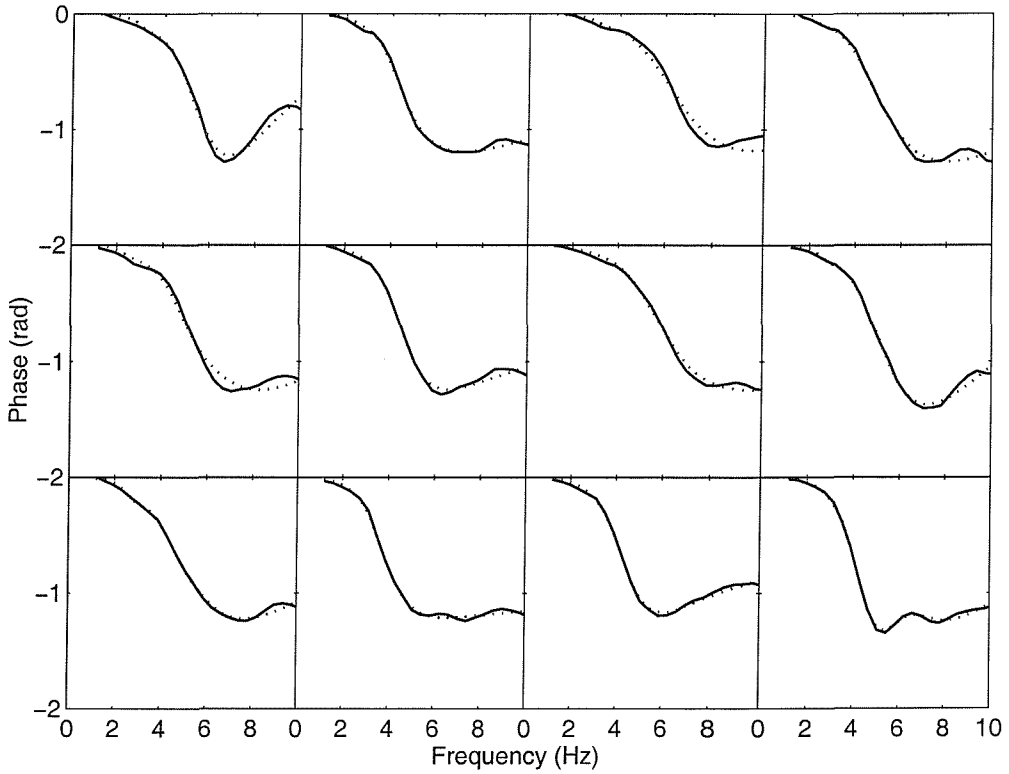

Figure 9.27 Vertical apparent masses phase of 12 subjects calculated from the model and obtained from the experiment in the average thigh contact posture: ———, experiment; ·····, model.

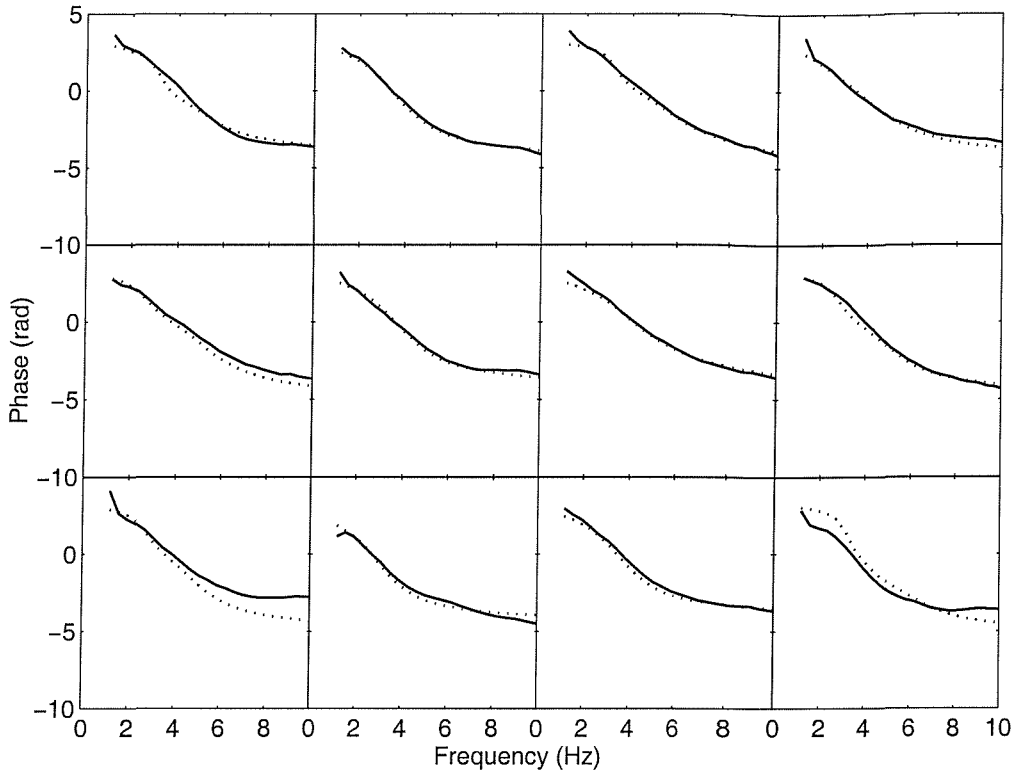

Figure 9.28 Fore-and-aft cross-axis apparent masses phase of 12 subjects calculated from the model and obtained from the experiment in the average thigh contact posture: —— , experiment; ····· , model.

The optimised parameters obtained for each individual from Model 5 are shown in Table 9.9 for the feet hanging posture and in Table 9.10 for the average thigh contact posture. The optimised parameters differed between subjects and showed high variability, especially with the feet hanging posture. This could be expected due to the high inter-subject variability found experimentally in the vertical apparent masses and the fore-and-aft cross-axis apparent masses. In the average thigh contact posture, the optimised parameters showed less variability between subjects than in the feet hanging posture. Moreover, the optimised parameters in the average thigh contact posture are of a similar order between subjects (except for subject 12). The experimental data showed less inter-subject variability in the average thigh contact posture than in the feet hanging posture (see, for example, Figure 4.4, Chapter 4). It is possible that in the feet hanging posture, swinging in the lower legs contributed to the force measured on the seat in the fore-and-aft direction. Since, the effect of the swinging of the feet is not accounted for when deriving the equations of the model, it will be reflected in the optimised parameters. This might have contributed to the high variability in the parameters between subjects in the feet hanging posture.

Table 9.9 Parameters obtained from Model 5 in the feet hanging posture, (m_1=0).

Subject	m_2 (kg)	m_3 (kg)	J_2 (kgm^2)	k_{1x} (N/m)	k_2 (Nm)	k_{3z} (N/m)	c_{1x} (Ns/m)	c_2 (Nsm)	c_{3z} (Ns/m)	e (m)	α (rad)
1	19	45	6.85	75239	5011	59103	1106	687	633	0.60	1.03
2	28	61	14.75	69586	6423	65037	956	145	891	0.43	1.18
3	32	52	18.06	32433	10838	78783	432	94	816	0.50	1.36
4	25	50	0.72	68572	228	64860	1048	4	866	0.11	1.34
5	18	44	0.24	76590	71	59661	1002	2	857	0.09	1.35
6	25	46	0.18	46203	49	38514	730	15	283	0.09	0.73
7	30	51	0.30	95174	125	70681	1807	2	833	0.05	1.17
8	20	44	0.10	50647	27	57593	811	2	738	0.06	1.28
9	34	44	9.77	56065	6273	36967	1081	194	318	0.41	0.75
10	23	53	7.15	65973	1424	45023	1165	75	666	0.34	1.29
11	31	55	3.75	49170	1555	43722	988	64	620	0.23	0.98
12	15	91	3.07	46350	3246	91985	553	23	2295	0.45	1.42

Table 9.10 Parameters obtained from Model 5 in the average thigh contact posture, (m_1=0).

Subject	m_2 (kg)	m_3 (kg)	J_2 (kgm^2)	k_{1x} (N/m)	k_2 (Nm)	k_{3z} (N/m)	c_{1x} (Ns/m)	c_2 (Nsm)	c_{3z} (Ns/m)	e (m)	α (rad)
1	26	26	0.29	26024	142	25631	2879	2	344	0.07	1.00
2	24	45	0.12	32887	76	44264	551	7	406	0.07	0.99
3	21	43	0.18	69002	90	74587	1132	1	1135	0.06	1.35
4	16	44	0.14	33170	41	48193	694	4	787	0.09	1.33
5	14	35	1.14	41203	414	40549	558	14	679	0.28	1.39
6	20	37	0.17	29561	145	36458	636	11	296	0.09	0.93
7	20	39	0.08	37212	67	64479	660	5	409	0.06	0.96
8	17	36	0.51	44320	186	35845	1167	4	545	0.10	1.25
9	17	42	0.13	49202	49	40155	758	1	786	0.06	1.27
10	24	35	0.13	19457	36	21967	514	8	149	0.07	0.61
11	24	43	0.21	32545	162	37923	744	14	445	0.09	0.98
12	23	64	9.41	38990	12409	52602	469	127	936	0.49	1.32

9.3.2.3 Parameter sensitivity tests

In this section, the effect of a change in the optimised parameters (masses, stiffness, and damping coefficients) of the model on the resonance frequencies and the magnitudes at resonance in both the vertical apparent mass and the fore-and-aft cross-axis apparent mass was studied. For each individual subject, each model parameter was allowed to change by ±40% from the obtained optimised value, while the rest of the parameters were

fixed at the optimised values. This helps in identifying the parts of the model producing the resonance behaviour.

9.3.2.3.1 Vertical apparent mass

The changes in the resonance frequencies and the magnitude at resonance as a result of ±40% change in the optimised model parameters are given in Appendix F for all subjects in the feet hanging posture and the average thigh contact posture. Table 9.11 shows the cases where there were statistically significant differences (Wilcoxon, $p < 0.05$) between the resonance frequency and magnitude at resonance of the vertical apparent mass obtained initially from the optimised model parameters and the resonance frequency and magnitude at resonance of the vertical apparent mass obtained when the optimised parameters were changed by ±40%. The table shows that the vertical apparent mass resonance frequency and apparent mass magnitude at resonance are affected by the change in mass 3 and the stiffness and damping coefficients of the spring and damper beneath mass 3 (i.e. k_{3z} and c_{3z}). The magnitude of the vertical apparent mass at resonance but not the resonance frequency is also affected by changes in k_2 and mass 2. Since there might be minor and major contributors to the resonance, as was shown in previous studies (e.g. Matsumoto and Griffin, 2001), the amount of change in the resonance frequency and the magnitude at resonance with the change in model parameters is needed before coming to a conclusion about what causes the resonance.

Table 9.11 Cases of statistically significant differences (SD) between the resonance frequency (f) and magnitude at resonance of the vertical apparent mass (m) obtained using the optimised model parameters (initial) and the resonance frequencies and magnitude at resonance obtained by changing the model parameters by ±40%. H: feet hanging, Av: average thigh contact, s: significant, -: not significant; N/A: not applicable.

Parameter	Posture	Resonance frequency, f		Magnitude at resonance, m		No. of SD (Out of 4)	Total No. of SD (Out of 8)
		Initial / -40%	Initial / +40%	Initial / -40%	Initial / +40%		
k_{1x}	H	-	-	-	s	f: 0	f: 0, m: 1
	Av	-	-	-	-	m: 1	
c_{1x}	H	-	-	-	-	f: 0	
	Av	-	-	-	-	m: 0	
k_2	H	-	-	s	s	f: 0	f: 1, m: 4
	Av	-	-	s	s	m: 4	
c_2	H	-	-	-	-	f: 1	
	Av	s	-	-	-	m: 0	
k_{3z}	H	s	s	s	s	f: 4	f: 8, m: 8
	Av	s	s	s	s	m: 4	
c_{3z}	H	s	s	s	s	f: 4	
	Av	s	s	s	s	m: 4	
m_2	H	-	-	s	s	f: 0	N/A
	Av	-	-	s	s	m: 4	
m_3	H	s	s	s	s	f: 4	N/A
	Av	s	s	s	s	m: 4	

The ratios between the resonance frequencies and magnitudes at resonance obtained after the ±40% change in the optimised parameters, and the initial resonance frequencies and initial magnitudes at resonance obtained from the optimised parameters were calculated for each subject. Table 9.12 shows the median and inter-quartile ranges for the calculated ratios. The table shows that the largest changes in the resonance frequencies of the apparent mass occurred with the changes in k_{3z} and m_3. The table also shows that the largest changes in the vertical apparent mass at resonance resulted from changes in k_{3z}, c_{3z}, m_3 and m_2, with the greatest changes in the apparent mass at resonance accompanying the changes in c_{3z} and m_3. The effect of m_2 on the magnitude of the apparent mass at resonance is believed to be due to a change in the total mass of the system rather than direct involvement in the resonance phenomenon. Although statistically significant differences were found in the magnitude of the apparent mass at resonance with changes in k_2, the change in the magnitude at resonance with change in k_2 was small (Table 9.12). It can be concluded that the resonance frequency of the vertical apparent mass is mainly produced by the single degree of freedom system represented by k_{3z}, c_{3z}, and m_3 with minor contribution from the other degrees of freedom.

Table 9.12 Medians (Med) and inter-quartile ranges (IQR) of ratios between the resonance frequency and magnitude at resonance of the vertical apparent mass obtained using the optimised model parameters (initial) and the resonance frequencies and magnitude at resonance obtained by changing the model parameters by ±40%.

		Feet hanging				Average thigh contact			
		Frequency		Magnitude		Frequency		Magnitude	
		-40% / initial	+40% / initial	-40% / initial	+40% / initial	-40% / initial	+40% / initial	-40% / initial	+40% / initial
	Med.	1.00	1.00	1.00	1.01	1.00	1.00	1.00	1.01
k_{1x}	IQR	0.00	0.00	0.01	0.02	0.00	0.00	0.01	0.01
	Med.	1.00	1.00	1.00	1.00	1.00	1.00	0.99	1.00
c_{1x}	IQR	0.00	0.00	0.01	0.01	0.00	0.00	0.01	0.00
	Med.	1.00	1.00	1.01	0.99	1.00	1.00	1.01	0.98
k_2	IQR	0.00	0.00	0.01	0.01	0.00	0.00	0.02	0.01
	Med.	1.00	1.00	1.00	1.00	1.00	1.00	1.00	1.00
c_2	IQR	0.08	0.00	0.01	0.00	0.08	0.00	0.01	0.05
	Med.	0.76	1.23	0.87	1.11	0.75	1.25	0.9	1.09
k_{3z}	IQR	0.06	0.06	0.03	0.04	0.03	0.01	0.06	0.02
	Med.	1.07	0.93	1.36	0.85	1.08	0.97	1.31	0.87
c_{3z}	IQR	0.02	0.07	0.16	0.04	0.04	0.08	0.16	0.03
	Med.	1.00	1.00	0.92	1.08	1.00	1.00	0.89	1.11
m_2	IQR	0.00	0.00	0.04	0.05	0.08	0.00	0.06	0.07
	Med.	1.23	0.86	0.62	1.39	1.26	0.90	0.65	1.34
m_3	IQR	0.07	0.05	0.07	0.16	0.05	0.10	0.10	0.16

9.3.2.3.2 Fore-and-aft cross-axis apparent mass

The changes in the resonance frequencies and the magnitude at resonance of the fore-and-aft cross-axis apparent mass with a change of ±40% in the optimised parameters are shown in Appendix F for all subjects. Using the results shown in Appendix F, statistical analysis was conducted to identify the parameters contributing to the resonance behaviour in the fore-and-aft cross-axis apparent mass. Table 9.13 shows statistically significant differences between the resonance frequencies calculated from the optimised parameters and the resonance frequencies calculated after changing the value of k_{1x}, k_{3z}, c_{3z}, or m_3 by ±40% of the optimised value. No significant effect on the resonance frequency was found when changing the value of k_2, c_2, or m_2. The magnitude of the fore-and-aft cross-axis apparent mass at resonance was affected by the change in any parameter (Table 9.13). However, the magnitude of the change in the resonance frequency and the magnitude at resonance must also be investigated.

Table 9.13 Cases of statistically significant differences (SD) between the resonance frequency (f) and magnitude at resonance of the cross-axis apparent mass (m) obtained using the optimised model parameters (initial) and the resonance frequencies and magnitude at resonance obtained by changing the model parameters by ±40%. H: feet hanging, Av: average thigh contact, s: significant, -: not significant; N/A: not applicable.

Parameter	Posture	Resonance frequency, f		Magnitude at resonance, m		No. of SD (Out of 4)	Total No. of SD (Out of 8)
		Initial / -40%	Initial / +40%	Initial / -40%	Initial / +40%		
k_{1x}	H	s	s	s	s	f: 4	f: 5, m: 8
	Av	s	s	s	s	m: 4	
c_{1x}	H	-	-	s	s	f: 1	
	Av	s	-	s	s	m: 4	
k_2	H	-	-	s	s	f: 0	f: 0, m: 8
	Av	-	-	s	s	m: 4	
c_2	H	-	-	s	s	f: 0	
	Av	-	-	s	s	m: 4	
k_{3z}	H	s	s	-	s	f: 3	f: 6, m: 6
	Av	s	-	-	s	m: 2	
c_{3z}	H	s	-	s	s	f: 3	
	Av	s	s	s	s	m: 4	
m_2	H	-	-	s	s	f: 0	N/A
	Av	-	-	s	s	m: 4	
m_3	H	s	s	s	s	f: 4	N/A
	Av	s	s	s	s	m: 4	

The ratios between the cross-axis apparent mass resonance frequencies and magnitudes of cross-axis apparent mass at resonance obtained after the ±40% change in each optimised parameter and the initial resonance frequencies and initial magnitudes of the cross-axis apparent mass at resonance obtained using the optimised parameters were

calculated for each subject. Table 9.14 shows the median and inter-quartile ranges for the calculated ratios. It can be seen from the table that changes in the resonance frequencies of the cross-axis apparent mass occurred with the change in k_{1x} k_{3z}, and m_3. All parameters showed some effect on the magnitude of the cross-axis apparent mass at resonance although the extent of this effect differed between the parameters: major effect came from changing the parameters of the horizontal degree-of-freedom beneath mass 1 and the vertical degree-of-freedom beneath mass 3.

Table 9.14 Medians (Med) and inter-quartile ranges (IQR) of ratios between the resonance frequency and magnitude at resonance of the fore-and-aft cross-axis apparent mass obtained using the optimised model parameters (initial) and the resonance frequencies and magnitude at resonance obtained by changing the model parameters by ±40%.

		Feet hanging				Average thigh contact			
		Frequency		Magnitude		Frequency		Magnitude	
		-40% / initial	+40% / initial	-40% / initial	+40% / initial	-40% / initial	+40% / initial	-40% / initial	+40% / initial
k_{1x}	Med.	0.90	1.09	0.61	1.24	0.81	1.10	0.59	1.46
	IQR	0.14	0.05	0.09	0.17	0.28	0.03	0.20	0.42
c_{1x}	Med.	1.00	1.00	1.47	0.81	1.00	1.00	1.41	0.87
	IQR	0.02	0.09	0.06	0.04	0.09	0.10	0.07	0.07
k_2	Med.	1.00	1.00	0.93	1.06	1.00	1.00	0.94	1.06
	IQR	0.00	0.00	0.05	0.08	0.00	0.02	0.05	0.05
c_2	Med.	1.00	1.00	1.09	0.92	1.00	1.00	1.16	0.90
	IQR	0.00	0.00	0.10	0.07	0.09	0.00	0.21	0.12
k_{3z}	Med.	0.90	1.09	0.98	0.80	0.87	1.00	1.11	0.85
	IQR	0.08	0.08	0.15	0.12	0.07	0.15	0.32	0.15
c_{3z}	Med.	1.07	1.00	1.33	0.82	1.09	0.92	1.31	0.87
	IQR	0.08	0.02	0.27	0.07	0.09	0.09	0.34	0.13
m_2	Med.	1.00	1.00	0.74	1.13	1.00	1.00	0.82	1.06
	IQR	0.02	0.00	0.08	0.07	0.00	0.02	0.05	0.05
m_3	Med.	1.26	0.86	0.38	1.82	1.38	0.83	0.41	1.71
	IQR	0.09	0.06	0.10	0.38	0.19	0.05	0.11	0.24

9.4 MODELLING THE FORE-AND-AFT APPARENT MASS AND THE VERTICAL CROSS AXIS APPARENT MASS DURING FORE-AND-AFT VIBRATION

In this section, a model to quantify the fore-and-aft apparent mass and the vertical cross-axis apparent mass measured on the seat during fore-and-aft vibration is proposed. The development of this model started by using Model 4 and Model 5, which were developed for vertical vibration, to predict the fore-and-aft apparent mass and the vertical cross-axis apparent mass obtained experimentally during fore-and-aft excitation. Neither Model 4 nor Model 5 responses were in good agreement with the experimental data, especially in the vertical cross-axis phase. Other alternative models were tried and the best fit was obtained when the vertical degree-of-freedom of mass 3 was replaced by a vertical degree-of-freedom at the base. The proposed model, hence, is a three degree-of-freedom model with rotational capability and with vertical and fore-and-aft degrees of freedom (Model 6, Figure 9.29). Model 6 was also used to predict the vertical apparent mass and the fore-and-aft cross-axis apparent mass during vertical excitation. The prediction was not in good agreement, especially the phase, with the measured responses. The vertical degree-of-freedom beneath mass 1 in Model 6 was not sufficient to predict the responses during vertical excitation: mass 3 and the vertical spring and damper beneath it (shown in Model 5) were needed to predict the responses during vertical excitation.

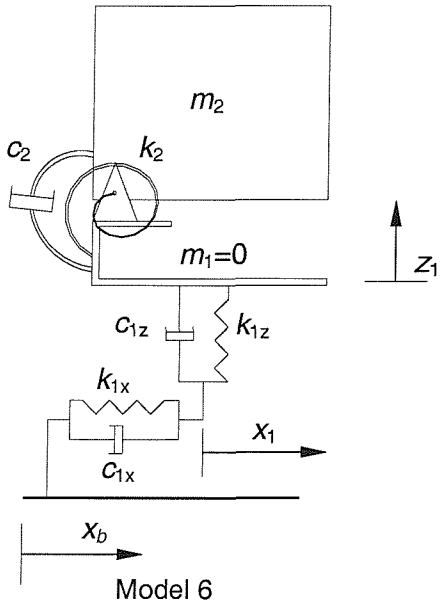

Figure 9.29 Proposed model to predict the fore-and-aft apparent mass and the vertical cross-axis apparent mass during fore-and-aft excitation.

The error function and the optimisation method were the same as those used for vertical vibration models. The results obtained for the individual data are shown in Figures 9.30 to Figure 9.33 for the feet hanging posture and in Figures 9.34 to Figure 9.37 for the average thigh contact posture.

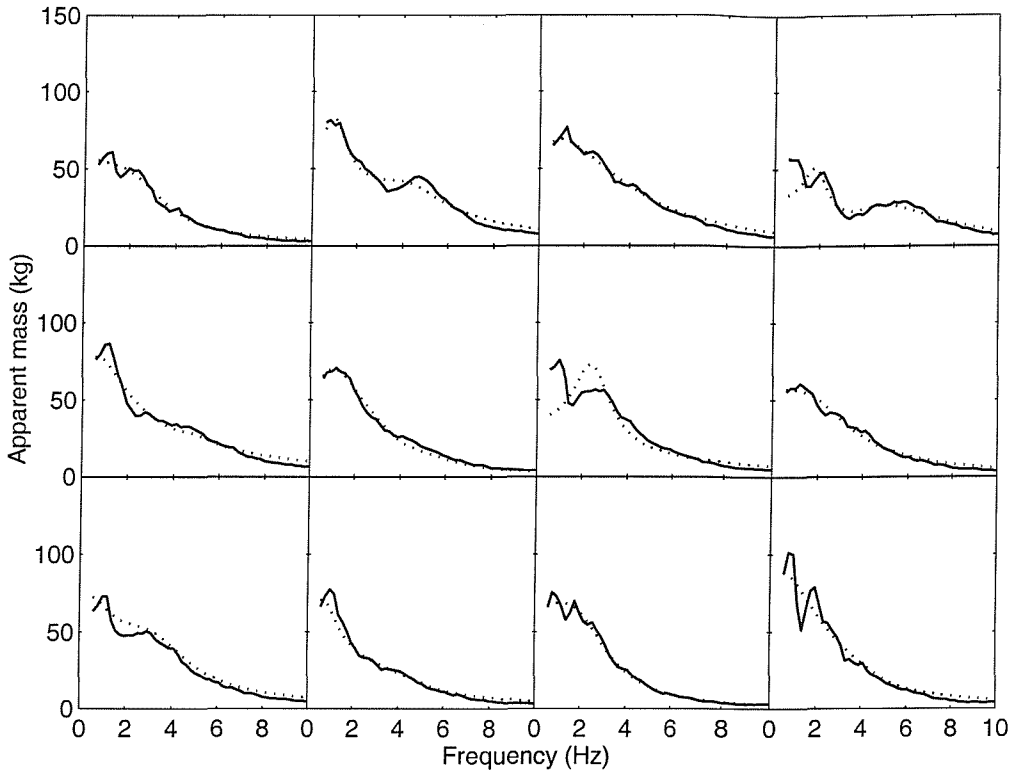

Figure 9.30 Fore-and-aft apparent masses of 12 subjects calculated from Model 6 and obtained from the experiment in the feet hanging posture: ———, experiment; ·····, model.

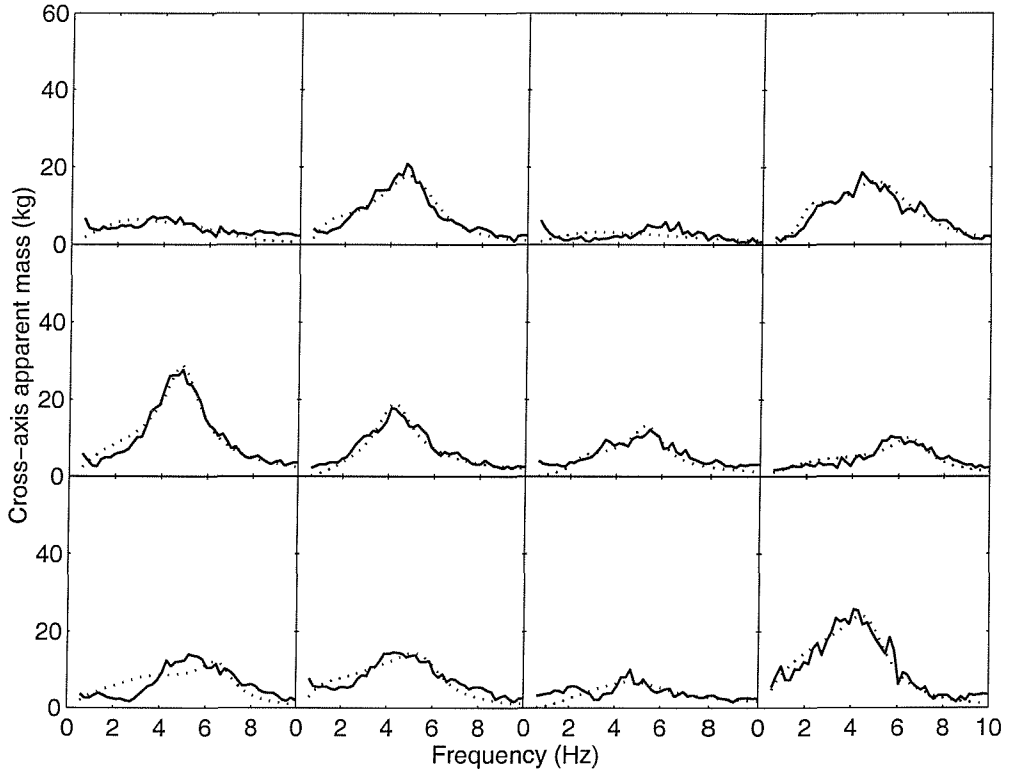

Figure 9.31 Vertical cross-axis apparent masses of 12 subjects calculated from Model 6 and obtained from the experiment in the feet hanging posture: ———, experiment; ·····, model.

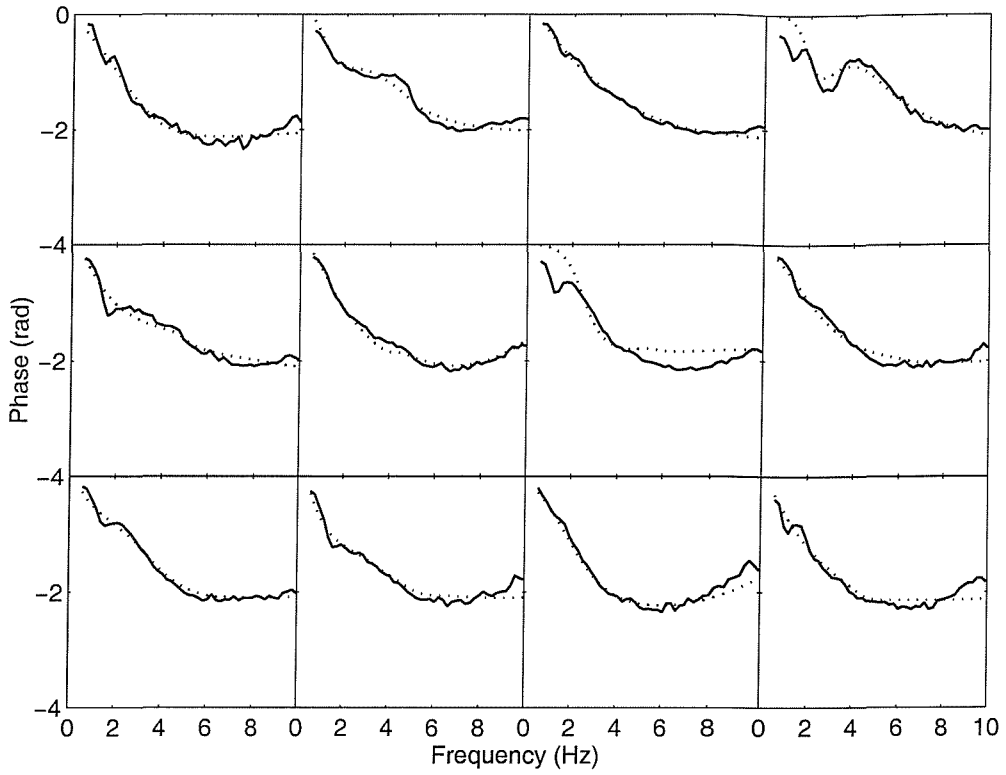

Figure 9.32 Fore-and-aft apparent masses phase of 12 subjects calculated from Model 6 and obtained from the experiment in the feet hanging posture: ———, experiment; ·····, model.

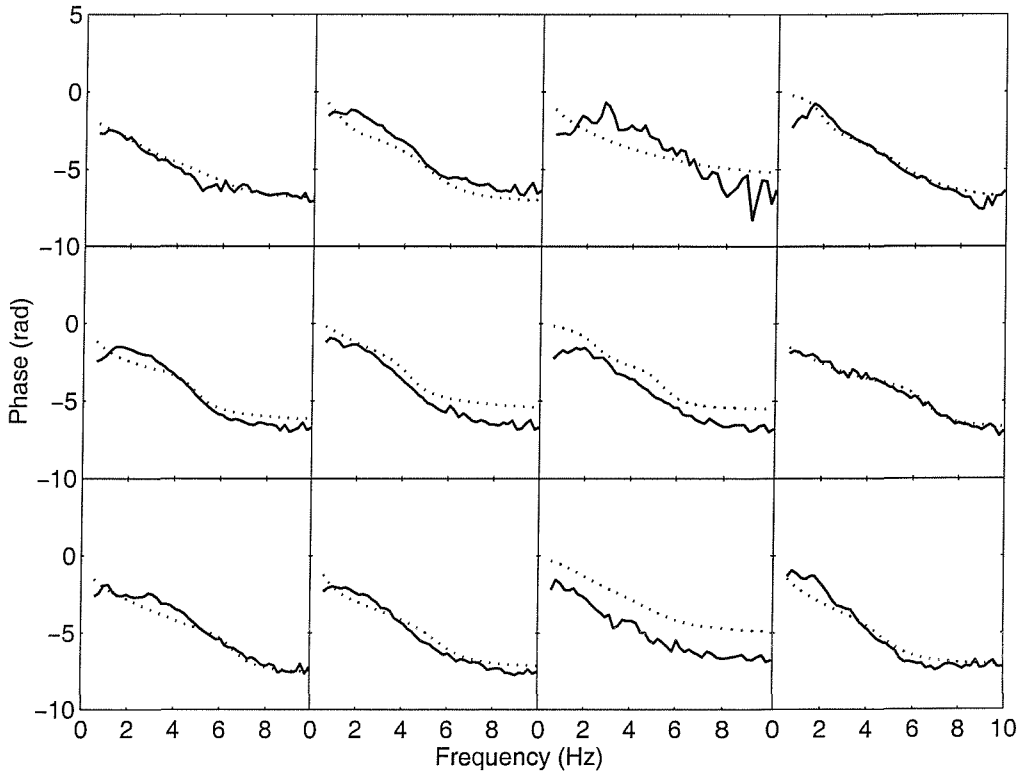

Figure 9.33 Vertical cross-axis apparent masses phase of 12 subjects calculated from Model 6 and obtained from the experiment in the feet hanging posture: ———, experiment; ·····, model.

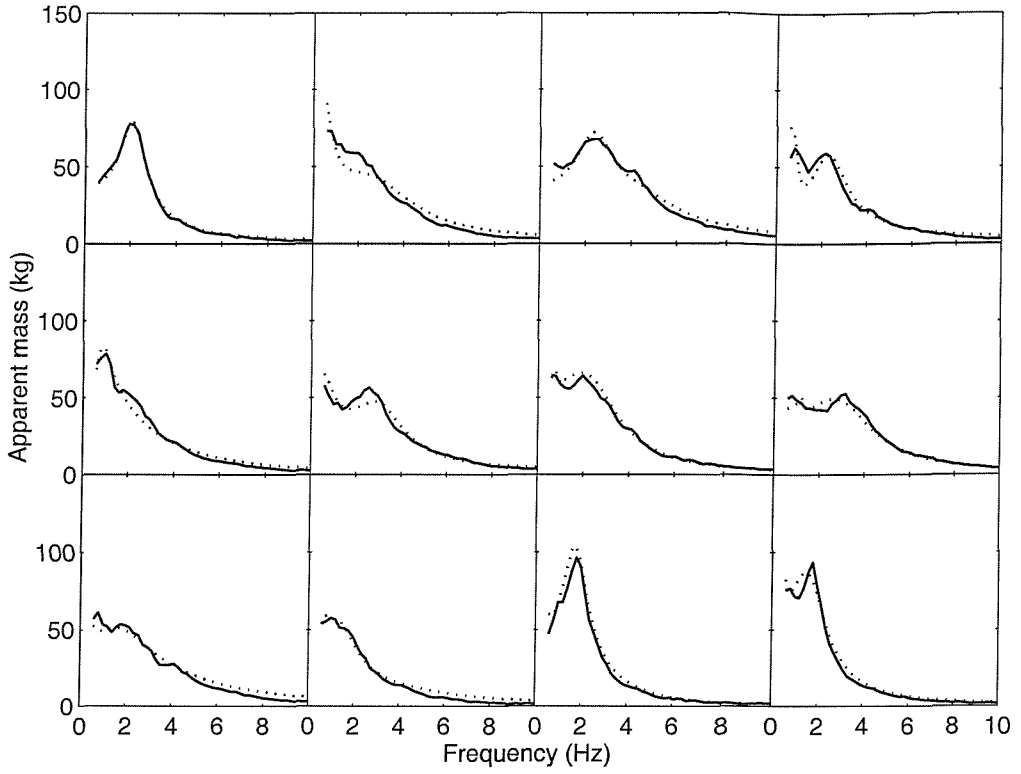

Figure 9.34 Fore-and-aft apparent masses of 12 subjects calculated from Model 6 and obtained from the experiment in the average thigh contact posture: ———, experiment; ·····, model.

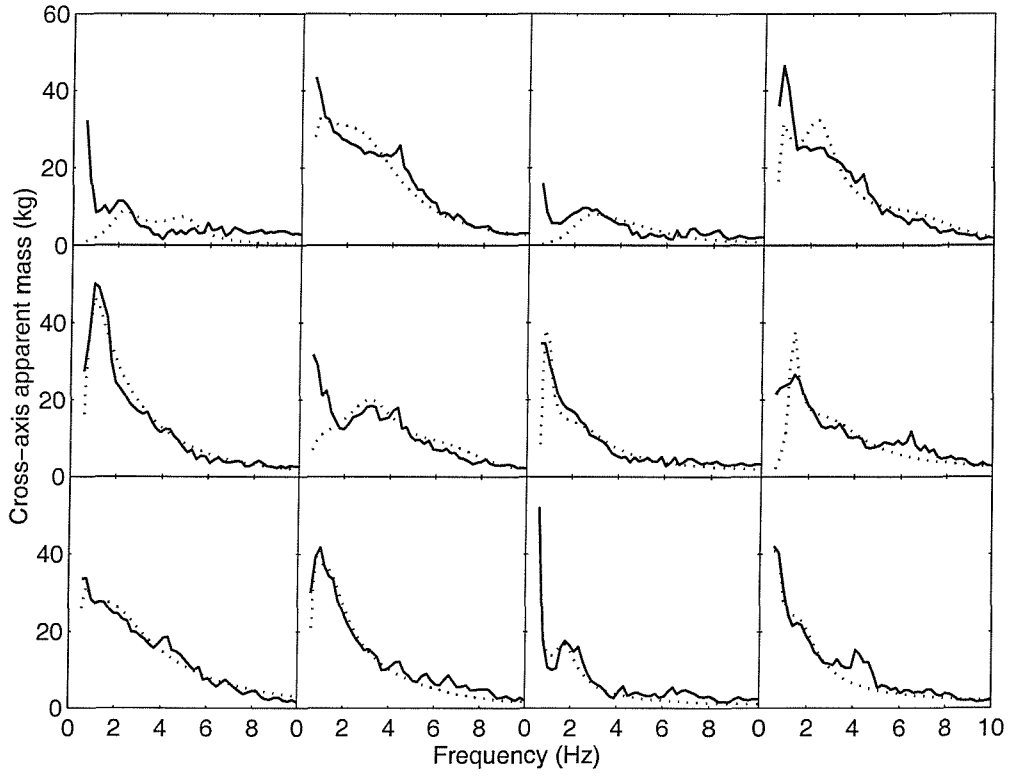

Figure 9.35 Vertical cross-axis apparent masses of 12 subjects calculated from Model 6 and obtained from the experiment in the average thigh contact posture: ———, experiment; ·····, model.

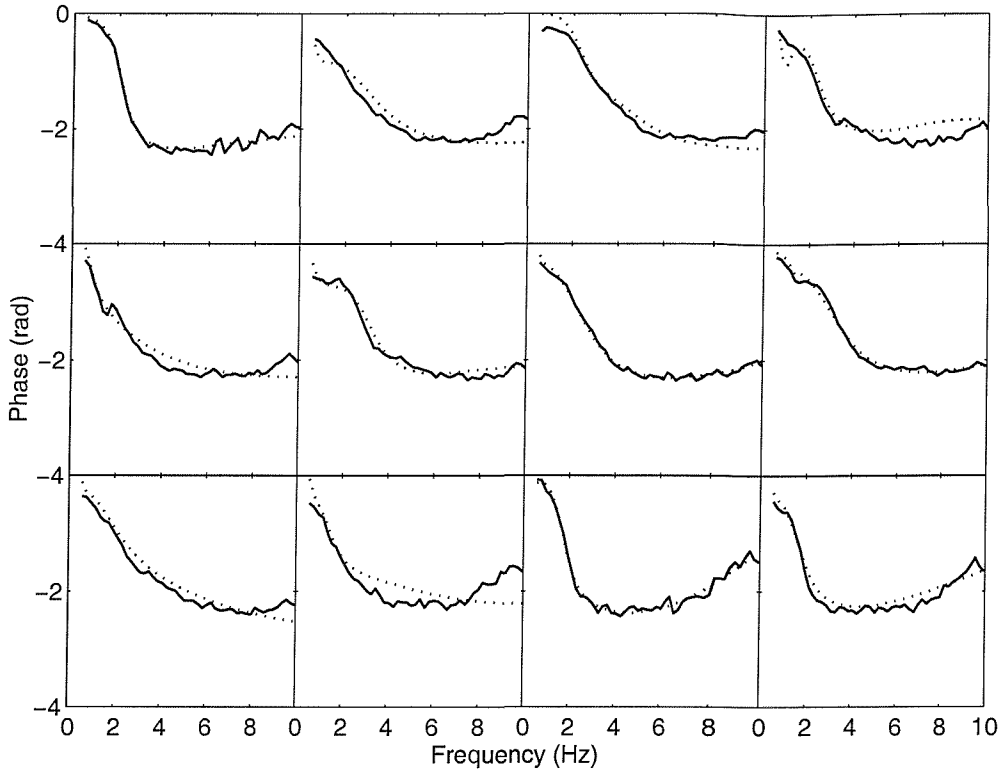

Figure 9.36 Fore-and-aft apparent masses phase of 12 subjects calculated from Model 6 and obtained from the experiment in the average thigh contact posture: ———, experiment; ·····, model.

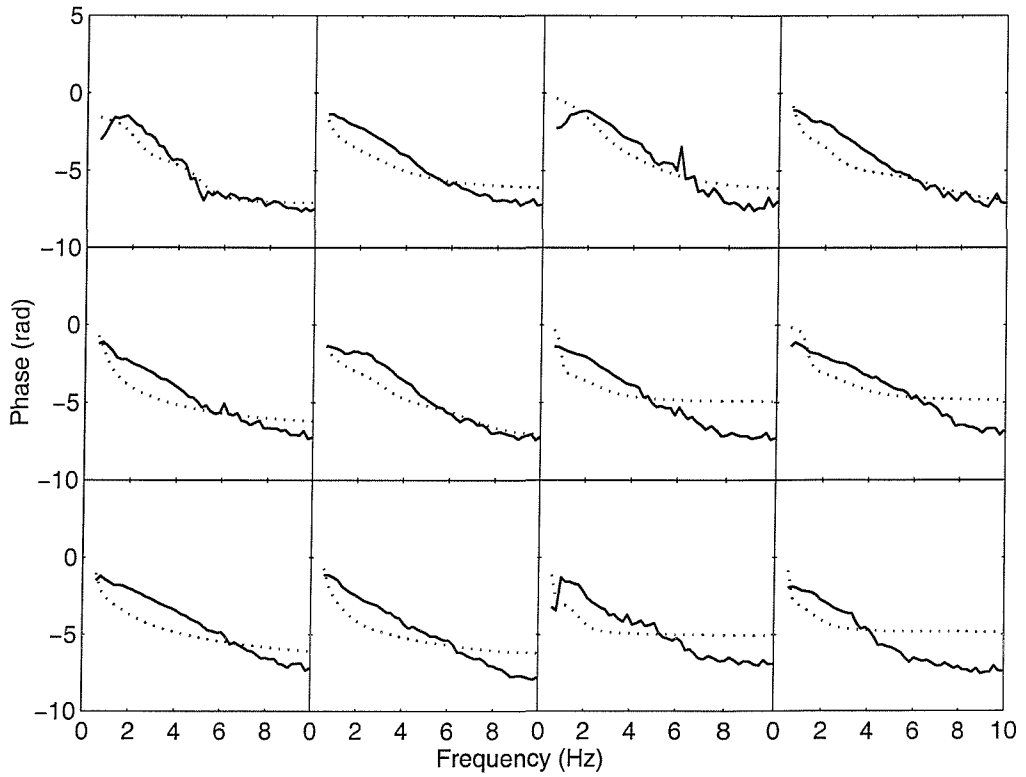

Figure 9.37 Vertical cross-axis apparent masses phase of 12 subjects calculated from Model 6 and obtained from the experiment in the average thigh contact posture: ———, experiment; ·····, model.

As can be seen from the figures, high subject variability was evident in the fore-and-aft apparent mass and the vertical cross-axis apparent mass in both the feet hanging posture and the average thigh contact posture. The figures also show that the fitting obtained with the feet hanging posture is better than that obtained in the average thigh contact posture, especially for the cross-axis apparent mass magnitude and phase at low frequencies. The high vertical cross-axis apparent mass found experimentally at low frequencies in the average thigh contact posture was attributed to the subjects trying to stabilise their body by exerting greater force on the footrest when moving forward and greater force on the seat when moving backward. Some subjects also reported difficulty in preventing themselves from sliding on the seat when the body was less supported and said they needed to push down on the footrest and the seat to prevent sliding. The proposed model may therefore not be sufficient to account for such a force at low frequencies. The parameters obtained from the model are shown in Table 9.15 for the feet hanging posture and in Table 9.16 for the average thigh contact posture and described as follows:

m_1 and m_2 are the masses of mass 1 (equals to zero) and mass 2, respectively
J_2 is the moment of inertia of mass 2 about the connection point
k_{1z} and c_{1z} are the vertical stiffness and damping beneath mass 1
k_{1x} and c_{1x} are the fore-and-aft stiffness and damping beneath mass 1
k_2 and c_2 are the rotational stiffness and damping of mass 2
e is the distance between the centre of gravity of mass 2 and the connection point
α is the angle that e has with the horizontal when the model is in equilibrium

Table 9.15 Parameters obtained from Model 6 in the feet hanging posture.

Subject	m_2 (kg)	J_2 (kgm^2)	k_{1x} (N/m)	k_2 (Nm)	k_{1z} (N/m)	c_{1x} (Ns/m)	c_2 (Nsm)	c_{1z} (Ns/m)	e (m)	α (rad)
1	56	6.29	9635	0	76063	192	49	1055	0.27	1.46
2	64	0.29	25371	14	69310	400	2	847	0.05	1.43
3	60	24.11	27726	993	937	277	333	4291	0.55	1.51
4	31	0.45	22809	74	33740	252	3.8	614	0.09	1.26
5	67	31.22	53790	982	64721	91	348	605	0.68	1.45
6	56	37.20	2928	16865	42041	747	139	470	0.77	1.41
7	38	0.76	72762	194	43711	97381	8	311	0.14	1.50
8	53	36.25	18500	582	90809	239	495	486	0.77	1.49
9	65	13.20	17773	218	111619	308	110	533	0.35	1.46
10	57	17.31	12871	425	72117	194	132	618	0.48	1.43
11	67	30.28	0	8454	69269	929	77	1339	0.65	1.51
12	76	43.51	15295	755	72436	232	390	727	0.66	1.38

Table 9.16 Parameters obtained from Model 6 in the average thigh contact posture.

Subject	m_2 (kg)	J_2 (kgm^2)	k_{1x} (N/m)	k_2 (Nm)	k_{1z} (N/m)	c_{1x} (Ns/m)	c_2 (Nsm)	c_{1z} (Ns/m)	e (m)	α (rad)
1	36	2.68	6802	40	34703	137	78	210	0.20	1.14
2	72	1.40	15814	21	2171	183	5	1155	0.13	1.04
3	39	1.69	20357	458	861	217	25	1036	0.14	1.26
4	53	0.74	7555	17	71020	265	2	663	0.09	0.93
5	53	30.08	13145	1173	1328	124	57	405	0.72	0.77
6	54	24.35	10891	437	96966	201	131	889	0.52	1.24
7	60	3.20	0	282	2203	1156	0	90	0.23	0.63
8	42	3.40	102	549	3632	1295	0	143	0.28	0.69
9	41	25.38	20364	667	826	38	0	218	0.77	0.51
10	41	2.96	11080	94	945	115	0	224	0.26	0.60
11	49	0.90	8596	1535	914	799	0	40	0.79	0.50
12	71	0.83	0	38	1559	1260	0	115	0.11	0.67

9.5 GENERAL REMARKS AND CONCLUSIONS

Previous studies have shown that the vertical apparent mass could be reasonably modelled by two degree-of-freedom lumped parameter models with the masses of the model moving only in the vertical direction (e.g. Wei and Griffin, 1998). Other studies used models with more than two degrees-of-freedom with the masses of the model moving only in the vertical direction (e.g. Payne and Band, 1971; Mertens and Vogt, 1978). The models investigated in this chapter showed that the vertical apparent mass obtained experimentally could also be obtained theoretically by using lumped parameter two degrees-of-freedom models with vertical and rotational motions as opposed to motion only in the vertical direction. However, the position of each degree-of-freedom in the model is important to obtain an agreement between the experimental and theoretical results, as has been shown by Model 1 and Model 2 (see Figure 9.18 and Figure 9.19). This chapter also showed that a two degree-of-freedom model consisting of a rotational degree-of-freedom and a fore-and-aft degree-of-freedom would be sufficient to reproduce the vertical apparent mass obtained experimentally with vertical excitation, as has been shown by the response of Model 3 (Figure 9.18 and Figure 9.19).

Despite the agreement between the apparent mass obtained from Model 2 and Model 3 and the apparent mass obtained experimentally, neither the cross-axis apparent mass obtained from Model 2 nor the cross-axis apparent mass obtained from Model 3 were in agreement with the cross-axis apparent mass measured experimentally, especially with

the phase response. The combination of the degrees-of-freedom of Model 2 and Model 3 (to produce Model 4) was needed to obtain good agreement between the apparent mass obtained theoretically and experimentally and between the cross-axis apparent mass obtained theoretically and experimentally, as seen in Model 4 and Model 5. Model 4 and Model 5 suggest that the human body undergoes a fore-and-aft movement on the seat when exposed to vertical excitation, which may indicate shear deformation of the tissue of the ischial tuberosities. This conclusion is consistent with the conclusion of Broman *et al.* (1996) who modelled the transmissibility to L3 using vertical, horizontal and rotational sub-systems and concluded that all vertical, rotational and horizontal sub-systems ('that allows the subject to slide on the seat') were needed to produce the experimentally measured transmissibility to L3. Using a finite element model of the human body, Kitazaki and Griffin (1997) also referred to shear deformation of the tissues of the buttocks at the principal resonance frequency. They reported that 'a principal resonance of the human body at about 5 Hz consisted of an entire body mode, in which the skeleton moved vertically due to axial and shear deformations of buttocks tissue, in phase with a vertical visceral mode, and a bending mode of the upper thoracic and cervical spine'.

Although the models investigated in this chapter were not intended to be mechanistic models, the masses m_2 and m_3 seem convincingly similar to the masses of the pelvis (and the part of the legs supported on the seat) and the upper body without the pelvis, respectively, bearing in mind the simplicity of the model. This is clearer in the masses obtained for the average thigh contact posture than in the feet hanging posture. In the feet hanging posture there was more variability in the individual parameters than in the average thigh contact posture, as was shown in Section 9.3.2.2. The values of the moment of inertia (except for subject 12), and the geometrical parameters of mass 2 with respect to a reference located at the ischial tuberosities seem also to be similar to those of the pelvis, given the simplicity and the assumptions made when deriving the equations of the model. For example, in the model, the springs and dampers used were assumed to be linear and the parameters were assumed to be independent of time and frequency while this might not be true. Moreover, when deriving the equations of motion, the effect of gravity was not taken into account. This means that, since the models are linear models, the effect of gravity will be included in the value given by the rotational stiffness, as both the stiffness term and the gravity term in the equations of motion are proportional to the rotational displacement, θ, for linear models. It was also assumed that the centre of gravity of mass 2 and the centre of gravity of mass 3 have the same fore-and-aft distance from the connection point, while this might not be necessarily the case, if mass 2 and mass 3 were the pelvis and the upper body and the connection point was the ischial tuberosities.

The vibration modes needed in Model 5 to reproduce the experimental data in this thesis are similar to modes suggested in previous studies. Hagena *et al.* (1985) measured the transmissibility between a vibrating seat and the spine, and between the sacrum and the spine and reported that the principal resonance frequency measured at 4 to 5 Hz corresponded to motion of the entire upper body. If mass 2 and mass 3 in Model 5 were considered to represent the pelvis and the upper body respectively, then the conclusion of Hagena *et al.* is in agreement with the results obtained from Model 5, where mass 3 and the vertical degree-of-freedom beneath it were the main contributors to the principal resonance frequency at about 5 Hz. Matsumoto and Griffin (2001) modelled the apparent mass and vertical and fore-and-aft transmissibilities to different locations on the spine using models with rotational capabilities (see Section 2.7.2.2) and concluded that the resonance frequency at around 5 Hz was 'attributed to a vibration mode consisting of vertical motion of the pelvis and legs and a pitch motion of the pelvis, both of which cause vertical motion of the upper-body above the pelvis, a bending motion of the spine and vertical motion of the viscera'. However, a parameter sensitivity test showed that axial deformation of tissue beneath the legs and pelvis (not included in Model 5 of this study) was the main contributor to the resonance frequency of the apparent mass, with some contribution from the vertical motion of the viscera, while the pitch degree-of-freedom made little contribution to the resonance frequency. A parameter sensitivity test for Model 5 in this thesis showed that the pitch motion of mass 2 made little contribution to the principal resonance frequency of the apparent mass at 5 Hz. However, based on the observations of Matsumoto and Griffin, one would not rule out that pitch or fore-and-aft motion of the pelvis (i.e. mass 2) of Model 5 in this thesis contributed to the resonance frequency of the apparent mass.

A parameter sensitivity test for Model 5 showed that the resonance of both the vertical apparent mass and the fore-and-aft cross-axis apparent mass were affected when changing the parameters of the vertical degree-of-freedom in Model 5. This is consistent with the experimental results (Chapter 4) where the resonance of the vertical apparent mass and the fore-and-aft cross-axis apparent mass were found to be correlated. However, it is possible that no common mode will be found between the vertical apparent mass and the fore-and-aft cross-axis apparent mass if the data in Chapter 8 are considered, as the resonances of the vertical apparent mass and the fore-and-aft cross-axis apparent mass were not correlated. Figure 9.38 and Figure 9.39 show the vertical apparent mass and the cross-axis apparent mass obtained with the average thigh contact posture in Chapter 4 and with a seat angle of 0° in Chapter 8. In both experiments, the upper legs were horizontal. However, the lower legs were vertical and the feet were resting on a horizontal footrest in Chapter 4 while the lower legs were stretched and the

feet resting on an inclined footrest in Chapter 8. This could have produced the difference between the responses shown in Figure 9.38 and 9.39 as was explained in Chapter 8 (see also Section 10.5). Based on the differences seen in the figures, it is expected that the parameters of the model, and possibly the vibration modes needed in the model, would change with a change in the position of the lower legs.

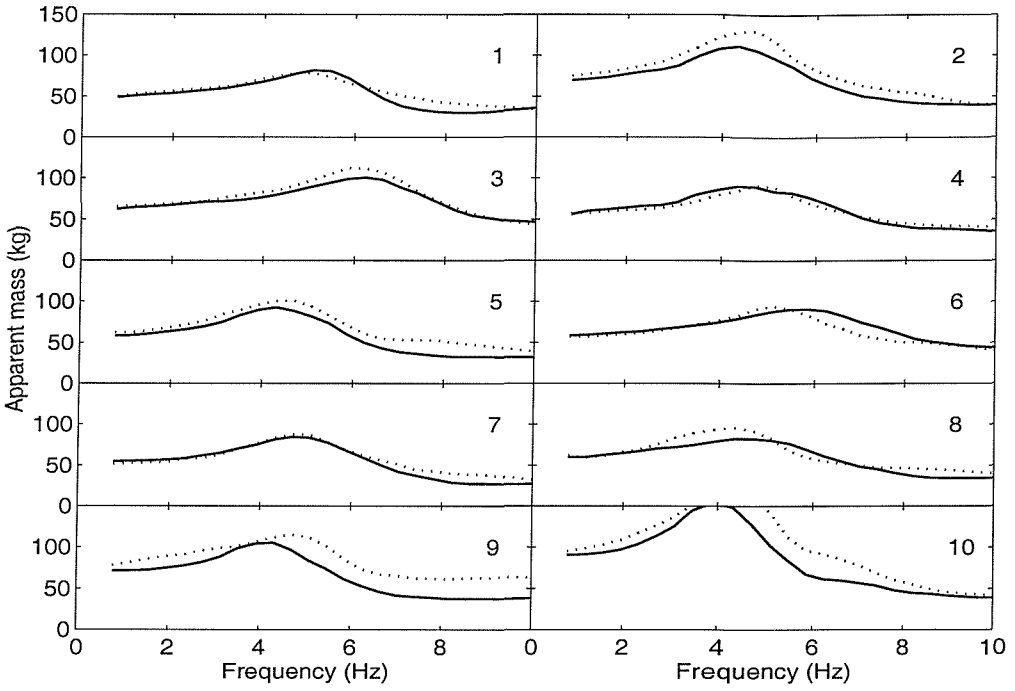

Figure 9.38 Apparent masses of 10 seated subjects measured at 1.25 ms^{-2} r.m.s. ———, with average thigh contact posture (Chapter 4); ·····, with seat angle of 0° (Chapter 8).

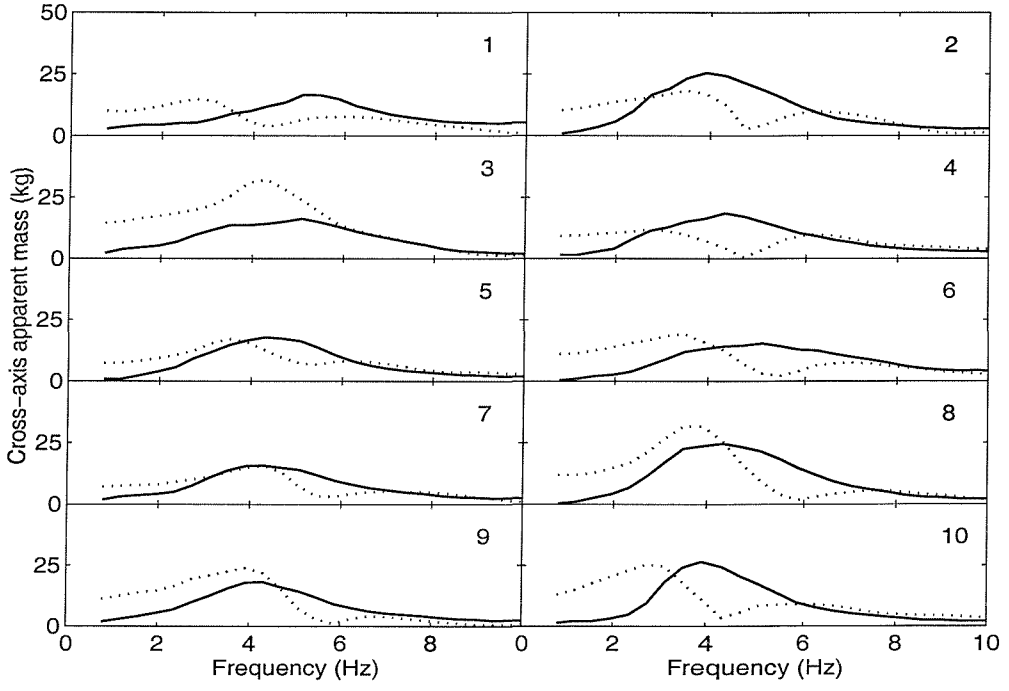

Figure 9.39 Cross-axis apparent masses of 10 seated subjects measured at 1.25 ms^{-2} r.m.s.. ———, with average thigh contact posture (Chapter 4); ·····, with seat angle of 0° (Chapter 8).

CHAPTER 10 GENERAL DISCUSSION

10.1 INTRODUCTION

In each of the previous chapters, a discussion section was used to explain the findings in each chapter and to compare the results obtained in this thesis with those reported in previous studies. This chapter presents a summary of the main findings from each chapter as well as a general discussion on the use of linear methods to analyse the responses of humans to vibration. This chapter also discusses the possibility of using the inequality between the vertical cross-axis forces and the fore-and-aft cross-axis forces as an indication of the non-linearity of the human body at a specific vibration magnitude. A comparison between the findings obtained in Chapter 4 and Chapter 8 will also be discussed.

10.2 SUMMARY OF THE MAIN FINDINGS

During vertical excitation, the vertical apparent mass on the seat showed a resonance in the vicinity of 5 Hz, which is consistent with findings in previous studies. The fore-and-aft cross-axis apparent masses on the seat and at the backrest were as high as 60% of the static masses of the subjects at some frequencies. The vertical apparent mass at the backrest and the lateral cross-axis apparent masses on both the seat and backrest were small compared to those measured in the vertical and fore-and-aft directions on the seat and in the fore-and-aft direction at the backrest. The apparent mass at the feet showed three vibration modes: around 5, 7.5 and 11 Hz. In all directions, the responses in all directions were non-linear: the resonance frequencies decreased with increasing the vibration magnitude.

During fore-and-aft excitation, the fore-and-aft apparent mass on the seat suggested three vibration modes when no backrest was used: around 1 Hz, between 1 and 3 Hz, and between 3 Hz and 5 Hz. When a backrest was used, only two modes were evident when the feet were not supported and only one mode when the feet were supported. The fore-and-aft apparent mass at the back suggested a main resonance between 3 and 5 Hz. The vertical cross-axis apparent masses on the seat reached as high as 70% of the static masses of the subjects and showed dependency on the height of the footrest. However, the vertical cross-axis apparent mass at the backrest and the lateral cross-axis apparent mass on the seat and backrest were very small compared to the vertical cross-axis apparent mass on the seat. The fore-and-aft apparent mass and the vertical cross-axis apparent mass at the feet were affected by the use of a backrest. The apparent

mass and cross-axis apparent mass on the seat, backrest and footrest were non-linear with vibration magnitude.

The effect of seat surface angle on the 'vertical apparent mass' and 'fore-and-aft cross-axis apparent mass' was studied with vertical excitation. The effect of seat surface angle was more pronounced in the 'fore-and-aft cross-axis apparent mass' than in the 'vertical apparent mass'. The 'fore-and-aft cross-axis apparent mass' increased with increasing seat surface angle. Increasing seat surface angle decreased the non-linearity in the 'fore-and-aft' direction, possibly due to an increase in the shear stiffness of the buttocks tissue.

The linear models developed in this thesis suggested that two degrees-of-freedom (rotational and vertical or rotational and fore-and-aft) were needed to predict the vertical apparent mass of seated subject while three degrees-of-freedom (rotational, vertical and fore-and-aft) were needed to predict the vertical apparent mass and the fore-and-aft cross-axis apparent mass simultaneously. The modelling suggested a fore-and-aft sliding motion (or possibly deformation of tissue in contact with the seat) of the human body on the seat when exposed to vertical excitation.

The cross-axis forces during vertical and fore-and-aft excitation indicate that the seated human body moves in two-dimensions when exposed to either vertical excitation or fore-and-aft excitation. The cross-axis forces were found to depend on several factors such as vibration frequency, vibration magnitude, sitting posture and seating condition (e.g. using a backrest or a footrest).

10.3 USE OF LINEAR TECHNIQUES (CROSS-SPECTRAL DENSITY METHOD)

Linear techniques, such as the cross-spectral density (CSD) method are frequently used to analyse biodynamic responses of the human body to vibration, even though observations suggest that the human body responds non-linearly. When using the CSD method, although a different response is found at different vibration magnitudes, there is generally high coherency between the input acceleration and the force measured in the same direction on the seat or at the backrest at any one magnitude. This has sometimes been assumed to imply that the body behaves approximately linearly at any specific vibration magnitude but differently at another magnitude: when the vibration magnitude changes, the human body might adjust to the new vibration magnitude (by postural change, muscular change or some other change), in which case the use of linear methods would be appropriate when analysing the response at one vibration magnitude.

However, a non-linear response when the body is exposed at only one vibration magnitude is also likely.

If the human body may behave non-linearly when exposed to a particular magnitude of vibration, it is of interest to compare the use of the cross-spectral density (CSD) method and the power spectral density (PSD) method for computing the apparent mass. For example, Figure 10.1 compares the fore-and-aft apparent mass of one subject measured on the seat and backrest at 0.25 ms^{-2} r.m.s. with the minimum thigh contact posture calculated using the CSD method and the PSD method (see Section 3.4.1). The figure also shows the vertical cross-axis apparent mass on the seat calculated using the CSD and PSD methods, as well as the coherency in the fore-and-aft direction and the vertical direction. In the fore-and-aft direction, the coherency was calculated after subtraction in the time domain the fore-and-aft force arising from the mass of the force plate (on the seat or the backrest) from the total measured fore-and-aft force. The coherency was high in all conditions in the fore-and-aft direction. In the vertical direction, the coherency was lower than that in the fore-and-aft direction and there were some differences between the results obtained using the CSD and PSD methods, consistent with a non-linearity in the body response (Figures 10.1 and 10.2).

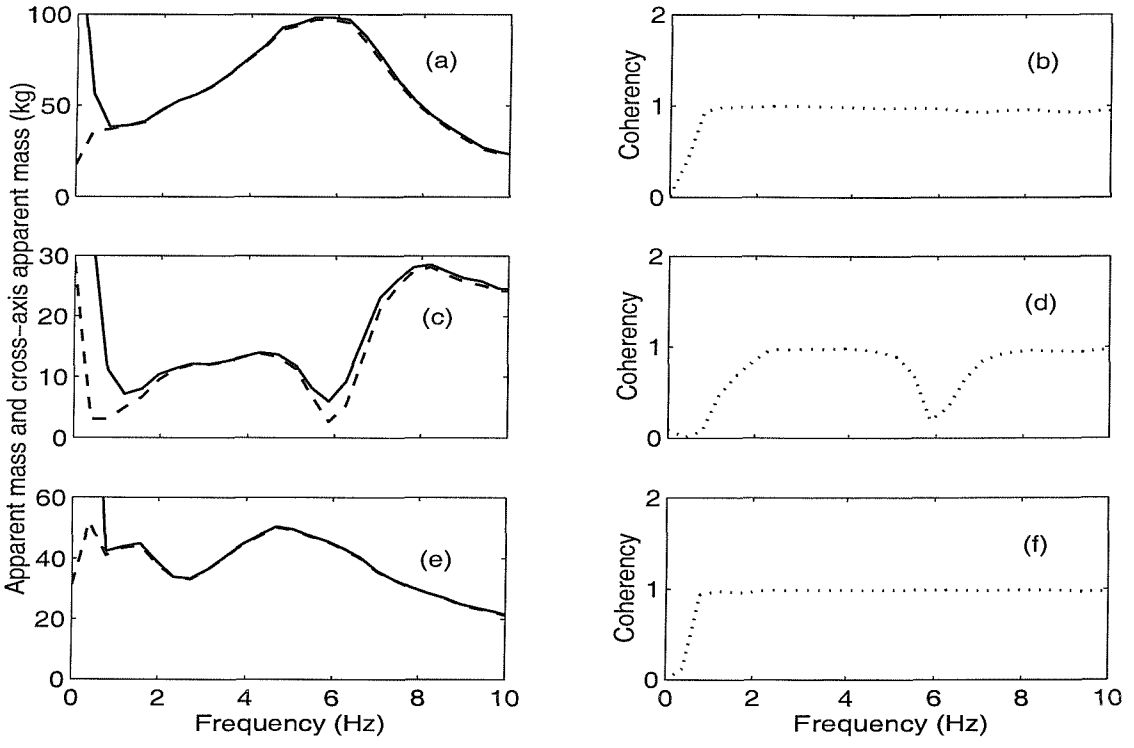

Figure 10.1 Fore-and-aft apparent masses, vertical cross-axis apparent mass, and coherences of one subject at 0.25 ms^{-2} r.m.s. with the minimum thigh contact posture. (a) and (b) fore-and-aft apparent mass on the seat, (c) and (d) vertical cross-axis apparent mass on the seat, (e) and (f) fore-and-aft apparent mass at the backrest. ———, PSD method; – – – –, CSD method; ·····, coherency.

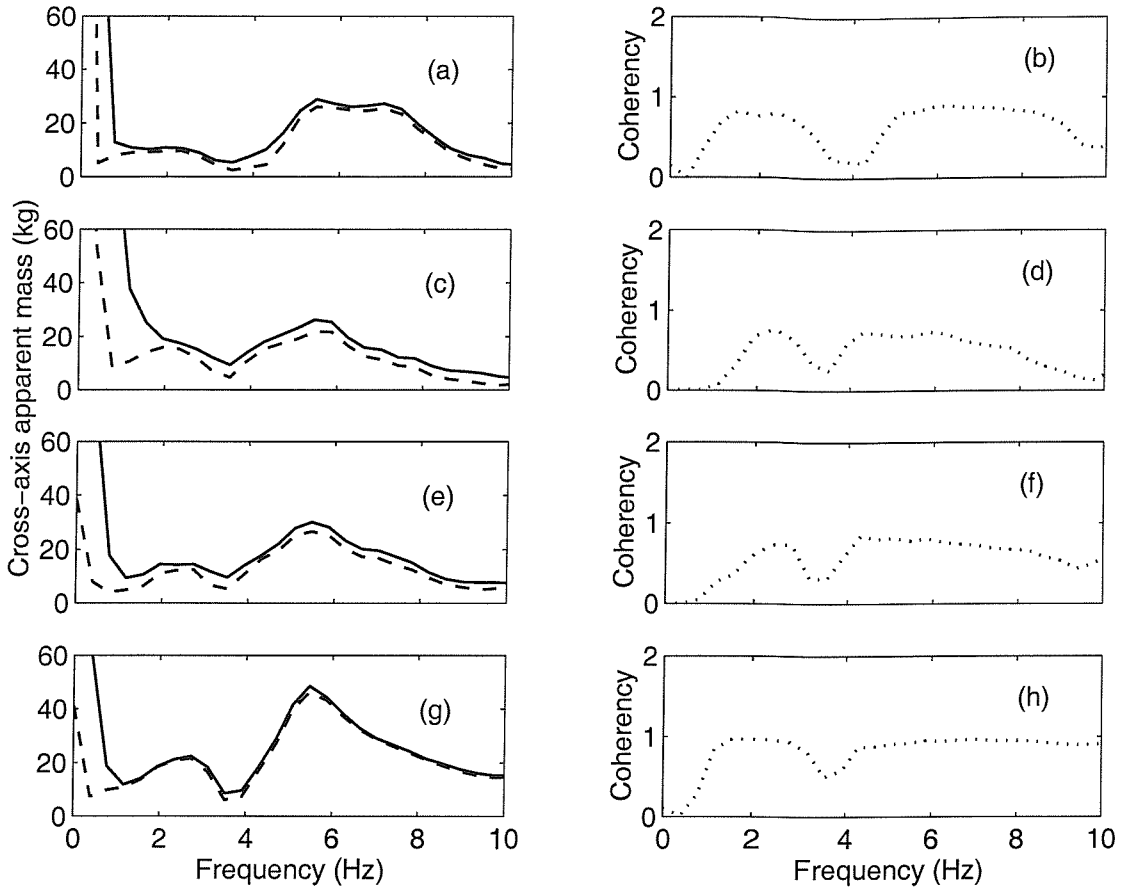

Figure 10.2 Vertical cross-axis apparent mass and coherences of one subject measured at 0.25 ms^{-2} r.m.s. with four different sitting postures. (a) and (b) feet hanging, (c) and (d) maximum thigh contact, (e) and (f) average thigh contact, (g) and (h) minimum thigh contact. ———, PSD method; – – – –, CSD method; ·····, coherency.

It may be seen that the CSD and PSD methods gave very similar results in the fore-and-aft direction (direction of vibration excitation). This suggests that, whether or not the body behaves linearly at the vibration magnitudes investigated, the use of linear techniques in this study has not produced misleading findings. In the vertical direction, the trends found with both methods, as well as the peaks and troughs, were similar, although there are some differences in the magnitudes of the vertical cross-axis apparent mass. This indicates the need for further investigation of the non-linearity, but the principal findings reported in this thesis from the use of linear methods appear relevant. This conclusion was tested for different subjects, different excitation magnitudes and directions and different postures and found to be consistent.

10.4 INVESTIGATING THE NON-LINEARITY OF THE HUMAN BODY USING THE PRINCIPLE OF RECIPROCITY AND THE CROSS-AXIS FORCES

10.4.1 Introduction

The non-linearity of the human body was indicated in this thesis, and in previous studies, as change in the resonance frequency of the body with a change in vibration magnitude. Some previous studies (see Section 2.3.1.2.1., Hinz and Seidel, 1987) used sinusoidal input excitation of a seat and obtained non-sinusoidal forces on the seat and non-sinusoidal acceleration on the body, indicating a non-linear system despite the high coherency always obtained at a specific vibration magnitude. In this section, an approach based on a property of a linear system (reciprocity) will be used to investigate the non-linearity of the human body at a specific vibration magnitude.

10.4.2 Principle of reciprocity

A linear dynamic system is shown in Figure 10.3 where a force f_1 applied to mass m_1 and a force f_2 applied to mass m_2 (The theory described in this section is obtained from Beards,1996).

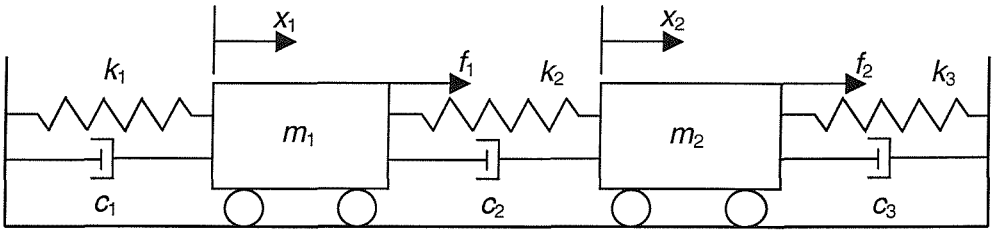

Figure 10.3 Two degree-of-freedom system with forced excitation (Beards, 1996).

For the undamped system, if $f_1 = F_1 \sin \omega t$ and f_2 is zero, the equations of motion can be written as:

$$m_1\ddot{x}_1 + (k_1 + k_2)x_1 - k_2x_2 = f_1 \qquad (10.1)$$

$$m_2\ddot{x}_2 + (k_2 + k_3)x_2 - k_2x_1 = 0 \qquad (10.2)$$

Assuming that $x_1 = X_1 \sin \omega t$ and $x_2 = X_2 \sin \omega t$ and substituting into the equations of motion we obtain:

$$(k_1 + k_2 - m_1\omega^2)X_1 + (-k_2)X_2 = F_1 \qquad (10.3)$$

and

$$(k_2 + k_3 - m_2\omega^2)X_2 + (-k_2)X_1 = 0 \tag{10.4}$$

Solving the two equations together for X_1/F_1 gives

$$\alpha_{11} = \frac{X_1}{F_1} = \frac{k_2 + k_3 - m_2\omega^2}{\Delta} \tag{10.5}$$

where

$$\Delta = (k_1 + k_2 - m_1\omega^2)(k_2 + k_3 - m_2\omega^2) - k_2^2 \tag{10.6}$$

The term α_{11} is called a direct receptance of the system. A cross receptance, α_{21}, can also be obtained by solving for X_2/F_1.

$$\alpha_{21} = \frac{X_2}{F_1} = \frac{k_2}{\Delta} \tag{10.7}$$

Two more receptances can be obtained for this system by applying a force $f_2 = F_2 \sin \omega t$ to the second body, m_2 and solve for α_{22} (i.e. X_2/F_2) and α_{12} (i.e. X_1/F_2). For a linear system the cross receptances are equal (i.e. $\alpha_{12} = \alpha_{21}$; Beards, 1996). This equality is referred to as the principle of reciprocity.

10.4.3 Applying the principle of reciprocity to Model 5 using the cross-axis apparent mass

Model 5 developed in Chapter 9 is a linear model and, hence, the principle of reciprocity is expected to apply to Model 5. This was tested using the fore-and-aft cross-axis apparent mass measured during vertical excitation and the vertical cross-axis apparent mass measured during fore-and-aft excitation. The optimised parameters for subject 11 using Model 5 (using the vertical apparent mass and the cross-axis apparent mass as described in Chapter 9) were used to calculate the vertical cross-axis apparent mass produced if Model 5 was exposed to fore-and-aft excitation. The fore-and-aft cross-axis apparent mass obtained from the model was then compared with the vertical cross-axis apparent mass calculated from the model. For a linear model, the two cross-axis apparent masses are equal at all frequencies, which is true for Model 5, as shown in Figure 10.4. The measured cross-axis apparent mass may then be used to identify if the human body is a linear or a non-linear system: if the measured vertical cross-axis apparent mass is different from the measured fore-and-aft cross-axis apparent mass then the system is non-linear. However, if the measured vertical cross-axis apparent mass is equal to the measured fore-and-aft cross-axis apparent mass, no conclusion can be drawn about the non-linearity of the system.

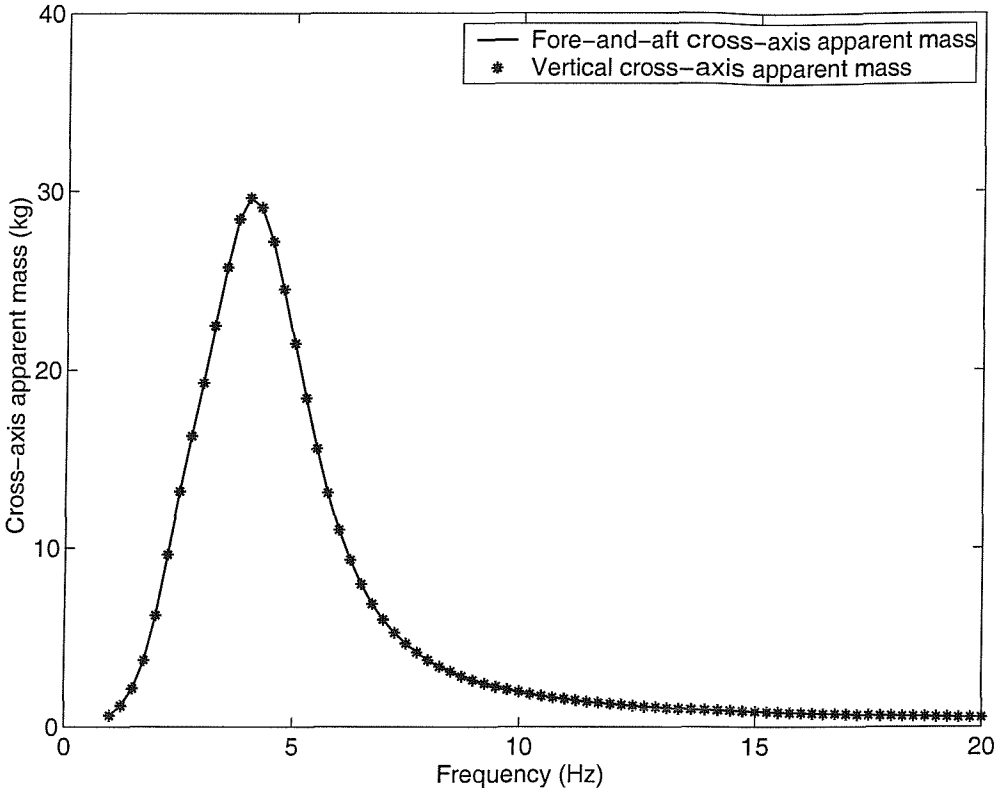

Figure 10.4 Cross-axis apparent masses calculated from Model 5 using the optimised parameters for subject 11. Conditions: posture, feet hanging with no backrest; vibration magnitude, 1.25 ms^{-2} r.m.s.

10.4.4 Testing the non-linearity of the human body using the cross-axis apparent mass

Previous studies have depended mainly on a shift in the resonance frequency of the human body with change in vibration magnitude to demonstrate the non-linearity of the human body. In this thesis, the resonance frequency of the apparent mass as well as the resonance frequency of the cross-axis apparent mass have been found to change with a change in vibration magnitude. However, the high coherency and the good agreement between the PSD and the CSD methods may imply that the human body behaves like a linear system at any particular vibration magnitude, as discussed in Section 10.3. In this section, the non-linearity of the human body at a specific vibration magnitude will be discussed using the cross-axis apparent mass: the fore-and-aft cross-axis apparent mass (measured during vertical excitation) will be compared with the vertical cross-axis apparent mass (measured during fore-and-aft excitation).

If a system is linear then the cross receptances are equal (i.e. the principle of reciprocity applies). However, an equality between the cross receptances is not proof of the linearity of a system: if the fore-and-aft cross-axis apparent mass is equal to the vertical cross-axis

apparent mass, no conclusion about the linearity of the human body (whether linear or non-linear) can be drawn. However, an inequality between the fore-and-aft cross-axis apparent mass and the vertical cross-axis apparent mass indicates that the human body is a non-linear system.

Figures 10.5 to 10.8 compare the fore-and-aft cross-axis apparent mass and the vertical cross-axis apparent mass for 10 subjects with four different vibration magnitudes when the subjects adopted the feet hanging posture. The comparison between the two functions is meaningful only at frequencies where the functions have high and identical (or very similar) coherencies: if the coherencies are not the same, the difference between the fore-and-aft cross-axis apparent mass and the vertical cross-axis apparent mass could be due to the different coherencies. Figures 10.9 to 10.12 show the coherencies obtained for the conditions in Figures 10.5 to 10.8.

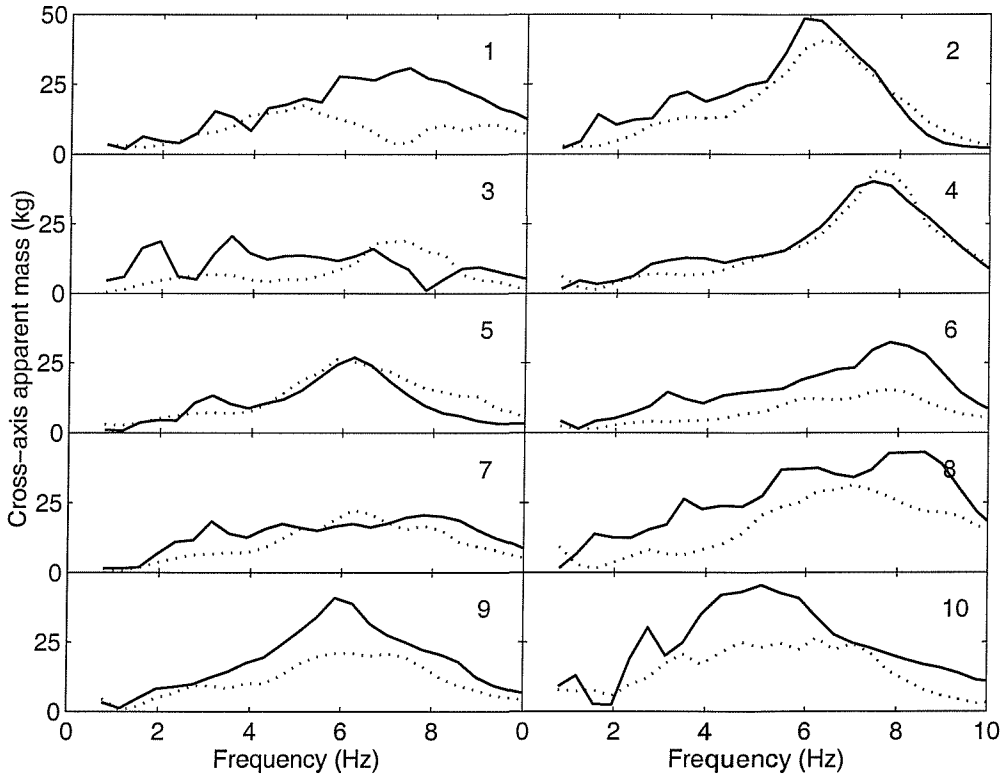

Figure 10.5 Cross-axis apparent masses of ten seated subjects measured at 0.125 ms^{-2} r.m.s. with the feet hanging posture. ———, fore-and-aft cross-axis apparent mass; ·····, vertical cross-axis apparent mass.

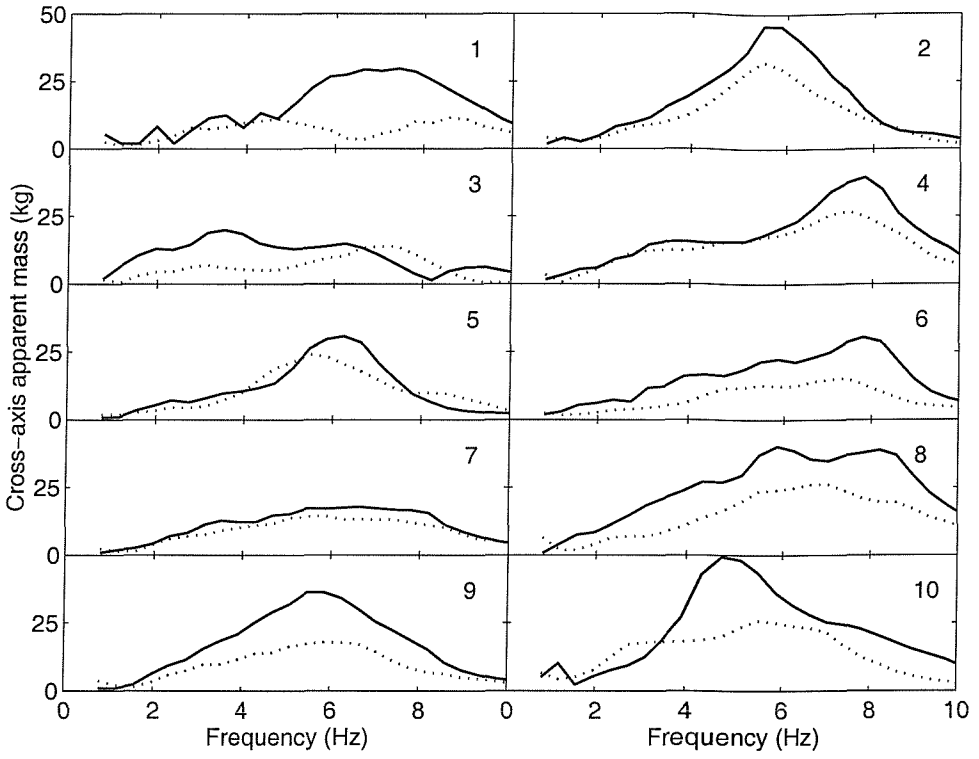

Figure 10.6 Cross-axis apparent masses of ten seated subjects measured at 0.25 ms^{-2} r.m.s. with the feet hanging posture. ———, fore-and-aft cross-axis apparent mass; ·····, vertical cross-axis apparent mass.

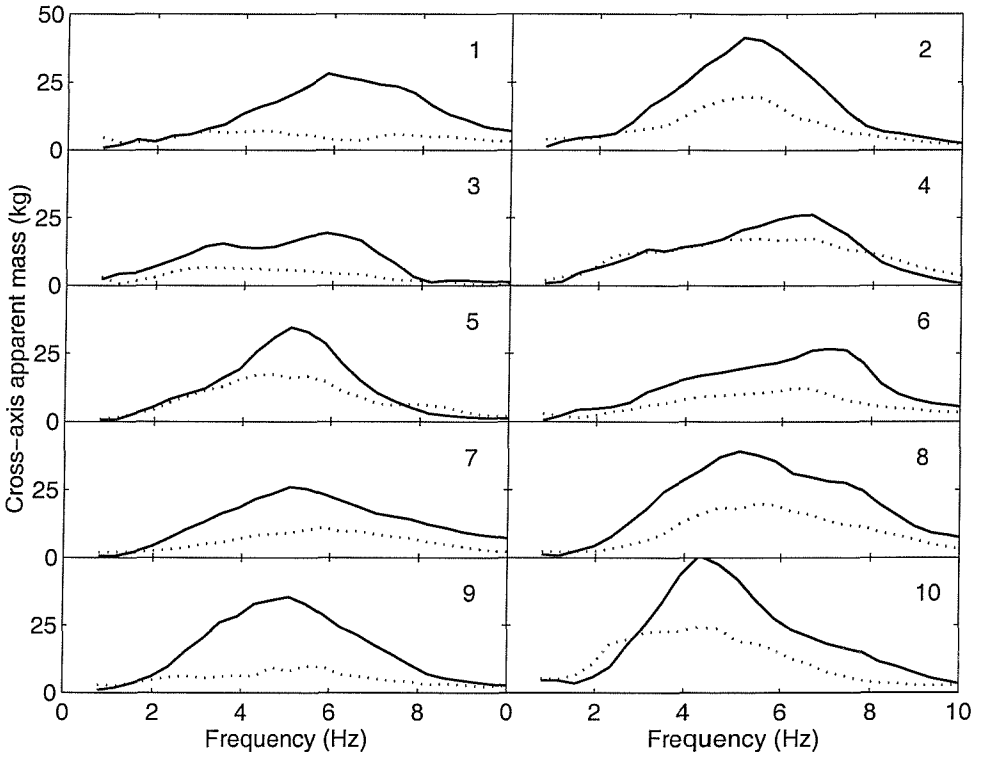

Figure 10.7 Cross-axis apparent masses of ten seated subjects measured at 0.625 ms^{-2} r.m.s. with the feet hanging posture. ———, fore-and-aft cross-axis apparent mass; ·····, vertical cross-axis apparent mass.

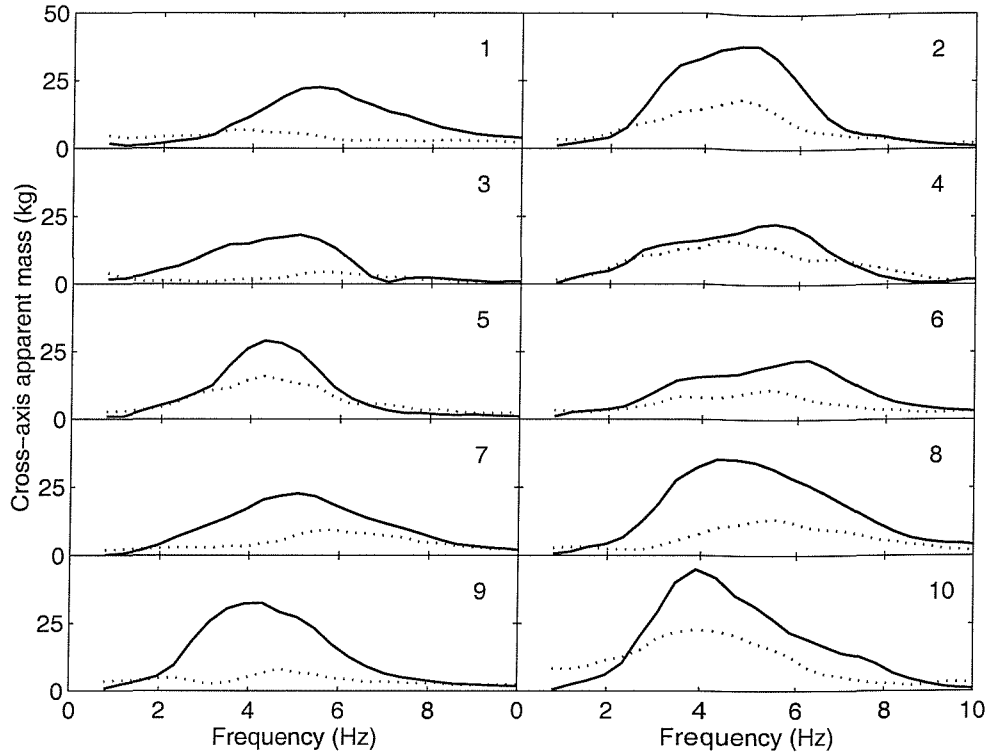

Figure 10.8 Cross-axis apparent masses of ten seated subjects measured at 1.25 ms^{-2} r.m.s. with the feet hanging posture. ———, fore-and-aft cross-axis apparent mass; ·····, vertical cross-axis apparent mass.

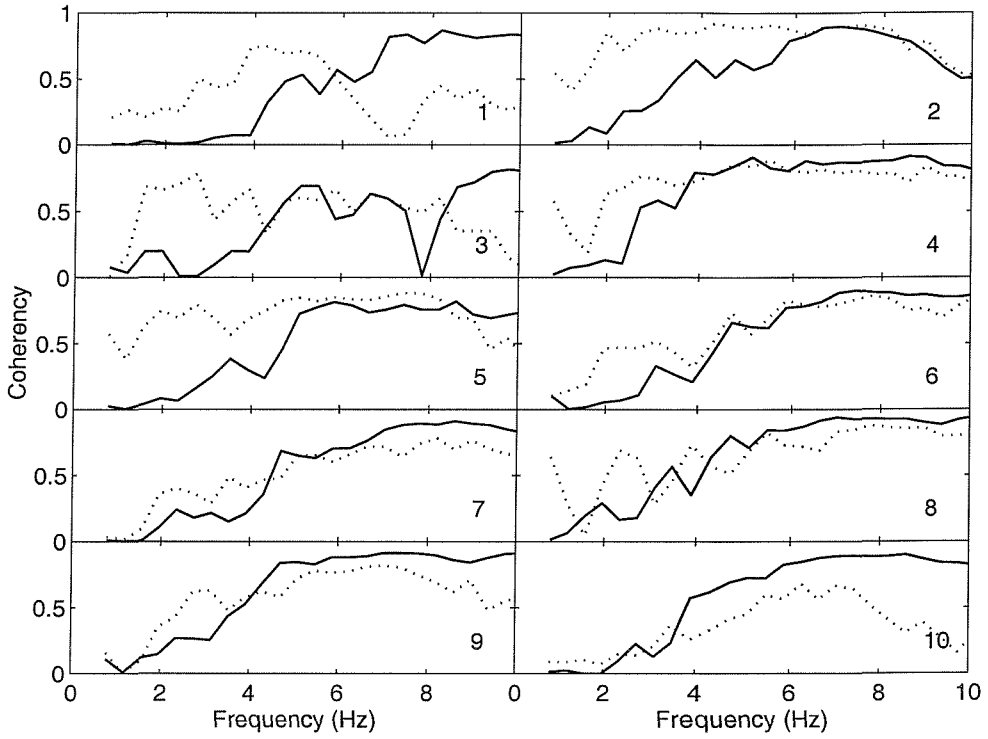

Figure 10.9 Coherencies of cross-axis apparent mass of ten seated subjects measured at 0.125 ms^{-2} r.m.s. with the feet hanging posture. ———, coherency of the fore-and-aft cross-axis apparent mass; ·····, coherency of vertical cross-axis apparent mass.

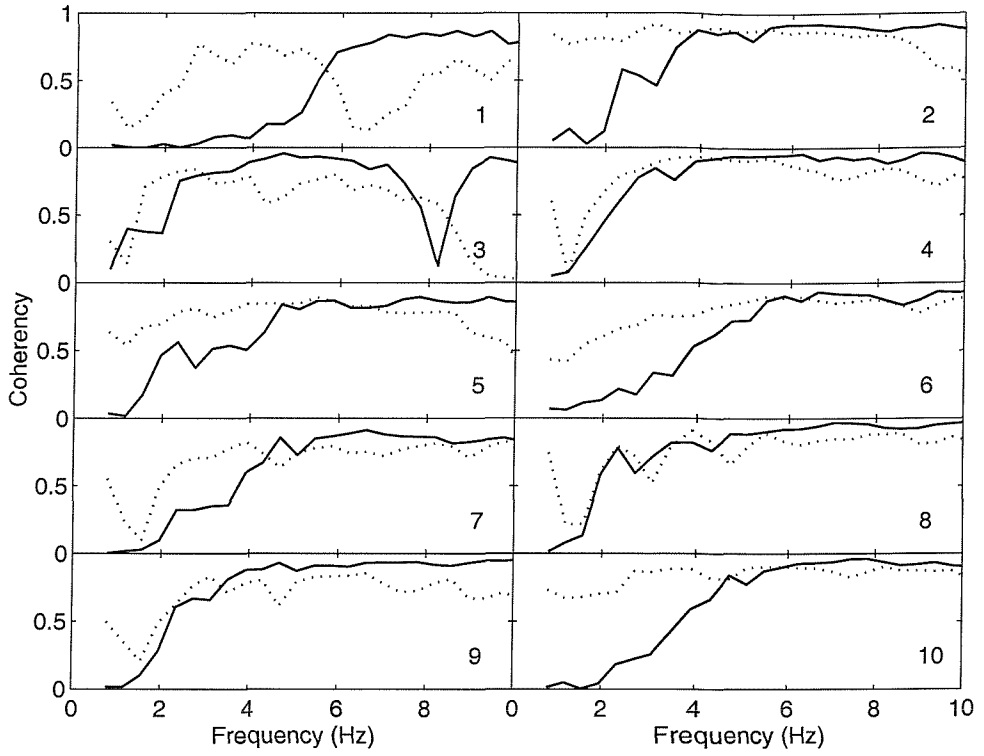

Figure 10.10 Coherencies of cross-axis apparent mass of ten seated subjects measured at 0.25 ms^{-2} r.m.s. with the feet hanging posture. ———, coherency of the fore-and-aft cross-axis apparent mass; ·····, coherency of vertical cross-axis apparent mass.

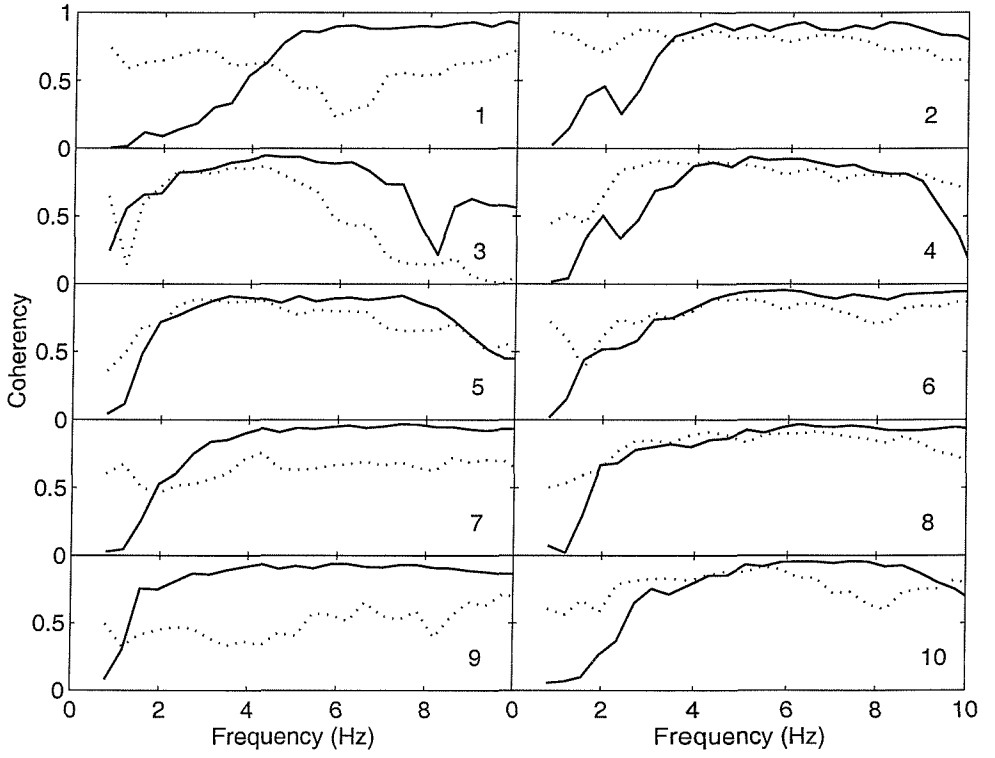

Figure 10.11 Coherencies of cross-axis apparent mass of ten seated subjects measured at 0.625 ms^{-2} r.m.s. with the feet hanging posture. ———, coherency of the fore-and-aft cross-axis apparent mass; ·····, coherency of vertical cross-axis apparent mass.

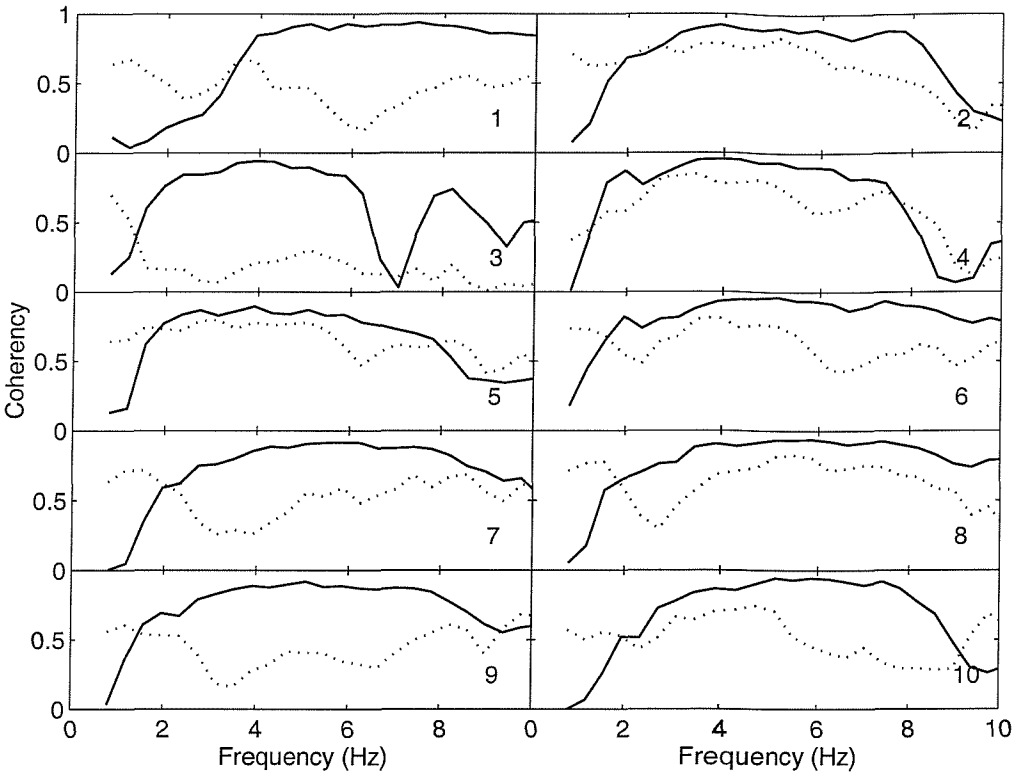

Figure 10.12 Coherencies of cross-axis apparent mass of ten seated subjects measured at 1.25 ms^{-2} r.m.s. with the feet hanging posture. ———, coherency of the fore-and-aft cross-axis apparent mass; ·····, coherency of vertical cross-axis apparent mass.

In most cases, where the coherencies of the fore-and-aft cross-axis apparent mass and the vertical cross-axis apparent mass were high and identical at a specific vibration magnitude, the values of the fore-and-aft cross-axis apparent mass and vertical cross-axis apparent mass were not equal (see Table 10.1 for selected examples). This may be indicative of a non-linearity in the human body despite the high coherency usually obtained for the apparent mass at a specific vibration magnitude, as was shown in Section 10.3. The non-linearity of the human body may depend on the excitation frequency and, hence, the indications of the non-linearity of the human body shown above cannot be generalised to frequencies other than those used in the comparison between the fore-and-aft cross-axis apparent mass and the vertical cross-axis apparent mass. The results may also indicate that including the responses of humans to vertical and fore-and-aft excitation in a single model (i.e. same model parameters apply to responses to vertical excitation and responses to fore-and-aft excitation) requires non-linear models.

Table 10.1 Conditions of high and identical coherencies for the fore-and-aft cross-axis apparent mass (F) and the vertical cross-axis apparent mass (V).

Vibration magnitude ms^{-2} r.m.s.	Subject	Frequency range (Hz)	Note
0.125	2	6 to 7.2	F is greater than V
	4	4 to 6	4 to 4.5 Hz: F is greater than V 4.5 to 6 Hz F is very similar to V
0.250	2	4 to 6	F is greater than V
	5	4.5 to 7	4.5 to 5.25 Hz: V is greater than F 5.25 to 7 Hz F is greater than V
0.625	3	2.5 to 3.5	F is greater than V
	10	4 to 6	F is greater than V

10.5 EFFECT OF SEATING CONDITION ON THE CORRELATION BETWEEN THE RESONANCE FREQUENCIES OF THE VERTICAL APPARENT MASS AND THE FORE-AND-AFT CROSS-AXIS APPARENT MASS

In Chapter 4, the resonance frequencies of the vertical apparent mass were correlated with the resonance frequencies of the fore-and-aft cross-axis apparent mass. In Chapter 8, however, the resonance frequencies of the 'vertical apparent mass' and the 'fore-and-aft cross-axis apparent mass' were not correlated. The different postures and different seating arrangements used in the experiments described in Chapter 4 and Chapter 8 might be the reason for this discrepancy. The mechanisms (or vibration modes) that contribute to the resonance frequencies may change with a change in posture or seating condition such that common mechanisms contribute to both resonances in certain conditions (posture or seating arrangement) and a correlation can be found while no common mechanisms (or modes) contribute to both resonances in other postures or seating conditions and hence, no correlation can be found. Figure 10.13 and Figure 10.14 compare between the results obtained in Chapter 4 (for the average thigh contact posture) and Chapter 8 (for seat angle of 0°). The difference between the two conditions is the lower leg and the foot positions: the lower legs were vertical and the feet were resting on a horizontal footrest in Chapter 4 while the lower legs were stretched and the feet resting on an inclined footrest in Chapter 8.

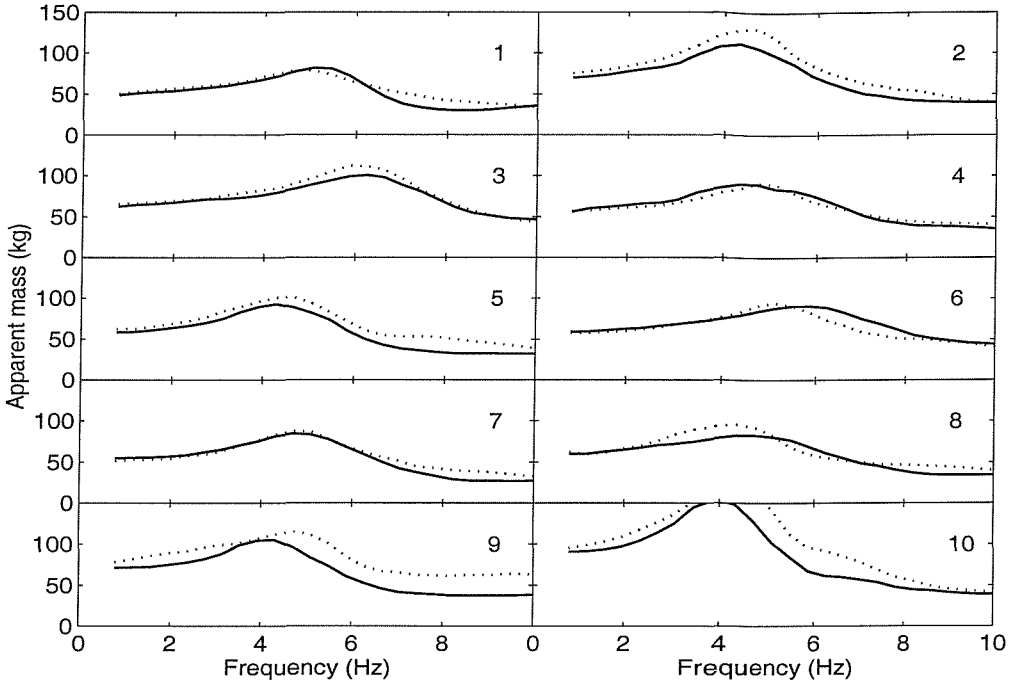

Figure 10.13 Apparent masses of 10 seated subjects measured at 1.25 ms^{-2} r.m.s. ——, with average thigh contact posture (Chapter 4); ·····, with seat angle of 0° (Chapter 8).

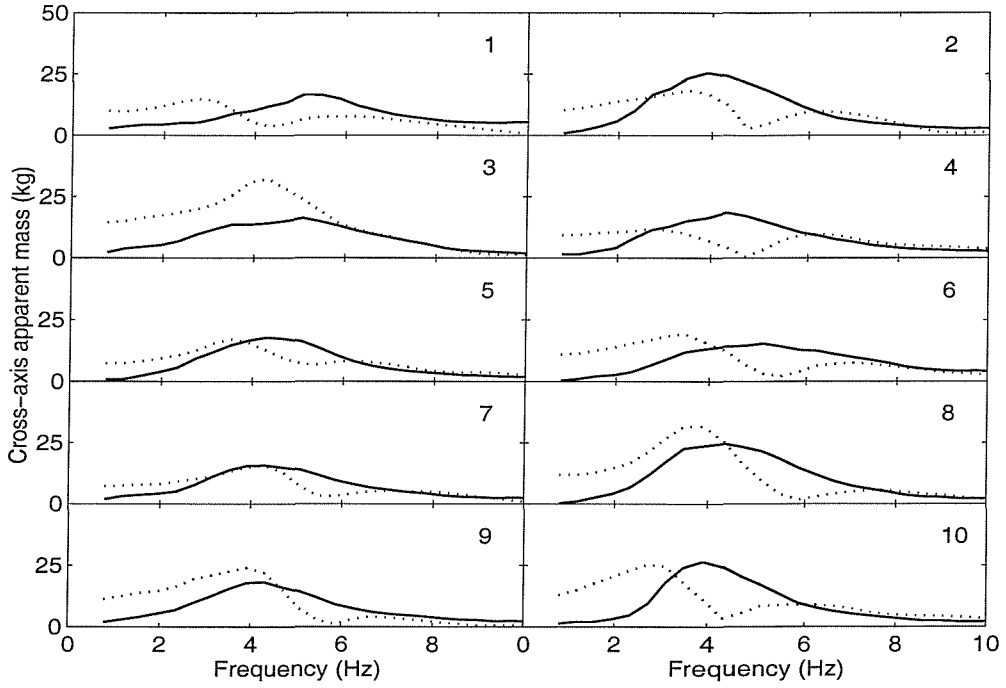

Figure 10.14 Cross-axis apparent masses of 10 seated subjects measured at 1.25 ms^{-2} r.m.s.. ———, with average thigh contact posture (Chapter 4); ·····, with seat angle of 0° (Chapter 8).

Matsumoto and Griffin (1998b) reported that for standing subjects, the apparent mass resonance frequency differed between standing postures: 5.5 Hz in a normal standing posture, 3.75 Hz for a one-leg posture and 2.75 Hz for a legs bent posture. Matsumoto and Griffin stated that 'in the normal standing posture, the transmissibilities to the fourth lumbar vertebra and to the iliac crests were similar to that of the apparent mass at low frequencies. In the leg bent posture, a pitching or bending mode of the upper body, together with a bending motion of the legs at the knees, appeared to contribute to the resonance frequency. When standing on one leg, rotational motion of the upper body about the hip joint may have contributed to the resonance frequency'.

It is possible that the frequencies of the modes contributing to the principal mode are different with different postures. It is also possible that some of the modes that contribute to the principal mode do not change their frequency while others change their frequency with a change in posture or seating condition, which leads to a change in the principal mode frequency. For example, Kitazaki and Griffin (1998) reported that in a normal sitting posture, the principal mode of the apparent mass occurred at 4.9 Hz and consisted of an entire body mode, in which axial and shear deformations of the buttocks tissue produced vertical motion of the head, spinal column and pelvis in phase with a vertical visceral mode and a bending mode of the upper thoracic and cervical spine. In a slouched sitting posture the principal mode, which occurred at 4.4 Hz, was 'separated into an entire body mode at 4.0 Hz and the combination of the visceral mode and the bending mode of the upper spine at 4.9 Hz': the modes at both 4.9 Hz and 4.0 Hz seemed to contribute to the resonance frequency of the apparent mass at 4.4 Hz. However, the shift in the resonance frequency from 4.9 Hz to 4.4 Hz when the body posture changed from normal to slouched was produced by the shift of the entire body mode. It may then be hypothesised that a similar behaviour happened when the subject changed posture and seating arrangements between Chapter 4 and Chapter 8, so that the correlation between the resonance frequencies of the vertical apparent mass and the cross-axis apparent mass was affected.

CHAPTER 11 GENERAL CONCLUSIONS AND RECOMMENDATIONS FOR FUTURE WORK

11.1 INTRODUCTION

This chapter is divided into two sections. The first section presents general conclusions and summarise the findings drawn across the different studies in the thesis. The second section provides recommendations for future work based on the results and findings in this thesis. Some recommendations for further research identified from the literature review are also provided.

11.2 GENERAL CONCLUSIONS

The main conclusion from this study is that the human body moves in two directions when exposed to vertical excitation or fore-and-aft excitation. This conclusion is based on the presence of fore-and-aft cross-axis forces and vertical cross-axis forces during exposure of the human body to vertical excitation and fore-and-aft excitation, respectively. Modelling of the vertical apparent mass and the fore-and-aft cross-axis apparent mass during vertical excitation required a vertical vibration mode, a pitch vibration mode and a fore-and-aft vibration mode, which implies that vertical excitation of the human body caused rotational motion of some parts of the body as well as shear deformation of the tissues, possibly the buttocks tissue, in contact with the seat. The need for a fore-and-aft degree-of-freedom near the vertically excited base may alternatively indicate that the human body slides on the seat when exposed to vertical excitation.

During vertical excitation and fore-and-aft excitation, the dynamic responses in all directions (vertical, fore-and-aft and lateral) showed a non-linear behaviour. The extent of the non-linearity depended on the posture, the vibration frequency and measurement location and direction. The non-linearity of the human body is implied by the differences between the cross-axis apparent masses: the inequality between the fore-and-aft cross-axis apparent mass and the vertical cross-axis apparent mass indicates that the human body is a non-linear system in spite of the obtained high coherency.

Two mechanisms were suggested to contribute to the non-linearity of the human body: axial deformation of the tissue beneath the pelvis may have contributed to the non-linearity found in the vertical apparent mass (see Chapter 4) while shear deformation of the same tissue may have contributed to the fore-and-aft 'cross-axis apparent mass' during vertical excitation. Modelling the vertical apparent mass and the cross-axis

apparent mass measured on the seat during vertical excitation also suggested the involvement of the tissue beneath the pelvis in the non-linearity of the human body.

Seating conditions (e.g. the presence of a backrest, using a footrest, footrest height, and seat surface angles) all have an effect on the responses of humans to whole-body vertical and fore-and-aft excitation. It is, therefore, a necessity to control the sitting posture and describe precisely the seating conditions used in experiments measuring the responses of humans to vibration.

11.3 RECOMMENDATIONS FOR FUTURE WORK

Responses to vibration in the lateral, pitch, roll, or yaw directions are not common in the literature. Excitation in the lateral, pitch, roll, and yaw directions may involve considerable cross-axis movements which, if identified, could improve the dynamic modelling of human responses to vibration. For example, lateral vibration, which is dominant in trains, could cause vertical cross-axis force on the seat. Vertical cross-axis forces could also occur during lateral acceleration produced by cornering in a vehicle. It will be interesting to identify the cross-axis forces (on the seat and backrest) during lateral excitation. Improving seat design with good body support and attenuation of vibration may depend on understanding how the body moves in all directions.

Rigid seats and rigid backrests were used in the experiments described in this thesis. Therefore, the results obtained in this thesis are not necessarily applicable to compliant seats: with compliant seats, the relative motion between the body and the seat cushion is expected to be different from the relative motion between the body and a rigid seat. Fore-and-aft forces produced on a compliant backrest during vertical excitation are expected to be of two sources. The first source of the fore-and-aft force will be the pitching movements of the upper body due to a vertical excitation on the seat and the second source will be the force applied by the compliant backrest on the body. This may imply the need to develop methods to measure or predict the forces on compliant seats are used in vehicles.

It is of interest to compare the apparent mass measured in a specific direction using multi-axis vibration condition with the apparent mass measured with a single axis excitation. The hypothesis will be that the apparent mass in a specific direction obtained in a multi-axis vibration condition will be different from that obtained in that specific direction due to excitation only in that specific direction. The hypothesis is based on the different forces involved in calculating the apparent mass in the two different conditions.

For example, the vertical forces obtained on a seat during pure vertical excitation are produced by the vertical force applied to the body by the seat as well as by the vertical component of the pitching movements of the upper body. If the multi-axis vibration condition, in a car for example, was assumed to be dominated by vertical and horizontal excitation, then the forces measured on the seat in the vertical direction are produced by vertical components similar to those produced due to single axis excitation in addition to a vertical cross-axis force produced by fore-and-aft excitation and possibly due to lateral excitation. The vertical apparent mass of the human body measured in real vehicle could also be affected by the usually inclined cushioned backrest used in real vehicles as oppose to the vertical rigid backrest employed in this study.

In this thesis the cross-axis apparent mass was quantified for seated subjects. People are also exposed to whole-body vibration while standing. Although a few studies reported the driving point responses of the standing human body to vertical excitation, no known study to have measured the cross-axis forces at the feet of standing subjects.

Three main modes of vibration were found in the fore-and-aft apparent mass measured during fore-and-aft excitation. The mechanisms that cause these modes are difficult to identify using only driving point responses. These mechanisms may be identified by measuring transmissibilities to different locations on the body and comparing the resonances of these parts with the resonances in the apparent mass. There is no known work to have reported transmissibility to the different parts of the body (except to the head) during horizontal excitation. The parts of the body contributing to the different modes may also be identified by varying the properties of the parts of the body in a mathematical model and observing the changes to the resonance frequency. No such mechanistic model to represent the response of humans to horizontal excitation is currently available in the literature.

The effect of seat surface inclination on the 'vertical apparent mass' and the 'fore-and-aft cross-axis apparent mass' was studied in this thesis. The experiments were conducted without a backrest and with a vertical rigid backrest. Since the human body and the seat act like a coupled system when exposed to vibration, the effect of changing the backrest angle together with seat surface angle may be more representative to the real situation in vehicles.

A vertical backrest was used in this work in all experiments where a backrest was employed. The backrest was fixed and not adjustable to subject height. This could have

increased the inter-subject variability especially in the measurements taken at the backrest due to the different areas of contact between the subjects and the backrest. This is of significance since the measurements taken at the backrest (especially during vertical excitation), which may also affect the measurements on the seat, are caused mainly by rotational modes. It is therefore recommended to consider adjusting the height of the backrest in future study.

Some studies reported an effect of gender on the mechanical impedance of the human body measured in the direction of vibration (e.g. Holmlund and Lundström, 1998). All subjects used in this thesis were male subjects. It will be interesting to test for the effect of gender on the cross-axis forces.

A three degree-of-freedom lumped parameter model was sufficient to predict the experimental results (apparent mass and cross-axis apparent mass) obtained during vertical excitation without a backrest. The fore-and-aft forces were best predicted when a fore-and-aft degree-of-freedom close to the vertically vibrating base was included in the model (see Model 5 in Chapter 9). Mechanistic models such as that reported by Matsumoto and Griffin (2001, see Figure 2.47), where vertical and fore-and-aft transmissibilities to different locations on the upper body were modelled together with the apparent mass, may be improved by adding a fore-and-aft degree-of-freedom near the base. In the model of Matsumoto and Griffin, the added fore-and-aft degree-of-freedom near the base can be thought of as representing the shear deformation of the buttocks tissue.

The models developed in this thesis accommodated the forces measured only on the seat in the fore-and-aft and vertical directions. The thesis, however, provides measurements of forces on the backrest and footrest which can be used to improve the developed models.

APPENDICES

APPENDIX A

INDIVIDUAL DATA: VERTICAL EXCITATION WITHOUT A BACKREST (CHAPTER 4)

APPENDIX A Vertical excitation without a backrest (Chapter 4)

A.1 Characteristics of subjects

Table A.1 Characteristics of subjects used in the experiment described in Chapter 4.

Subject No.	Mass (kg)	Stature (m)	Age (year)
1	64.0	1.75	23
2	86.0	1.82	37
3	80.0	1.86	46
4	70.0	1.69	40
5	57.0	1.70	47
6	67.0	1.75	25
7	74.0	1.77	33
8	61.0	1.68	30
9	75.0	1.84	26
10	73.5	1.84	20
11	82.5	1.85	25
12	106.9	1.86	28

A.2 Instructions given to the subjects prior exposure to vibration

- The goal of this experiment is to measure the forces on the seat in three axes (vertical, fore-and-aft and lateral) and at the feet in the vertical direction during whole-body vertical vibration.

- You will be seated on a rigid seat and exposed to random vertical vibration at different vibration magnitudes and in four different postures.

The adopted postures will be:

a. Normal sitting while feet hanging in the air.
b. Sitting with the upper leg horizontal, the lower legs vertical, and the feet supported on the footrest mounted on the vibrating table. Subject must be barefooted.
c. Sitting with minimum thigh contact with the seat by raising the footrest while keeping the lower legs in a vertical position. Subject must be barefooted.
d. Sitting with maximum thigh contact such that the feet are just touching the footrest. The lower legs are also vertical in this case. Subject must be barefooted.

- In each of the sitting conditions mentioned above you will be exposed to four random vibrations. The experimenter will show you the order in which the above conditions will be adopted.

- During the exposure to vibration, you can stop the vibration at any time by pressing the red STOP button that you will be holding throughout the experiment.

Thank you for taking part in this experiment.

A.3 Individual results

A.3.1 Vertical apparent mass on the seat

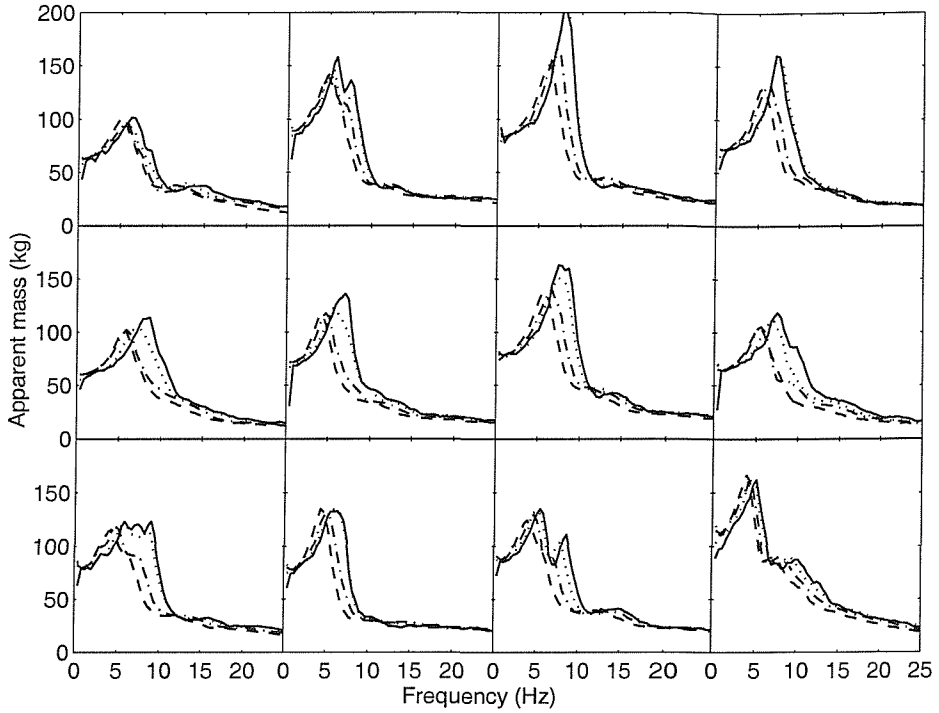

Figure A.1 Vertical apparent masses of 12 subjects measured on the seat in the feet hanging posture at four vibration magnitudes. ———, 0.125 ms^{-2} r.m.s.; ·····, 0.25 ms^{-2} r.m.s.; –·–·–·–, 0.625 ms^{-2} r.m.s.; – – – –, 1.25 ms^{-2} r.m.s.

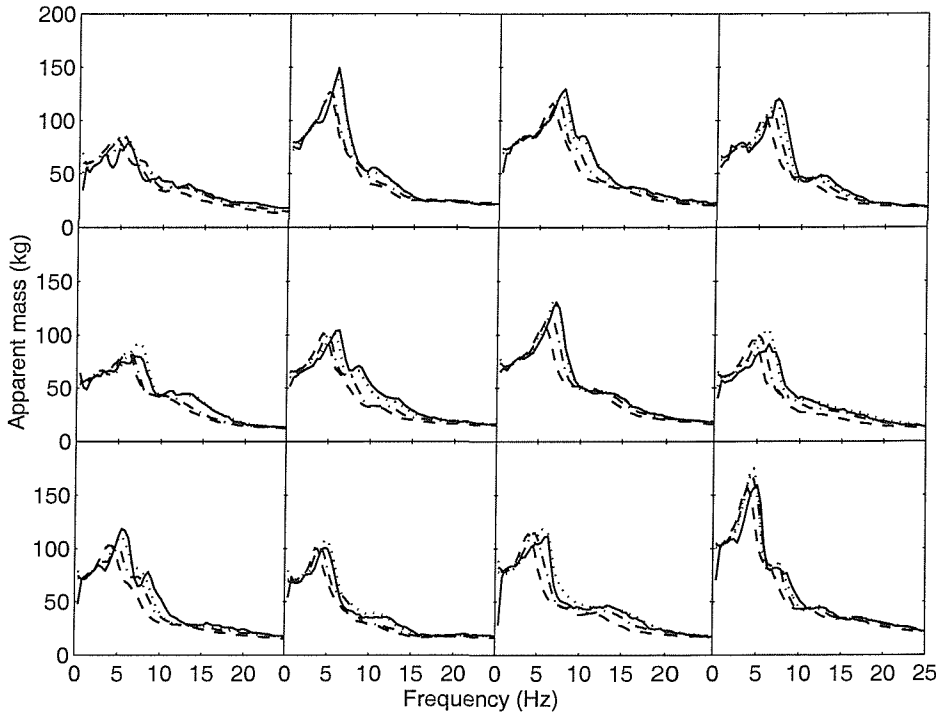

Figure A.2 Vertical apparent masses of 12 subjects measured on the seat in the maximum thigh contact posture at four vibration magnitudes. ———, 0.125 ms^{-2} r.m.s.; ·····, 0.25 ms^{-2} r.m.s.; –·–·–·–, 0.625 ms^{-2} r.m.s.; – – – –, 1.25 ms^{-2} r.m.s.

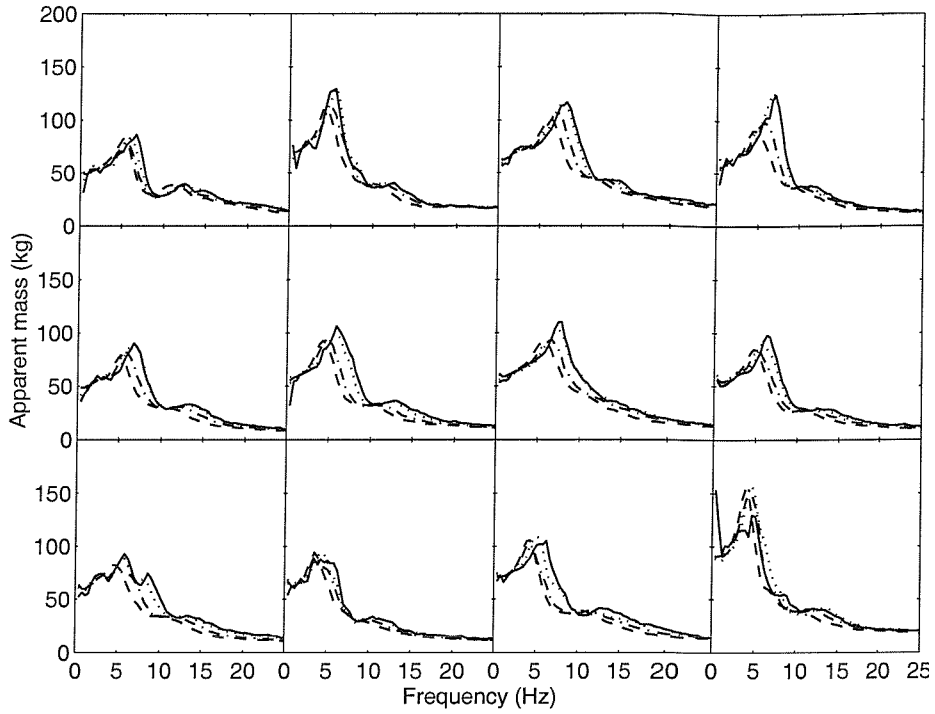

Figure A.3 Vertical apparent masses of 12 subjects measured on the seat in the average thigh contact posture at four vibration magnitudes. ———, 0.125 ms^{-2} r.m.s.; ·····, 0.25 ms^{-2} r.m.s.; –·–·–, 0.625 ms^{-2} r.m.s.; – – – –, 1.25 ms^{-2} r.m.s.

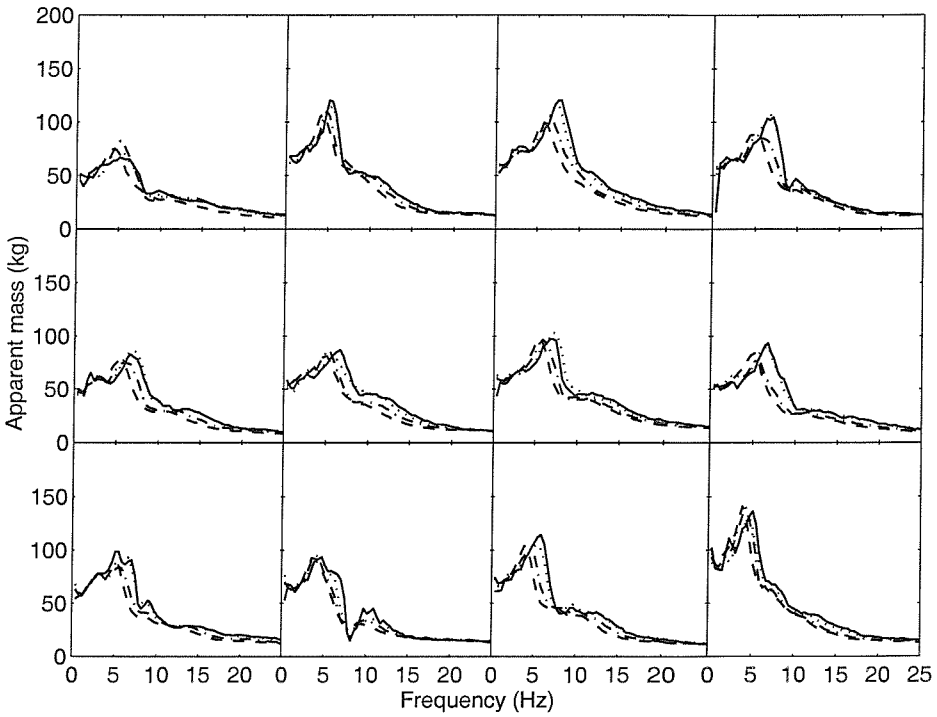

Figure A.4 Vertical apparent masses of 12 subjects measured on the seat in the minimum thigh contact posture at four vibration magnitudes. ———, 0.125 ms^{-2} r.m.s.; ·····, 0.25 ms^{-2} r.m.s.; –·–·–, 0.625 ms^{-2} r.m.s.; – – – –, 1.25 ms^{-2} r.m.s.

A.3.2 Fore-and-aft cross-axis apparent mass on the seat

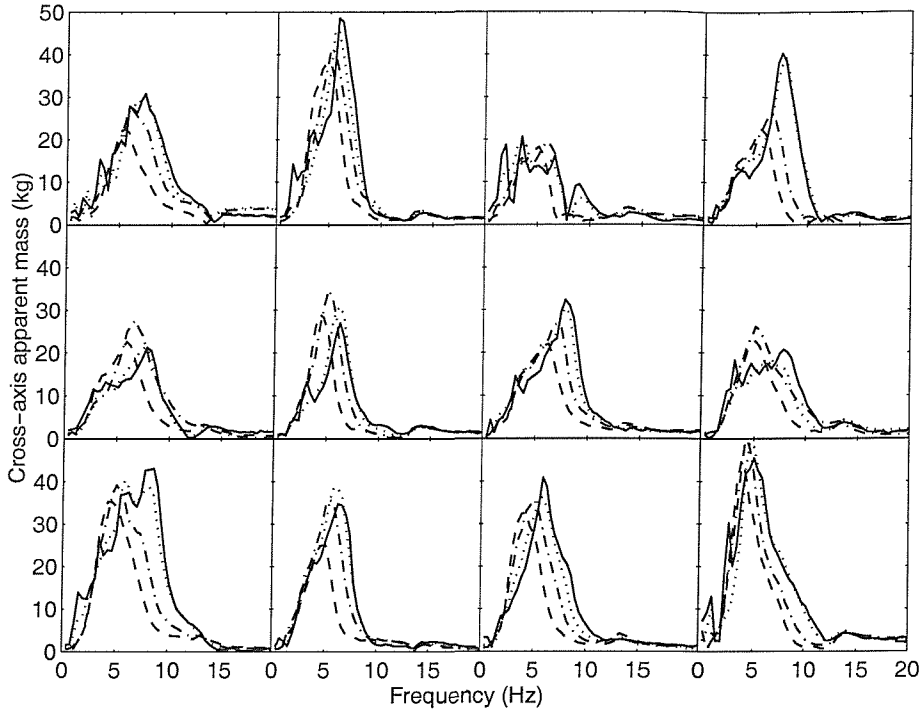

Figure A.5 Fore-and-aft cross-axis apparent masses of 12 subjects measured in the feet hanging posture at four vibration magnitudes. ———, 0.125 ms^{-2} r.m.s.; ·····, 0.25 ms^{-2} r.m.s.; –·–·–, 0.625 ms^{-2} r.m.s.; – – – –, 1.25 ms^{-2} r.m.s.

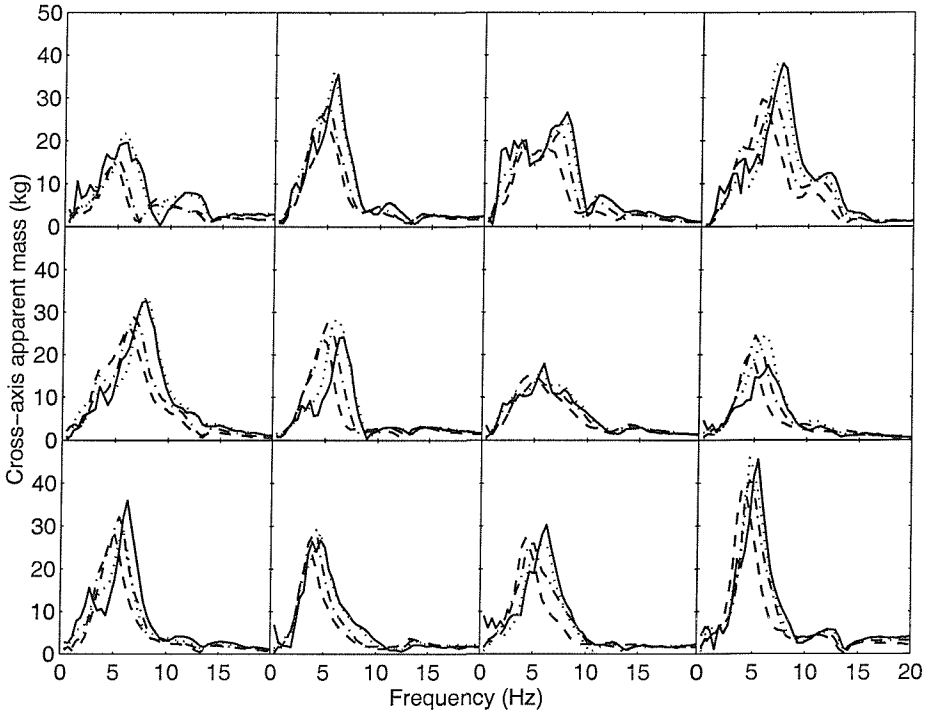

Figure A.6 Fore-and-aft cross-axis apparent masses of 12 subjects measured in the maximum thigh contact posture at four vibration magnitudes. ———, 0.125 ms^{-2} r.m.s.; ·····, 0.25 ms^{-2} r.m.s.; –·–·–, 0.625 ms^{-2} r.m.s.; – – – –, 1.25 ms^{-2} r.m.s.

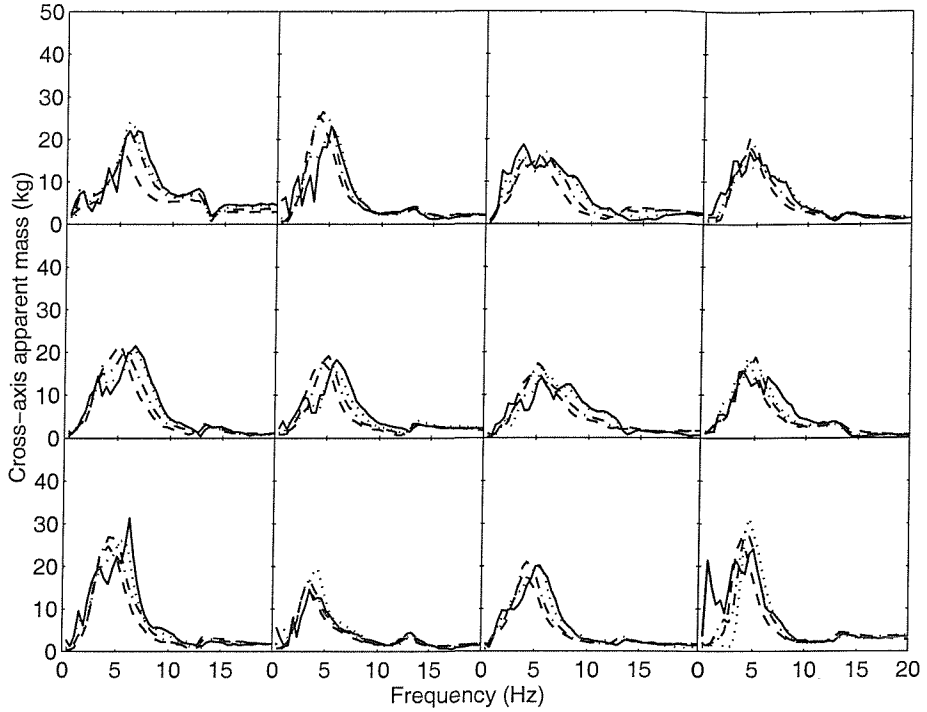

Figure A.7 Fore-and-aft cross-axis apparent masses of 12 subjects measured in the average thigh contact posture at four vibration magnitudes. ———, 0.125 ms^{-2} r.m.s.; ·····, 0.25 ms^{-2} r.m.s.; –·–·–, 0.625 ms^{-2} r.m.s.; – – – –, 1.25 ms^{-2} r.m.s.

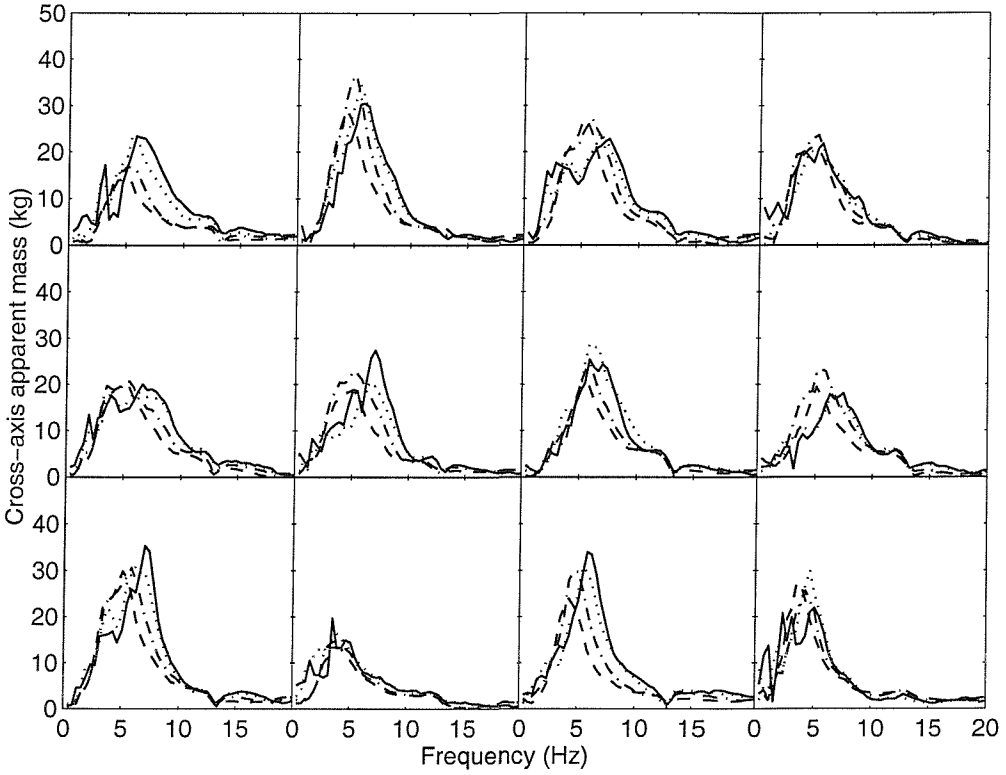

Figure A.8 Fore-and-aft cross-axis apparent masses of 12 subjects measured in the minimum thigh contact posture at four vibration magnitudes. ———, 0.125 ms^{-2} r.m.s.; ·····, 0.25 ms^{-2} r.m.s.; –·–·–, 0.625 ms^{-2} r.m.s.; – – – –, 1.25 ms^{-2} r.m.s.

A.3.3 Lateral cross-axis apparent mass on the seat

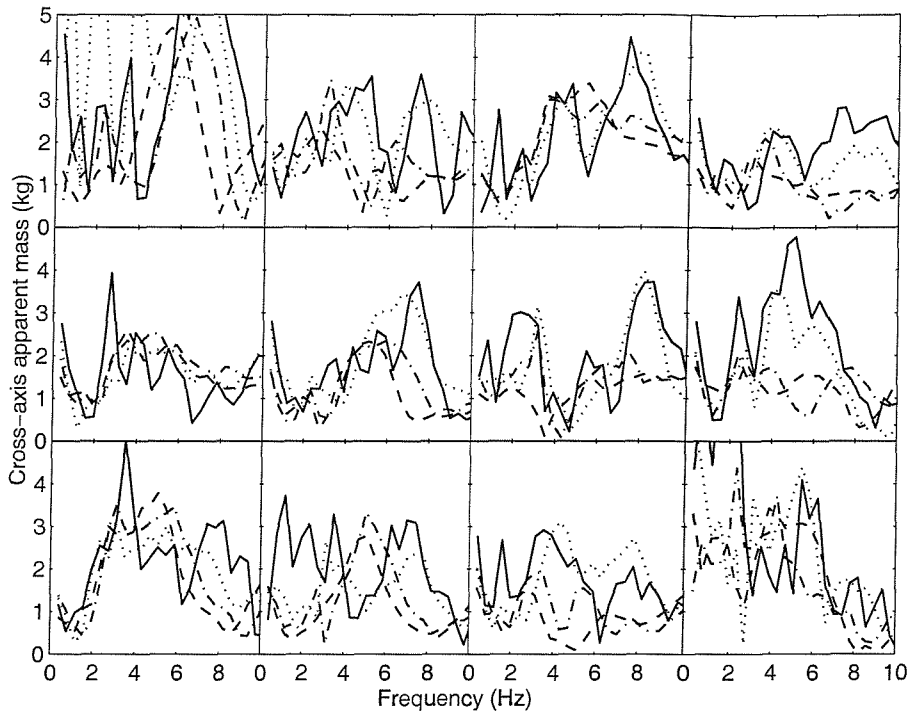

Figure A.9 Lateral cross-axis apparent masses of 12 subjects measured in the feet hanging posture at four vibration magnitudes. ———, 0.125 ms^{-2} r.m.s.; ·····, 0.25 ms^{-2} r.m.s.; –·–·–, 0.625 ms^{-2} r.m.s.; – – – –, 1.25 ms^{-2} r.m.s.

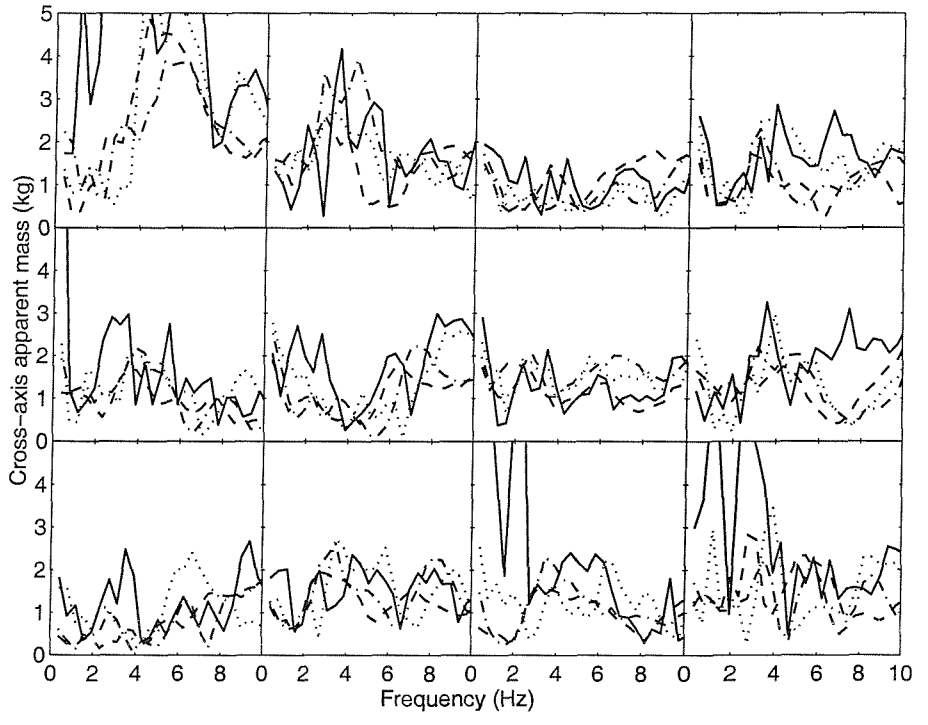

Figure A.10 Lateral cross-axis apparent masses of 12 subjects measured in the maximum thigh contact posture at four vibration magnitudes. ———, 0.125 ms^{-2} r.m.s.; ·····, 0.25 ms^{-2} r.m.s.; –·–·–, 0.625 ms^{-2} r.m.s.; – – – –, 1.25 ms^{-2} r.m.s.

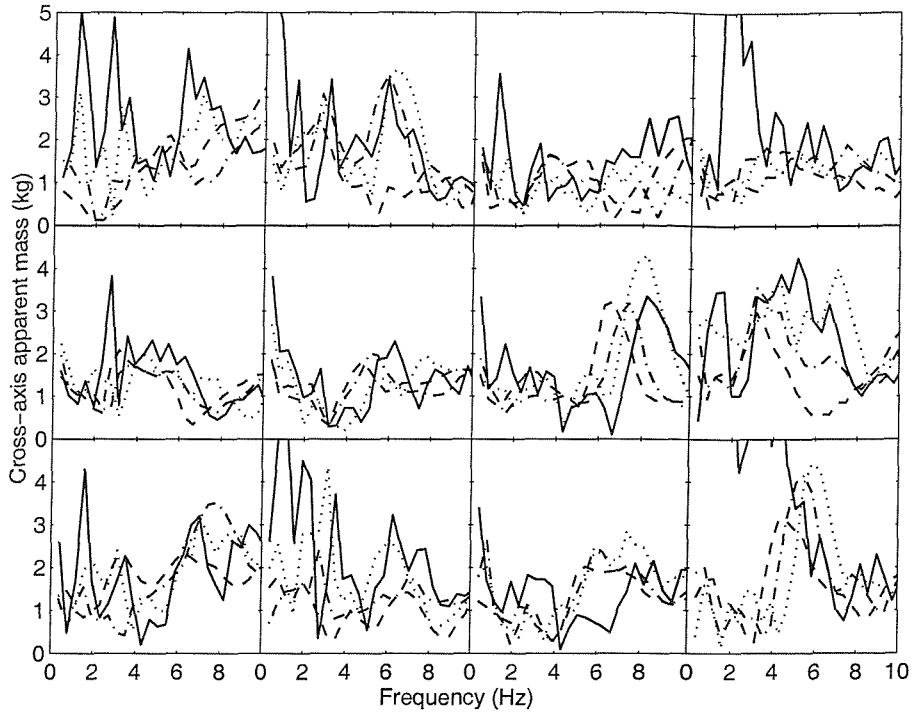

Figure A.11 Lateral cross-axis apparent masses of 12 subjects measured in the average thigh contact posture at four vibration magnitudes. ———, 0.125 ms^{-2} r.m.s.; ·····, 0.25 ms^{-2} r.m.s.; –·–·–, 0.625 ms^{-2} r.m.s.; – – – –, 1.25 ms^{-2} r.m.s.

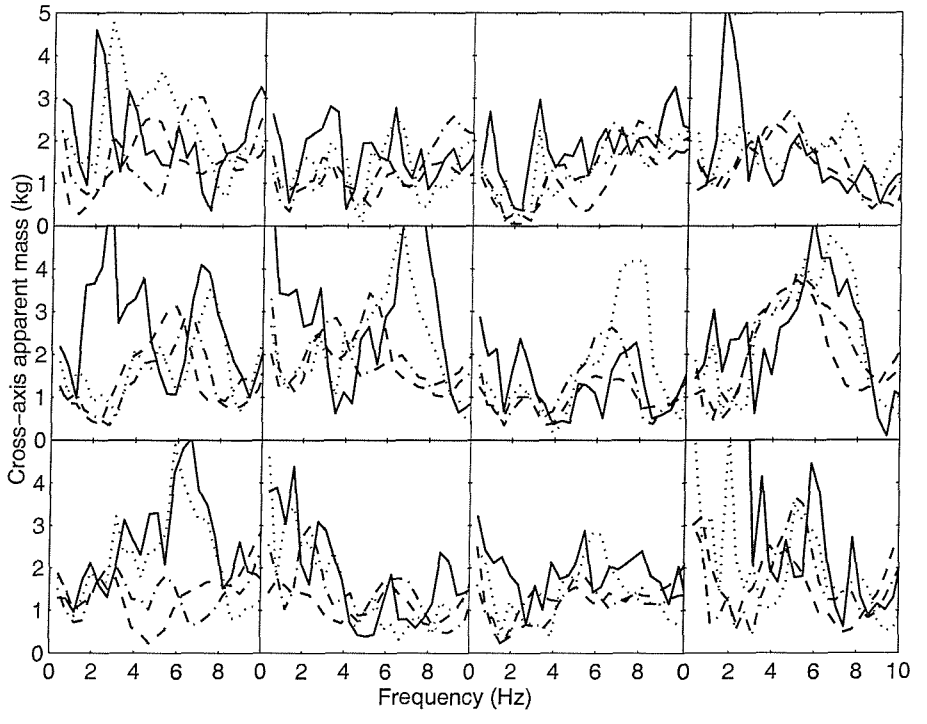

Figure A.12 Lateral cross-axis apparent masses of 12 subjects measured in the minimum thigh contact posture at four vibration magnitudes. ———, 0.125 ms^{-2} r.m.s.; ·····, 0.25 ms^{-2} r.m.s.; –·–·–, 0.625 ms^{-2} r.m.s.; – – – –, 1.25 ms^{-2} r.m.s.

A.3.4 Vertical apparent mass at the footrest

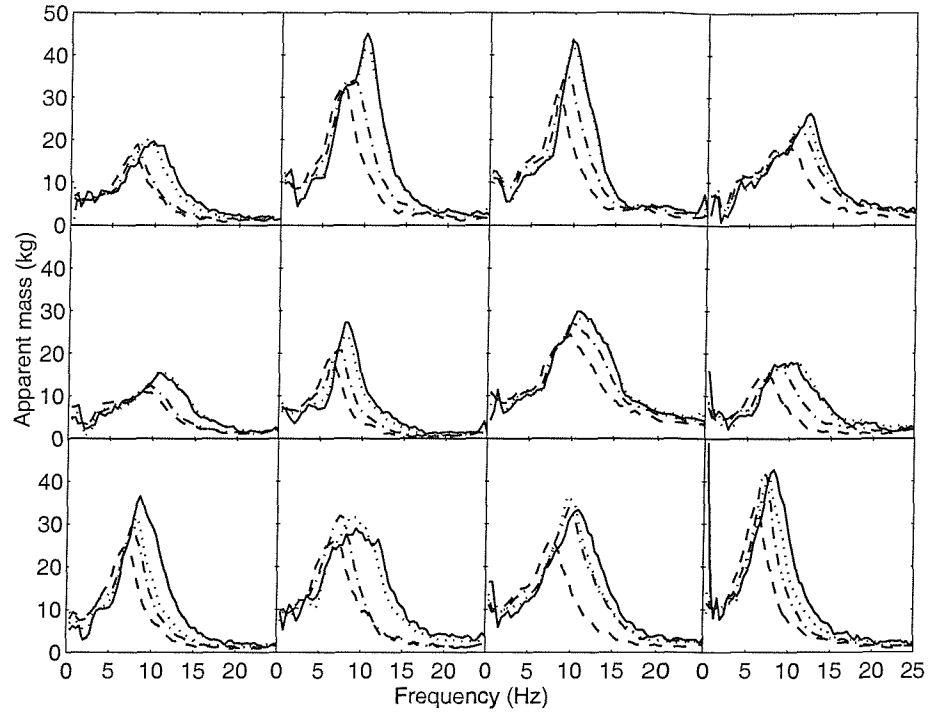

Figure A.13 Vertical apparent masses at the feet of 12 subjects in the maximum thigh contact posture measured at four vibration magnitudes. ———, 0.125 ms^{-2} r.m.s.; ·····, 0.25 ms^{-2} r.m.s.; –·–·–, 0.625 ms^{-2} r.m.s.; – – – –, 1.25 ms^{-2} r.m.s.

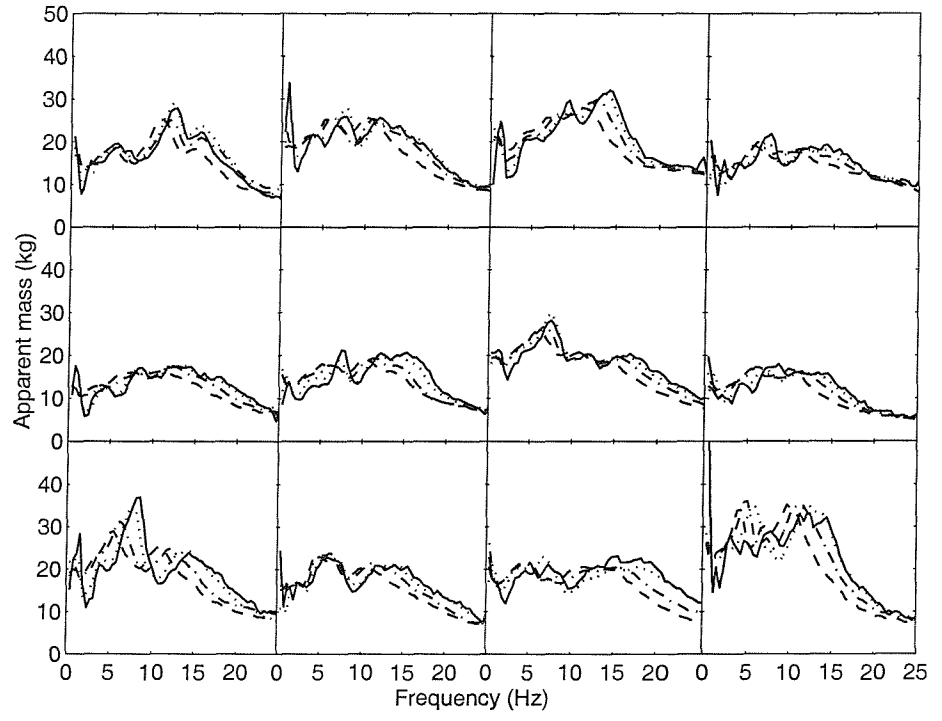

Figure A.14 Vertical apparent masses at the feet of 12 subjects in the average thigh contact posture measured at four vibration magnitudes. ———, 0.125 ms^{-2} r.m.s.; ·····, 0.25 ms^{-2} r.m.s.; –·–·–, 0.625 ms^{-2} r.m.s.; – – – –, 1.25 ms^{-2} r.m.s.

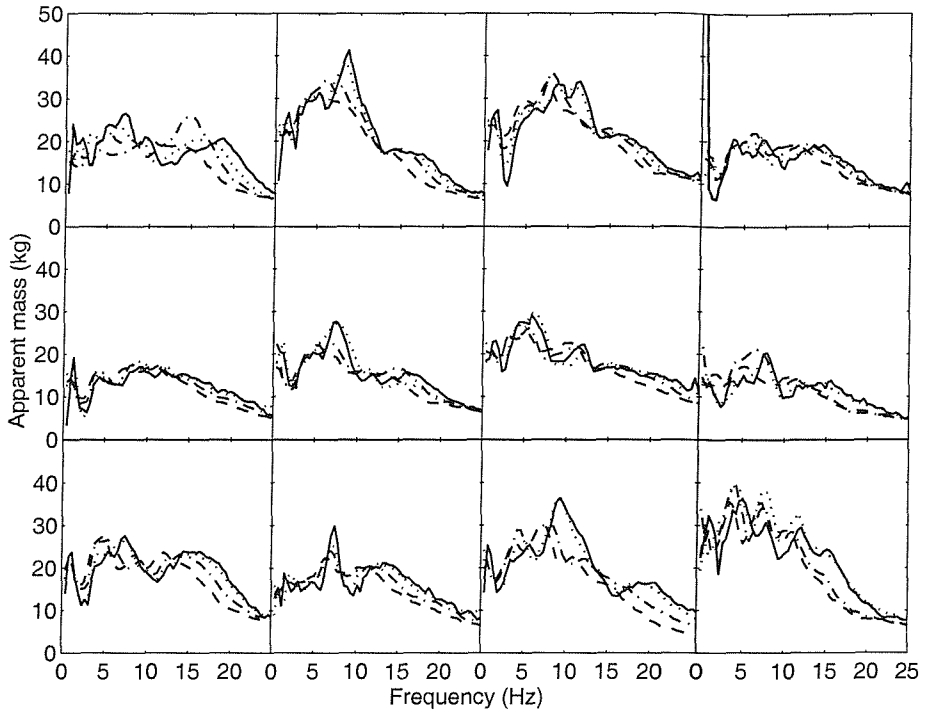

Figure A.15 Vertical apparent masses at the feet of 12 subjects in the minimum thigh contact posture measured at four vibration magnitudes. ———, 0.125 ms^{-2} r.m.s.; ·····, 0.25 ms^{-2} r.m.s.; –·–·–, 0.625 ms^{-2} r.m.s.; – – – –, 1.25 ms^{-2} r.m.s.

A.3.5 Coherencies of the fore-and-aft cross-axis apparent mass

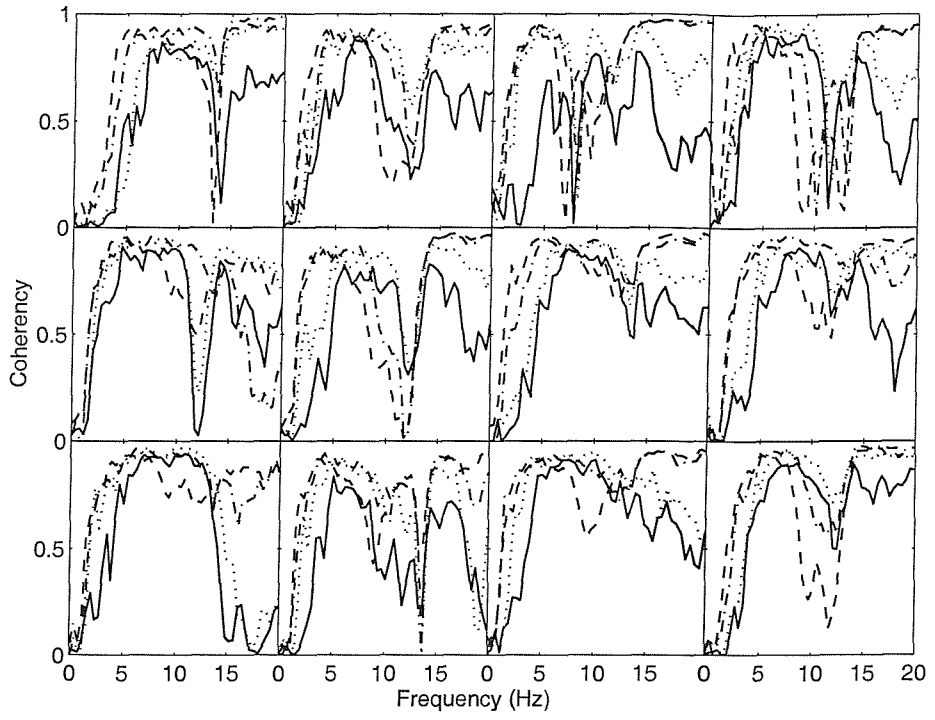

Figure A.16 Coherencies of fore-and-aft cross-axis apparent mass of 12 subjects in the feet hanging posture measured at four vibration magnitudes. ———, 0.125 ms^{-2} r.m.s.; ·····, 0.25 ms^{-2} r.m.s.; –·–·–, 0.625 ms^{-2} r.m.s.; – – – –, 1.25 ms^{-2} r.m.s.

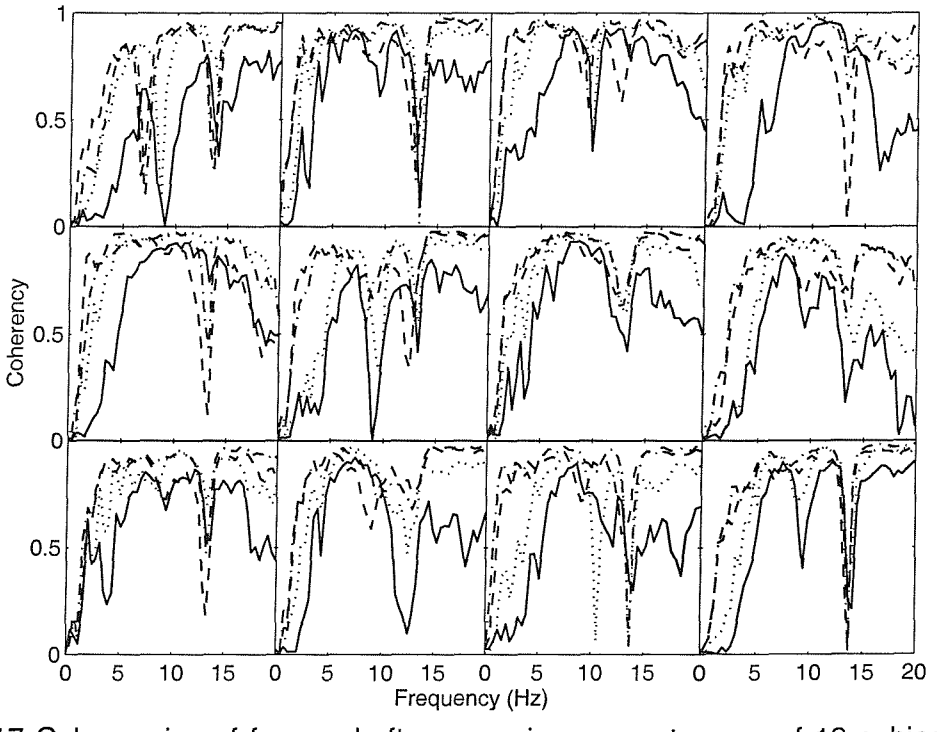

Figure A.17 Coherencies of fore-and-aft cross-axis apparent mass of 12 subjects in the maximum thigh contact posture measured at four vibration magnitudes. ———, 0.125 ms^{-2} r.m.s.; ·····, 0.25 ms^{-2} r.m.s.; –·–·–, 0.625 ms^{-2} r.m.s.; – – – –, 1.25 ms^{-2} r.m.s.

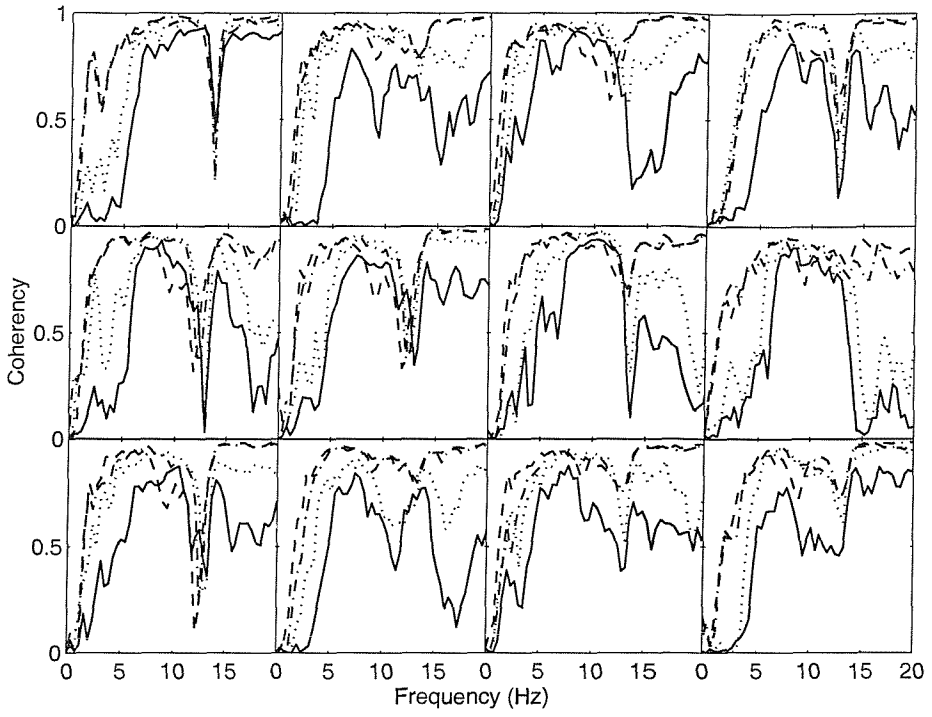

Figure A.18 Coherencies of fore-and-aft cross-axis apparent mass of 12 subjects in the average thigh contact posture measured at four vibration magnitudes. ———, 0.125 ms^{-2} r.m.s.; ·····, 0.25 ms^{-2} r.m.s.; –·–·–, 0.625 ms^{-2} r.m.s.; – – – –, 1.25 ms^{-2} r.m.s.

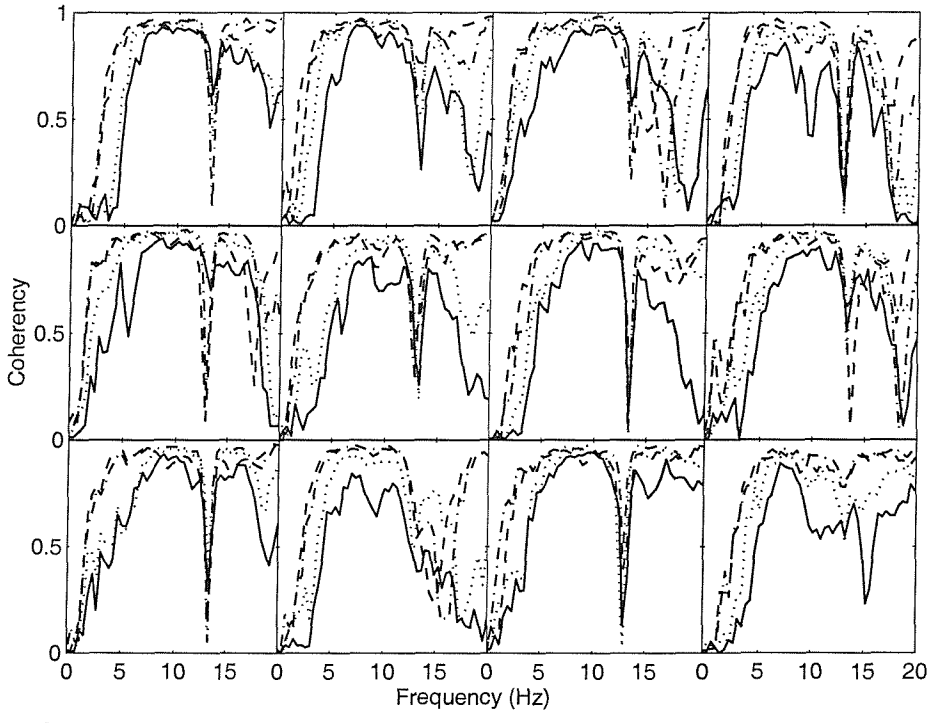

Figure A.19 Coherencies of fore-and-aft cross-axis apparent mass of 12 subjects in the minimum thigh contact posture measured at four vibration magnitudes. ———, 0.125 ms^{-2} r.m.s.; ·····, 0.25 ms^{-2} r.m.s.; –·–·–, 0.625 ms^{-2} r.m.s.; – – – –, 1.25 ms^{-2} r.m.s.

APPENDIX B

INDIVIDUAL DATA: VERTICAL EXCITATION WITH A BACKREST (CHAPTER 5)

APPENDIX B Vertical excitation with backrest (Chapter 5)

B.1 Instructions given to the subjects prior exposure to vibration

- The goal of this experiment is to measure the forces at the back of human subjects exposed to vertical vibration and to study the effect of different feet heights on those forces by calculating the apparent mass of the back. Forces on the seat in three directions are also measured.

- You will be seated on a rigid seat with a rigid backrest and exposed to random vertical vibration at different vibration magnitudes and with four different foot positions.

The adopted postures which will give different feet heights are:

a. Normal sitting while feet hanging in the air.
b. Sitting with the upper leg horizontal, the lower legs vertical, and the feet supported on the footrest mounted on the vibrating table. Subject must be barefooted.
c. Sitting with minimum thigh contact with the seat, by raising the footrest while keeping the lower legs in a vertical position. Subject must be barefooted.
d. Sitting with maximum thigh contact such that the feet are just touching the footrest. The lower legs are also vertical in this case. Subject must be barefooted.

- In each of the sitting conditions mentioned above you will be exposed to four random vibrations. The experimenter will show you the order in which the above conditions will be adopted.

- During the experiment you need to sit in an upright and relaxed position with your back against the backrest.

- Keeping the same sitting posture throughout the experiment is a very important and key factor for getting correct measurements that represent the posture of interest. Any voluntary movements of any part of the body (such as using your hand to scratch your head during the experiment) has an effect.

- During the exposure to vibration, you can stop the vibration at any time by pressing the red STOP button that you will be holding throughout the experiment.

Thank you for taking part in this experiment.

B.2 Individual results

B.2.1 Vertical apparent mass on the seat

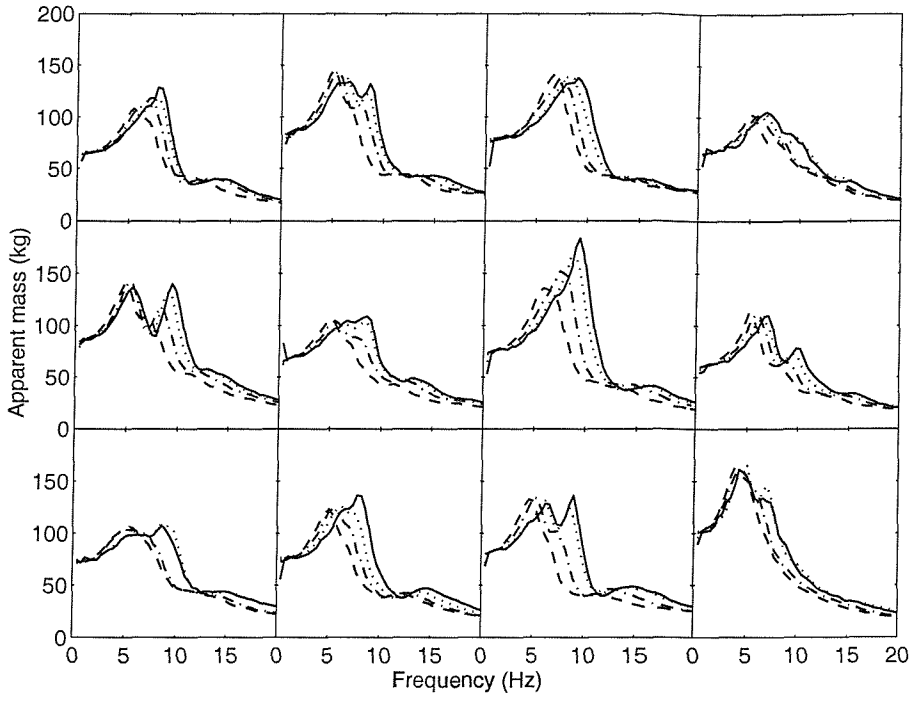

Figure B.1 Vertical apparent masses of 12 subjects measured on the seat with backrest in the feet hanging posture at four vibration magnitudes. ———, 0.125 ms^{-2} r.m.s.; ·····, 0.25 ms^{-2} r.m.s.; –·–·–, 0.625 ms^{-2} r.m.s.; – – – –, 1.25 ms^{-2} r.m.s.

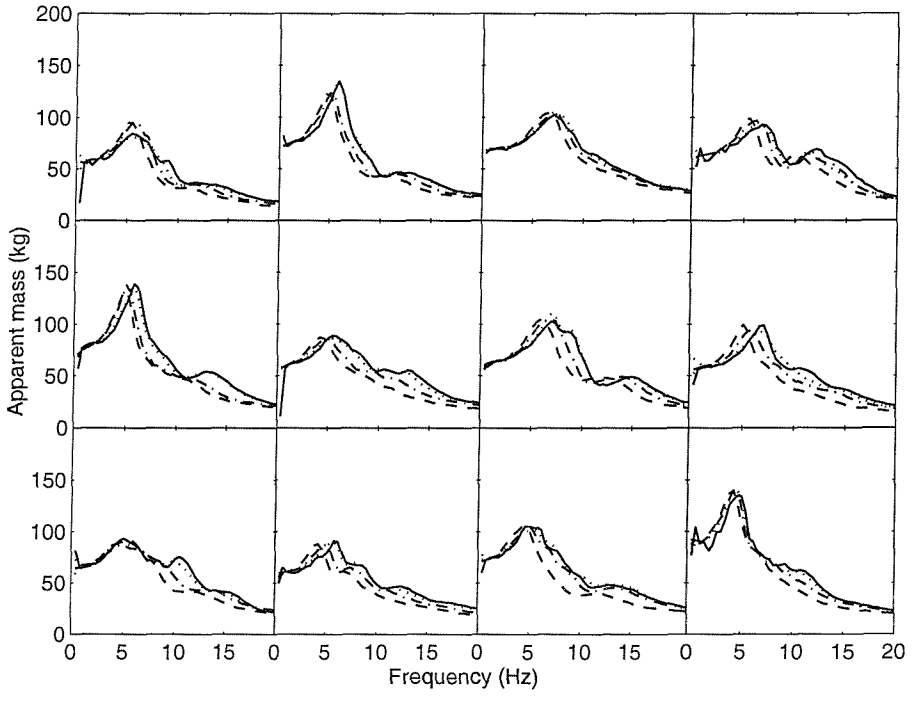

Figure B.2 Vertical apparent masses of 12 subjects measured on the seat with backrest in the maximum thigh contact posture at four vibration magnitudes. ———, 0.125 ms^{-2} r.m.s.; ·····, 0.25 ms^{-2} r.m.s.; –·–·–, 0.625 ms^{-2} r.m.s.; – – – –, 1.25 ms^{-2} r.m.s.

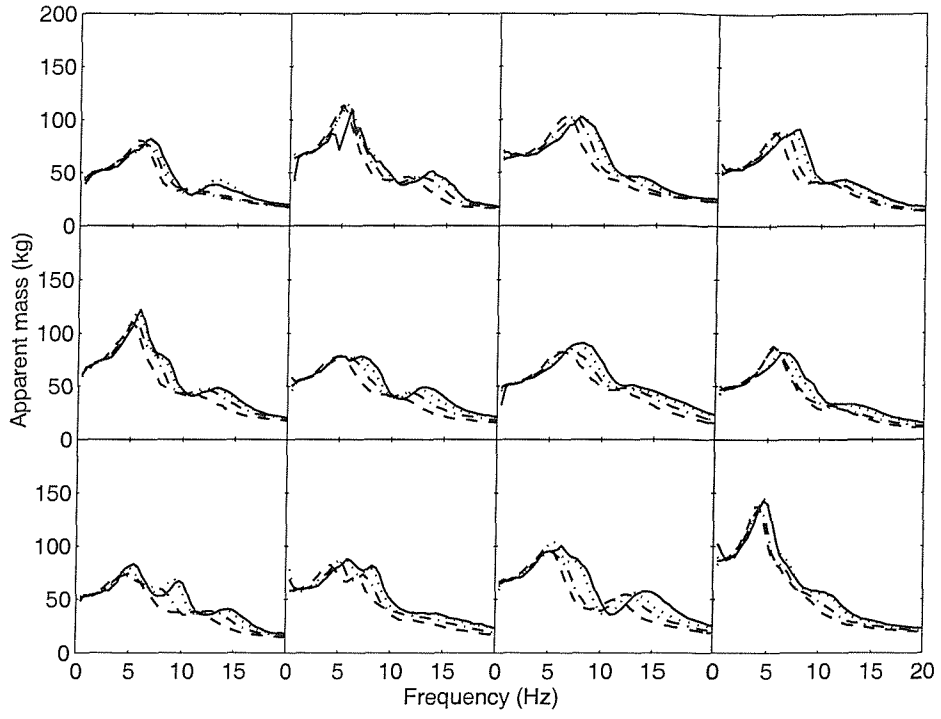

Figure B.3 Vertical apparent masses of 12 subjects measured on the seat with backrest in the average thigh contact posture at four vibration magnitudes. ———, 0.125 ms^{-2} r.m.s.; ·····, 0.25 ms^{-2} r.m.s.; –·–·–, 0.625 ms^{-2} r.m.s.; – – – –, 1.25 ms^{-2} r.m.s.

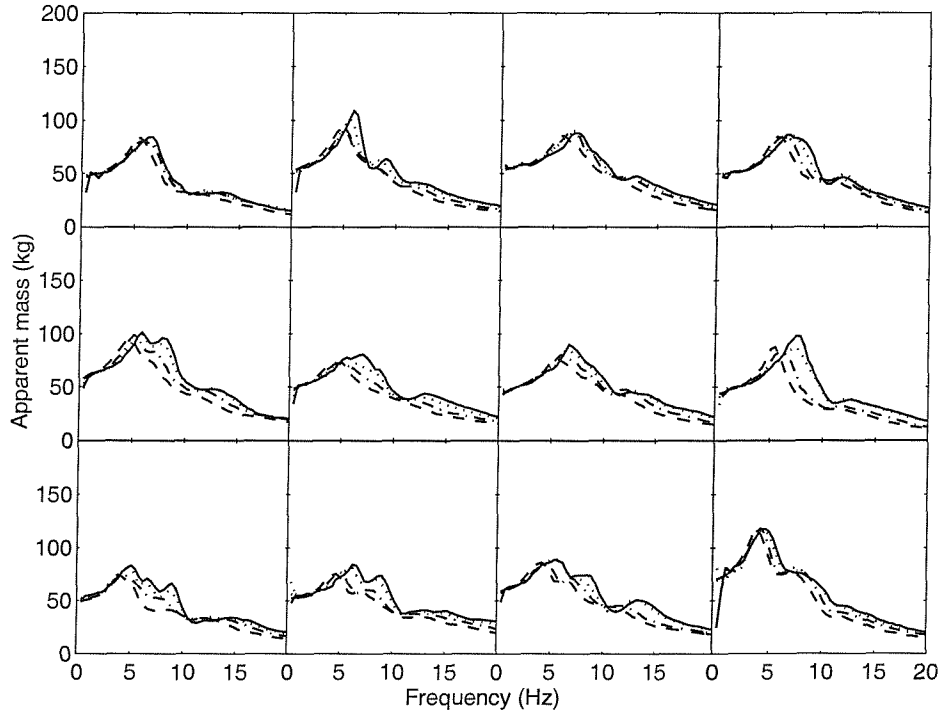

Figure B.4 Vertical apparent masses of 12 subjects measured on the seat with backrest in the minimum thigh contact posture at four vibration magnitudes. ———, 0.125 ms^{-2} r.m.s.; ·····, 0.25 ms^{-2} r.m.s.; –·–·–, 0.625 ms^{-2} r.m.s.; – – – –, 1.25 ms^{-2} r.m.s.

B.2.2 Fore-and-aft cross-axis apparent mass on the seat

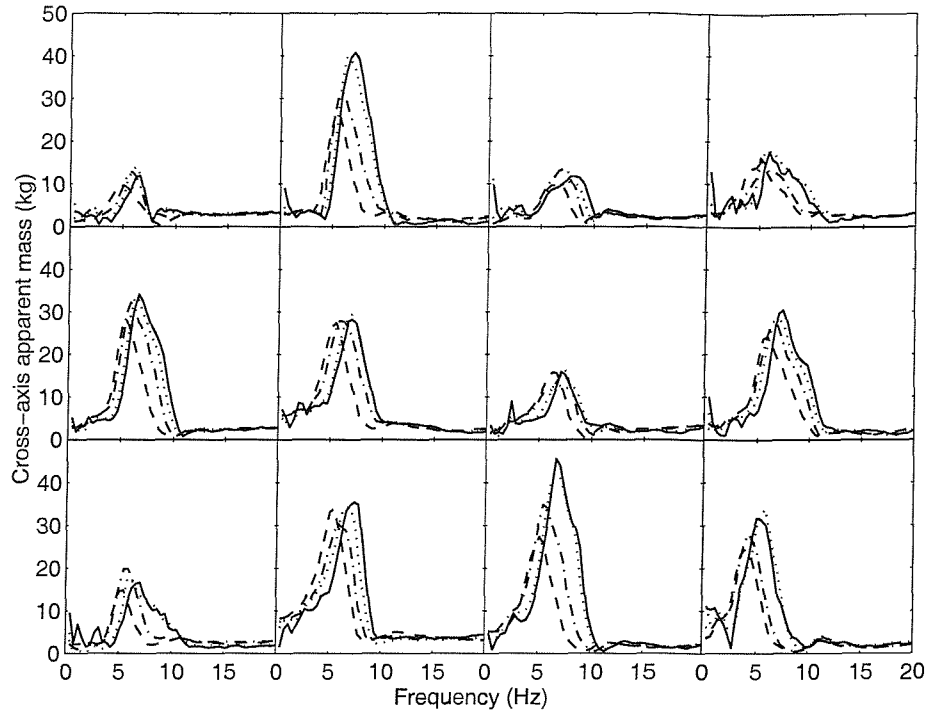

Figure B.5 Fore-and-aft cross-axis apparent masses of 12 subjects measured on the seat in the feet hanging posture at four vibration magnitudes. ———, 0.125 ms^{-2} r.m.s.; ·····, 0.25 ms^{-2} r.m.s.; –·–·–, 0.625 ms^{-2} r.m.s.; – – – –, 1.25 ms^{-2} r.m.s.

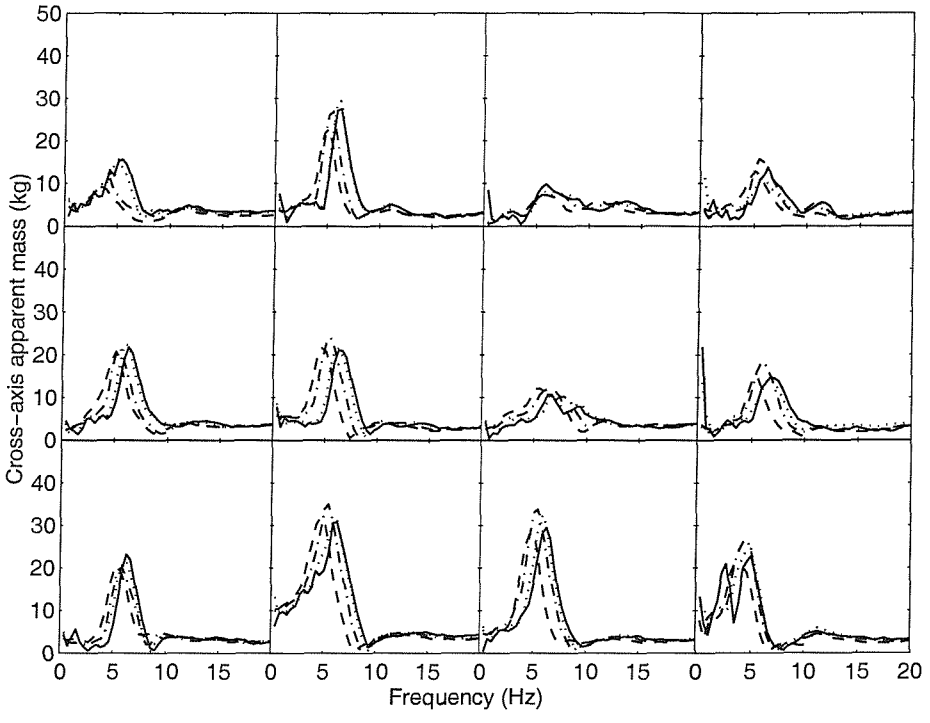

Figure B.6 Fore-and-aft cross-axis apparent masses of 12 subjects measured on the seat in the maximum thigh contact posture at four vibration magnitudes. ———, 0.125 ms^{-2} r.m.s.; ·····, 0.25 ms^{-2} r.m.s.; –·–·–, 0.625 ms^{-2} r.m.s.; – – – –, 1.25 ms^{-2} r.m.s.

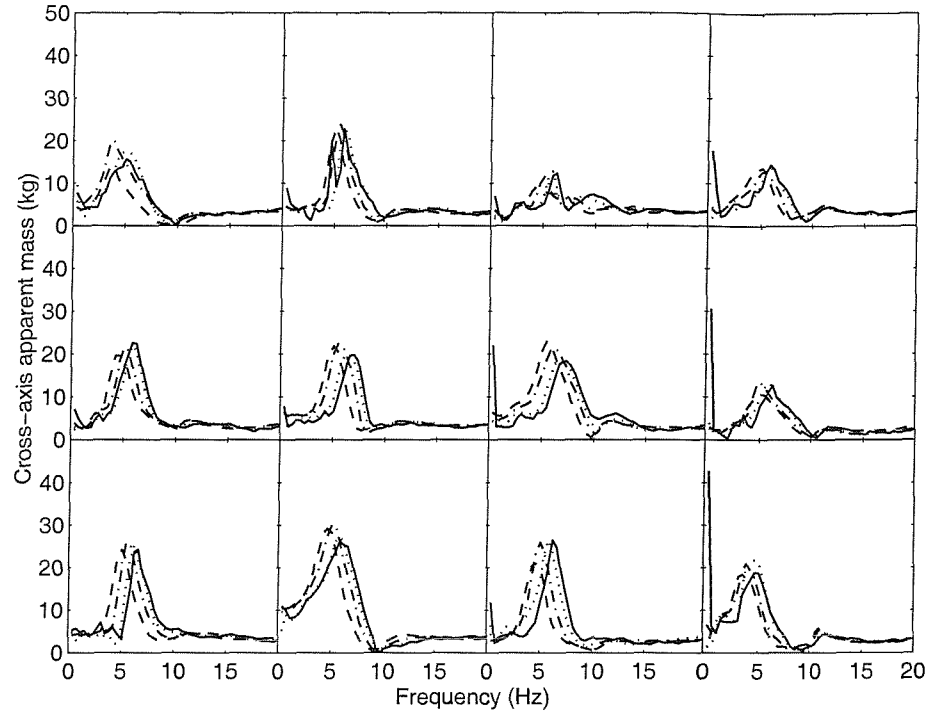

Figure B.7 Fore-and-aft cross-axis apparent masses of 12 subjects measured on the seat in the average thigh contact posture at four vibration magnitudes. ———, 0.125 ms^{-2} r.m.s.; ·····, 0.25 ms^{-2} r.m.s.; –·–·–, 0.625 ms^{-2} r.m.s.; – – – –, 1.25 ms^{-2} r.m.s.

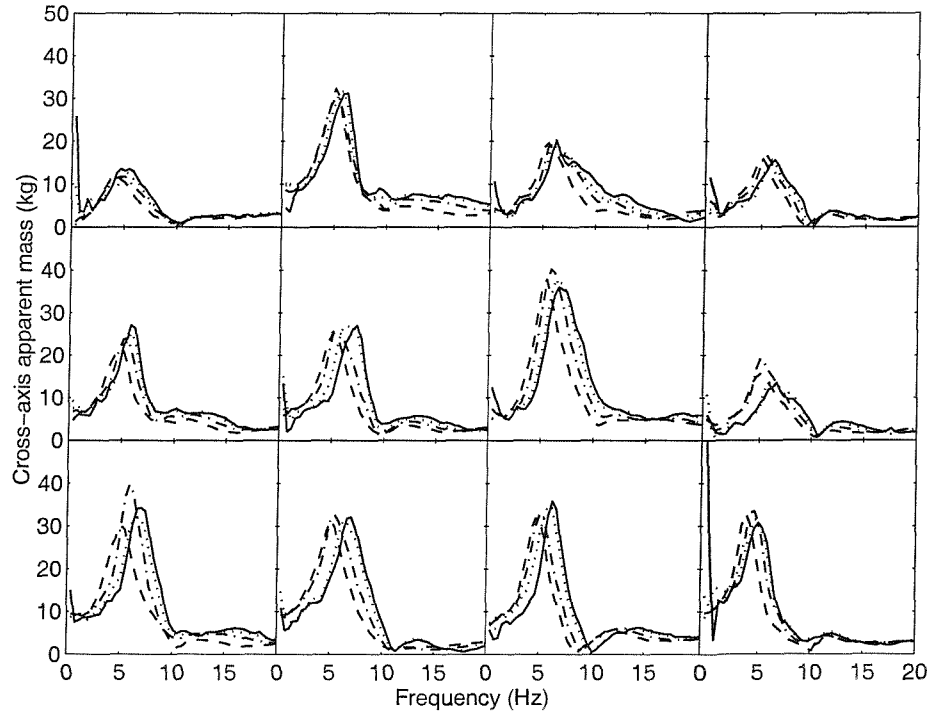

Figure B.8 Fore-and-aft cross-axis apparent masses of 12 subjects measured on the seat in the minimum thigh contact posture at four vibration magnitudes. ———, 0.125 ms^{-2} r.m.s.; ·····, 0.25 ms^{-2} r.m.s.; –·–·–, 0.625 ms^{-2} r.m.s.; – – – –, 1.25 ms^{-2} r.m.s.

B.2.3 Lateral cross-axis apparent mass on the seat

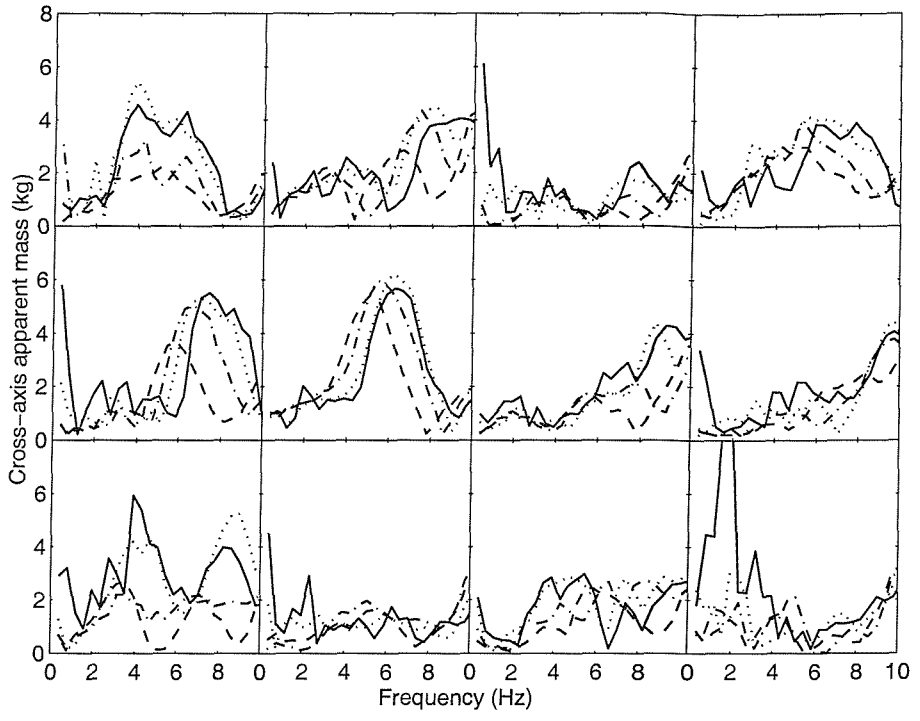

Figure B.9 Lateral cross-axis apparent masses of 12 subjects measured on the seat in the feet hanging posture at four vibration magnitudes. ———, 0.125 ms^{-2} r.m.s.; ·····, 0.25 ms^{-2} r.m.s.; –·–·–, 0.625 ms^{-2} r.m.s.; – – – –, 1.25 ms^{-2} r.m.s.

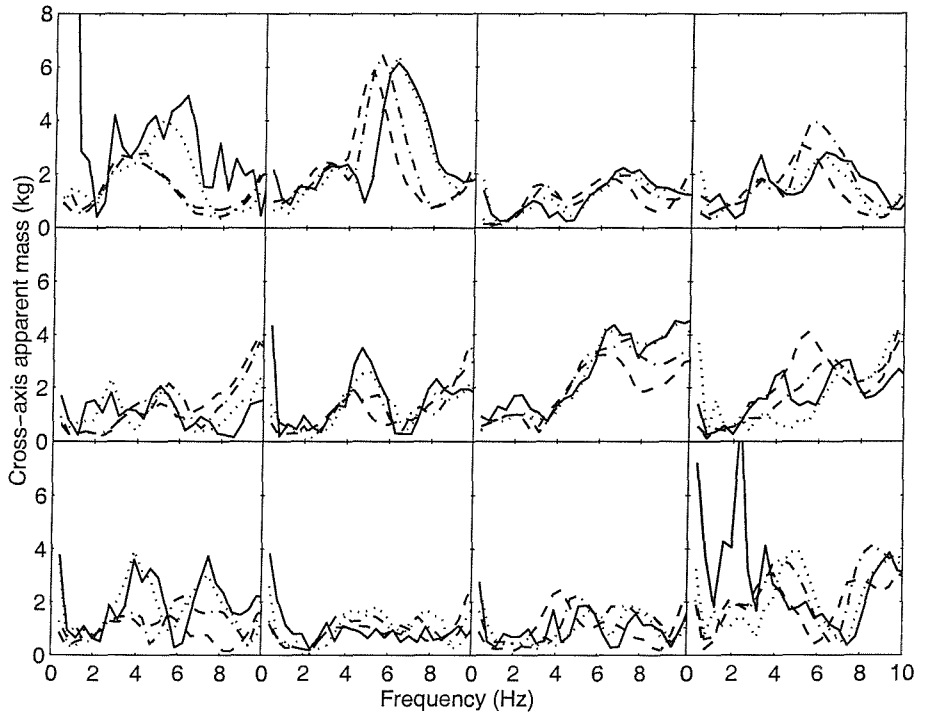

Figure B.10 Lateral cross-axis apparent masses of 12 subjects measured on the seat in the maximum thigh contact posture at four vibration magnitudes. ———, 0.125 ms^{-2} r.m.s.; ·····, 0.25 ms^{-2} r.m.s.; –·–·–, 0.625 ms^{-2} r.m.s.; – – – –, 1.25 ms^{-2} r.m.s.

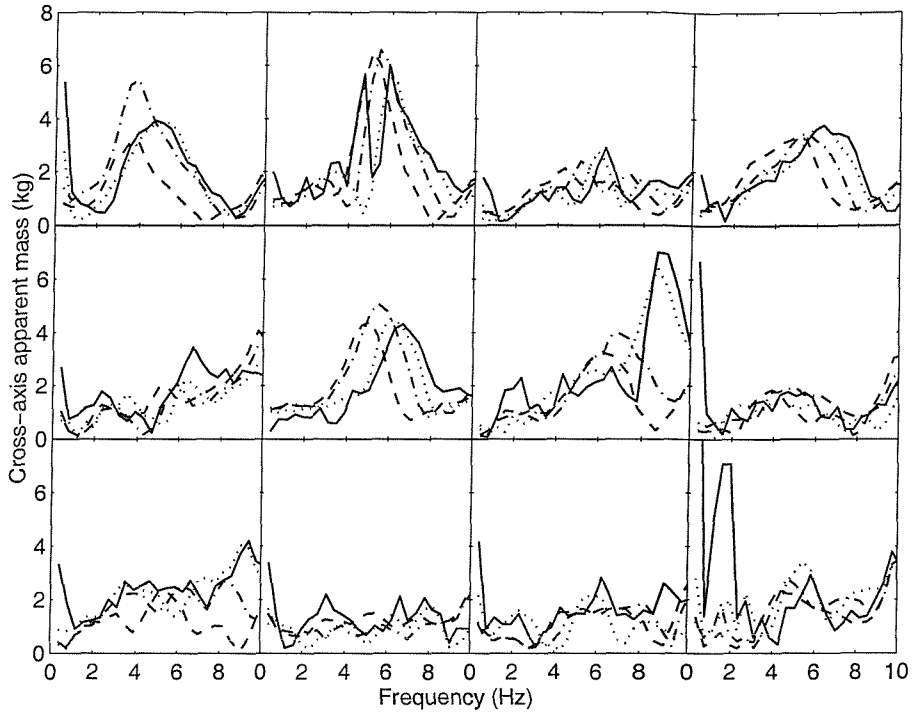

Figure B.11 Lateral cross-axis apparent masses of 12 subjects measured on the seat in the average thigh contact posture at four vibration magnitudes. ———, 0.125 ms^{-2} r.m.s.; ·····, 0.25 ms^{-2} r.m.s.; –·–·–, 0.625 ms^{-2} r.m.s.; – – – –, 1.25 ms^{-2} r.m.s.

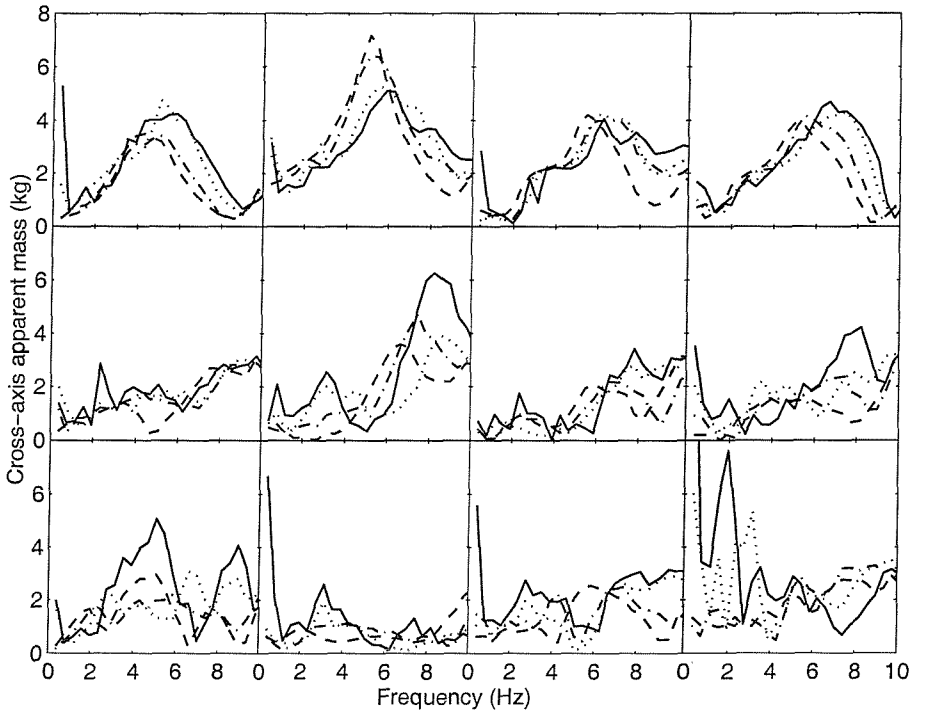

Figure B.12 Lateral cross-axis apparent masses of 12 subjects measured on the seat in the minimum thigh contact posture at four vibration magnitudes. ———, 0.125 ms^{-2} r.m.s.; ·····, 0.25 ms^{-2} r.m.s.; –·–·–, 0.625 ms^{-2} r.m.s.; – – – –, 1.25 ms^{-2} r.m.s.

B.2.4 Vertical apparent mass at the backrest

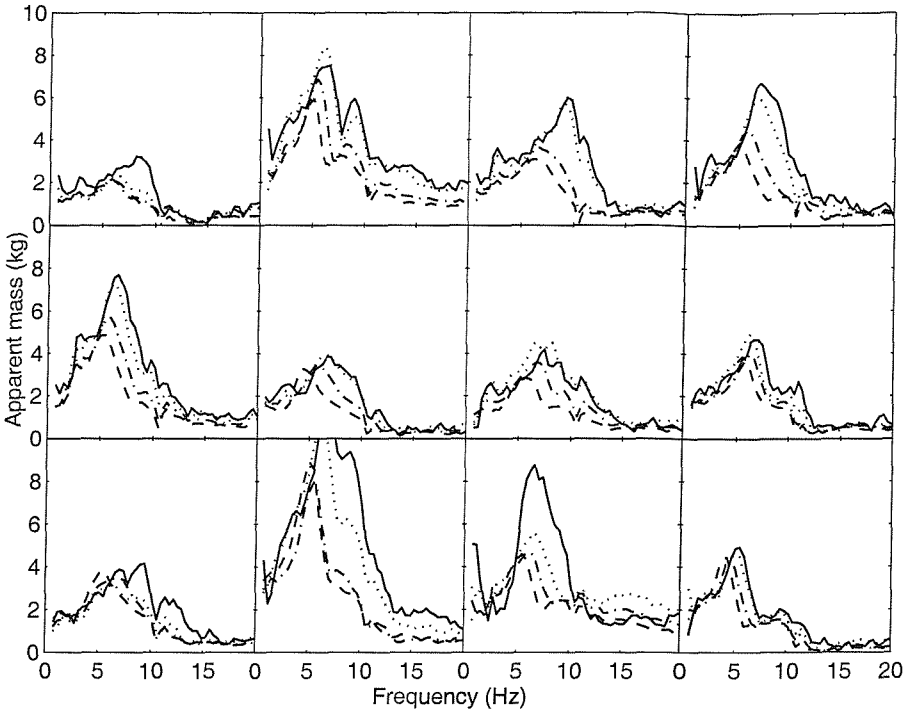

Figure B.13 Vertical apparent masses of 12 subjects measured at the back in the feet hanging posture at four vibration magnitudes. ———, 0.125 ms^{-2} r.m.s.; ·····, 0.25 ms^{-2} r.m.s.; –·–·–, 0.625 ms^{-2} r.m.s.; – – – –, 1.25 ms^{-2} r.m.s.

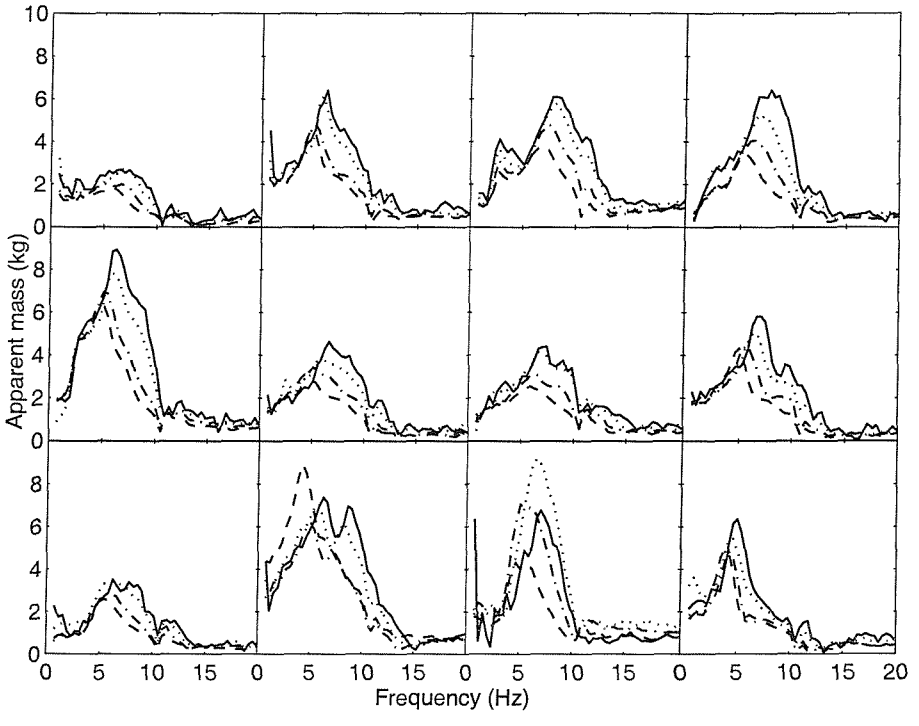

Figure B.14 Vertical apparent masses of 12 subjects measured at the back in the average thigh contact posture at four vibration magnitudes. ———, 0.125 ms^{-2} r.m.s.; ·····, 0.25 ms^{-2} r.m.s.; –·–·–, 0.625 ms^{-2} r.m.s.; – – – –, 1.25 ms^{-2} r.m.s.

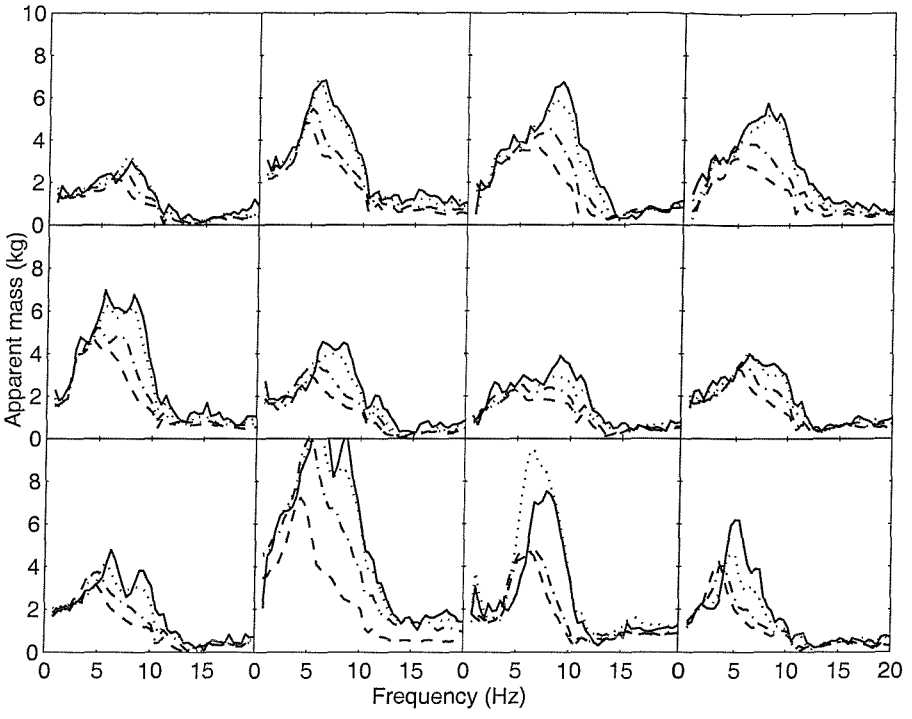

Figure B.15 Vertical apparent masses of 12 subjects measured at the back in the maximum thigh contact posture at four vibration magnitudes. ———, 0.125 ms^{-2} r.m.s.; ·····, 0.25 ms^{-2} r.m.s.; —·—·—, 0.625 ms^{-2} r.m.s.; – – – –, 1.25 ms^{-2} r.m.s.

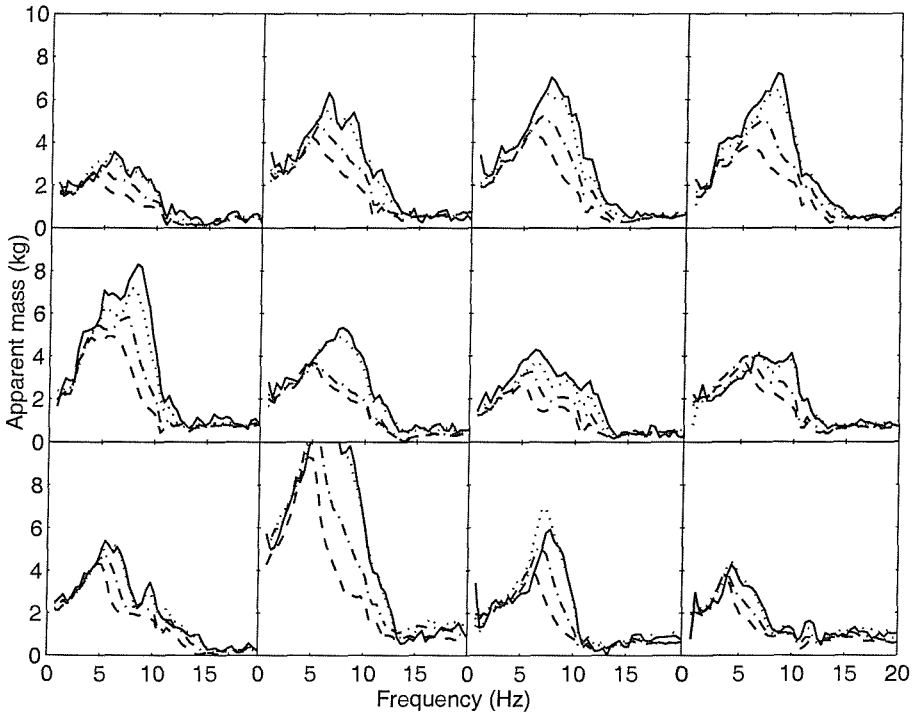

Figure B.16 Vertical apparent masses of 12 subjects measured at the back in the minimum thigh contact posture at four vibration magnitudes. ———, 0.125 ms^{-2} r.m.s.; ·····, 0.25 ms^{-2} r.m.s.; —·—·—, 0.625 ms^{-2} r.m.s.; – – – –, 1.25 ms^{-2} r.m.s.

B.2.5 Fore-and-aft cross-axis apparent mass at the back

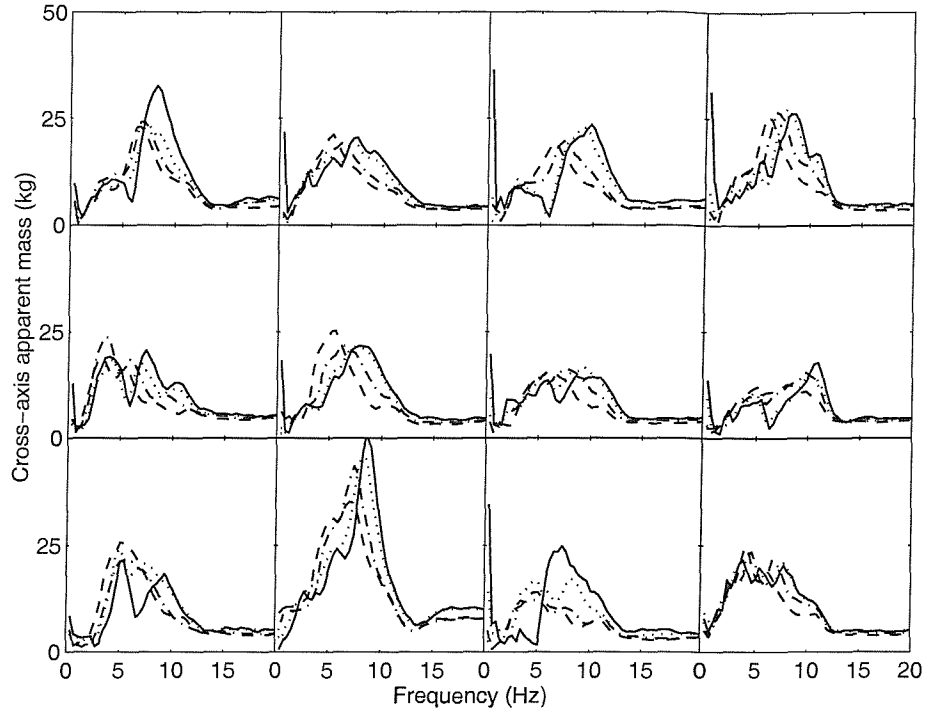

Figure B.17 Fore-and-aft cross-axis apparent masses of 12 subjects measured at the back in the feet hanging posture at four vibration magnitudes. ———, 0.125 ms^{-2} r.m.s.; ·····, 0.25 ms^{-2} r.m.s.; –·–·–, 0.625 ms^{-2} r.m.s.; – – – –, 1.25 ms^{-2} r.m.s.

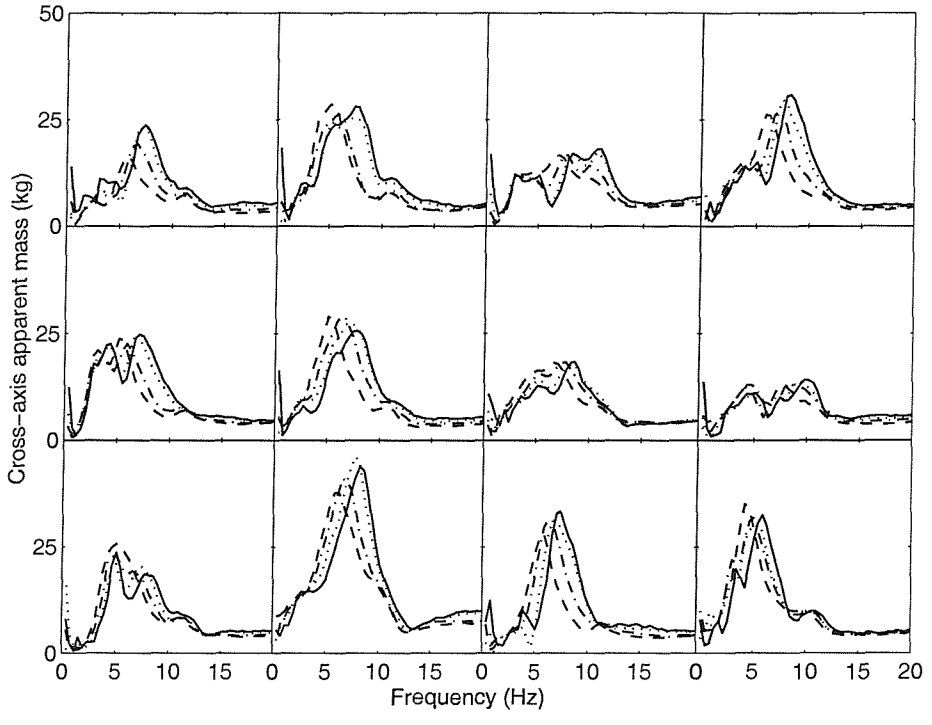

Figure B.18 Fore-and-aft cross-axis apparent masses of 12 subjects measured at the back in the maximum thigh contact posture at four vibration magnitudes. ———, 0.125 ms^{-2} r.m.s.; ·····, 0.25 ms^{-2} r.m.s.; –·–·–, 0.625 ms^{-2} r.m.s.; – – – –, 1.25 ms^{-2} r.m.s.

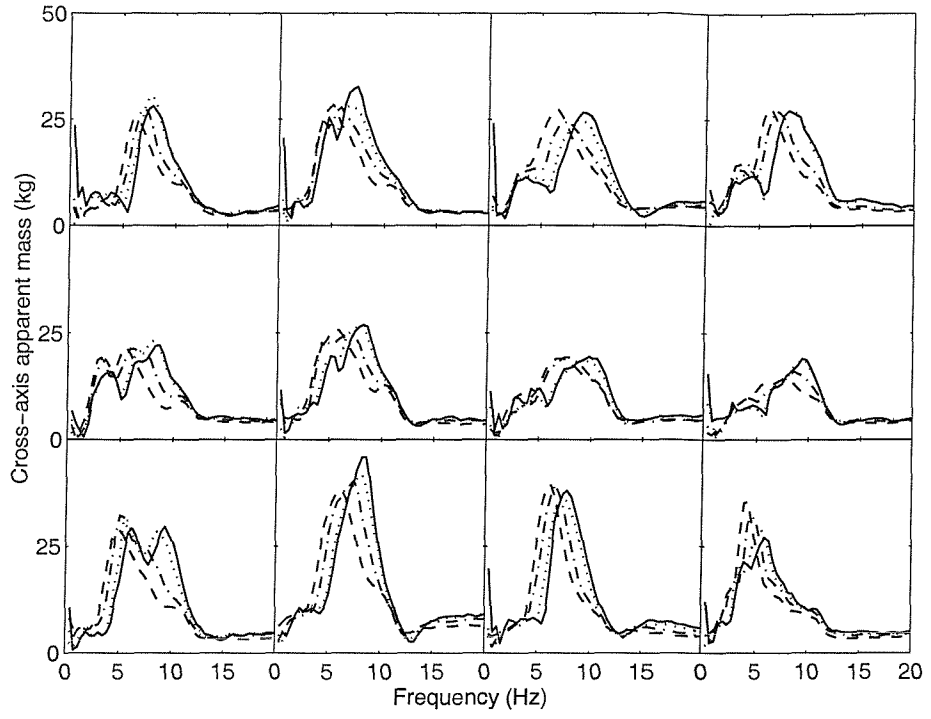

Figure B.19 Fore-and-aft cross-axis apparent masses of 12 subjects measured at the back in the average thigh contact posture at four vibration magnitudes. ———, 0.125 ms^{-2} r.m.s.; ·····, 0.25 ms^{-2} r.m.s.; —·—·—, 0.625 ms^{-2} r.m.s.; – – – –, 1.25 ms^{-2} r.m.s.

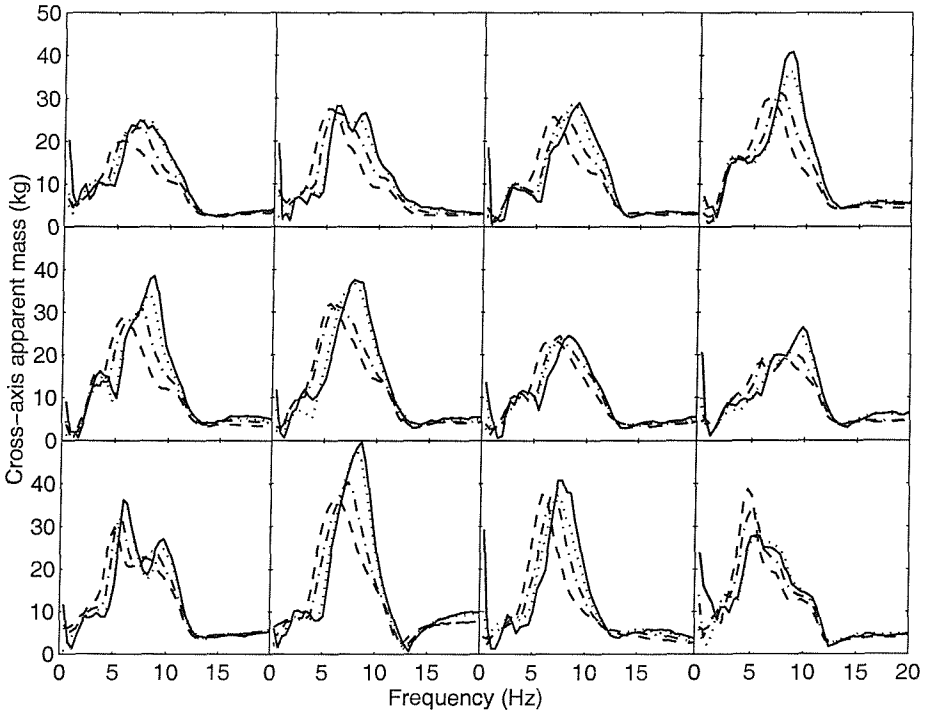

Figure B.20 Fore-and-aft cross-axis apparent masses of 12 subjects measured at the back in the minimum thigh contact posture at four vibration magnitudes. ———, 0.125 ms^{-2} r.m.s.; ·····, 0.25 ms^{-2} r.m.s.; —·—·—, 0.625 ms^{-2} r.m.s.; – – – –, 1.25 ms^{-2} r.m.s.

B.2.6 Lateral cross-axis apparent mass at the back

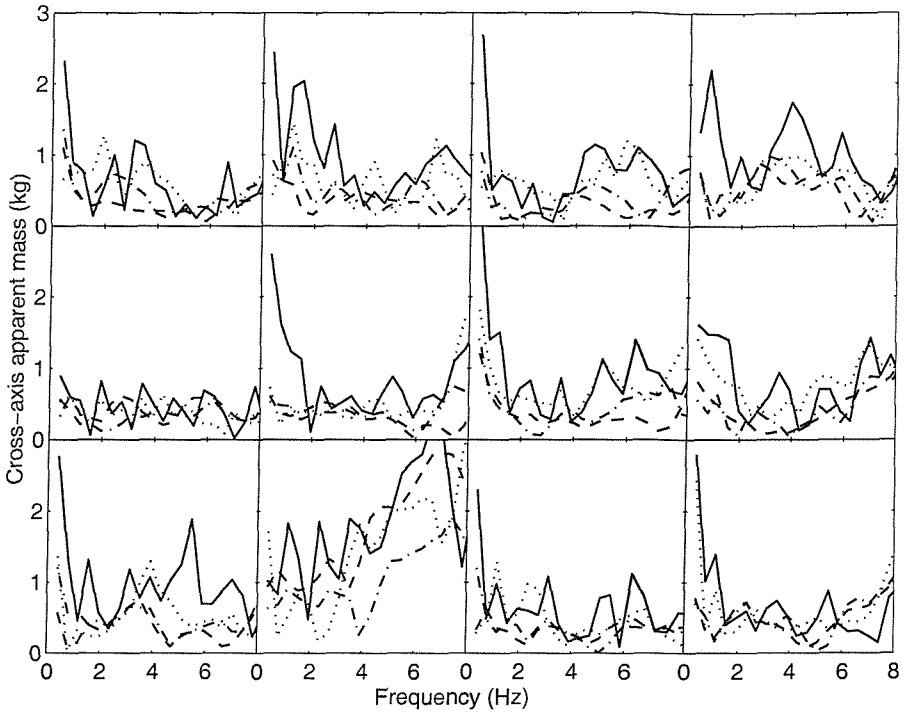

Figure B.21 Lateral cross-axis apparent mass measured at the back of 12 subjects in the feet hanging posture at four vibration magnitude. ———, 0.125 ms^{-2} r.m.s.; ·····, 0.25 ms^{-2} r.m.s.; –·–·–, 0.625 ms^{-2} r.m.s.; – – – –, 1.25 ms^{-2} r.m.s.

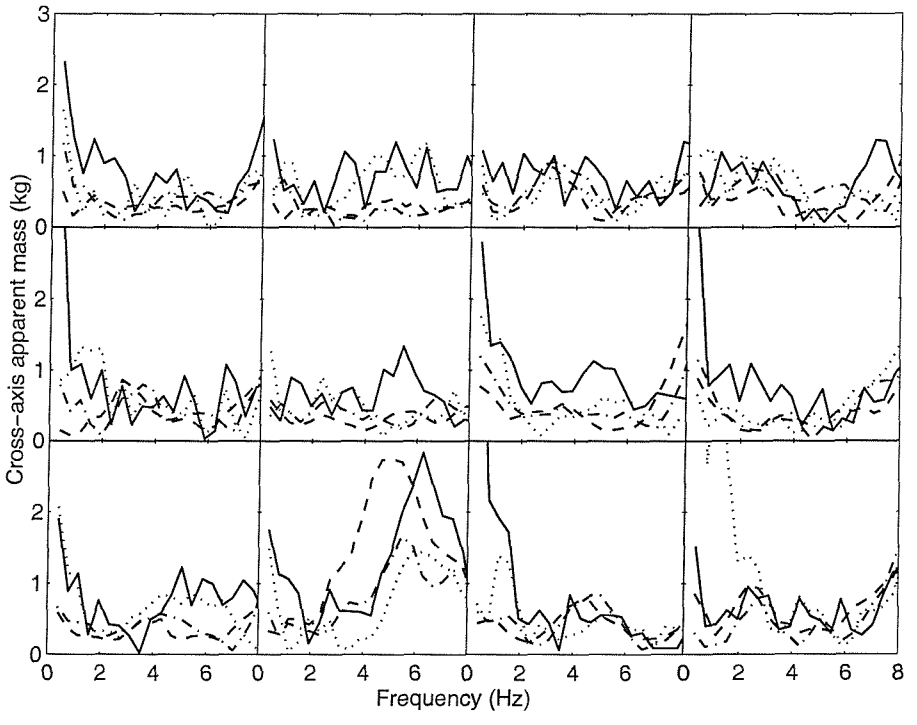

Figure B.22 Lateral cross-axis apparent mass measured at the back of 12 subjects in the maximum thigh contact posture at four vibration magnitude. ———, 0.125 ms^{-2} r.m.s.; ·····, 0.25 ms^{-2} r.m.s.; –·–·–, 0.625 ms^{-2} r.m.s.; – – – –, 1.25 ms^{-2} r.m.s.

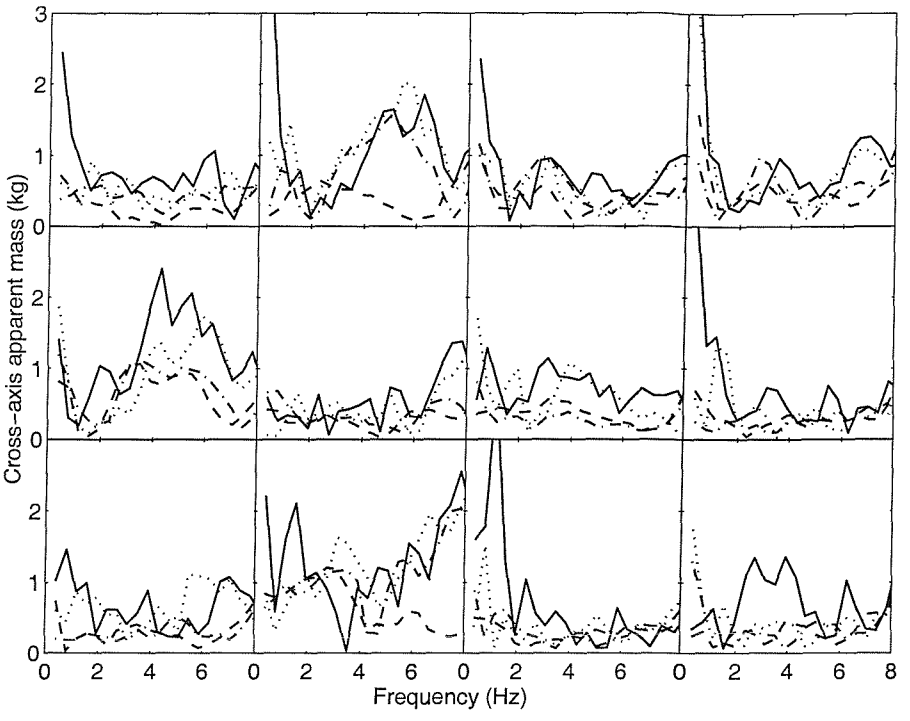

Figure B.23 Lateral cross-axis apparent mass measured at the back of 12 subjects in the average thigh contact posture at four vibration magnitude. ———, 0.125 ms^{-2} r.m.s.; ·····, 0.25 ms^{-2} r.m.s.; –·–·–, 0.625 ms^{-2} r.m.s.; – – – –, 1.25 ms^{-2} r.m.s.

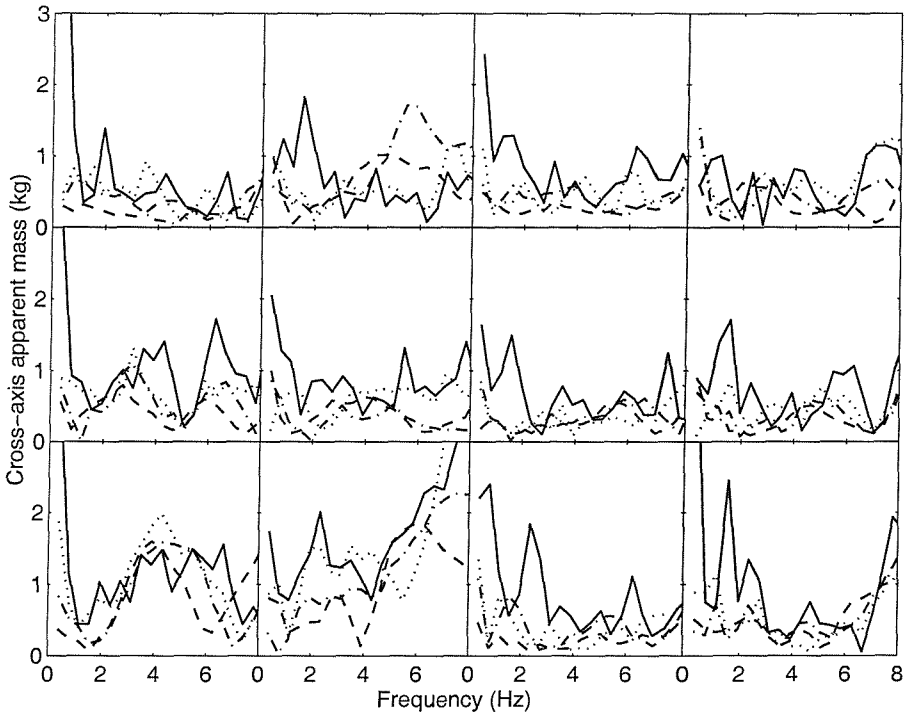

Figure B.24 Lateral cross-axis apparent mass measured at the back of 12 subjects in the minimum thigh contact posture at four vibration magnitude. ———, 0.125 ms^{-2} r.m.s.; ·····, 0.25 ms^{-2} r.m.s.; –·–·–, 0.625 ms^{-2} r.m.s.; – – – –, 1.25 ms^{-2} r.m.s.

B.2.7 Coherencies of the fore-and-aft cross-axis apparent mass at the back

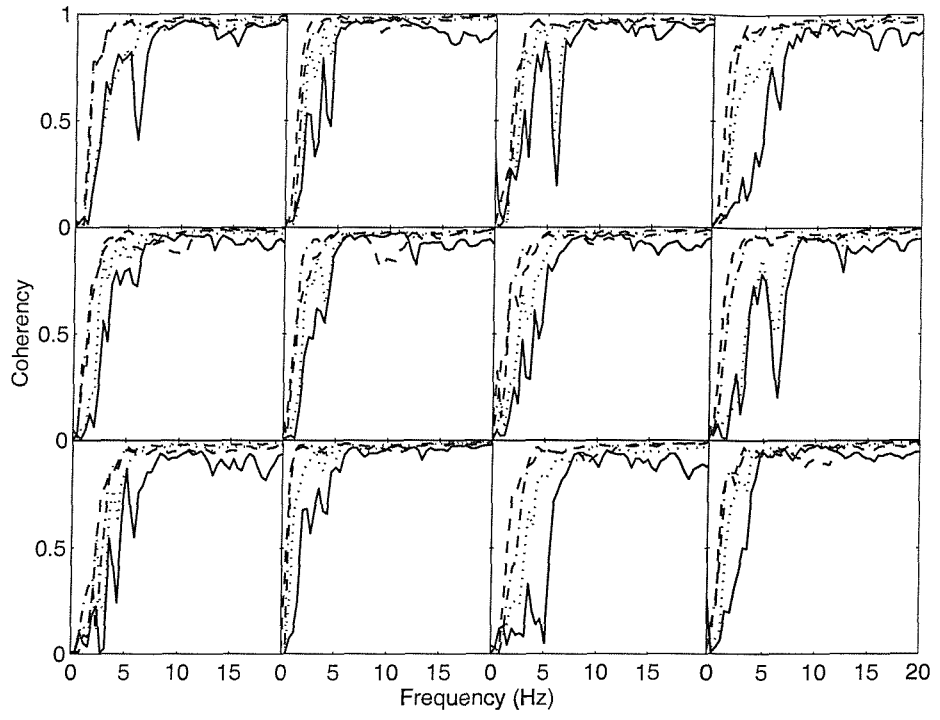

Figure B.25 Coherencies of fore-and-aft cross-axis apparent mass measured at the backs of 12 subjects in the feet hanging posture at four vibration magnitudes. ———, 0.125 ms^{-2} r.m.s.; ·····, 0.25 ms^{-2} r.m.s.; –·–·–, 0.625 ms^{-2} r.m.s.; – – – –, 1.25 ms^{-2} r.m.s.

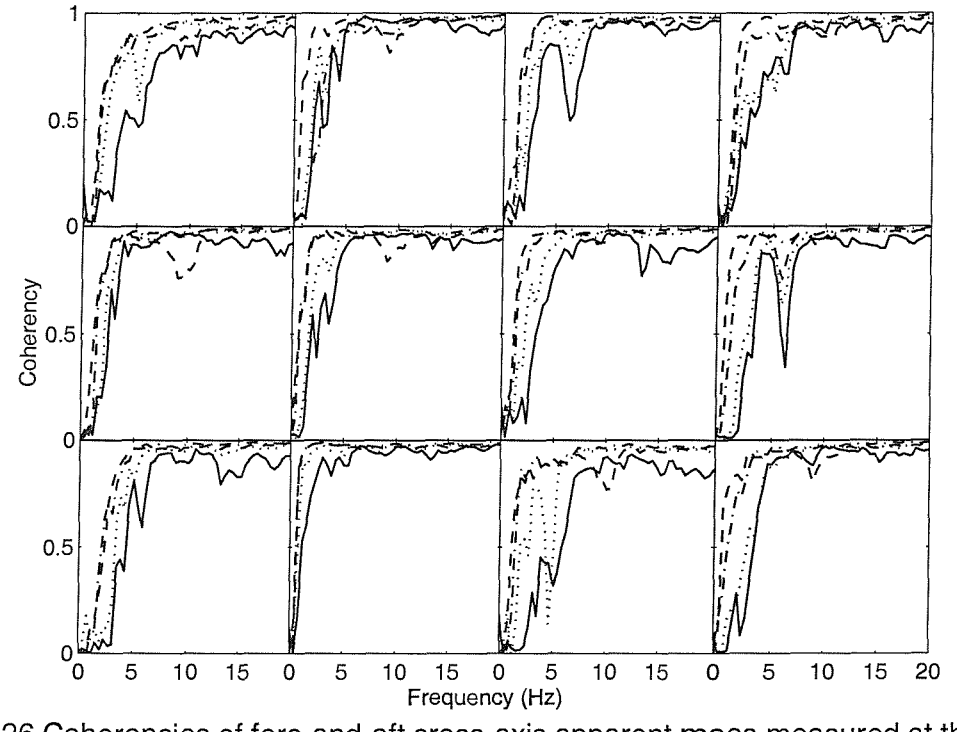

Figure B.26 Coherencies of fore-and-aft cross-axis apparent mass measured at the backs of 12 subjects in the maximum thigh contact posture at four vibration magnitudes. ———, 0.125 ms^{-2} r.m.s.; ·····, 0.25 ms^{-2} r.m.s.; –·–·–, 0.625 ms^{-2} r.m.s.; – – – –, 1.25 ms^{-2} r.m.s.

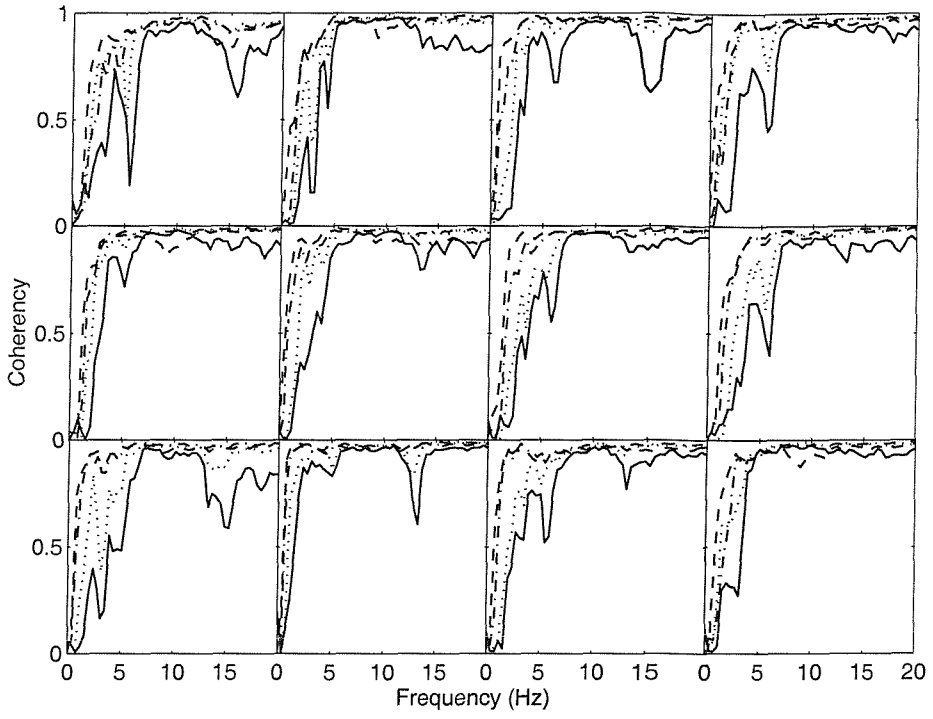

Figure B.27 Coherencies of fore-and-aft cross-axis apparent mass measured at the backs of 12 subjects in the average thigh contact posture at four vibration magnitudes. ———, 0.125 ms^{-2} r.m.s.; ·····, 0.25 ms^{-2} r.m.s.; –·–·–, 0.625 ms^{-2} r.m.s.; – – – –, 1.25 ms^{-2} r.m.s.

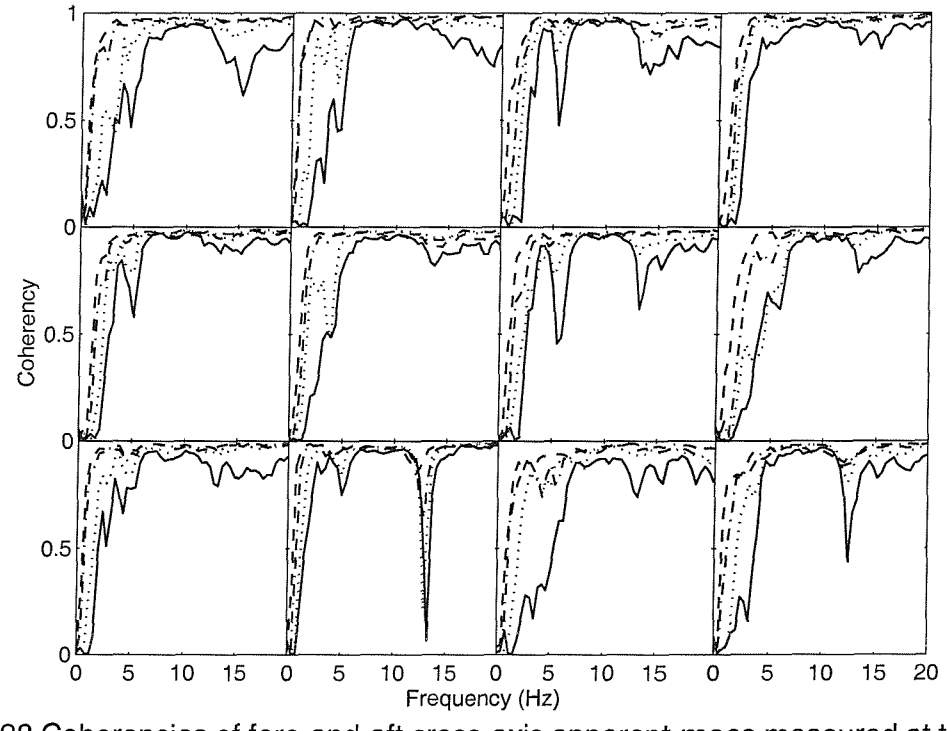

Figure B.28 Coherencies of fore-and-aft cross-axis apparent mass measured at the backs of 12 subjects in the minimum thigh contact posture at four vibration magnitudes. ———, 0.125 ms^{-2} r.m.s.; ·····, 0.25 ms^{-2} r.m.s.; –·–·–, 0.625 ms^{-2} r.m.s.; – – – –, 1.25 ms^{-2} r.m.s.

APPENDIX C

INDIVIDUAL DATA: FORE-AND-AFT EXCITATION WITHOUT A BACKREST (CHAPTER 6)

APPENDIX C Fore-and-aft excitation without backrest (Chapter 6)

C.1 Characteristics of subjects

Table C.1 Characteristics of subjects used in the first experiment described in Chapter 6

Subject No.	Mass (kg)	Stature (m)	Age (year)
1	67.0	1.75	24
2	88.0	1.82	38
3	79.0	1.86	47
4	70.0	1.69	41
5	88.0	1.72	29
6	71.0	1.75	26
7	76.0	1.77	34
8	63.0	1.68	31
9	72.0	1.84	27
10	65.0	1.91	24
11	85.0	1.85	26
12	106.0	1.86	26

Table C.2 Characteristics of subjects used in the second experiment described in Chapter 6

Subject No.	Mass (kg)	Stature (m)	Age (year)
1	56.0	1.63	21
2	65.0	1.70	32
3	87.0	1.83	38
4	73.0	1.70	25
5	75.0	1.68	26
6	72.0	1.75	26

C.2 Instructions given to the subjects prior exposure to vibration

- This experiment is designed to measure the forces on the seat in three axes (vertical, fore-and-aft and lateral) during whole-body fore-and-aft vibration.

- You will be seated on a rigid seat and exposed to random fore-and-aft vibration at different vibration magnitudes and in four different postures.

The adopted postures will be:

a. Normal sitting while feet hanging in the air.
b. Sitting with the upper leg horizontal, the lower legs vertical, and the feet supported on the footrest mounted on the vibrating table. Subject must be barefooted.
c. Sitting with minimum thigh contact with the seat by raising the footrest while keeping the lower legs in a vertical position. Subject must be barefooted.
d. Sitting with maximum thigh contact such that the heels are just touching the footrest. The lower legs are also vertical in this case. Subject must be barefooted.

- In each of the sitting conditions mentioned above you will be exposed to four random vibrations. The experimenter will show you the order in which the above conditions will be adopted.

- During the exposure to vibration, you can stop the vibration at any time by pressing the red STOP button that you will be holding throughout the experiment.

Thank you for taking part in this experiment.

C.3 Individual results

C.3.1 Fore-and-aft apparent mass on the seat

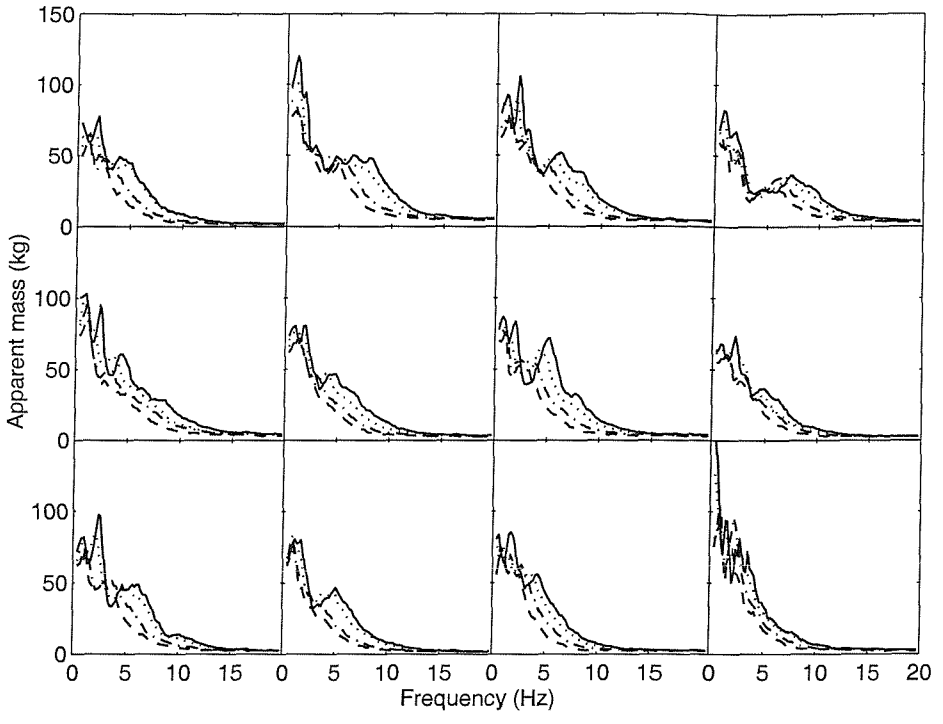

Figure C.1 Fore-and-aft apparent masses of 12 subjects measured on the seat in the feet hanging posture at four vibration magnitudes. ———, 0.125 ms^{-2} r.m.s.; ·····, 0.25 ms^{-2} r.m.s.; —·—·—, 0.625 ms^{-2} r.m.s.; – – – –, 1.25 ms^{-2} r.m.s.

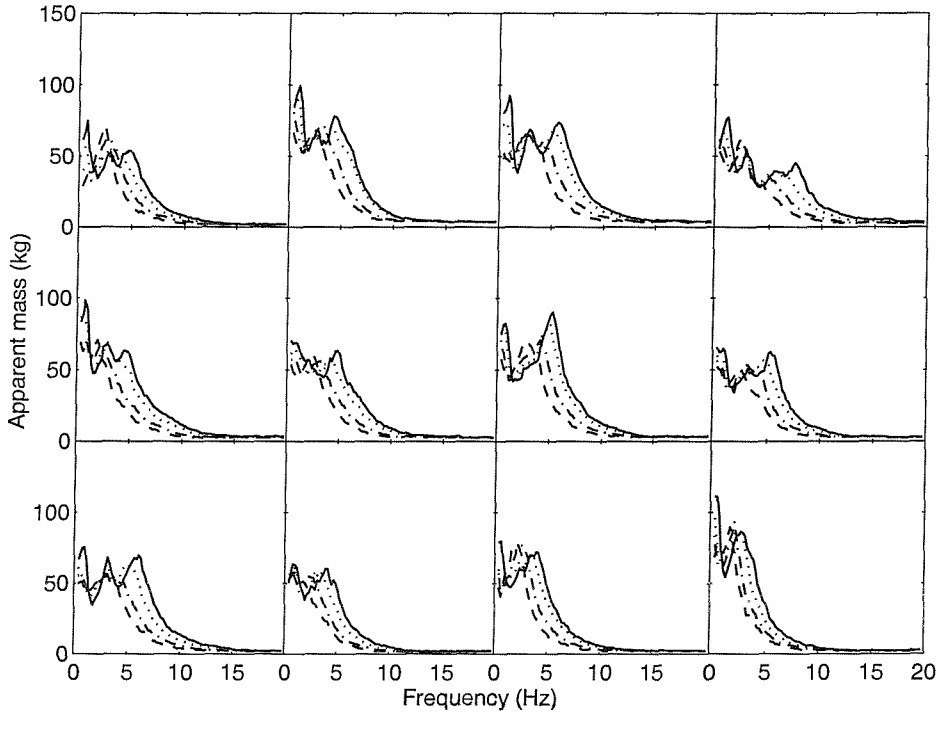

Figure C.2 Fore-and-aft apparent masses of 12 subjects measured on the seat in the maximum thigh contact posture at four vibration magnitudes. ———, 0.125 ms^{-2} r.m.s.; ·····, 0.25 ms^{-2} r.m.s.; —·—·—, 0.625 ms^{-2} r.m.s.; – – – –, 1.25 ms^{-2} r.m.s.

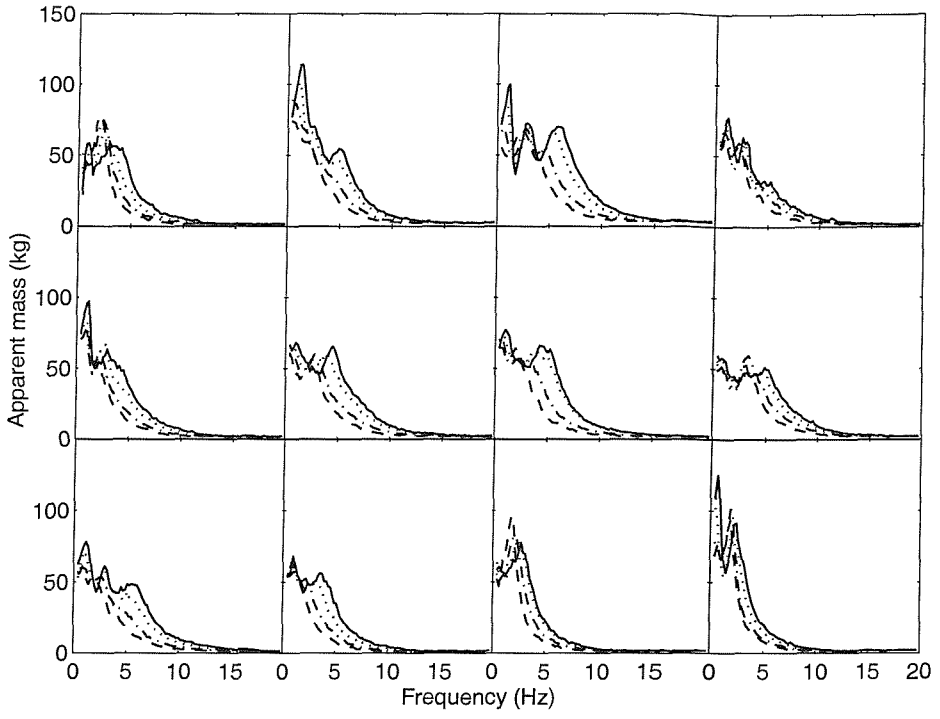

Figure C.3 Fore-and-aft apparent masses of 12 subjects measured on the seat in the average thigh contact posture at four vibration magnitudes. ———, 0.125 ms^{-2} r.m.s.; ·····, 0.25 ms^{-2} r.m.s.; –·–·–, 0.625 ms^{-2} r.m.s.; – – – –, 1.25 ms^{-2} r.m.s.

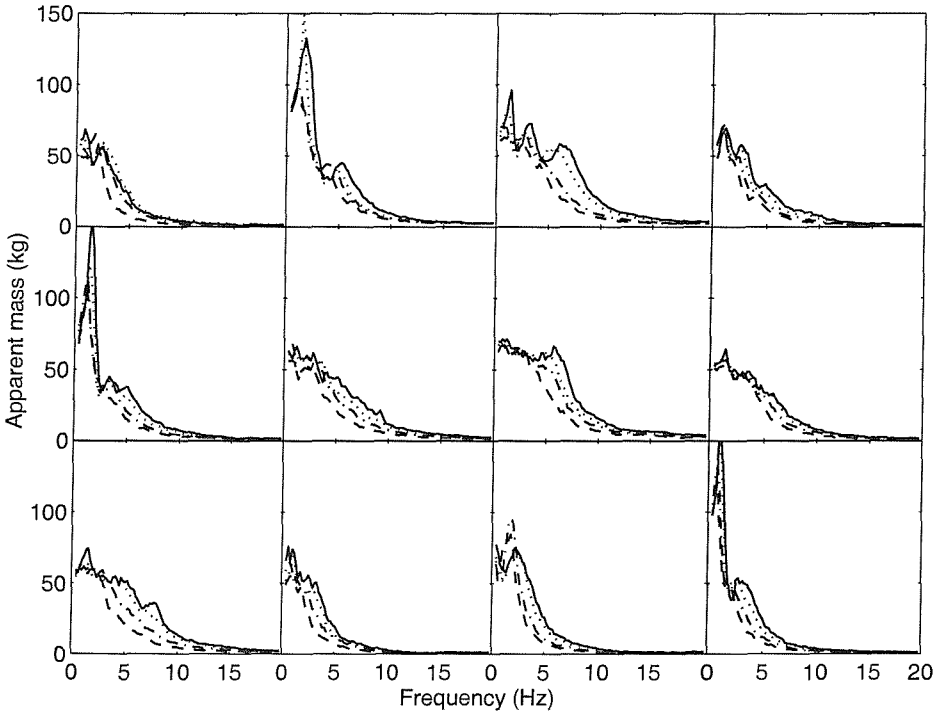

Figure C.4 Fore-and-aft apparent masses of 12 subjects measured on the seat in the minimum thigh contact posture at four vibration magnitudes. ———, 0.125 ms^{-2} r.m.s.; ·····, 0.25 ms^{-2} r.m.s.; –·–·–, 0.625 ms^{-2} r.m.s.; – – – –, 1.25 ms^{-2} r.m.s.

Table C.3 Peak frequencies in the apparent masses of 12 subjects adopting the feet hanging posture and exposed to horizontal vibration at four vibration magnitudes.

Subject	Vibration Magnitude (ms^{-2} r.m.s.)	Mode 1 (Below 1 Hz)	Mode 2 (Between1 and 3 Hz)	Mode 3 (Above 3 Hz)
1	0.125	0.39	1.95	3.91
	0.250	0.78	1.56, 2.73	4.49
	0.625	0.98	2.54	-
	1.250	-	1.17, 1.95	-
2	0.125	0.98	1.76, 2.54	4.69, 6.25, 8.00
	0.250	0.98	2.34	4.10
	0.625	0.59	1.17	5.27
	1.250	0.78	-	4.69
3	0.125	0.98	2.15	3.13, 6.05
	0.250	0.98	1.95, 2.73	5.47
	0.625	0.59	1.17, 2.73	4.69
	1.250	-	1.17, 2.34	-
4	0.125	0.78	1.95	4.49, 7.23
	0.250	0.78	1.56, 2.34	7.23
	0.625	0.59	1.17, 2.15	6.25
	1.250	0.98	2.15	5.66
5	0.125	0.98	2.34	4.49
	0.250	0.78	1.76	3.32
	0.625	0.98	-	3.32
	1.250	-	1.17	-
6	0.125	0.98	1.95	4.69
	0.250	0.98	1.76	3.71
	0.625	-	1.37	-
	1.250	-	1.17	-
7	0.125	0.78	1.95	5.08, 7.81
	0.250	0.78	1.56	4.30
	0.625	0.59	1.17, 2.93	-
	1.250	0.98	2.54	-
8	0.125	0.78	2.15	4.69
	0.250	0.78	2.15	5.08
	0.625	-	1.17, 2.73	-
	1.250	-	1.17, 2.73	-
9	0.125	0.98	2.34	4.69, 5.86
	0.250	0.98	1.95	5.08
	0.625	-	1.17	3.32
	1.250	-	1.17	-
10	0.125	-	1.17, 1.76	5.08
	0.250	-	1.17	-
	0.625	0.98	-	-
	1.250	0.98	-	-
11	0.125	0.59	1.76	4.30
	0.250	-	1.17, 2.54	3.52
	0.625	0.98	1.95, 2.73	-
	1.250	0.78	1.76	-
12	0.125	0.39	1.37, 2.73	3.52
	0.250	0.39	1.37, 2.34	-
	0.625	0.98	2.15	-
	1.250	0.78	1.95	-

Table C.4 Peak frequencies in the apparent masses of 12 subjects adopting the maximum thigh contact posture and exposed to horizontal vibration at four vibration magnitudes.

Subject	Vibration Magnitude (ms^{-2} r.m.s.)	Mode 1 (Below 1 Hz)	Mode 2 (Between1 and 3 Hz)	Mode 3 (Above 3 Hz)
1	0.125	0.78	2.73	4.88
	0.250	0.39	2.93	-
	0.625	-	2.73	-
	1.250	-	2.34	-
2	0.125	0.98	2.54	4.30
	0.250	0.78	2.34	4.10
	0.625	-	-	3.13
	1.250	-	2.73	-
3	0.125	0.98	2.93	5.66
	0.250	0.59	2.93	5.08
	0.625	0.78	2.73	4.10
	1.250	-	2.93	-
4	0.125	-	1.17, 2.73	5.47, 7.42
	0.250	0.78	2.93	5.47
	0.625	-	2.34	4.88
	1.250	-	2.34	4.30
5	0.125	0.78	2.93	4.69
	0.250	0.78	2.93	-
	0.625	0.59	2.34	-
	1.250	0.98	1.95	-
6	0.125	0.78	1.95	4.88
	0.250	0.78	-	4.10
	0.625	0.78	-	3.13
	1.250	-	2.34	-
7	0.125	0.78	2.54	5.27
	0.250	0.59	2.73	4.88
	0.625	-	-	4.10
	1.250	-	2.93	-
8	0.125	0.98	-	3.13, 5.27
	0.250	0.98	-	3.13, 4.69
	0.625	0.78	-	3.13
	1.250	0.78	2.54	-
9	0.125	0.98	-	3.13, 6.05
	0.250	0.39	-	3.13, 5.08
	0.625	0.78	-	3.13
	1.250	0.78	2.15, 2.93	-
10	0.125	0.78	2.54	3.91
	0.250	0.98	2.93	3.52
	0.625	0.78	2.34	-
	1.250	0.78	1.76	-
11	0.125	0.59	2.34	3.32
	0.250	0.78	2.34	3.52
	0.625	-	2.54	-
	1.250	-	2.15	-
12	0.125	0.39	2.73	-
	0.250	0.39	2.34	-
	0.625	-	2.15	-
	1.250	0.78	1.76	-

Table C.5 Peak frequencies in the apparent masses of 12 subjects adopting the average thigh contact posture and exposed to horizontal vibration at four vibration magnitudes.

Subject	Vibration Magnitude (ms^{-2} r.m.s.)	Mode 1 (Below 1 Hz)	Mode 2 (Between1 and 3 Hz)	Mode 3 (Above 3 Hz)
1	0.125	0.98	2.93	-
	0.250	0.78	2.34	-
	0.625	0.59	2.34	-
	1.250	-	1.95	-
2	0.125	-	1.37, 2.34	4.88
	0.250	-	1.17, 2.15	4.69
	0.625	0.59	-	-
	1.250	-	-	-
3	0.125	-	1.17, 2.93	5.86
	0.250	0.98	2.93	5.08
	0.625	0.59	2.73	4.69
	1.250	-	2.54	-
4	0.125	-	1.17, 2.54	4.69
	0.250	0.98	2.73	4.88
	0.625	0.78	2.15	-
	1.250	0.78	2.15	-
5	0.125	-	1.17, 2.93	-
	0.250	0.78	2.73	-
	0.625	0.78	2.15	-
	1.250	0.98	1.76	-
6	0.125	0.98	-	4.49
	0.250	0.98	-	3.91
	0.625	-	2.73	-
	1.250	-	1.17, 2.54	-
7	0.125	0.98	-	4.30
	0.250	0.78	-	4.10
	0.625	0.59	2.34	-
	1.250	0.59	1.95	-
8	0.125	0.78	-	3.13, 5.08
	0.250	0.78	2.93	4.49
	0.625	-	-	3.32
	1.250	0.78	-	3.13
9	0.125	-	1.17, 2.93	5.47
	0.250	0.98	2.93	5.08
	0.625	0.78	2.34	-
	1.250	0.78	1.76	4.10
10	0.125	0.98	-	3.52
	0.250	0.98	2.54	-
	0.625	0.78	2.15	-
	1.250	0.98	-	-
11	0.125	-	2.73	-
	0.250	0.39	2.54	-
	0.625	-	2.15	-
	1.250	-	1.76	-
12	0.125	0.59	2.34	-
	0.250	0.39	1.95	-
	0.625	-	1.76	-
	1.250	0.78	1.76	-

Table C.6 Peak frequencies in the apparent masses of 12 subjects adopting the minimum thigh contact posture and exposed to horizontal vibration at four vibration magnitudes.

Subject	Vibration Magnitude (ms^{-2} r.m.s.)	Mode 1 (Below 1 Hz)	Mode 2 (Between1 and 3 Hz)	Mode 3 (Above 3 Hz)
1	0.125	0.78	2.54	-
	0.250	0.59	2.40	-
	0.625	0.59	2.34	-
	1.250	-	1.76	-
2	0.125	-	1.76	5.27
	0.250	-	1.56	4.88
	0.625	-	1.17	3.91
	1.250	-	1.17	4.30
3	0.125	-	1.37	3.32, 6.04
	0.250	0.98	2.93	4.88
	0.625	0.78	2.73	-
	1.250	-	1.17, 2.54	-
4	0.125	-	1.17, 2.54	4.88
	0.250	-	1.17, 2.34	4.69
	0.625	0.98	2.15	-
	1.250	0.98	-	-
5	0.125	-	1.56	3.32
	0.250	-	1.37	3.32
	0.625	-	1.17	3.32
	1.250	-	1.17	-
6	0.125	-	-	-
	0.250	0.98	2.15	3.71
	0.625	0.78	1.95	3.32
	1.250	0.78	2.73	-
7	0.125	-	-	-
	0.250	0.78	2.15	3.32
	0.625	0.78	2.34	3.91
	1.250	0.78	2.54	-
8	0.125	-	-	-
	0.250	-	1.56, 2.73	5.47
	0.625	-	1.38, 2.73	-
	1.250	-	1.17, 2.93	-
9	0.125	-	1.56	-
	0.250	-	1.17	-
	0.625	-	1.17, 2.93	-
	1.250	0.78	1.95	-
10	0.125	0.98	-	-
	0.250	-	1.17, 2.54	-
	0.625	0.78	1.95	-
	1.250	-	1.17	-
11	0.125	-	2.15	-
	0.250	-	2.34	-
	0.625	-	1.76	-
	1.250	-	1.76	-
12	0.125	0.98	2.73	-
	0.250	0.98	2.34	-
	0.625	0.78	2.15	-
	1.250	0.78	1.76	-

C.3.2 Vertical cross-axis apparent mass on the seat

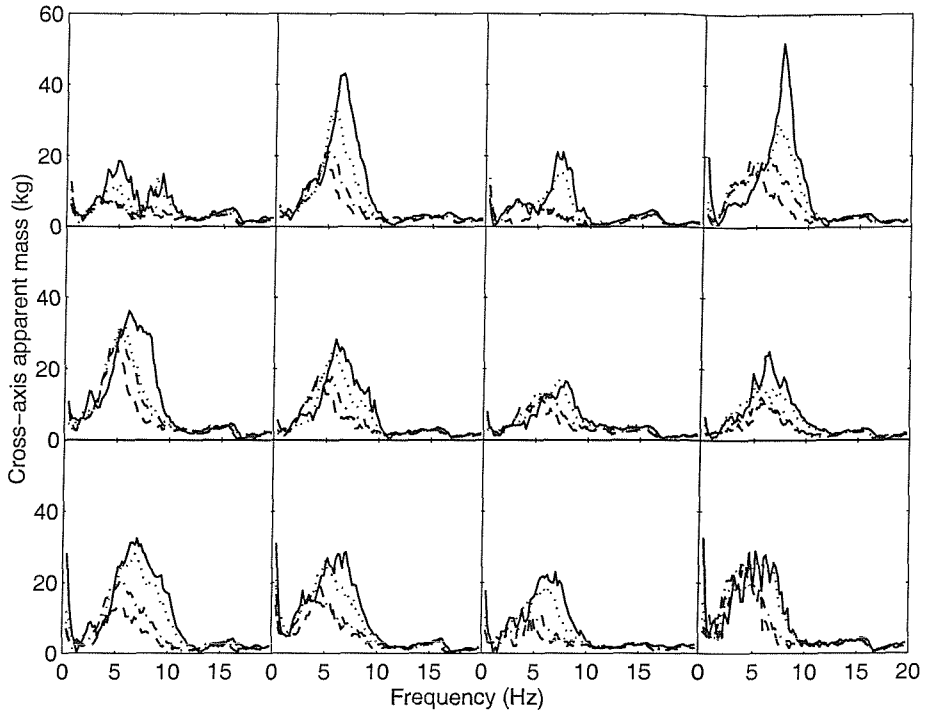

Figure C.5 Vertical cross-axis apparent masses of 12 subjects measured on the seat in the feet hanging posture at four vibration magnitudes. ———, 0.125 ms^{-2} r.m.s.; ·····, 0.25 ms^{-2} r.m.s.; –·–·–, 0.625 ms^{-2} r.m.s.; – – – –, 1.25 ms^{-2} r.m.s.

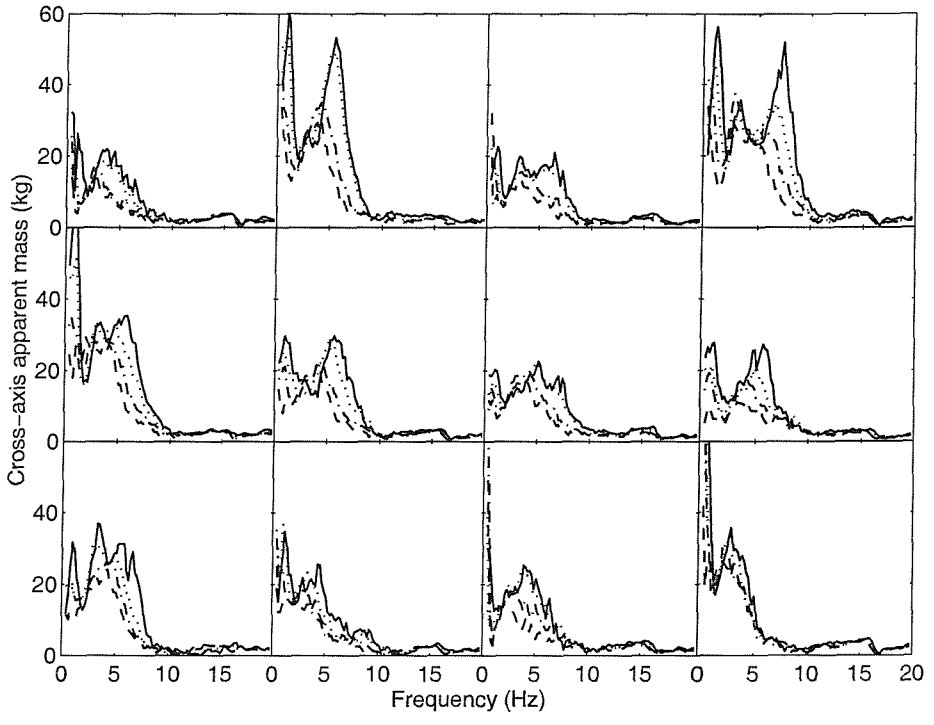

Figure C.6 Vertical cross-axis apparent masses of 12 subjects measured on the seat in the maximum thigh contact posture at four vibration magnitudes. ———, 0.125 ms^{-2} r.m.s.; ·····, 0.25 ms^{-2} r.m.s.; –·–·–, 0.625 ms^{-2} r.m.s.; – – – –, 1.25 ms^{-2} r.m.s.

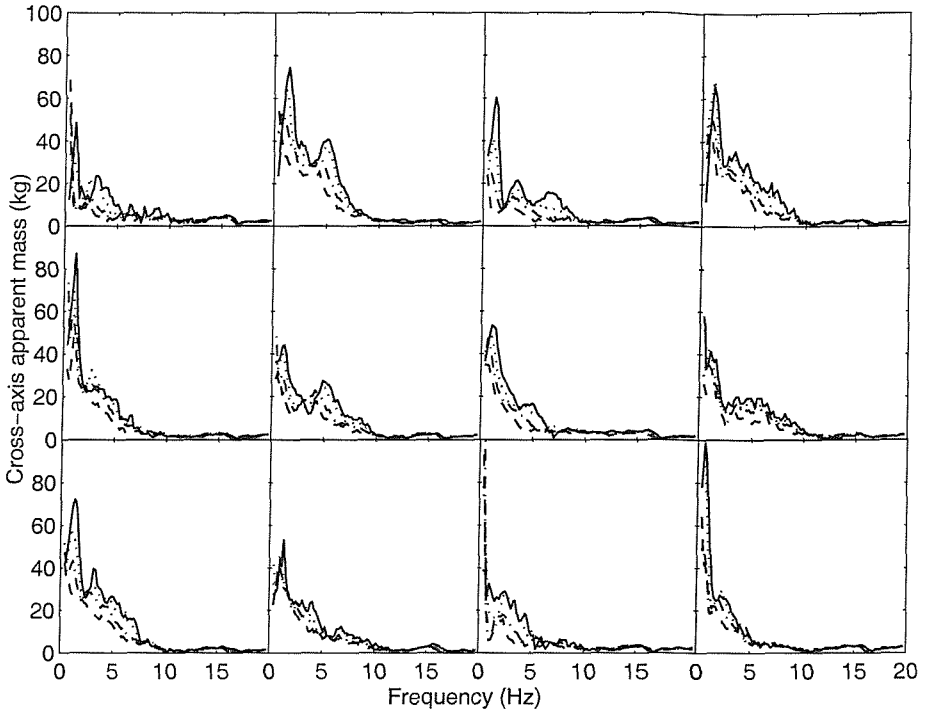

Figure C.7 Vertical cross-axis apparent masses of 12 subjects measured on the seat in the average thigh contact posture at four vibration magnitudes. ———, 0.125 ms^{-2} r.m.s.; ·····, 0.25 ms^{-2} r.m.s.; –·–·–, 0.625 ms^{-2} r.m.s.; – – – –, 1.25 ms^{-2} r.m.s.

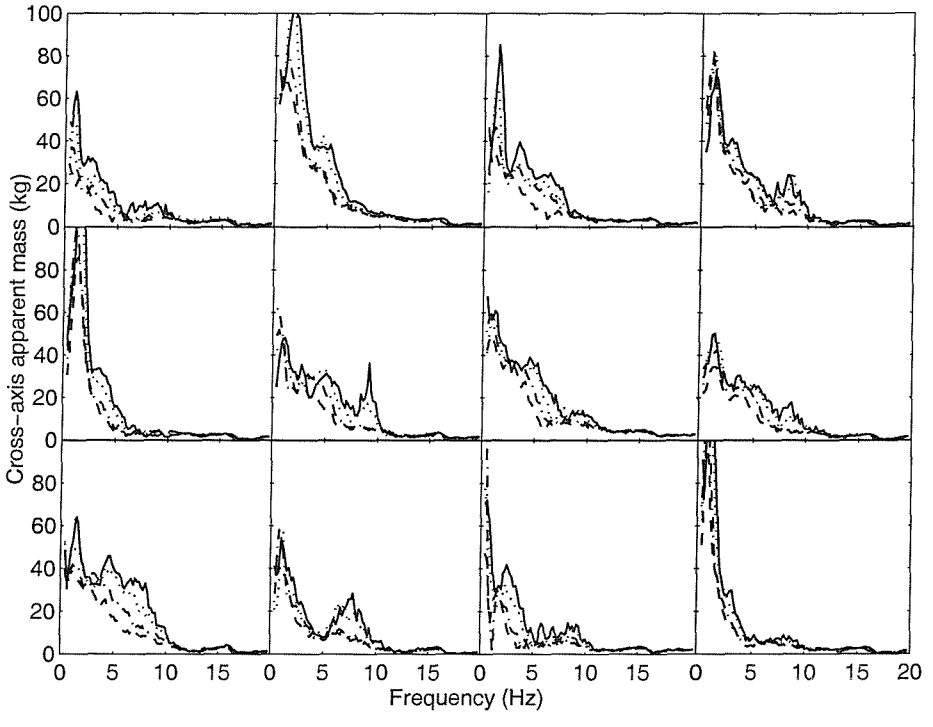

Figure C.8 Vertical cross-axis apparent masses of 12 subjects measured on the seat in the minimum thigh contact posture at four vibration magnitudes. ———, 0.125 ms^{-2} r.m.s.; ·····, 0.25 ms^{-2} r.m.s.; –·–·–, 0.625 ms^{-2} r.m.s.; – – – –, 1.25 ms^{-2} r.m.s.

Table C.7 Peak frequencies and magnitudes in the vertical cross-axis apparent masses of 12 subjects adopting the feet hanging posture and exposed to horizontal vibration at four vibration magnitudes. f: frequency; mag: magnitude.

Subject	Vibration Magnitude (ms^{-2} r.m.s.)	f1, mag1	f2, mag2	f3, mag3
1	0.125	2.93, 8.2	4.88, 18.6	9.18, 14.8
	0.250	2.93, 8.7	4.49, 11.6	8.59, 14.1
	0.625	-	4.10, 7.9	7.42, 6.24
	1.250	3.52, 7.2	-	-
2	0.125	3.71, 13.6	6.45, 43.1	-
	0.250	2.92, 9.5	5.47, 33.5	-
	0.625	-	4.88, 21.2	-
	1.250	-	4.30, 18.3	-
3	0.125	3.13, 7.7	7.42, 21.0	-
	0.250	3.13, 7.7	7.23, 15.5	-
	0.625	2.93, 7.3	-	-
	1.250	-	6.05, 5.8	-
4	0.125	2.93, 7.2	7.62, 51.8	-
	0.250	2.93, 13.0	7.23, 29.3	-
	0.625	2.93, 13.0	4.88, 18.6	-
	1.250	-	4.30, 18.5	-
5	0.125	2.34, 13.7	6.05, 36.2	-
	0.250	1.95, 8.5	5.66, 31.9	-
	0.625	-	5.08, 30.1	-
	1.250	-	4.88, 27.6	-
6	0.125	2.54, 7.2	5.86, 28.4	-
	0.250	-	5.66, 24.8	-
	0.625	-	5.47, 17.6	-
	1.250	-	4.10, 17.9	-
7	0.125	-	6.05, 12.8	7.81, 16.4
	0.250	-	4.88, 12.4	7.23, 16.8
	0.625	-	-	6.25, 12.7
	1.250	-	3.52, 9.5	5.47, 12.2
8	0.125	2.93, 6.7	6.45, 24.8	-
	0.250	-	5.08, 16.4	-
	0.625	-	5.66, 12.0	-
	1.250	-	5.66, 10.3	-
9	0.125	2.73, 8.9	7.03, 32.3	-
	0.250	2.54, 7.1	6.84, 28.1	-
	0.625	-	5.47, 20.8	-
	1.250	-	5.27, 14.0	-
10	0.125	2.93, 17.7	6.25, 28.1	-
	0.250	-	5.08, 26.3	-
	0.625	-	4.49, 19.3	-
	1.250	-	4.30, 14.5	-
11	0.125	2.73, 10.1	7.03, 22.8	-
	0.250	-	5.86, 18.6	-
	0.625	-	4.69, 11.8	-
	1.250	2.15, 5.7	4.69, 10.0	-
12	0.125	1.37, 9.5	5.27, 28.9	-
	0.250	3.71, 18.9	5.66, 26.2	-
	0.625	-	3.91, 25.3	-
	1.250	-	4.10, 25.6	-

Table C.8 Peak frequencies and magnitudes in the vertical cross-axis apparent masses of 12 subjects adopting the maximum thigh contact posture and exposed to horizontal vibration at four vibration magnitudes. f: frequency; mag: magnitude.

Subject	Vibration Magnitude (ms^{-2} r.m.s.)	f1, mag1	f2, mag2	f3, mag3
1	0.125	0.98, 26.2	3.71, 21.8	-
	0.250	-	3.71, 18.5	-
	0.625	-	2.93, 15.6	-
	1.250	-	2.54, 16.8	-
2	0.125	0.98, 60.4	2.93, 27.2	5.47, 53.3
	0.250	0.78, 53.5	2.73, 25.9	5.27, 47.0
	0.625	-	-	4.30, 34.9
	1.250	-	-	4.10, 30.7
3	0.125	0.98, 22.5	3.13, 19.9	-
	0.250	0.98, 15.8	3.13, 18.6	5.66, 16.9
	0.625	-	3.32, 15.5	-
	1.250	-	3.32, 13.0	-
4	0.125	1.17, 56.3	3.32, 35.6	7.42, 52.1
	0.250	0.98, 45.0	3.13, 30.8	6.64, 34.7
	0.625	-	2.73, 37.6	5.66, 27.6
	1.250	-	2.54, 30.6	-
5	0.125	0.98, 68.5	3.32, 33.4	5.86, 35.4
	0.250	0.98, 51.3	2.93, 33.8	4.88, 32.3
	0.625	0.98, 31.3	2.54, 29.3	4.10, 28.9
	1.250	0.98, 26.8	1.95, 29.1	4.10, 27.2
6	0.125	0.98, 29.7	-	5.66, 29.7
	0.250	0.78, 25.3	-	5.08, 28.0
	0.625	0.98, 21.1	-	4.10, 22.6
	1.250	-	-	4.10, 22.2
7	0.125	0.98, 20.0	-	5.08, 22.5
	0.250	0.78, 16.8	3.13, 14.65	4.88, 22.4
	0.625	0.59, 15.3	-	4.10, 19.8
	1.250	0.78, 11.6	3.13, 18.4	-
8	0.125	1.17, 27.8	3.52, 16.9	5.66, 27.3
	0.250	0.98, 21.5	-	5.08, 21.2
	0.625	0.78, 19.2	-	4.10, 17.4
	1.250	0.78, 9.8	-	4.30, 11.2
9	0.125	0.98, 31.7	3.32, 36.9	5.66, 31.4
	0.250	0.98, 20.1	3.13, 32.4	4.88, 28.8
	0.625	0.98, 19.0	-	4.69, 26.4
	1.250	0.78, 12.6	-	4.30, 24.2
10	0.125	1.17, 34.9	3.71, 21.4	4.3, 25.5
	0.250	0.98, 36.8	3.32, 23.3	-
	0.625	0.98, 24.9	2.73, 18.7	-
	1.250	-		
11	0.125	-	3.91, 25.3	-
	0.250	-	3.71, 24.2	-
	0.625	-	3.32, 18.9	-
	1.250	-	2.15, 14.6	-
12	0.125	-	2.93, 35.7	-
	0.250	-	2.34, 31.0	-
	0.625	-	2.15, 30.6	-
	1.250	-	1.95, 26.7	-

Table C.9 Peak frequencies and magnitudes in the vertical cross-axis apparent masses of 12 subjects adopting the average thigh contact posture and exposed to horizontal vibration at four vibration magnitudes. f: frequency; mag: magnitude.

Subject	Vibration Magnitude (ms^{-2} r.m.s.)	f1, mag1	f2, mag2	f3, mag3
1	0.125	0.98, 48.4	2.93, 23.5	-
	0.250	0.78, 34.2	2.34, 22.5	-
	0.625	-	2.54, 12.7	-
	1.250	-	2.15, 11.4	-
2	0.125	1.37, 74.2	2.54, 39.5	5.08, 40.8
	0.250	1.17, 63.7	2.54, 34.4	4.88, 37.1
	0.625	0.78, 53.2	-	4.30, 31.2
	1.250	-	-	-
3	0.125	1.17, 60.2	3.32, 21.6	6.25, 15.7
	0.250	0.98, 41.0	3.32, 17.3	-
	0.625	0.59, 25.3	2.93, 13.9	-
	1.250	-	2.34, 9.65	-
4	0.125	1.17, 65.9	3.13, 35.4	-
	0.250	1.17, 68.8	2.93, 33.4	-
	0.625	0.78, 50.5	-	-
	1.250	0.78, 46.5	-	-
5	0.125	1.17, 87.1	-	-
	0.250	0.98, 69.1	2.73, 32.4	-
	0.625	0.98, 58.7	2.54, 27.4	-
	1.250	0.98, 50.1	-	-
6	0.125	1.17, 44.1	-	4.88, 27.3
	0.250	0.98, 40.3	-	5.08, 24.2
	0.625	0.98, 30.0	-	4.10, 23.0
	1.250	0.59, 31.7	-	-
7	0.125	0.98, 53.2	-	4.88, 16.7
	0.250	0.98, 48.0	-	-
	0.625	0.59, 47.2	-	-
	1.250	-		
8	0.125	0.98, 41.3	3.32, 19.8	-
	0.250	0.98, 43.3	3.52, 16.8	-
	0.625	-	-	-
	1.250	1.37, 26.5	-	-
9	0.125	1.37, 71.9	3.13, 39.5	-
	0.250	0.98, 58.4	3.32, 30.5	-
	0.625	1.17, 43.2	2.93, 28.4	-
	1.250			
10	0.125	1.37, 53.3	-	-
	0.250	1.17, 40.9	2.93, 25.3	-
	0.625	0.98, 37.2	-	-
	1.250	0.98, 41.7	-	-
11	0.125	-	2.15, 28.2	-
	0.250	-	2.54, 27.8	-
	0.625	-	2.34, 18.1	-
	1.250	-	1.75, 17.6	-
12	0.125	-	2.15, 27.2	-
	0.250	-	2.34, 29.8	-
	0.625	-	1.95, 25.7	-
	1.250		1.56, 22.2	-

Table C.10 Peak frequencies and magnitudes in the vertical cross-axis apparent masses of 12 subjects adopting the minimum thigh contact posture and exposed to horizontal vibration at four vibration magnitudes. f: frequency; mag: magnitude.

Subject	Vibration Magnitude (ms^{-2} r.m.s.)	f1, mag1	f2, mag2	f3, mag3
1	0.125	0.98, 63.2	2.15, 32.4	-
	0.250	0.98, 47.1	2.93, 23.7	-
	0.625	0.78, 36.6	2.54, 18.8	-
	1.250	1.37, 23.4	-	-
2	0.125	1.76, 108.1	-	4.10, 37.1
	0.250	1.56, 132.9	-	4.49, 42.6
	0.625	1.17, 82.4	-	-
	1.250	0.98, 67.4	-	-
3	0.125	1.37, 85.0	3.32, 39.4	-
	0.250	1.17, 67.1	3.32, 28.7	-
	0.625	0.98, 46.4	2.93, 29.3	-
	1.250	1.17, 32.8	-	-
4	0.125	1.17, 71.0	2.73, 41.0	-
	0.250	1.17, 81.0	2.34, 39.7	-
	0.625	0.98, 81.9	-	-
	1.250	0.98, 78.3	-	-
5	0.125	1.56, 155.3	3.32, 33.7	-
	0.250	1.37, 122.3	-	-
	0.625	1.17, 105.2	-	-
	1.250	1.37, 86.1	-	-
6	0.125	1.17, 48.2	2.15, 32.1	-
	0.250	0.98, 46.9	2.34, 30.6	4.88, 33.4
	0.625	-	3.32, 31.1	-
	1.250	-	2.73, 25.5	-
7	0.125	1.17, 60.55	3.13, 37.0	-
	0.250	1.17, 56.7	3.32, 36.3	-
	0.625	0.78, 57.8	-	-
	1.250	0.98, 49.4	-	-
8	0.125	1.37, 50.2	-	-
	0.250	1.56, 48.6	-	-
	0.625	1.56, 42.5	-	-
	1.250	1.37, 34.6	-	-
9	0.125	1.56, 63.9	-	4.69, 45.9
	0.250	1.56, 49.6	-	4.30, 40.9
	0.625	1.17, 41.8	-	-
	1.250	1.17, 39.0	-	-
10	0.125	0.98, 53.7	-	7.81, 28.5
	0.250	1.17, 57.5	-	7.03, 23.6
	0.625	0.78, 58.2	-	-
	1.250	1.17, 41.4	-	-
11	0.125	-	2.54, 41.8	-
	0.250	-	2.34, 32.6	-
	0.625	1.56, 27.6	-	-
	1.250	1.76, 29.8	-	-
12	0.125	0.98, 134.9	-	-
	0.250	0.98, 129.3	-	-
	0.625	0.78, 113.1	-	-
	1.250	0.78, 109.4	-	-

C.3.3 Lateral cross-axis apparent mass on the seat

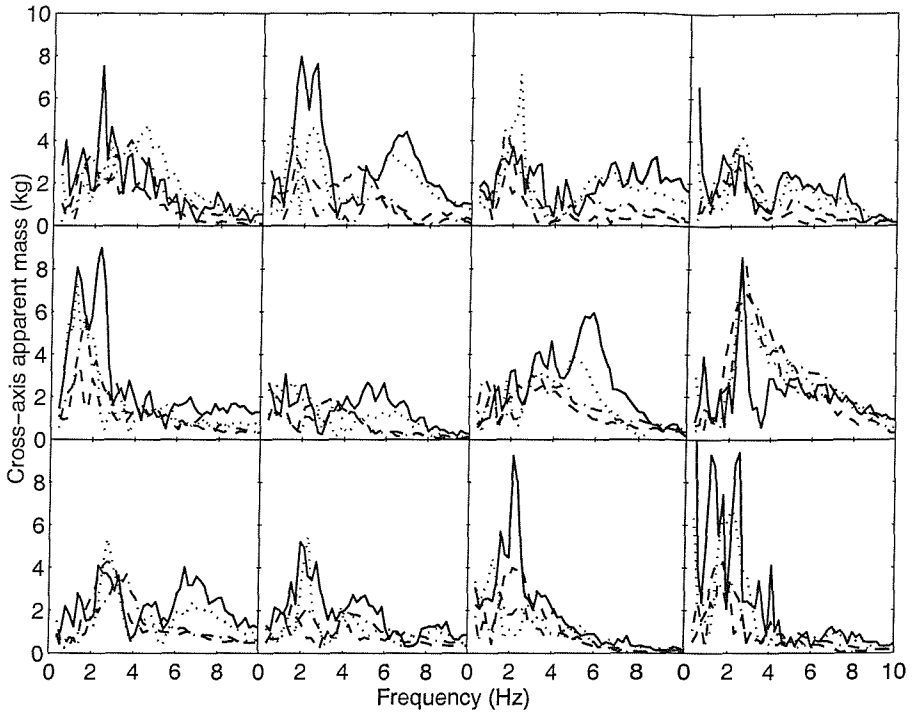

Figure C.9 Lateral cross-axis apparent masses of 12 subjects measured on the seat in the feet hanging posture at four vibration magnitudes. ———, 0.125 ms^{-2} r.m.s.; ·····, 0.25 ms^{-2} r.m.s.; –·–·–, 0.625 ms^{-2} r.m.s.; – – – –, 1.25 ms^{-2} r.m.s.

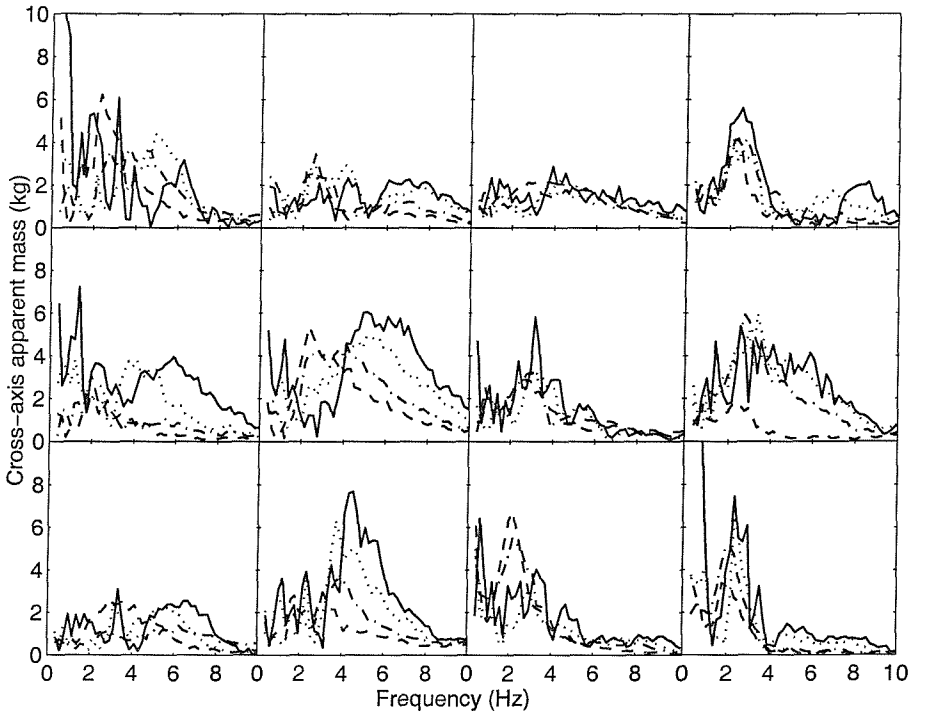

Figure C.10 Lateral cross-axis apparent masses of 12 subjects measured on the seat in the maximum thigh contact posture at four vibration magnitudes. ———, 0.125 ms^{-2} r.m.s.; ·····, 0.25 ms^{-2} r.m.s.; –·–·–, 0.625 ms^{-2} r.m.s.; – – – –, 1.25 ms^{-2} r.m.s.

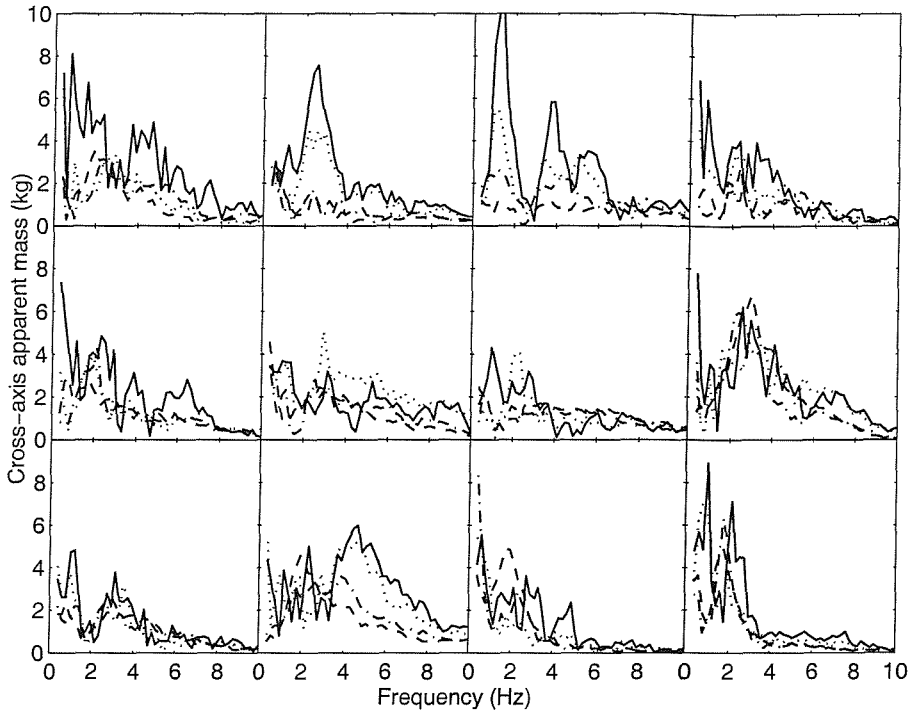

Figure C.11 Lateral cross-axis apparent masses of 12 subjects measured on the seat in the average thigh contact posture at four vibration magnitudes. ———, 0.125 ms^{-2} r.m.s.; ·····, 0.25 ms^{-2} r.m.s.; –·–·–, 0.625 ms^{-2} r.m.s.; – – – –, 1.25 ms^{-2} r.m.s.

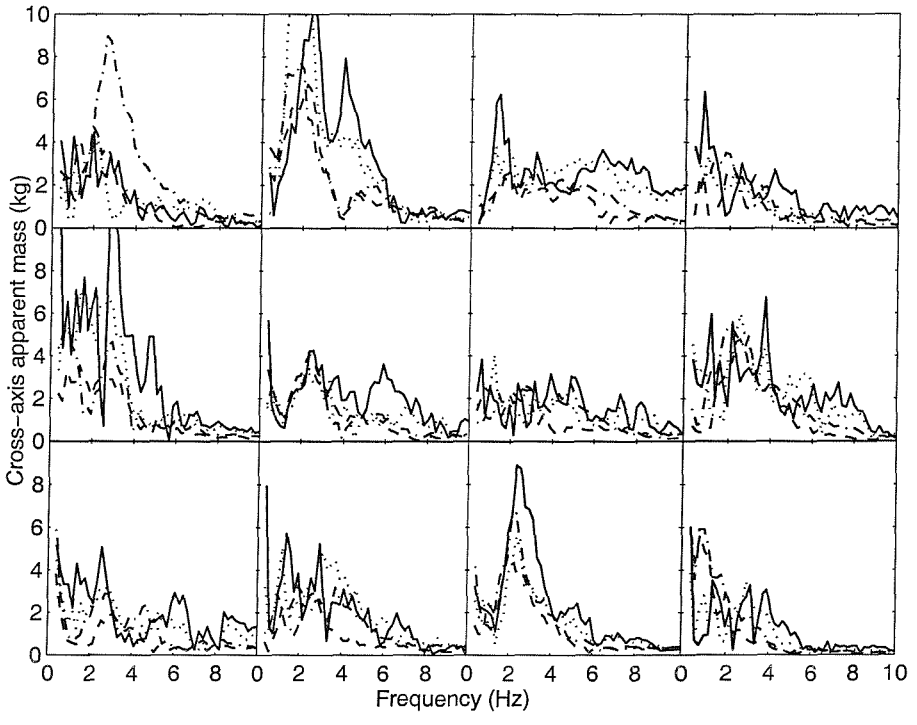

Figure C.12 Lateral cross-axis apparent masses of 12 subjects measured on the seat in the minimum thigh contact posture at four vibration magnitudes. ———, 0.125 ms^{-2} r.m.s.; ·····, 0.25 ms^{-2} r.m.s.; –·–·–, 0.625 ms^{-2} r.m.s.; – – – –, 1.25 ms^{-2} r.m.s.

C.3.4 Coherencies of the vertical cross-axis apparent mass

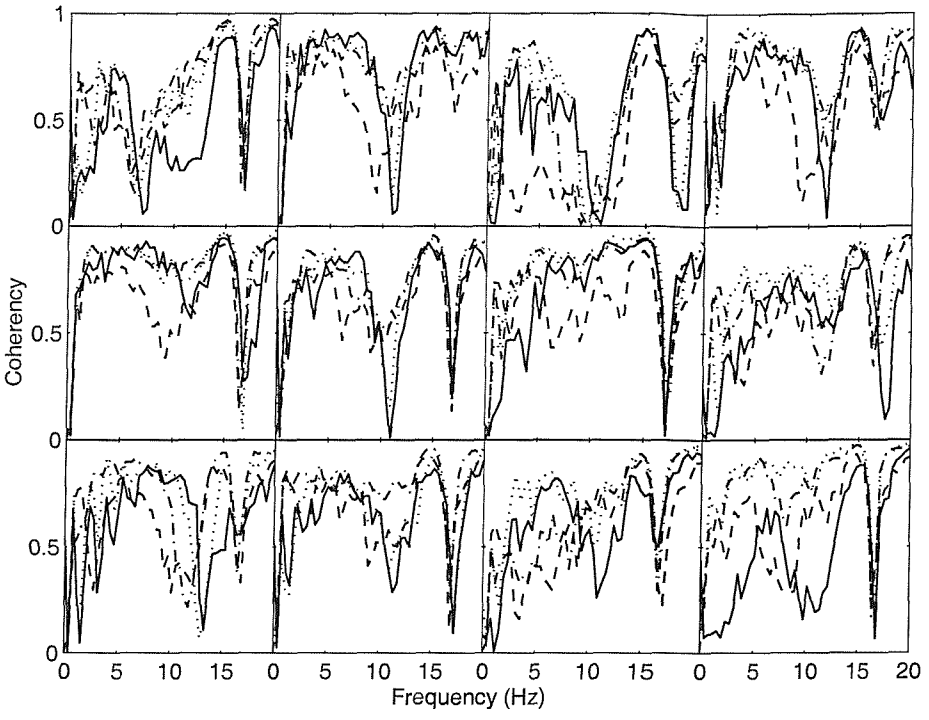

Figure C.13 Coherencies of vertical cross-axis apparent masses of 12 subjects measured on the seat in the feet hanging posture at four vibration magnitudes. ———, 0.125 ms^{-2} r.m.s.; ·····, 0.25 ms^{-2} r.m.s.; –·–·–, 0.625 ms^{-2} r.m.s.; – – – –, 1.25 ms^{-2} r.m.s.

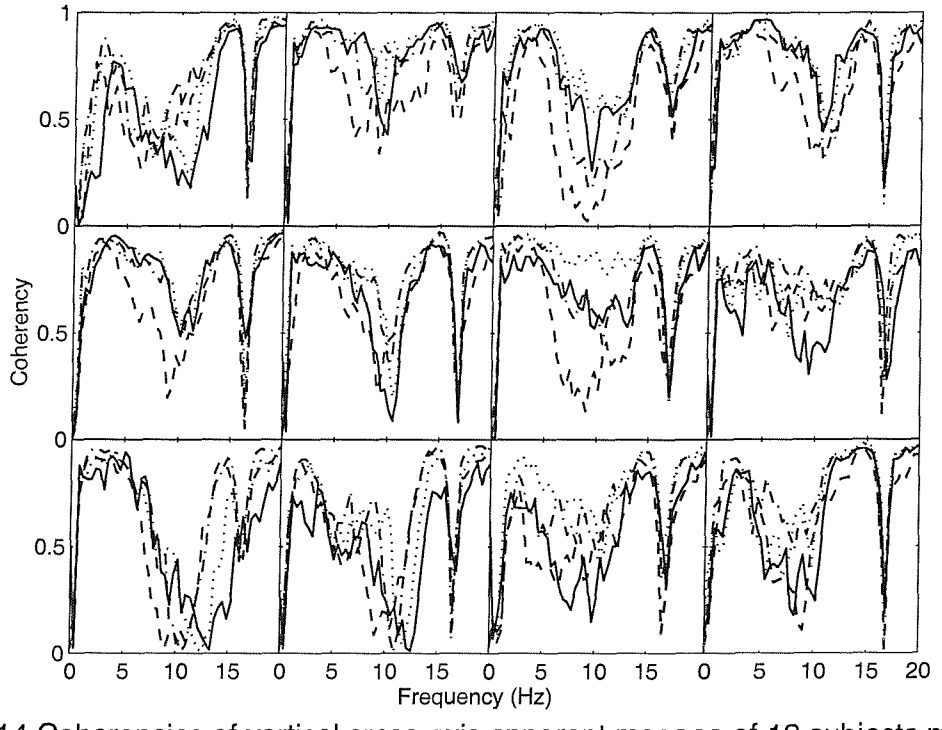

Figure C.14 Coherencies of vertical cross-axis apparent masses of 12 subjects measured on the seat in the maximum thigh contact posture at four vibration magnitudes. ———, 0.125 ms^{-2} r.m.s.; ·····, 0.25 ms^{-2} r.m.s.; –·–·–, 0.625 ms^{-2} r.m.s.; – – – –, 1.25 ms^{-2} r.m.s.

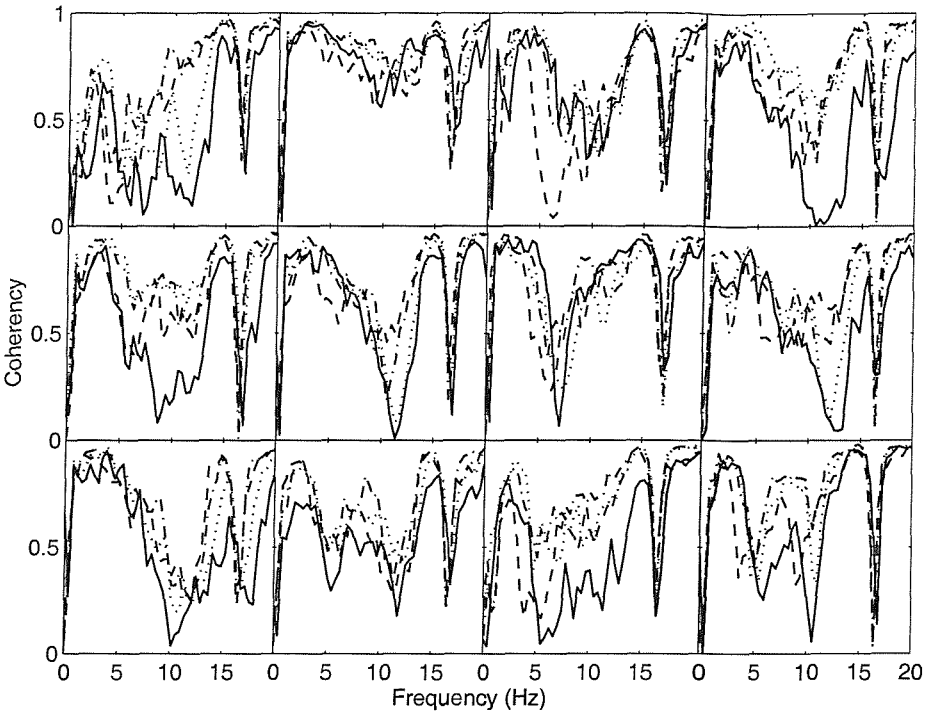

Figure C.15 Coherencies of vertical cross-axis apparent masses of 12 subjects measured on the seat in the average thigh contact posture at four vibration magnitudes. ———, 0.125 ms^{-2} r.m.s.; ·····, 0.25 ms^{-2} r.m.s.; –·–·–, 0.625 ms^{-2} r.m.s.; – – – –, 1.25 ms^{-2} r.m.s.

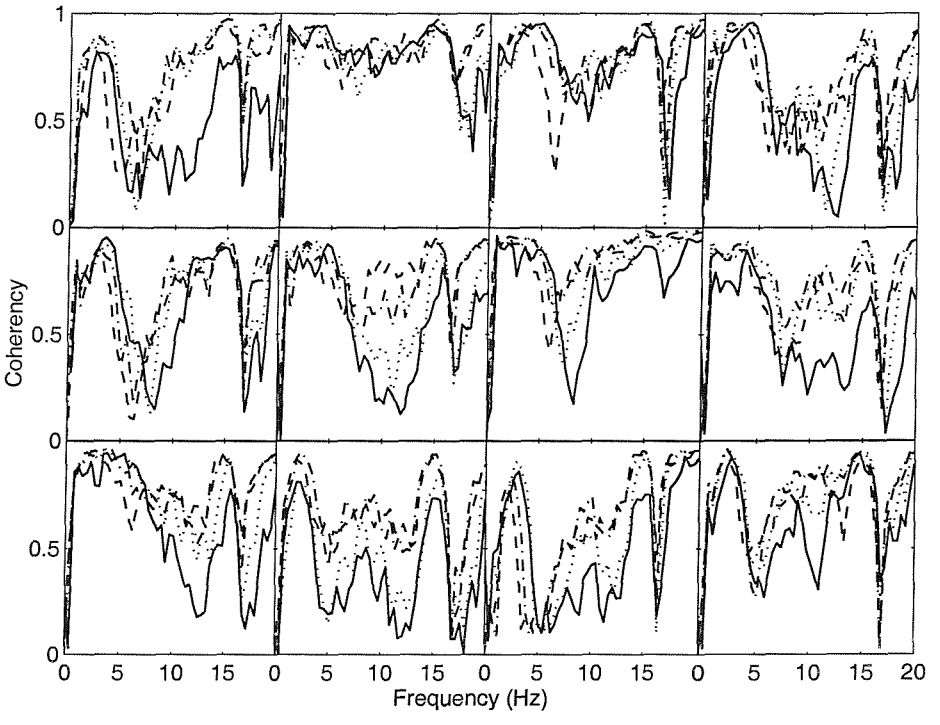

Figure C.16 Coherencies of vertical cross-axis apparent masses of 12 subjects measured on the seat in the minimum thigh contact posture at four vibration magnitudes. ———, 0.125 ms^{-2} r.m.s.; ·····, 0.25 ms^{-2} r.m.s.; –·–·–, 0.625 ms^{-2} r.m.s.; – – – –, 1.25 ms^{-2} r.m.s.

APPENDIX D

INDIVIDUAL DATA: FORE-AND-AFT EXCITATION WITH A BACKREST (CHAPTER 7)

APPENDIX D Fore-and-aft excitation with backrest (Chapter 7)

D.1 Instructions given to the subjects prior exposure to vibration

- The aim of this experiment is to measure the forces on the seat and at the backrest during exposure to fore-and-aft vibration and to study the effect of different feet heights and vibration magnitude on these forces.

- You will be seated on a rigid seat with a rigid backrest and exposed to random fore-and-aft vibration at different vibration magnitudes and with four different foot positions.

The adopted postures which will give different feet heights are:

a. Normal sitting while feet hanging in the air.
b. Sitting with the upper leg horizontal, the lower legs vertical, and the feet supported on the footrest mounted on the vibrating table. Subject must be barefooted.
c. Sitting with minimum thigh contact with the seat, by raising the footrest while keeping the lower legs in a vertical position. Subject must be barefooted.
d. Sitting with maximum thigh contact such that the feet are just touching the footrest. The lower legs are also vertical in this case. Subject must be barefooted.

- In each of the sitting conditions mentioned above you will be exposed to four random vibrations. The experimenter will show you the order in which the above conditions will be adopted.

- During the experiment you need to sit in an upright and relaxed position with your back against the backrest.

- Keeping the same sitting posture throughout the experiment is a very important and key factor for getting correct measurements that represent the posture of interest. Any voluntary movements of any part of the body (such as using your hand to scratch your head during the experiment) has an effect.

- Please keep your eyes open during the experiment.

- During the exposure to vibration, you can stop the vibration at any time by pressing the red STOP button that you will be holding throughout the experiment.

Thank you for taking part in this experiment.

D.2 Individual results

D.2.1 Fore-and-aft apparent mass on the seat

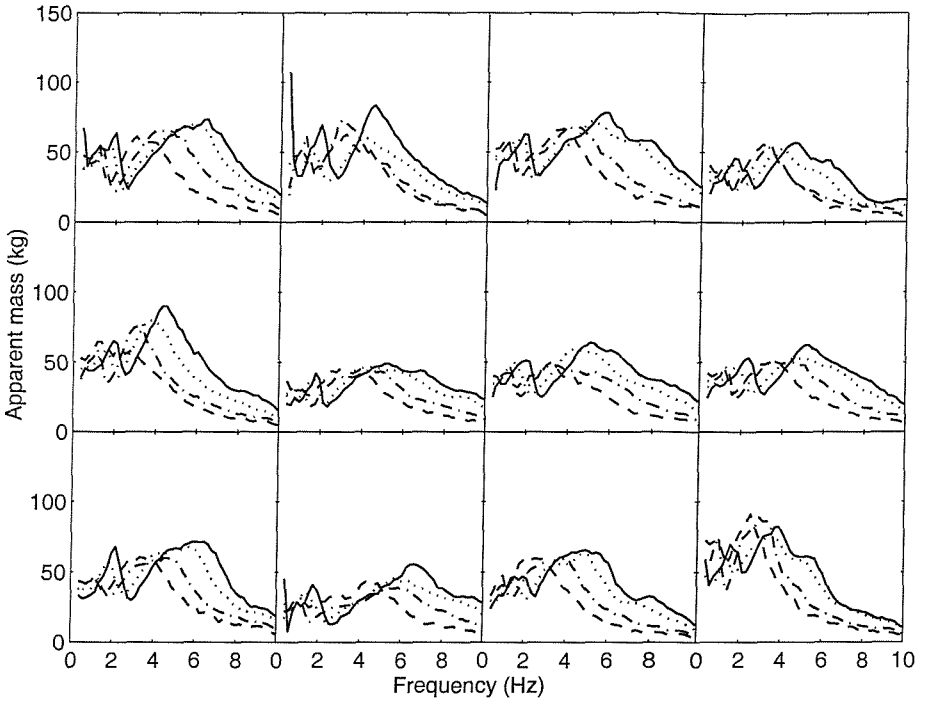

Figure D.1 Fore-and-aft apparent masses of 12 subjects measured on the seat in the feet hanging posture at four vibration magnitudes. ———, 0.125 ms^{-2} r.m.s.; ·····, 0.25 ms^{-2} r.m.s.; –·–·–, 0.625 ms^{-2} r.m.s.; – – – –, 1.25 ms^{-2} r.m.s.

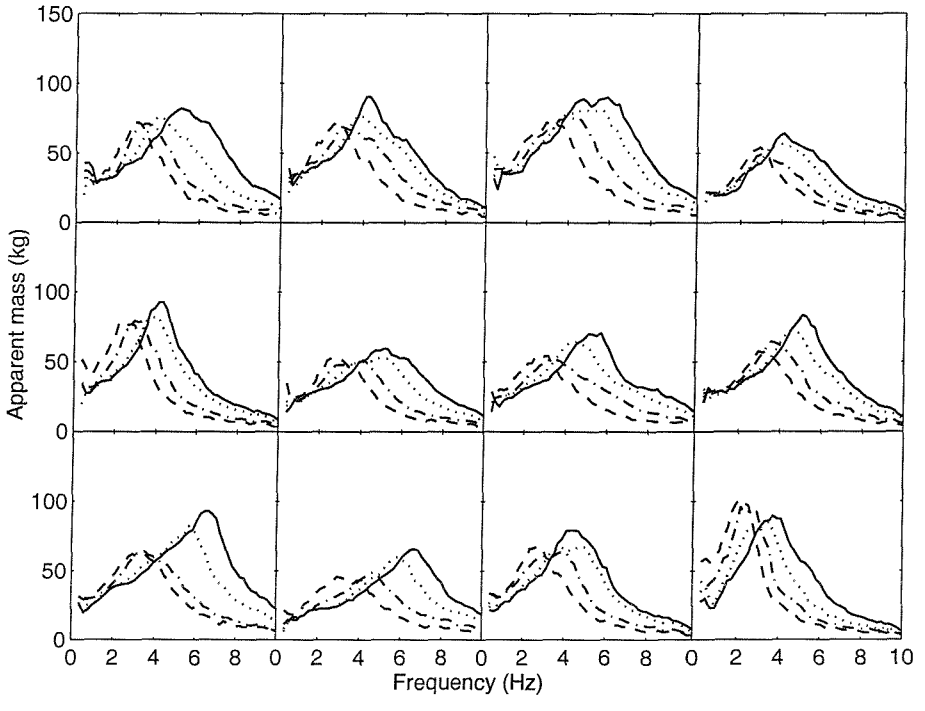

Figure D.2 Fore-and-aft apparent masses of 12 subjects measured on the seat in the maximum thigh contact posture at four vibration magnitudes. ———, 0.125 ms^{-2} r.m.s.; ·····, 0.25 ms^{-2} r.m.s.; –·–·–, 0.625 ms^{-2} r.m.s.; – – – –, 1.25 ms^{-2} r.m.s.

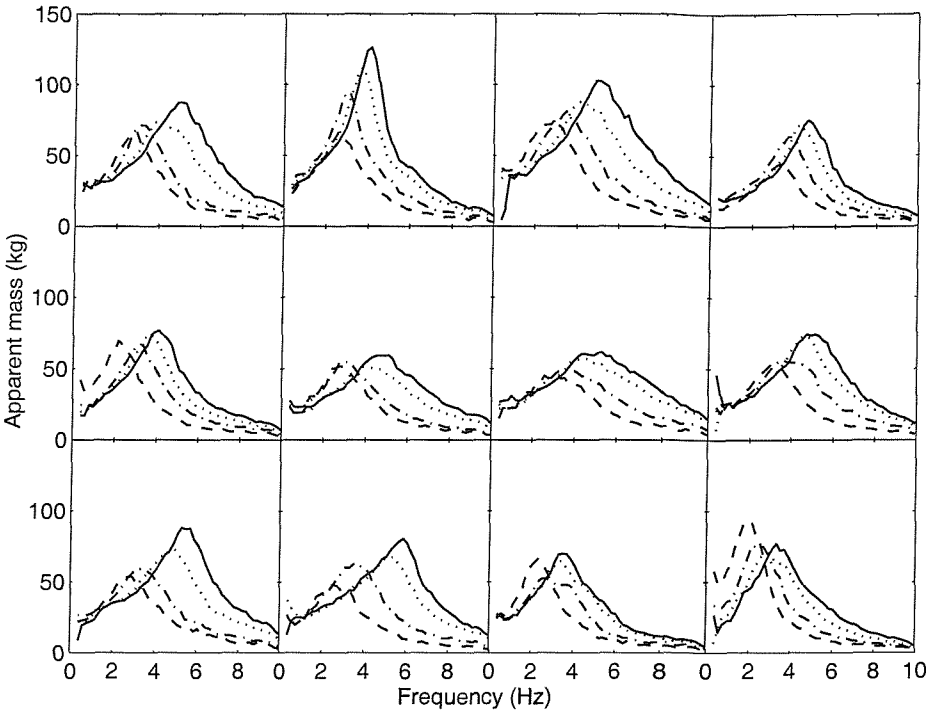

Figure D.3 Fore-and-aft apparent masses of 12 subjects measured on the seat in the average thigh contact posture at four vibration magnitudes. ———, 0.125 ms^{-2} r.m.s.; ·····, 0.25 ms^{-2} r.m.s.; –·–·–, 0.625 ms^{-2} r.m.s.; – – – –, 1.25 ms^{-2} r.m.s.

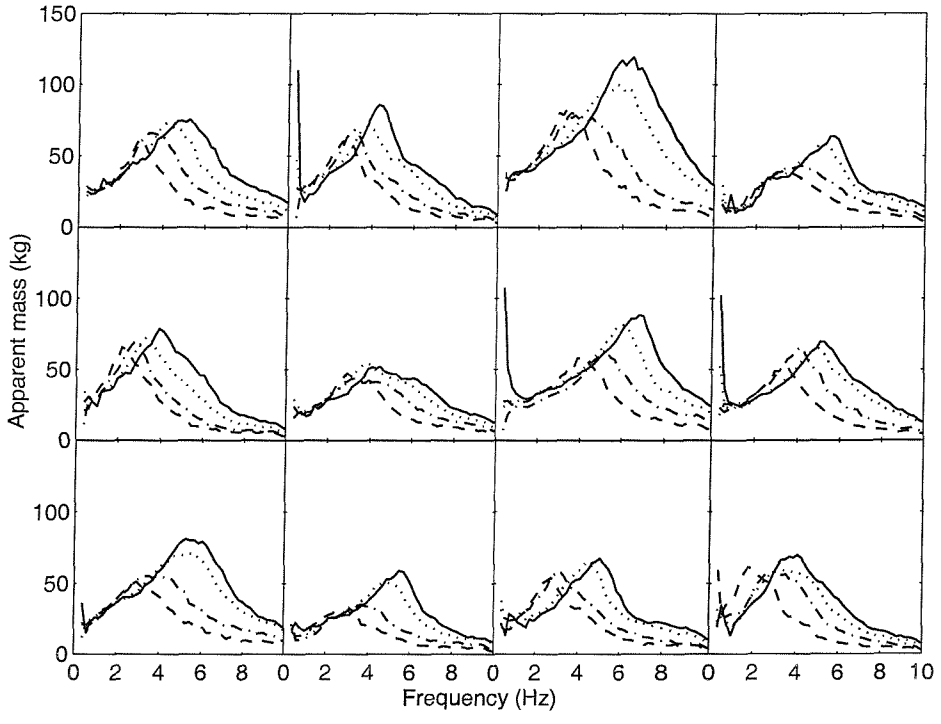

Figure D.4 Fore-and-aft apparent masses of 12 subjects measured on the seat in the minimum thigh contact posture at four vibration magnitudes. ———, 0.125 ms^{-2} r.m.s.; ·····, 0.25 ms^{-2} r.m.s.; –·–·–, 0.625 ms^{-2} r.m.s.; – – – –, 1.25 ms^{-2} r.m.s.

D.2.2 Fore-and-aft apparent mass at the back

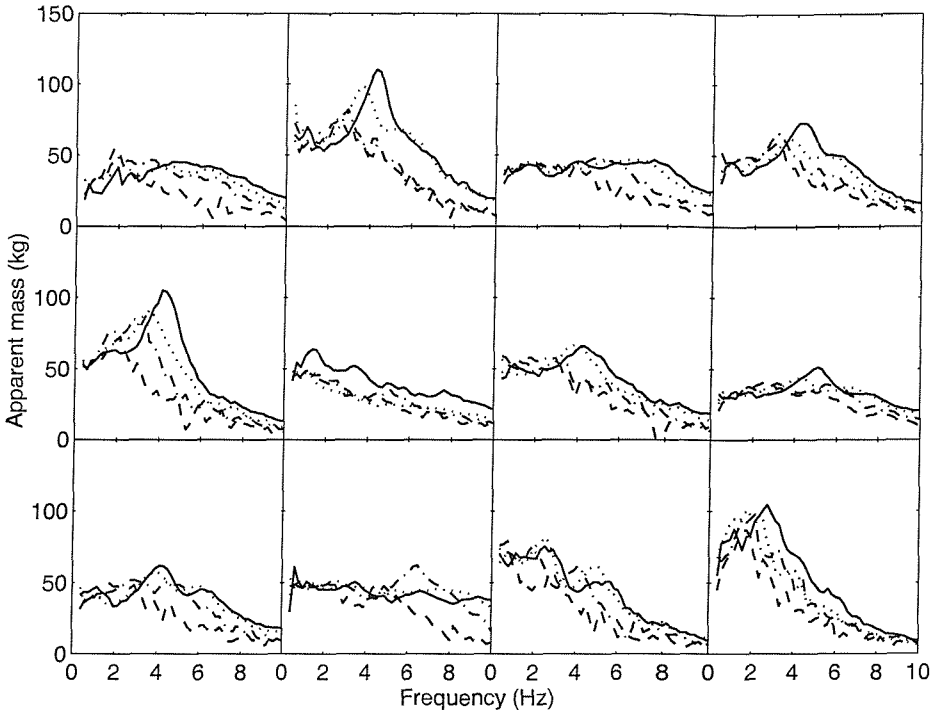

Figure D.5 Fore-and-aft apparent masses measured at the backs of 12 subjects in the feet hanging posture at four vibration magnitudes. ———, 0.125 ms^{-2} r.m.s.; ·····, 0.25 ms^{-2} r.m.s.; –·–·–, 0.625 ms^{-2} r.m.s.; – – – –, 1.25 ms^{-2} r.m.s.

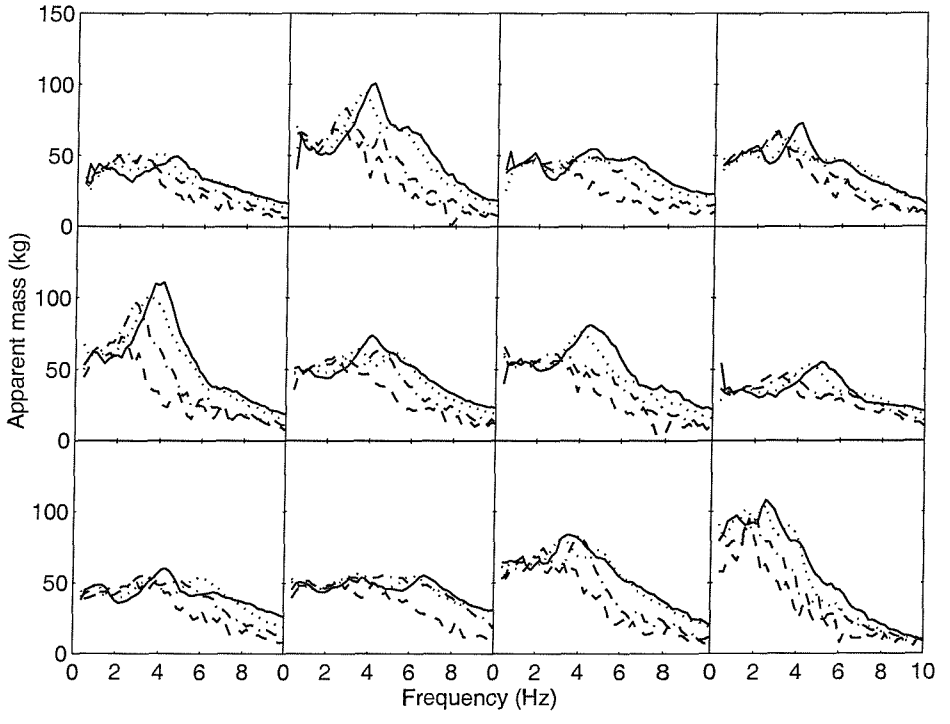

Figure D.6 Fore-and-aft apparent masses measured at the backs of 12 subjects in the maximum thigh contact posture at four vibration magnitudes. ———, 0.125 ms^{-2} r.m.s.; ·····, 0.25 ms^{-2} r.m.s.; –·–·–, 0.625 ms^{-2} r.m.s.; – – – –, 1.25 ms^{-2} r.m.s.

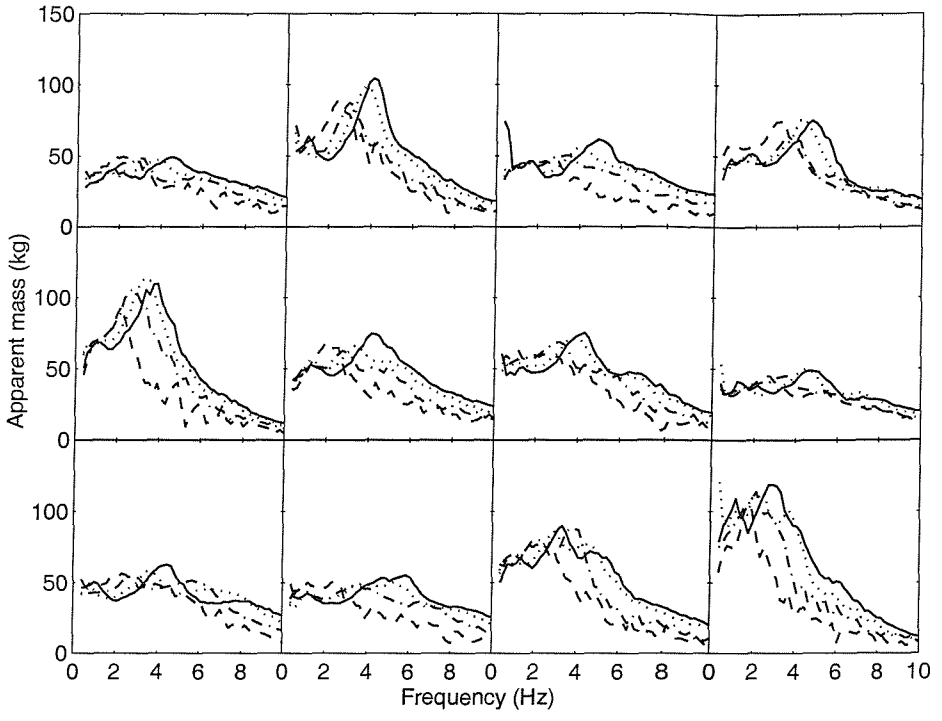

Figure D.7 Fore-and-aft apparent masses measured at the backs of 12 subjects in the average thigh contact posture at four vibration magnitudes. ———, 0.125 ms^{-2} r.m.s.; ·····, 0.25 ms^{-2} r.m.s.; –·–·–, 0.625 ms^{-2} r.m.s.; – – – –, 1.25 ms^{-2} r.m.s.

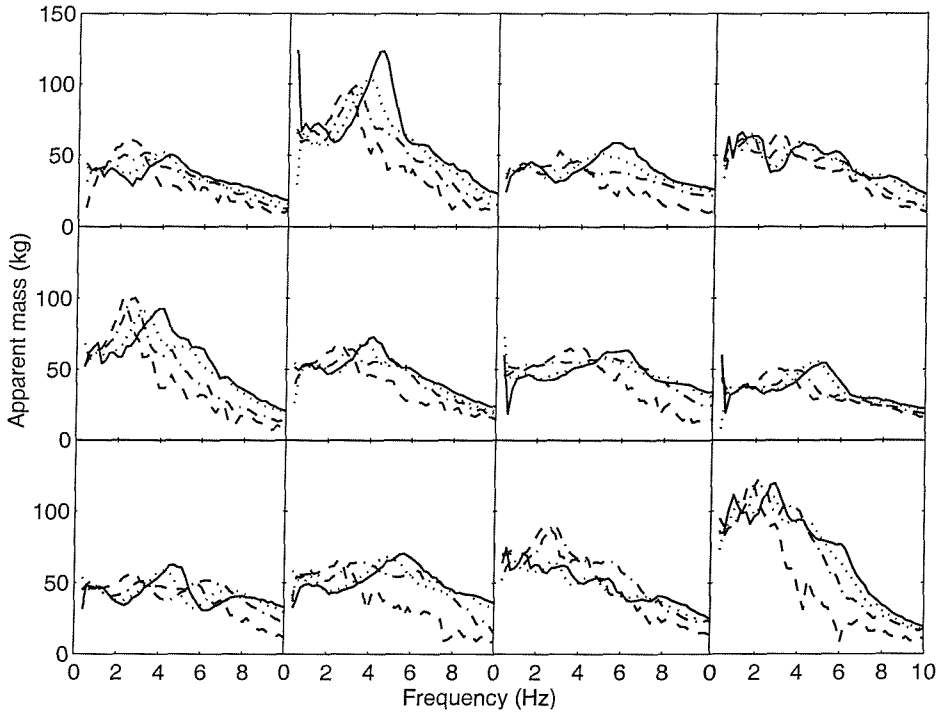

Figure D.8 Fore-and-aft apparent masses measured at the backs of 12 subjects in the minimum thigh contact posture at four vibration magnitudes. ———, 0.125 ms^{-2} r.m.s.; ·····, 0.25 ms^{-2} r.m.s.; –·–·–, 0.625 ms^{-2} r.m.s.; – – – –, 1.25 ms^{-2} r.m.s.

D.2.3 Vertical cross-axis apparent mass on the seat

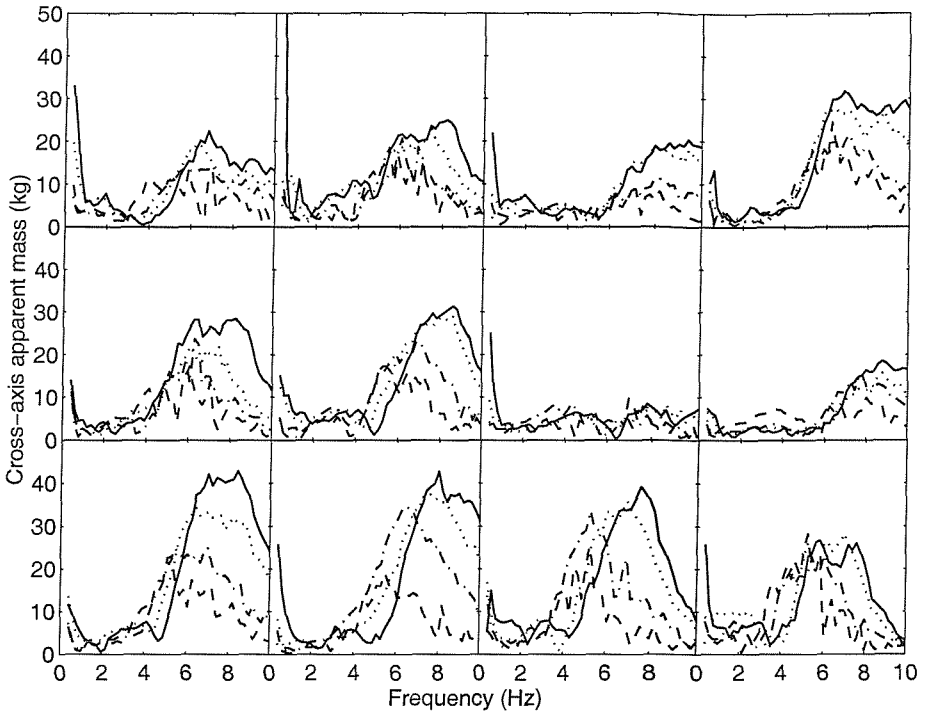

Figure D.9 Vertical cross-axis apparent masses of 12 subjects measured on the seat in the feet hanging posture at four vibration magnitudes. ———, 0.125 ms^{-2} r.m.s.; ·····, 0.25 ms^{-2} r.m.s.; —·—·—, 0.625 ms^{-2} r.m.s.; – – – –, 1.25 ms^{-2} r.m.s.

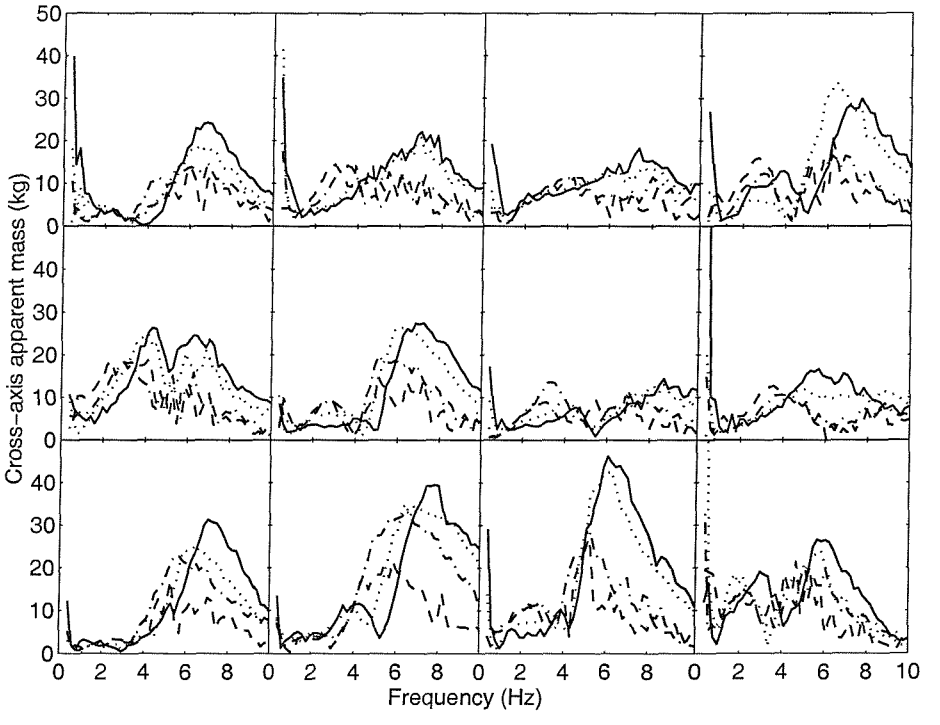

Figure D.10 Vertical cross-axis apparent masses of 12 subjects measured on the seat in the maximum thigh contact posture at four vibration magnitudes. ———, 0.125 ms^{-2} r.m.s.; ·····, 0.25 ms^{-2} r.m.s.; —·—·—, 0.625 ms^{-2} r.m.s.; – – – –, 1.25 ms^{-2} r.m.s.

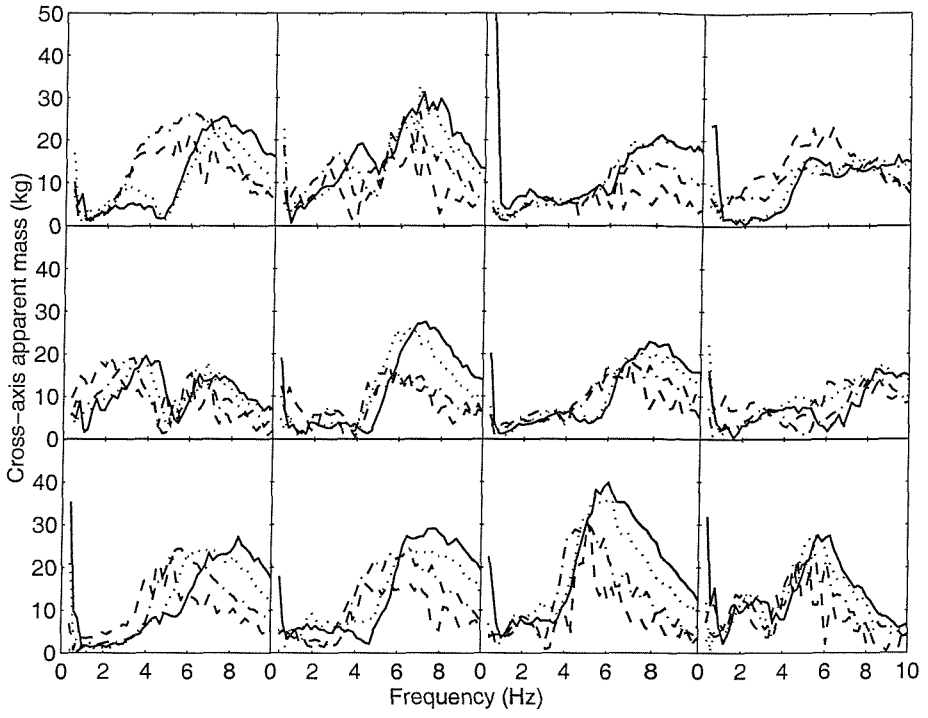

Figure D.11 Vertical cross-axis apparent masses of 12 subjects measured on the seat in the average thigh contact posture at four vibration magnitudes. ———, 0.125 ms^{-2} r.m.s.; ·····, 0.25 ms^{-2} r.m.s.; –·–·–, 0.625 ms^{-2} r.m.s.; – – – –, 1.25 ms^{-2} r.m.s.

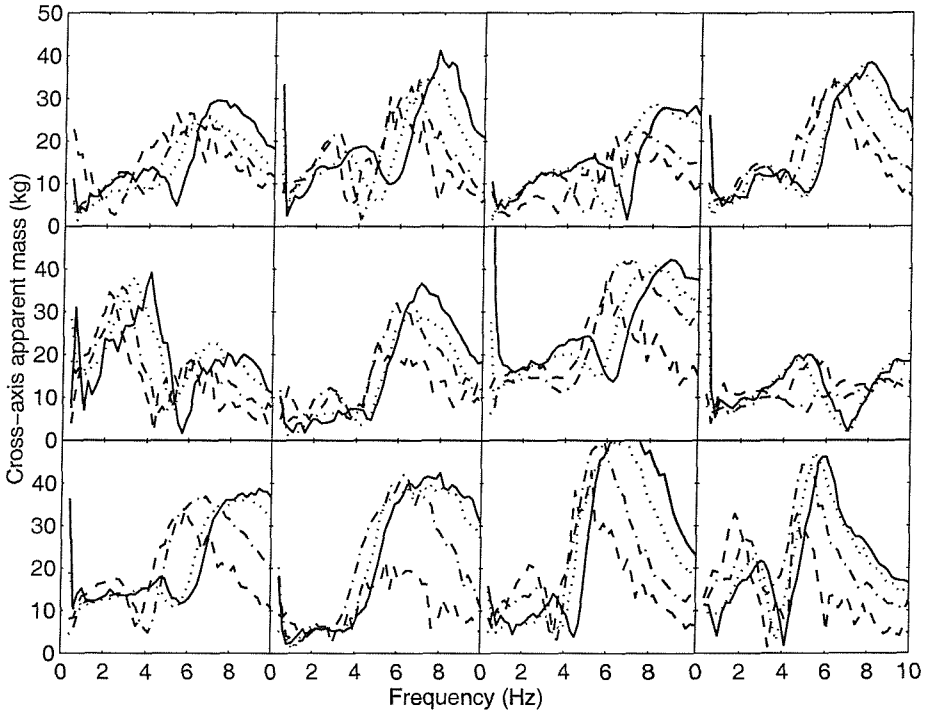

Figure D.12 Vertical cross-axis apparent masses of 12 subjects measured on the seat in the minimum thigh contact posture at four vibration magnitudes. ———, 0.125 ms^{-2} r.m.s.; ·····, 0.25 ms^{-2} r.m.s.; –·–·–, 0.625 ms^{-2} r.m.s.; – – – –, 1.25 ms^{-2} r.m.s.

D.2.4 Lateral cross-axis apparent mass on the seat

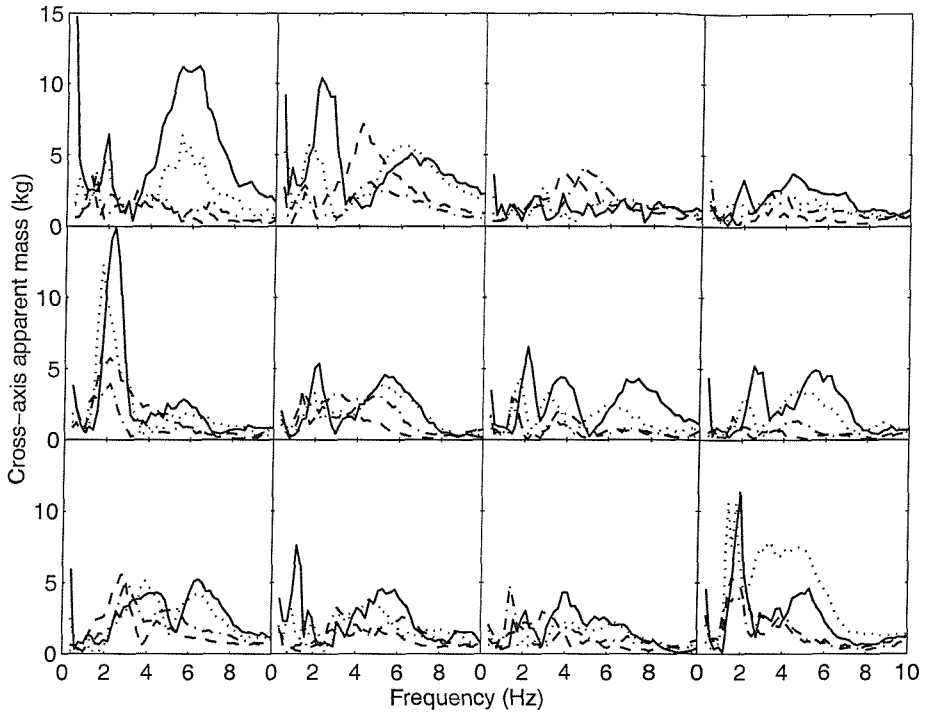

Figure D.13 Lateral cross-axis apparent masses of 12 subjects measured on the seat in the feet hanging posture at four vibration magnitudes. ———, 0.125 ms^{-2} r.m.s.; ·····, 0.25 ms^{-2} r.m.s.; –·–·–, 0.625 ms^{-2} r.m.s.; – – – –, 1.25 ms^{-2} r.m.s.

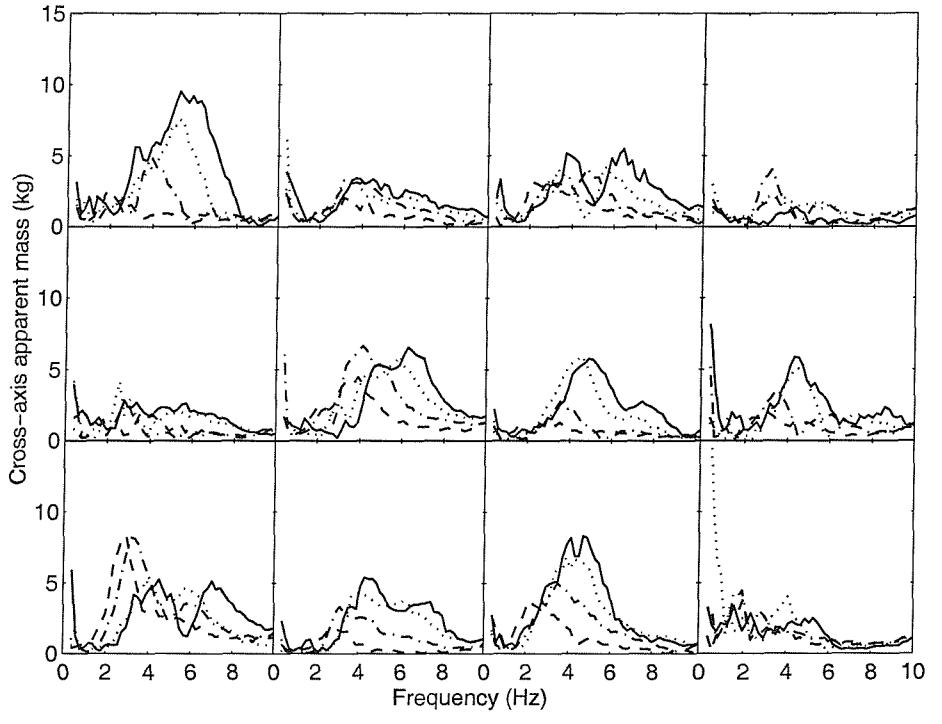

Figure D.14 Lateral cross-axis apparent masses of 12 subjects measured on the seat in the maximum thigh contact posture at four vibration magnitudes. ———, 0.125 ms^{-2} r.m.s.; ·····, 0.25 ms^{-2} r.m.s.; –·–·–, 0.625 ms^{-2} r.m.s.; – – – –, 1.25 ms^{-2} r.m.s.

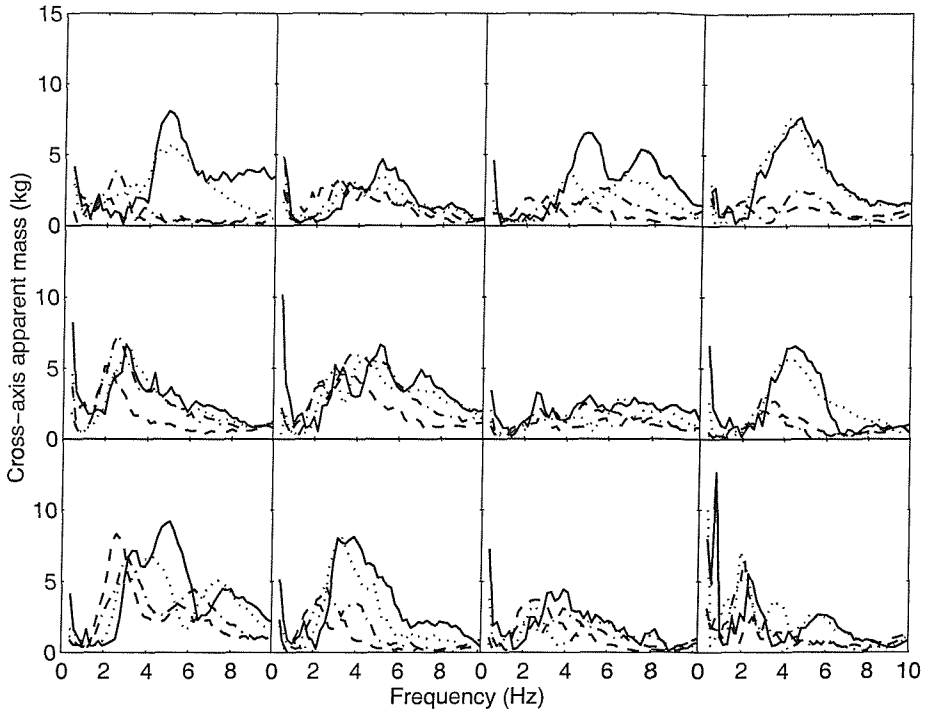

Figure D.15 Lateral cross-axis apparent masses of 12 subjects measured on the seat in the average thigh contact posture at four vibration magnitudes. ———, 0.125 ms^{-2} r.m.s.; ·····, 0.25 ms^{-2} r.m.s.; –·–·–, 0.625 ms^{-2} r.m.s.; – – – –, 1.25 ms^{-2} r.m.s.

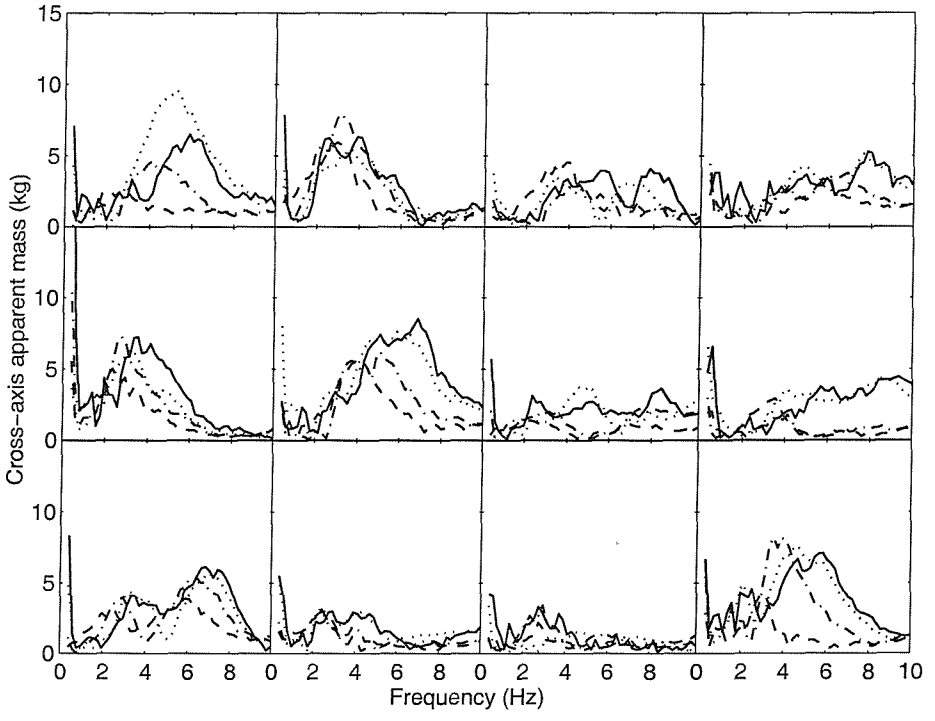

Figure D.16 Lateral cross-axis apparent masses of 12 subjects measured on the seat in the minimum thigh contact posture at four vibration magnitudes. ———, 0.125 ms^{-2} r.m.s.; ·····, 0.25 ms^{-2} r.m.s.; –·–·–, 0.625 ms^{-2} r.m.s.; – – – –, 1.25 ms^{-2} r.m.s.

D.2.5 Coherencies of the fore-and-aft apparent mass at the back

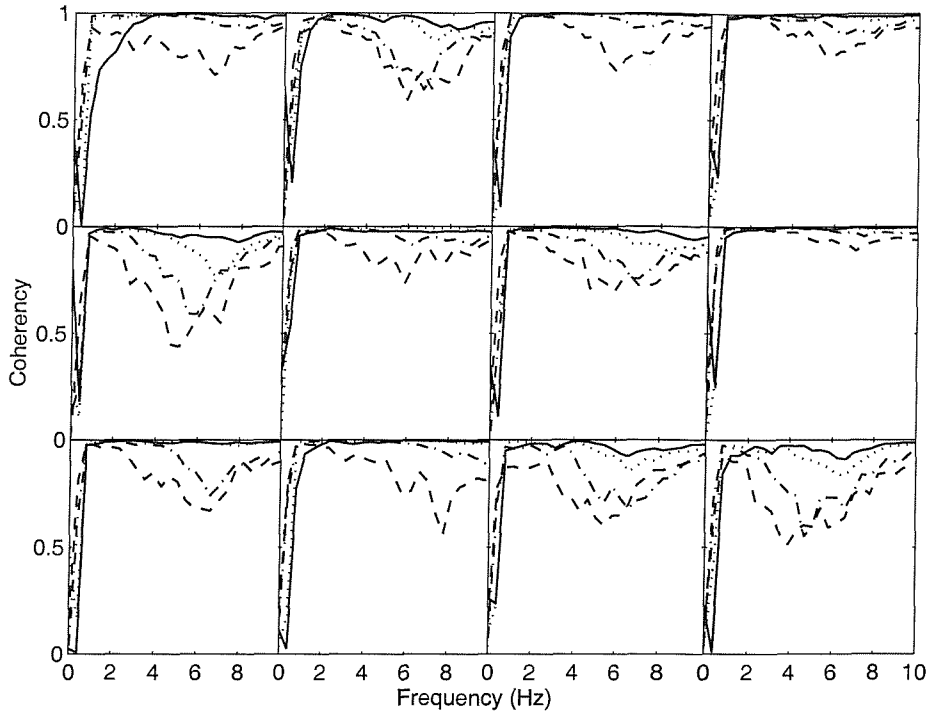

Figure D.17 Coherencies of apparent masses of 12 subjects measured at the back in the feet hanging posture at four vibration magnitudes. ———, 0.125 ms^{-2} r.m.s.; ·····, 0.25 ms^{-2} r.m.s.; –·–·–, 0.625 ms^{-2} r.m.s.; – – – –, 1.25 ms^{-2} r.m.s.

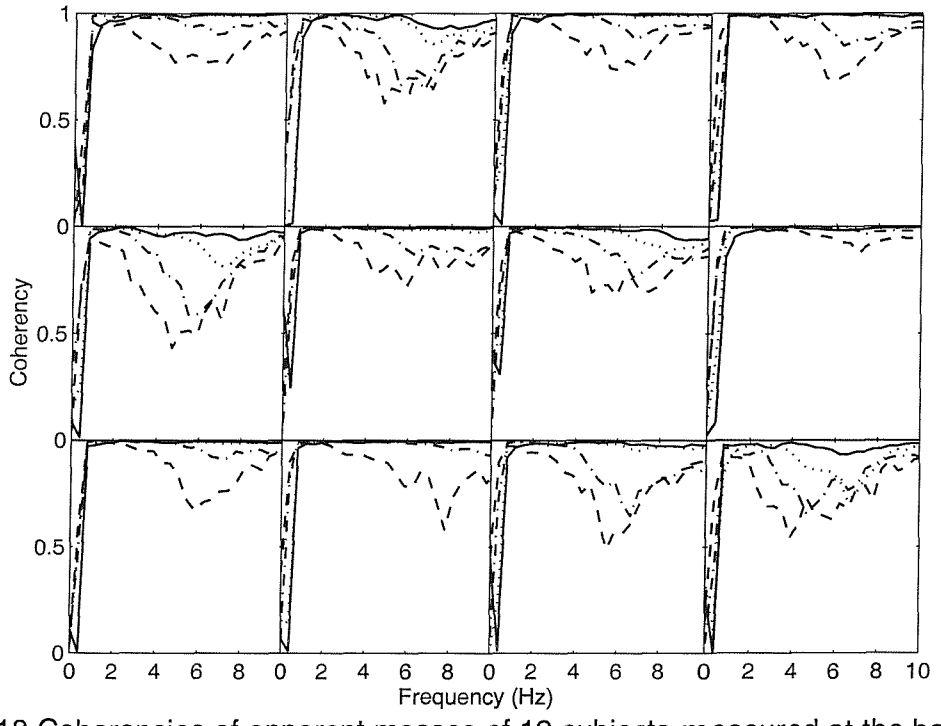

Figure D.18 Coherencies of apparent masses of 12 subjects measured at the back in the maximum thigh contact posture at four vibration magnitudes. ———, 0.125 ms^{-2} r.m.s.; ·····, 0.25 ms^{-2} r.m.s.; –·–·–, 0.625 ms^{-2} r.m.s.; – – – –, 1.25 ms^{-2} r.m.s.

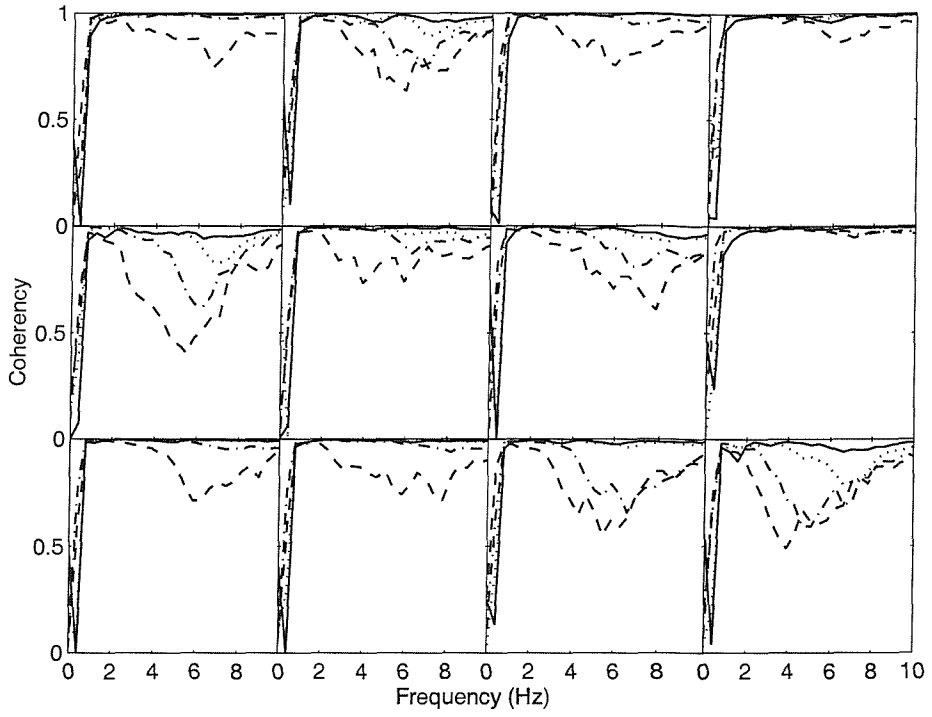

Figure D.19 Coherencies of apparent masses of 12 subjects measured at the back in the average thigh contact posture at four vibration magnitudes. ———, 0.125 ms^{-2} r.m.s.; ·····, 0.25 ms^{-2} r.m.s.; —·—·—, 0.625 ms^{-2} r.m.s.; – – – –, 1.25 ms^{-2} r.m.s.

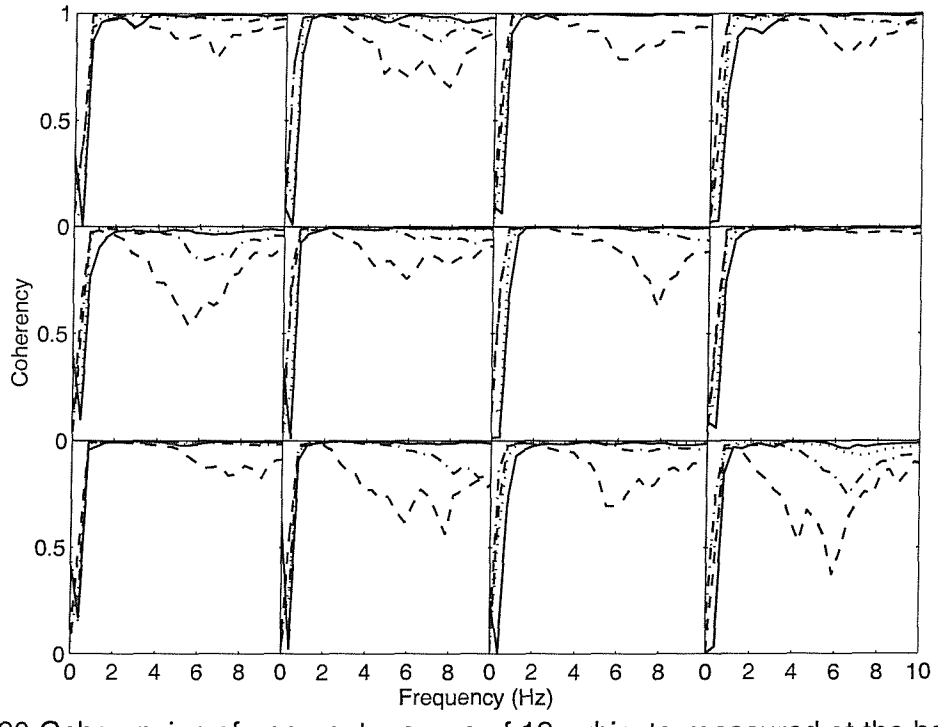

Figure D.20 Coherencies of apparent masses of 12 subjects measured at the back in the minimum thigh contact posture at four vibration magnitudes. ———, 0.125 ms^{-2} r.m.s.; ·····, 0.25 ms^{-2} r.m.s.; —·—·—, 0.625 ms^{-2} r.m.s.; – – – –, 1.25 ms^{-2} r.m.s.

APPENDIX E

INDIVIDUAL DATA: VERTICAL EXCITATION WITH DIFFERENT SEAT SURFACE ANGLES (CHAPTER 8)

APPENDIX E Vertical excitation with different seat surface angles (Chapter 8)

E.1 Characteristics of subjects

Table E.1 Characteristics of subjects used in the experiment described in Chapter 8.

Subject No.	Mass (kg)	Stature (m)	Age (year)
1	90.0	1.82	38
2	69.0	1.75	26
3	74.0	1.77	34
4	77.0	1.86	47
5	103.0	1.86	26
6	68.0	1.69	41
7	76.0	1.75	24
8	66.0	1.75	24
9	67.5	1.64	27
10	88.0	1.85	26
11	75.0	1.84	27
12	65.0	1.68	31

E.2 Instructions given to the subjects prior exposure to vibration

- The goal of this experiment is to find out the effect of seat surface angle on the forces measured on the seat in the 'vertical' and 'fore-and-aft' directions during whole-body vertical vibration.

- You will be seated on a rigid seat adopting an upright posture and exposed to random vertical vibration at different vibration magnitudes. At each vibration magnitude, four different seat angles (0, 5, 10, and 15°) will be tested once with a backrest and once without a backrest. The experimenter will show you the order in which the above conditions will be used.

- During the exposure to vibration, you can stop the vibration at any time by pressing the red STOP button that you will be holding throughout the experiment.

Thank you for taking part in this experiment.

E.3 Individual results

E.3.1 'Vertical apparent mass' on the seat measured without using a backrest

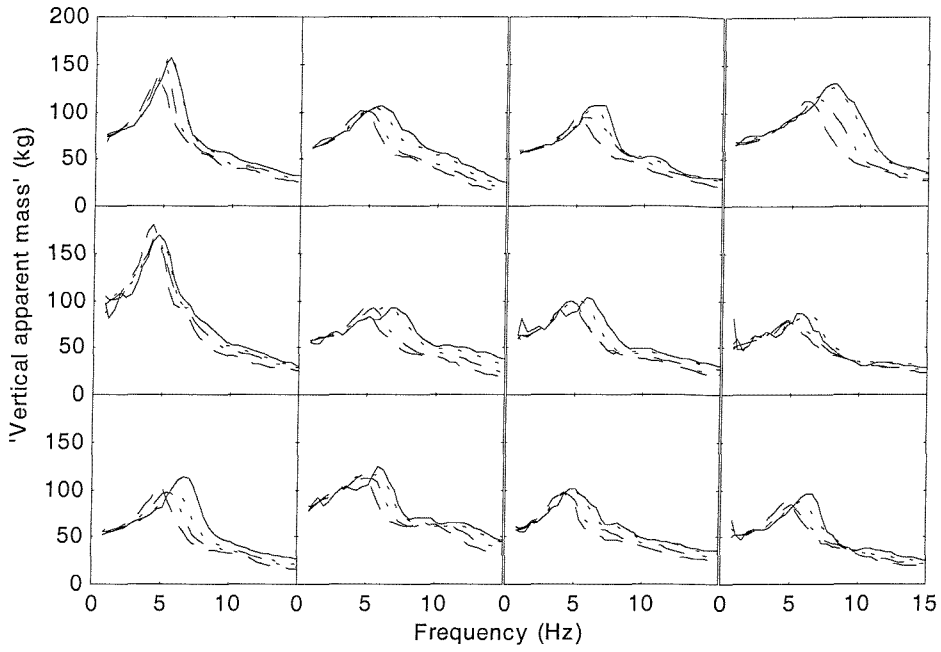

Figure E.1 'Vertical apparent masses' of twelve subjects measured without a backrest with seat surface angle of 0°: ———, 0.125 ms^{-2} r.m.s.; ·····, 0.25 ms^{-2} r.m.s.; —·—·—, 0.625 ms^{-2} r.m.s.; – – – –, 1.25 ms^{-2} r.m.s.

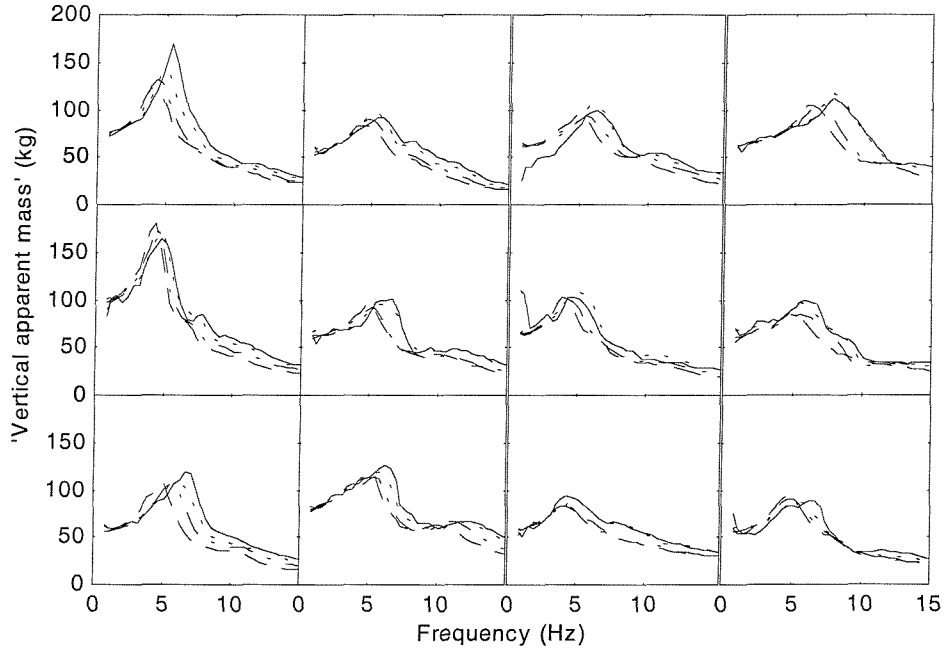

Figure E.2 'Vertical apparent masses' of twelve subjects measured without a backrest with seat surface angle of 5°: ———, 0.125 ms^{-2} r.m.s.; ·····, 0.25 ms^{-2} r.m.s.; —·—·—, 0.625 ms^{-2} r.m.s.; – – – –, 1.25 ms^{-2} r.m.s.

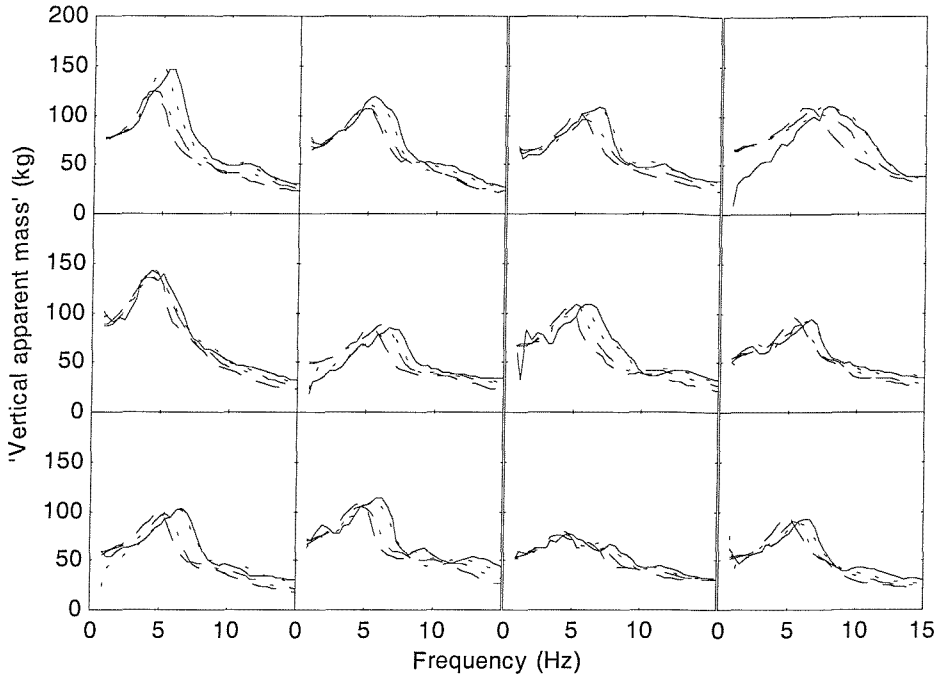

Figure E.3 'Vertical apparent masses' of twelve subjects measured without a backrest with seat surface angle of 10°: ———, 0.125 ms^{-2} r.m.s.; ·····, 0.25 ms^{-2} r.m.s.; —·—·—, 0.625 ms^{-2} r.m.s.; – – – –, 1.25 ms^{-2} r.m.s.

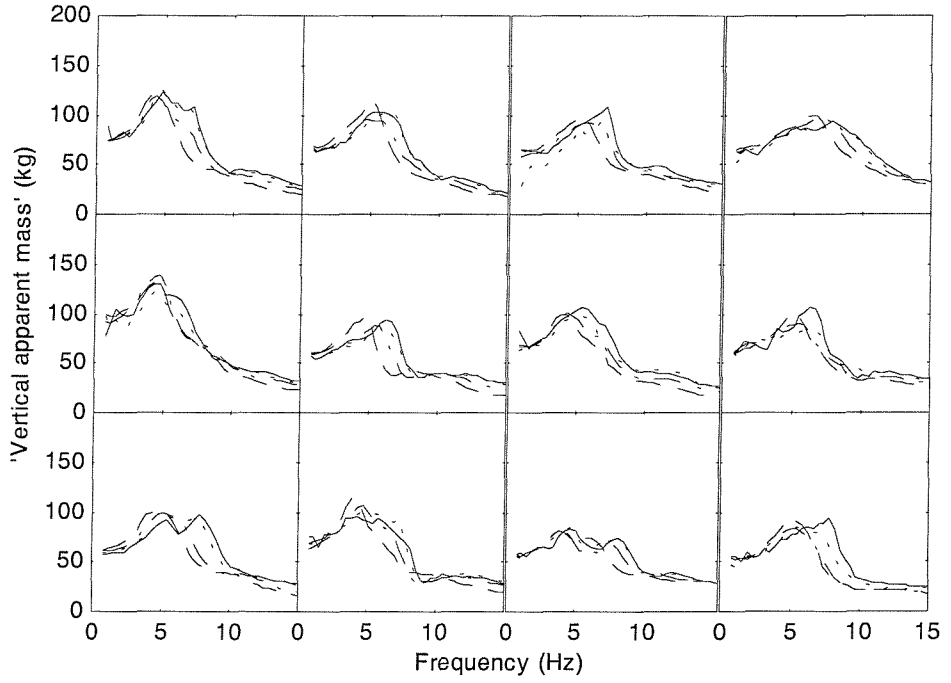

Figure E.4 'Vertical apparent masses' of twelve subjects measured without a backrest with seat surface angle of 15°: ———, 0.125 ms^{-2} r.m.s.; ·····, 0.25 ms^{-2} r.m.s.; —·—·—, 0.625 ms^{-2} r.m.s.; – – – –, 1.25 ms^{-2} r.m.s.

E.3.2 'Vertical apparent mass' on the seat measured with using a backrest

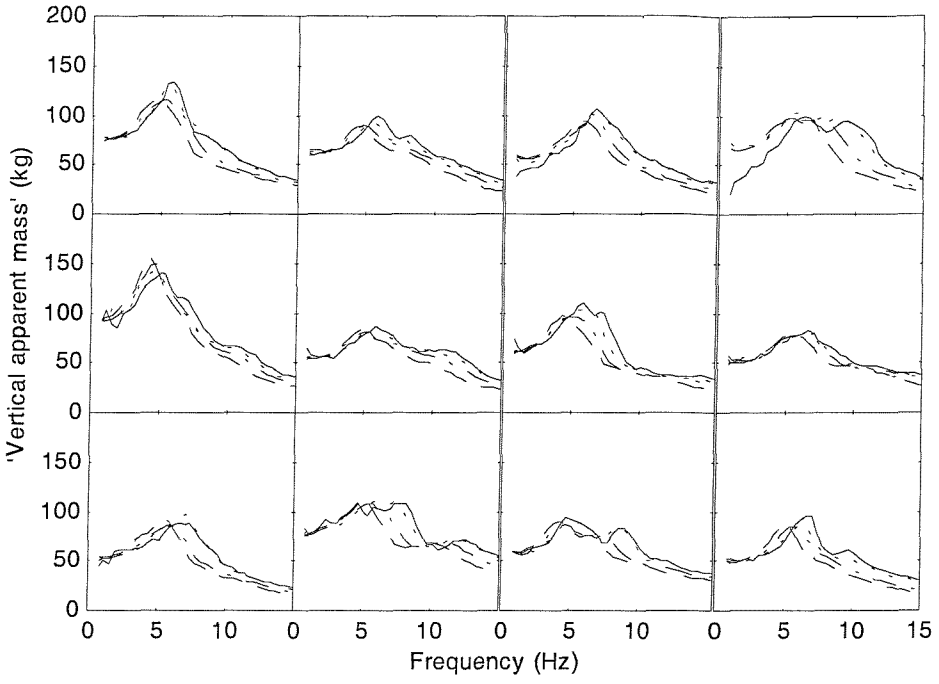

Figure E.5 'Vertical apparent masses' of twelve subjects measured with a backrest and with seat surface angle of 0°: ———, 0.125 ms^{-2} r.m.s.; ·····, 0.25 ms^{-2} r.m.s.; —·—·—, 0.625 ms^{-2} r.m.s.; – – – –, 1.25 ms^{-2} r.m.s.

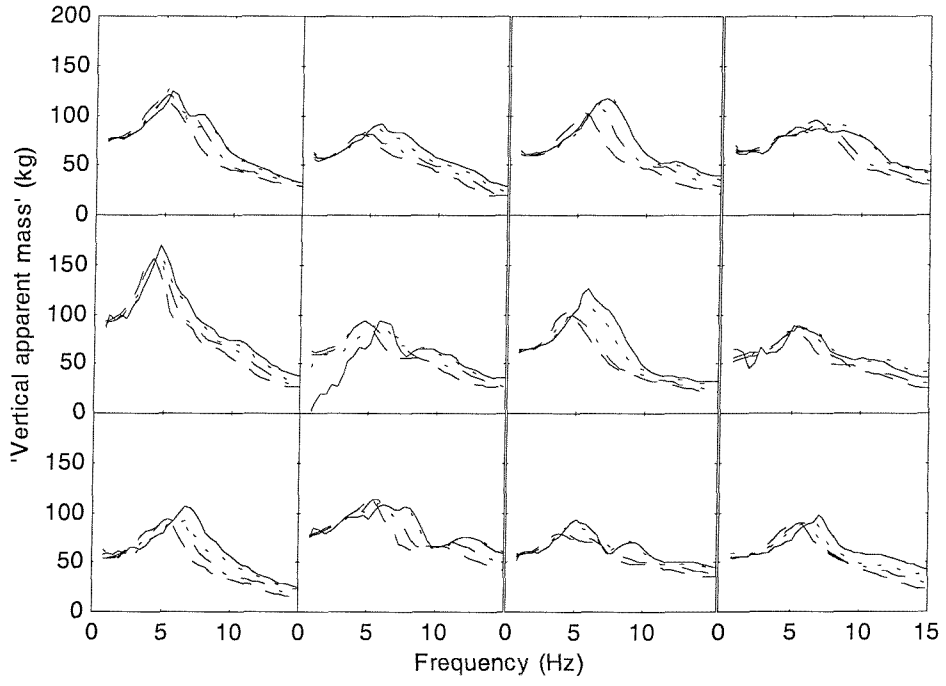

Figure E.6 'Vertical apparent masses' of twelve subjects measured with a backrest and with seat surface angle of 5°: ———, 0.125 ms^{-2} r.m.s.; ·····, 0.25 ms^{-2} r.m.s.; —·—·—, 0.625 ms^{-2} r.m.s.; – – – –, 1.25 ms^{-2} r.m.s.

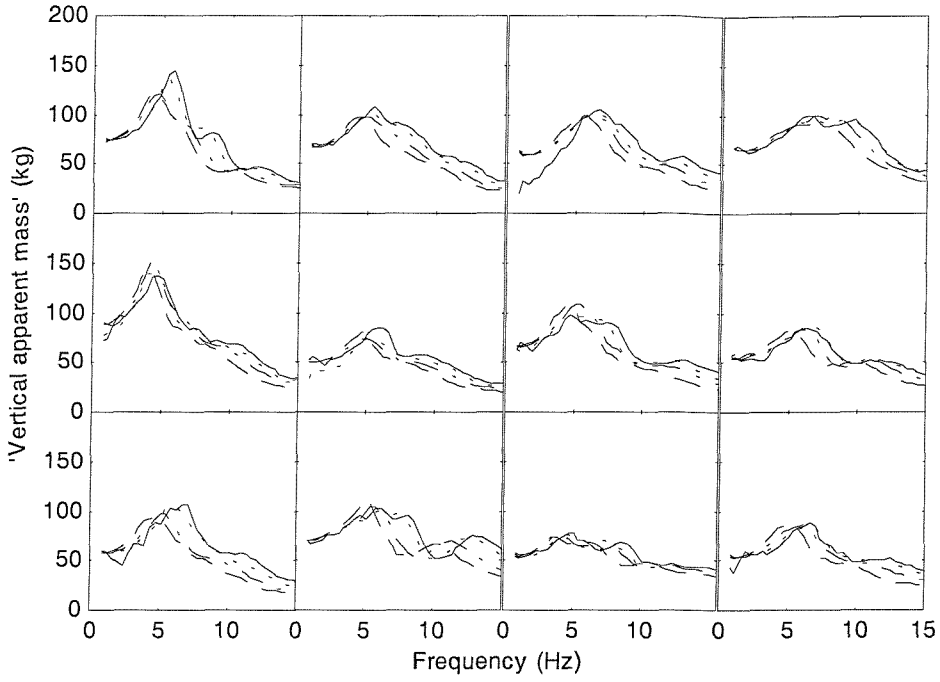

Figure E.7 'Vertical apparent masses' of twelve subjects measured with a backrest and with seat surface angle of 10°: ———, 0.125 ms^{-2} r.m.s.; ·····, 0.25 ms^{-2} r.m.s.; —·—·—, 0.625 ms^{-2} r.m.s.; – – – –, 1.25 ms^{-2} r.m.s.

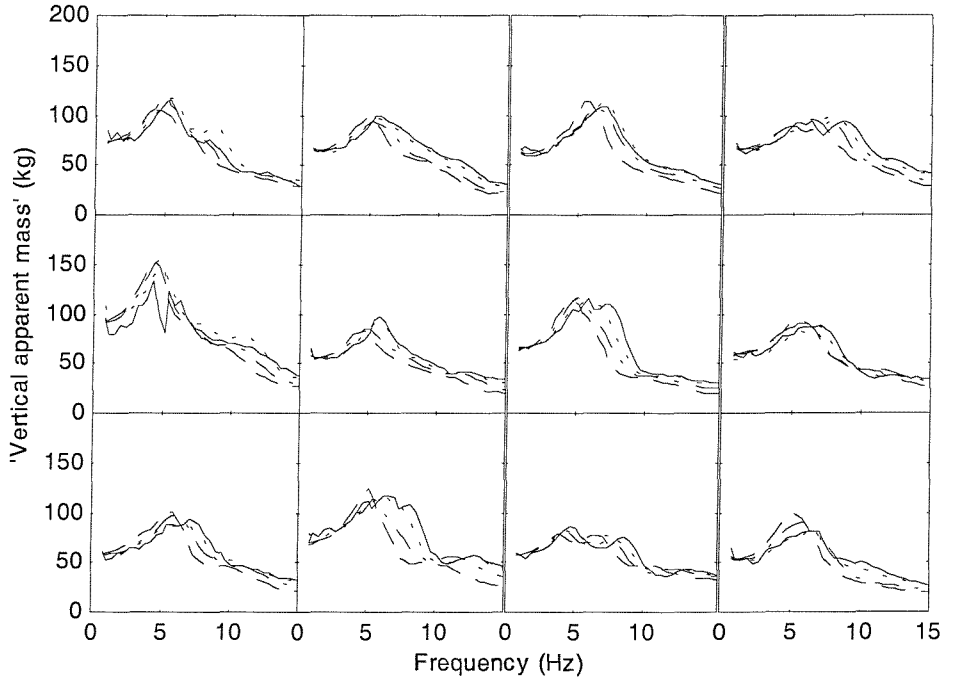

Figure E.8 'Vertical apparent masses' of twelve subjects measured with a backrest and with seat surface angle of 15°: ———, 0.125 ms^{-2} r.m.s.; ·····, 0.25 ms^{-2} r.m.s.; —·—·—, 0.625 ms^{-2} r.m.s.; – – – –, 1.25 ms^{-2} r.m.s.

E.3.3 'Fore-and-aft cross-axis apparent mass' on the seat measured without using a backrest

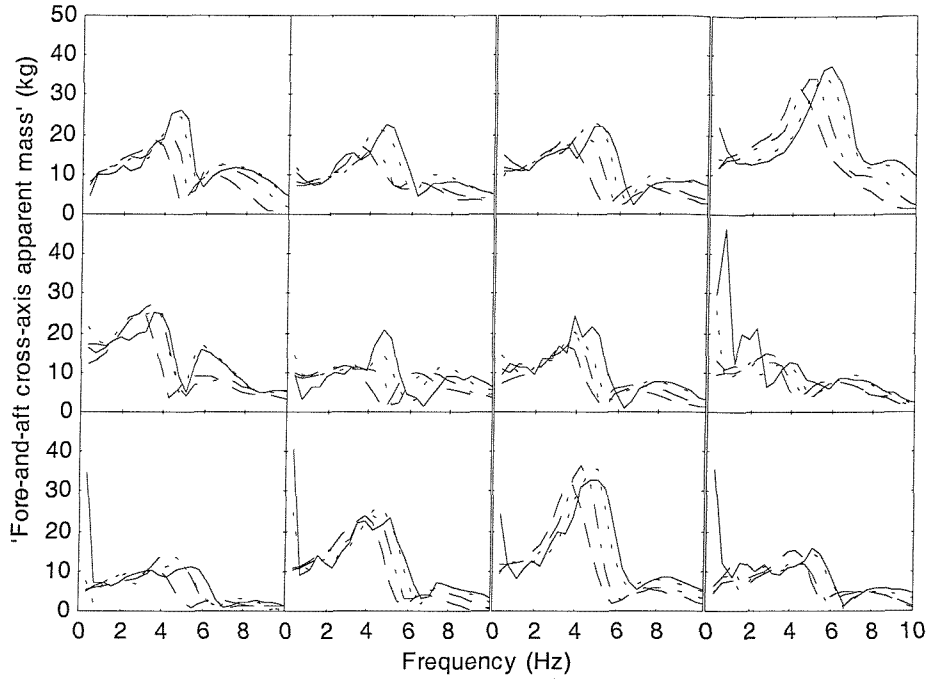

Figure E.9 'Fore-and-aft cross-axis apparent masses' of twelve subjects measured without a backrest with seat surface angle of 0°: ———, 0.125 ms^{-2} r.m.s.; ·····, 0.25 ms^{-2} r.m.s.; –·–·–, 0.625 ms^{-2} r.m.s.; – – – –, 1.25 ms^{-2} r.m.s.

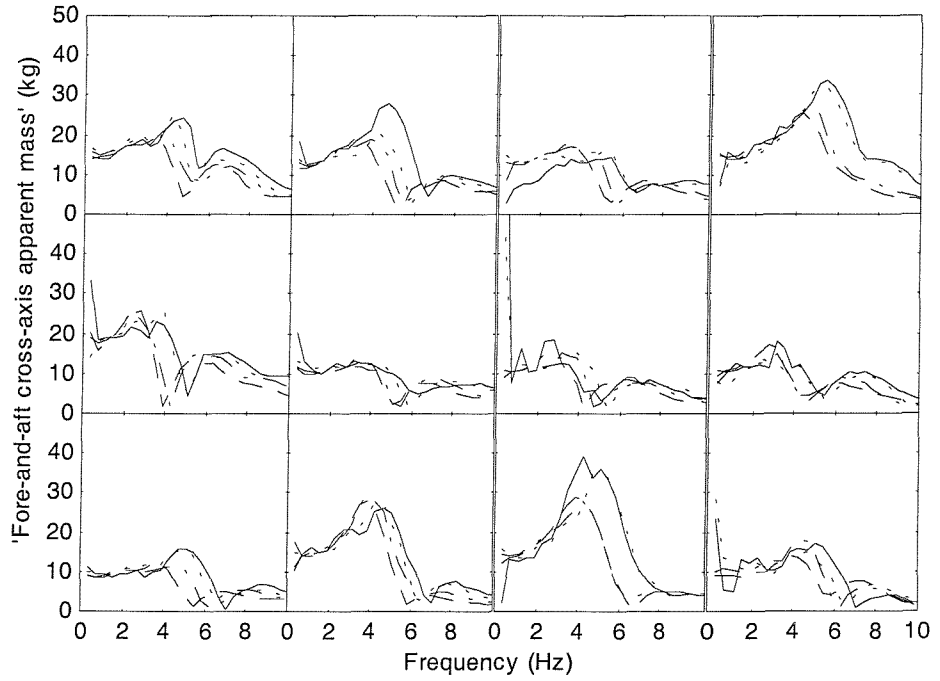

Figure E.10 'Fore-and-aft cross-axis apparent masses' of twelve subjects measured without a backrest with seat surface angle of 5°: ———, 0.125 ms^{-2} r.m.s.; ·····, 0.25 ms^{-2} r.m.s.; –·–·–, 0.625 ms^{-2} r.m.s.; – – – –, 1.25 ms^{-2} r.m.s.

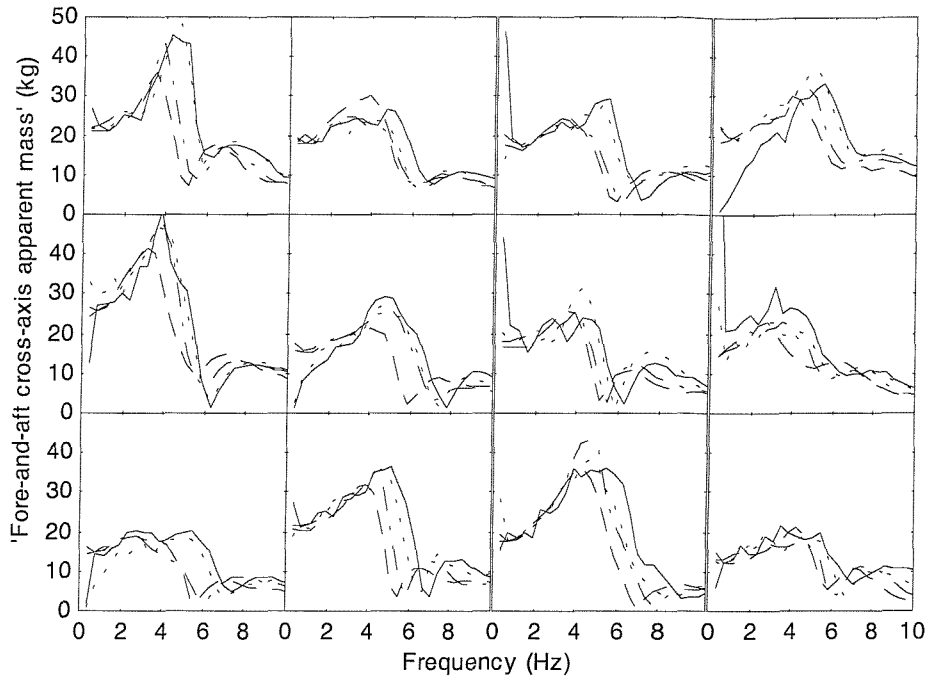

Figure E.11 'Fore-and-aft cross-axis apparent masses' of twelve subjects measured without a backrest with seat surface angle of 10°: ———, 0.125 ms^{-2} r.m.s.; ·····, 0.25 ms^{-2} r.m.s.; –·–·–, 0.625 ms^{-2} r.m.s.; – – – –, 1.25 ms^{-2} r.m.s.

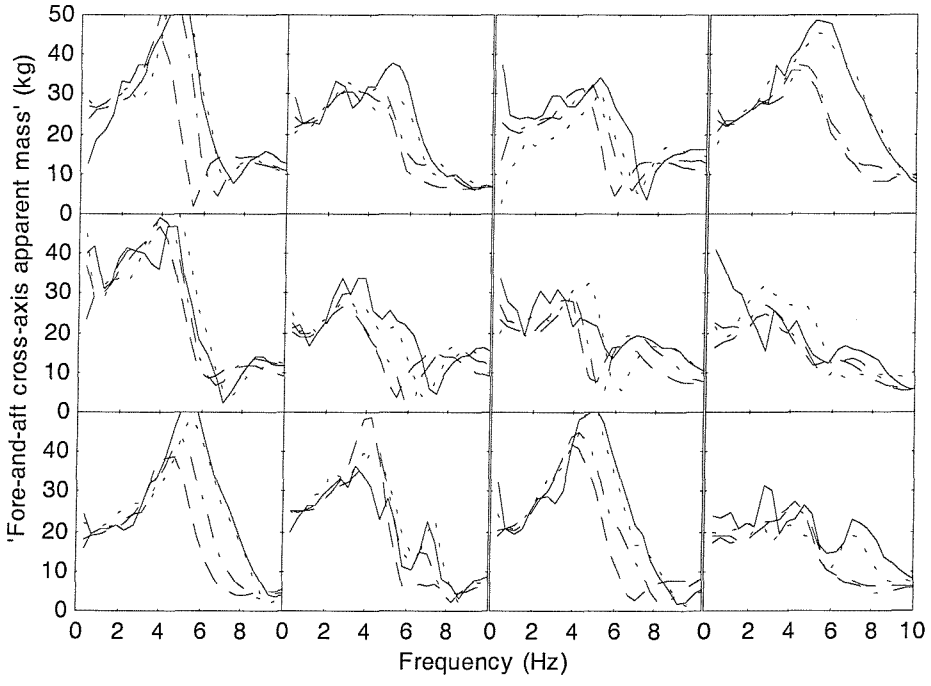

Figure E.12 'Fore-and-aft cross-axis apparent masses' of twelve subjects measured without a backrest with seat surface angle of 15°: ———, 0.125 ms^{-2} r.m.s.; ·····, 0.25 ms^{-2} r.m.s.; –·–·–, 0.625 ms^{-2} r.m.s.; – – – –, 1.25 ms^{-2} r.m.s.

E.3.4 'Fore-and-aft cross-axis apparent mass' on the seat measured with using a backrest

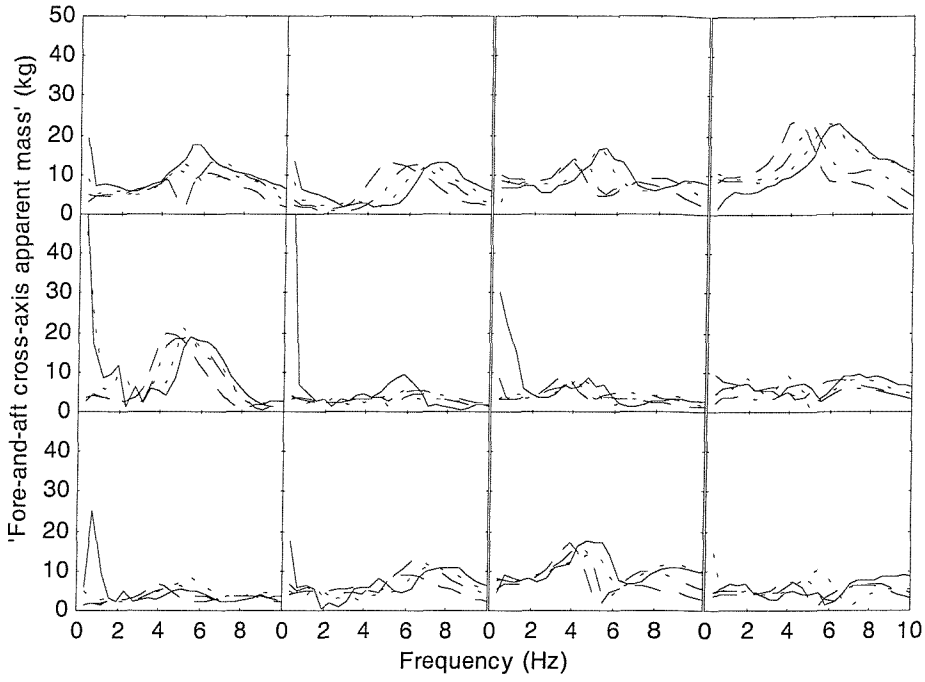

Figure E.13 'Fore-and-aft cross-axis apparent masses' of twelve subjects measured with a backrest and with seat surface angle of 0°: ———, 0.125 ms^{-2} r.m.s.; ·····, 0.25 ms^{-2} r.m.s.; —·—·—, 0.625 ms^{-2} r.m.s.; – – – –, 1.25 ms^{-2} r.m.s.

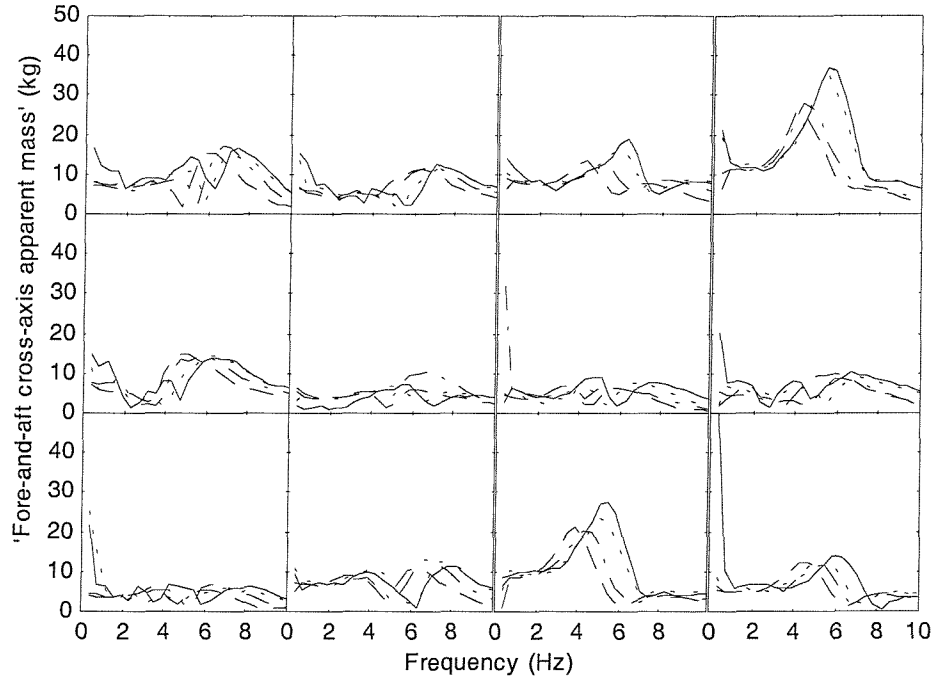

Figure E.14 'Fore-and-aft cross-axis apparent masses' of twelve subjects measured with a backrest and with seat surface angle of 5°: ———, 0.125 ms^{-2} r.m.s.; ·····, 0.25 ms^{-2} r.m.s.; —·—·—, 0.625 ms^{-2} r.m.s.; – – – –, 1.25 ms^{-2} r.m.s.

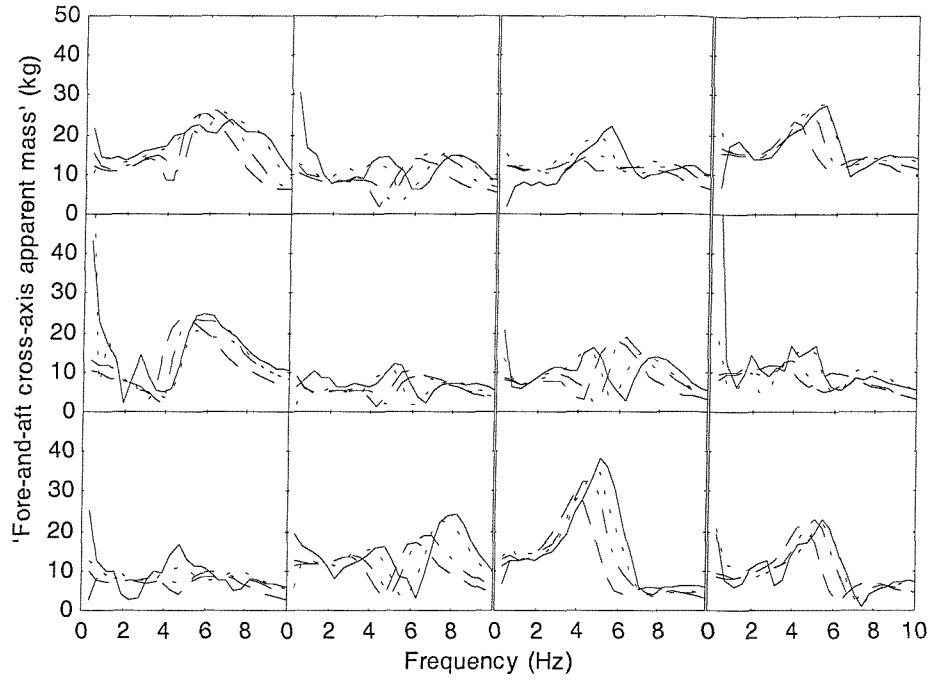

Figure E.15 'Fore-and-aft cross-axis apparent masses' of twelve subjects measured with a backrest and with seat surface angle of 10°: ———, 0.125 ms^{-2} r.m.s.; ·····, 0.25 ms^{-2} r.m.s.; –·–·–, 0.625 ms^{-2} r.m.s.; – – – –, 1.25 ms^{-2} r.m.s.

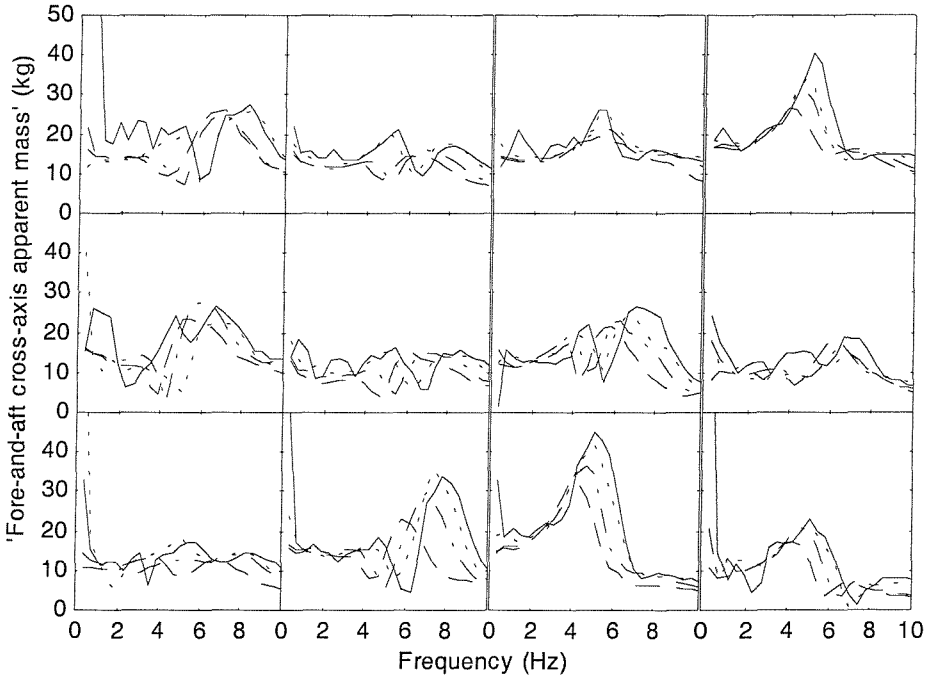

Figure E.16 'Fore-and-aft cross-axis apparent masses' of twelve subjects measured with a backrest and with seat surface angle of 15°: ———, 0.125 ms^{-2} r.m.s.; ·····, 0.25 ms^{-2} r.m.s.; –·–·–, 0.625 ms^{-2} r.m.s.; – – – –, 1.25 ms^{-2} r.m.s.

APPENDIX F

INDIVIDUAL DATA: MODELLING RESULTS

(CHAPTER 9)

APPENDIX F RESULTS FROM MODELS

F.1 Results from model 1

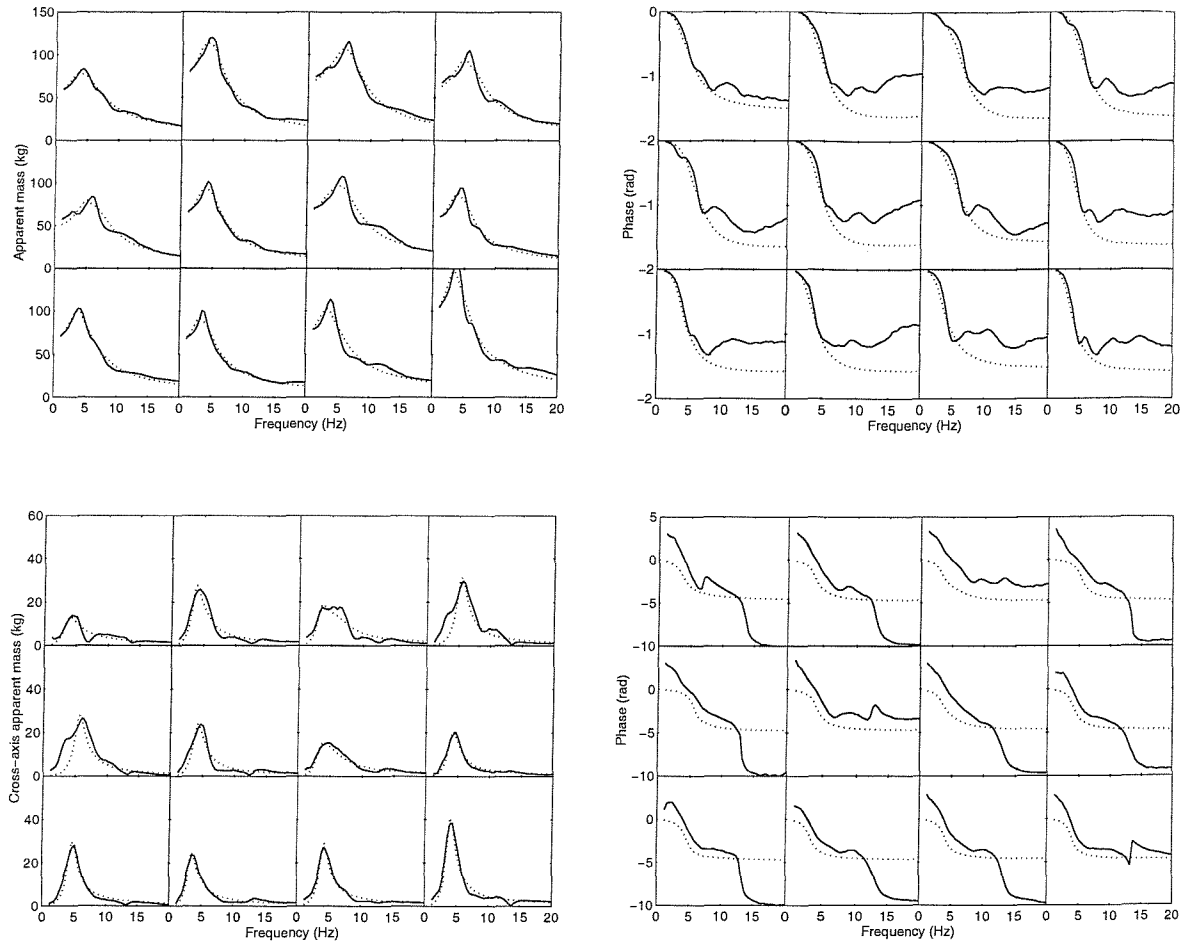

Figure F.1 Apparent masses and fore-and-aft cross-axis apparent masses of 12 subjects calculated from the model and obtained from the experiment in the maximum thigh contact posture: ———, experiment; ·····, model.

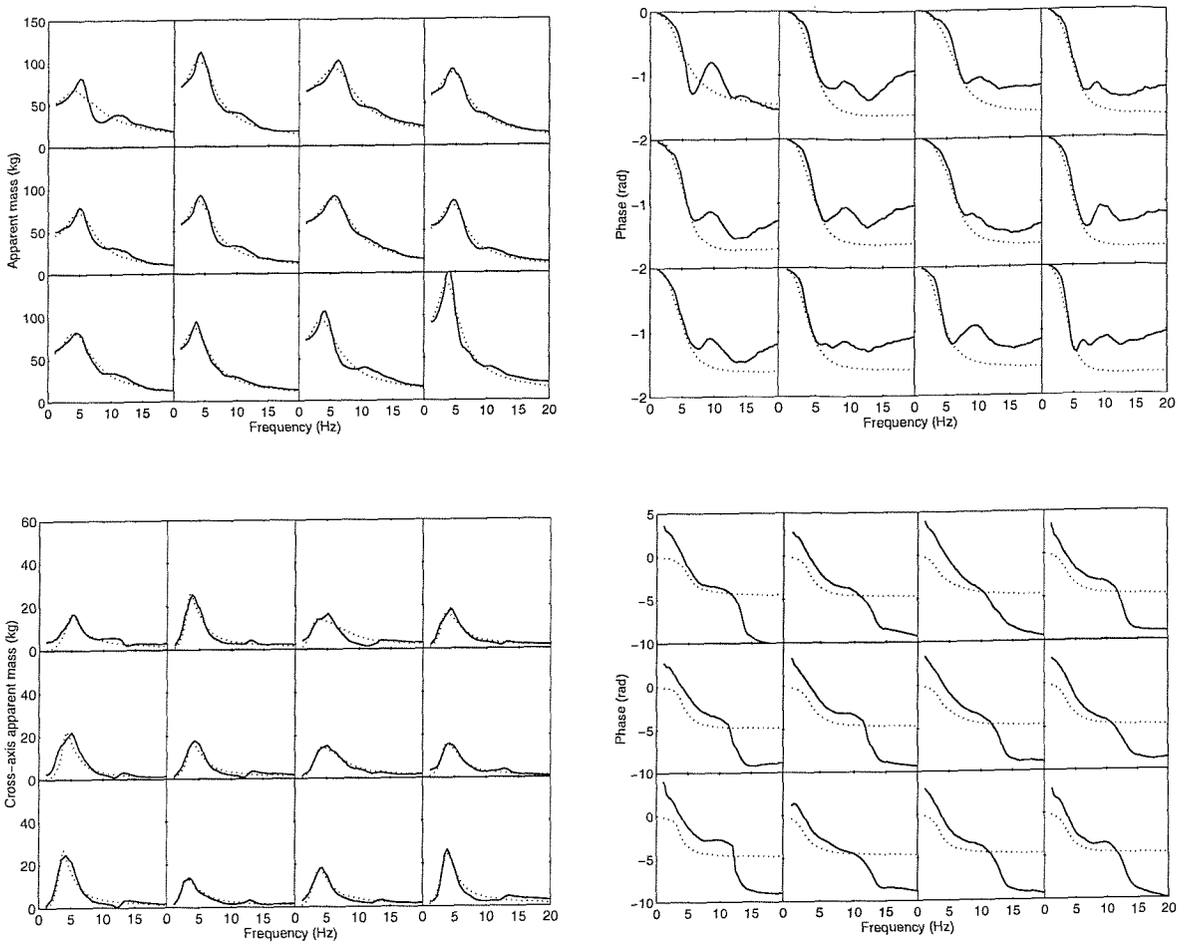

Figure F.2 Apparent masses and fore-and-aft cross-axis apparent masses of 12 subjects calculated from the model and obtained from the experiment in the average thigh contact posture: ———, experiment; ·····, model.

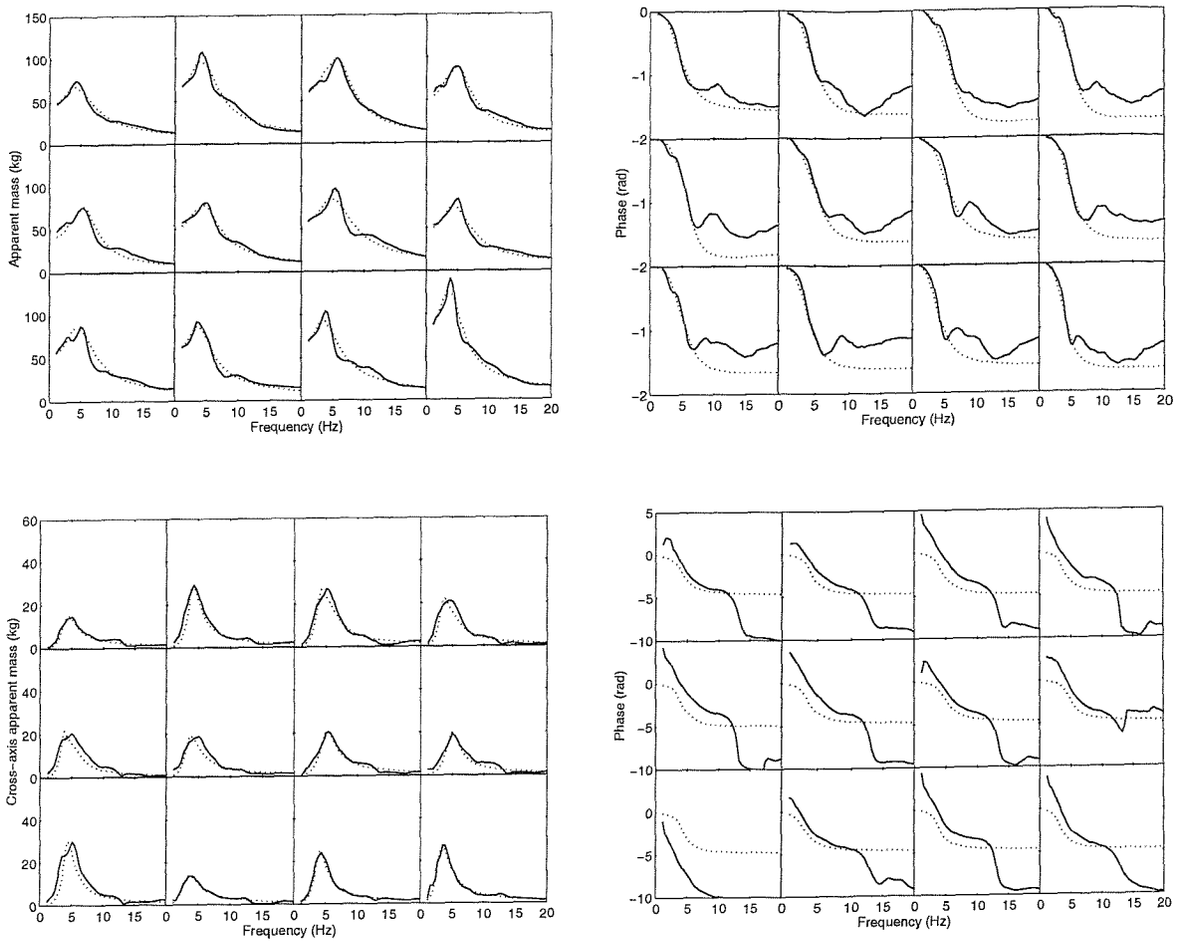

Figure F.3 Apparent masses and fore-and-aft cross-axis apparent masses of 12 subjects calculated from the model and obtained from the experiment in the minimum thigh contact posture: ———, experiment; ·····, model.

F.2 Effect of ±40% change in the parameters of Model 5 on the resonance frequency and the magnitude at resonance of the vertical apparent mass.

Table F.1 Effect of ±40% change in the mass of m_2 on the resonance frequency and the magnitude at resonance of the vertical apparent mass.

	Feet hanging						Average thigh contact					
	Frequency (Hz)			Magnitude (kg)			Frequency (Hz)			Magnitude (kg)		
Subject	-40%	Initial	+40%	-40%	Initial	+40%	-40%	Initial	+40%	-40%	Initial	+40%
1	5.08	5.08	5.08	92.8	103.8	115.3	5.08	4.69	4.69	71.3	84.8	97.5
2	5.08	5.08	5.08	136.7	149.7	161.7	4.69	4.69	4.69	98.1	114.9	131.9
3	5.86	5.86	5.86	146.6	158.9	171.0	5.86	5.86	5.86	88.7	97.0	105.0
4	5.47	5.47	5.08	121.3	129.9	138.6	5.08	4.69	4.69	86.6	94.8	102.3
5	5.47	5.47	5.47	95.5	103.0	109.7	5.08	4.69	4.69	72.6	78.7	84.6
6	4.30	4.30	4.30	105.6	125.2	143.8	4.30	4.69	4.69	83.4	96.5	110.1
7	5.86	5.47	5.47	128.8	141.6	154.3	6.25	6.25	6.64	82.6	98.1	114.1
8	5.47	5.47	5.47	100.5	109.5	117.8	4.69	4.69	4.69	81.3	89.7	97.2
9	5.08	4.69	4.69	103.6	135.1	163.4	4.69	4.30	4.30	80.6	89.1	97.3
10	4.30	4.30	4.30	132.5	143.4	153.0	3.91	3.91	4.30	84.8	107.2	132.2
11	4.30	4.30	4.30	113.5	134.5	153.1	4.30	4.30	4.30	95.4	108.6	122.1
12	3.52	3.52	3.52	155.8	147.3	150.8	3.91	3.91	3.91	147.2	151.3	157.6

Table F.2 Effect of ±40% change in the mass of m_3 on the resonance frequency and the magnitude at resonance of the vertical apparent mass.

	Feet hanging						Average thigh contact					
	Frequency (Hz)			Magnitude (kg)			Frequency (Hz)			Magnitude (kg)		
Subject	-40%	Initial	+40%	-40%	Initial	+40%	-40%	Initial	+40%	-40%	Initial	+40%
1	6.64	5.08	4.30	68.2	103.8	136.9	5.86	4.69	4.30	56.3	84.8	111.6
2	5.86	5.08	4.30	94.2	149.7	198.6	6.25	4.69	3.52	82.4	114.9	140.3
3	7.03	5.86	5.08	94.7	158.9	230.6	7.03	5.86	5.08	60.7	97.0	136.8
4	6.64	5.47	4.69	78.3	129.9	188.5	5.86	4.69	4.30	58.6	94.8	132.3
5	6.64	5.47	4.69	61.8	103.0	148.8	5.86	4.69	4.30	48.2	78.7	112.4
6	5.86	4.30	3.52	91.2	125.2	150.1	6.25	4.69	3.52	69.3	96.5	119.6
7	6.64	5.47	5.08	87.5	141.6	197.0	8.20	6.25	5.08	71.7	98.1	116.6
8	6.64	5.47	4.69	67.2	109.5	152.7	5.86	4.69	4.30	55.2	89.7	123.7
9	5.86	4.69	4.30	104.1	135.1	144.9	5.47	4.30	3.91	56.3	89.1	122.0
10	5.47	4.30	3.91	84.5	143.4	206.0	5.08	3.91	3.52	85.9	107.2	120.2
11	5.47	4.30	3.52	93.1	134.5	162.3	5.47	4.30	3.52	74.3	108.6	141.8
12	5.86	3.52	3.12	85.7	147.3	241.9	4.69	3.91	3.52	85.9	151.3	235.9

Table F.3 Effect of ±40% change in k_{1x} on the resonance frequency and the magnitude at resonance of the vertical apparent mass.

	Feet hanging						Average thigh contact					
	Frequency (Hz)			Magnitude (kg)			Frequency (Hz)			Magnitude (kg)		
Subject	-40%	Initial	+40%	-40%	Initial	+40%	-40%	Initial	+40%	-40%	Initial	+40%
1	5.08	5.08	5.47	102.9	103.8	103.9	4.69	4.69	4.69	84.8	84.8	84.9
2	5.08	5.08	5.08	151.0	149.7	152.8	4.69	4.69	4.30	115.0	114.9	117.1
3	5.86	5.86	5.86	159.2	158.9	158.4	5.86	5.86	5.86	97.0	97.0	97.4
4	5.47	5.47	5.47	130.4	129.9	130.5	4.69	4.69	4.69	94.7	94.8	95.9
5	5.47	5.47	5.47	102.4	103.0	103.8	5.08	4.69	5.08	78.5	78.7	79.7
6	4.30	4.30	4.69	122.6	125.2	127.1	4.69	4.69	4.69	95.6	96.5	99.0
7	5.47	5.47	5.47	141.3	141.6	142.4	6.25	6.25	6.25	98.4	98.1	98.1
8	5.47	5.47	5.47	110.0	109.5	110.5	4.69	4.69	4.69	89.4	89.7	90.2
9	5.08	4.69	4.69	136.6	135.1	140.8	4.69	4.30	4.69	88.2	89.1	89.9
10	4.30	4.30	4.30	142.2	143.4	144.1	3.91	3.91	3.91	107.3	107.2	107.9
11	4.30	4.30	4.30	133.8	134.5	138.3	4.30	4.30	4.30	107.5	108.6	110.7
12	3.52	3.52	3.12	154.5	147.3	154.7	3.91	3.91	3.91	151.7	151.3	145.1

Table F.4 Effect of ±40% change in c_{1x} on the resonance frequency and the magnitude at resonance of the vertical apparent mass.

	Feet hanging						Average thigh contact					
	Frequency (Hz)			Magnitude (kg)			Frequency (Hz)			Magnitude (kg)		
Subject	-40%	Initial	+40%	-40%	Initial	+40%	-40%	Initial	+40%	-40%	Initial	+40%
1	5.47	5.08	5.08	104.9	103.8	103.2	4.69	4.69	4.69	84.3	84.8	85.1
2	4.69	5.08	5.08	147.1	149.7	151.1	4.69	4.69	4.69	113.3	114.9	116.1
3	5.86	5.86	5.86	159.0	158.9	158.8	5.86	5.86	5.86	96.5	97.0	97.2
4	5.47	5.47	5.47	128.9	129.9	130.3	4.69	4.69	4.69	93.9	94.8	95.3
5	5.47	5.47	5.47	103.0	103.0	103.2	4.69	4.69	5.08	78.8	78.7	78.9
6	4.30	4.30	4.30	125.4	125.2	124.8	4.69	4.69	4.69	95.2	96.5	97.1
7	5.47	5.47	5.47	141.1	141.6	141.9	6.25	6.25	6.25	97.2	98.1	99.0
8	5.47	5.47	5.47	108.2	109.5	110.2	4.69	4.69	4.69	89.4	89.7	89.9
9	4.69	4.69	4.69	130.7	135.1	136.9	4.30	4.30	4.30	89.6	89.1	88.9
10	4.30	4.30	4.30	143.8	143.4	143.3	3.91	3.91	3.91	106.2	107.2	107.9
11	4.30	4.30	4.30	131.9	134.5	135.6	4.30	4.30	4.30	108.0	108.6	108.7
12	3.52	3.52	3.12	151.3	147.3	148.8	3.91	3.91	3.91	153.1	151.3	150.0

Table F.5 Effect of ±40% change in k_2 on the resonance frequency and the magnitude at resonance of the vertical apparent mass.

	Feet hanging						Average thigh contact					
	Frequency (Hz)			Magnitude (kg)			Frequency (Hz)			Magnitude (kg)		
Subject	-40%	Initial	+40%	-40%	Initial	+40%	-40%	Initial	+40%	-40%	Initial	+40%
1	5.47	5.08	5.08	104.7	103.8	103.2	4.69	4.69	5.08	85.7	84.8	83.5
2	5.08	5.08	5.08	153.1	149.7	145.0	4.69	4.69	4.69	118.4	114.9	111.5
3	5.86	5.86	5.86	159.8	158.9	157.3	5.86	5.86	5.86	97.4	97.0	96.4
4	5.47	5.47	5.47	130.4	129.9	129.2	4.69	4.69	4.69	95.4	94.8	94.2
5	5.47	5.47	5.47	103.4	103.0	102.6	4.69	4.69	4.69	79.0	78.7	78.3
6	4.30	4.30	4.30	126.4	125.2	123.9	4.69	4.69	4.30	99.6	96.5	94.9
7	5.47	5.47	5.47	142.8	141.6	140.0	6.25	6.25	6.25	101.2	98.1	95.0
8	5.47	5.47	5.47	110.3	109.5	108.6	4.69	4.69	4.69	90.7	89.7	88.3
9	4.69	4.69	4.69	145.8	135.1	123.0	4.30	4.30	4.30	90.2	89.1	87.7
10	4.30	4.30	4.30	144.3	143.4	142.4	3.91	3.91	3.91	109.7	107.2	104.6
11	4.30	4.30	4.30	139.6	134.5	128.5	4.30	4.30	4.30	110.3	108.6	107.5
12	4.69	3.52	3.91	142.6	147.3	165.2	3.91	3.91	3.91	136.1	151.3	156.4

Table F.6 Effect of ±40% change in c_2 on the resonance frequency and the magnitude at resonance of the vertical apparent mass.

	Feet hanging						Average thigh contact					
	Frequency (Hz)			Magnitude (kg)			Frequency (Hz)			Magnitude (kg)		
Subject	-40%	Initial	+40%	-40%	Initial	+40%	-40%	Initial	+40%	-40%	Initial	+40%
1	5.47	5.08	5.08	98.0	103.8	108.8	4.69	4.69	4.69	85.6	84.8	84.2
2	5.08	5.08	5.08	151.1	149.7	148.9	5.08	4.69	4.69	112.1	114.9	121.4
3	5.86	5.86	5.86	159.5	158.9	158.3	5.86	5.86	5.86	97.1	97.0	96.9
4	5.47	5.47	5.47	130.2	129.9	129.6	5.08	4.69	4.69	94.7	94.8	95.6
5	5.47	5.47	5.47	103.3	103.0	102.9	4.69	4.69	4.69	78.6	78.7	78.7
6	4.69	4.30	4.30	118.6	125.2	134.5	5.08	4.69	4.69	88.3	96.5	104.3
7	5.47	5.47	5.47	142.3	141.6	141.1	7.03	6.25	6.25	98.5	98.1	103.3
8	5.47	5.47	5.47	110.1	109.5	109.3	4.69	4.69	4.69	90.2	89.7	89.4
9	5.08	4.69	4.69	143.9	135.1	133.8	4.30	4.30	4.30	89.2	89.1	89.1
10	4.30	4.30	4.30	144.0	143.4	143.1	4.30	3.91	3.91	112.1	107.2	112.3
11	4.69	4.30	4.30	135.8	134.5	135.3	4.30	4.30	4.30	100.6	108.6	114.5
12	3.12	3.52	3.52	148.7	147.3	147.0	3.91	3.91	3.91	153.6	151.3	150.2

Table F.7 Effect of ±40% change in k_{3z} on the resonance frequency and the magnitude at resonance of the vertical apparent mass.

	Feet hanging						Average thigh contact					
	Frequency (Hz)			Magnitude (kg)			Frequency (Hz)			Magnitude (kg)		
Subject	-40%	Initial	+40%	-40%	Initial	+40%	-40%	Initial	+40%	-40%	Initial	+40%
1	3.91	5.08	6.25	95.8	103.8	108.5	3.91	4.69	5.86	73.1	84.8	94.2
2	3.91	5.08	6.25	129.5	149.7	169.1	3.52	4.69	5.86	111.2	114.9	124.8
3	4.69	5.86	7.03	131.3	158.9	179.2	4.30	5.86	7.03	86.5	97.0	106.0
4	3.91	5.47	6.64	113.7	129.9	144.6	3.52	4.69	5.86	85.3	94.8	104.7
5	3.91	5.47	6.64	89.8	103.0	113.4	3.52	4.69	5.86	69.9	78.7	86.2
6	3.52	4.30	5.47	118.6	125.2	127.8	3.52	4.69	5.86	93.5	96.5	100.9
7	4.30	5.47	6.64	122.5	141.6	158.0	4.30	6.25	7.81	92.9	98.1	107.1
8	3.91	5.47	6.64	96.7	109.5	122.3	3.52	4.69	5.86	77.2	89.7	99.6
9	3.52	4.69	5.86	112.3	135.1	158.0	3.52	4.30	5.47	78.3	89.1	97.5
10	3.12	4.30	5.47	121.5	143.4	158.0	2.73	3.91	5.08	100.2	107.2	116.5
11	3.12	4.30	5.47	117.8	134.5	151.0	3.12	4.30	5.08	102.2	108.6	112.4
12	2.73	3.52	5.86	149.1	147.3	154.8	3.12	3.91	4.30	135.5	151.3	151.0

Table F.8 Effect of ±40% change in c_{3z} on the resonance frequency and the magnitude at resonance of the vertical apparent mass.

	Feet hanging						Average thigh contact					
	Frequency (Hz)			Magnitude (kg)			Frequency (Hz)			Magnitude (kg)		
Subject	-40%	Initial	+40%	-40%	Initial	+40%	-40%	Initial	+40%	-40%	Initial	+40%
1	5.47	5.08	5.08	130.1	103.8	91.2	5.08	4.69	4.69	115.5	84.8	73.1
2	5.08	5.08	4.69	202.5	149.7	127.5	5.08	4.69	4.30	137.3	114.9	102.6
3	6.25	5.86	5.47	226.8	158.9	130.6	6.25	5.86	5.47	130.5	97.0	84.2
4	5.47	5.47	5.08	181.9	129.9	109.5	5.08	4.69	4.30	128.1	94.8	81.5
5	5.86	5.47	5.08	142.3	103.0	87.2	5.08	4.69	4.69	106.4	78.7	67.8
6	4.69	4.30	4.30	143.8	125.2	113.1	4.69	4.69	4.30	112.2	96.5	87.0
7	5.86	5.47	5.47	198.9	141.6	119.3	6.64	6.25	5.86	117.4	98.1	87.2
8	5.86	5.47	5.08	149.3	109.5	92.7	5.08	4.69	4.69	124.0	89.7	75.6
9	5.08	4.69	4.69	163.6	135.1	119.7	4.69	4.30	4.30	118.7	89.1	77.6
10	4.69	4.30	4.30	201.8	143.4	118.5	4.30	3.91	3.91	121.8	107.2	97.8
11	4.69	4.30	3.91	170.3	134.5	117.8	4.30	4.30	3.91	129.6	108.6	96.7
12	5.08	3.52	2.73	177.4	147.3	136.8	3.91	3.91	3.91	194.1	151.3	128.5

F.3 Effect of ±40% change in the parameters of Model 5 on the resonance frequency and the magnitude at resonance of the cross-axis apparent mass.

Table F.9 Effect of ±40% change in the mass of m_2 on the resonance frequency and the magnitude at resonance of the fore-and-aft cross-axis apparent mass.

	Feet hanging						Average thigh contact					
	Frequency (Hz)			Magnitude (kg)			Frequency (Hz)			Magnitude (kg)		
Subject	-40%	Initial	+40%	-40%	Initial	+40%	-40%	Initial	+40%	-40%	Initial	+40%
1	5.86	5.47	5.47	13.8	21.0	25.7	3.12	5.47	5.47	8.3	10.0	12.8
2	4.69	4.69	4.69	24.0	32.5	36.2	3.91	3.91	3.91	19.5	23.1	22.5
3	3.52	3.91	3.91	21.9	16.7	12.9	3.12	5.47	5.47	8.0	9.9	10.6
4	5.08	5.08	5.08	11.9	15.8	17.7	4.30	4.30	4.30	10.8	13.1	13.8
5	5.86	5.86	5.86	11.6	15.7	18.1	5.08	5.08	5.08	11.8	14.2	15.0
6	4.30	4.30	4.30	18.5	27.6	31.7	4.30	4.30	4.30	13.0	16.5	17.5
7	5.86	5.86	5.86	11.8	17.0	20.4	4.69	4.30	4.30	11.3	13.6	13.2
8	5.08	5.08	5.08	13.5	17.0	18.2	4.69	4.69	4.69	8.0	11.0	12.8
9	4.69	4.69	4.69	24.4	35.9	41.7	4.69	4.69	4.69	12.6	17.0	19.4
10	4.69	4.69	4.69	13.8	20.2	24.6	3.52	3.52	3.91	10.2	12.7	13.7
11	4.30	3.91	3.91	21.7	29.3	32.6	3.91	3.91	4.30	13.2	17.0	17.9
12	3.52	3.12	3.12	59.7	72.0	68.5	3.91	3.52	4.30	27.3	31.5	32.1

Table F.10 Effect of ±40% change in the mass of m_3 on the resonance frequency and the magnitude at resonance of the fore-and-aft cross-axis apparent mass.

	Feet hanging						Average thigh contact					
	Frequency (Hz)			Magnitude (kg)			Frequency (Hz)			Magnitude (kg)		
Subject	-40%	Initial	+40%	-40%	Initial	+40%	-40%	Initial	+40%	-40%	Initial	+40%
1	7.03	5.47	4.69	10.0	21.0	31.5	7.42	5.47	4.30	4.9	10.0	17.1
2	5.86	4.69	3.91	11.1	32.5	60.4	5.47	3.91	3.12	8.9	23.1	39.4
3	4.30	3.91	3.52	3.2	16.7	35.3	7.03	5.47	4.69	3.1	9.9	20.3
4	6.64	5.08	4.30	5.2	15.8	31.0	5.08	4.30	3.52	5.1	13.1	23.4
5	7.03	5.86	5.08	5.8	15.7	29.1	6.25	5.08	4.30	5.0	14.2	27.4
6	5.86	4.30	3.91	13.6	27.6	38.1	6.25	4.30	3.52	7.8	16.5	26.6
7	7.42	5.86	5.08	6.1	17.0	32.1	8.20	4.30	3.91	6.0	13.6	22.7
8	6.25	5.08	4.30	6.2	17.0	31.0	6.25	4.69	3.91	4.0	11.0	20.6
9	6.25	4.69	3.91	17.4	35.9	51.2	5.86	4.69	3.91	6.0	17.0	32.2
10	5.86	4.69	3.91	7.8	20.2	36.5	5.47	3.52	2.73	7.3	12.7	19.6
11	5.47	3.91	3.52	11.4	29.3	49.6	5.86	3.91	3.52	7.4	17.0	27.9
12	3.52	3.12	3.12	32.3	72.0	92.7	5.08	3.52	3.12	15.3	31.5	44.3

Table F.11 Effect of ±40% change in k_{1x} on the resonance frequency and the magnitude at resonance of the fore-and-aft cross-axis apparent mass.

	Feet hanging						Average thigh contact					
	Frequency (Hz)			Magnitude (kg)			Frequency (Hz)			Magnitude (kg)		
Subject	-40%	Initial	+40%	-40%	Initial	+40%	-40%	Initial	+40%	-40%	Initial	+40%
1	5.08	5.47	6.25	12.5	21.0	25.8	5.47	5.47	5.47	9.5	10.0	10.5
2	3.52	4.69	5.08	21.9	32.5	40.0	3.12	3.91	4.30	11.7	23.1	37.8
3	3.52	3.91	4.30	10.1	16.7	23.1	3.12	5.47	6.25	9.5	9.9	12.0
4	2.34	5.08	5.86	10.4	15.8	19.8	3.12	4.30	4.69	8.4	13.1	18.2
5	4.69	5.86	6.25	10.7	15.7	16.9	3.91	5.08	5.47	9.5	14.2	16.8
6	3.91	4.30	4.69	13.0	27.6	40.6	4.30	4.30	4.69	8.8	16.5	26.1
7	5.47	5.86	6.25	11.3	17.0	20.1	3.52	4.30	5.08	7.4	13.6	21.4
8	3.91	5.08	5.47	10.0	17.0	23.7	2.73	4.69	5.08	8.1	11.0	12.8
9	4.69	4.69	5.08	19.6	35.9	51.0	3.52	4.69	5.08	13.0	17.0	18.5
10	4.30	4.69	5.08	13.6	20.2	20.9	3.91	3.52	3.91	7.0	12.7	21.4
11	3.12	3.91	4.69	18.0	29.3	39.8	4.30	3.91	4.30	9.3	17.0	26.0
12	3.52	3.12	3.52	36.4	72.0	89.1	4.30	3.52	3.91	14.7	31.5	58.4

Table F.12 Effect of ±40% change in c_{1x} on the resonance frequency and the magnitude at resonance of the fore-and-aft cross-axis apparent mass.

	Feet hanging						Average thigh contact					
	Frequency (Hz)			Magnitude (kg)			Frequency (Hz)			Magnitude (kg)		
Subject	-40%	Initial	+40%	-40%	Initial	+40%	-40%	Initial	+40%	-40%	Initial	+40%
1	5.47	5.47	5.47	31.1	21.0	16.8	5.08	5.47	5.47	10.0	10.0	10.1
2	4.69	4.69	4.69	48.7	32.5	25.4	3.52	3.91	3.91	32.6	23.1	19.1
3	3.91	3.91	3.52	21.2	16.7	14.5	5.47	5.47	3.12	14.6	9.9	8.9
4	5.08	5.08	5.08	23.9	15.8	12.5	3.91	4.30	4.30	18.8	13.1	11.0
5	5.86	5.86	5.47	23.6	15.7	12.4	5.08	5.08	5.08	20.8	14.2	11.2
6	4.30	4.30	4.69	40.9	27.6	21.7	3.91	4.30	4.69	22.8	16.5	14.6
7	5.47	5.86	5.86	24.4	17.0	14.1	4.30	4.30	5.47	19.2	13.6	11.6
8	4.69	5.08	5.08	24.7	17.0	13.9	4.69	4.69	4.69	15.4	11.0	9.3
9	4.30	4.69	5.08	50.0	35.9	30.2	4.69	4.69	4.69	25.3	17.0	13.5
10	4.69	4.69	4.69	29.8	20.2	16.1	3.12	3.52	3.91	17.4	12.7	12.0
11	3.91	3.91	4.30	43.3	29.3	24.1	3.91	3.91	4.30	22.8	17.0	15.0
12	3.12	3.12	3.52	97.9	72.0	63.3	3.52	3.52	3.91	39.4	31.5	28.9

Table F.13 Effect of ±40% change in k_2 on the resonance frequency and the magnitude at resonance of the fore-and-aft cross-axis apparent mass.

	Feet hanging						Average thigh contact					
	Frequency (Hz)			Magnitude (kg)			Frequency (Hz)			Magnitude (kg)		
Subject	-40%	Initial	+40%	-40%	Initial	+40%	-40%	Initial	+40%	-40%	Initial	+40%
1	5.47	5.47	5.47	20.6	21.0	21.4	5.47	5.47	5.08	8.7	10.0	11.7
2	4.69	4.69	4.69	28.7	32.5	37.1	3.91	3.91	3.91	21.7	23.1	24.4
3	3.52	3.91	4.30	13.8	16.7	18.7	5.47	5.47	3.52	8.7	9.9	13.2
4	5.08	5.08	5.08	14.5	15.8	17.4	4.30	4.30	3.91	12.5	13.1	13.9
5	5.86	5.86	5.86	14.9	15.7	16.5	5.08	5.08	5.08	13.3	14.2	15.1
6	4.30	4.30	4.30	27.3	27.6	27.9	4.30	4.30	4.30	15.6	16.5	17.4
7	5.86	5.86	5.47	15.5	17.0	18.8	4.30	4.30	4.30	12.7	13.6	14.3
8	5.08	5.08	5.08	16.1	17.0	17.8	4.69	4.69	4.69	9.8	11.0	12.5
9	4.69	4.69	4.69	34.4	35.9	37.2	4.69	4.69	4.69	15.3	17.0	19.1
10	4.69	4.69	4.69	19.1	20.2	21.4	3.52	3.52	3.52	12.4	12.7	13.0
11	4.30	3.91	3.91	26.7	29.3	32.6	3.91	3.91	3.91	16.1	17.0	17.8
12	2.73	3.12	4.30	64.1	72.0	52.6	3.52	3.52	3.52	42.4	31.5	20.8

Table F.14 Effect of ±40% change in c_2 on the resonance frequency and the magnitude at resonance of the fore-and-aft cross-axis apparent mass.

	Feet hanging						Average thigh contact					
	Frequency (Hz)			Magnitude (kg)			Frequency (Hz)			Magnitude (kg)		
Subject	-40%	Initial	+40%	-40%	Initial	+40%	-40%	Initial	+40%	-40%	Initial	+40%
1	5.47	5.47	5.47	25.9	21.0	17.5	5.47	5.47	5.47	10.2	10.0	9.7
2	4.69	4.69	4.69	34.7	32.5	30.4	3.52	3.91	3.91	28.6	23.1	19.1
3	3.91	3.91	3.91	20.2	16.7	14.2	3.12	5.47	5.47	12.7	9.9	9.5
4	5.08	5.08	5.08	16.2	15.8	15.4	3.91	4.30	4.30	14.9	13.1	11.7
5	5.86	5.86	5.86	16.1	15.7	15.2	5.08	5.08	5.08	14.9	14.2	13.4
6	4.30	4.30	4.30	31.3	27.6	24.5	3.91	4.30	4.30	20.9	16.5	13.8
7	5.86	5.86	5.86	17.5	17.0	16.4	4.30	4.30	4.69	17.7	13.6	10.9
8	5.08	5.08	5.08	18.3	17.0	15.7	4.69	4.69	4.69	11.5	11.0	10.5
9	4.69	4.69	4.69	39.6	35.9	32.8	4.69	4.69	4.69	17.9	17.0	16.2
10	4.69	4.69	4.69	21.2	20.2	19.1	3.12	3.52	3.52	14.2	12.7	11.4
11	3.91	3.91	3.91	32.8	29.3	26.3	3.91	3.91	4.30	22.3	17.0	13.8
12	3.12	3.12	3.52	85.2	72.0	62.3	4.30	3.52	3.52	37.4	31.5	28.3

Table F.15 Effect of ±40% change in k_{3z} on the resonance frequency and the magnitude at resonance of the fore-and-aft cross-axis apparent mass.

	Feet hanging						Average thigh contact					
	Frequency (Hz)			Magnitude (kg)			Frequency (Hz)			Magnitude (kg)		
Subject	-40%	Initial	+40%	-40%	Initial	+40%	-40%	Initial	+40%	-40%	Initial	+40%
1	5.08	5.47	6.25	16.8	21.0	19.1	3.12	5.47	6.25	11.0	10.0	10.2
2	4.30	4.69	4.69	31.6	32.5	25.9	3.52	3.91	3.52	32.5	23.1	17.3
3	3.91	3.91	3.91	24.5	16.7	13.3	3.12	5.47	3.12	11.0	9.9	8.5
4	4.69	5.08	5.47	14.9	15.8	12.7	3.91	4.30	4.30	14.1	13.1	11.1
5	5.08	5.86	6.25	12.1	15.7	15.1	4.30	5.08	5.08	12.0	14.2	12.8
6	3.91	4.30	4.69	29.2	27.6	19.8	3.52	4.30	4.30	21.0	16.5	12.1
7	4.69	5.86	6.64	16.1	17.0	14.8	4.30	4.30	4.30	20.1	13.6	10.9
8	4.30	5.08	5.08	17.7	17.0	13.5	3.91	4.69	5.47	10.7	11.0	9.9
9	3.91	4.69	5.47	38.3	35.9	26.7	3.91	4.69	4.69	14.3	17.0	15.8
10	3.91	4.69	5.08	15.2	20.2	19.7	3.12	3.52	4.69	19.9	12.7	8.7
11	3.52	3.91	4.30	31.0	29.3	23.2	3.52	3.91	4.30	20.0	17.0	13.0
12	3.12	3.12	3.52	71.0	72.0	67.7	3.52	3.52	4.30	31.3	31.5	29.5

Table F.16 Effect of ±40% change in c_{3z} on the resonance frequency and the magnitude at resonance of the fore-and-aft cross-axis apparent mass.

	Feet hanging						Average thigh contact					
	Frequency (Hz)			Magnitude (kg)			Frequency (Hz)			Magnitude (kg)		
Subject	-40%	Initial	+40%	-40%	Initial	+40%	-40%	Initial	+40%	-40%	Initial	+40%
1	5.86	5.47	5.47	28.3	21.0	16.9	5.47	5.47	5.47	15.8	10.0	7.3
2	5.08	4.69	4.69	43.0	32.5	26.1	3.91	3.91	3.52	25.3	23.1	21.1
3	3.91	3.91	3.91	17.5	16.7	15.8	5.86	5.47	3.12	13.6	9.9	9.0
4	5.47	5.08	5.08	23.4	15.8	12.4	4.69	4.30	3.91	16.3	13.1	11.6
5	5.86	5.86	5.47	24.7	15.7	12.0	5.08	5.08	4.69	21.0	14.2	11.2
6	4.30	4.30	4.30	32.0	27.6	24.1	4.69	4.30	3.91	18.9	16.5	14.8
7	5.86	5.86	5.47	26.5	17.0	12.9	4.69	4.30	4.30	14.1	13.6	13.0
8	5.47	5.08	4.69	22.8	17.0	14.1	5.08	4.69	4.30	16.8	11.0	8.5
9	5.08	4.69	4.69	44.8	35.9	30.0	4.69	4.69	4.30	25.2	17.0	13.3
10	4.69	4.69	4.69	32.0	20.2	15.0	3.91	3.52	3.52	14.2	12.7	11.7
11	4.30	3.91	3.91	38.2	29.3	24.7	4.30	3.91	3.91	21.2	17.0	14.7
12	3.52	3.12	3.12	82.8	72.0	66.0	4.30	3.52	3.52	43.6	31.5	26.8

REFERENCES

Bearrds CF (1996) Structural vibration: Analysis and damping. London: Arnold.

Belytschko T and Privitzer E (1978) A three dimensional discrete element dynamic model of the spine, head and torso. AGARD conference proceeding No. 253 A9-1-15.

Boileau PE and Rakheja S (1998) Whole-body vertical biodynamic response characteristics of the seated vehicle driver-Measurement and model development. International Journal of Industrial Ergonomics 22, 449-472.

Boileau PE, Rakheja S and Wu X (2002) A body mass dependent mechanical impedance model for applications in vibration seat testing. Journal of Sound and Vibration 253 (1), 243-264.

Boileau PE, Wu X and Rakheja S (1998) Definition of a range of idealised values to characterize seated body biodynamic response under vertical vibration. Journal of Sound and Vibration 215 (4), 841-862.

British Standards Institution (1987) British Standard guide to measurement and evaluation of human exposure to whole-body vibration and repeated shock. British Standard BS 6841.

Broman H, Pope M and Hansson T (1996) A mathematical model of the impact response of the seated subject. Med. Eng. Phys. 18, 410-419.

Clegg F (1990) Simple statistics: A course book for the social sciences. Cambridge: Cambridge University press.

Coermann RR (1962) The mechanical impedance of the human body in sitting and standing positions at low frequencies. Human Factors 4 (10), 227-253.

Deursen DL, Lengsfeld M, Snijders CJ, Evers JJM and Goossens RHM (2000) Mechanical effects of continuous passive motion on the lumbar spine in seating. Journal of Biomechanics 33, 695-699.

Donati PM and Bonthoux C (1983) Biodynamic response of the human body in the sitting position when subjected to vertical vibration. Journal of Sound and Vibration 90 (3), 423-442.

Fairley T (1986) Predicting the dynamic performance of seats. Ph.D. thesis, University of Southampton, England.

Fairley T and Griffin MJ (1989) The apparent mass of the seated human body: vertical vibration. Journal of Biomechanics 22 (2), 81-94.

Fairley T and Griffin MJ (1990) The apparent mass of the seated human body in the fore-and-aft and lateral directions. Journal of Sound and Vibration 139 (2), 299-306.

Fritz M (2000) Description of the relation between the forces acting in the lumbar spine and whole-body vibrations by means of transfer functions. Clinical Biomechanics 15, 234-240.

Griffin MJ (1975) Vertical vibration of seated subjects: effect of posture, vibration level and frequency. Aviation, Space and Environmental Medicine 46 (3), 269-276.

Griffin MJ (1990) Handbook of Human Vibration. London: Academic Press Limited.

Griffin MJ (2001) The validation of biodynamic models. Clinical Biomechanics 16 (1), 81-92.

Griffin MJ and Brett MW (1997) Effects of fore-and-aft, lateral and vertical whole-body vibration on head-positioning task. Aviation, space and environmental medicine 68 (12), 1115-1122.

Griffin MJ, Lewis CH, Parsons KC and Whitham EM (1978) The biodynamic response of the human body and its application to standards. AGARD Conference Proceeding No. 253, A28-1-18.

Gunston TP (2003) The apparent mass of the seated human body in response to lateral and roll vibration. 38th United Kingdom Conference on Human Response to Vibration, Institute of Naval Medicine, Alverstoke, Gosport, PO12 2DL, England, 17-19 September.

Hagena FW, Wirth CJ, Piehler J, Plitz W, Hofmann GO and Zwingers T (1985) In vivo experiments on the response of the human spine to sinusoidal Gz-vibration. AGARD Conference Proceedings 378.

Hay JG (1994) The biomechanics of sports techniques. Prentice hall.

Hinz B and Seidel H (1987) The nonlinearity of the human body's dynamic response during sinusoidal whole-body vibration. Industrial Health 25, 169-181.

Hinz B, Seidel H, Brauer D, Menzel G, Blüthner R and Erdmann U (1988) Bidimensional accelerations of lumbar vertebrae and estimation of internal spinal load during sinusoidal vertical whole-body vibration: a pilot study. Clinical Biomechanics 3, 241-248.

Holmlund P (1998) Absorbed power and mechanical impedance of the seated human exposed to whole-body vibration in horizontal and vertical directions. Ph.D. thesis, Umea University, Sweden.

Holmlund P and Lundström R (1998) Mechanical impedance of the human body in the horizontal direction. Journal of Sound and Vibration 215 (4), 801-812.

Holmlund P, Lundström R and Lindberg L (2000) Mechanical impedance of the human body in vertical direction. Applied Ergonomics 31, 415-422.

Holmlund P and Lundström R (2001) Mechanical impedance of the sitting human body in single-axis compared to multi-axis whole-body vibration exposure. Clinical Biomechanics 16 (1), S101-S110.

Holmlund P, Lundström R and Lindberg L (1995) Whole-body vibration. Mechanical impedance of human body in the vertical direction. United Kingdom Informal Group Meeting on Human Response to Vibration, Silsoe, Bedford, United Kingdom, 18-20 September.

Howarth HVC (2003) A laboratory study of the effect of posture on head movement during low frequency fore-and-aft oscillation. 38th United Kingdom Conference on Human Response to Vibration, Institute of Naval Medicine, Alverstoke, Gosport, PO12 2DL, England, 17-19 September.

International Organization for Standardization (1981) Vibration and shock - mechanical driving point impedance of the human body. ISO 5982.

International Organization for Standardization (1987) Vibration and shock - mechanical transmissibility of the human body in the z-direction. ISO 7982.

International Organization for Standardization (1997) Vibration and shock - evaluation of human exposure to whole-body vibration. ISO 2631.

International Organization for Standardization (2001) Vibration and shock - mechanical driving point impedance of the human body. Final Draft ISO 5982.

Ji TJ (1995) A continuous model for the vertical vibration of the human body in a standing position. United Kindom Informal Group Meeting on Human Response to Vibration, 18-20 September.

Kitazaki S (1992) Application of experimental modal analysis to the human whole-body vibration. United Kingdom Informal Group Meeting on Human Response to Vibration, Institute of Sound and Vibration Research, University of Southampton, Southampton, United Kingdom, 28-30 September.

Kitazaki S (1994) Modelling mechanical responses to human whole-body vibration. Ph.D. thesis, University of Southampton, England.

Kitazaki S (1997) The apparent mass of the foot and prediction of floor carpet transfer function. United Kingdom Group Meeting on Human Response to Vibration, University of Southampton, Southampton, United Kingdom, 17-19 September.

Kitazaki S and Griffin MJ (1995) A data correction method for surface measurement of vibration on the human body. Journal of biomechanics 28 (7), 885-890.

Kitazaki S and Griffin MJ (1997) A modal analysis of whole-body vertical vibration using a finite element model of the human body. Journal of Sound and Vibration 200 (1), 83-103.

Kitazaki S and Griffin MJ (1998) Resonance behaviour of the seated human body and effects of posture. Journal of Biomechanics 31, 143-149.

Lakie M (1986) Vibration causes stiffness changes (thixotropic behaviour) in relaxed human muscle. Proceedings of the United Kingdom Informal Group Meeting on Human Response to Vibration, Loughborough University of Technology, Loughborough, England, 22-23 September.

Latham F (1957) A study in body ballistics: seat ejection. Proceedings of the Royal Society, B 147, 121-139.

Lee RA and Pradko F (1968) Analytical analysis of human vibration. Automotive Engineering Congress, Detroit, Mich., U.S.A, 8-12 January.

Lewis CH (2001) An adaptive electro-mechanical model for simulating the driving point force response of the human body with different input motions. 36th United Kingdom Group Meeting on Human Response to Vibration, Centre for Human Sciences, QinetiQ, Farnborough, UK, 12-14 September.

Lewis CH and Griffin MJ (1996) The transmission of vibration to the occupants of a car seat with a suspended back-rest. Proc Instn Mech Engrs 210, 199-207.

Li TF, Advani SH and Lee Y-C (1971) The effect of initial curvature on the dynamic response of the spine to axial acceleration. Symposium on Biodynamic Models and their Applications, Wright-Patterson Air Force Base, Ohio.

Liu YK and Murray JD (1966) A theoretical study of the effect of impulse on the human torso. Proceeding of the Symposium on Biomechanics, New York.

Lundström R and Holmlund P (1998) Absorption of energy during whole-body vibration exposure. Journal of Sound and Vibration 215 (4), 789-799.

Lundström R and Lindberg L (1983) Whole-body vibrations in road construction vehicles. The Swedish National Board of Occupational Safety and Health. Report No. 18.

Magnusson M, Pope M, Rostedt M and Hansson T (1993) Effect of backrest inclination on the transmission of vertical vibrations through the lumbar spine. Clinical Biomechanics 8, 5-12.

Mansfield NJ (1994) The apparent mass of the human body in the vertical direction-the effect of vibration magnitude. Proceedings of the United Kingdom Informal Group Meeting

on Human Response to Vibration, Institute of Naval Medicine, Alverstoke, Gosport, Hampshire, United Kingdom, 19-21 September.

Mansfield NJ (1997) A consideration of alternative non-linear lumped parameter models of the apparent mass of a seated person. United Kingdom Group Meeting on Human Response to Vibration, ISVR, University of Southampton, Southampton, 17-19 September.

Mansfield NJ (1998) Non-linear dynamic response of the seated person to whole-body vibration. Ph.D. thesis, University of Southampton, England.

Mansfield NJ and Griffin MJ (1998) Effect of magnitude of vertical whole-body vibration on absorbed power for the seated human body. Journal of Sound and Vibration 215 (4), 813-825.

Mansfield NJ and Griffin MJ (2000) Non-linearities in apparent mass and transmissibility during exposure to whole-body vertical vibration. Journal of Biomechanics 33, 933-941.

Mansfield NJ and Griffin MJ (2002) Effects of posture and vibration magnitude on apparent mass and pelvis rotation during exposure to whole-body vertical vibration. Journal of Sound and Vibration 253 (1), 93-107.

Mansfield NJ, Holmlund P and Lundström R (2001) Apparent mass and absorbed power during exposure to whole-body vibration and repeated shocks. Journal of Sound and Vibration 248 (3), 427-440.

Mansfield NJ and Lundström R (1998) Variability in the apparent mass of the seated person to horizontal vibration. United Kingdom Group Meeting on Human Response to Vibration, Buxton, Derbyshire, England, 16-18 September.

Mansfield NJ and Lundström R (1999a) The apparent mass of the human body exposed to non-orthogonal horizontal vibration. Journal of Biomechanics 32, 1269-1278.

Mansfield NJ and Lundström R (1999b) Models of the apparent mass of the seated human body exposed to horizontal whole-body vibration. Aviation Space and Environmental Medicine 70 (12), 1166-1172.

Matsumoto Y (1996) The influence of posture on the apparent mass of standing subjects exposed to vertical vibration. United Kingdom Informal Group Meeting on Human Response to Vibration, MIRA, England, 18-20 September.

Matsumoto Y (1999) Dynamic response of standing and seated persons to whole-body vibration: principal resonance of the body. Ph.D. thesis, University of Southampton.

Matsumoto Y and Griffin MJ (1998a) Movement of the upper-body of seated subjects exposed to vertical whole-body vibration at the principal resonance frequency. Journal of Sound and Vibration 215 (4), 743-762.

Matsumoto Y and Griffin MJ (1998b) Dynamic response of the standing human body exposed to vertical vibration: influence of posture and vibration magnitude. Journal of Sound and Vibration 212 (1), 85-107.

Matsumoto Y and Griffin MJ (2000) Comparison of biodynamic responses in standing and seated human bodies. Journal of Sound and Vibration 238 (4), 691-704.

Matsumoto Y and Griffin MJ (2001) Modelling the dynamic mechanisms associated with the principal resonance of the seated human body. Clinical Biomechanics 16 (1), 31-44.

Matsumoto Y and Griffin MJ (2002a) Effect of muscle tension on non-linearities in the apparent masses of seated subjects exposed to vertical whole-body vibration. Journal of Sound and Vibration 253 (1), 77-92.

Matsumoto Y and Griffin MJ (2002b) Non-linear characteristics in the dynamic responses of seated subjects exposed to vertical whole-body vibration. Journal of Biomechanical Engineering 124, 527-532.

Matsumoto Y and Griffin MJ (2003) Mathematical models for the apparent masses of standing subjects exposed to vertical whole-body vibration. Journal of Sound and Vibration 260, 431-451.

Mertens H (1978) Nonlinear behavior of sitting humans under increasing gravity. Aviation, Space, and Environmental Medicine 49 (1), 287-298.

Mertens H and Vogt L (1978) The response of a realistic computer model for sitting humans to different types of shocks. AGARD Conference Proceedings No. 253, A26-1-17.

Miwa T (1975) Mechanical impedance of human body in various postures. Industrial Health 13, 1-22.

Moore KL and Agur AMR (2002) Essential clinical anatomy. Baltimore: Lippincott Williams and Wilkins.

Muksian R and Nash CD (1974) A model for the response of seated humans to sinusoidal displacements of the seat. Journal of Biomechanics 7, 209-215.

National Aeronautics and Space Administration (1978) NASA Reference publication 1024. Anthropometric source book, volume I: anthropometry for designers.

Nicol JJ, Morrison J, Roddan G and Rawicz A (1995) The application of an artificial neural network to modeling seat to spine transmission of acceleration. The United Kingdom Informal Group meeting on Human Response to Vibration, Silsoe Research Institute, Wrest Park, Silsoe, Bedford, United Kingdom, 18-20 September.

Nishiyama S, Uesugi N, Takeshima T, Kano Y and Togii H (2000) Research on vibration characteristics between human body and seat, steering wheel, and pedals (effects of seat position on ride comfort). Journal of Sound and Vibration 236 (1), 1-21.

Paddan GS (1995) Hand displacements during exposure to whole-body lateral vibration. United Kingdom Informal Group Meeting on Human Response to Vibration, Silsoe, Bedford, United Kingdom, 18-20 September.

Paddan GS and Griffin MJ (1988a) The transmission of translational seat vibration to the head.I. Vertical seat vibration. Journal of Biomechanics 21 (3), 191-197.

Paddan GS and Griffin MJ (1988b) The transmission of translational seat vibration to the head. II. Horizontal seat vibration. Journal of Biomechanics 21 (3), 199-206.

Paddan GS and Griffin MJ (1994) Transmission of roll and pitch seat vibration to the head. Ergonomics 37 (9), 1513-1531.

Paddan GS and Griffin MJ (2000) Transmission of yaw seat vibration to the head. Journal of Sound and Vibration 229 (5), 1077-1095.

Panjabi MM, Anderson GBJ, Jorneus L, Hult E and Mattsson L (1986) In vivo measurements of spinal column vibrations. Journal of Bone and Joint Surgery, Incorporated 68A (5), 695-702.

Pankoke S, Buck B and Woelfel HP (1998) Dynamic FE model of sitting man adjustable to body height, body mass and posture used fro calculating internal forces in the lumbar vertebral disks. Journal of Sound and Vibration 215 (4), 827-839.

Parsons KC, Griffin MJ and Whitham EM (1982) Vibration and comfort III. Translational vibration of the feet and back. Ergonomics 25 (8), 705-719.

Payne PR (1965) Personnel restraint and support system dynamics. Aerospace Medical Research Laboratories, Wright-Patterson Air Force Base. Report no. AMRL-TR-65-127.

Payne PR and Band EGU (1971) A four-degree-of-freedom lumped parameter model of the seated human body. Aerospace Medical Research Laboratory, Wright-Patterson Air Force Base. Report No. AMRL-TR-70-35.

Pope MH, Wilder DG and Magnusson ML (1999) A review of studies on seated whole-body vibration and low back pain. Proc Instn Mech Engrs 213 Part H, 435-446.

Pradko F, Lee R and Kaluza V (1966) Theory of human vibration response. ASME. Paper No. 66-WA/BHF-15.

Rakheja S, Stiharu I and Boileau PE (2002) Seated occupant apparent mass characteristics under automotive postures and vertical vibration. Journal of Sound and Vibration 253 (1), 57-75.

Sandover J (1978) Modelling human responses to vibration. Aviation Space and Environmental Medicine 49 (1), 335-339.

Sandover J and Dupuis H (1987) A reanalysis of spinal motion during vibration. Ergonomics 30 (6), 975-985.

Seidel H, Blüthner R and Hinz B (2001) Application of finite-element models to predict forces acting on the lumbar spine during whole-body vibration. Clinical Biomechanics 16 (1), 57-63.

Siegel S and Castellan NJ (1988) Nonparametric statistics for the behavioral sciences. Singapore: McGraw-Hill.

Singley GT and Haley JL (1978) The use of mathematical modeling in crashworthy helicopter seating system. AGARD Conference Proceedings No. 253, A22-1-21, Paris, France, 6-10 November.

Smith SD (1993) Comparison of the driving point impedance and transmissibility techniques in describing human response to whole-body vibration. Proceeding of the United Kingdom Informal Group Meeting on Human Response to Vibration, Army Personnel Research Establishment, Ministry of Defence, Farnborough, UK, 20-22 September.

Smith SD (1994) Nonlinear resonance behaviour in the human exposed to whole-body vibration. Shock and Vibration 1 (5), 439-450.

Smith SD (1995) The effects of whole-body vibration on human biodynamic response. Journal of Gravitational Physiology 2 (1), P96-P99.

Smith SD (2000) Modelling differences in the vibration response characteristics of the human body. Journal of Biomechanics 33, 1513-1516.

Suggs CW, Abrams CF and Stikeleather LF (1969) Application of a damped spring-mass human vibration simulator in vibration testing of vehicle seats. Ergonomics 12 (1), 79-90.

Toward MGR (2002) Apparent mass of the human body in the vertical direction: effect of input spectra. Presented at the 37th United Kingdom Conference on Human Response to Vibration, Department of Human Sciences, Loughborough University, UK, 17-19 September.

Toward MGR (2003) Apparent mass of the human body in the vertical direction: effect of seat backrest. Presented at the 38th United Kingdom Conference on Human Response to Vibration, Institute of Naval Medicine, Alverstoke, Gosport, PO12 2DL, England, 17-19 September.

Vogt HL, Coermann RR and Fust HD (1968) Mechanical impedance of the sitting human under sustaind acceleration. Aerospace Medicine 39 (7), 675-679.

Vogt HL, Krause H, Hohlweck H and May E (1973) Mechanical impedance of supine humans under sustained acceleration. Aerospace Medicine 44 (2), 123-128.

Wei L (2000) Predicting transmissibility of car seats from seat impedance and the apparent mass of the human body. Ph.D. thesis, University of Southampton, England.

Wei L and Griffin MJ (1998a) The influence of seat cushion inclination on subject apparent mass and seat transmissibility. United Kingdom Group Meeting on Human Response to Vibration, Health and Safety Executive, Buxton, Derbyshire, England, 16-18 September.

Wei L and Griffin MJ (1998b) Mathematical models for the apparent mass of the seated human body exposed to vertical vibration. Journal of sound and vibration 212 (5), 855-874.

Wei L and Griffin MJ (1999) Modelling the effect of backrest angle on the vertical apparent mass of seated subjects. United Kingdom Group Meeting on Human Response to Vibration, Ford Motor Company, Dunton, Essex, England, 22-24 September.

Wittmann TJ and Phillips NS (1969) Human body nonlinearity and mechanical impedance analysis. Journal of Biomechanics 2, 281-288.